THE JOURNAL
OF
CHEMICAL PHYSICS

VOLUME 18, NUMBER 3 MARCH, 1950

Paramagnetic Susceptibilities and Electronic Structures of Aqueous Cations of Elements 92 to 95

JEROME J. HOWLAND, JR.[1] AND MELVIN CALVIN
Radiation Laboratory and Department of Chemistry, University of California, Berkeley, California

(Received June 25, 1949)

Magnetic susceptibilities per gram atomic weight of elements 92 to 95 in most of their oxidation states were measured at 20°C on 0.1 ml of solution which was 0.005 to 0.09*M* in heavy element. The values obtained (all paramagnetic) in units $\times 10^6$ were: U(IV), 3690; Np(VI), 2060; Np(V), 4120; Np(IV), 4000; Pu(IV), 1610; Pu(III), 370; Am(III), 720. The results could be interpreted only on the basis of electronic configurations $5f^n$, even though susceptibilities were generally lower than the theoretical values and lower than experimental values for corresponding lanthanide $4f^n$ cations. The lower values should be expected as a result of the Stark effect produced by electric fields of anions and of water dipoles. Failure of the Russell-Saunders approximation to the coupling between electrons may account for some of the error in the theoretical calculations. That the susceptibilities of Pu(III) and Am(III) are manyfold lower than those of Sm(III) and Eu(III), respectively, is attributed to wider multiplet splitting in the actinide atoms.

CHEMICAL and physical properties and theoretical calculations have indicated that elements of about $Z=90$ and higher constitute a series in which the $5f$ orbitals are filled as Z increases. These heavy elements have been called actinides in analogy to the name lanthanides for the rare earth elements.[2] It was of interest to determine whether corresponding aqueous cations of actinide and lanthanide elements have the same outer electronic configurations even though the actinide concept might not require that they be identical.

If an atom has its electrons in question (i.e., those in addition to the inert gas structure) in inner orbitals, the electrons may be electrostatically shielded from neighboring atoms to the extent that the magnetic susceptibility of a solution of such atoms can be deduced from quantum numbers of the ground state of the electronic configuration. Sometimes the converse, deduction of ground state quantum numbers from the susceptibility, will yield a unique answer. The method was successful for the lanthanide tripositive ions which have as outer configurations $4f^{1-14}5s^25p^6$.

Susceptibilities of U(IV) and U(III) solutions were reported by Lawrence.[3] Solid uranium compounds have been studied by numerous investigators.[4] At room temperature the susceptibility of U(IV) solutions and salts approximates the theoretical value derived from the spin magnetic moment of atoms with two unpaired electrons. Since this type of calculation was successful in accounting for the susceptibility of the first row transition element ions which have partially filled $3d$ electron orbitals, the observed susceptibility of U(IV) was usually interpreted as evidence for a $5d^2$ electron configuration. This deduction was inconsistent with the fact that the observed susceptibilities of cations of heavier transition elements (those with partially filled $4d$ or $5d$ orbitals) are generally manyfold smaller than the "spin only" calculations, and later studies of general properties of U, Np, and Pu made $6d$ configurations improbable. Hutchison and Elliott[5] have interpreted their recent measurements of uranium(IV) susceptibilities on the basis of a $5f^2$ structure.

Shortly after plutonium became available, the susceptibilities of dilute Pu(VI), Pu(V), Pu(IV), and

[1] Now at Brookhaven National Laboratory, Upton, Long Island, New York.

[2] Some of the properties of the recently discovered heavy transition elements were reviewed and the name actinides was suggested by G. T. Seaborg, Chem. and Eng. News **23**, 2190 (1945); Science **104**, 379 (1946). W. H. Zachariasen, Phys. Rev. **73**, 1104 (1948) used the name actinide for the +3 ions only, thorides for +4 ions, etc., in reporting his x-ray diffraction studies which showed that the solid compounds have the crystal structures and ionic radii consistent with assumption of $5f$ electronic configurations. We use Seaborg's nomenclature.

[3] R. W. Lawrence, J. Am. Chem. Soc. **56**, 776 (1934).

[4] See reference 5 for keys to this literature.

[5] C. A. Hutchison, Jr., and N. Elliott, J. Chem. Phys. **16**, 920 (1948).

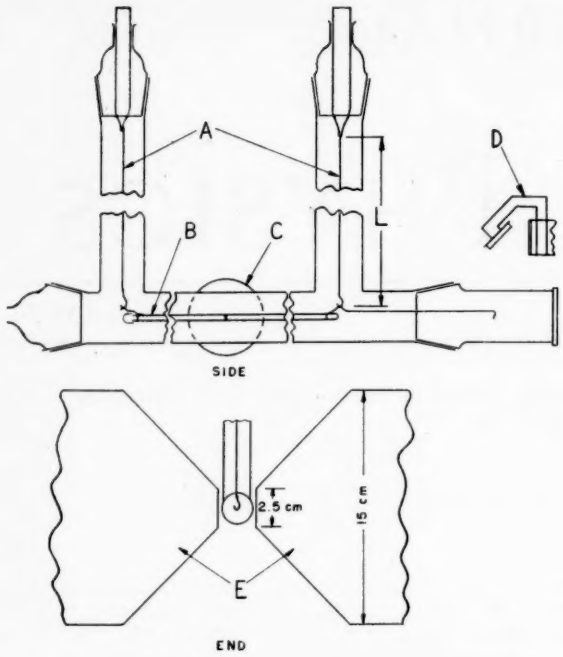

FIG. 1. Apparatus for measurement of magnetic susceptibility: A, glass fibers, 0.005×140 cm; B, glass capillary, 0.2×16 cm; C, magnet pole faces, 2.5 cm diam.; D, mirror and microscope; E, magnet pole pieces, 15 cm diam.

Pu(III) solutions were measured[6] with the expectation that they might closely parallel those of Pr(III) through Sm(III) if the actinide element ions also had f^n electronic configurations. The measurement of Pu(V) was very crude because of the instability of that state.[7] For the other three plutonium oxidation states there was no close agreement with expectations of particular electronic structures. More actinide elements which exist in one or more oxidation states could be used in the present study.

EXPERIMENTAL

Magnetic susceptibility measurements were made on 0.1 ml samples which were of the order of 0.01M in heavy element by use of a bifilar suspension method developed from one described by Theorell.[8] A divided glass capillary was suspended as shown in Fig. 1. A solution was in the left compartment; distilled water was in the right or rear compartment. The capillary moved a distance of the order of 0.1 cm when the current through the magnet coils was 40 amp. (Field strength directly between the pole faces was about 17,000 Gauss.)

The horizontal force, F, on the capillary very nearly equals wD/L, where w is the weight of the capillary, L is the fiber length, and D is the horizontal displacement which was observed in a microscope equipped with a traveling cross hair. One scale division on the knob corresponded to a distance of 8×10^{-5} cm or to a force of 6×10^{-7} g if the load was a 0.5-g capillary.

Each solution was measured several times at magnet coil currents of 20, 30, and 40 amp. in order to establish that susceptibilities were always independent of field strength.

The molar susceptibility, χ, of a substance equals I_m/H where I_m is the magnetic moment of a gram atomic weight of the bulk material and H is the magnetic field strength. The total force acting on a long cylinder of solution with cross section A and whose axis passes through an inhomogeneous field is

$$wD/L=F=\chi MA(H_2^2-H_1^2)/2000, \qquad (1)$$

where M is the molar concentration and H_1 and H_2 are the field strengths on the ends of the solution.

Equation (1) would hold only for a homogeneous sample; it was used for rough estimation of the field strength H_2 from the displacements of nickel chloride solutions. Susceptibilities of other substances were calculated on the assumption that the displacement of a given filled capillary was proportional to χM if H_1 and H_2 were held constant. The displacement was measured for each actinide element solution in the same capillary and at the same magnet coil current (±0.2 amp.) as was done for a standard nickel chloride solution. Correction for diamagnetism of the solvent (including anions) and for non-uniformity of the capillary was made by subtraction of an experimentally determined displacement for the solvent only in the rear compartment. If the molar susceptibility of nickel chloride at 20°C is taken as 4436×10^{-6} units,[9] then for any cation

$$\chi=4436\times10^{-6}D'M_{NiCl_2}/(MD'_{NiCl_2}), \qquad (2)$$

where D' is the displacement after application of the correction.

The U(IV) solution was prepared by dissolution of weighed, distilled UCl_4 in oxygen-free hydrochloric acid solution. The last step in the preparation of the neptunium, plutonium, and americium solutions was dissolution of a hydroxide which had been precipitated with ammonium hydroxide. The plutonium concentrations were based on a weighing. The neptunium and americium solutions were assayed by measurement of the rate of alpha-particle emission of a small aliquot. The specific activities in counts minutes^{-1} micrograms^{-1} were taken as 790 for Np[10] and 3.36×10^6 for Am[11] if a thin sample is mounted on platinum and a counter

[6] M. Calvin, Plutonium Project Report CK-2411 (1944). Calvin, Kasha, and Sheline, AECD-2002 (1948).

[7] Connick, Kasha, McVey, and Sheline, "The +5 oxidation state of plutonium," Plutonium Project Record, Vol. 14B, No. 3.15 (to be published).

[8] H. Theorell, Arkiv f. Kemi. Min. Geol. **16A**, No. 1 (1943). Our apparatus was essentially the one used but not described by G. N. Lewis, and M. Calvin, J. Am. Chem. Soc. **67**, 1232 (1945).

[9] H. R. Nettleton, and S. Sugden, Proc. Roy. Soc. (London) **A173**, 313 (1939).

[10] L. B. Magnusson, and T. J. LaChapelle, J. Am. Chem. Soc. **70**, 3534 (1948).

[11] B. B. Cunningham, Plutonium Project Report CC-3876, Sect. 2.2 (1948).

TABLE I. Typical data; displacement of capillary for 40-ampere magnet coil current.

Material in rear compart.	Displacement D	D'	Suscept. units $\times 10^6$
0.36M HCl	−030		
0.0392M $NiCl_2$ in 0.36M HCl	+991	1021	4436[a]
0.50M HCl	−030		
0.0600M Pu(III) in 0.5M Cl^-	+099	129	370
0.50M H_2SO_4	−089		
0.0507M Pu(IV) in 0.5M HSO_4^-	+389	478	1610

[a] Magnetic standard, reference 9.

geometry of "50 percent" is used.[12] These values are said to be better than ±5 percent. If other specific activities are reported at a later date, the magnetic susceptibilities should be corrected proportionately. The quantity of neptunium or plutonium which was not in the desired oxidation state was shown to be less than 1 percent by measurement of the characteristic optical absorption maxima[13] on a Beckman spectrophotometer.

The 0.03920M nickel chloride solution which served as magnetic standard was prepared by dissolution of 0.2301 g of nickel rod (Johnson Matthey and Company, 99.97 percent Ni) in 5 ml of refluxing 10M HCl. After the solution had been diluted to 100.0 ml, the excess HCl concentration was found to be 0.360M.

Although the measured displacements were reproducible to about one scale division, the precision for determination of the molar susceptibilities is about 2 percent or 30×10^6 units, whichever is larger, because of the direct dependence upon determination of actinide element concentration and because of the presence in the solutions of an unknown amount of diamagnetic ammonium ion. The large negative displacements found for some examples of solvent only in the rear compartments were due to non-uniformity of the glass capillary. These large negative subtractions do not increase the percent error if the gross displacement of the actinide solution is positive.

RESULTS AND INTERPRETATION

Some typical data are given in Table I, and the results are summarized in Table II. In Fig. 2 experimental χ of the actinide element cations are compared with simple theoretical χ_J for the assumed ground quantum states of the electronic configurations $5f^n$ and $5f^{n-1}6d$. The experimental χ follow the χ_J for configurations f^n to a significant degree, though not as closely as had been found for most of the lanthanide cations.[14,15] The susceptibility of Am(III) is much higher than the theoretical value of zero, but that is also true of the corresponding lanthanide ion, Eu(III). It will be discussed in a later section of this paper. The susceptibilities of the cations are, of course, dependent upon the anion to a secondary degree.[3]

The ground states of the cations Np(VI), Np(V), Np(IV), Pu(IV), Pu(III), and Am(III) were concluded to be those on which the theoretical curve B was based, i.e., $^2F_{5/2}$, $^3H_4$, $^4I_{9/2}$, $^5I_4$, $^6H_{5/2}$, and $^7F_0$ respectively as n is 1 through 6.

While the atomic quantum numbers of a state may be those which are expected for a definite configuration, f^n, the state can belong partly to another configuration of the same parity.[16] Susceptibility measurements can show only that the ground state has certain L, S, and J quantum numbers; identification of the state with a configuration is a useful approximate concept. To the extent that quantum states of complicated atoms can be attributed to a single electronic configuration, the known aqueous cations of uranium and higher elements must have as the outer part of their ground configurations, $5f^n6s^26p^6$ ($n5f$ electrons which are more or less inside the configuration for the inert gas element 86).

APPROXIMATE NATURE OF THEORETICAL CALCULATIONS

The factors which account for the limited accuracy of our theoretical calculations should be mentioned.

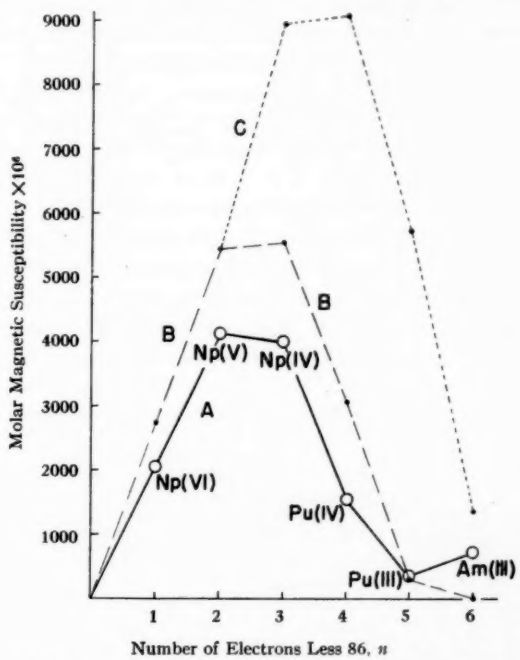

FIG. 2. Comparison at 20°C of magnetic susceptibilities of actinide elements cations with theoretical susceptibilities: A, experimental; B, theoretical for ground states of $5f^n$; C, theoretical for ground states of $5f^{n-1}6d$.

[12] About 52 percent of the disintegrations are counted, Cunningham, Ghiorso, and Hindman, "Back-scattering of Pu^{239} alpha-particles from platinum," Plutonium Project Record, Vol. **14B**, No. 16.3 (to be published).

[13] J. C. Hindman, and D. P. Ames, "Absorption spectra of ionic species of plutonium," Plutonium Project Record, Vol. **14B**, No. 4.1; Hindman, Magnusson, and LaChapelle, "Chemistry of element 93, III. Absorption spectrum studies of aqueous ions of neptunium," Ibid., No. 15.2.

[14] F. Hund, Zeits. f. Physik **33**, 855 (1925).

[15] J. H. Van Vleck, Phys. Rev. **31**, 587 (1928).

[16] E. U. Condon, Phys. Rev. **36**, 1121 (1930).

Quantum statistically the susceptibility is given by the relation[15]

$$\chi=\frac{I_m}{H}=\frac{N_0}{H}\frac{\Sigma\partial W_i/\partial H\exp(-W_i/kT)}{\Sigma\exp(-W_i/kT)}, \quad (3)$$

where N_0 is Avogadro's number and the summations are over-all quantum states of energies W_i. If the energy levels are simply those resulting from the Zeeman splitting of an isolated (on the energy scale) state of a free atom, their energies might be assumed to be

$$W_i-W_i^0=Hg\beta M, \quad (4)$$

where $\beta=eh/4\pi mc$ and $M=J,\ J-1,\ \cdots -J$. Since $2Hg\beta J\ll kT$ Eq. (3) yields

$$\chi_J=Ng^2\beta^2J(J+1)/3kT.^{17} \quad (5)$$

If the angular momenta of the several electrons are coupled according to the Russell-Saunders scheme (*LS* coupling)

$$g=[3J(J+1)+S(S+1)-L(L+1)]/2J(J+1). \quad (6)$$

Equations (5) and (6) were used to calculate the theoretical points of Fig. 2. The ground state of a configuration was assumed by application of Hund's rules. The limited agreement of theoretical and experimental susceptibilities indicates that each paramagnetic atom interacts with other surrounding atoms as well as with the external magnetic field used for the measurements. Since most of the surrounding atoms are diamagnetic, the interaction is generally electrostatic in nature.

Penney and Schlapp attempted to calculate the effect of crystal electric fields on the magnetic susceptibility of iron group compounds and rare earth salts.[18,19] Qualitatively it is a Stark splitting which is of the order of kT whereas the Zeeman splitting is small compared to kT. Although the calculations are not perfected,[20] it is clear that the summation (3) can be much smaller than its evaluation by Eq. (5). Similarly in solutions the electric fields of neighbor anions and water dipoles will lower the magnetic susceptibility of an actinide element cation compared to its corresponding lanthanide ion since the $5f$ electrons of the former should be outside the valence shell more often than are the $4f$ electrons in the latter. Since Np(VI) is essentially a one-electron case, the complications to be mentioned later cannot be important, and the 25 percent lowering of the susceptibility from the theoretical χ_J must be due to the Stark splitting. It might be assumed tentatively that the Stark effect is the most important single complication tending to lower the susceptibility of all the actinide element cations.

Our theoretical calculations may be inadequate also on account of incorrect assumptions about the interactions between the several $5f$ electrons within one actinide atom. Ground quantum states of the $4f^n$ configurations were deduced by Hund[14] from rules which are correct for atoms of small Z in which case it is a good approximation to derive atomic states from the states of individual electrons by means of the *LS* or Russell-Saunders coupling model (vanishingly weak spin-orbit interaction). In the spectra of gaseous uranium[21,22] the multiplet splitting is wider than the separation of the centers of gravity of *LS* states. By definition this is strong spin-orbit interaction. The experimental g's of low lying states of the $5f^36d7s^2$ configuration of uranium are fairly close to g_{LS}, however.

It is interesting to see what happens to the energy levels as the spin-orbit interaction increases and the interelectronic interaction approaches the limiting case of *jj* coupling. Column 2 of Table III lists some states which should lie very low in the configurations $5f^{1-6}$. The state listed first lies deepest according to Hund's rules. For $5f^2$, $5f^3$, and $5f^4$ the state listed second was selected because it belongs both to the next group according to *LS* coupling and to the lowest group of *jj* coupling states. The ground state of $5f^5$ or of $5f^6$ becomes more isolated as *jj* coupling is approached. In the case of $5f^6$ the two lowest multiplets of ^7F were selected because the spacing between $J=0$ and $J=1$ would be only 1/21 of the total multiplet splitting according to

TABLE II. Molar susceptibilities of actinide element cations at 20°C in aqueous solution.

Cation in solution	Anion in solution	Cation suscept. units $\times10^6$
U(IV)	0.5*M* Cl^-	3690[a]
Np(VI)	0.5*M* HSO_4^-	2060
Np(V)	0.2*M* Cl^-	4120[a]
Np(IV)	0.2*M* HSO_4^-	4000[b]
Pu(IV)	0.5*M* HSO_4^-	1610
Pu(III)	0.5*M* Cl^-	370
Am(III)	0.5*M* NO_3^-	720

[a] For Pu(VI) (same number of electrons as U(IV) and Np(V)) susceptibility is 3540×10^{-6}, reference 6.
[b] For U(III) (same number of electrons as Np(IV)), susceptibility is 4340×10^{-6}, reference 3.

[17] The small contribution to susceptibility from the atomic magnetic moment induced by the applied field was not added to the theoretical χ_J's. It would be only about -50×10^{-6} for monatomic ions represented by Pu^{+3} and Am^{+3} and possibly as much as $+50\times10^{-6}$ for molecular types such as NpO_2^+ and NpO_2^{++}.

[18] W. G. Penny, and R. Schlapp, Phys. Rev. **41**, 194 (1932); R. Schlapp and W. G. Penny, Ibid. **42**, 667 (1932). These authors pointed out the absence of any fundamental significance of the empirical Weiss-Curie relation, $\chi=C/(T+\Delta)$. Many investigators have calculated "effective atomic magnetic moments" as $\mu_{eff}=(Ck/N)^{\frac{1}{2}}$ and compared this "experimental" moment with $\mu=g\beta[J(J+1)]^{\frac{1}{2}}$. These μ_{eff} can have no more meaning than C, which sometimes approaches $N\mu^2/3k$ when Δ is nearly zero. It seems preferable to present all results as susceptibilities and then compare theoretical values with the directly observed quantities even though the discrepancies appear twice as great when the device of square root extraction is not used.

[19] A. Frank, Phys. Rev. **48**, 765 (1935).

[20] For more recent discussions see W. G. Penny, and G. J. Kynch, Proc. Roy. Soc. (London) **A170**, 112 (1939) and L. J. F. Broer, Physica **12**, 642 (1946).

[21] Kiess, Humphreys, and Laun, J. Opt. Soc. Am. **36**, 357 (1946); J. Research Nat. Bur. Standards **37**, 57 (1946).

[22] Ph. Schuurmans, Physica **11**, 475 (1946); Schuurmans, van den Bosch, and Dijkwel, Ibid. **13**, 117 (1947).

TABLE III. Theoretical susceptibilities of possible low energy states of actinide ions.

Assumed elect. config.	Possible low energy states	Theor. χ_J's LS coupl. 20°C	Theor. χ_J's jj coupl. 20°C
$5f^1$	$^2F_{5/2}$	2730	2730
$5f^2$	$^3H_4$; $^3F_2$	5420; 1130	6210; 1870
$5f^3$	$^4I_{9/2}$; $^4G_{5/2}$	5540; 1210	7680; 2730
$5f^4$	$^5I_4$; $^5G_2$	3040; 280	6210; 1870
$5f^5$	$^6H_{5/2}$	300	2730
$5f^6$	$^7F_0$; $^7F_1$	0; 1900	0; 1900
$5f6d$	$^3H_4$; $^3G_3$	5420; 2860	
$5f^26d$	$^4K_{11/2}$; $^4I_{9/2}$	8950; 5540	
$5f^36d$	$^5L_6$; $^5K_5$	9070; 5670	
$5f^46d$	$^6L_{11/2}$; $^6K_{9/2}$	5730; 3130	
$5f^56d$	$^7K_4$; $^7I_3$	1350; 320	

the Landé interval rule. The relative importance of the probably second lowest states is not known at the present time except that $^7F_1$ must be significantly populated in Am(III) at 20°C.

Theoretical χ_J's for each ground state of the $5f^n$ configurations were calculated for both coupling approximations, and the two results diverge as n increases from 2 to 5. Since the two χ_J's differ directly as g_{LS}^2 and g_{jj}^2 differ, the experimental χ of Pu(III), the example of $5f^5\,{}^6H_{5/2}$, shows unambiguously that g is much nearer to g_{LS} than to g_{jj}. This is consistent with previously mentioned results for the gaseous uranium atom.

Equation (5) depends on the validity of Eq. (4) for the Zeeman splitting. For each low energy state of Sm(III) and Eu(III) it was necessary[23] to use a more complete equation for χ_J which had been derived by Van Vleck[15] from considerations equivalent to taking the Zeeman splitting to the second-order terms in H. He obtained Eq. (5) with the following added on the right:

$$\frac{N\beta^2}{6(2J+1)}\left\{\frac{f(J)}{h\nu(J-1:J)}+\frac{f(J+1)}{h\nu(J+1;J)}\right\}, \qquad (5a)$$

where $f(J)=[(S+L+1)^2-J^2][J^2-(S-L)^2]/J$. For sufficiently large $h\nu$'s this addition is negligible except that when S and L are large and J is small the $f/h\nu$ terms are extremely large. In the examples Pu(III) and Am(III) the susceptibilities are greater than theoretical χ_J's for $^6H_{5/2}$ and $^7F_0$ as obtained with Eq. (5). The $f/h\nu$ terms must be significant for low lying states of both cations. While the $^7F_1$ state must be well populated in Am(III), it is much less so than in Eu(III) where the multiplet splitting is narrower. Thus the same discrepancies with simplest theory that were important in Sm(III) and in Eu(III) can be detected in Pu(III) and Am(III). The analogy is shown clearly in Fig. 3 where experimental susceptibilities of lanthanide and actinide element cations are compared directly.

[23] J. H. Van Vleck, and A. Frank, Phys. Rev. **34**, 1494, 1625 (1929).

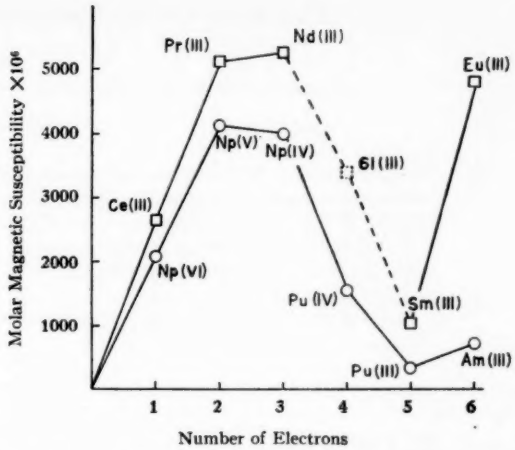

FIG. 3. Comparison of experimental magnetic susceptibilities of lanthanide and actinide element cations at 20°C. The values for the lanthanides were calculated from some of the "effective magnetic moments" compiled by Yost, Russell, and Garner, *The Rare Earth Elements and Their Compounds* (John Wiley, and Sons, Inc., New York, 1947), p. 14. The point for 61(III) is from the theoretical calculation by Van Vleck and Frank (see reference 23).

ACKNOWLEDGMENT

The neptunium and americium were available for this study through the cooperation of T. J. LaChapelle, L. B. Magnusson, L. B. Asprey, and Dr. B. B. Cunningham, who had isolated these materials in very pure form for various research purposes. Many others contributed, of course, to the production of these special materials.[24] We are especially grateful to Professor G. T. Seaborg for his efforts toward making the work reported here possible.

This paper is based on work performed under the auspices of the AEC at the Radiation Laboratory, University of California.

[24] *Note added in proof:* See Plutonium Project Record, Volume 14B. This collection of papers has recently been published under the title *The Transuranium Elements*, Seaborg, Katz, and Manning, Ed., (McGraw Hill Book Company, Inc., New York, 1949)

The Absorption Spectrum and the Dissociation of H_2O_2

RUDOLPH EDSE
Cryogenic Laboratory and Department of Chemistry, The Ohio State University, Columbus, Ohio
(Received June 29, 1949)

Although Holt, McLane, and Oldenberg state that they were unable to observe a sharp cut in the absorption spectrum of hydrogen peroxide vapor, it is shown that their measurements indicate a rather abrupt increase of the absorption coefficient at 1920A.

It is doubtful that the dissociation energy of hydrogen peroxide can be derived from its absorption spectrum. However, it seems possible that the photo-chemical decomposition of hydrogen peroxide gives an upper limit for its dissociation energy.

Our measurements of the absorption coefficient of hydrogen peroxide agree well with the results of Holt, McLane, and Oldenberg.

IN a recent paper Holt, McLane, and Oldenberg[1] remark that the absence of a "sharp cut" in the absorption spectrum of hydrogen proxide vapor according to their measurements obviates the necessity of placing a limit on the energy of dissociation of water vapor, which has been done by Damköhler and Edse.[2] However, it seems to me that the measurements of Holt and coworkers rather indicate a sharp cut than prove its absence and that the authors overlooked the fact that the sharp cut is not the only basis for the derivation of an upper limit.[3]

Sharma[4] himself did not explain what he meant by sharp cut. Presumably he referred to a discontinuity of the slope of the curve of the absorption coefficient. Sharma found an abrupt increase of the absorption coefficient of hydrogen peroxide vapor at 2055A and ascribed this phenomenon to the photo-chemical dissociation of gaseous hydrogen peroxide into two OH radicals:

$$(H_2O_2)\text{gas}+h\nu(2055\text{A})\rightarrow OH(^2\Pi)+OH(^2\Sigma) \quad +139.0 \text{ kcal.}$$
$$OH(^2\Sigma)\rightarrow OH(^2\Pi) \quad -92.7 \text{ kcal.}^5$$
$$(H_2O_2)\text{gas} \rightarrow 2OH(^2\Pi) \quad +46.3 \text{ kcal.} \quad (1)$$

Sharma rejected this interpretation of his observations, however, after he found that the dissociation energy of hydrogen peroxide is much lower according to the following reactions

$$(H_2O_2)\text{gas}\rightarrow(H_2O)\text{gas}+\tfrac{1}{2}O_2 \quad -25.2 \text{ kcal.}$$
$$2(H_2O)\text{gas}\rightarrow H_2+2OH \quad +121.0 \text{ kcal.}$$
$$H_2+\tfrac{1}{2}O_2 \rightarrow(H_2O)\text{gas} \quad -57.0 \text{ kcal.}$$
$$(H_2O_2)\text{gas}\rightarrow 2OH(^2\Pi) \quad +38.8 \text{ kcal.} \quad (2)$$

Therefore he postulated that the photo-chemical decomposition of hydrogen peroxide must be expressed by the equation

$$(H_2O_2)\text{gas}+h\nu(2055\text{A})\rightarrow 2H+O_2. \quad (3)$$

He based this reaction on the assumption that the structure of hydrogen peroxide is H–O=O–H. It is obvious that this assumption is not justified and that reaction 3 is very improbable. Actually the discrepancy which Sharma found between reactions 1 and 2 disappears when modern data are used for the calculation of 2:

$$(H_2O_2)\text{gas}\rightarrow(H_2O)\text{gas}+\tfrac{1}{2}O_2 \quad -25.6 \text{ kcal.}$$
(see Table I.)
$$2(H_2O)\text{gas}\rightarrow H_2+2OH \quad +129.0 \text{ kcal.}$$
$$H_2+\tfrac{1}{2}O_2 \rightarrow(H_2O)\text{gas} \quad -57.1 \text{ kcal.}^6$$
$$(H_2O_2)\text{gas}\rightarrow 2OH(^2\Pi) \quad +46.3 \text{ kcal.} \quad (2a)$$

This calculation is based on the assumption that the dissociation energy of water according to the reaction

$$(H_2O)\text{gas}\rightarrow\tfrac{1}{2}H_2+OH$$

TABLE I. Calculation of heat of reaction.[a]

$(H_2O_2)\text{liq}\rightarrow(H_2O)\text{liq}+\frac{1}{2}O_2$	$\Delta H_{293.1}'=-23.5\pm0.1$ kcal.[b]
$(H_2O_2)\text{gas}\rightarrow(H_2O_2)\text{liq}$	$-\lambda_{293.1}=-11.8\pm0.3$ kcal.[c]
$(H_2O)\text{liq}\rightarrow(H_2O)\text{gas}$	$\lambda_{293.1}=10.6$ kcal.[d]
$(H_2O_2)\text{gas}\rightarrow(H_2O)\text{gas}+\frac{1}{2}O_2$	$\Delta H_{293.1}=-24.7\pm0.4$ kcal.

$$\Delta H_0=\Delta H_{293.1}-[(H-E_0)_{293.1}^{H_2O}+\tfrac{1}{2}(H-E_0)_{293.1}^{O_2}-(H-E_0)_{293.1}^{H_2O_2}]$$
$$\Delta H_0=-24.7-[2.324+1.016-2.381]=-25.6\pm0.4 \text{ kcal.}$$

[a] The enthalpy of hydrogen peroxide was calculated according to the Planck-Einstein function. For the vibrational levels of hydrogen peroxide [see C. R. Bailey and R. R. Gordon, Trans. Faraday Soc. **34**, 1133–1138 (1938)].
[b] G. L. Matheson, and O. Maass, J. Am. Chem. Soc. **51**, 674–687 (1929). Roth, Grau, and Meichsner. Zeit. f. anorg. allgem. Chemie **193**, 161–175 (1930).
[c] O. Maass, and P. G. Hiebert, J. Am. Chem. Soc. **46**, 2693–2700 (1924). O. Maass, and W. H. Hatcher, J. Am. Chem. Soc. **42**, 2548–2569 (1920).
[d] Osborne, Stimson, and Ginnings, J. Res. N.B.S. **23**, 261–270 (1939).

[1] Holt, McLane, and Oldenberg, J. Chem. Phys. **16**, 225–229 (1948); **16**, 638 (1948).
[2] G. Damköhler, and R. Edse, Die Naturwiss. **31**, 310–314 (1943).
[3] R. Edse, F-TR-2125-ND, Wright Field No. 18 (1948).
[4] R. S. Sharma, Proc. Acad. Sci. U. P. Agra and Oudh, India, **4**, 51–58 (1934/35).
[5] L. Grebe, and O. Holtz, Ann. d. Physik **39**, 1246–1250 (1912); H. L. Johnston, and D. H. Dawson, Phys. Rev. **43**, 980–991 (1933).
[6] F. D. Rossini, J. Res. N.B.S. **34**, 143–161 (1945).

amounts to 64.5 kcal.[3] Since this value is in good agreement with other measurements it seems justified to prefer Sharma's first interpretation (Eq. (1)) to his second one (Eq. (3)). Whether Sharma's sharp cut is identical with the abrupt increase of the absorption coefficient measured by Holt, McLane, and Oldenberg, cannot be derived from Sharma's paper. In the diagram of the absorption coefficient that was published by Holt, McLane, and Oldenberg, a sudden increase of the absorption coefficient obviously occurs near 1920A. The discontinuity becomes more pronounced when the absorption coefficient is plotted against the wave numbers rather than wave-lengths and it seems that the points of measurement lie on two straight lines which intersect at 1920A (Fig. 1). Whether the increase is abrupt or smooth can be shown only by additional measurements at 1920A and shorter wave-lengths. Even if there is an abrupt increase of the absorption coefficient, however, it cannot be said at present in which way this phenomenon is related to the dissociation of hydrogen peroxide into two OH molecules because we do not possess sufficient knowledge concerning the structure of the hydrogen peroxide spectrum. Therefore, the sudden increase of the absorption coefficient of hydrogen peroxide, found by Sharma at 2055A and evident in the diagram of Holt, McLane, and Oldenberg at 1920A, must be considered a rather uncertain criterion for the dissociation of hydrogen peroxide. Positive evidence for the dissociation of hydrogen peroxide into two OH molecules was furnished by Urey, Dawsey, and Rice[7] who illuminated hydrogen peroxide with light from 2138A to 2025A. From the appearance of the 3064A band in the resulting fluorescence the authors concluded that their experiments showed definitely that the dissociation of hydrogen peroxide into one normal and one electronically excited OH molecule is one possible way in which light dissociates this molecule. The dissociation of hydrogen peroxide into OH molecules is corroborated by studies concerning the electric discharge in hydrogen peroxide vapor.[8] Recent investigations on the decomposition of organic peroxides[9] also indicate that the primary dissociation of peroxides occurs at the O—O bond. The measurements of Urey and coworkers lead to $\Delta H_0^{H_2O}=64.5 \pm 0.9$ kcal. for the dissociation energy of water according to the reaction $H_2O \rightarrow \frac{1}{2}H_2+OH$. This value represents an upper limit for the dissociation energy of water because the photo-chemical decomposition of hydrogen peroxide vapor gives an upper limit for the dissociation energy of hydrogen peroxide† (see Eq. (1)).

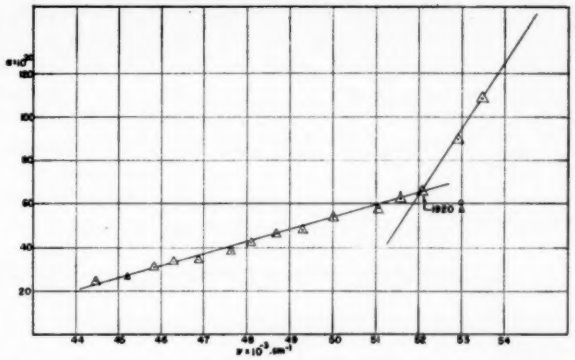

FIG. 1. Absorption coefficient, α, of H_2O_2 vapor according to the measurements of Holt, McLane, and Oldenberg, replotted against wave number.

The result is in agreement with most of the older data but approximately 2 kcal. lower than the recent measurement by Dwyer and Oldenberg.[10] This discrepancy cannot be explained at present.

As a partial result of our search for data of the energy of dissociation of hydrogen peroxide into two OH molecules we found in 43 experiments on the ultraviolet absorption of hydrogen peroxide vapor in the region of 2000 to 2100A that there is no sharp cut of the absorption coefficient in this region.[11] We measured the absorption of hydrogen peroxide, with and without presence of water vapor, at room temperature and slightly higher. The liquid 100 percent pure hydrogen peroxide was kept in a quartz vessel at constant temperature. The quartz vessel was connected with one end of the absorption tube of quartz which was 190 cm long and 3 cm wide. The other end of the tube led to a capillary, from there to a liquid air trap and then to a vacuum pump. The hydrogen peroxide vapor flowing through the tube was collected in the cooling trap and then analyzed. The gaseous products of the decomposing vapor were also collected and analyzed. The absorption tube was sealed by quartz windows which were 2 mm thick. An air-cooled hydrogen discharge tube served as light source and the Model Q24 quartz spectrograph of Zeiss was employed. The intensity of the light source was carefully controlled by means of a photo-cell. Our results agree well with the measurements of Holt, McLane, and Oldenberg for the limited range of wave-lengths that we investigated.

I wish to express my appreciation to Dr. Charles W. Beckett for reading the manuscript and making several helpful suggestions.

[7] Urey, Dawsey, and Rice, J. Am. Chem. Soc. **51**, 1371–1383 (1929).

[8] A. A. Frost, and O. Oldenberg, J. Chem. Phys. **4**, 781–784 (1936).

[9] Raley, Rust, and Vaughan, J. Am. Chem. Soc. **70**, 88–95 (1948).

† If the photo-chemical decomposition of hydrogen peroxide were not a monomolecular process but the result of a secondary reaction ($H_2O_2+H_2O_2$ or H_2O_2+M), the dissociation energy of hydrogen peroxide could no longer be derived from the measurements of Urey and co-workers. According to our present knowledge of the reaction kinetics of H_2O_2, however, it is very improbable that a secondary process is involved in the photo-chemical decomposition of this molecule. Of course, further experimental studies are necessary for a final solution of this problem, which is analogous to the photo-chemical dissociation of carbon monoxide.

[10] R. J. Dwyer and O. Oldenberg, J. Chem. Phys. **12**, 351–361 (1944).

[11] R. Edse and H. G. Wolfhard, "The reaction $H_2O_2 \rightarrow 2OH$" (not published).

Statistical Mechanics of Adsorption. IX. Adsorption Thermodynamics and Solution Thermodynamics†

TERRELL L. HILL*
Department of Chemistry, University of Rochester, Rochester, New York
(Received June 29, 1949)

This paper is a generalization of Part V of this series. We show here that the usual solution thermodynamics can be recast into an equivalent but alternative form which is more natural and useful in adsorption work. Relations between the two systems of thermodynamics are pointed out. The extension to the case of sorption from a mixture of gases is included.

I. INTRODUCTION

IF we consider a list of sorption systems such as argon-graphite, hydrogen-tungsten, hydrogen-charcoal, hydrogen-palladium, benzene-rubber, water-sodium chloride, and water-sulfuric acid, it is clear that, from the point of view of pure thermodynamics, no really significant division of these systems into separate classes can be made, and therefore that the same thermodynamic treatment should apply to the entire list. This is a well-known point of view, and has been especially emphasized by Coolidge.[1] Thus, ordinary solution thermodynamics can quite correctly be applied, for example, to the phase argon-graphite (this phase being in equilibrium with argon vapor).

We are interested, however, not only in obtaining correct thermodynamic data but also in *understanding* the data. For this latter purpose, solution thermodynamics leaves something to be desired when applied to a system such as argon-graphite because the argon-graphite phase is treated *symmetrically* in the two components.[2] This is a perfectly natural arrangement for a solution of sugar in water or rubber in benzene, but is very unnatural for argon-graphite, where the two components obviously play completely different roles in the condensed phase (and in the vapor phase). We should therefore anticipate that an alternative but equivalent thermodynamic system which is properly *asymmetric* in the two components might be more directly useful in interpreting data relating to a large number of sorption systems. The above conclusion is confirmed by the fact that, as far as the author is aware, all statistical mechanical theories of physical and chemical adsorption which have been proposed up to the present time treat the condensed phase as a *one component* system of adsorbed molecules in a potential field presented by the adsorbent. The asymmetric thermodynamic system referred to above thus turns out to be the same system which is implicit in statistical mechanical theories.[3]

In paper V of this series[4] we have used this asymmetric point of view almost exclusively in a detailed discussion of the thermodynamics of adsorption of a single gas on an inert adsorbent (approximated in physical adsorption). In the present paper we now wish to give proper emphasis to the generality of the method (as applied, say, to any of the systems in the list above) (Section II), to the relations between solution thermodynamics and the alternative system (Section II), and to sorption from a mixture of gases[4a] (Section III).

II. ONE-COMPONENT SORBATE[5]

Consider a two-component ("A" and "1") condensed phase in equilibrium with gaseous "1," "A" being nonvolatile.[6] The condensed phase has energy E, entropy S, etc., and contains N_A and N_1 molecules of the two types. We include only those cases in which E is completely determined by S, V, N_A and N_1. This requires no further comment if A is a liquid (e.g., A = sulfuric acid, 1 = water) or a solid (e.g., A = palladium, 1 = hydrogen) such that surface effects are negligible compared to bulk effects. However, if A is, for example, a finely divided solid with appreciable surface effects (the case of primary interest) it is to be understood that in all of the thermodynamic processes contemplated a change

† Presented at an American Chemical Society Meeting, Atlantic City, September 20, 1949.
* Present address: Naval Medical Research Institute, Bethesda, Maryland.
[1] A. S. Coolidge, J. Am. Chem. Soc. **48**, 1795 (1926).
[2] See, for example, Eq. (1).
[3] See, for example, R. H. Fowler and E. A. Guggenheim, *Statistical Thermodynamics* (Cambridge University Press, Cambridge, 1939), Chapter X.
[4] T. L. Hill, J. Chem. Phys. **17**, 520 (1949); see also J. Chem. Phys. **17**, 507 (1949).
[4a] It is rather obvious that sorption from a liquid solution bears a considerable thermodynamic resemblance to sorption from a gas. We shall not discuss sorption from a solution here but we hope to at some other time.
[5] We use "sorption" as a general term to include adsorption and absorption. As in paper V, "sorbate" refers to sorbed molecules and does *not* include gas molecules in equilibrium with sorbed molecules.
[6] There is no difficulty in extending the present paper to cases in which all components are volatile *provided* all significant surface properties (e.g., the "surface area" of a volatile finely divided solid) of the "sorbent" (*one* component must be chosen as sorbent) are independent of amount of sorbent volatilization. In practice, except as an approximation, this probably means that the all-volatile case must be restricted to systems with *no* significant surface properties; that is, to solutions. But in this case adsorption thermodynamics (see reference 10) does not at present seem to have anything to recommend it.
Equations such as Eqs. (48) and (59) are unchanged in the all-volatile case. The determinants in equations such as Eqs. (46) and (58) have one more row and column.

in N_A, dN_A, refers to an addition of pure A in the same state of subdivision, etc., as the pure A used in preparing the original sample. Thus, in cases where the term "surface area" has meaning, the area is proportional to N_A and is not an additional independent variable.[7] The use of N_A in place of $\mathfrak{A}$ as an independent variable is the fundamental step allowing the generality of paper V to be extended to cases in which the adsorbent is perturbed by the absorbate,[8] and to systems (such as hydrogen-palladium) without an "area."

We now review very briefly an application of solution thermodynamics.[9] We have

$$dE=TdS-PdV+\mu_1dN_1+\mu_AdN_A, \tag{1}$$

$$dF=-SdT+VdP+\mu_1dN_1+\mu_AdN_A, \tag{2}$$

$$d\mu_1=-\bar{S}_1dT+\bar{v}_1dP+(\partial\mu_1/\partial\Gamma)_{T,P}d\Gamma, \tag{3}$$

where

$$\Gamma=N_1/N_A, \quad \bar{S}_1=(\partial S/\partial N_1)_{N_A,P,T}, \quad \text{etc.}$$

P is the *hydrostatic* pressure, exerted by a hypothetical inert piston or (in part) by a hypothetical inert additional gas (see also Appendix I). At equilibrium with gas, $d\mu_1=d\mu_G$,[9a] and

$$-\bar{S}_1dT+\bar{v}_1dP+(\partial\mu_1/\partial\Gamma)_{T,P}d\Gamma = -S_GdT+v_Gdp \tag{4}$$

$$=[-S_G+(H_G-H_G^*)/T]dT+kTd\ln f, \tag{5}$$

where p is the equilibrium vapor pressure, f the vapor fugacity, $S_G=S_G/N_G$, etc. H_G^* is the value of H_G as $p\to 0$ (same temperature). Hence

$$(\partial p/\partial T)_\Gamma=(S_G-\bar{S}_1)/(v_G-\bar{v}_1) \quad (P=p) \tag{6}$$

$$(\partial p/\partial T)_{\Gamma,P}=(S_G-\bar{S}_1)/v_G \tag{7}$$

$$(\partial\ln f/\partial T)_{\Gamma,P}=[(S_G-\bar{S}_1)/kT]+[(H_G^*-H_G)/kT^2] =(H_G^*-\bar{H}_1)/kT^2. \tag{8}$$

The "isosteric heat" of adsorption terminology is defined here as $q_{st}=H_G-\bar{H}_1=T(S_G-\bar{S}_1)$.

Equations (6), (7) and (8) all give in the usual approximation (perfect gas, $\bar{v}_1=0$)

$$(\partial\ln p/\partial T)_\Gamma=(S_G-\bar{S}_1)/kT =(H_G-\bar{H}_1)/kT^2=q_{st}/kT^2. \tag{9}$$

We now turn to adsorption thermodynamics.[10] We consider a sample of *pure* A with the *same state of subdivision, etc.*, as used in preparing the "solution" of Eq. (1), and with the same N_A, P and T:

$$dE_{0A}=TdS_{0A}-PdV_{0A}+\mu_{0A}dN_A. \tag{10}$$

We *define*

$$E_s\equiv E-E_{0A} \quad V_s\equiv V-V_{0A}$$
$$S_s\equiv S-S_{0A} \quad \Phi\equiv\mu_{0A}-\mu_A. \tag{11}$$

On subtracting Eq. (10) from Eq. (1), we find

$$dE_s=TdS_s-PdV_s-\Phi dN_A+\mu_1dN_1. \tag{12}$$

By use of this simple device we now have a pseudo one component (component "1") system in place of the two component solution. Φ plays the role of a second "pressure." In the special case of adsorption on an inert adsorbent (paper V), E_s, for example, according to Eqs. (11), is just the energy of a system of adsorbed molecules in the potential field of the surface (the energy of the adsorbent subtracts out *except* for the interaction energy between adsorbent and adsorbed molecules which is left in E_s); also, $\Phi N_A=\varphi\mathfrak{A}$.[8]

We *define* the Gibbs free energy $F_s\equiv N_1\mu_1$. On integrating Eq. (12),

$$F_s=E_s-TS_s+PV_s+\Phi N_A, \tag{13}$$

$$=A_s+PV_s+\Phi N_A, \quad A_s\equiv E_s-TS_s. \tag{14}$$

We *define* $H_s\equiv F_s+TS_s$. Hence

$$H_s=E_s+PV_s+\Phi N_A. \tag{15}$$

These definitions of F_s and H_s insure that

$$H_G-H_s=T(S_G-S_s) \tag{16}$$

at equilibrium between gas and sorbate, where $H_s=H_s/N_1$, etc.

From Eqs. (12) and (13),

$$dF_s=-S_sdT+V_sdP+N_Ad\Phi+\mu_1dN_1. \tag{17}$$

Equations (2) and (17) give

$$\mu_1=(\partial F/\partial N_1)_{T,P,N_A}=\bar{F}_1=\bar{H}_1-T\bar{S}_1 \tag{18}$$

$$=(\partial F_s/\partial N_1)_{T,P,\Phi}=F_s/N_1=F_s=H_s-TS_s. \tag{19}$$

At equilibrium between gas and sorbate,

$$d\mu_1=-S_sdT+v_sdP+(1/\Gamma)d\Phi =d\mu_G=-S_GdT+v_Gdp =[-S_G+(H_G-H_G^*)/T]dT+kTd\ln f. \tag{20}$$

Hence

$$(\partial p/\partial T)_\Phi=(S_G-S_s)/(v_G-v_s) \quad (P=p) \tag{21}$$

$$(\partial p/\partial T)_{\Phi,P}=(S_G-S_s)/v_G \tag{22}$$

[7] The area $\mathfrak{A}$ is *not* necessarily constant if N_A is constant (e.g., swelling): $\mathfrak{A}=N_Af(T, P, N_1/N_A)$.

[8] See Appendix I.

[9] See, for example, F. H. MacDougall, *Thermodynamics and Chemistry* (John Wiley and Sons, Inc., New York, 1939), Chapter X.

[9a] In the adsorption, say, of H_2 on tungsten, if H_2 is chosen as the single independent component of *both* the gas and adsorbed phase, then the equations given in this paper apply. If it is convenient from a statistical mechanical point of view to choose H_2 as the independent component for the gas and H as the independent component for the adsorbed phase, then $\mu_1=\frac{1}{2}\mu_G$, as is well known, and a factor of $\frac{1}{2}$ or 2 will appear in various thermodynamic equations. This of course does not alter the essential *thermodynamic* content of these equations.

[10] For want of a better term, we shall refer hereafter to the alternative asymmetric system of thermodynamics as "adsorption thermodynamics," as contrasted to "solution thermodynamics." Although both systems apply to both adsorption and solution, the names emphasize the principal field of usefulness.

$$(\partial \ln f/\partial T)_{\Phi,P}=[(S_G-S_s)/kT]+[(H_G^*-H_G)/kT^2] =(H_G^*-H_s)/kT^2. \quad (23)$$

In the usual approximation (perfect gas, $v_s=0$)

$$(\partial \ln p/\partial T)_\Phi=(S_G-S_s)/kT =(H_G-H_s)/kT^2\equiv q_\Phi/kT^2. \quad (24)$$

Equation (23), for example, is analogous to

$$(\partial \ln f/\partial T)_P=(H_G^*-H_L)/kT^2 \quad (25)$$

for the equilibrium between a pure liquid (or solid) and its vapor.

We may also derive from Eq. (20)

$$d\Phi=\Gamma(v_G-v_s)dp \quad (P=p,\ T \text{ const.}) \quad (26)$$

$$=\Gamma v_G dp=\Gamma kT d\ln f \quad (P,\ T \text{ const.}) \quad (27)$$

$$(\partial\Phi/\partial T)_p=\Gamma(S_s-S_G) \quad (P=p). \quad (28)$$

By definition $\Phi=0$ when $p=0$, so we have the usual approximate integral form (due to Bangham) of the "Gibbs equation"

$$\Phi=kT\int_0^p \Gamma d\ln p \quad (T \text{ const.}). \quad (29)$$

It is clear that this equation is not exclusively a "surface" equation. Indeed, this is precisely the well-known relation giving the activity of one component (A) of a solution when the activity of the other (1) is known[11,12] (see also Appendix III).

It is important to keep in mind that the calculation of Φ or any other thermodynamic function from experimental data alone can never give us any information about the existence or magnitude of sorbent perturbation. If it is present, it will automatically be included in the thermodynamic functions. Non-thermodynamic experiments or theoretical calculations are necessary to investigate this question.

TABLE I. Entropy of adsorption.

Source	Quantity derived
A. 1. Statistical mechanics	S_s
2. Heat capacity*	$S_s(T_2)-S_s(T_1)$
3. q_Φ, etc.	S_s
B. 1. q_{st}	$(\partial S_s/\partial N_1)_{T,N_A}$
2. Calorimetric*	$(\partial S_s/\partial N_1)_{T,N_A}$

*See Section III and paper V.

[11] See, for example, G. N. Lewis and M. Randall, *Thermodynamics* (McGraw-Hill Book Company, Inc., New York, 1923), Eq. XXII-20. It may also be noted that Eq. XXII-24 resembles Eq. (3) of G. Jura and W. D. Harkins, J. Am. Chem. Soc. **66**, 1356 (1944).

[12] When adsorption thermodynamics is applied to a perfect solution with only one volatile component (or a semi-permeable membrane), the sorption isotherm is just Raoult's law and

$$\Phi=kT\ln[(N_1+N_A)/N_A].$$

Discussion

In physical adsorption we presumably have, to a satisfactory order of *approximation*, essentially the case of adsorption on an inert (unperturbed) adsorbent. In any case, all theories advanced in this field up to the present time have made this assumption. Even with this simplification the problem is much more complicated than the theory of an isotropic liquid. Thus the statistical mechanical model of an adsorbate in the external field presented by an inert adsorbent will presumably be a common one for some time to come. Even in chemisorption (and in solutions such as hydrogen-palladium) or in cases intermediate between chemisorption and physical adsorption this model has been and will no doubt continue to be used extensively as a valuable first approximation.

Adsorption thermodynamics finds its most natural application in the above special case. Thus, if nitrogen is adsorbed on graphite we are primarily interested in measuring and interpreting the entropy, energy, etc. of the *assembly of nitrogen molecules alone* in terms of intermolecular interactions, configurations of the assembly, rotations and vibrations of the molecules, etc. These functions are just the S_s, E_s, etc. defined and are the functions which are obtained from statistical mechanical partition functions for this model using the standard relations between statistical mechanics and thermodynamics (e.g., $A_s=-kT\ln Q$). *This entropy S_s of the adsorbed molecules alone (inert adsorbent)*[13] *is obtained from experimental data by direct use of Eq. (24) and not Eq. (9).*

For a system such as water-sulfuric acid, adsorption thermodynamics is perfectly correct but no longer has particular usefulness, as far as the writer is aware at the present time. In the gradual transition from physical adsorption systems to solution systems it is not yet clear at what point adsorption thermodynamics loses its relative advantages.

An interesting intermediate case is exemplified by benzene-rubber (or water-protein, etc.). At low benzene vapor pressures this system is no doubt fairly well characterized as sorption on an inert sorbent. At higher benzene pressures we have a solution of rubber in benzene.[14] In studies where the low pressure sorption aspect is of primary interest it may prove advantageous

[13] Equation (24) gives in any case $S_s=S-S_{0A}$. If adsorbent perturbations are appreciable S_s is of course still a well-defined quantity but with a less direct physical significance.

[14] A related system is the type water-sodium chloride. At low pressures water is adsorbed on salt. At a certain intermediate pressure we will have salt in equilibrium with a saturated solution of salt in water as the condensed "phase." The adsorption isotherm is perpendicular here. Above this pressure all the salt will have dissolved—water vapor is in equilibrium with an unsaturated salt solution. This region is a "solution isotherm." See, for example, R. H. Stokes and R. A. Robinson, J. Am. Chem. Soc. **70**, 1870 (1948). Equation (29) applies, of course, to the entire range in p. Contributions to the integral from pressures greater than the vapor pressure of the saturated solution will be relatively large. Surface properties of the salt affect the isotherm only below this vapor pressure.

to use adsorption thermodynamics at low pressures and, for the sake of continuity, carry its use over into the high pressure solution region.

A significant general property of S_s and H_s is the following. The quantity $H_G-H_s=T(S_G-S_s)$ of Eq. (24) is the equilibrium heat of sorption which is analogous to the usual ΔH of fusion, vaporization, etc. of a pure substance (Eq. (25)). ΔH refers to a reversible process at constant pressure while H_G-H_s, by analogy, refers to constant P and Φ (see Section III). In both cases *all* intensive properties stay constant during the vaporization (desorption) process.

The isosteric heat q_{st} of Eq. (9) gives[15]

$$\bar{S}_1=(\partial S/\partial N_1)_{P,T,N_A}=(\partial S_s/\partial N_1)_{P,T,N_A}\cong(\partial S_s/\partial N_1)_{T,N_A} \quad (33)$$

since S_{0A} is independent of N_1, and the dependence on P is usually negligible. Thus q_{st} gives a differential S_s while q_Φ gives the "integral" $S_s(=N_1S_s)$. This suggests an alternative method of calculating S_s from experimental data.[16] We write

$$q_{st}=T(S_G-\bar{S}_1),$$

multiply by dN_1 and integrate from $N_1=0$ to N_1. Using

$$\mu_G=H_G-TS_G$$
$$d\mu_G=kTd\ln p \quad (T \text{ const.})$$

and a partial integration, we find

$$T(S_G-S_s)=\frac{1}{N_1}\int_0^{N_1} q_{st}dN_1-(\Phi/\Gamma) \quad (N_A, T \text{ const.}) \quad (34)$$

Eq. (34) also follows from Eq. (V–91).

Being a differential entropy, $\bar{S}_1=(\partial S_s/\partial N_1)_{T,N_A}$ contains less thermodynamic information than S_s. This is of course related to the fact that more work is involved in using Eq. (24) than Eq. (9), as Φ must first be calculated by integration from Eq. (29) (which requires low pressure experimental data). Indeed, there is no way of avoiding an integration if S_s is to be found. Eqs. (34) and (37) involve *two* integrations each, the extra integration in each case having been introduced for computational convenience. In the language of solution thermodynamics, the entropy S of the solution is not known unless *both* $\bar{S}_1$ and $\bar{S}_A$ are known:

$$S=N_1\bar{S}_1+N_A\bar{S}_A. \quad (35)$$

However, from isotherm data alone we can obtain no information about S_{0A} so the best we can expect to do in this case is to find $S-S_{0A}=S_s$. Thus, we get $\bar{S}_1$ from Eq. (9) (if $S_G(p)$ is known) and $\bar{S}_A-S_{0A}$ from integration of

$$d\bar{S}_A=-(N_1/N_A)d\bar{S}_1 \quad (T \text{ const.}). \quad (36)$$

Integration of this equation is inconvenient, but using $Td\bar{S}_A=d\bar{H}_A-d\mu_A$ we have

$$T(\bar{S}_A-S_{0A})=\Phi-\int_{\bar{H}_1^0}^{\bar{H}_1}(N_1/N_A)d\bar{H}_1 \quad (T \text{ const.}), \quad (37)$$

where $\bar{H}_1^0$ is the value of $\bar{H}_1$ at $p=0$. Substitution of Eq. (37) into Eq. (35) gives $S-S_{0A}$ in terms of calculable quantities.

Finally, in this section, we wish to emphasize that entropies calculated in adsorption work fall into two classes. In Table I we list various sources of entropy data and the type of quantity which is derived in each case. It is obviously incorrect, for example, to compare directly an experimental entropy calculated from q_{st} with the statistical mechanical entropy (this has been done several times in the literature). To make a comparison either S_s must be differentiated[17] or $(\partial S_s/\partial N_1)_{T,N_A}$ integrated (Eq. (34)), or Eq. (24) or (68) may be used.

III. MULTI-COMPONENT SORBATE

Some of the most important practical applications of adsorption involve adsorption from a mixture of gases. In order to gain a fundamental understanding of this field it will eventually be necessary to compare statistical mechanical theories with thermodynamic quantities derived from experimental data. In physical adsorption we may anticipate that the theory of liquid solutions will have to be extended in the same way that the theory of liquids will have to be extended to treat a one component sorbate. Very little fundamental work has been done on mixtures so far.[18–20,20a] Measurements at neighboring temperatures are especially lacking.

In the physical adsorption of, say, a mixture of two gases on a solid, the condensed phase is a three-component phase but for the same reasons as before it is illuminating to treat this phase as a pseudo two-component phase, using adsorption thermodynamics.

It is the purpose of this section, then, to generalize the previous work (above; and paper V) to mixtures, pointing out the type of thermodynamic data which might be useful in interpretation and which can be derived from experiment. We first treat isotherm data,[21] and then calorimetric data.

---

[15] We might note here that $H=E+PV\cong E$ but $H_s\neq E_s$ in general (ΦN_A is not negligible). Also $H_s\neq H-H_{0A}$ and $F_s\neq F-F_{0A}$.

[16] Four other ways were pointed out in paper V: Eqs. (66), (85), (88), and (112).

[17] For example, this was done in effect by Davis and DeWitt, J. Am. Chem. Soc. **70**, 1135 (1948). Incidentally, the expression they give for q_{st} (BET theory) can be shown to be identical with a simpler equation for q_{st} in paper VII of this series (J. Chem. Phys. **17**, 772 (1949)).

[18] T. L. Hill, J. Chem. Phys. **14**, 268 (1946).

[19] J. R. Arnold, J. Am. Chem. Soc. **71**, 104 (1949).

[20] L. White and C. H. Schneider, J. Am. Chem. Soc. **71**, 2593 (1949).

[20a] S. Brunauer, *Adsorption of Gases and Vapors* (Princeton University Press, Princeton, 1943), Chapter 14.

[21] We might emphasize at the outset that with gas mixtures there are a large number of possible useful equations of the Clausius-Clapeyron type. We shall give only a few which appear to the writer to be most important; others can be written down using the same general methods.

Solution Thermodynamics

The condensed phase has components 1, 2, $\cdots i, \cdots m$ and $a, b, \cdots \alpha, \cdots z$ of which only 1, 2, $\cdots i, \cdots m$ are volatile.[6] We restrict ourselves to cases such that E, say, is completely determined by S, V, N_1, N_2, $\cdots N_m$, N_A where $N_A=\sum N_\alpha$. That is, the pure sorbent has constant composition, state of subdivision, etc., in all processes to be considered; hence there is only *one* independent variable of the type N_α; we choose N_A. If an "area" exists, it is proportional to N_A. The case of most interest is of course a one component sorbent, as in Section II.

We have

$$dE=TdS-PdV+\sum\mu_i dN_i+\mu_A dN_A, \tag{42}$$

$$dF=-SdT+VdP+\sum\mu_i dN_i+\mu_A dN_A, \tag{43}$$

where μ_A is defined as $(\partial E/\partial N_A)_{S,V,N_i}$.

At equilibrium, $d\mu_i=d\mu_{iG}$ for $i=1, \cdots m$. Now μ_i is a function of T, P, Γ_1, $\cdots\Gamma_m$ where $\Gamma_i=N_i/N_A$ and μ_{iG} is a function of T, p, x_1, $\cdots x_{m-1}$, where x_i is a gas composition variable. With $P\neq p$ there are then $2m+2$ variables, with m equilibrium relations, giving $m+2$ degrees of freedom.[22] In writing, for example, $\partial p/\partial T$, then, we must specify $m+1$ variables to be held constant. If $P=p$, m variables must be held constant.

We may write $(d\mu_i=d\mu_{iG})$

$$-\bar{S}_i dT+\bar{v}_i dP+\sum_{k=1}^{m}(\partial\mu_i/\partial\Gamma_k)d\Gamma_k = -\bar{S}_{iG}dT+\bar{v}_{iG}dp+\sum_{k=1}^{m-1}(\partial\mu_{iG}/\partial x_k)dx_k \qquad (i=1, \cdots m). \tag{45}$$

For brevity we shall let n denote the composition of the condensed phase $(\Gamma_1, \cdots\Gamma_m)$ and n_G the composition of the gas $(x_1, \cdots x_{m-1})$. Holding n and P constant, and dividing by dT, Eqs. (45) may be regarded as m linear non-homogeneous equations in the m unknowns $\partial p/\partial T$ and $\partial x_k/\partial T$. Then

$$\left(\frac{\partial p}{\partial T}\right)_{n,P}=\frac{\begin{vmatrix} \bar{S}_{1G}-\bar{S}_1 & \dfrac{\partial\mu_{1G}}{\partial x_1} & \cdots & \dfrac{\partial\mu_{1G}}{\partial x_{m-1}} \\ \cdot & \cdot & & \cdot \\ \cdot & \cdot & & \cdot \\ \cdot & \cdot & & \cdot \\ \bar{S}_{mG}-\bar{S}_m & \dfrac{\partial\mu_{mG}}{\partial x_1} & \cdots & \dfrac{\partial\mu_{mG}}{\partial x_{m-1}} \end{vmatrix}}{\begin{vmatrix} \bar{v}_{1G} & \dfrac{\partial\mu_{1G}}{\partial x_1} & \cdots & \dfrac{\partial\mu_{1G}}{\partial x_{m-1}} \\ \cdot & \cdot & & \cdot \\ \cdot & \cdot & & \cdot \\ \cdot & \cdot & & \cdot \\ \bar{v}_{mG} & \dfrac{\partial\mu_{mG}}{\partial x_1} & \cdots & \dfrac{\partial\mu_{mG}}{\partial x_{m-1}} \end{vmatrix}}. \tag{46}$$

[22] See reference 9, pp. 140–141. No "new" phase rule is necessary.

Using fugacities f_i we have alternatively

$$-\bar{S}_i dT+\bar{v}_i dP+\sum_{k=1}^{m}(\partial\mu_i/\partial\Gamma_k)d\Gamma_k = [-\bar{S}_{iG}+(\bar{H}_{iG}-H_{iG}^*)/T]dT+kTd\ln f_i \qquad (i=1, \cdots m). \tag{47}$$

With n and P constant, these equations have a particularly simple solution:

$$(\partial\ln f_i/\partial T)_{n,P}=[(\bar{S}_{iG}-\bar{S}_i)/kT]+[(H_{iG}^*-\bar{H}_{iG})/kT^2] =(H_{iG}^*-\bar{H}_i)/kT^2 \quad (i=1, \cdots m). \tag{48}$$

For a perfect gas and taking $\bar{v}_i=0$,

$$(\partial\ln p_i/\partial T)_n=(S_{iG}-\bar{S}_i)/kT=(H_{iG}-\bar{H}_i)/kT^2 =q_{s\,t(\bar{v})}/kT^2 \quad (i=1, \cdots m), \tag{49}$$

where p_i is a partial pressure, and S_{iG} and H_{iG} are the entropy and heat content per molecule of (perfect) pure i gas at p_i and T. In Eq. (46), in this special case, we have $\bar{v}_{iG}=kT/p$, $\bar{S}_{iG}=S_{iG}$ and, taking the x_i as mole fractions with $x_m=1-x_1-x_2-\cdots-x_{m-1}$,

$$\partial\mu_{iG}/\partial x_i=kT/x_i, \quad \partial\mu_{iG}/\partial x_j=0, \qquad (i,j=1, 2, \cdots m-1)$$

$$\partial\mu_{mG}/\partial x_i=-kT/x_m.$$

Equations (46), (48), and (49) are "isosteric" equations. An equation analogous to Eq. (46) but with *gas* composition constant (as in the experiments of Arnold[19]) is

$$\left(\frac{\partial p}{\partial T}\right)_{n_G,\Gamma_1,P}=\frac{\begin{vmatrix} \bar{S}_{1G}-\bar{S}_1 & -\dfrac{\partial\mu_1}{\partial\Gamma_2} & \cdots & -\dfrac{\partial\mu_1}{\partial\Gamma_m} \\ \cdot & \cdot & & \cdot \\ \cdot & \cdot & & \cdot \\ \cdot & \cdot & & \cdot \\ \bar{S}_{mG}-\bar{S}_m & -\dfrac{\partial\mu_m}{\partial\Gamma_2} & \cdots & -\dfrac{\partial\mu_m}{\partial\Gamma_m} \end{vmatrix}}{\begin{vmatrix} \bar{v}_{1G} & -\dfrac{\partial\mu_1}{\partial\Gamma_2} & \cdots & -\dfrac{\partial\mu_1}{\partial\Gamma_m} \\ \cdot & \cdot & & \cdot \\ \cdot & \cdot & & \cdot \\ \cdot & \cdot & & \cdot \\ \bar{v}_{mG} & -\dfrac{\partial\mu_m}{\partial\Gamma_2} & \cdots & -\dfrac{\partial\mu_m}{\partial\Gamma_m} \end{vmatrix}}. \tag{50}$$

If $P=p$, the subscript P is omitted in Eqs. (46) and (50), and $\bar{v}_{iG}$ is replaced by $\bar{v}_{iG}-\bar{v}_i$.

Adsorption Thermodynamics

Equations (10) and (42), with μ_{0A} defined as $(\partial E_{0A}/\partial N_A)_{S_{0A},V_{0A}}$ and $N_A=\sum N_\alpha$, give

$$dE_s=TdS_s-PdV_s-\Phi dN_A+\sum\mu_i dN_i \tag{51}$$

$$dF_s=-S_s dT+V_s dP+N_A d\Phi+\sum\mu_i dN_i \tag{52}$$

$$F_s\equiv\sum N_i\mu_i. \tag{53}$$

We define

$$\bar{G}_i^* = (\partial G_s/\partial N_i)_{T,P,\Phi,N_j} \tag{54}$$

(this asterisk when combined with the "bar" in this way has nothing to do with the $p \to 0$ notation). This is an obvious generalization of the usual definition of a partial molal quantity. Thus, from Eq. (52), at equilibrium

$$\begin{aligned}\mu_i &= \bar{F}_i^* = \bar{H}_i^* - T\bar{S}_i^* \\ &= \bar{H}_i - T\bar{S}_i = \mu_{iG} = \bar{H}_{iG} - T\bar{S}_{iG},\end{aligned} \tag{55}$$

where, as usual,

$$\bar{G}_i = (\partial G/\partial N_i)_{P,T,N_j,N_A}.$$

It is clear that $G_s = G_s(\Phi, P, T, N_i)$ is a homogeneous function of degree one in the N_i at constant Φ, P, T. Hence,

$$G_s = \sum \bar{G}_i^* N_i; \tag{56}$$

Eq. (53) is an example. For a one component sorbate, $\bar{G}_1^* = G_s/N_1 = G_s$.

Now μ_i is a function of T, P, Φ, $y_1, \cdots y_{m-1}$ where y_i is a composition variable *for the sorbate.*[5] For example, for the y_i, one might use N_2/N_1, N_3/N_1, $\cdots N_m/N_1$. We let n_s represent the composition of the sorbate.[5] From Eq. (52) we obtain, for the equilibrium between gas and sorbate,

$$\begin{aligned}d\mu_i &= -\bar{S}_i^* dT + \bar{v}_i^* dP + \bar{N}_{Ai}^* d\Phi + \sum_{k=1}^{m-1} (\partial \mu_i/\partial y_k) dy_k \\ &= d\mu_{iG} = -\bar{S}_{iG} dT + \bar{v}_{iG} dp + \sum_{k=1}^{m-1} (\partial \mu_{iG}/\partial x_k) dx_k \\ &= [-\bar{S}_{iG} + (\bar{H}_{iG} - H_{iG}^*)/T] dT + kT d \ln f_i \\ &\qquad (i = 1, \cdots m).\end{aligned} \tag{57}$$

We can now easily derive equations analogous to Eqs. (46), (48), and (50), respectively:

$$\left(\frac{\partial p}{\partial T}\right)_{n_s,\Phi,P} = \frac{\begin{vmatrix} \bar{S}_{1G} - \bar{S}_1^* & \frac{\partial \mu_{1G}}{\partial x_1} & \cdots & \frac{\partial \mu_{1G}}{\partial x_{m-1}} \\ \cdot & \cdot & & \cdot \\ \cdot & \cdot & & \cdot \\ \cdot & \cdot & & \cdot \\ \bar{S}_{mG} - \bar{S}_m^* & \frac{\partial \mu_{mG}}{\partial x_1} & \cdots & \frac{\partial \mu_{mG}}{\partial x_{m-1}} \end{vmatrix}}{\begin{vmatrix} \bar{v}_{1G} & \frac{\partial \mu_{1G}}{\partial x_1} & \cdots & \frac{\partial \mu_{1G}}{\partial x_{m-1}} \\ \cdot & \cdot & & \cdot \\ \cdot & \cdot & & \cdot \\ \cdot & \cdot & & \cdot \\ \bar{v}_{mG} & \frac{\partial \mu_{mG}}{\partial x_1} & \cdots & \frac{\partial \mu_{mG}}{\partial x_{m-1}} \end{vmatrix}}. \tag{58}$$

$$\begin{aligned}(\partial \ln f_i/\partial T)_{n_s,\Phi,P} &= [(\bar{S}_{iG} - \bar{S}_i^*)/kT] \\ &\quad + [(H_{iG}^* - \bar{H}_{iG})/kT^2] = (H_{iG}^* - \bar{H}_i^*)/kT^2 \\ &\qquad (i = 1, \cdots m).\end{aligned} \tag{59}$$

$$\left(\frac{\partial p}{\partial T}\right)_{n_G,\Phi,P} = \frac{\begin{vmatrix} \bar{S}_{1G} - \bar{S}_1^* & -\frac{\partial \mu_1}{\partial y_1} & \cdots & -\frac{\partial \mu_1}{\partial y_{m-1}} \\ \cdot & \cdot & & \cdot \\ \cdot & \cdot & & \cdot \\ \cdot & \cdot & & \cdot \\ \bar{S}_{mG} - \bar{S}_m^* & -\frac{\partial \mu_m}{\partial y_1} & \cdots & -\frac{\partial \mu_m}{\partial y_{m-1}} \end{vmatrix}}{\begin{vmatrix} \bar{v}_{1G} & -\frac{\partial \mu_1}{\partial y_1} & \cdots & -\frac{\partial \mu_1}{\partial y_{m-1}} \\ \cdot & \cdot & & \cdot \\ \cdot & \cdot & & \cdot \\ \cdot & \cdot & & \cdot \\ \bar{v}_{mG} & -\frac{\partial \mu_m}{\partial y_1} & \cdots & -\frac{\partial \mu_m}{\partial y_{m-1}} \end{vmatrix}}. \tag{60}$$

In the usual approximation we omit P, replace f_i by p_i, $\bar{S}_{iG}$ by S_{iG}, and put $H_{iG}^* = \bar{H}_{iG}$ in Eq. (59). If $P = p$, the subscript P is omitted in Eqs. (58) and (60) and $\bar{v}_{iG}$ is replaced by $\bar{v}_{iG} - \bar{v}_i^*$.

If we replace $d\Phi$ in Eq. (57) by $Td(\Phi/T) + (\Phi/T)dT$ we have

$$\left(\frac{\partial \ln f_i}{\partial T}\right)_{n_s,\Phi/T,P} = \frac{T(\bar{S}_{iG} - \bar{S}_i^*) + \bar{N}_{Ai}^* \Phi + H_{iG}^* - \bar{H}_{iG}}{kT^2} \qquad (i = 1, \cdots m). \tag{61}$$

For a perfect gas and $\bar{v}_i^* = 0$ this becomes

$$(\partial \ln p_i/\partial T)_{n_s,\Phi/T} = (E_{iG} + kT - \bar{E}_i^*)/kT^2 \qquad (i = 1, \cdots m). \tag{62}$$

We now derive the "Gibbs equation." From Eqs. (52) and (53),

$$\sum N_i d\mu_i = \sum N_i d\mu_{iG} = -S_s dT + V_s dP + N_A d\Phi \tag{63}$$

$$d\Phi = \sum \Gamma_i kT d \ln f_i \quad (P, T \text{ const.}). \tag{64}$$

For a perfect gas and $V_s = 0$,

$$d\Phi = \sum \Gamma_i kT d \ln p_i \quad (T \text{ const.}). \tag{65}$$

Φ is obtained in practice by integration of Eq. (65) from $p_1 = \cdots = p_m = 0$ ($\Phi = 0$) to $p_1, \cdots p_m$. Φ is a function of the state of the system only so various alternative paths may be used in carrying out the integration. For example, if the *composition* of the gas is held constant,[19] Eq. (65) becomes, in integral form,

$$\Phi = kT \int_0^p (\sum \Gamma_i) d \ln p \quad (T, n_G \text{ const.}). \tag{66}$$

Another obvious path is to increase p_1 from $p_1=0$ to $p_1=p_1'$ keeping $p_2=0$ ($m=2$), then increase p_2 from $p_2=0$ to $p_2=p_2'$ keeping[20] $p_1=p_1'$, thus reaching the final state p_1', p_2', T.

Equation (65), as applied to adsorption, has been discussed previously, for example, by Kemball, Rideal, and Guggenheim[23] and Innes and Rowley.[24]

Finally, we shall obtain explicit relations between $\bar{S}_i$ and $\bar{S}_i^*$, etc. We have $\mu_i=\mu_i(P, \Phi, T, n_s)$, in which we may regard $\Phi=\Phi(P, T, n)$. This gives

$$\left(\frac{\partial\mu_i}{\partial T}\right)_{P,n}=\left(\frac{\partial\mu_i}{\partial T}\right)_{P,\Phi,n_s}+\left(\frac{\partial\mu_i}{\partial\Phi}\right)_{P,T,n_s}\left(\frac{\partial\Phi}{\partial T}\right)_{P,n} \quad (67)$$

or

$$\bar{S}_i=\bar{S}_i^*-\bar{N}_{Ai}^*(\partial\Phi/\partial T)_{P,n} \quad (i=1, \cdots m). \quad (68)$$

For a one component sorbate, $\bar{S}_1^*=S_s$ and $\bar{N}_{A1}^*=1/\Gamma$. Interchanging P and T in Eq. (67) gives

$$\bar{v}_i=\bar{v}_i^*+\bar{N}_{Ai}^*(\partial\Phi/\partial P)_{T,n} \quad (i=1, \cdots m). \quad (69)$$

Also,

$$\bar{H}_i=\bar{H}_i^*-T\bar{N}_{Ai}^*(\partial\Phi/\partial T)_{P,n} \quad (i=1, \cdots m) \quad (70)$$

follows from Eqs. (68) and (55).

Various equations, which may be of some use, involving $\partial\Phi/\partial T$, $\partial\Phi/\partial p$, etc. can be written down from Eq. (57) if desired.

Two Component Perfect Gas; $\bar{v}_i=\bar{v}_i^*=0$

This is the most important case, so we give a few additional results here (these can be generalized) which should be helpful in interpreting experimental data.

First, we write, from Eq. (47),

$$-\bar{S}_1dT+(\partial\mu_1/\partial\Gamma_1)d\Gamma_1+(\partial\mu_1/\partial\Gamma_2)d\Gamma_2 = -S_{1G}dT+kTd\ln p_1. \quad (71)$$

This corresponds to $p_1=p_1(\Gamma_1, \Gamma_2, T)$. Now suppose we want instead $p_1=p_1(\Gamma_1, u, T)$, where $u=p_2$, p_1/p_2 or p $(=p_1+p_2)$. Then we use

$$d\Gamma_2=(\partial\Gamma_2/\partial\ln p_1)d\ln p_1+(\partial\Gamma_2/\partial u)du+(\partial\Gamma_2/\partial T)dT \quad (72)$$

in place of $d\Gamma_2$ in Eq. (71). Hence

$$\left(\frac{\partial\ln p_1}{\partial T}\right)_{\Gamma_1,u}=\frac{S_{1G}-\bar{S}_1+(\partial\mu_1/\partial\Gamma_2)_{T,\Gamma_1}(\partial\Gamma_2/\partial T)_{p_1,p_2}}{kT-(\partial\mu_1/\partial\Gamma_2)_{T,\Gamma_1}(\partial\Gamma_2/\partial\ln p_1)_{u,T}}. \quad (73)$$

$u=p_1/p_2$ in Arnold's work,[19] $u=p_2$ in the paper of White and Schneider,[20] and $u=p$ in the work of Markham and Benton.[25]

White and Schneider[20] also plot Γ_1 against p_2 at constant p_1. We derive, as above, for this case

$$\left(\frac{\partial\ln p_2}{\partial T}\right)_{\Gamma_1,u}=\frac{S_{2G}-\bar{S}_2+(\partial\mu_2/\partial\Gamma_2)_{\Gamma_1,T}(\partial\Gamma_2/\partial T)_{p_1,p_2}}{kT-(\partial\mu_2/\partial\Gamma_2)_{\Gamma_1,T}(\partial\Gamma_2/\partial\ln p_2)_{u,T}}, \quad (74)$$

where $u=p_1$ (White and Schneider), p_1/p_2 or p.

From Eq. (57),

$$-\bar{S}_1^*dT+\bar{N}_{A1}^*d\Phi+(\partial\mu_1/\partial y)dy = -S_{1G}dT+kTd\ln p_1. \quad (75)$$

Putting $y=y(\ln p_1, u, T)$ (alternatively, y can be replaced by Φ), we find

$$\left(\frac{\partial\ln p_1}{\partial T}\right)_{\Phi,u}=\frac{S_{1G}-\bar{S}_1^*+(\partial\mu_1/\partial y)_{T,\Phi}(\partial y/\partial T)_{p_1,p_2}}{kT-(\partial\mu_1/\partial y)_{T,\Phi}(\partial y/\partial\ln p_1)_{u,T}}, \quad (76)$$

where $u=p_2$, p_1/p_2 or p.

Arnold found it helpful to plot $\Gamma_1+\Gamma_2(=\Gamma_{12})$ against p at constant p_1/p_2. Here, in place of Eq. (71), we use

$$\begin{aligned}-\bar{S}_1dT+(\partial\mu_1/\partial\Gamma_{12})d\Gamma_{12}+(\partial\mu_1/\partial y)dy &= -S_{1G}dT+kTd\ln p+kTd\ln x\\ -\bar{S}_2dT+(\partial\mu_2/\partial\Gamma_{12})d\Gamma_{12}+(\partial\mu_2/\partial y)dy &= -S_{2G}dT+kTd\ln p+kTd\ln(1-x),\end{aligned} \quad (77)$$

where x is the mole fraction of component 1 in the gas. Then

$$\left(\frac{\partial\ln p}{\partial T}\right)_{\Gamma_{12},x}=\frac{\begin{array}{r}(\partial\mu_2/\partial y)_{\Gamma_{12},T}(S_{1G}-\bar{S}_1)\\ -(\partial\mu_1/\partial y)_{\Gamma_{12},T}(S_{2G}-\bar{S}_2)\end{array}}{kT[(\partial\mu_2/\partial y)_{\Gamma_{12},T}-(\partial\mu_1/\partial y)_{\Gamma_{12},T}]}. \quad (78)$$

In a complete thermodynamic treatment we want S_s. If the individual $\bar{S}_i^*$ are found from say, Eq. (59), then

$$S_s=\sum N_i\bar{S}_i^*. \quad (79)$$

Also, using a generalization of Eq. (34), we can find $S_s(N_1, N_2, \cdots)-S_s(0, N_2, \cdots)$. By using m successive integrations of this type we get finally $S_s(N_1, N_2, \cdots)$ itself.

Summary: Clausius-Clapeyron Equations for Mixtures

Workers who obtain isotherm data for mixtures will be interested in making calculations of the Clausius-Clapeyron type and in knowing just what thermodynamic quantities they are obtaining from such calculations. Equations (46)–(78) answer the latter question for the most obvious types of calculation. The final equations fall into four classes:

(1) Equations (49) and (59) give the simplest and most useful results: individual ΔS_i's.

(2) The quantities obtained from Eqs. (46) and (48) involve all the ΔS_i's, and, in addition, certain properties of the equilibrium vapor, which, however, are easily evaluated if the vapor is a perfect gas mixture.

(3) Equations (73), (74), and (76) give individual

[23] Kemball, Rideal, and Guggenheim, Trans. Faraday Soc. **44**, 948 (1948). A somewhat simplified version of their statistical model has been used to check many of the equations of Section III.

[24] W. B. Innes and H. H. Rowley, J. Phys. Chem. **49**, 411 (1945).

[25] E. C. Markham and A. F. Benton, J. Am. Chem. Soc. **53**, 497 (1931).

ΔS_i's, but certain derivatives (e.g., $(\partial\Gamma_2/\partial T)_{p_1,p_2}$) have to be evaluated from isotherm data and others (e.g., $(\partial\mu_1/\partial\Gamma_2)_{T,\Gamma_1}$) have to be evaluated from theory or from isotherm data (using—provided $\mu_{1G}(p_1, T)$ is known—the fact that, for example, $\mu_1=\mu_{1G}$ at equilibrium*). In any case, in comparing an explicit statistical theory with experiment, the right-hand members of all the equations in (1)–(4), regardless of complexity, can of course be calculated from the theoretical model and compared with left-hand members calculated from experimental data.

(4) Equations (50), (60), and (78) contain quantities of the type mentioned in (2), and, in addition, derivatives involving μ_i, as in (3).

Calorimetric Quantities

In this section it will be seen that the calorimetric equations of paper V actually apply without formal change to sorption on any type of sorbent, regardless of sorbent perturbation, etc. The equations are also extended to gas mixtures.

Integral heat of sorption. Suppose we have a system consisting of a closed container immersed in a large isolated constant temperature bath. The bath has an initial energy E_b. The container is divided into two parts connected by a stop-cock. Initially one part contains $N_1^0, N_2^0, \cdots$ molecules of a perfect gas mixture and the other part contains $N_A=\sum N_\alpha$ molecules of an evacuated sorbent. The stop-cock is opened and equilibrium is eventually established. Initially the total energy of the complete system is $E_b+E_{0A}(P=0)+\sum N_i^0 E_{iG}$. Let E_b' be the internal energy of the bath in the final equilibrium state and suppose N_i molecules of type i have been sorbed. Then the total final energy of the system is $E_b'+E+\sum(N_i^0-N_i)E_{iG}$. But

$$E_b+E_{0A}(P=0)+\sum N_i^0 E_{iG} = E_b'+E+\sum(N_i^0-N_i)E_{iG} \quad (80)$$

so

$$Q=E_b'-E_b=\sum N_i E_{iG}-E_s = \sum N_i(E_{iG}-\bar{E}_i^*) \quad (T, N_A \text{ const.}), \quad (81)$$

where Q is the integral heat of sorption and the difference between $E_{0A}(P=0)$ and $E_{0A}(p)$ has been ignored.

Differential and isothermal heat of sorption. We have a container as above. The perfect gas mixture is in equilibrium with sorbate. Let V_c be the volume of the container: $V_c=V_G+V$. A frictionless piston forms one wall of the container. The piston is moved (T constant) so that V_c changes by dV_c and a new equilibrium state is reached. Let E_t be the total initial internal energy of the complete system:

$$E_t=E_b+E+\sum(N_i^0-N_i)E_{iG} \quad (82)$$

$$dE_t=-pdV_c=dE_b+dE-\sum E_{iG}dN_i. \quad (83)$$

Now E is a function of P, T, N_i, N_A. N_A and T are constant in Eq. (83) and the effect of $dP=dp$ is neglected, so we write

$$dE=\sum(\partial E/\partial N_i)_{N_j,N_A,T}dN \cong \bar{E}_i dN_i \quad (84)$$

and

$$dE_b=\sum q_{d(i)}dN_i-pdV_c \quad (T, N_A \text{ const.}) \quad (85)$$

$$q_{d(i)}=E_{iG}-\bar{E}_i. \quad (86)$$

We digress to note that[15] (Eq. (49))

$$q_{st(i)}=H_{iG}-\bar{H}_i \cong E_{iG}+kT-\bar{E}_i=q_{d(i)}+kT. \quad (87)$$

dE_b in Eq. (85) is the isothermal heat of sorption for a volume change dV_c. If the piston is omitted and the expansion dV_c takes place irreversibly through a stop-cock, say, then the external work term pdV_c is omitted from Eq. (85) and the resulting dE_b is the differential heat of sorption for a volume change dV_c. In either case we wish to evaluate dN_i in terms of dV_c. We have

$$p_i(V_c-V)=(N_i^0-N_i)kT \quad (i=1, \cdots m) \quad (88)$$

$$p_i dV_c+V_G dp_i=-kTdN_i \quad (i=1, \cdots m), \quad (89)$$

where we neglect dV. Also, using the equilibrium adsorption isotherm data in the form $N_i=N_i(p_1, p_2, \cdots, T)$, we have

$$dN_i=\sum_k(\partial N_i/\partial p_k)dp_k \quad (i=1, \cdots m). \quad (90)$$

Equations (89) and (90) constitute $2m$ linear nonhomogeneous equations in the $2m$ unknowns dN_i, dp_i. Thus we can easily solve for each

$$dN_i=dV_c f(p_k, T, V_G, \partial N_j/\partial p_k).$$

For a one-component sorbate Eq. (85) reduces to

$$(\partial E_b/\partial N_1)_{N_A,T}=q_{th}=q_{st}+[V_G/(\partial N_1/\partial p)_T]. \quad (91)$$

We may note that in the special case $dp=0$, $q_{th}=q_{st}=H_G-\bar{H}_1$ as expected for a reversible constant pressure process. Of course in general $dp\neq 0$.

Professor J. G. Aston has pointed out to the writer that a calorimeter[26] which gives directly ΔH of vaporization of a pure liquid should, when used in adsorption work, give q_{th} of Eq. (91) and *not* q_d. With such a calorimeter the uncertainty in calorimetric measurements mentioned in paper V would appear to be removed.

"Equilibrium" heat and entropy of sorption. In the reversible process we now describe all intensive properties remain constant, giving what we may call the "equilibrium" entropy of sorption (since it is analogous to the entropy of vaporization, etc., carried out reversibly—maintaining the same equilibrium point between liquid and vapor).

The following equations are exact (perfect gas not assumed, etc.). We have a container as in the "iso-

* Thus, in Eq. (73) (perfect gas),

$$\mu_1=\mu_{1G}=\mu_{1G}^0(T)+kT\ln p_1$$

$$\left(\frac{\partial\mu_1}{\partial\Gamma_2}\right)_{T,\Gamma_1}=kT\left(\frac{\partial\ln p_1}{\partial\Gamma_2}\right)_{T,\Gamma_1}.$$

[26] See, for example, Aston *et al.*, J. Am. Chem. Soc. **66**, 1171 (1944); **68**, 52 (1946); Giauque and Johnston, J. Am. Chem. Soc. **51**, 2300 (1929).

thermal" arrangement, but with the following modification: there is an additional hypothetical piston which separates $N_A^0-N_A$ molecules of pure sorbent from N_A molecules of sorbent in contact with sorbate. That is, this piston prevents the sorbate from spreading over the entire sorbent—it is impermeable to sorbate but, when the *piston* moves, stationary sorbent can pass through it (see Appendix III). When the gas piston is moved by an amount dV_c, the sorbent piston is moved an "amount" dN_A such that *all* intensive properties are kept constant—doing external work ΦdN_A. We have

$$E_t=E_b+E(N_A, N_i, p, T)+E_{0A}(N_A^0-N_A, p, T)+\sum(N_i^0-N_i)\bar{E}_{iG}. \quad (92)$$

Now

$$E_{0A}(N_A^0-N_A, p, T)=E_{0A}(N_A^0, p, T)-E_{0A}(N_A, p, T) \quad (93)$$

and

$$E_s=\sum N_i\bar{E}_i^*,$$

so

$$E_t=E_b+\sum N_i\bar{E}_i^*+E_{0A}(N_A^0, p, T)+\sum(N_i^0-N_i)\bar{E}_{iG} \quad (94)$$

$$dE_t=-pdV_c-\Phi dN_A=dE_b+\sum(\bar{E}_i^*-\bar{E}_{iG})dN_i. \quad (95)$$

Also

$$V_c=V_G+V(N_A, N_i, p, T)+V_{0A}(N_A^0-N_A, p, T)=\sum(N_i^0-N_i)\bar{v}_{iG}+\sum N_i\bar{v}_i^*+V_{0A}(N_A^0, p, T) \quad (96)$$

$$dV_c=\sum(\bar{v}_i^*-\bar{v}_{iG})dN_i \quad (97)$$

and

$$dN_A=\sum\bar{N}_{Ai}^*dN_i. \quad (98)$$

Putting Eqs. (97) and (98) into Eq. (95) gives

$$dE_b=\sum[(\bar{E}_{iG}+p\bar{v}_{iG})-(\bar{E}_i^*+p\bar{v}_i^*+\Phi\bar{N}_{Ai}^*)]dN_i=\sum(\bar{H}_{iG}-\bar{H}_i^*)dN_i=\sum T(\bar{S}_{iG}-\bar{S}_i^*)dN_i. \quad (99)$$

As this is a reversible process, the entropy change in the material inside the container must be $-dE_b/T$. This entropy change in the above process may easily be calculated independently and is found to check Eq. (99). The dN_i in Eq. (99) are not all independent. In fact, $N_i/N_A=\Gamma_i=$ const., so $dN_i=\Gamma_i dN_A$.

Heat capacity and entropy. We have a perfect gas mixture in equilibrium with sorbate in a container of constant volume. The temperature of the entire system (container plus bath) is changed by dT owing to an absorption of heat in amount q from an external source. Then Eq. (82) holds and

$$dE_t=q=dE_b+dE+\sum N_{iG}dE_{iG}-\sum E_{iG}dN_i \quad (100)$$

where, neglecting pressure effects,

$$dE=\sum[(\partial E/\partial N_i)_{N_j,T,N_A}dN_i]+(\partial E/\partial T)_{N_i,N_A}dT. \quad (101)$$

Writing $E=E_s+E_{0A}$, Eq. (101) becomes

$$dE=\sum\bar{E}_i dN_i+C_n dT+C_{0A}dT,$$

where the definitions of C_n and C_{0A} are obvious. As we are ignoring pressure effects, C_{0A} is also the heat capacity of the *evacuated* pure sorbent. Returning to Eq. (100),

$$C_n=(q/dT)-C_b-\sum C_{iGV}-C_{0A}+\sum q_{d(i)}(dN_i/dT) \quad (N_A, V_c \text{ const.}), \quad (102)$$

where C_b is the heat capacity of the bath and C_{iGV} is the heat capacity at constant volume of the $i-th$ component of the gas. The dN_i/dT may be found from (see Eqs. (88) and (90))

$$V_G dp_i=kN_{iG}dT-kTdN_i \quad (i=1, \cdots m) \quad (103)$$

$$dN_i=\sum_k[(\partial N_i/\partial p_k)_{p_j,T}dp_k]+(\partial N_i/\partial T)_{p_k}dT \quad (i=1, \cdots m). \quad (104)$$

The dN_i/dT will depend on the $(\partial N_i/\partial T)_{p_k}$, among other things. These derivatives may be more easily evaluated from isotherm data using

$$\left(\frac{\partial N_i}{\partial T}\right)_{p_k}=-\left(\frac{\partial N_i}{\partial p_i}\right)_{p_j,T}\left(\frac{\partial p_i}{\partial T}\right)_{p_j,\Gamma_i}. \quad (105)$$

We now relate S_s to C_n. We have

$$dE_s=TdS_s+\sum\mu_i dN_i=\sum(\partial E_s/\partial N_i)dN_i+C_n dT \quad (N_A \text{ const.}) \quad (106)$$

$$(\partial S_s/\partial T)_n=C_n/T \quad (107)$$

$$dS_s=\sum[(\partial S_s/\partial N_i)dN_i]+(\partial S_s/\partial T)dT=\sum\bar{S}_i dN_i+(C_n/T)dT \quad (N_A \text{ const.}), \quad (108)$$

where the dN_i are given by Eqs. (103) and (104). Integration of this equation between T_1 and T_2 gives $S_s(N_i(T_2), T_2)-S_s(N_i(T_1), T_1)$ (see paper V). In order to use Eq. (102), C_{0A} must be measured. Hence $S_{0A}(T_2)-S_{0A}(T_1)$ and $S(T_2)-S(T_1)$ are also available (indeed, if we do not use $E=E_s+E_{0A}$ in Eq. (101), dS is obtained directly in place of dS_s in Eq. (108)).

I am indebted to Drs. J. G. Aston, P. H. Emmett, G. Halsey, G. Jura and G. B. Kistiakowsky for very stimulating discussions and comments.

APPENDIX I

We discuss here some relations with surface thermodynamics. Gibbs' treatment[27] of surfaces is of course classical. Guggenheim[28] has given an equivalent but alternative treatment of surface thermodynamics which is more satisfactory from a physical point of view, and which can more readily be compared with the present paper than Gibbs' work. Guggenheim considers the thermodynamic functions for a surface region σ between two phases, σ extending into each phase far enough to reach the homogeneous region of the phase, but otherwise being arbitrary in extent. We now characterize

[27] E. A. Guggenheim, *Modern Thermodynamics* (Methuen and Company, London, 1933), Chapter XII.

[28] E. A. Guggenheim, Trans. Faraday Soc. **36**, 397 (1940).

our special case. In the first place, we take one of the homogeneous phases as a gas,[4a] neglect molecular interactions between the gas and the condensed phase, and take σ as the *entire* condensed phase. Similarly, we take an equivalent (see discussion preceding Eq. (10)) sample of pure sorbent and call it σ_0. We then subtract thermodynamic properties of σ_0 from those of σ to obtain S_s, E_s, etc. In our notation, Guggenheim writes in general for σ,

$$dE=TdS-PdV+\gamma' d\mathfrak{A}+\sum\mu_i' dN_i+\sum\mu_\alpha' dN_\alpha, \quad (109)$$

where γ', μ_i' and μ_α' are defined as derivatives by Eq. (109), and $\mathfrak{A}$ is a further *independent* variable. In our special case each N_α is determined by $\mathfrak{A}$ (but our discussion is more general in that we are not restricted to "surface" problems—$\mathfrak{A}$ is replaced by N_A), so

$$dE=TdS-PdV+\gamma d\mathfrak{A}+\sum\mu_i dN_i, \quad (110)$$

where γ and μ_i are defined as derivatives by Eq. (110). Also,

$$dE_{0A}=TdS_{0A}-PdV_{0A}+\gamma_0 d\mathfrak{A} \quad (111)$$

$$dE_s=TdS_s-PdV_s-\varphi d\mathfrak{A}+\sum\mu_i dN_i \quad (112)$$

$$\varphi=\gamma_0-\gamma. \quad (113)$$

If we are concerned with strictly surface effects it is obviously not necessary to take σ and σ_0 as including the entire sorbent, but it has the considerable advantage of extending the generality to solutions, etc.

The concept of "area" is useful, when it can be defined, so long as the only perturbations of the sorbent by the sorbate are non-structural: that is, the volume and equilibrium molecular structure of the sorbent stay essentially constant (as in most physical and chemisorptions) but vibration frequencies of surface atoms, rotational and electronic energy levels, etc. may change. With structural perturbations, Eq. (112) must be replaced by Eq. (51).

Guggenheim points out that in general with curved interfaces there is ambiguity in P in the external work term $-PdV$. However, in our special case there is no ambiguity because the only PV external work the condensed phase can do is against the vapor pressure or an additional hydrostatic pressure exerted, say, by an inert gas. From another point of view, since adsorption systems are thermodynamically indistinguishable from solution systems, the pressure P exerted on an adsorbent-adsorbate has precisely the same significance as the pressure P exerted on a solution.

Finally, it must be pointed out that for some systems the ***volume*** of the condensed phase cannot be defined precisely because of the importance of surface configurations down to the molecular level. Using the approximate guide that the transfer of a certain number of molecules from the gas phase to the condensed phase increases the volume of the condensed phase by an amount equal to the concomitant decrease in free volume available to the (remaining) gas molecules, it is clear that this effect is in general not important. The rigorous way of avoiding this difficulty, however, is to use the Gibbs or Guggenheim[28] treatment of the surface region between bulk gas and bulk condensed phase; or to treat gas plus condensed phase, combined, as the "thermodynamic system."

APPENDIX II

We discuss briefly here a "fugacity" of the sorbate: a generalization of Φ in the same sense that gas fugacity is a generalization of gas pressure.[29] The concept does not seem to be particularly useful for present purposes but may be important in other connections. For simplicity we shall consider a one-component sorbate only, the extension to any number of components being straightforward.

For a sufficiently small pressure p^*, we assume that Henry's law holds:[30]

$$\Gamma^*=a(P, T)p^*, \quad (114)$$

where P is the hydrostatic pressure on the "solution" and the asterisk refers to the limiting case $p\rightarrow 0$. Then, from Eq. (27),

$$\Phi^*=akTp^*=\Gamma^* kT. \quad (115)$$

Now

$$\mu_G{}^*=\mu_G{}^0(T)+kT\ln p^* = \mu_1{}^*=\mu_G{}^0(T)+kT\ln(\Phi^*/akT). \quad (116)$$

Hence,

$$\mu_1{}^*=\mu_1{}^0(P, T)+kT\ln\Phi^* \quad (117)$$

with

$$\mu_1{}^0(P, T)=\mu_G{}^0(T)-kT\ln a(P, T)kT. \quad (118)$$

Noting the analogy between Eq. (116) and Eq. (117), we *define* a fugacity f_s by the equations

$$\mu_1=\mu_1{}^0(P, T)+kT\ln f_s \qquad f_s\rightarrow\Phi \quad \text{as} \quad \Phi\rightarrow 0 \quad (p\rightarrow 0). \quad (119)$$

We have immediately the properties of f_s

$$\left(\frac{\partial \ln f_s}{\partial \mu_1}\right)_{P,T}=\frac{1}{kT}, \quad \left(\frac{\partial \ln f_s}{\partial \Phi}\right)_{P,T}=\frac{1}{\Gamma kT}. \quad (120)$$

Also, one finds with no difficulty

$$\left(\frac{\partial \ln f_s}{\partial T}\right)_{P,\Phi}=\frac{H_s{}^*-H_s}{kT^2}, \quad \left(\frac{\partial \ln f_s}{\partial P}\right)_{T,\Phi}=\frac{v_s-v_s{}^*}{kT}. \quad (121)$$

---

[29] W. B. Innes and H. H. Rowley, J. Phys. Chem. **46**, 548 (1942). These authors have already discussed the unimolecular case (strictly two-dimensional systems).

[30] If, owing to dissociation (or association) of the gas molecules on the surface, $\Gamma^*=a(P, T)p^{*1/n}$, where Γ^* is the surface concentration taking the dissociated species as the fundamental component on the surface (e.g. $n=2$ for $H_2\rightarrow 2H$ on adsorption), then from (Eq. (27))

$$d\Phi=(1/n)\Gamma kTd\ln f \quad (P, T \text{ const.})$$

we get $\Phi^*=akTp^{*1/n}=\Gamma^* kT$. Using $n\mu_1{}^*=\mu_G{}^*$, Eq. (117) is obtained again with

$$\mu_1{}^0(P, T)=[\mu_G{}^0(T)/n]-kT\ln akT.$$

It is of interest to consider μ_1 as a function of T, P and $\ln f_s$ so that

$$d\mu_1=\left(\frac{\partial\mu_1}{\partial T}\right)_{P,f_s}dT+\left(\frac{\partial\mu_1}{\partial P}\right)_{T,f_s}dP+\left(\frac{\partial\mu_1}{\partial \ln f_s}\right)_{T,P}d\ln f_s \quad (122)$$

$$=[-S_s+(H_s-H_s^*)/T]dT+v_s^*dP+kTd\ln f_s \quad (123)$$

$$=d\mu_G=[-S_G+(H_G-H_G^*)/T]dT+kTd\ln f. \quad (124)$$

Hence, in analogy with Eq. (23),

$$\left(\frac{\partial\ln f}{\partial T}\right)_{f_s,P}=\frac{H_G^*-H_s^*}{kT^2}. \quad (125)$$

At *any* vapor pressure p this equation merely gives the information that Eq. (23) already gives at *low* pressures. The reason for this is clear from the following:

$$\mu_1=\mu_G$$
$$\mu_1^0(P,T)+kT\ln f_s=\mu_G^0(T)+kT\ln f$$
$$K(P,T)=f_s/f=\exp\{[\mu_G^0(T)-\mu_s^0(P,T)]/kT\} \quad (126)$$
$$=a(P,T)kT, \quad (127)$$

where K is an "equilibrium constant," independent of p, which can be evaluated from Eq. (114). Thus, at any pressure p, f_s is essentially determined by the behavior of the adsorption isotherm at low pressures.

In solution thermodynamics, in place of f_s the fugacity $f_1=f$ would of course be used.

APPENDIX III

We discuss here the relation between Φ and the osmotic pressure. Referring to Eqs. (92)–(99) and the related discussion, we note that pure sorbent A at P and T is separated from a solution of sorbate in sorbent at P and T by a kind of semi-permeable piston. The chemical potential of pure sorbent is μ_{0A} and of sorbent in the solution is μ_A. We define (as usual) the osmotic pressure Π as the excess hydrostatic pressure on the solution needed in order to increase μ_A up to the value μ_{0A}. We find

$$\mu_{0A}-\mu_A=\Phi=\int_P^{P+\Pi}\bar{v}_AdP \quad (T, n \text{ const.}). \quad (128)$$

If $\bar{v}_A$ is essentially constant between P and $P+\Pi$, $\Phi=\Pi\bar{v}_A$. For an inert adsorbent with a well-defined surface area $\mathcal{A}$, $\bar{v}_A=v_{0A}$ to a very high approximation and

$$\Phi N_A=\varphi\mathcal{A}=\Pi V_{0A},$$
$$\Phi dN_A=\varphi d\mathcal{A}=\Pi dV_{0A}. \quad (129)$$

There are two unusual features about the present osmotic system: (1) the solvent (sorbent) is non-volatile, and (2) it is the escaping or diffusing tendency of the solute (sorbate) which is *in effect* operative when the hypothetical sorbent piston moves. This is especially clear when the spreading pressure $\varphi=\gamma_0-\gamma$ has meaning.

THE JOURNAL OF CHEMICAL PHYSICS VOLUME 18, NUMBER 3 MARCH, 1950

The Occurrence of Hypsochromic Shifts on Alkyl Substitution: Structure and Color of Methylated Derivatives of Azulene

BERNARD PULLMAN, MARCEL MAYOT, AND GASTON BERTHIER
Institut du Radium, and Institut d'Astrophysique, Paris, France
(Received June 2, 1949)

While two methylated derivatives of azulene show the usual bathochromic shift with respect to azulene itself, the remaining three isomers show an unusual displacement of the visible spectrum toward shorter wave-lengths. No steric effects can be claimed to account for these last results which are considered as representing genuine hypsochromic shifts brought about by alkyl substitution and due to the particularities of the structure of azulene and its derivatives. It is then shown by molecular orbital method calculations that Mulliken's $N \rightarrow V$ theory of color accounts satisfactorily for the observed facts. In the methylated derivatives showing a bathochromic shift, the calculated excitation energy of the $N \rightarrow V_1$ transition appears to be smaller than the corresponding energy in azulene itself, while the reverse is true for the compounds exhibiting a hypsochromic shift. The general conditions necessary for the occurence of hypsochromic shifts upon alkylation and a few predictions of such shifts in other hydrocarbons are given.

IT is well known that the substitution of a methyl group for the H atoms of the usual ethylenic or aromatic hydrocarbons produces generally a more or less pronounced shift of the spectrum toward longer wave-lengths (a bathochromic shift).[1] A few exceptions to this rule, corresponding to isolated cases in which methyl substitution brings about a displacement of the spectrum toward shorter wave-lengths (a hypsochromic shift), are generally attributed to steric interference with the coplanarity necessary for the existence of full conjugation effects. The classical examples of such exceptions are the α- or β-alkylated derivatives of stilbene in which the presence of a methyl group on the ethylenic double bond produces a partial rotation of one of the phenyl rings with respect to the other and thus destroys the full resonance of the molecule.[2]

The appearance of a bathochromic shift with alkyl substitution has been attributed to two principal effects: the hyperconjugation and the inductive effects of the methyl group.[3] In the molecular orbital method which is generally employed in the quantum-mechanical investigation of this problem, the two effects are related, respectively,[4] to the attribution of a particular exchange integral to the $C=H_2$ or $C\equiv H_3$ bonds, considered as quasi-double or quasi-triple bonds, and to the differences in the values of the Coulomb integrals of the C_{arom}, C_{aliph}, and H_2 or H_3 atoms, caused by differences in their electronegativities. As a matter of fact, the distinction should be made, as it is here, between hyperconjugation and the inductive effect and not, as it sometimes is,[5] between hyperconjugation and "charge transfert" because it has been explicitly shown that hyperconjugation alone may produce in some cases appreciable charge transfert, the existence, the magnitude, and the direction of such an electronic displacement depending mostly upon the geometrical configuration of the molecule.[6]

The degree of the bathochromic shift is related to the value of the energy difference between the ground (N) and the excited (V) state of the substance. In the usual alkylated hydrocarbons, hyperconjugation of the methyl group produces *a raising* of the highest filled orbital and a parallel *lowering* of the lowest empty one, while the inductive effect produces *a differential raising* of the two orbitals, the changes of the ground one being the more pronounced. This is not necessarily the only possible way in which these two effects modify the distribution of the energy levels, and the mode of their influence is in fact determined largely by the geometrical shape of the hydrocarbons.[7] Nevertheless, in all hitherto investigated compounds, the electronic interactions between an alkyl group and the mobile electrons of an unsaturated hydrocarbon seemed to result always in a bathochromic shift, the only exceptions being the previously mentioned cases of steric perturbation of coplanarity.

Recently, however, Plattner and co-workers[8] have studied in detail the visible (and ultraviolet) spectra of methylated derivatives of azulene and have observed the unusual fact that though there is presumably no appreciable steric inhibition of resonance in any of these

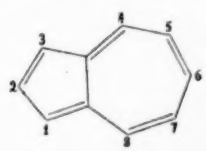

FIG. 1. Azulene.

[1] For a review of experimental evidence see N. Jones, Chem. Rev. **32**, 1 (1943).
[2] B. Arends, Ber. **64**, 1936 (1931).
[3] R. S. Mulliken, J. Chem. Phys. **7**, 339 (1939); Rev. Mod. Phys. **14**, 265 (1942). See also A. D. Walsh, Ann. Rep. **44**, 32 (1947); Quart. Rev. **2**, 73 (1948).
[4] Mulliken, Rieke, and Brown, J. Am. Chem. Soc. **63**, 41 (1941); R. S. Mulliken and C. A. Rieke, J. Am. Chem. Soc. **63**, 1770 (1941).
[5] W. C. Price and A. D. Walsh, Proc. Roy. Soc. **A179**, 209 (1941); T. M. Sugden and A. D. Walsh, Trans. Faraday Soc. **41**, 76 (1945).
[6] The case of cyclic dienes and trienes is a particularly good illustration of this statement: a. G. Berthier and B. Pullman at the International Colloquium on the Polarization of Matter, Paris, April, 1949 [Bull. Soc. Chim. **76**, 457 (1949)]. b. See also G. Berthier and B. Pullman, Trans. Faraday Soc. **45**, 484 (1949).
[7] Here, too, the example of cyclic polyenes is the most illustrative: A. Pullman and G. Berthier, Bull. Soc. Chim. (in press).
[8] A. Plattner and E. Heilbronner, Helv. Chim. Acta **30**, 910 (1947) and the references given there.

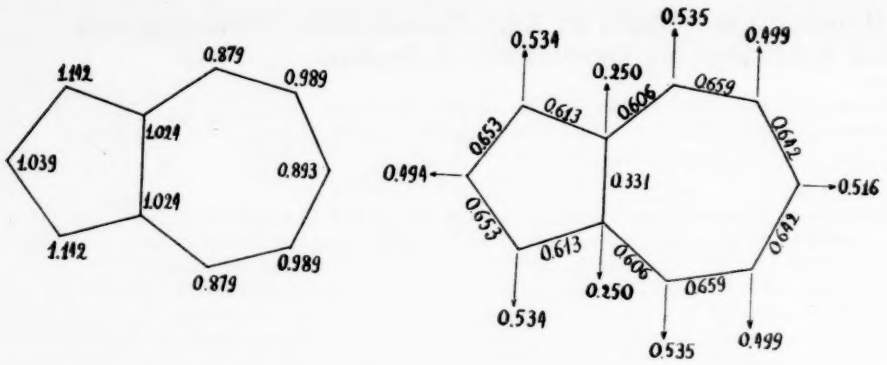

FIG. 2. (a) Charge distribution in azulene. (b) Bond orders and free valence in azulene.

compounds, only two of them manifest the usual bathochromic displacement, while the three remaining isomers show a hypsochromic shift in respect to azulene itself. Following the numbering of Fig. 1, the bathochromic shift corresponds to derivatives methylated at the positions 1 and 5 and the hypsochromic one to derivatives substituted at carbons 2, 4, and 6. The most pronounced displacement of visible color toward longer wave-lengths is observed for the 1-methyl compound, while the hypsochromic shift is the greatest, in the visible spectrum, for the 2- and the smallest for the 4-methyl derivative. *Obviously no steric interference with coplanarity may be claimed to explain this unusual result and the reason for these genuine hypsochromic shifts has to be looked for in the particularities of the structure of azulene itself and in the specific nature of the interactions of the alkyl groups with the mobile electrons of this hydrocarbon.*

THE STRUCTURE OF AZULENE AND OF ITS METHYLATED DERIVATIVES

In fact, azulene belongs to the group of the non-benzenoid aromatic hydrocarbons and quantum-mechanical investigation of these compounds[9] has shown that their electronic configuration differs profoundly from that of the ordinary aromatic molecules. Thus, these compounds show intramolecular charge displacements in their ground state and possess an appreciable dipole moment whenever their geometrical shape does not prevent its appearance, while no such charge displacements are found in the usual benzenoid hydrocarbons. They also generally show a marked diminution of the $N \rightarrow V_1$ excitation energy with respect to their benzenoid isomers.[10] In what concerns the particular case of azulene, its electronic structure has been studied in the molecular orbital method by Coulson and Longuet-Higgins[11] and by Brown[12] in the usual approximation in which the exchange integrals of the C—C bonds have all been put uniformly equal to β and the Coulomb integrals of the C atoms equal all to α. A better approximation has been obtained by Pullman and Berthier[13] who have taken into account the particular nature of the binuclear bond, much more "single" than the other C—C links, and assumed its exchange integral to be equal to 0.8β. In this approximation the distribution of electrical charges and of bond orders and free valence[14] is shown in Figs. 2(a) and 2(b), respectively. There is an appreciable charge shift corresponding to the fundamental tendency of mobile electrons to leave heptagonal rings and to concentrate in pentagonal ones.[6a] Quite recently, Wheland and Mann[15] have carried out a still more refined treatment of azulene by taking into consideration the variations of the exchange integrals of all the C—C bonds and by introducing also differences in the Coulomb terms of the C atoms. In such a way they reach a theoretical dipole moment which is in better agreement with the experimental one than those previously evaluated. In the calculations carried out in the present paper we have limited ourselves, however, to

TABLE I. Energies of molecular orbitals in methylated azulenes

Azulene	1-methyl-azulene	2-methyl-azulene	4-methyl-azulene	5-methyl-azulene	6-methyl-azulene
		Antibonding $(E-\alpha)/\beta$			
	−2.3287	−2.3129	−2.3427	−2.3271	−2.3238
−1.9817	−1.9541	−1.9817	−1.9412	−1.9710	−1.9817
−1.8864	−1.8481	−1.8565	−1.8081	−1.8147	−1.8167
−1.5868	−1.5434	−1.5231	−1.5843	−1.5649	−1.5531
−0.7172	−0.7204	−0.7271	−0.7209	−0.7239	−0.7271
−0.4361	−0.4365	−0.4441	−0.4499	−0.4369	−0.4533
		Bonding $(E-\alpha)/\beta$			
0.5046	0.4517	0.5046	0.4983	0.4804	0.5046
0.8354	0.8237	0.7602	0.8195	0.8292	0.7990
1.3943	1.3687	1.3943	1.3002	1.3509	1.3943
1.6458	1.5974	1.5740	1.6304	1.5650	1.5034
	1.9735	1.9985	1.9940	2.0516	2.0693
2.2284	2.3150	2.3038	2.3043	2.2814	2.2736

[9] For a general account see reference 6a.

[10] A. Pullman and B. Pullman, International Colloquium on the Nature of the Chemical Bond, Paris, April, 1948 [J. de Chim. Phys. **46**, 212 (1949)].

[11] C. A. Coulson and H. C. Longuet-Higgins, Rev. Sci. Inst. **85**, 929 (1947).

[12] R. D. Brown, Trans. Faraday Soc. **44**, 984 (1948).

[13] A. Pullman and G. Berthier, Comptes Rendus **227**, 677 (1948).

[14] For the definition of bond order and free valence in the molecular orbital method see C. A. Coulson, Faraday Soc. Disc. **2**, 9 (1947). N_{max} is, however, taken in the present paper as equal to 4, 8 following B. Pullman and G. Berthier, Bull. Soc. Chim. **16**, 145 (1949).

[15] G. W. Wheland and D. E. Mann, J. Chem. Phys. **17**, 269 (1949). *Added in proof:* See however, G. Berthier and A. Pullman, Comptes Rendus **229**, 567 (1949).

the approximation of Pullman and Berthier. As we are essentially interested in the relative values of the energies of the molecular orbitals in different methylated azulenes with respect to azulene itself, the eventual introduction of the refinements used by Wheland and Mann would not alter greatly our principal conclusions. It would simply change the absolute values of the molecular orbitals and probably only slightly as the energies are less sensible to refinements in calculations than are the charge distributions (see the discussion of the results).*

In order to evaluate the energies of the molecular orbitals in methylated azulenes, definite assumptions have to be adopted in what concerns the parameters to be employed in order to account for the electronic interactions which occur between the alkyl group and the hydrocarbon. Following the work of Mulliken and Rieke on hyperconjugation,[4] we have adopted 2β for the exchange integral of the $C{\equiv}H_3$ bond and 0.7β for the exchange integral of $C_{arom}-C_{aliph}$ "single" bond, and, following the calculations of Wheland,[16] Crawford,[17] and others,[18] we have assumed the Coulomb integral of the H_3 group as equal to $\alpha-0.2\beta$ and that of the C atom to which the methyl group is attached as equal to $\alpha-0.1\beta$. This group of parameters has already been used in different calculations involving methyl and has led to satisfactory results. It enables one, for instance, to reproduce exactly the experimental dipole moment of toluene (see reference 18).

The calculations were then carried out in the usual way (see, e.g., reference 18) and the energies of the molecular orbitals found by solving the appropriate secular equations. The overlap between adjacent atomic orbitals being neglected, the energies are of the form: $E=\alpha+k\beta$. As β is numerically negative, positive values of k correspond to bonding and negative values to antibonding orbitals. The results of the calculations are summed up in Table I.

DISCUSSION OF THE RESULTS

In the ground state of the molecules the mobile electrons occupy in pairs all the bonding orbitals. The different excited states are obtained by taking an electron from a bonding orbital and placing it on an antibonding one. The first excited state corresponds to the transition of one of the electrons from the highest bonding orbital to the lowest antibonding one. The transition is called $N\rightarrow V_I$ in the notation of Mulliken and Rieke and the corresponding excitation energy determines the longest wave-length of absorption. The values of the $N\rightarrow V_I$ transitions are listed in Table II.

TABLE II.

Compound	$N\rightarrow V_I$ (in β-units)
Azulene	0.9407
1-methyl-azulene	0.8882
2-methyl-azulene	0.9487
4-methyl-azulene	0.9482
5-methyl-azulene	0.9173
6-methyl-azulene	0.9579

It is seen that the $N\rightarrow V_I$ excitation energies of the derivatives substituted at the positions 1 and 5 are smaller but that those of the derivatives substituted at the positions 2, 4, and 6 are greater than the $N\rightarrow V_I$ excitation energy of azulene itself. The occurence of the corresponding bathochromic and hypsochromic shifts is thus fully accounted for. The bathochromic shifts are produced in the usual way by a differential raising of the N and V_I states, the displacement being more pronounced for the N level. Two cases can be distinguished in the appearance of the hypsochromic shifts. In the 2- and 6-methylated compounds the displacement of the spectrum toward shorter wave-lengths is due to the fact that the substitution does not bring about any appreciable change in the energy of the ground state and produces only the raising of the excited V_I state.† In the 4-methylated derivative we observe the customary differential raising of the two states but it is their relative displacement which is unusual: the excited state is raised much more than the ground one.

The *quantitative* evaluation of the magnitude of the spectral displacements and its comparison with the values found by Plattner and co-workers leads to only a limited agreement between theory and experiment. The agreement is, in fact, excellent for the two compounds showing a bathochromic shift but is much less satisfactory for the derivatives which manifest the hypsochromic displacement. Thus, when a suitable value ($=-43.5$ kcal./mole) is adopted for the parameter β so as to account for the position of the longest wave-length of absorption in azulene itself,‡ the calculated shift is of 41 mμ in 1-methyl-azulene (observed 41 mμ) and of 20 mμ in 5-methyl-azulene (observed 18 mμ). In the second class of derivatives, the greatest calculated hypsochromic shift corresponds to the 6-methyl-azulene (calculated 13 mμ, observed 16 mμ), while experimentally it is found in the 2-methyl derivative (calculated 6 mμ, observed 21 mμ). In 4-methyl-azulene the observed shift is 17 mμ, the calculated one 6 mμ. The calculated value is thus in a strong disagreement with

* *Note added in proof:* Since this paper was submitted for publication, a molecular orbital study of the spectrum of azulene has been carried out by Mann, Platt, and Klevens, J. Chem. Phys. 17, 481 (1949). The energies of the molecular orbitals in azulene given by these authors differ slightly from those calculated by ourselves. This is obviously due to different assumptions in setting up the secular equation. In particular, Mann, Platt, and Klevens assumed all the C–C exchange integrals to be equal among themselves and have included the overlap integral in their calculations.

[16] G. W. Wheland, J. Am. Chem. Soc. **64**, 900 (1942).

[17] Private communication.

[18] A. Pullman and J. Metzger, Bull. Soc. Chim. **15**, 1021 (1948); J. Metzger and A. Pullman, Bull. Soc. Chim. **15**, 1166 (1948).

† In fact, there is probably a small raising of the N state due to the perturbations produced by the substituents in the Coulomb integrals of the orthocarbon atoms.

‡ This value of β was obtained on neglecting the singlet-triplet separation in the excited state.

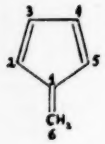

FIG. 3. Fulvene.

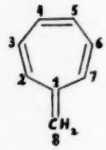

FIG. 4. Methylenecycloheptatriene.

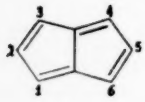

FIG. 5. Pentalene.

the experimental one for two compounds. The introduction of more developed refinements in the calculations, such as those as have been used by Wheland and Mann,[15] does not bring about any important improvement of these results. Thus, assuming the Coulomb integrals of the C atoms to be of the form $\alpha+\delta_i\beta$ and the δ_i's equal to the net charges on the C atoms [of Fig. 2(a)], the excitation energy of azulene itself is reduced to 0.8044β and the hypsochromic shifts, calculated in a similar way as previously, are equal to 16 mμ in 6-methyl-azulene, to 10 mμ in 4-methylazulene, and to 8 mμ in 2-methyl-azulene. This is thus a point which needs further study.

Leaving now the particular case of methylated azulenes, some general remarks may be made about the conditions necessary for the occurrence of genuine hypsochromic shifts following the substitution of a methyl group in a conjugated system. Theoretical considerations of which an account will be given later enable the following statements to be made:

(1) The existence of such a displacement is strictly dependent on the modification brought by the substituent in the value of the Coulomb integral of the C atom to which it is attached. *Thus the hypsochromic shift is closely related to the inductive effect of the alkyl group.*

(2) *No production of a hypsochromic shift by alkyl substitution may be expected in the case of ordinary conjugated hydrocarbons* ("alternant hydrocarbons" in the notation of Coulson and Rushbrooke[19]) as it can be shown that in this group of compounds the relative displacement of the N state is always greater than the displacement of the V_I state.

(3) The occurrence of a hypsochromic shift may, on the contrary, be encountered on alkyl substitution of certain positions of some other "non-alternant" (aromatic non-benzenoid) hydrocarbons. *Thus it can be predicted that a hypsochromic shift should occur upon the substitution of an H atom by CH_3 at the position 6 in fulvene and at the corresponding position in dibenzofulvene and even in benzofulvene, though this last molecule lacks the symmetry properties of the other two*[20] (Fig. 3). No hypsochromic shift is expected in case of alkyl derivatives of the hypothetical methylenecycloheptatriene[21] (Fig. 4). In the hypothetical pentalene[22] (Fig. 5) a hypsochromic shift should be obtained for alkyl substitution at positions 1, 3, 4, and 6.

CONCLUSIONS

The possible production of a hypsochromic shift by alkyl substitution shows the dependence of the changes which may occur in the energies of the molecular orbitals of a hydrocarbon upon its particular geometrical and electronic configuration. This conclusion completes our previous results obtained in the field of simple, unsubstituted resonating molecules. We have already shown in different examples[10] that while the resonance energy always increases in a given family of hydrocarbons with the increase of the number of conjugated double bonds,[23] the $N\rightarrow V_I$ excitation energy may follow in the same conditions quite a different evolution. Thus, while the $N\rightarrow V_I$ transition decreases from benzene to naphthalene, it increases from fulvene (isomer of benzene) to benzofulvene (isomer of naphthalene).[20] In the same way, the $N\rightarrow V_I$ transition increases in the series of paraquinodimethanes with fused rings and decreases in the paraquinodimethanes with conjugated rings.[24] The present results concerning alkylated compounds show the general character of our previous observation and enable one to realize the importance of the geometrical configuration of the basic skeleton in determining the outstanding spectroscopic properties of conjugated systems.*

[19] C. A. Coulson and G. S. Rushbrooke, Proc. Camb. Phil. Soc. **36**, 193 (1940).

[20] For the electronic structure of these compounds see Pullman, Pullman, and Rumpf, Bull. Soc. Chim. **15**, 280 (1948); **15**, 757 (1948).

[21] For its electronic structure see G. Berthier and B. Pullman, Trans. Faraday Soc. **45**, 484 (1949).

[22] For its electronic structure see references 20 and 6a.

[23] The statement by L. G. S. Brooker, Rev. Mod. Phys. **14**, 275 (1942), that the resonance energy of the symmetrical cyanines decreases with the increase of the number of (CH=CH) groups does not seem to be justified.

[24] Pullman, Berthier, and Pullman, Bull. Soc. Chim. **15**, 450 (1948).

* *Added in proof:* A further interesting example of a genuine hypsochromic shift brought about by increasing the size of the conjugated system is given by the feris dibiphenylene-ethylene, dibiphenylene butadiene. See B. Pullman and G. Berthier, Comptes Rendus **229**, 717 (1949).

The Thermal Stabilization and Sintering of Gold Smoke Deposits*

LOUIS HARRIS, DAVID JEFFRIES, AND BENJAMIN M. SIEGEL**
Department of Chemistry, Massachusetts Institute of Technology, Cambridge, Massachusetts
(Received August 29, 1949)

Gold smokes made by evaporation in an inert gas atmosphere are initially in a thermodynamically unstable state. A theory based on diffusion of vacant sites to the surface of the crystallites has been developed to describe the process by which the deposit approaches equilibrium. Measurement at different temperatures of the change of resistance associated with the loss of vacant sites gives a value of 23.5 kcal./g atom for the activation energy of this process.

When heated above 100°C the deposits sinter rapidly and undergo pronounced changes in optical properties. However, a gold smoke deposit can be stabilized, by heat treatment at 70°C, so that sintering proceeds at an appreciably slower rate.

INTRODUCTION

GOLD smoke deposits prepared under certain conditions are of particular interest because they are excellent absorbers of infra-red radiation with very low reflectance.[1,2] Electron microscopy studies reveal that a deposit consists of aggregates of individual spheroidal particles of varying size, the mean diameter in any given deposit being in the range of 40A to 200A, depending on the conditions of preparation.[3] Preliminary observations[1] on changes occurring in gold smoke deposits at elevated temperatures showed that the reflectance of the smokes increased markedly upon being heated to 120°C. A more detailed study of the effect of heating has now been made.

A slow decrease in the resistance of a deposit is observed at room temperature, and at higher temperatures pronounced changes in the optical characteristics occur which depend on the previous history of the specimen. It has been found necessary to treat the effects observed in the lower and higher temperature ranges as the results of two different processes. In the lower temperature (up to 80°C) process, the electrical resistance decreases with time, dropping to less than 0.3 of its original value, while the only change in the optical properties is a small decrease in the infra-red transmission. This process effects a stabilization of the system. The second process, which occurs at higher temperatures (greater than 100°C), produces not only an additional decrease in the electrical resistance but also pronounced changes in the optical characteristics. This process is to be associated with a sintering of the deposit.

MECHANISM OF STABILIZATION

The stabilization of the system must be associated with internal changes in the individual particles observed with the electron microscope. Three types of internal structure suggest themselves as probable ones in a freshly formed deposit.

1. Each particle consists of a number of crystallites surrounded by disordered regions. During stabilization the disordered region becomes ordered with a consequent increase in size of the crystallites. Such a model and mechanism have been used by Suhrmann and his co-workers[4,5] to describe the irreversible resistance changes of thin metallic deposits prepared in a high vacuum and condensed on surfaces cooled to as low as 20°K.

2. Each particle consists of a large number of smaller nuclei. During stabilization the nuclei grow to a single crystallite.

3. Each particle consists of a single crystallite having a non-equilibrium lattice. Energy considerations indicate that for such a model a lattice containing an excess of vacant sites over the number present in the equilibrium lattice is more probable than a distorted lattice with atoms in interstitial positions. Seitz and Huntington[6,7] have made calculations on self-diffusion in copper. Their results show that it would require about 9.5 ev to place a copper atom in an interstitial position in the lattice, while the creation of a vacant site requires only 1.23 ev. These results should also be applicable, qualitatively, to the gold lattice. Therefore it is to be expected that in such a non-equilibrium lattice, which is not too greatly disordered, the lattice will have an excess of vacant sites and should approach the equilibrium state as the excess vacant sites diffuse to the surface of the particle.

Model (1) can be excluded here since the rate of approach to equilibrium, as observed by Suhrmann and his co-workers,[4,5] for the deposits condensed at low temperatures is very much more rapid than the rate observed here for the smokes.

It is possible to decide between models (2) and (3) quite conclusively by x-ray diffraction patterns taken from a fresh deposit and from the same deposit after

* This work has been supported by the Navy Department, Bureau of Ships under contract NObs 25391.
** Present address, Cornell University, Ithaca, New York.
[1] Harris, McGinnies, and Siegel, J. Opt. Soc. Am. **38**, 582 (1948).
[2] E. K. Plyler and J. J. Ball, J. Opt. Soc. Am. **38**, 988 (1948).
[3] Harris, Jeffries, and Siegel, J. App. Phys. **19**, 791 (1948).
[4] R. Suhrmann and G. Barth, Zeits. f. Physik **103**, 133 (1936).
[5] R. Suhrmann and H. Schnackenberg, Zeits. f. Physik **119**, 287 (1942).
[6] H. B. Huntington and F. Seitz, Phys. Rev. **61**, 315 (1942).
[7] H. B. Huntington, Phys. Rev. **61**, 325 (1942).

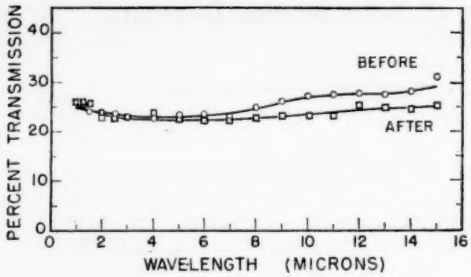

FIG. 1. Infra-red transmission before and after thermal stabilization.

stabilization. Particles made up of very small nuclei should give diffraction patterns with very broad diffuse rings which sharpen upon stabilization. In the case of non-equilibrium particles which are single crystallites with only an excess of lattice vacancies, the line breadth of the diffraction pattern from the fresh deposit should give a particle size correlating with the average diameter observed in the electron microscope, and this line breadth should not change with stabilization of the deposit. Line breadth measurements were made on the (111) diffraction line of gold using Cu radiation and a "Norelco" recording spectrometer. The natural line breadth for the setting of the slits used was 0.27° and a freshly prepared deposit gave a line breadth of 1.07°. Using the modification of the Debye-Scherrer formula given by Warren[8] the average particle size was found to be 120A which checks well within the range observed for such particles with the electron microscope. No sharpening of this line was observed after keeping the deposit at 62°C for a total of 27 hours during which time the resistance dropped to ~30 percent of its original value.

The excess vacant site lattice arrangement in the non-equilibrium particle is further substantiated by the low temperature coefficient of resistivity observed in gold smoke deposits. The temperature coefficient of resistivity has been measured between 70° and 25°C and found to be about 0.1 percent per degree C, or one-third that of massive gold. The effect of the excess vacant sites on the resistivity of the deposit will be discussed in detail further on, but since these vacant sites must act as scatterers of the conduction electrons, they should lower the temperature coefficient of resistivity in the same manner as foreign atoms in the lattice.

DIFFUSION OF VACANT SITES

The stabilization process by the diffusion of excess vacant sites to the surface of the particles can be derived if we restrict the calculations to spherical particles of uniform size in which the surfaces of equal concentration are concentric. The diffusion equation in spherical coordinates is

$$\frac{\partial C}{\partial t}=D\left(\frac{\partial^2 C}{\partial r^2}+\frac{2}{r}\frac{\partial C}{\partial r}\right) \tag{1}$$

where C is the excess concentration of vacant sites above the equilibrium concentration; D is the diffusion coefficient for vacant sites and is given by

$$D=\frac{N}{N+N'}\frac{\nu_s\delta^2}{6}\exp(-\epsilon/kT), \tag{2}$$

where δ is the lattice parameter and $(\nu_s/6)\exp(-\epsilon/kT)$ is the probability that a vacant site will change places with an atom. ν_s is the vibrational frequency of the lattice atoms and ϵ is the activation energy required for the passage of an atom from one site to an adjacent vacant site. If the ratio of the number of vacant sites, N', to the number of atoms, N, is small, as is generally the case, $N/(N+N')\simeq 1$.

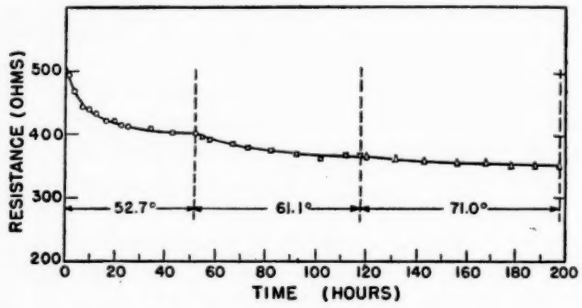

FIG. 2. Resistance change of a deposit at different temperatures.

Taking the boundary conditions as

1. $C=0$, at $r=a$, for all values of t (a represents the particle radius)
2. $C=$finite, at $r=0$, for all values of t
3. Uniform distribution of sites, C_0, at $t=0$,

the solution of Eq. (2) is

$$C=C_0\sum_{n=1}^{\infty}(-1)^{n+1}\frac{\frac{2a}{n\pi}\sin\left(\frac{n\pi}{a}r\right)}{r}\exp(-n^2\lambda t), \tag{3}$$

where

$$\lambda=(\nu_s/6)(\pi^2/a^2)\delta^2\exp(-\epsilon/kT). \tag{3a}$$

The ratio of the total number of vacant sites to the total number of atoms as a function of time is obtained by integrating C in Eq. (3) over the volume of the sphere.

$$\frac{N'-N_e'}{N}=4\pi\int_0^a Cr^2dr=4\pi C_0\int_0^a\sum_{n=1}^{\infty}(-1)^{n+1}\times\frac{2a}{n\pi}r\sin\left(\frac{n\pi}{a}r\right)\exp(-n^2\lambda t)dr. \tag{4}$$

If N_0' is the total number of vacant sites in the volume at $t=0$, and N_e' is the number at equilibrium, then the integration over the volume gives

$$\frac{N'-N_e'}{N_0'-N_e'}=A\sum_{n=1}^{\infty}\frac{1}{n^2}\exp(-n^2\lambda t), \tag{4a}$$

[8] B. E. Warren, Zeits. f. Krist. 99, 448 (1938).

where

$$A=\frac{1}{\sum_{n=1}^{\infty}(1/n^2)}=\frac{6}{\pi^2}.$$

At large t, only the first term in the series is significant and the relation reduces to

$$\ln\frac{N'-N_e'}{N_0'-N_e'}=-\lambda t+\ln A. \tag{4b}$$

MEASUREMENT OF RATE OF STABILIZATION

The stabilization process is characterized by a decrease in the electrical resistance of a deposit and this change in resistance is to be correlated with the change in the number of vacant sites. A vacant site will disrupt the periodicity of the lattice and will act as a scatterer of conducting electrons. If Q_v is the cross section of scattering by a vacant site, then in a particle of volume V with N' vacant sites, the mean-free path, L_v, for scattering by vacant sites is given by[9]

$$1/L_v=(N'Q_v/V). \tag{5}$$

Since electrical resistance is inversely proportional to the mean-free path of the conducting electrons there will be a resistance, R', associated with the presence of vacant sites, which is directly proportional to the number of vacant sites, and if R_0' is this resistance at $t=0$

$$R'/R_0'=N'/N_0' \tag{6}$$

or, in terms of the differences from the equilibrium resistance, R_e', associated with the number of vacant sites at equilibrium,

$$\frac{R'-R_e'}{R_0'-R_e'}=\frac{N'-N_e'}{N_0'-N_e'}. \tag{7}$$

It can be shown that the total resistance of a deposit at time t is given by

$$R_t=R'+R_c, \tag{8}$$

where R_c is the normal resistance due to the thermal motion of the atoms and is thus time-independent. After stabilization the resistance of a smoke deposit will be

$$R_\infty=R_c+R_e', \tag{9}$$

and the change in the number of vacant sites can thus be related to the measured resistance by

$$\frac{N'-N_e'}{N_0'-N_e'}=\frac{R'-R_e'}{R_0'-R_e'}=\frac{R_t-R_\infty}{R_0-R_\infty}. \tag{10}$$

From Eq. (4a)

$$\frac{R_t-R_\infty}{R_0-R_\infty}=A\sum_{n=1}^{\infty}\frac{1}{n^2}\exp(-n^2\lambda t) \tag{11}$$

and at large t

$$\ln\frac{R_t-R_\infty}{R_0-R_\infty}=-\lambda t+\ln A. \tag{12}$$

EXPERIMENTS ON STABILIZATION OF DEPOSITS

Deposits weighing 50 to 100×10^{-6} grams/cm², with mean particle diameter between 200 and 300A, were prepared. These deposits showed a decrease in resistance to as low as twenty percent of their original value when heated to less than 80°C and showed only a small decrease in transmission for wave-lengths greater than 5μ and no measurable change in reflectivity. The infrared transmission before and after heating a deposit of gold-black on rock salt at 67.5°C for 18 hours is shown in Fig. 1. The resistance of this deposit decreased to 27 percent of its original value after the heat treatment.

Figure 2 shows the change of total resistance at three temperatures for a gold smoke deposited at a moderate rate, in an atmosphere of nitrogen (pressure 3 mm of mercury) on a glass slide ~0.2 mm thick. The slide was placed inside a massive metal block maintained to within ±0.2°C during the experiment. The resistances were recorded continuously.

In Fig. 3 are shown, as encircled points, values of $(R_t-R_\infty)/(R_0-R_\infty)$ at different values of t, as calculated from the data of Fig. 2, and using the R_∞ value corrected for temperature. R_∞ was taken as the resistance of a deposit that had been maintained at 72°C for at least 100 hours. (Heating at 80°C produced no further change in resistance.) λ and A were determined by successive approximations so that Eq. (11) gave a curve which best fitted the experimental points. The calculated curves are shown by the solid lines in Fig. 3; the dashed lines represent the limiting Eq. (12). The initial time for the 61.1°C calculated curve was obtained from the relation $(\lambda t)_{52.7°C}=(\lambda t)_{61.1°C}$, so that 52 hours at 52.7° is equivalent to 19.3 hours at 61.1°.

The average of the observed values for A is 0.38; according to Eq. (4a), $A=6/\pi^2=0.61$. The observed

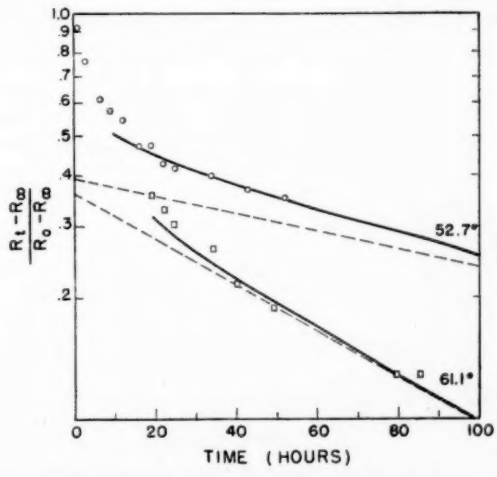

FIG. 3. $(R_t-R_\infty)/(R_0-R_\infty)$ *versus* time.

[9] F. Seitz, *Modern Theory of Solids* (McGraw-Hill Book Company, Inc., New York, 1940), pp. 541.

TABLE I. Values of λ, sec.$^{-1}$, and ϵ, kcal./g atom, at different temperatures for three different smoke deposits.

Deposit	Atmosphere	λ's sec.$^{-1}$		ϵ kcal./g atom
#11 *B*	3 mm Nitrogen	$\lambda_{52.7°C}=.180\times10^{-5}$	$\lambda_{61.1°C}=.450\times10^{-5}$	23.8
12 *A*	3 mm Nitrogen	$\lambda_{52.7°C}=.170\times10^{-5}$	$\lambda_{61.1°C}=.400\times10^{-5}$	22.2
10 *C*	4 mm Helium	$\lambda_{50.4°C}=.133\times10^{-5}$	$\lambda_{60.1°C}=.396\times10^{-5}$	24.2
10 *C*	4 mm Helium	$\lambda_{60.1°C}=.396\times10^{-5}$	$\lambda_{70.8°C}=1.24\times10^{-5}$	24.3
10 *C*	4 mm Helium	$\lambda_{50.4°C}=.133\times10^{-5}$	$\lambda_{70.8°C}=1.24\times10^{-5}$	23.5
			Mean	23.5 kcal./g atom.

discrepancy may be due to non-uniform concentration of vacant sites at t_0.

The calculated values of $(R_t-R_\infty)/(R_0-R_\infty)$ for small values of t were, in most cases, less than the observed values. This discrepancy may be attributed to a non-uniform initial distribution of vacant sites or to a particle size distribution which has been neglected in the derivation of Eq. (3).

EVALUATION OF THE ACTIVATION ENERGY, ϵ

The energy ϵ necessary to permit an atom to move from a lattice site to an adjacent vacant site can be evaluated from the λ-values at two temperatures since from Eq. (3a) we have the relation

$$\epsilon=\frac{T_1T_2}{T_2-T_1}R\ln(\lambda_1/\lambda_2). \tag{13}$$

Measurements on many deposits showed considerable variation in the value of λ from deposit to deposit in spite of all attempts to prepare them under the same conditions. Therefore to obtain values of ϵ from Eq. (12), λ_1 and λ_2 must be obtained on the same deposit measured at different temperatures. An example of such a measurement has already been shown in Figs. 2 and 3. In Table I are listed some pairs of λ's which have been obtained on typical deposits. The mean value of the activation energy ϵ was found to be 23.5 kcal./g atom.

THE SINTERING OF GOLD SMOKE DEPOSITS

The electron microscope observations show the particles of gold smoke in contact with each other, forming loose aggregates which make up a spongy structure. When a deposit is heated sufficiently above the temperature at which only the stabilization of individual particles occurs, there is a continued decrease in the resistance of the deposit and at the same time a pronounced change in its optical characteristics. We attribute this change to sintering due to the coalescence of the particles. It has been found that the minimum temperature and time required to sinter a given deposit depend first on the particle size in the deposit (determined by the conditions of preparation), and second, on the thermal history of the specimen.

Fresh deposits of gold smoke, prepared at low pressures and low rates of evaporation, have a very small particle size (mean diameter 15–40A),[3] and such deposits sinter at temperatures as low as 40–50°C. A typical example is a specimen prepared in 0.4 mm of nitrogen at a slow rate. The infra-red reflectance increased from 19 percent to 52 percent during a 40-hour treatment at 50°C.

Deposits prepared under conditions producing large particles (mean diameter 100–200A) show negligible sintering below 80°C (the stabilization process which occurs has already been described). At temperatures above ~100°C, however, behavior of these deposits depends to a great extent on the degree of previous stabilization. Figure 4 shows the change of infra-red reflectance at 150° for two similarly prepared deposits: *A* was freshly made whereas *B* was thoroughly stabilized.

Above 175° stabilized deposits show appreciable sintering within a few hours. Figure 5 shows the change of infra-red reflectance *versus* time at three temperatures for similarly prepared and stabilized deposits.

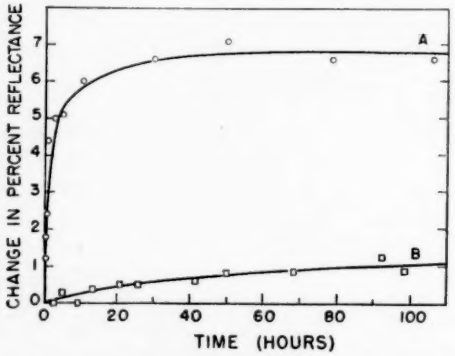

FIG. 4. Reflectance change at 150°C for a stabilized (*B*) and an unstabilized (*A*) deposit.

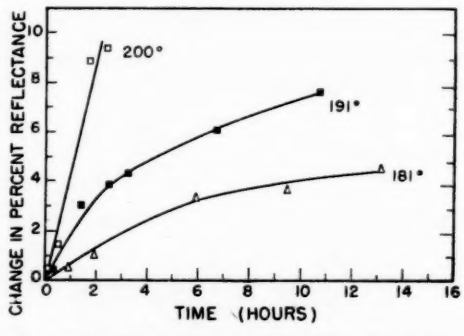

FIG. 5. Reflectance change at high temperature for stabilized deposits.

DISCUSSION

It would be of considerable interest to obtain a value of the energy involved in the sintering process. This process in which the spheroidal particles coalesce undoubtedly proceeds by a process of self-diffusion.[10] ϵ'', the energy required for self-diffusion by the vacancy mechanism in a crystalline lattice, is equal to the sum of ϵ' and ϵ, where ϵ' is the energy required to move an atom from an interior lattice site to the surface, and ϵ is the activation energy required for an atom to move from one site in the lattice to an adjacent vacant site. ϵ' would thus be given by the difference in ϵ'' and ϵ. Also since the equilibrium ratio of the number of vacant sites to the total number of atoms is

$$N_e'/N \simeq \exp(-\epsilon'/kT) \qquad (14)$$

a knowledge of the magnitude of ϵ' would permit calculation of the equilibrium number of vacant sites.

Unfortunately, it has not been possible to relate satisfactorily the change in resistance or reflectance observed during the sintering process to any mechanism involving the coalescence of the particles.

If ϵ has the same value for massive gold as for gold smoke, then ϵ' for massive gold would be 27.5 kcal./g atom, since ϵ'' for massive gold is 51 kcal./g atom.[11] This value of ϵ' is to be compared with the value of 28 kcal./g atom, calculated by Huntington[6] for the energy required to move a copper atom from an interior site to the surface. The energies for the copper lattice should be somewhat higher than for gold since the measured value of self-diffusion in copper is 57 kcal./g atom.[12] For gold smoke, however, ϵ' must be considerably smaller than 27.5 kcal./g atom in order to account for the rapid changes observed at temperatures below 200°C. When a smoke deposit is stabilized by heating below 80°C, the number of vacant sites is decreased and ϵ' is increased correspondingly. The difference in behavior above 100°C, shown in Fig. 4 at 150°C, between an untreated and a stabilized deposit indicates that the increase in energy required for the process after stabilization is probably of the order of magnitude of 5 to 10 kcal./g atom.

ACKNOWLEDGMENTS

We are indebted to Mr. John K. Beasley for many helpful discussions during the course of this investigation, and to Professor John T. Norton for the x-ray studies.

[10] J. Frenkel, J. Phys. U.S.S.R. **9**, 385 (1945).

[11] H. McKay, Trans. Faraday Soc. **34**, 845 (1938).

[12] Steigman, Shockley, and Nix, Phys. Rev. **56**, 13 (1939).

THE JOURNAL OF CHEMICAL PHYSICS VOLUME 18, NUMBER 3 MARCH, 1950

Some Studies in Molecular Orbital Theory

I. Resonance Structures and Molecular Orbitals in Unsaturated Hydrocarbons*

H. C. LONGUET-HIGGINS
Department of Physics, University of Chicago,† Chicago, Illinois

(Received June 13, 1949)

The predictions of qualitative resonance theory, as to the electronic structures of unsaturated hydrocarbons, are analyzed in terms of LCAO molecular orbital theory. The following results are proved for "alternant" hydrocarbons, that is, hydrocarbons containing no odd-membered unsaturated rings:

(1) The number of unpaired electrons present in the ground state is at least as great as the number of carbon atoms having a deficiency of valence bonds in any principal resonance structure.

(2) With a few special exceptions, these odd electrons are distributed over just those atoms which have a deficiency of valence bonds in one or more of the principal resonance structures.

(3) In singly charged hydrocarbon anions or cations the ionic charge is located on just those atoms which bear charges in the various principal resonance structures.

It follows that enumeration of the principal resonance structures of a hydrocarbon molecule or ion gives much valuable information as to its electronic structure; and in particular, an alternant hydrocarbon possessing no normal Kekulé-type structure must have a paramagnetic ground state, and behave as a radical or multiradical.

These results do not depend on the neglect of overlap, or the assumption of a constant carbon-carbon resonance integral.

1. NOTATION

THE following is a summary of the notation used in this paper:

ϕ_t, ϕ_u are $2p$ atomic orbitals (AO) on the carbon atoms t, u.
N is the number of such AO.
T is the maximum number of double bonds (a triple bond being counted as two double bonds) occurring in any resonance structure.
ψ is a molecular orbital (MO) of form $\Sigma_t c_t\phi_t$; its binding energy is ϵ.
r is any "starred" carbon atom in an alternant hydrocarbon.
s is any "unstarred" carbon atom.
μ is any "active" carbon atom.
ν is any "normal" carbon atom.
R is the total number of starred atoms.

* Work done under ONR, Task Order IX of Contract N6ori-20, with the University of Chicago.

† Now at the Department of Chemistry, Manchester University, Manchester, England.

N_μ is the total number of active atoms.
N_ν is the total number of normal atoms.
R_ν is the number of normal starred atoms r_ν.
S_ν is the number of normal unstarred atoms s_ν.
A is the matrix formed by the resonance integrals β_{tu}.
A_μ is the matrix formed by the resonance integrals $\beta_{t\mu}$.
B is the matrix formed by the resonance integrals β_{rs}.
B_μ is the matrix formed by the resonance integrals β_{rs_μ}.
B_ν is the matrix formed by the resonance integrals β_{rs_ν}.
C is the matrix formed by the resonance integrals β_{sr}.
C_μ is the matrix formed by the resonance integrals β_{sr_μ}.
U is the rank of A.
U_μ is the rank of A_μ.
$\Pi^P\beta_{rs}$, $\Pi^Q\beta_{sr}$, $\Pi^{P_\mu}\beta_{rs_\mu}$, $\Pi^{Q_\mu}\beta_{sr_\mu}$, are products of P, Q, P_μ, Q_μ finite terms from different rows and columns of B, C, B_μ, C_μ.

2. INTRODUCTION

Because of their great simplicity and appeal to intuition, classical valence structures will probably long continue to be used for the description of molecules in the ground state. For this reason it is important to examine theoretically the various empirical rules which are used for correlating the properties of molecules with their classical valence structures.

An outstanding question in this connection is the following: Why are there relatively few stable molecules for which it is impossible to write some classical valence structure? This is perhaps the most fundamental problem in structural chemistry, and still awaits complete solution. In this paper it will be shown that the question can be answered more or less completely for unsaturated hydrocarbons containing no odd-membered rings, and that the answer throws much light on the theory of hydrocarbon free radicals and ions.

3. NOMENCLATURE

Before discussing the problem in detail, it is necessary to establish an unambiguous nomenclature.

For simplicity we shall restrict attention at first to unsaturated hydrocarbons in which all the carbon and hydrogen atoms lie in one plane, every carbon atom being of the sp^2-type, bonded to three other atoms. From this class we shall further select (for reasons that will appear shortly) those hydrocarbons which contain no odd-membered rings; and these will be referred to as *alternant hydrocarbons*.[1] According to this definition benzene, naphthalene, butadiene, and cyclobutadiene are alternant hydrocarbons, and so are most known planar hydrocarbons, but azulene and fulvene are not alternant.

(I)

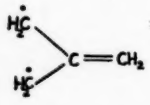

(II)

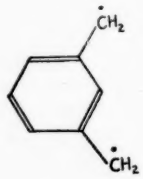

(III)

[1] See C. A. Coulson and H. C. Longuet-Higgins, Proc. Roy. Soc. A192, 16 (1947).

If hyperconjugation is neglected, an alternant hydrocarbon may have two kinds of resonance structure, namely (i) Kekulé-type or *K-structures*, in which each hydrogen atom is attached by a single bond to the adjacent carbon atom, and each carbon atom is involved in three single bonds and one double bond, and (ii) excited or *E-structures*, in which at least one carbon atom is joined to its three neighbors by single bonds only.

According to this nomenclature, benzene has two K-structures and several E-structures, whereas triphenylmethyl and the allyl radical have only E-structures. In the general case, an alternant hydrocarbon will have K-structures if and only if $N=2T$, where N is the number of carbon atoms in the molecule and T is the maximum number of double bonds occurring in any resonance structure. This is because in a K-structure each carbon atom is involved in one double bond, and each double bond links two carbon atoms.

Those resonance structures which contain the greatest possible number, T, of double bonds will be described as *principal resonance structures*. In benzene ($T=3$, $N=6$) the principal resonance structures are just the two Kekulé structures, whereas in the allyl radical the principal resonance structures are of the E-type, namely,

$$\dot{C}H_2-CH=CH_2 \quad \text{and} \quad CH_2=CH-\dot{C}H_2.$$

A further concept will be found useful later on. Carbon atoms which are doubly bonded in *all* the principal resonance structures will be described as *normal* carbon atoms, and all others will be described as *active* carbon atoms, to anticipate later results. Thus in benzene, all the carbon atoms are normal, whereas in allyl the two terminal atoms are active.

4. SCOPE OF THIS PAPER

The first problem to be discussed may now be formulated as follows: Why are alternant hydrocarbons with no K-structures so rarely stable? Consider, for example, the hydrocarbons (I), (II), and (III), none of which has hitherto been prepared. The only anomaly in their structures is the fact that they have no K-structures; each one has an unstrained skeleton of σ-bonds and an even number of π-electrons. Clar,[2] who first drew attention to molecule (I), supposed that it would be impossible to prepare because of having no Kekulé structures. As far as the author is aware, the attempt has not been made, and it would be of great interest to know the outcome; but (II) and (III), at any rate, are almost certainly unstable, according to the experimental evidence. The question is, why?

In approaching this problem theoretically, either the valence bond method or the method of molecular orbitals might be used. Superficially, the following answer, in

[2] E. Clar, *Aromatische Kohlenwasserstoffe* (Verlag. Julius Springer, Berlin, 1941), p. 311.

FIG. 1.

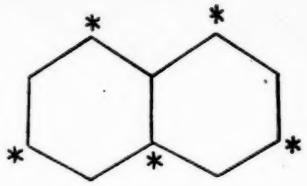

terms of the valence bond method, might appear plausible:

It is known that in benzene most of the resonance energy arises from the K-structures, the E-structures being relatively unimportant. One might therefore expect that in (I), where there are no K-structures, the resonance energy would be considerably reduced, and that this molecule would be relatively unstable. However, calculations by the French school[3] show that as a molecule becomes bigger the contribution of K-structures to its ground state becomes less and less significant; and that even in molecules the size of anthracene almost all the resonance energy arises from E-structures.

The breakdown of this argument suggests that the valence bond method is not a very promising approach to the problem in hand; so the molecular orbital method has been used as a basis for discussion, in spite of the apparent lack of connection between resonance structures and molecular orbitals. As will be seen, it can be proved by MO theory (i) that an alternant hydrocarbon must have at least $N-2T$ unpaired electrons in its ground state, and (ii) that of these, at least $N-2T$ will be distributed over the active carbon atoms only, in the sense of Section 3. It follows that any diamagnetic alternant hydrocarbon must have $N=2T$, and must therefore possess at least one K-structure. In view of the fact that paramagnetic molecules usually behave as free radicals, these results provide a theoretical explanation for the rarity of stable alternant hydrocarbons possessing no Kekulé-type structures.

5. BASIS OF ARGUMENT

In discussing the electron configuration of an unsaturated hydrocarbon, it is usual to begin by dividing the electrons into two classes, σ and π. In the ground state the σ-electrons will form a closed shell since their orbitals have lower energy than the upper π-orbitals; and any unpaired electrons which may be present in the ground state will tend to occupy π-orbitals. The σ-electrons will therefore be ignored in the following discussion.

In determining the configuration of the π-electrons, each π-orbital is expressed as a linear combination of atomic orbitals of the correct symmetry. In this approximation (LCAO approximation) the total number of π-molecular orbitals in a hydrocarbon equals the total number of π-electrons, since both are equal to the number of available carbon $2p$ atomic orbitals.

There is one particular kind of unsaturated hydrocarbon in which the π-orbitals are distributed in a specially simple way, namely, the alternant hydrocarbons defined earlier. It has been shown[4] that in an alternant hydrocarbon the π-molecular orbitals of non-zero binding energy occur in pairs with opposite energies; for example, in benzene the orbital energies are $\pm 2\beta$, $\pm\beta$, $\pm\beta$. In an alternant hydrocarbon with N carbon atoms, there will be N π-electrons and N π-molecular orbitals, in LCAO approximation. Therefore, if there are M π-orbitals of negative energy, there will be $N-2M$ π-orbitals of zero energy. In the ground state the electrons tend to occupy the orbitals of lowest energy, so as a rule each MO of negative energy will contain two electrons with opposed spins, leaving $N-2M$ to be distributed among the $N-2M$ orbitals of zero energy. By Hund's rule, the most stable configuration is that with the highest multiplicity; so in the ground state there will be just one electron in each zero-energy molecular orbital. The number of unpaired electrons in an alternant hydrocarbon therefore equals the number of π-molecular orbitals of zero energy.

There is one loophole in the above argument. It is possible that there may be a pair of MO with binding energies $+\epsilon$ and $-\epsilon$, where ϵ is very small but not equal to zero. In such cases an electron will overflow from the lower into the upper MO if the exchange integral between the two is numerically greater than 2ϵ. Thus in the ground state there may be more unpaired electrons than indicated in the last paragraph. However, the following discussion is mainly concerned with finding a lower limit to the number of unpaired electrons, so this possibility does not matter.

6. MOLECULAR ORBITALS IN AN ALTERNANT HYDROCARBON

The electronic structures of alternant hydrocarbons have been studied by Coulson and Rushbrooke,[4] and by Coulson and Longuet-Higgins.[1] The distinguishing feature of an alternant hydrocarbon is that its sp^2 carbon atoms can be divided into two sets, such that no two carbon atoms in the same set have their $2p$ orbitals overlapping. This is illustrated by naphthalene in Fig. 1, where the carbon atoms of one set have been marked with stars, and the unstarred ones constitute those of the other set. This classification into "starred" and "unstarred" atoms has nothing to do with our earlier classification of carbon atoms into "normal" and "active;" thus all the carbon atoms in naphthalene are normal, but only half (which half does not matter) are starred.

Let us label the $2p$ orbitals of the starred atoms ϕ_1 to ϕ_R, and those of the unstarred atoms ϕ_{R+1} to ϕ_N. If the π-orbitals are now expressed in the form

$$\psi=\sum_{i=1}^{N} c_i\phi_i, \qquad (1)$$

then the secular equations for the binding energy ϵ and

[3] A. and B. Pullman, Rev. Sci. Inst. 84, 145 (1946).

[4] C. A. Coulson and S. Rushbrooke, Proc. Camb. Phil. Soc. 36, 193 (1940).

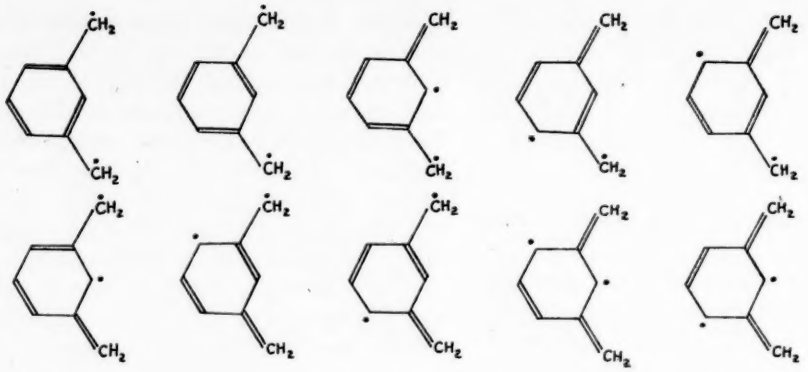

FIG. 2.

the coefficients c_i^r fall into two sets, namely,

$$-\epsilon c_r+\sum_{s=R+1}^{N}\beta_{rs}c_s=0, \quad r=1, 2, \cdots, R \tag{2}$$

and

$$-\epsilon c_s+\sum_{r=1}^{R}\beta_{sr}c_r=0, \quad s=R+1, \cdots, N. \tag{3}$$

These two sets of equations correspond to the two sets of atomic orbitals, those of the starred atoms being denoted collectively by ϕ_r, and those of the unstarred atoms by ϕ_s. It can now easily be seen why the MO of non-zero energy occur in pairs with opposite energies. For if $\epsilon=\epsilon^j\neq 0$, $c_r=c_r{}^j$, $c_s=c_s{}^j$ is a solution of (2) and (3), then $\epsilon=-\epsilon^j\neq\epsilon^j$, $c_r=c_r{}^j$, $c_s=-c_s{}^j$ is also a solution, distinct from the first.

As for the MO of zero energy, these are obtained by solving Eqs. (4) and (5), obtained by putting $\epsilon=0$ in (2) and (3).

$$\sum_{s=R+1}^{N}\beta_{rs}c_s=0, \quad r=1, 2, \cdots, R, \tag{4}$$

$$\sum_{r=1}^{R}\beta_{sr}c_r=0, \quad s=R+1, \cdots, N. \tag{5}$$

The number of zero-energy MO equals the number of linearly independent solutions of (4) and (5); and this is given[5] by $N-U$, where U is the rank of the matrix A in Eq. (6). The rank of a matrix is said to be U if all its minors of order $U+1$ or greater have vanishing determinants, while there is at least one minor of order U whose determinant does not vanish. An upper limit for the rank of A may be obtained as follows:

$$A=\begin{bmatrix} 0 & B \\ C & 0 \end{bmatrix}=\left[\begin{array}{ccc|ccc} 0, & \cdots, & 0 & \beta_{1,R+1}, & \cdots, & \beta_{1,N} \\ \vdots & & \vdots & \vdots & & \vdots \\ 0, & \cdots, & 0 & \beta_{R,R+1}, & \cdots, & \beta_{R,N} \\ \hline \beta_{R+1,1}, & \cdots, & \beta_{R+1,R} & 0, & \cdots, & 0 \\ \vdots & & \vdots & \vdots & & \vdots \\ \beta_{N,1}, & \cdots, & \beta_{N,R} & 0, & \cdots, & 0 \end{array}\right]. \tag{6}$$

Consider a typical non-vanishing term in the expansion of any one of the minors of A. Such a term will be of the form (7)

$$\pm\Pi^P\beta_{rs}\Pi^Q\beta_{sr}, \tag{7}$$

where $\Pi^P\beta_{rs}$ represents a product of P non-vanishing terms from B, and $\Pi^Q\beta_{sr}$ is a product of Q factors from C. Neither r nor s can take the same value more than once in either product; furthermore, each factor β_{rs} or β_{sr} must correspond to a pair of adjacent atomic orbitals ϕ_r and ϕ_s, or (7) would vanish. Therefore if the P pairs of atoms represented in $\Pi^P\beta_{rs}$ are joined by formal double bonds, we obtain a possible resonance structure for the molecule, and similarly for $\Pi^Q\beta_{sr}$. Conversely, any permissible resonance structure containing P double bonds defines a P-fold product of elements from B (or C), such that no two elements lie in the same row or column. Now T was defined as the maximum number of double bonds occurring in any resonance structure.

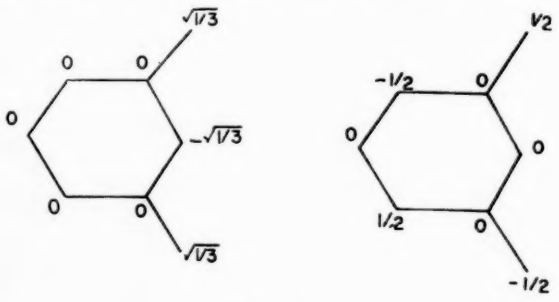

FIG. 3.

[5] See, for instance, H. A. Bôcher, *Higher Algebra* (The Macmillan Company, New York, 1922).

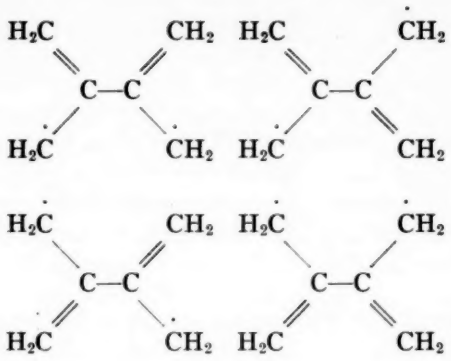

FIG. 4.

Therefore neither P nor Q can exceed T, and so the number of factors in (7) cannot exceed $2T$. Therefore A has no non-vanishing minors of order greater than $2T$, and the rank of A cannot exceed $2T$. Hence there are at least $N-2T$ MO of zero energy.

This proves our first result, namely, that the number of unpaired electrons in the ground state of an alternant hydrocarbon is not less than $N-2T$; this being just the number of carbon atoms without double bonds in any principal resonance structure.

In the important case that the number R of starred atoms is not equal to the number $N-R$ of unstarred atoms, it can simply be shown that $N-2T$ is not less than the difference between these numbers. Suppose, without loss of generality, that R exceeds $N-R$. Then T is not greater than $N-R$, since any double bond must join a starred atom to an unstarred atom. Therefore $N-2T$ is not less than $N-2(N-R)=R-(N-R)$. From this result it can be seen at once that all the molecules (I), (II), and (III) contain not fewer than two unpaired electrons each.

7. EXAMPLES

(1) The hypothetical molecule *m*-phenylene-dimethylene (III) has no K-structures; its principal resonance structures are shown in Fig. 2. The dots denote π-electrons with unspecified spin functions. For this molecule $N=8$, $T=3$, so there must be at least two MO of zero energy, each containing one unpaired electron in the ground state. It turns out that there are just two such MO, and Fig. 3 gives their AO coefficients c_t, normalized to unity.

(2) The molecule tetramethylene-ethylene (IV) would have $N=6$, $T=2$; its principal resonance structures are shown in Fig. 4. Each of these structures has just two carbon atoms which lack double bonds, and there are in fact exactly two zero-energy MO, with coefficients shown in Fig. 5.

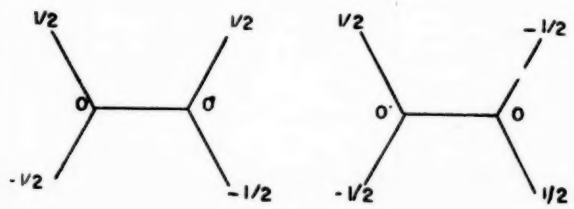

FIG. 5.

(3) Clar's hydrocarbon (III) has $N=22$, and it is quite easily verified that this molecule has no resonance structures with more than 10 double bonds. Therefore there must be at least $22-20=2$ MO of zero energy, each containing one unpaired electron in the ground state. Hence, if it could be prepared, this molecule would be paramagnetic, having the character of a biradical. The AO coefficients for the two MO of zero energy are given in Fig. 6. Any two orthonormal combinations of these would, of course, do equally well.

(4) Cyclobutadiene (V), for which $N=4$, has two K-structures, each having two double bonds, so $N=2T$, and no conclusion can be drawn as to its number of zero-energy MO. Calculation shows that in fact this molecule has two zero-energy MO, with AO coefficients as shown in Fig. 7.

This last example shows that the absence of K-structures in an alternant hydrocarbon is a sufficient but not a necessary condition for the molecule to be paramagnetic in the ground state. This is an important point to be borne in mind when free radical character is being discussed from the point of view of qualitative resonance theory.

8. FORM OF THE ZERO-ENERGY MOLECULAR ORBITALS

In the above examples there is one point which is immediately striking, namely, that in three of the four examples quoted, the AO coefficients in the zero-energy MO vanish at the normal carbon atoms, in the sense of Section 2. In other words, according to MO theory, the unpaired electrons in these molecules are associated with just those carbon atoms at which, from the principal resonance structures, one would expect them to be located. This fact was noted as a curiosity by Coulson and Longuet-Higgins[1] for the particular case of the benzyl radical, but there seemed no obvious reason why it should be true in general.

We shall now show, as an extension of what has already been proved, that if N and T have their usual meanings, then any alternant hydrocarbon has at least $N-2T$ zero-energy MO of the form (8)

$$\psi=\sum_{\mu} c_{\mu}\phi_{\mu}, \tag{8}$$

where μ denotes an active carbon atom.

Since the active carbon atoms are by definition those which are not normal any MO can certainly be written in the form (9),

$$\psi=\sum_{\mu} c_{\mu}\phi_{\mu}+\sum_{\nu} c_{\nu}\phi_{\nu}, \tag{9}$$

where ν refers to a normal carbon atom. Therefore it will be sufficient to prove that there are at least $N-2T$ zero-

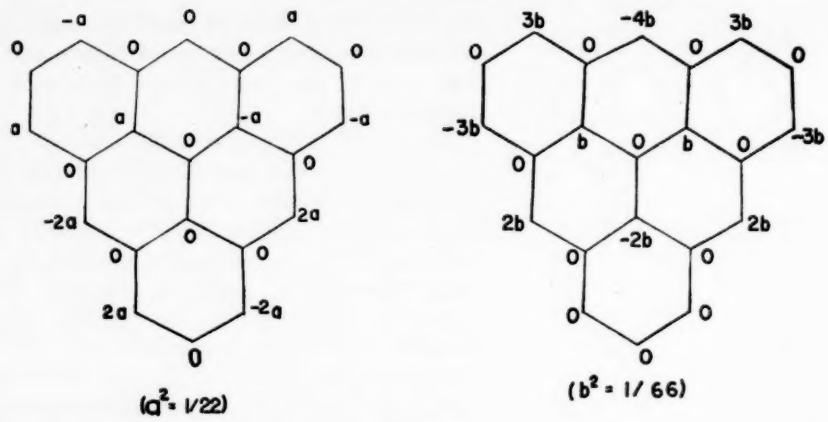

FIG. 6.

energy MO satisfying the condition that $c_\nu=0$ for every normal carbon atom. Inserting this condition into Eqs. (4) and (5), we obtain (10) and (11),

$$\sum_{s_\mu} \beta_{rs_\mu} c_{s_\mu}=0, \quad r=1, 2, \cdots, R \tag{10}$$

$$\sum_{r_\mu} \beta_{sr_\mu} c_{r_\mu}=0, \quad s=R+1, \cdots, N \tag{11}$$

where r_μ, s_μ denote active carbon atoms in the starred and unstarred sets, respectively. The matrix A_μ of the β's in Eqs. (10) and (11) may be written in the form (12),

$$A_\mu=\begin{bmatrix} 0 & B_\mu \\ C_\mu & 0 \end{bmatrix}, \tag{12}$$

where B_μ and C_μ are obtained from B and C by striking out those columns which correspond to the normal carbon atoms. A_μ is therefore an N by N_μ matrix, N_μ being the total number of active carbon atoms; and the number of zero-energy MO of form (8) equals $N_\mu-U_\mu$ where U_μ is the rank of A_μ.

An upper limit may be obtained from U_μ by considering a typical non-vanishing term in the expansion of any minor of A_μ. Such a term will be of the form (13),

$$\pm\Pi^{P_\mu}\beta_{rs_\mu}\Pi^{Q_\mu}\beta_{sr_\mu}, \tag{13}$$

where $\Pi^{P_\mu}\beta_{rs_\mu}$ is a product of P_μ terms from B_μ, and $\Pi^{Q_\mu}\beta_{sr_\mu}$ is a product of Q_μ terms from C_μ. In the next section it will be proved that $P_\mu\leqslant T-S_\nu$, $Q_\mu\leqslant T-R_\nu$, where R_ν and S_ν are the numbers of normal carbon atoms in the starred and unstarred sets, respectively. Taking this for granted, it follows that no non-vanishing term in the expansion of a minor of A can contain more than $2T-S_\nu-R_\nu=2T-N_\nu$ factors, where N_ν is the total number of normal carbon atoms. Hence U_μ cannot exceed $2T-N_\nu$, and the number of zero-energy MO of the form $\sum_\mu c_\mu\phi_\mu$ cannot be less than $N_\mu-(2T-N_\nu)$ $=N-2T$. This is the required result.

A zero-energy MO which is not of this form will be called a *supernumerary* zero-energy MO, and in this sense the zero-energy MO in cyclobutadiene are supernumerary.

9. PROOF THAT $P_\mu\leqslant T-S_\nu$

We shall now show that if $P_\mu>T-S_\nu$, it must be possible to construct a principal resonance structure in which not all the normal carbon atoms are doubly bonded.

We first introduce the idea of a "zigzag." Denote the product $\Pi^{P_\mu}\beta_{rs_\mu}$ by E_1; and denote by E_0 any product of T elements from B corresponding to the double bonds in a principal resonance structure. Then the factors of E_0 and E_1 are grouped into sets such that (a) a factor of E_0 and a factor of E_1 lie in the same set if they lie in the same row or in the same column, or are identical; (b) the number of elements in each set is a minimum, subject to condition (a). These sets are appropriately called zigzags, and have the following properties:

(i) Every element of E_0 or E_1 lies in exactly one zigzag, if it is allowed that a zigzag may consist of one element only.

(ii) The numbers of elements of E_0 and E_1 in a given zigzag cannot differ by more than one, since such elements occur alternately in the zigzag.

(iii) No two separate zigzags can contain elements in the same row or column.

Now E_0 has T factors, and E_1 has $P_\mu(\leqslant T)$; therefore by (ii) there must be $T-P_\mu$ zigzags ζ', or more, containing one more element of E_0 than of E_1. Define E_2 as the product of those elements of E_0 which lie in the zigzags ζ' with those elements of E_1 which lie in all the other zigzags ζ''.

By taking the elements of E_0 rather than those of E_1 from the zigzags ζ', we have made the number of factors of E_2 greater by $T-P_\mu$ than the number of factors of E_1. Therefore the total number of factors in E_2 is P_μ $+(T-P_\mu)$, $=T$. Further, since the zigzags ζ' and ζ'' span different rows and columns, E_2 cannot contain

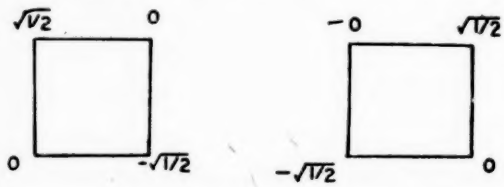

FIG. 7.

more than one element in any row or column. E_2 therefore corresponds to a principal resonance structure.

Denote by B_ν the S_ν columns of B which correspond to normal carbon atoms, these being excluded from B_μ. Then E_1 contains no factors in B_ν, and all those factors of E_2 lying in B_ν must be derived from E_0. But all such factors occur in the $T-P_\mu$ zigzags ζ', and no zigzag can have more than one element in B_ν. Therefore E_2 cannot have more than $T-P_\mu$ elements in B_ν. But by hypothesis $P_\mu > T-S_\nu$: that is, $T+P_\mu < S_\nu$; so at least one column of B_ν contains no factor of E_2.

Hence E_2 corresponds to a principal resonance structure in which at least one normal carbon atom is not doubly bonded; and this is absurd. It follows, by *reductio ad absurdum*, that $P_\mu \leqslant T-S_\nu$; and it can similarly be shown that $Q_\nu \leqslant T-R_\nu$.

10. SUMMARY OF RESULTS

The results so far obtained are:

(1) In LCAO approximation an alternant hydrocarbon has at least $N-2T$ π-molecular orbitals of zero energy, this being the number of carbon atoms (if any) lacking double bonds in any given principal resonance structure.

(2) At least $N-2T$ of these zero-energy MO are of the form $\sum_\mu c_\mu \phi_\mu$, the summation being confined to those carbon atoms which lack a double bond in one or more principal resonance structures.

(3) In the ground state there will be just one electron in each MO of zero energy, and if there are two or more such electrons, their spins will be parallel.

In proving these results it has not been assumed that the carbon-carbon resonance integral has the same value for all bonds. On the other hand, overlap has been neglected, and all the carbon atoms have been assumed to be in the (sp^2, p) state of hybridization. It will now be shown that neither of these latter assumptions is necessary to the validity of the results.

11. INCLUSION OF OVERLAP

If overlap is taken into account, the secular equations for the π-molecular orbitals take the form (14),

$$(\alpha-E)c_t+\sum_{u\neq t}(\beta_{tu}-S_{tu}E)c_u=0, \qquad (14)$$

where α is the Coulomb integral for a carbon atomic $2p$ orbital (assumed constant), E is the absolute energy of an electron in the molecular orbital, and S_{tu} is the overlap integral between ϕ_t and ϕ_u.

If it is assumed‡ that

$$S_{tu}=k\beta_{tu}, \qquad (15)$$

where k is the same for all the bonds tu, then (14) may be written

$$-\epsilon c_t+\sum_{u\neq t}\beta_{tu}c_u=0, \qquad (16)$$

where now ϵ is understood to mean the quantity $(E-\alpha)/(1-kE)$. It follows that the "true" binding energy $E-\alpha$ of a MO is given by the expression $\epsilon(1-k\alpha)/(1+k\epsilon)$, where ϵ is the "apparent" binding energy, calculated on the assumption that $S_{tu}=0$. Hence the sign of $E-\alpha$ is the same as that of ϵ, and the numbers of MO of positive, zero, and negative binding energy are correctly given by the secular equations in which overlap is formally neglected.

Equations (16) show that the ratio of the coefficients c_t is not affected by the inclusion of overlap, although the absolute values of c_t will in general depend on S_{tu} because of the normalization condition

$$\sum_t\sum_u c_t S_{tu} c_u=1.$$

Hence any molecular orbital which vanishes at the normal carbon atoms when overlap is neglected will still do so when overlap is taken into account; and result (2) of the last section remains true.

12. EXTENSION TO MORE COMPLEX HYDROCARBONS

It is possible to extend the results of Section 10 to hydrocarbons containing sp^3 and sp carbon atoms, provided due account is taken of geometrical considerations. If hyperconjugation is neglected, a tetrahedral sp^3 carbon atom will not contribute to the π-molecular orbitals, and may be ignored in discussing the π-electrons. For example, it is a good approximation to take the π-molecular orbitals of diphenyl-methane as being identical with those of two benzene molecules.

On the other hand, an (sp, p^2) carbon atom—that is, an acetylenic or allenic carbon atom—has two $2p$ atomic orbitals, and both of these may take part in π-conjugation. So the number of $2p$ atomic orbitals differs from the number of unsaturated carbon atoms, and N will be used to denote the former quantity, not the latter. An alternant hydrocarbon is redefined as one which contains no odd-membered ring of mutually overlapping $2p$ atomic orbitals; so that according to this definition the secular equations for an alternant hydrocarbon may still be written in the form (2), (3), where r and s now refer to the two sets of *atomic orbitals*. In discussing molecular orbitals in relation to resonance structures, it is necessary to exclude from consideration any formal resonance structures whose multiple bonds do not correspond to non-zero elements of B and C. The quantity T is then redefined as the maximum number of such factors in any product of such elements; and since a triple bond corresponds to two pairs of overlapping $2p$ orbitals, T equals the maximum value of (the number of double bonds plus twice the number of triple bonds) occurring in any permissible resonance structure.

The importance of geometrical considerations is well illustrated by the example of allene, C_3H_4. This molecule is known to have its CH_2 groups in perpendicular planes,

‡ This assumption is certainly much better than the assumption that $S_{tu}=0$; and R. S. Mulliken (private communication) has found that it is quite accurately true in various two-center cases.

and is assigned the K-structure (VI).

$$H_2C=C=CH_2.$$
(VI)

The double bonds correspond to two mutually overlapping pairs of $2p$ orbitals: the central carbon atom has two perpendicular $2p$ orbitals, one of which overlaps the $2p$ orbital of the left-hand carbon atom, and the other of which overlaps the $2p$ orbital of the right-hand carbon atom. However, if allene were planar, the K-structure (VI) would be inadmissible; this is because only one of the $2p$ orbitals of the central atom would have the correct symmetry to overlap either of the terminal $2p$ orbitals, so that the above K-structure would not correspond to a non-vanishing product of terms from the matrix B. Instead, the principal resonance structures would contain one double bond each, and be as shown in Fig. 8. So in the ground state there would be two

$$H_2\dot{C}-\dot{C}=CH_2 \qquad H_2C=\dot{C}-\dot{C}H_2$$

FIG. 8.

unpaired electrons, distributed over the "active" $2p$ orbitals, namely, the $2pz$ orbital of the central atom and the $2py$ orbitals of the terminal carbon atoms. (The z axis is taken perpendicular to the molecular plane, and the x direction along the molecular axis.) Therefore if allene were planar, it would have a paramagnetic (triplet) ground state.

Two other examples will be given, to illustrate what happens in molecules containing triple bonds.

In phenyl-acetylene, $N=10$, and $T=5$ since the conventional K-structure does correspond to a possible division of the $2p$ orbitals into mutually overlapping pairs. There is therefore no reason to expect unpaired electrons in the ground state, and this molecule is indeed diamagnetic. The second example is the hypothetical linear molecule C_3H_2, which has the following principal resonance structures:

$$H-\dot{C}=C=\dot{C}-H$$

$$H-\dot{C}-C\equiv C-H$$

$$H-C\equiv C-\dot{C}-H.$$

For this molecule $N=6$, $T=2$, so there must be two unpaired electrons in the ground state, and these will be distributed over the $2p$ atomic orbitals of the terminal carbon atoms.

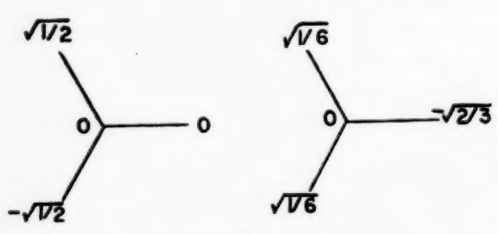

FIG. 9.

13. DISCUSSION OF RESULTS

The results established above provide what has been lacking for a long time in the theory of conjugated systems, namely, a bridge between molecular orbital theory and the essentially different concepts of classical resonance theory. There are, it is true, certain divergences between the two theories, as noted already in the case of cyclobutadiene, for which molecular orbital theory predicts a triplet ground state. However, from the principal resonance structures of an alternant hydrocarbon, it is possible to derive a correct lower limit for the number of unpaired electrons in the ground state, and in general to decide at which atoms these electrons are located.

The question at once arises: What experimental predictions can be made on the basis of these theoretical results?

One prediction, following immediately from Section 10, is that an alternant hydrocarbon with no classical structure of the K-type should be paramagnetic in the ground state. For a molecule with an odd number of valence electrons this is trivial; but for Clar's hydrocarbon (I) and such molecules as (II) and (III), the result is of great interest, and leads to further conclusions. One feature in common between paramagnetic molecules is their tendency to react with one another. For example, methyl, triphenyl-methyl, nitrogen dioxide, and chlorine trioxide all dimerize to varying extents, and most free radicals react with oxygen and nitric oxide, although the last two molecules themselves show little tendency to polymerize. In particular, there seems to be no exception to the rule that paramagnetic hydrocarbon molecules (radicals or multiradicals) react extremely easily with oxygen; so that any attempt to prepare such molecules in the presence of air will probably be unsuccessful. However, it is to be hoped that the hydrocarbon (I) will be prepared, and its magnetic susceptibility measured.

Another interesting prediction concerns the effect of bond twisting on the ground state of an alternant hydrocarbon. The discussion of the last section shows that if allene is twisted into a planar configuration, its ground state becomes a triplet. This is a special case of a more general phenomenon: if a diamagnetic alternant hydrocarbon undergoes internal twisting through 90° about a carbon-carbon bond that is formally double in *all* the principal resonance structures, the twisted molecule will have a triplet ground state. This is because twisting the molecule about the bond in question destroys the overlap between the $2p$ orbitals forming the double bond, so that all the principal resonance structures of the undistorted molecule become inadmissible when the molecule is twisted. Therefore T is decreased by one, and $N-2T$ is raised from zero to two. From this it follows that excitation of the undistorted molecule into a triplet level will lower the barrier to rotation

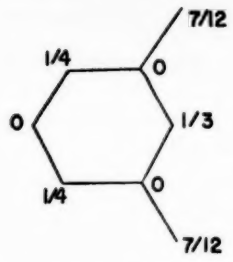

FIG. 10.

about any double bond; and it may be possible to induce *cis-trans*-isomerization by irradiation with photons whose energy is considerably less than the energy that would be required to twist the molecule if it remained all the time in the singlet state.

It can also be predicted, though with less certainty, which positions should be involved in the polymerization or oxidation of an unsaturated hydrocarbon radical. It is reasonable to suppose that those positions at which the density of unpaired electrons is highest will be the initial points of attack. Generally these positions are the "active" carbon atoms, which may be identified by enumerating principal resonance structures, if so desired. However, a more reliable procedure for predicting the reactive positions, is actually to solve the secular equations for the zero-energy molecular orbitals (this is not at all difficult or laborious as will be shown in the Appendix). One can then calculate the *odd-electron density* at atom t from the equation

$$q_t^* = \sum_z (c_t^z)^2, \qquad (17)$$

the summation being taken over the zero-energy MO ψ^z. This procedure has the advantage of being quantitative; but, more important, it avoids the omission of supernumerary unpaired electrons such as occur in cyclobutadiene. Equation (17) is suitable as a definition of odd-electron density, as q_t^* is then invariant under an orthogonal transformation applied to the MO ψ^z, any set of orthogonal combinations of the ψ^z being equally valid as a description of the zero-energy MO.

To illustrate this procedure, consider molecules (II), (III), and (I), in that order.

The zero-energy MO of (II) are as shown in Fig. 9, if all the atoms are supposed to lie in one plane. The odd-electron density is therefore two-thirds at each external carbon atom, these being the active carbon atoms. Molecule (II) will therefore tend to polymerize through these atoms, or, more likely, to undergo ring closure with formation of methylene-cyclopropane (VII), which is known to be stable.

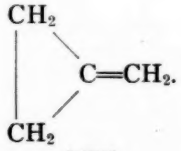

(VII)

The odd-electron densities in (III) may be calculated from the orbitals shown in Fig. 3. They are given in Fig. 10. It is reassuring to find that the unpaired electrons are most dense at the external positions; one would be very surprised to find that polymerization involved the carbon atoms in the ring.

Clar's hydrocarbon (I) has odd-electron densities as shown in Fig. 11. The most active positions in free radical reactions should therefore be the meso positions.

A third prediction which can be made concerns the behavior of carbonium ions derived from alternant hydrocarbon radicals by loss of one electron. The ionized electron will be one that was unpaired in the radical, because the orbitals of the unpaired electrons are less stable than the other occupied orbitals. Now in a neutral alternant hydrocarbon the net charge at every carbon atom is zero, as proved by Coulson and Rushbrooke.[4] Therefore ionization of an electron in an orbit $\sum_\mu c_\mu \phi_\mu$ will leave a net positive charge of c_μ^2 at each active carbon atom. We conclude that in the cation the positive charge will be distributed entirely over the active carbon atoms, if the parent radical contained no supernumerary unpaired electrons. But the ionized electron is equally likely to have come from any one of the zero-energy orbitals ψ^z, so the probable net charge in ϕ_μ is given by $(1/Z)\sum_z (c_\mu^z)^2$, where Z is the number of zero-energy MO. A similar argument can be used for anions. For example, if Clar's hydrocarbon could be singly ionized, the probable net charges at the various atoms would be half the numbers given in Fig. 11.

Our third prediction may therefore be stated as follows: In singly charged anions or cations derived from alternant hydrocarbon radicals containing no supernumerary zero-energy MO, the ionic charge is distributed entirely over those carbon atoms which bear formal charges in one or more of the principal resonance structures. This prediction depends on the tacit assumption that the Coulomb integrals of the carbon atoms are the same in an ion as in a neutral hydrocarbon, and this cannot be strictly true; but it will be a better approximation the larger the ion.

14. SUPERNUMERARY ZERO-ENERGY MO

One further comment should be made on the generality of the results obtained in this paper. The proofs given in

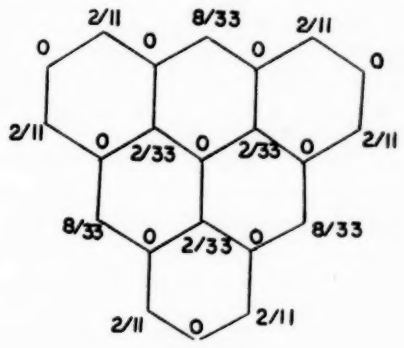

FIG. 11.

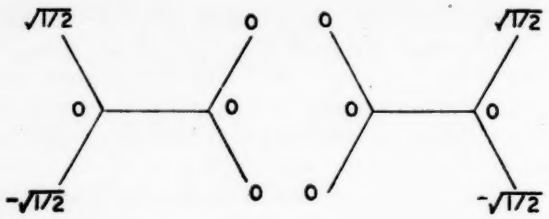

FIG. 12.

Sections 6 and 8 depend on the fact that a determinant vanishes if all the terms in its expansion vanish; and the existence of supernumerary MO arises from the fact that the converse is not true in general. It might therefore reasonably be asked: Is it not possible to find a stronger condition for the vanishing of one of the minors of B or C, which will give the exact number z of zero-energy MO in the general case? The answer seems to be as follows. Any stronger condition for the vanishing of a minor of B must necessarily imply some numerical relationship between the elements of B, and hence between the resonance integrals of the various carbon-carbon bonds. However, none of the arguments in this paper depend on the assumption of equal or related resonance integrals for the various bonds, so it would be necessary to sacrifice a certain amount of generality in order to obtain an exact expression for the total number of zero-energy MO in an alternant hydrocarbon. As an illustration, the conclusion that cyclobutadiene has two zero-energy MO depends on the assumption that all four carbon-carbon bonds have equal resonance integrals, so that there is an "accidental" cancellation of the terms of B corresponding to the two K-structures. However, if this molecule were rectangular instead of square (which is by no means out of the question), the energy of the corresponding MO would not be zero any longer. A precisely similar argument can be applied to cyclooctatetraene; if this molecule were a regular octagon it would have two zero-energy MO, and therefore behave as a diradical. On the other hand, if it has a non-planar configuration with alternating bond lengths, there is no reason to anticipate a paramagnetic ground state.

To sum up, the conventional procedure of enumerating principal resonance structures in order to determine the number and distribution of unpaired electrons or electric charges in hydrocarbon molecules and ions, is justified with remarkable completeness by molecular orbital theory; and in particular, it is now possible to understand more deeply why hydrocarbon molecules without normal classical structures are so rare.

APPENDIX

It is usually much easier to determine the form of the zero-energy MO in an alternant hydrocarbon than to do the same for a MO of finite energy. This is because one can always obtain the solutions of (4) and (5) in the form $\sum_r c_r\phi_r$ or $\sum_s c_s\phi_s$ to begin with,* and then express the zero-energy MO as linear combinations of these, having the symmetry appropriate to some irreducible representation of the molecular symmetry group. To show that this is possible, consider the general solution of (4) and (5), namely,

$$\psi=\sum_r c_r\phi_r+\sum_s c_s\phi_s,$$

where at least one coefficient c_r and one coefficient c_s do not vanish. Then, by the arguments of Section 6, another solution of (4) and (5) is

$$\psi'=\sum_r c_r\phi_r-\sum_s c_s\phi_s,$$

linearly independent of ψ. It follows that, with suitable normalization factors, the combinations

$$\sum_r c_r\phi_r \quad \text{and} \quad \sum_s c_s\phi_s$$

are also solutions of (4) and (5), and may be linearly combined to give again ψ and ψ'.

As an example of the use of this procedure, consider again the molecule (IV).

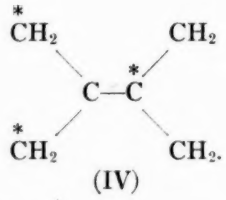

(IV)

It is easy to verify that (4) and (5) have one solution of the form $\sum_r c_r\phi_r$ and one of the form $\sum_s c_s\phi_s$, these being as shown in Fig. 12. To obtain MO of the correct symmetry properties with respect to the molecular group, it is merely necessary to take the sum and the difference of these, suitably normalized; this gives the forms shown in Fig. 5.

The author would like to express his gratitude to Professors J. R. Platt and R. S. Mulliken for much helpful discussion and criticism.

* As before, the starred atoms are denoted collectively by r, and the unstarred ones by s.

Some Studies in Molecular Orbital Theory

II. Ionization Constants in Heteroaromatic Amines and Related Compounds*

H. C. LONGUET-HIGGINS
Department of Physics, University of Chicago,† Chicago, Illinois
(Received June 13, 1949)

The relative basicities of a series of mono-aza-aromatic amines are calculated by a very simple application of LCAO molecular orbital theory. Rough quantitative agreement between theory and experiment is obtained if the heterocyclic nitrogen atom is supposed to take up the proton; on the other hand, if the amine group is assumed to add the proton in the first ionization, the observed basicities are negatively correlated with theory.

It is also shown how the qualitative differences in reactivity between methyl-aza-hydrocarbons and between heteroaromatic phenols may be understood in similar very simple terms.

1. INTRODUCTION

IN recent years much valuable experimental data[1–3] has been obtained as to the basic strengths of aromatic amines. In particular, a comprehensive collection of data has been published by Albert, Goldacre, and Phillips,[1] who recorded ionization constants for 120 heterocyclic bases belonging to 30 different, completely unsaturated ring systems. These authors assumed that in heterocyclic amines such as the amino-pyridines, the first proton adds to the heterocyclic nitrogen atom rather than to the amino group; and on this assumption they interpreted their results qualitatively in terms of resonance possibilities in the amine and its cation.

In this paper the ionization constants given by Albert, Goldacre, and Phillips will be discussed quantitatively in terms of LCAO molecular orbital theory. Attention will be confined to those bases which are derived from cata-condensed hydrocarbons by replacing a CH group by N, and attaching an NH_2 at some external position. The results confirm the view that the heterocyclic nitrogen adds the first proton; and quantitative calculation shows that the observed differences in basicity are mainly caused by differences in resonance energy, in agreement with Albert, Goldacre, and Phillips.

In interpreting the experimental results theoretically, first-order perturbation theory has been used, for two reasons: (1) because it minimizes the number of unknown parameters that have to be introduced into the calculations—indeed, only one unknown parameter enters into the final results; and (2) because the use of perturbation theory tremendously simplifies the mathematics.

2. POSTULATES

Any comparison of the dissociation constants of two bases B_1 and B_2 in a given solvent at a given temperature amounts to a consideration of the equilibrium

$$B_1H^+ + B_2 \rightleftharpoons B_1 + B_2H^+.$$

Hammett[4] has discussed in detail how the equilibrium constant for such a reaction is related to the kinetic and potential energies of reaction. Let

$$\Delta G^0 = -RT \log K$$

be the standard free energy change in the reaction, K being the equilibrium constant. Then, as Hammett points out, if the partition functions of the species B_1H^+, B_1, B_2H^+, and B_2 are related by the equation

$$\frac{f_{B_1H^+}}{f_{B_1}} = \frac{f_{B_2H^+}}{f_{B_2}},$$

it is possible to use ΔG_0 as a measure of the potential energy change ΔE_P occurring in the reaction. (Strictly speaking, this would only be true in a solvent of infinite dielectric constant, and electrostatic interaction terms should be taken into account; but these will be less important the more alike the charge distributions in B_1H^+ and B_2H^+.)

Now for bases of the type discussed in this paper, the change in potential energy ΔE_P will be principally due to the difference in unsaturation energy between the species on the right-hand side of the equation and those on the left. For simplicity it will be assumed that strict equality holds, that is:

$$\Delta E_P = \Delta \mathcal{E}_2 - \Delta \mathcal{E}_1,$$

where $\Delta \mathcal{E}_2$ is the difference in unsaturation energy between B_2H^+ and B_2, and $\Delta \mathcal{E}_1$ is defined similarly. This assumption cannot be entirely correct, but it is a reasonable initial hypothesis, and may be tested by its consequences.

In order to establish a connection with the experimental data, it is further necessary to assume that Hammett's condition holds, i.e., that f_{BH^+}/f_B has the same value for all the bases considered; this amounts to

* Work done under ONR, Task Order IX of Contract N6ori-20, with the University of Chicago.
† Now at the Department of Chemistry, Manchester University, Manchester, England.
[1] Albert, Goldacre, and Phillips, J. Chem. Soc. 2240 (1948).
[2] A. Albert and R. J. Goldacre, J. Chem. Soc. 706 (1946).
[3] A. Albert and R. J. Goldacre, J. Chem. Soc. 454 (1943).
[4] L. P. Hammett, *Physical Organic Chemistry* (McGraw-Hill Book Company, Inc., New York, 1940).

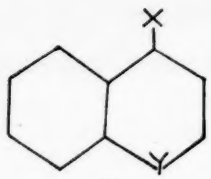

(I)

saying that the entropies of ionization of heteroaromatic amines are roughly equal. This is an optimistic assumption, but cannot be avoided, as no entropy data are available at present.

The above postulates may be summarized in the equations

$$\Delta\mathcal{E}_2-\Delta\mathcal{E}_1\simeq\Delta E_F\simeq\Delta G^0=-RT\log K$$
$$=2.3RT(pKa_1-pKa_2)$$

or, dropping suffixes,

$$2.3RT\,pKa=\text{const.}-\Delta\mathcal{E}.$$

3. METHOD OF CALCULATING $\Delta\mathcal{E}$

The principle of the method is to assume that the wave function for the π-electrons in a conjugated molecule containing one or two heteroatoms is the same as in the "parent" hydrocarbon—that is, the hydrocarbon with the same arrangement of atomic p orbitals and the same number of π-electrons. The unsaturation energy $\mathcal{E}$ of the heteromolecule is then obtained from the π-wave function of the parent hydrocarbon by first-order perturbation theory, assuming that structural differences between the heteromolecule and its parent hydrocarbon may be regarded as perturbations applied to the Hamiltonian of the latter.

The procedure is probably best illustrated by an example. Consider the set of molecules (I) where X stands for H, CH_3, CH_2^-, NH_2, or NH_3^+, and Y stands for CH, N, NH^+, or NR^+. If hyperconjugation is neglected, the molecules with X=H, CH_3, or NH_3^+ have naphthalene (II) as their parent hydrocarbon, whereas those with X=CH_2^- or NH_2 are derived from the carbanion (III). Now it is known[5] that if r is an atom in a conjugated system, and if the Coulomb integral of atom r is altered by a small amount $\delta\alpha_r$, then the change in unsaturation energy of the system is given by

$$\delta\mathcal{E}=q_r\delta\alpha_r,$$

where q_r is the π-electron density at position r. It follows that on passing from (II) or (III) to one of the heteromolecules (I), the change in unsaturation energy can be

TABLE I. Unsaturation energies in molecules of Type (I).

X =	H or CH_3	NH_3^+	CH_2^-	NH_2
Y=CH	$\mathcal{E}_0$	$\mathcal{E}_0+z$	$\mathcal{E}_1$	$\mathcal{E}_1+q_0y$
N	$\mathcal{E}_0+x$	$\mathcal{E}_0+x+z$	$\mathcal{E}_1+q_4x$	$\mathcal{E}_1+q_4x+q_0y$
NH^+ or NR^+	$\mathcal{E}_0+y$	$\mathcal{E}_0+y+z$	$\mathcal{E}_1+q_4y$	$\mathcal{E}_1+q_4y+q_0y$

[5] C. A. Coulson and H. C. Longuet-Higgins, Proc. Roy. Soc. A191, 39 (1947).

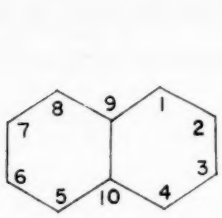

(II)

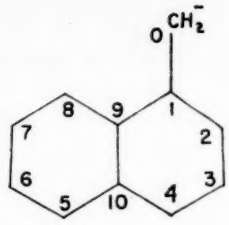

(III)

expressed in terms of the electron densities in the parent hydrocarbon and the changes in Coulomb integral at the affected atoms.

The π-electron densities are known to be unity at every position in naphthalene;[6] but the π-electron densities in (III) will not necessarily be equal to one, and their values at the CH_2^- group and the four-position may be denoted by q_0 and q_4, respectively. Then, if $\mathcal{E}_0$ and $\mathcal{E}_1$ denote the unsaturation energies of (II) and (III), the unsaturation energies of the molecules (I) will be as listed in Table I.

In Table I, x denotes the difference in Coulomb integral between aromatic CH and N, y denotes the difference in Coulomb integral between

$-CH_2^-$ and $-NH_2$, CH and NH^+,

or

CH and NR^+,

TABLE II. Changes in unsaturation energy for some ionization reactions.

(1) 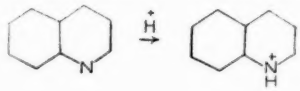 ; $\Delta\mathcal{E}=y-x$

(2) 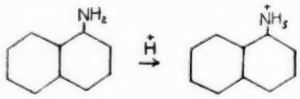 ; $\Delta\mathcal{E}=\begin{cases}\mathcal{E}_0-\mathcal{E}_1\\+z-q_0y\end{cases}$

(3) 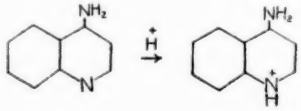 ; $\Delta\mathcal{E}=q_4(y-x)$

(4) 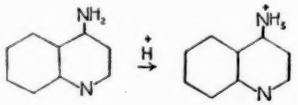 ; $\Delta\mathcal{E}=\begin{cases}\mathcal{E}_0-\mathcal{E}_1\\+x+z\\-q_4x-q_0y\end{cases}$

(5) 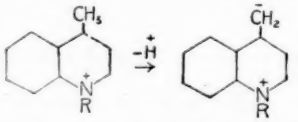 $+H^+$; $\Delta\mathcal{E}=\begin{cases}\mathcal{E}_1-\mathcal{E}_0\\+q_4y-y\end{cases}$

[6] C. A. Coulson and S. Rushbrooke, Proc. Camb. Phil. Soc. 36, 193 (1940).

TABLE III. Base strengths of some heterocyclic systems.

Base	*pKa* in aqueous solution	*pKa* in 50 percent aquenous ethanol
Pyridine	5.23	—
Quinoline	4.94	—
Acridine	5.60	4.11*
Isoquiyoline	5.14	—
5,6-benzquinoline	5.15	3.90
6,7-benzquinoline	5.05	3.84
7,8-benzquinoline	4.25	3.15
Phenanthridine	—	3.30
3,4-benzacridine	4.70	4.16
2,3-benzacridine	—	4.52
1,2-benzacridine	—	3.45

* This figure is taken from Albert and Goldacre (see reference 2).

and z is the change in Coulomb integral of an aromatic CH group when the H atom is replaced by $-NH_3^+$. (It is assumed that methyl substitution does not affect appreciably the Coulomb integral of aromatic carbon.)

From Table I it is possible to deduce $\Delta\mathcal{E}$, the change in unsaturation energy in some ionization reactions; and Table II gives values of $\Delta\mathcal{E}$ for five different possible ionizations.

(In reactions (3) and (5) the species on the right-hand side have important resonance structures in which the charges are disposed in a different way from that shown in Table II. However, this fact is irrelevant when these reactions are discussed in terms of molecular orbital theory: the additional stabilization arising from such resonance is implicit in the expressions given for $\Delta\mathcal{E}$.)

The data in Table II lead to some interesting conclusions. For reaction (1) the change in $\mathcal{E}$ is seen to be independent of $\mathcal{E}_0$ and $\mathcal{E}_1$; and is simply equal to the difference in Coulomb integral between the groups N and NH^+. The essential reason for this is that in naphthalene the π-electron density is unity at the four-position, and this is a special case of the Coulson-Rushbrooke theorem[6] that in any hydrocarbon containing no odd-membered rings the π-electron density is unity at every position. It follows from this theorem that to a first approximation the value of $\Delta\mathcal{E}$ and hence of *pKa* should be the same for all mono-aza-derivatives of such hydrocarbons under given conditions. Table III gives the *pKa* values for all the alternant aza-hydrocarbons so far studied experimentally; the data are taken from Albert, Goldacre, and Phillips,[1] and refer to 20°C. It will be seen that apart from acridine, which has a high value of *pKa* in water but not in aqueous alcohol, the figures in the two columns of Table III show little variation. The observed differences are relatively small when compared to those occurring in the amino-derivatives discussed below, and may be in part due to differences in activity coefficient, associated with the large differences in solubility between the various bases.[7] In any case, discrepancies would be expected in view of the severe approximations made in Section 2.

Another important feature of Table II is that it provides a theoretical basis for deciding whether, in a given series of amines, ionization involves the heterocyclic nitrogen atom or the amine group. Craig and Short,[8] from a study of electronic absorption spectra, established that in the amino-acridines it is the nuclear nitrogen atom which first adds a proton; but it is not known how widely this is true for heteroaromatic amines. Consider, for example, the various aza-derivatives of 1-naphthylamine, all of which have the carbanion (III) as their parent hydrocarbon. (The following argument would not hold for the various amino-quinolines, as these are not all derived from the same parent hydrocarbon.) If the ionization of r-aza-1-naphthylamine is represented by Eq. (3) in Table II, then $\Delta\mathcal{E}_r$ is given by

$$\Delta\mathcal{E}_r = q_r(y-x),$$

where q_r is the π-electron density at position r in (III). Now NH^+ is more electron-attracting than N, so $y-x$ is negative; hence a plot of $\Delta\mathcal{E}_r$ against q_r for various values of r should have a negative slope. But by hypothesis

$$2.3RT\,pKa = \text{const.} - \Delta\mathcal{E},$$

so if Eq. (3) represents the ionization correctly, a plot of *pKa* against q_r should have a positive slope. Suppose, on the contrary, that the ionization of r-aza-1-naphthylamine is correctly represented by Eq. (4). In this case we have

$$\Delta\mathcal{E} = \mathcal{E}_0 - \mathcal{E}_1 + x + z - q_r x + q_0 y.$$

Here all the terms except q_r are the same for different values of r, so the last equation may be written

$$\Delta\mathcal{E} = -q_r x + \text{const.}$$

But N attracts electrons more strongly than CH, so x is negative, and a plot of *pKa* against q_r should have a

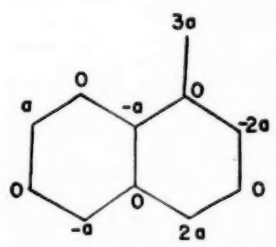

$(20\alpha^2 = 1.)$

(IV)

[7] Kolthoff, Lingane, and Larson, J. Am. Chem. Soc. **60**, 2512 (1938).

[8] D. P. Craig and L. N. Short, J. Chem. Soc. 419 (1945).

TABLE IV. Values of net charge and acidity constant for some aza-1-naphthylamines.

Amine	q_r-1	pKa in water at 20°
2-aza-1-naphthylamine (1-amino-isoquinoline)	0.200	7.62
4-aza-1-naphthylamine (α-amino-quinoline)	0.200	9.17
5-aza-1-naphthylamine (5-amino-quinoline)	0.050	5.46
8-aza-1-naphthylamine (8-amino-quinoline)	0.000	3.99

negative slope. Therefore, in order to distinguish between the posibilities (3) and (4), it is only necessary to determine whether a plot of pKa against q_r has a positive or a negative slope, assuming, of course, that the ionization proceeds by the same mechanism for the different amines in the series.

4. CALCULATION OF q_0 AND q_r

Before discussing the other ionizations formulated in Table II, we shall show how the electron densities q_0 and q_r may be calculated for the carbanions of Type (III). The calculation is made extremely simple by the following general theorems:[9]

(i) In a singly ionized carbanion containing no odd-membered rings, the net negative charge q_r-1 at atom r is given by

$$q_r-1=(c_r^0)^2,$$

TABLE V.

Serial No.	Amine	Parent carbanion	(q_r-1)	pKa in water at 20°C	Anomaly (if any)
12	2-amino-pyridine	*A*	1/7=0.143	6.86	Ortho
13	3-amino-pyridine	*A*	0=0.000	5.98	—
14	4-amino-pyridine	*A*	1/7=0.143	9.17	—
16	2-amino-quinoline	*C*	4/17=0.235	7.34	Ortho
17	3-amino-quinoline	*C*	0=0.000	4.95	—
18	4-amino-quinoline	*B*	4/20=0.200	9.17	—
19	5-amino-quinoline	*B*	1/20=0.050	5.46	—
20	6-amino-quinoline	*C*	0=0.000	5.63	—
21	7-amino-quinoline	*C*	1/17=0.059	6.65	—
22	8-amino-quinoline	*B*	0=0.000	3.99	Peri
26	5-amino-acridine	*D*	4/14=0.286	9.99	—
27	4-amino-acridine	*E*	4/42=0.095	6.04	—
28	3-amino-acridine	*F*	0=0.000	5.88	—
29	2-amino-acridine	*F*	4/34=0.118	8.04	—
30	1-amino-acridine	*E*	0=0.000	4.40	Peri
36	8-amino-1-aza-phenanthrene	*H*	1/54=0.019	5.20	—
38	5-amino-1-aza-phenanthrene	*L*	0=0.000	5.03	—
46	3-amino-1-aza-anthracene	*F*	0=0.000	4.78	—
54	9-amino-phenan-thridine	*G*	16/56=0.286	7.31	Ortho
60	1-amino-isoquinoline	*B*	4/20=0.200	7.62	Ortho
64	8-amino-2,3-benzacridine	*Q*	9/99=0.091	7.42	—
75	8-amino-1,2-benzacridine	*P*	9/102=0.088	6.72	—

[9] H. C. Longuet-Higgins, Paper I of this series, J. Chem. Phys. 18, 265 (1950).

TABLE VI.

Serial No.	Amine	Parent carbanion	(q_r-1)	pKa at 20°C in 50 percent ethanol	Anomaly (if any)
26	5-amino-acridine	*D*	4/14=0.286	9.45*	—
27	4-amino-acridine	*E*	4/42=0.095	5.50*	—
28	3-amino-acridine	*F*	0=0.000	5.03*	—
29	2-amino-acridine	*F*	4/34=0.118	7.61*	—
30	1-amino-acridine	*E*	0=0.000	3.59*	Peri
32	4-amino-1-aza-phenanthrene	*L*	9/51=0.176	7.99	—
36	8-amino-1-aza-phenanthrene	*H*	1/54=0.019	4.10	—
37	7-amino-1-aza-phenanthrene	*J*	0=0.000	4.02	—
41	4-amino-1-aza-acridine	*E*	9/42=0.214	8.75	—
46	3-amino-1-aza-acridine	*F*	0=0.000	3.73	—
48	1-amino-4-aza-phenanthrene	*H*	9/54=0.167	7.68	—
54	9-amino-phenanthridine	*G*	16/56=0.286	6.75	Ortho
62	5-amino-3,4-benzacridine	*M*	36/144=0.250	8.41	—
63	7-amino-3,4-benzacridine	*P*	0=0.000	5.03	—
64	8-amino-3,4-benzacridine	*Q*	9/99=0.091	6.51	—
68	5-amino-2,3-benzacridine	*R*	36/120=0.300	9.72	—
70	7-amino-2,3-benzacridine	*S*	0=0.000	5.38	—
73	5-amino-1,2-benzacridine	*N*	36/156=0.231	8.13	—
74	7-amino-1,2-benzacridine	*Q*	0=0.000	4.05	—
75	8-amino-1,2-benzacridine	*P*	9/102=0.088	5.97	—

where $\psi^0=\sum_r c_r^0\phi_r$ is the highest occupied molecular orbital.

(ii) If the carbanion contains an odd number of p atomic orbitals, the orbital ψ^0 has zero binding energy, and, furthermore, the coefficients c_r^0 have non-zero

TABLE VII.

Serial No.	Amine	Parent carbanion	(q_r-1)	pKa at 20°C in 50 percent ethanol	Anomaly (if any)
33	4-amino-2-methyl-1-aza-phenanthrene	*L*	9/51=0.176	8.45	—
35	2-amino-4-methyl-1-aza-phenanthrene	*J*	9/46=0.195	6.51	Ortho
42	4-amino-2-methyl-1-aza-anthracene	*E*	9/42=0.214	9.45	—
49	1-amino-3-methyl-4-aza-phenanthrene	*H*	9/54=0.167	7.96	—
50	3-amino-1-methyl-4-aza-phenanthrene	*K*	9/49=0.184	6.02	Ortho
51	9-amino-3-methyl-4-aza-phenanthrene	*G*	0=0.000	5.23	—
52	8-amino-3-methyl-4-aza-phenanthrene	*H*	0=0.000	4.75	—
55	2-amino-9-methyl-phenanthridine	*J*	1/46=0.022	5.66	—
56	7-amino-9-methyl-phenanthridine	*J*	0=0.000	5.23	—

values only at those atoms r which bear a formal charge in one or more of the principal resonance structures.

As an illustration, consider again the carbanion (III). To calculate the π-electron densities we must first find the coefficients c_r^0. By (ii), these coefficients will vanish at positions 1, 3, 6, 8, and 10, as these are separated from the CH_2^- group by odd numbers of bonds, and therefore cannot bear a negative charge in any of the principal resonance structures. Now, as is well known,[10] the coefficients c_r in a MO must satisfy the equations

$$-\epsilon c_r+\sum_{s\neq r}\beta_{rs}c_s=0, \text{ for all positions } r,$$

where ϵ is the binding energy and β_{rs} is the resonance integral between orbitals ϕ_r and ϕ_s. For the orbital ψ^0, ϵ is zero; so the equations become

$$\sum_{s\neq r}\beta_{rs}c_s^0=0, \text{ for all } r.$$

Further, β_{rs} will have roughly the same value β for all bonded pairs of atoms, and will be zero if r and s are not bonded. It follows that for each atom r, the coefficients c_s^0 at the adjacent atoms must add up to zero. Returning to the example (III), we see that if the coefficient c_7^0 equals a, the other coefficients c_r^0 must be as shown in (IV). The normalization condition requires that $20a^2=1$, so that $a=1/(20)^{\frac{1}{2}}$. Therefore in (III) the net charges are: 9/20 at the CH_2 group, 4/20 at the 2 and 4 positions, 1/20 at the 5, 7, and 9 positions, and zero elsewhere.

5. RELATION BETWEEN q_r AND pKa

Table IV gives a comparison between the acidity constants of various aza-1-naphthylamines, determined by Albert, Goldacre, and Phillips, and the appropriate values of q_r-1, determined in the previous section. The function pKa is seen to increase with q_r, except that the first amine is less basic than the second, and this exception may be explained as an "ortho" anomaly in 1-amino-isoquinoline. It follows from the argument of Section 3, that the proton adds to the heterocyclic nitrogen atom rather than to the amino group.

Tables V–VII give values of q_r-1 and pKa for a wide variety of amines, derived from eleven different heteroaromatic ring systems. The first column gives the serial number allotted to each amine by Albert, Goldacre, and Phillips. The letter in the third column denotes which of the carbanions in the Appendix is the "parent" hydrocarbon; the fourth column gives the net charge q_r-1 obtained from this carbanion; the fifth column gives the experimental pKa value. All the values of pKa are taken from Albert, Goldacre, and Phillips,[1] except for those marked with an asterisk, which are taken from Albert and Goldacre.[2] The measurements were all made at 20°C; those in Table V refer to aqueous solution, and those in Tables VI and VII to solution in 50 percent ethanol. All the amines considered contain just one NH_2 group and one heterocyclic nitrogen atom, and are derived from even-membered ring systems; the amines in Table VII contain also a methyl group attached to the aromatic system, but amines containing other side groups have not been considered. Within the field defined by these restrictions, all the available experimental data are presented in Tables V–VII; and Figs. 1–3 give the same data plotted in graphical form.

DISCUSSION OF RESULTS

Although the points in Figs. 1–3 are somewhat scattered, there does seem to be a roughly linear relationship

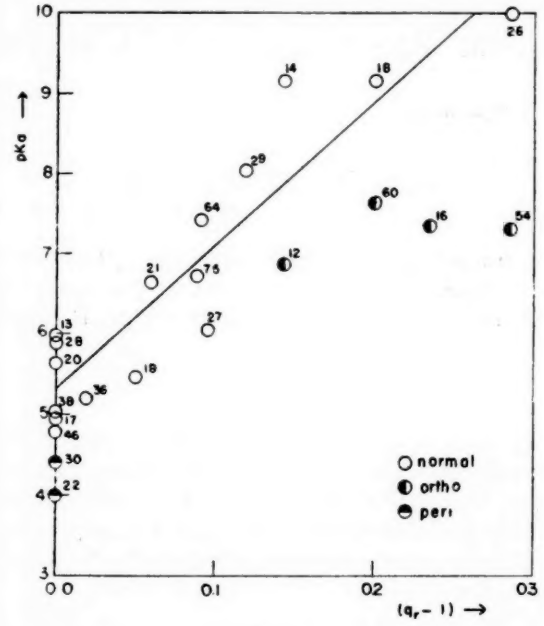

FIG. 1.

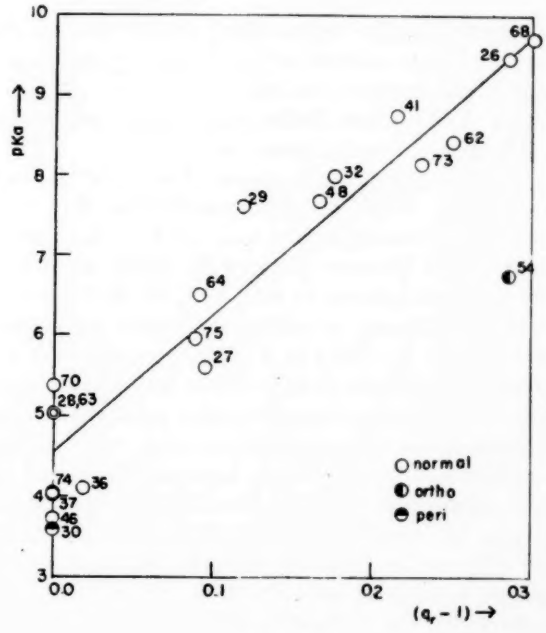

FIG. 2.

[10] C. A. Coulson and H. C. Longuet-Higgins, Proc. Roy. Soc. A192, 16 (1947).

between pKa and q_r for those amines in which the NH_2 group is not too close to the heterocyclic nitrogen atom. The bases which deviate most widely from the general trend are, almost without exception, those in which the NH_2 group is either in the *ortho* or in the *peri* position with respect to the nuclear nitrogen; and, as suggested by Albert and Goldacre,[2] this anomaly is probably an instance of the well-known and widely occurring "ortho effect." With this comment, such anomalous molecules will be dismissed from further consideration. The straight lines in Figs. 1–3 have been drawn to give the

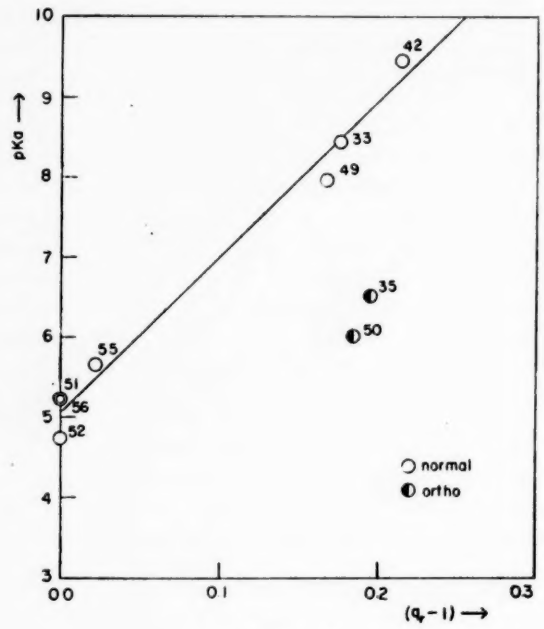

FIG. 3.

best general fit with the remaining points; the fact that these lines have a positive rather than a negative slope is strong evidence that the ionization of the amines in Tables V–VII involves the nuclear nitrogen rather than the NH_2 group, as anticipated earlier.

In judging the present simple theory by the data given in Figs. 1–3, it must be remembered that many serious approximations have been made in establishing the correlation between q_r and pKa. Quite apart from the usual errors inherent in simple LC AO MO theory, it cannot, for instance, be correct to regard the replacement of CH_2^- by NH_2 as a small perturbation; also addition of the proton to the nuclear nitrogen atom will certainly modify the π-wave function considerably, and introduce second-order corrections to the energy. However, there is a compensating factor which makes the former assumption, at least, less drastic than it would otherwise be. This factor is the influence of the charge at an atom on its Coulomb integral. If the charges in 1-naphthylamine, for instance, are anywhere near those calculated for the carbanion (III), the excess electron density at the nitrogen atom will reduce its electron affinity considerably, perhaps to a value which hardly differs from the value for aromatic carbon; and the charge distribution calculated for (III) may even be a better approximation for the amine than for the carbanion.

Again, it cannot be strictly correct to assume that the difference in free energy of ionization between two bases, is equal to the difference between their values of $\Delta\mathcal{E}$: differences in entropy of ionization and electrostatic energy terms should really be taken into consideration. So it would be naïve to expect a precise linear relation between the theoretical q_r and the experimental pKa; indeed, when all the possible errors are considered, it is encouraging that the observed correlation is as good as it is.

One other point may be noted here, as it illustrates the fundamental agreement between qualitative resonance theory and molecular orbital theory. The form of the zero-energy MO ψ^0 demands that the net charge q_r-1 be zero at every atom separated from the amino group by an odd number of bonds. Therefore all amines, in which there is an odd number of bonds between the heterocyclic atom and the amino group, should have approximately the same base strength, in agreement with qualitative resonance theory. This expectation is roughly confirmed by the experimental results.

CALCULATION OF $y-x$

From the slope of the graphs in Figs. 1–3, it is possible to obtain an order of magnitude for $y-x$, the difference in Coulomb integral between heterocyclic $\diagdown\!\!=\!\!\diagup$N and heterocyclic $\diagdown\!\!=\!\!\diagup$NH$^+$. The theoretical slope is determined by the equations

$$(q_r-q_r')(y-x)=\Delta\mathcal{E}-\Delta\mathcal{E}'$$
$$=\Delta F-\Delta F'=RT\log_e Ka/Ka'$$
$$=-2.3RT(pKa-pKa'),$$

where primed and unprimed quantities refer to two different bases. The observed slopes of the three lines are 18, 18, and 20 $\log s_{10}$ per unit of charge. It follows that

$$(y-x)/(2.3RT)=18,$$

whence $y-x$ is approximately 24,000 cal./mole. The usual value assigned to β, the carbon-carbon resonance integral, is 20,000 cal./mole, so $y-x$ is approximately 1.2β. The probable error in this figure is large, perhaps ± 20 percent, but the value may be found useful in later computations.

RELATED REACTIONS

There are other important types of reaction that can be discussed in terms of the theoretical ideas put

forward in this paper. Consider, for example, the ionization of methyl groups attached to heteroaromatic systems. This process is represented by reaction (5) in Table II, and involves a change in unsaturation energy given by

$$\Delta\mathcal{E}=\mathcal{E}_1-\mathcal{E}_0+q_r y-y-z.$$

This equation implies that ionization of a methyl group attached to a heteroaromatic system proceeds more easily the greater the charge q_r at the heteroatom. But, as shown already, q_r is positively correlated with the basic strength of the corresponding heteroaromatic amine. Therefore, given a series of s-amino-r-aza-derivatives (where s is fixed and r varies), it may be predicted that the more basic the amino-derivative, the more easily ionized will be the CH_3 group of the corresponding methyl derivative, especially when the nuclear nitrogen atom is quaternated. This has been known as a qualitative fact for some time: for example, the high reactivity of the *N*-methyl-4-methyl-quinolinium ion is naturally interpreted as due to easy ionization of the 4-methyl group; but there seem to be no quantitative data at present to confirm or contradict the prediction that the values of $\Delta\mathcal{E}$ for the two types of reaction should be linearly related.

Or again, consider the ionization of a heteroaromatic phenol. There is good evidence that the $-O^-$ group conjugates much more strongly with an aromatic system than the $-OH$ group; and this is presumably due to the high electron affinity of OH relative to O^-, which makes structures involving $=O$ more stable than those involving $=OH^+$. Denote by v the change in Coulomb integral of a CH group when the H atom is replaced by OH, and denote by w the difference in Coulomb integral between $-CH_2^-$ and $-O^-$. Then, by similar arguments to those of Section 3, the change in unsaturation energy on ionization of an r-aza-phenol is given by

$$\begin{aligned}\Delta\mathcal{E}&=(\mathcal{E}_1+q_0w+q_rx)-(\mathcal{E}_0+v+x)\\&=\mathcal{E}_1-\mathcal{E}_0+q_rx+q_0w-x-v.\end{aligned}$$

That is, in a series of r-aza-derivatives of a given aromatic phenol, the acidity of the OH group will be greater the greater the electron density at the r-position. Now the greater q_r, the greater also the basicity of the heterocyclic nitrogen atom; and indeed it is found that in molecules such as 4-hydroxy-pyridine or 5-hydroxy-acridine, for which the value of q_r in the parent carbanion is high, the phenolic proton actually migrates from the OH group to the nuclear nitrogen atom, giving a pyridone or acridone. As yet, very little quantitative data is available as to the ionization constants of heteroaromatic phenols; from the theoretical standpoint such data would be of great interest.

CONCLUSION

The perturbation theory outlined here makes it possible to calculate relative rate constants and equilibrium constants for many types of reaction without having to solve completely the secular equations. For example, in calculating $\Delta\mathcal{E}$ for each amine in Tables V–VII it was only necessary to find atomic orbital coefficients c_r^0 for a molecular orbital of zero binding energy; the net charge q_r-1 was then obtained simply by squaring the appropriate coefficient. As already shown, these atomic orbital coefficients may be written down with great rapidity, and herein lies the usefulness of the method.

In the next paper of this series we shall show how these atomic orbital coefficients can be used in calculating transition state energies for the substitution reactions of aromatic and heteroaromatic systems.

(See page 282 for Appendix of this paper.)

APPENDIX

Zero-Energy Molecular Orbitals in Some Carbanions

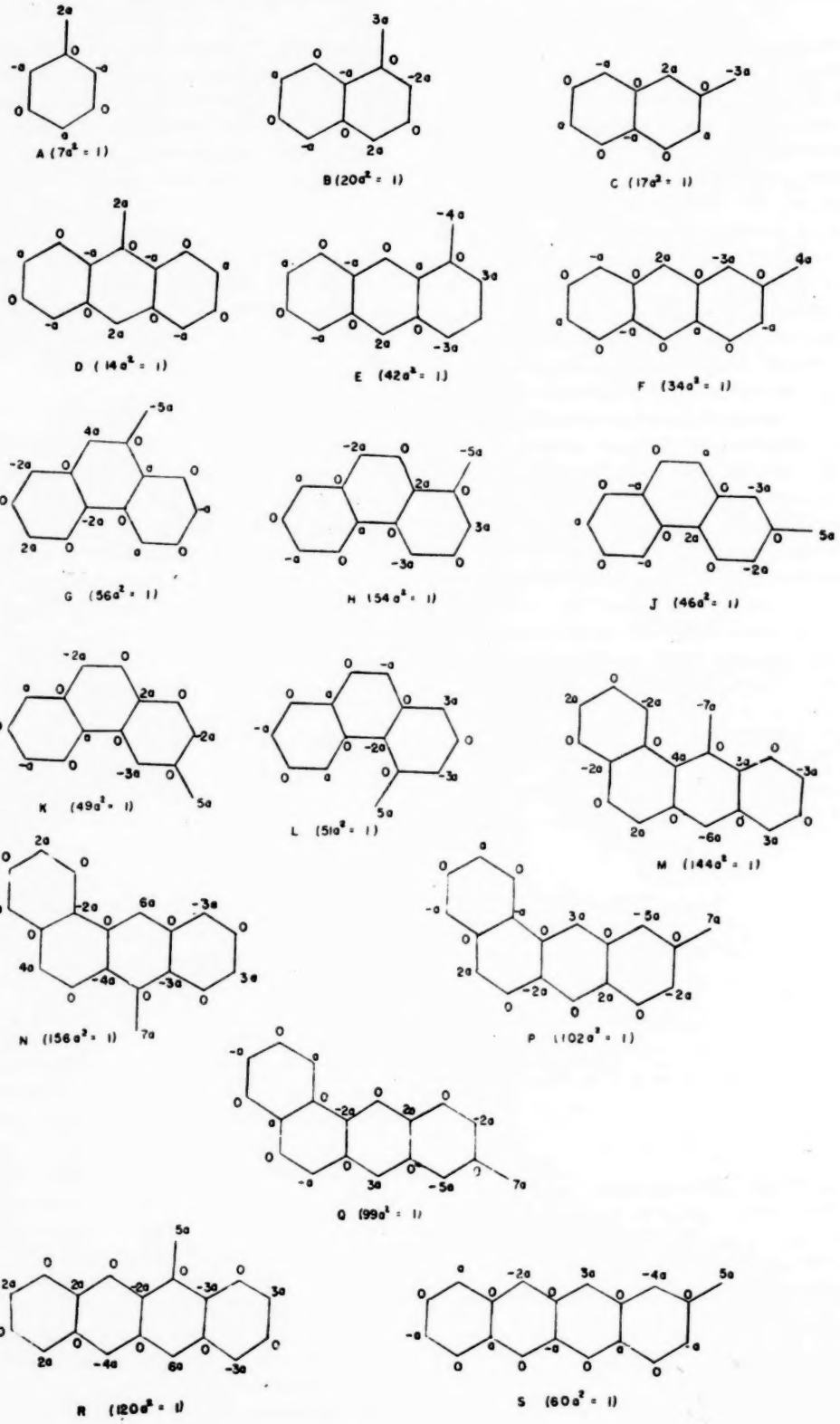

THE JOURNAL OF CHEMICAL PHYSICS VOLUME 18, NUMBER 3 MARCH, 1950

Some Studies in Molecular Orbital Theory
III. Substitution in Aromatic and Heteroaromatic Systems*

H. C. LONGUET-HIGGINS
Department of Physics, University of Chicago,† Chicago, Illinois
(Received June 13, 1949)

It is shown that LCAO molecular orbital theory, when combined with first-order perturbation theory, provides a very simple procedure for estimating how far electronic effects will modify the transition state energies for substitution reactions in alternant molecules. This procedure is shown to lead to the same qualitative predictions as resonance theory, but has the advantage that it gives at the same time quantitative information as to the relative effects of substitution at different points in a complex system. The theoretical results agree well with experiment as far as can be ascertained at present.

The approximations involved, and their relation to those of resonance theory, are discussed in detail.

1. INTRODUCTION

THE theory of resonance between classical valence-bond structures has proved triumphantly successful in explaining the stabilities and reactivities of organic molecules in terms of their electronic structures. However, up to the time of writing, the qualitative successes of the theory have not been extensively followed up with quantitative calculations.‡ This is primarily because in discussing molecules containing atoms other than carbon and hydrogen it is necessary to take into account ionic structures, and the contributions of such structures to the wave function and energy of a molecule are not easy to estimate by the valence-bond method. Almost all the quantitative calculations made in the past on polyatomic heteromolecules have been carried out by the method of molecular orbitals; and although the results generally agree with those of resonance theory, few attempts have been made to unite the ideas which lie behind the two approaches, or to discover how far agreement may be expected to extend beyond the special cases worked out.

In this paper it will be shown that the most significant general predictions of resonance theory, as to the reactivity of conjugated systems, do indeed follow from a combination of molecular orbital theory and perturbation theory; and that with the latter combination of theoretical tools it is possible to calculate quite simply the relative stabilities of isomeric systems containing heteroatoms. Such systems include both individual molecules and reaction complexes, so one can discuss both energies and rates of reaction in this way.

2. SUBSTITUTION IN AROMATIC SYSTEMS

The attack of electrophilic (cationoid) and nucleophilic (anionoid) reagents on conjugated systems has been discussed quantitatively from two points of view. On the one hand, calculations have been made[1] on the unsaturation energy of the transition complexes involved in substitution reactions; and it has been found that for a given reagent R and a series of different positions of attack on a given substrate S, the rate of reaction is higher the lower the energy of the π-electrons in the transition state RS. Such calculations justify the view that differences in substitution rate in conjugated systems are indeed determined principally by the changes in energy of the π-electrons; and this assumption will be made throughout the present paper. On the other hand,[2,3] it has been demonstrated that if two positions in a conjugated molecule differ considerably in "π-electron density" q, then the position with the higher value of q is more susceptible to attack by electrophilic reagents, whereas nucleophilic reagents substitute more easily at the position of lower electron density.

Calculations on the transition state are of course more reliable than calculations of electron density for predicting the relative rates of analogous reactions, and in the following pages the former approach will be adopted as far as possible; but for certain types of substitution electron density calculations are much easier to make, and provide a useful supplement to the more rigorous approach.

3. SCOPE OF THIS PAPER

For the most part we shall be concerned with heterolytic substitution reactions, that is, bimolecular reactions of the type

$$A+BC\rightarrow AB+C,$$

where A is an electrophilic or nucleophilic reagent and BC is a conjugated molecule, not necessarily a hydrocarbon. Reactions of the above general type in which A is electrophilic have been called S_E2 reactions by

* Work done under ONR, Task Order IX of Contract N6ori-20, with the University of Chicago.
† Now at the Department of Chemistry, Manchester University, Manchester, England.
‡ The procedure of counting resonance structures in order to estimate resonance energy has no basis in quantum theory, and should be relegated to the limbo of what Guggenheim has called "sesqui-empirical methods."

[1] G. W. Wheland, J. Am. Chem. Soc. **64**, 900 (1942).
[2] G. W. Wheland and L. Pauling, J. Am. Chem. Soc. **57**, 2091 (1935).
[3] H. C. Longuet-Higgins and C. A. Coulson, Trans. Faraday Soc. **43**, 87 (1947).

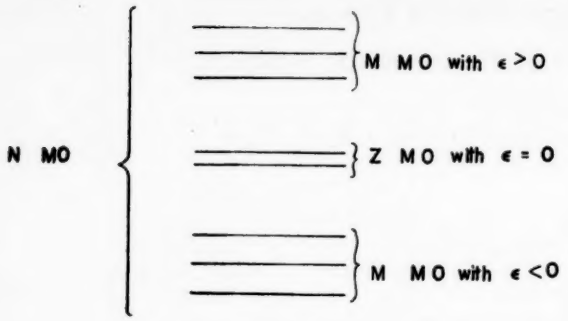

FIG. 1.

Hughes and Ingold[4] and their school:¶ a typical S_E2 reaction is the nitration of an aromatic compound, represented by the equation

$$NO_2^+ + ArH \rightarrow ArNO_2 + H^+.$$

If the substrate ArH contains $2m$ π-electrons distributed over n atomic orbitals, then the transition complex NO_2ArH^+ will have $2m-2$ π-electrons distributed over $n-1$ atomic orbitals. (The π-electrons of the nitro group are not counted, since they are not conjugated with the aromatic π-electrons in the transition state.) This statement applies to all S_E2 reactions in which A attacks an unsaturated carbon atom of BC. On the other hand, for S_N2 reactions, in which A is nucleophilic, the electronic mechanism is essentially different. A typical S_N2 reaction is the hydrolysis of aryl chlorides to phenols, according to the equation

$$OH^- + ArCl \rightarrow ArOH + Cl^-.$$

In this type of reaction the transition complex $HOArCl^-$ contains the same number, $2m$, of π-electrons as the substrate, these electrons being again distributed over $n-1$ atomic orbitals.

The first problem that will be considered is:

What can be said about the difference in activation energy between two S_E2 reactions or two S_N2 reactions having precisely similar electronic mechanisms? To make the question clearer, it is necessary to introduce the idea of *isoaromatic* systems. If two conjugated systems have the same number of π-electrons, moving in geometrically similar sets of atomic p orbitals, the two systems are said to be isoaromatic. Thus naphthalene, quinoline, and isoquinoline are all isoaromatic, and nitrobenzene is isoaromatic with the benzoate ion. Two *reactions* are said to be isoaromatic if and only if both the substrates *and* the transition complexes are isoaromatic. Thus the nitration of benzene is isoaromatic with the nitration of toluene in any position, and the 1-chlorination of naphthalene is isoaromatic with the 5-chlorination of isoquinoline; but the 2-nitration of naphthalene would not be isoaromatic with the 1-nitration of the same molecule because the transition complexes have different geometry.

The above question may now be put in the form: What will be the difference in activation energy between two isoaromatic S_E2 or S_N2 reactions? This question will be discussed in Sections 5 and 6, and it will be shown that the relative stabilities of isoaromatic systems can be understood very simply in terms of LCAO molecular orbital theory.

Another problem of importance is to predict theoretically the relative rates of two reactions which are not strictly isoaromatic. This problem is discussed in Section 8, and, as would be expected, the theory is not quite so straightforward as for isoaromatic reactions. Nevertheless, if one assumes that the activation energy of a reaction is correlated with the change in unsaturation energy in the early stages of reaction, it is possible to predict differences in reactivity on the basis of electron density values; and in many important cases these electron density values may be calculated to a first approximation without having to solve any secular equations.

It is obviously desirable to understand as far as possible how the results obtained by these quantitative methods are related to those of qualitative resonance theory; so an attempt has been made to interpret the latter theory in terms of the former, where this is possible, and to discover to what extent the two theories rely on the same physical principles.

4. ALTERNANT HETEROMOLECULES

In what follows, we shall be mainly concerned with heteromolecules satisfying the conditions: (a) The number of π-electrons is even, all these electrons being paired. (b) No odd-membered rings of conjugated atoms are present. (c) In the isoaromatic hydrocarbon all the MO of negative energy are filled, and all the MO of positive energy are empty.

Of these conditions the first rules out free radicals, and the second defines the class of alternant molecules,

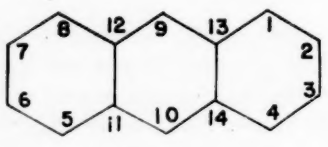

FIG. 2.

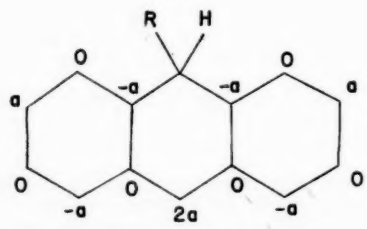

$(a^2 = 1/10)$

FIG. 3.

[4] E. D. Hughes and C. K. Ingold, J. Chem. Soc. 244 (1935).

¶ The symbols S_N2 and S_E2 have been most used in discussing substitution at a *saturated* carbon atom; but there seems to be no objection to removing this restriction.

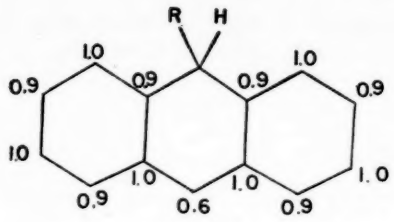

FIG. 4.

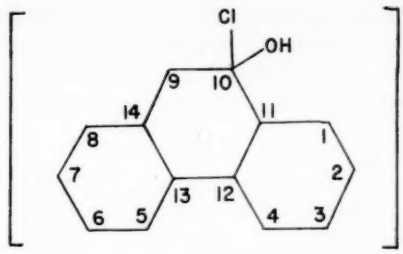

FIG. 5.

in the sense of Papers I* and II.† In order to see whether condition (c) holds for a given heteromolecule, it is necessary to find the arrangement of the MO energies in the isoaromatic hydrocarbon. Let N be the total number of MO (equal to the number of conjugated atomic orbitals), and let Z be the number of zero-energy MO. By the theorem quoted in Paper I, the numbers of MO of positive and negative energy must be equal, to M say; so $N=2M+Z$, and the arrangement of MO energies is as shown in Fig. 1. For the parent hydrocarbon not to contain unpaired electrons, the levels Z must either all be filled or all be empty. So if P is the number of π-electrons, the following three cases may be distinguished:

(1) $Z=0$, $P=2M$. Hence, according to the Coulson-Rushbrooke theorem,[5] $q_r=1$ at every position.

(2) $Z>0$, $P=2M$. The electron densities are then given by,

$$q_r=2\sum_m (c_r^m)^2, \tag{1}$$

where m refers to a MO of negative energy. But, as shown in Paper I,

$$1=2\sum_m (c_r^m)^2+\sum_z (c_r^z)^2, \tag{2}$$

where z refers to a MO of zero energy. Hence,

$$q_r=1-\sum_z (c_r^z)^2. \tag{3}$$

(3) $Z>0$, $P=2M+2Z$. In this case

$$q_r=2\sum_m (c_r^m)^2+2\sum_z (c_r^z)^2. \tag{4}$$

Combining (2) with (4) we get

$$q_r=1+\sum_z (c_r^z)^2. \tag{5}$$

Now, as shown in Paper I, the number Z of zero-energy MO in an alternant hydrocarbon and their AO coefficients c_r^z, may be obtained without evaluating the roots of the secular determinant. So, if conditions (a), (b), and (c) are satisfied, the electron densities q_r may be found very easily.

5. ISOAROMATIC REACTIONS

It will now be shown how first-order perturbation theory can be used to calculate approximately the difference in unsaturation energy between a heteromolecule and the isoaromatic hydrocarbon.

Denote by ϵ_0^j the energy of a π-electron in the MO ψ^j of the hydrocarbon. Then replacement of one or more carbon atoms by heteroatoms will change the value of ϵ_0^j to ϵ^j, say, where, by first-order perturbation theory,[6]

$$\epsilon^j=\epsilon_0^j+\int \psi^j H' \psi^j d\tau, \tag{6}$$

and H' denotes the difference between the effective 1-electron Hamiltonian for the hydrocarbon and the heteromolecule. Now in LCAO approximation,

$$\psi^j=\sum_r c_r^j \phi_r;$$

so the above equation becomes

$$\epsilon^j=\epsilon_0^j+\sum_r\sum_s c_r^j c_s^j \int \phi_r H' \phi_s d\tau.$$

The most important of the integrals under the double summation will be the Coulomb terms of the various heteroatoms, the Coulomb term of atom r being defined as $\int \phi_r H' \phi_r d\tau, = \alpha_r$, say. Hence, to a fair approximation,

$$\epsilon^j=\epsilon_0^j+\sum_r (c_r^j)^2 \alpha_r.$$

Summing over the π-electrons we get

$$\mathcal{E}=\mathcal{E}_0+\sum_r q_r \alpha_r, \tag{7}$$

where $\mathcal{E}$ is the unsaturation energy of the heteromolecule, $\mathcal{E}_0$ that of the parent hydrocarbon, and q_r is the π-electron density at position r in the latter. Equation (7) was used with success in Paper II for interpreting the basic strengths of heterocycles. It will now be used to calculate the relative rates of isoaromatic reactions.

Equation (7) implies that alteration of the Coulomb integral of atom r in a substrate changes the unsatura-

* H. C. Longuet-Higgins, J. Chem. Phys. 18, 265 (1950), hereafter referred to as Paper I.

† H. C. Longuet-Higgins, J. Chem. Phys. 18, 275 (1950), hereafter referred to as Paper II.

[5] C. A. Coulson and S. Rushbrooke, Proc. Camb. Phil. Soc. 36, 193 (1940).

[6] L. Pauling and E. B. Wilson, *Introduction to Quantum Mechanics* (McGraw-Hill Book Company, Inc., New York, 1935).

tion energy by approximately $q_r\alpha_r$, q_r being the π-electron density at atom r in the isoaromatic hydrocarbon. For a given reaction of this substrate the perturbation α_r will therefore lower the activation energy by an amount

$$\alpha_r(q_r-q_r'), \tag{8}$$

where q_r' is the electron density at position r in the transition complex, or rather, in the hydrocarbon isoaromatic with it. Thus, if the perturbation increases the electron affinity of atom r ($\alpha_r<0$), the reaction will be favored by a high value of q_r', but if $\alpha_r>0$, the reverse is true. The electron densities q_r and q_r' in Eq. (8) are calculated from the equations of Section 4.

6. EXAMPLES

(1) A typical problem in orientation theory is the following: To what extent will the rate of 9-nitration of anthracene be affected by methyl or aza-substitution at other positions in the molecule? For example, one might wish to estimate the relative rates at which 1-methyl, 2-methyl, 3-methyl, 4-methyl, and 10-methyl anthracenes nitrate in the 9-position, the numbering of the positions being as shown in Fig. 2. The effect of methyl substitution will be taken into account by supposing that it alters the Coulomb integral of the substituted carbon atom by an amount $\alpha>0$. Now the electron densities on the carbon atoms in anthracene are all unity, by the Coulson-Rushbrooke theorem, so any differences in nitration rate between the various methyl anthracenes will be due to differences in the electron densities q_r' in the transition complex. In the transition complex, position 9 is no longer conjugated with the rest of the molecule, and two π-electrons have been removed from the aromatic system to form a σ-bond with the nitro group; so 12 π-electrons are left, distributed over 13 carbon atoms. Using the relations between resonance structures and MO established in Paper I, we deduce that in the transition state there is one MO of zero energy, and that its AO coefficients are finite only at positions 2, 4, 5, 7, 10, 12, and 13, where the plus charge is located in the principal resonance structures. It is easily verified that these coefficients c_r^z are as shown in Fig. 3. For the transition complex $Z=1$ and $N=13$, so $2M=12=P$. So Eq. (3) applies, and the electron densities q_r' in the transition complex are as shown in Fig. 4.

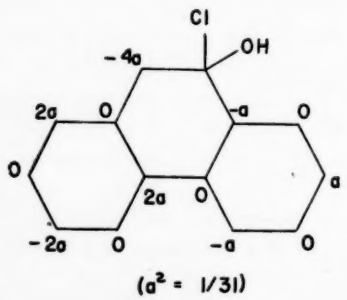

FIG. 6.

By Eq. (8), therefore, methyl substitution at the various positions lowers the activation energy by the following amounts:

1-methyl	$+0.0\alpha$
2-methyl	$+0.1\alpha$
3-methyl	$+0.0\alpha$
4-methyl	$+0.1\alpha$
10-methyl	$+0.4\alpha$.

Therefore, 10-methyl substitution lowers the activation energy for 9-nitration four times as much as 2-methyl or 4-methyl substitution, whereas 1- or 3-methyl substitution has no effect. Now in anthracene itself the 1 and 4 positions are obviously equivalent, and so are the 2- and 3-positions. From the experimental point of view, therefore, the significant predictions are that a 1-methyl group activates the 10-position but not the 9-position, a 2-methyl group activates the 9-position but not the 10-position, and a 10-methyl group activates the 9-position, the three energy shifts being in the ratio 1:1:4.

(2) A precisely analogous discussion is possible of how aza-substitution affects the anionoid activity of a given position in an aromatic system. Suppose we are interested in the relative effects of aza-substitution in different places on the hydrolysis of the chlorine atom in 10-chloro-phenanthrene. It is probably a good approximation to neglect the conjugation of the Cl atom with the aromatic system, in which case the π-electron densities q_r will be unity at all positions in the substrate. So here again, any differences in rate of hydrolysis between the various aza-derivatives will be ascribed to differences in q_r', and hence in energy, in the corresponding transition complexes. The transition complexes probably have the general structure shown in Fig. 5 with 14 π-electrons associated with 13 carbon atoms. The rules given in Paper I demand that there shall be one zero-energy MO, with AO coefficients vanishing at all positions except 2, 4, 6, 8, 9, 11, and 13; and it is easily checked that the coefficients c_r^z are in fact as shown in Fig. 6. So $Z=1$, $M=\frac{1}{2}(N-Z)=6$, $P=14=2M+2Z$, and Eq. (5) may be applied. The electron densities q_r' in the transition complex are therefore as given in Fig. 7. Now if α is the Coulomb term for aromatic nitrogen, the activating effect of aza-substitution at position r is, by Eq. (8),

$$\alpha(1-q_r').$$

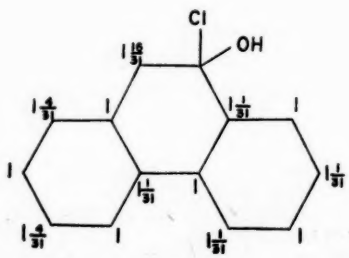

FIG. 7.

We conclude that aza-substitution in positions 1, 2, 3, 4, 5, 6, 7, 8, and 9 lowers the activation energy for the hydrolysis of the chlorine atom by amounts in the ratios 0:1:0:1:0:4:0:4:16. Whether these figures are quantitatively correct or not, they certainly agree well with the observation that 10-chloro-phenanthridine is much more easily hydrolyzed than other aza-10-chloro-phenanthrenes.

(3) The ionization of "reactive" methyl groups was discussed briefly in Paper II. This is not an aromatic substitution, of course, but nevertheless the present ideas may be applied. We may compare the energies of ionization of the methyl group in toluene and the methyl groups in the three aza-toluenes (picolines). Ionization of the methyl group gives a system isoaromatic with the benzyl anion, which has eight π-electrons and seven MO, one of which has zero energy; so the π-electron densities in the ion are given by Eq. (5). They are as shown in Fig. 8 (see Paper II). Hence aza-substitution at the meta-position does not affect the activity of the methyl group, whereas aza-substitution at the ortho or para positions activates the methyl group by an amount $(1/7)\alpha$. A further point is that the group $=NR^+$, which has a higher electron affinity than $=N$, will also have a larger value of α, and this is why quaternation of α- and γ-picolines greatly enhances the reactivity of their methyl groups.

(4) A more complicated example is the problem of where S_E2 substitution should occur in the molecule 2,4-diamino-pyridine. The presence of three heteroatoms in this molecule probably makes it less accurate to apply Eq. (7) than in the above three examples; but all the same it is interesting to see what the theory predicts. The numbering of the atoms is as shown in Fig. 9: the attacking reagent may enter in any one of positions 3, 4, or 6. The transition complexes formed by attack of an electrophilic reagent in positions 3, 4, and 6 are all isoaromatic, differing only in the position of the nuclear nitrogen atom. (This is, of course, why the example has been chosen.) The parent hydrocarbon of the three transition complexes would have seven MO (this being the number of conjugated AO), one having zero energy, with coefficients as shown in Fig. 10(a). There are eight π-electrons, so the zero-energy MO contains two electrons, and the π-electron densities are as shown in Fig. 10(b).

The electron density in the transition complex is therefore highest on one of the NH_2 groups and on the unsubstituted atom next to the position of attack. Aza-substitution of the latter atom will therefore lend the transition complex most stability, so 2,4-diamino-pyridine should be most sensitive to electrophilic reagents in the 6-position. What resonance theory would predict in this case is not at all clear, but it might be

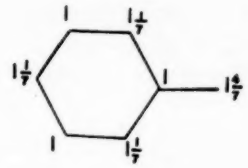

FIG. 8.

thought that the 4- and 6-positions would be deactivated by the nuclear heteroatom, and that S_E2 substitution would therefore occur at the 3-position. This is an interesting point which should be checked experimentally.

(5) The problem of orientation by substituents in the benzene ring has been solved qualitatively many times over, and semiquantitatively by Wheland and Pauling.[2] However, it is instructive to see how the results of the latter authors may be understood from the present viewpoint. The substituent X in C_6H_5X affects the aromatic ring in either or both of two ways: (1) it may alter the Coulomb integral of the adjacent carbon atom‡ (inductive effect), and (2) the atom or residue X may itself possess π-electrons which can conjugate with the ring π-electrons (electromeric effect). Insofar as the inductive effect is the more important, as it probably is in toluene and the anilinium ion, the ortho, meta, and para S_E2 or S_N2 reactions of C_6H_5X are isoaromatic, and may be discussed as follows:

The transition states for substitution at the ortho, meta, or para positions are all isoaromatic with a 5-carbon chain having four or six π-electrons according as S_E2 or S_N2 substitution is being considered. This 5-carbon chain has one zero-energy MO, with coefficients as shown in Fig. 11. Therefore, in S_E2 reactions the positive charge on the transition complex is located equally at the three positions ortho and para to the position being attacked, and the same applies to the negative charge in S_N2 reactions. The electron densities q_r' at the various positions in the three possible types of transition complex are therefore as follows:

	$q_1'=q_5'$	$q_2'=q_4'$	q_3'
S_E2	$\frac{2}{3}$	1	$\frac{2}{3}$
S_N2	$1\frac{1}{3}$	1	$1\frac{1}{3}$
S_R2	1	1	1.

(Here S_R2 means bimolecular substitution by free radicals. For such reactions the transition complex contains five mobile electrons, so by the Coulson-Rushbrooke theorem the electron density is unity at each of the five carbon atoms.) If we denote by α the difference

FIG. 9.

‡ Strictly speaking, the inductive effect also affects the other ring atoms; but this can be ignored in first approximation.

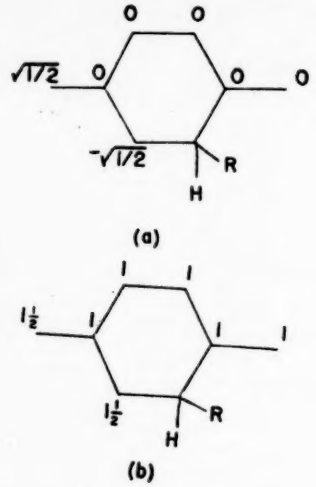

FIG. 10.

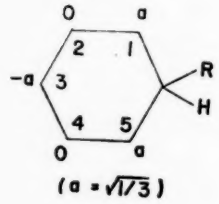

FIG. 11.

in Coulomb integral between the substituted carbon atom and the others, then the activating effects of the substituent X on the nine types of substitution are as follows:

	Ortho	Meta	Para
S_E2	$\frac{1}{3}\alpha$	0	$\frac{1}{3}\alpha$
S_N2	$-\frac{1}{3}\alpha$	0	$-\frac{1}{3}\alpha$
S_R2	0	0	0.

This shows that in first approximation S_R2 reactions are unaffected by inductive substituents, as are S_E2 and S_N2 reactions in the meta position. Substituents such as NR_3^+, for which $\alpha<0$ ($+I$ substituents) deactivate the ortho and para positions equally toward electrophilic reagents; whereas substituents such as CH_3 with $\alpha>0$ ($-I$ substituents) have precisely the opposite effect. The above argument follows similar lines to one given by Dewar[7] in his recent book, and perhaps makes clearer why the inductive effect discriminates between the meta positions and the others.

When the electromeric effect of X is more important than the inductive effect, the complication arises that the transition complexes corresponding to substitution in the ortho, meta, and para positions are not isoaromatic. In order to study the relative reactivities of these three positions, it is necessary either to solve the secular equations completely for the transition states, as was done by Wheland,[1] or to fall back on calculations of electron density at the different positions in the substrate, as done by Wheland and Pauling.[2] If the latter procedure is accepted as reliable, the electron densities can often be estimated without solving the secular equations, by the method outlined in Section 2, and this means a considerable saving of labor. This point will be taken up in Section 8.

[7] M. J. S. Dewar, *Electronic Theory of Organic Reactions* (Oxford University Press, London, 1949).

7. DISCUSSION

The conclusions arrived at so far may be summarized as follows: (1) For a given reaction, if the substrate has electron density q_r at position r, and the electron density is q_r' at the same position in the transition complex, then alteration of the Coulomb integral of atom r by an amount α will lower the activation energy for the reaction by an amount $\alpha(q_r-q_r')$. (2) For many types of reaction, such as those discussed in the preceding section, the electron densities q_r and q_r' depend only on the AO coefficients c_r^2 belonging to zero-energy MO, so the relative activating effects of $\pm I$ substituents at different positions may be quantitatively calculated without solving the secular equations.

There is for many types of reaction a correspondence between the above results and the predictions of qualitative resonance theory. For instance, in example (2) of the previous section the π-electron densities are unity at all positions in 10-chloro-phenanthrene, but the electron densities q_r' in the transition complex with the OH ion exceed unity at those atoms which bear the negative charge in one or more principal resonance structures. Therefore the transition complex is stabilized by an increased positive field at one of the charged positions; and this is precisely what is implied by the statement that resonance structures containing $\diagdown\!\overset{-}{\text{N}}\!\diagup$ are more stable than those containing $\diagdown\!\overset{-}{\text{CH}}\!\diagup$. The fundamental connecting link between the resonance and MO predictions is the fact, proved in Paper I, that in alternant hydrocarbon ions the ionic charge is distributed entirely over the atoms that bear the charge in the principal resonance structures. This result may be regarded as a kind of correspondence principle between resonance theory and LCAO MO theory, and is frequently illuminating when one wishes to interpret the former theory in terms of the latter.

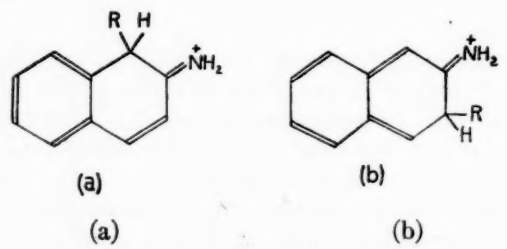

FIG. 12.

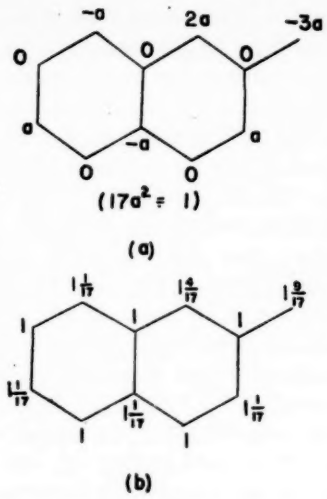

FIG. 13.

8. REACTIONS WHICH ARE NOT ISOAROMATIC

In the preceding sections we have seen how it is possible to estimate differences in activation energy for two or more reactions in which both the substrates and the transition complexes are isoaromatic. It is clearly desirable to see if an equally simple treatment can be given for reactions in which the transition complexes differ in their geometry. For example, it should be possible to understand in simple terms why 2-naphthylamine directs electrophilic reagents into position 1 rather than position 3, say. The most rigorous kind of calculation would be to solve the secular equations for the complexes (a) and (b) in Fig. 12, and thus obtain the difference in their unsaturation energies. If this is done, it does indeed turn out that (b) is less stable than (a); but this sort of calculation becomes prohibitively laborious when the aromatic system contains more than two rings. On the other hand, the electron distribution in a heteromolecule is often a good index of its behavior in S_E2 and S_N2 substitutions; so we shall now apply the methods outlined in Section 4 to the calculation of electron densities in heteromolecules.

To return to the example of 2-naphthylamine, two different extreme approximations can be made in calculating the π-electron densities in this molecule. The first is to assign the Coulomb integral of the nitrogen atom an infinite negative value; in this case two π-electrons would be localized on the NH_2 group, the remaining ten having the same distribution as in naphthalene, so that the π-electron density would be unity at every carbon atom. The other approximation is to assume that the nitrogen atom has the same Coulomb integral as aromatic carbon, so that we have in effect a carbanion with 11 atomic orbitals and 12 π-electrons. The principal resonance structures for this carbanion all have just one carbon atom bearing an unshared pair of π-electrons, so there is one zero-energy MO whose AO coefficients are finite only at these "active" atoms. According to the definitions of Section 5, therefore, $Z=1$, $2M=10$, $P=12=2M+2Z$, so the molecule is of Type (3), and the electron densities may be calculated from Eq. (5). To find the coefficients c_r^2 we first observe that in any principal resonance structure the negative charge must be located either at the external position or at a position separated from it by an even number of bonds; c_r^2 therefore vanishes at positions 2, 4, 5, 7, and 9. It is then obvious that the remaining AO coefficients have the values shown in Fig. 13(a) and that the π-electron densities are as given in Fig. 13(b).

The question is: will the electron densities in 2-naphthylamine be nearer to those shown in Fig. 13(b) or to those in naphthalene? The following argument suggests that Fig. 13(b) probably gives not too inaccurate a picture of the electron distribution in the amine. In calculating the coefficients given in Fig. 13(a), it has been assumed that the Coulomb integral of the external atom is the same as that of a ring atom. This assumption leads to a considerably greater negative charge on the external atom than on any of the ring atoms, so that the electron affinity of the external atom would be reduced more than that of the others. So a negative value of α for the external atom would be required to make the field self-consistent, and it is even possible that the electron distribution given in Fig. 13(b) is a better approximation for the amine than for the isoaromatic carbanion. Be that as it may, the actual electron densities in the amine almost certainly lie between those in naphthalene and those given in Fig. 13(b), and the latter probably gives a more or less correct picture of the relative net charges at the carbon atoms. Certainly the electron densities given in Fig. 13(b) accord well with the high reactivity of the 1-position in 2-naphthylamine toward electrophilic reagents as compared with any of the other positions.

The elementary calculations just described for 2-naphthylamine may be extended to disubstituted alternant hydrocarbons, provided that the heterosubstituents are separated by even numbers of unsaturated bonds. As an example, let us work out the electron distribution in the diamine depicted in Fig. 14. If we carry out the starting process described in Paper I, starting with one of the NH_2 groups, we find that the other NH_2 group is also starred, and that there are altogether 11 starred atoms and nine unstarred atoms. Therefore there must be $11-9=2$ zero-energy MO in the isoaromatic hydrocarbon; and both of these are distributed entirely over

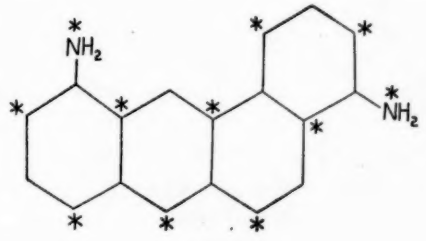

FIG. 14.

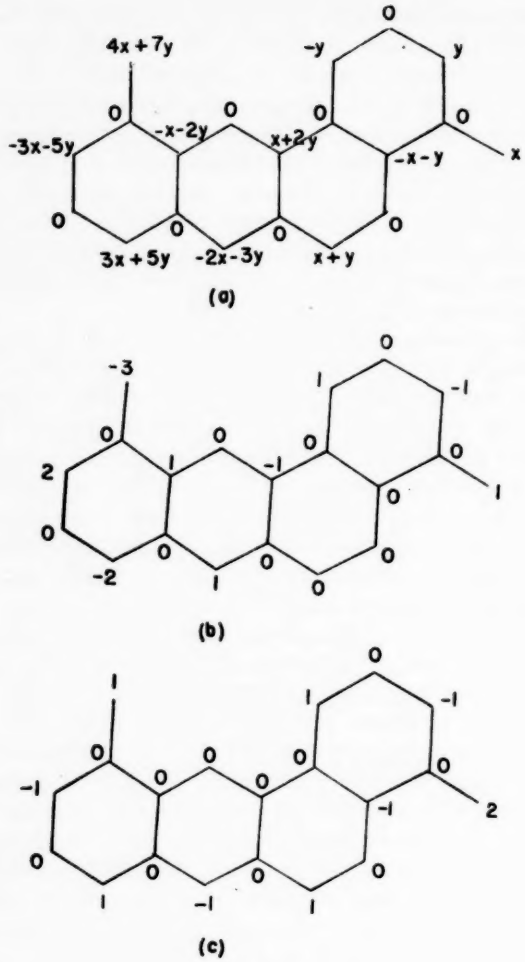

FIG. 15.

the starred atoms, since in every principal resonance structure there are nine double bonds, and every unstarred atom is therefore doubly bonded in all the structures. To find the net charges at the various atoms we require the AO coefficients for the two zero-energy MO only. These MO are not completely determined, —any orthonormal combination is equally valid—but the sum of the squares of their coefficients at a given atom is determinate, being invariant under an orthogonal transformation of the two MO. Denote by x and y the AO coefficients of a zero-energy MO at the left-hand NH_2 group and the ring position ortho to it. Then the other coefficients must be as shown in Fig. 15(a). Putting $x=1$, $y=-1$ and $x=2$, $y=-1$, we get the linearly independent (but not normalized or orthogonal) combinations of AO shown in Figs. 15(b) and 15(c), respectively. By well-known methods we can obtain from these combinations two orthonormal MO, and the sum of the squares of their AO coefficients at each position are given in Fig. 16.¶ In view of Eq. (7), the numbers in Fig. 16 also represent the net negative charges at the various positions, except at the nitrogen atoms, which have net positive charges equal to the differences of these numbers from unity. As in the case of 2-naphthylamine, the true π-electron densities are probably nearer to unity than the values in Fig. 16, but the order is probably more or less correct. The diamine should therefore be more reactive in the left-hand ring than in the right-hand one.

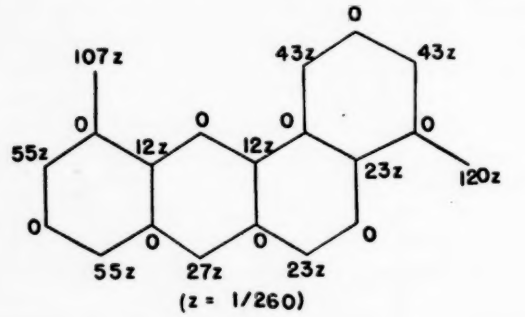

FIG. 16.

Although in the heteromolecules discussed, relative net charges may be calculated with little labor, this can by no means always be done, even for alternant molecules. If a molecule contains two heterosubstituents separated by odd numbers of unsaturated bonds, as in the hydroquinones, the isoaromatic hydrocarbon will not in general have any zero-energy MO, so Eq. (7) cannot be applied. But provided all the heteroatoms are in the same class when the starring process is carried out, the parent hydrocarbon will have enough zero-energy MO to accommodate all the extra electrons, and the approximate electron distribution may be calculated by the simple method just described.

9. CONCLUSIONS

Two quite different lines of thought have been pursued in this paper. On the one hand, it has been shown how differences in activation energy between isoaromatic reactions may be calculated by first-order perturbation theory, provided conditions (a), (b), and (c) of Section 4 are satisfied. On the other hand, it has been shown that the relative reactivities of different positions in a heteromolecule can be estimated from the calculated electron distribution in the parent hydrocarbon ion. It must be emphasized that calculations of the former kind are probably much more reliable than those of the latter sort. There are two main reasons for this. (1) As has already been said, calculations on the transition state provide a much firmer basis for predicting relative reaction rates than calculations of electron density in the substrate, although in a given substrate there often seems to be a close correspondence between the calculated electron distribution and the observed chemical

¶ Alternatively, we can use the result that if $\chi_1=\Sigma_r a_r\phi_r$ and $\chi_2=\Sigma_r b_r\phi_r$ are two linearly independent combinations of AO, and if $\Sigma_r c_r\phi_r$ and $\Sigma_r d_r\phi_r$ are two orthonormal combinations of χ_1 and χ_2, then

$$c_i^2+d_i^2=\frac{a_i^2\,\Sigma_r b_r^2-2a_ib_i\,\Sigma_r a_rb_r+b_i^2\,\Sigma_r a_r^2}{\Sigma_r a_r^2\,\Sigma_r b_r^2-(\Sigma_r a_rb_r)^2}.$$

behavior. (2) It is certainly not correct to neglect the Coulomb terms of the heteroatoms in working out the electron distribution in a heteromolecule. It might be argued that the latter objection applies as much to calculations of transition state energies as to calculations of electron distribution; however, this seems not to be so, for the following reasons. In calculating the unsaturation energy of a heteromolecule or transition complex by Eq. (7), we are essentially using first-order perturbation theory; and it is well known that the first-order correction to the energy of a perturbed system is obtained by integrating the perturbation over the unperturbed wave function. In other words, even an inaccurate wave function gives the energy fairly accurately if the right Hamiltonian is used, and this is the basis of Eq. (7). On the other hand, the electron densities in a heteromolecule depend on the AO coefficients in the π-orbitals, and these coefficients differ in first order between a heteromolecule and the parent hydrocarbon. So the electron densities calculated in Section 8 should not be taken too literally, although their relative values are probably correct.

Before concluding, it seems worth while to compare briefly the present ideas with those of qualitative resonance theory. The first point to be made is that neither approach pretends to do more than account for the energy changes due to electronic conjugation in a molecule; other energy terms, and all entropy terms, have to be ignored altogether. Therefore both theories should be most successful when used to account for the relative stabilities of two species, or the relative rates of two reactions, in which these other energy and entropy terms are nearly equal. Second, the results of Paper I establish, and the examples of Sections 6 and 8 illustrate, the fact that the approximate quantitative theory outlined here is bound to give qualitatively the same π-electron distribution in an alternant molecule as would arise from resonance among the principal resonance structures *only*, the higher excited structures being absent altogether. Third, Eq. (7) shows that a heteroatom confers most stability on a conjugated system if the isoaromatic hydrocarbon has a high electron density at the corresponding position; and this is physically equivalent to the statement that a heteroatom is relatively more stable with two unshared p electrons than a carbon atom. (A heteroatom here means an atom to the right of carbon in the Periodic Table.) So a large measure of agreement is to be expected in general between the results of MO theory and predictions based on the principal resonance structures only.

The methods of calculation outlined are not to be regarded as a substitute for the more precise method of Wheland[1] in cases for which (a) the required Coulomb integrals are all known with moderate certainty, and (b) solution of the secular equations is not prohibitively laborious; and, of course, there are many important molecules to which the present calculations cannot be applied, even in principle. However, for problems such as example 2 in Section 6, the labor involved in applying Eqs. (3) and (5) is infinitesimal compared with that required to set up and solve the secular equations for all the species involved; and the difference between the results of the two kinds of calculation is not likely to be as significant as the error due to uncertainty in the Coulomb term for aromatic nitrogen.[8] As is well known, the labor of solving the secular equations increases rapidly with the size of the molecule, particularly if there is no symmetry; and to solve the secular equations for all the possible transition states that could be formed by the diamine in Fig. 14 would be extremely tedious, and not very illuminating. The present method, it is hoped, provides a moderately balanced compromise between accuracy and speed for calculations on complex systems; and perhaps provides a clearer picture of why the more exact calculations come out in the way that they do.

My thanks are due Dr. J. R. Platt for much stimulating discussion.

[8] C. A. Coulson and H. C. Longuet-Higgins, Proc. Roy. Soc. **A192**, 16 (1947).

THE JOURNAL OF CHEMICAL PHYSICS VOLUME 18, NUMBER 3 MARCH, 1950

The Effect of the Electrostatic Polarization of the Solvent on Electronic Absorption Spectra in Solution

NOEL S. BAYLISS
Department of Chemistry, University of Western Australia, Nedlands, Western Australia
(Received June 29, 1949)

Regarding the solvent as a continuous dielectric medium, it is shown that its effect on the Franck-Condon absorption of light by solute molecules must be expressed in terms of the electronic polarization part of its dielectric constant, $K=n^2$. Using methods based both on quantum theory and on classical dispersion theory, it is shown that the red shift of absorption in solution depends directly on f, the oscillator strength, and inversely either on a^2 (a is the radius of the spherical solute molecule) or the polarizability α. The expression $\Delta\nu(\text{cm}^{-1})=\text{const.}\ (f/\nu a^3)[(n^2-1)/(2n^2+1)]$ with two possible values of the constant, and alternatively with the substitution of α for a^3, is tested on experimental data for isoprene, benzene, bromine, and iodine. Good quantitative agreement is obtained for the (V, N) transitions of isoprene and benzene. If the strong ultraviolet absorption of bromine and iodine solutions is regarded as the displaced (V, N) transition, the quantitative agreement is poor, although qualitatively in accordance with the theory. The weak λ2600 system of benzene, and the visible continua of bromine and iodine, show the expected smaller $\Delta\nu$ with smaller f, although quantitative comparison with theory is prevented by the superposition of other solvent effects which become important in weak absorption bands.

INTRODUCTION

THE red shift of visible and ultraviolet electronic absorption spectra in solution from their position in the gas state has long been related to the dielectric constant or to the refractive index of the solvent. This paper will develop a theory for the solvent shift in terms of the electrostatic or polarization forces of the solvent assuming it to be a continuous dielectric medium, bearing in mind that observed solvent displacements may well be the result of the superposition of several effects of which the electrostatic effect is only one. Two methods of approach will be used, the first based on quantum theory where the absorption process is visualized as an electrical displacement within the absorbing molecule, and the second based on classical dispersion theory in terms of the forced, damped vibration of an electron bound by elastic forces. It will be seen that both methods lead essentially to the same result.

In both cases it will be assumed that the absorption process is so rapid that only the electron polarization of the surrounding solvent medium can respond to it; i.e., we shall identify the effective dielectric constant K of the solvent with n^2, where n is its refractive index at the frequency concerned, and use K and n^2 interchangeably throughout. This assumption is obviously true in terms of the classical model of absorption, since the frequency of the vibrating electron is known to be too great to exert any orienting effect on permanent solvent dipoles. Its truth for the quantum theory model is indicated by the Franck-Condon principle, according to which the initial absorption is regarded as extremely rapid compared with nuclear motions. After the initial process, and during the relatively long life of the excited molecule, there will doubtless be time for any required re-orientation of solvent dipoles to occur, involving transfer of orientation polarization energy between solute and solvent. While this subsequent effect will be of importance in photo-chemical changes and in re-emission by fluorescence, it is without influence on the initial "vertical" Franck-Condon absorption, where the only transfer of energy between solute and solvent is by means of electron polarization.

THEORETICAL

Quantum-Mechanical Model

If an absorption transition occurs between states with wave functions ψ_1 and ψ_2, the electric dipole matrix element for an electronic displacement in the x direction,

$$\int \psi_1 ex \psi_2 d\tau = eQ \tag{1}$$

is a measure of the absorption intensity. It will be assumed in this paper that the transition integral Q is the same for absorption in the gas state as in solution, an assumption that is justified at least for strong transitions by the considerations of Mulliken and Rieke[1] and by the recent intensity measurements of Jacobs and Platt.[2] The red shift of absorption in solution can now be expressed in terms of the decreased electrostatic work required to produce the dipole $\mu=eQ$ in a dielectric medium as compared with the gas, or alternatively in terms of the lower electrostatic energy of this dipole in solution.

If an electric field F acting on a molecule produces a dipole $\mu=\alpha F$, where α is the polarizability, then the work required *in vacuum* is $\mu^2/2\alpha$.[3] With a naive interpretation of the dielectric constant K of the solvent, the corresponding work in solution is $\mu^2/2\alpha K$, leading to a shift of the absorption to lower frequencies

[1] R. S. Mulliken and C. A. Rieke, Rep. Prog. Phys. **8**, 231 (1941).
[2] L. E. Jacobs and J. R. Platt, J. Chem. Phys. **16**, 1137 (1948).
[3] J. C. Slater and N. H. Frank, *Introduction to Theoretical Physics* (McGraw-Hill Book Company, Inc., New York, 1933), p. 550.

given by (ν in cm^{-1}):[4]

$$\Delta\nu=(\mu^2/2\alpha hc)(1-1/K). \tag{2}$$

Onsager's work[5] has shown however that the solute dipole itself modifies the dielectric constant of the solvent in its immediate vicinity, and his treatment of the external effect of the dipole suggests that $1/K$ should be replaced by $3K/K(2K+1)$, leading to the following formula in which μ has been replaced by eQ:

$$\Delta\nu=(e^2Q^2/\alpha hc)[(K-1)/(2K+1)]. \tag{3}$$

Alternatively, if we regard the dipole as a point at the center of a spherical solute cavity of radius a, Fröhlich[6] has shown that its interaction energy with the surrounding solvent dielectric is $-\mu R/2$, where R is Onsager's reaction field on the solute dipole due to that dipole's effect on the solvent given by[5]

$$R=(\mu/a^3)(2K-2)/(2K+1). \tag{4}$$

If the lowered absorption frequency in solution is attributed to this interaction energy, one obtains

$$\Delta\nu=(e^2Q^2/a^3hc)[(K-1)/(2K+1)], \tag{5}$$

which would be identical with Eq. (3) if $a^3=\alpha$. It is more usual to relate α and a^3 by means of the "internal refractive index" n' of the solute molecule by $\alpha=a^3(n'^2-1)/(n'^2+2)$, where the factor involving n' is probably between $\frac{1}{3}$ and $\frac{1}{4}$.

The Classical Model

The classical dispersion equation[7] for the vibration of an electron bound elastically to an absorbing molecule in the gas state is

$$m\ddot{x}+mg\dot{x}+\omega_0^2mx=eF \tag{6}$$

where F represents the oscillating electric field of the light wave and is given by $F^0\exp(i\omega t)$, g is the damping coefficient, and where the elastic restoring force term $\omega_0=2\pi\nu_0c$ if ν_0 (cm^{-1}) is the frequency of maximum absorption. If the absorbing molecule is now regarded as placed in a dielectric solvent medium, F will be altered by the solvent, but the change will affect ω_0 only if the altered value of F contains a term in x. This is in fact the case, since Onsager[5] has shown that if the solute molecule is regarded as a spherical cavity of radius a in the surrounding solvent, then the Clausius-Mosotti field of the external field F is the sum of two parts, a cavity field and a reaction field. The former is independent of the solute dipole and may be represented by F' for our present purpose. The reaction field R however depends on the instantaneous dipole $\mu=ex$ of the solute molecule (see Eq. (4)).

If the absorption transition under consideration has the oscillator strength f, each absorbing molecule has f electrons of natural frequency ω_0, and hence in solution each solute molecule exerts a total reaction field,

$$fR=(fex/a^3)[(2K-2)/(2K+1)]. \tag{7}$$

Equation (6) becomes

$$m\ddot{x}+mg\dot{x}+\omega_0^2mx=e(F'+fR). \tag{8}$$

The terms in x become

$$mx\left[\omega_0^2-\frac{e^2f}{ma^3}\frac{(2K-2)}{(2K+1)}\right],$$

showing that the natural vibration frequency in solution is lowered by the amount

$$\Delta(\omega^2)=2\omega\Delta\omega=\frac{e^2f}{ma^3}\frac{(2K-2)}{(2K+1)} \tag{9}$$

which with the substitution $\omega=2\pi\nu c$ and $K=n^2$ gives

$$\Delta\nu=\frac{e^2}{4\pi^2c^2m}\cdot\frac{f}{\nu a^3}\cdot\frac{n^2-1}{2n^2+1}=7.14\times10^9\frac{f}{\nu a^3}\cdot\frac{n^2-1}{2n^2+1}. \tag{10}$$

Introducing the relationship between f and Q, namely,

$$f=(8\pi^2mc/3h)\nu Q^2$$

into Eqs. (3) and (5), we get

$$\Delta\nu=\frac{3e^2}{8\pi^2c^2m}\cdot\frac{f}{\nu\alpha}\cdot\frac{n^2-1}{2n^2+1}=10.71\times10^9\frac{f}{\nu\alpha}\cdot\frac{n^2-1}{2n^2+1} \tag{11}$$

$$\Delta\nu=\frac{3e^2}{8\pi^2c^2m}\cdot\frac{f}{\nu a^3}\cdot\frac{n^2-1}{2n^2+1}=10.71\times10^9\frac{f}{\nu a^3}\cdot\frac{n^2-1}{2n^2+1}, \tag{12}$$

respectively. The numerical constants are those appropriate if a and α are expressed in A and A^3, respectively. Equations (10)–(12) are identical except for the different numerical factor in (10), and the replacement of a^3 by α in (11).

DISCUSSION

Expressions with similar dependence on n and a have been derived previously. To take some recent examples, Sheppard,[8] in his review of the effect of the environment on the spectra of dyes, has suggested that $\Delta\nu=$ const. $(1-1/K)$ although the experimental results are somewhat more complex than predicted by this simple formula. In a treatment designed particularly for the case of vibration spectra, Kirkwood[9] has found $\Delta\nu$

[4] This formula, with an incorrect numerical factor, was presented by the author at the Perth (1947) meeting of the Australian and New Zealand Association for the Advancement of Science in a paper published by title only in the Proceedings, Vol. 24, p. 107. See also N. S. Bayliss, Nature (May, 1949).

[5] L. Onsager, J. Am. Chem. Soc. 58, 1486 (1936).

[6] H. Fröhlich, Trans. Faraday Soc. 44, 238 (1948).

[7] Reference 3, p. 276.

[8] S. E. Sheppard, Rev. Mod. Phys. 14, 303 (1942).

[9] J. G. Kirkwood, quoted by W. West and R. T. Edwards, J. Chem. Phys. 5, 14 (1937).

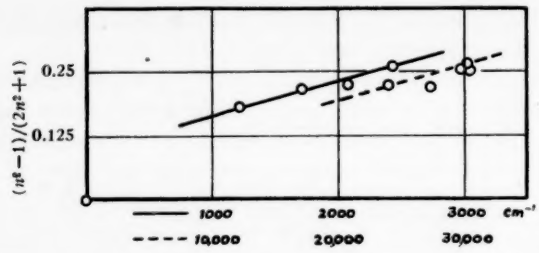

FIG. 1. Upper (full) line: Plot of $\Delta\nu$ against $(n^2-1)/(2n^2+1)$ for merocyanine in the solvents (left to right) *n*-hexane, carbon tetrachloride, benzene, carbon disulfide. Lower (broken) line: $\Delta\nu$ for ultraviolet absorption of bromine in the solvents (left to right) cyclohexane, carbon tetrachloride, benzene, chlorobenzene, toluene. Refractive index data for CCl_4 were available only in the visible; the true point for Br_2 in this solvent should be closer to the broken line. The $\Delta\nu$ scale for bromine is 10 times that for merocyanine.

$=C(K-1)/(2K+1)$, and for the model of a point dipole at the center of a sphere of radius a, his C closely resembles that of Eq. (10) without its explicit dependence on f. Sambursky and Wolfsohn[10] have discussed the solvent effect on the fluorescence of anthracene in terms of Onsager's dielectric theory, and find $\Delta\nu=A\mu^2/a^3$ where A is derived from the expression for the reaction field and contains K and the internal refractive index n'.

It is believed that this is the first time the dependence of $\Delta\nu$ on the oscillator strength f has been stated explicitly, although it is implicit in the inclusion of μ for the excited state in Sambursky and Wolfsohn's expression[10] and also in the treatment of the dispersion of solids and liquids by Slater and Frank.[11] Breit and Salant[12] put $\Delta\nu$ proportional to the absorption coefficient in the case of infra-red spectra.

When one compares the theoretical predictions with experiment, two qualifying factors must be borne in mind:

(a) Other solvent effects are almost certainly operative in addition to the electrostatic polarization effect considered here, including the solvent "cage" effect discussed by Bayliss and Rees[13] and by Rees,[14] and the electronic wave function overlap effect discussed generally by Breit and Salant.[12] The possibility of effects resulting from solvate formation must not be overlooked, although the author's opinion is that this effect, though present in certain cases, is less frequent than is commonly postulated.

(b) The absolute magnitude of the predicted $\Delta\nu$ depends very heavily on the geometry of Onsager's model of a point dipole at the center of a spherical solute molecule. Deviations from this model have, for example, a large effect on Kirkwood's constant C.[9] Most organic molecules are far from spherical, and in the case of strong transitions, where Q may be of the order of 1A, the dipole is far from being a point relative to the size of the solute molecule.

It must also be remembered that in spite of the mass of experimental data on absorption spectra in solution, there are not many examples which combine reliable f data with a systematic investigation of the effect of various solvents. The few typical examples considered here will serve to show the extent of the qualitative and quantitative validity of the theory, together with its limitations.

[10] S. Sambursky and G. Wolfsohn, Phys. Rev. **62**, 357 (1942).
[11] Reference 3, p. 280.
[12] G. Breit and E. O. Salant, Phys. Rev. **36**, 871 (1930).
[13] N. S. Bayliss and A. L. G. Rees, J. Chem. Phys. **8**, 377 (1940).
[14] A. L. G. Rees, J. Chem. Phys. **8**, 429 (1940).

Dependence on *n*

The example of a merocyanine dye in the gas state and in several solvents is taken from Sheppard's review.[8] The upper full line in Fig. 1, recalculated from Sheppard's figure, shows $\Delta\nu$ for the merocyanine (λ_{max}(gas) $=4800$A) plotted against $(n^2-1)/(2n^2+1)$ for four solvents, n_D being taken for n in each case. The points lie satisfactorily on a straight line, which, however does not pass through the origin as it should if Eqs. (10)–(12) accounted completely for the displacement. Sheppard's plot of λ against n does pass through the origin, but the fit of his points to a straight line is less satisfactory than in Fig. 1. The lower broken curve shows $\Delta\nu$ for the strong ultraviolet absorption of bromine solutions plotted similarly. The points lie on a straight line parallel to that of the merocyanine. This case will be discussed further.

(V, N) Transitions in Isoprene and Benzene

These examples have been chosen, since there are recent measurements in both the gas and in solution, together with reliable f data. The data summarized in Table I are taken from Jacobs and Platt[2] in the case of isoprene, from Price and Walsh[15] for the (V, N) band in benzene gas, and from Platt and Klevens[16] for benzene dissolved in *n*-heptane. Equations (10)–(12) have been used to calculate the values of a and α required by the theory, and these can now be compared with data from other experimental sources. Either of the values $a=2.57$A or $a=2.94$A is in good agreement with the known dimensions of the benzene molecule. In solid benzene, the molecules are known to pack as if the unsaturation electrons occupy an almost spherical

TABLE I. Molecular radius and polarization calculated from red frequency shifts of strong absorption bands.

	Isoprene[a]	Benzene	Bromine	Iodine
ν (gas) cm^{-1}	46500	55800[b]	64000[d]	56000[g]
ν (soln.) cm^{-1}	44900	54500[c]	34000[e]	33600[b]
Solvent	*n*-heptane	*n*-heptane	benzene	benzene
$\Delta\nu$ cm^{-1}	1600	1300	30000	22400
f	0.40	0.79[c]	0.18[e]	0.21[b]
n (solvent)	1.46(λ2250)	1.46(λ2250)	1.61(λ2900)[f]	1.61(λ2900)
a [Eq. (10)] in A	2.03	2.57	0.60	0.72
a [Eq. (12)] in A	2.31	2.94	0.69	0.83
α [Eq. (11)] in A^3	12.5	25.4	0.33	0.57

[a] Data from Jacobs and Platt, reference 2.
[b] Price and Walsh, reference 15.
[c] Platt and Klevens, reference 16.
[d] Estimated position of (V, N) transition, reference 1.
[e] Bayliss, Cole, and Green (unpublished results).
[f] Landolt-Börnstein, "Tabellen," HW II, p. 972.
[g] (V, N) transition, see reference 1.
[h] Green and Rees (unpublished results), also reference 20.

[15] W. C. Price and A. D. Walsh, Proc. Roy. Soc. **A191**, 22 (1947).
[16] J. R. Platt and H. B. Klevens, Chem. Rev. **41**, 301 (1947).

"dome" whose radius has been shown by Mack[17] to be 2.45A. If one regards liquid benzene as consisting of spherical molecules in closest packing, the molecular radius is found to be 3.0A. In testing Eq. (11), the difficulty arises of choosing the correct value of the polarizability α, which depends on the wave-length. It would obviously be best to calculate α for the wave-length corresponding to λ(max.), but the required refractive index is unknown. The benzene molecule is also markedly anisotropic. However the mean polarizability, presumably calculated with $n=n_D$, is 10.32.[18]

The isoprene molecule is more elongated, but if liquid isoprene consists of spherical molecules in closest packing, one finds $a=3.1$A, rather greater than either of the values in Table I. On the other hand, a short extrapolation from the data of Melaven and Mack[19] on collision areas of hydrocarbons suggests that the collision area of pentane (somewhat similar to isoprene) is about 20A^2, giving $a=2.5$A. Furthermore, using the refractive index of isoprene in the visible region, one calculates $\alpha=10.0$A^3 in good agreement with Table I, although as in the case of benzene it would be more satisfactory to use the refractive index in the neighborhood of the absorption band. While the agreement between theory and experiment is not as good here as in benzene, the molecule departs more widely from the spherical model. (See also following discussion of bromine and iodine.)

Ultraviolet Absorption of Bromine and Iodine Solutions

Both iodine dissolved in benzene,[20,21] and bromine dissolved in several solvents[22,23] show intense absorption ($f\approx0.2$) near 2900A and toward shorter wave-lengths. The respective gases absorb very weakly indeed in this region, and if the solution bands are displaced from bands that are intense in the gas, the only possible parent gas bands are the (V, N) transitions of rather greater predicted intensity[1] that lie in the vacuum ultraviolet. While the solution bands have been ascribed to other causes,* it is of interest to consider the consequences of the hypothesis that they are in fact displaced (V, N) transitions. The data based on this supposition regarding ν(max.) in the gas are set out in Table I. Owing to the very great postulated value of $\Delta\nu$, an average of the gas and solution ν's has been used in each case in applying Eqs. (10)–(12).

The $\Delta\nu$ data for bromine in several solvents are plotted also in Fig. 1 (lower broken line). The points lie on a straight line which, as in merocyanine, does not pass through the origin, although it is parallel to the merocyanine line, suggesting that the solvent displacements have the same cause in both cases. It should be noted that the scale of $\Delta\nu$ for bromine in Fig. 1 is ten times as great as for merocyanine, and the much greater "spread" between the solution maxima in bromine than in merocyanine (a fact that is independent of any hypothesis about the location of the gas absorption) shows that the parent gas absorption in bromine must be much further removed from the solution spectra than in merocyanine.

The calculated values of a (Table I) are all much smaller than the actual molecular radii (e.g., 2.5A for bromine). There is also a very great discrepancy in the polarizabilities, the ordinary experimental values being 8.0A^3 and 11.0A^3 for bromine and iodine, respectively. The model of a point dipole at the center of a spherical molecule may well be at fault, however. In a similar discussion by West and Edwards[9] of the solvent displacement of the infra-red absorption of HCl, Kirkwood's formula[9] required $a=0.62$A for HCl instead of the more reasonable value of 2A. Changing the model to locate the dipole off-center was able to bring about much better agreement. A similar treatment might resolve the difficulty in the iodine and bromine cases, since the plot of $\Delta\nu$ for bromine in Fig. 1 strongly suggests that we are dealing with a large solvent displacement. The case of iodine in benzene is admittedly complex.[20]

Weak Absorption Bands in Benzene, Bromine, and Iodine

Benzene, with its transitions of differing intensity at 1790A ($f=0.79$), 1980A ($f=0.1$),[16] and 2600A ($f=0.0006$),[24] offers the possibility of checking the theoretical dependence of $\Delta\nu$ on f by comparisons within the one molecule. Unfortunately, it is difficult to estimate $\Delta\nu$ from the published data on the 1980A transition in the gas[15] and in solution[16] except that it is apparently less than for the (V, N) transition, in qualitative agreement with theory. Data for the weak system at 2600A in the gas and in solution are quoted by Sponer,[25] from which $\Delta\nu$ appears to be about 300

[17] E. Mack, Jr., J. Am. Chem. Soc. **54**, 2141 (1932).
[18] Landolt-Börnstein, "Tabellen," Erg. Bd. III.1, p. 153.
[19] R. M. Melaven and E. Mack, Jr., J. Am. Chem. Soc. **54**, 888 (1932).
[20] J. H. Hildebrand and H. A. Benesi, J. Am. Chem. Soc. **70**, 2832 (1948).
[21] B. G. Green and A. L. G. Rees (private communication).
[22] Aickin, Bayliss, and Rees, Proc. Roy. Soc. **A169**, 234 (1948).
[23] Bayliss, Cole, and Green (unpublished results).

* Hildebrand and Benesi (reference 20) suggest that the iodine-benzene band is the result of solvate formation involving bonding with the π-electrons of the benzene molecule. This explanation is not so plausible in the case of bromine, which shows the strong absorption not only in aromatic solvents, but also in chloroform and cyclohexane. Mulliken and Rieke regard the bromine band as an example of extreme solvent perturbation on the very weak absorption exhibited by bromine gas in the same region. If this is so, it is an example that seems to be without parallel in other solution spectra. The phenomenon is of great interest, and further work is being undertaken to obtain more quantitative data. *Added in proof:* In a recent paper, which the author was privileged to see in manuscript, Mulliken (J. Am. Chem. Soc., Jan. 1950) has ascribed the UV solution bands of both bromine and iodine to solvates. The author proposes to deal further with the problem in a future publication.

[24] R. S. Mulliken, J. Chem. Phys. **7**, 353 (1939).
[25] H. Sponer, Chem. Rev. **41**, 281 (1947).

cm^{-1} to the red (solvent not specified). Sheppard[8] states, however, that while the shorter wave-length bands are displaced to the red (solvent unspecified), the longer wave-length bands move to the violet in solution.* From Eqs. (10)–(12), one would expect $\Delta\nu$ to be about 1/10,000 of $\Delta\nu$ for the (V, N) transition. When the electrostatic displacement becomes so small, other effects such as that of the solvent cage[12,13] become predominant, and the quantitative evaluation of $\Delta\nu$ becomes impossible.

For the well-known visible continua of bromine and iodine we have $f=0.0029$[26] and $f=0.015$,[21] respectively. If a is chosen as 0.6A to conform to the results for the (V, N) transition in Table I, Eq. (10) predicts $\Delta\nu=780$ cm^{-1} for bromine in n-hexane. With the actual value of $a=2.5$A, the predicted $\Delta\nu$ is about 10 cm^{-1}. The experimental value is 100 cm^{-1},[26] while for most solvents, particularly if they are associated, the displacements $\Delta\nu$ are to the violet ranging to 1400 cm^{-1}.[26] Similar experimental results obtain for iodine.[27] These are again cases where relatively small electrostatic displacements are superimposed by other influences such as the solvent cage effect[12,13,26] which causes displacements to the violet. Other authors[27] have ascribed the violet shift of the iodine continuum in associated solvents to solvate formation. Whether the true explanation be solvation or caging, these and the electrostatic polarization effect are of the same order of magnitude in weak bands, and the observed displacements must be regarded as their resultant.

Subject to the complications arising out of the superposition of the other effects particularly in weak bands, the qualitative dependence of the electrostatic polarization effect on f, a (or α), and n seems to be justified by the experimental results. The quantitative agreement is good for the (V, N) transitions in isoprene and benzene, although the data do not allow one to decide which of Eq. (10)–(12) is the best. The cases of the ultraviolet absorption of bromine and iodine are much less satisfactory from the quantitative viewpoint.

* *Added in proof:* K. Lauer and R. Oda (Berichte, **69**, 851 (1936)) give data for the 2600A benzene system in 11 solvents. The displacements to the red vary from 100 to 400 cm^{-1} and are qualitatively in agreement with the refractive index law.

[26] Bayliss, Cole, and Green, Australian J. Sci. Research, Series A **1**, 472 (1948).

[27] O. J. Walker, Trans. Faraday Soc. **31**, 1432 (1935).

THE JOURNAL OF CHEMICAL PHYSICS VOLUME 18, NUMBER 3 MARCH, 1950

The Vibrational Spectra of Molecules and Complex Ions in Crystals III. Ammonium Chloride and Deutero-Ammonium Chloride* †

E. L. WAGNER‡ AND D. F. HORNIG
Metcalf Research Laboratory, Brown University, Providence, Rhode Island

(Received July 11, 1949)

The infra-red spectra of thin non-scattering films of NH_4Cl and ND_4Cl were obtained at 28°, −78° and −190°C. A convenient low temperature transmission type cell usable for such films is described. No indication of fine structure due to free rotation of the NH_4^+ ions was found. Instead, evidence is presented for the existence, both above and below the λ-point, of a torsional lattice mode involving the NH_4^+ ions. The limiting frequencies of the torsional oscillations were observed at about 390 and 280 cm^{-1} for NH_4Cl and ND_4Cl, respectively. These values agree quite well with the frequencies calculated on the basis of a purely electrostatic potential function. The spectra of the low temperature modifications indicate strongly that the structures belong to the space group T_d^1 in which the NH_4^+ ion symmetry is T_d. Of the eight observed bands, two are assigned to the triply degenerate fundamentals ν_3 and ν_4, one to the overtone $2\nu_4$, one to the combination $\nu_2+\nu_4$ which resonates strongly with ν_3, one to the combination of the totally symmetric mode, ν_1, with the limiting lattice frequency, ν_b, and two to the combinations involving the lattice torsional mode, ν_6, i.e., $\nu_4+\nu_6$ and $\nu_2+\nu_6$. The spectra of the room temperature modifications are consistent with a structure in which the NH_4^+ ion tetrahedra are randomly distributed between the two possible equilibrium orientations in each unit cell. The λ-point transformations are probably simple order-disorder transitions between the two modifications.

I. INTRODUCTION

ALL of the simple ammonium salts have second-order phase transitions in the vicinity of −30° to −60°C, but the nature of these transitions has never been clarified. Pauling[1] has advanced the hypothesis that these transitions mark the onset of essentially free rotation, while Frenkel,[2] on the other hand, has suggested that such transformations are order-disorder transitions in the orientations.

In the case of NH_4Cl a considerable amount of experimental data is available. Lawson[3] has demonstrated that the evidence obtained from the measurement of

* Based in part on a thesis submitted by Edward L. Wagner in partial fulfillment of the requirements for the Ph.D. degree at Brown University (1948).

† This work was supported in part by ONR under Contract N6ori-88, T.O. 1.

‡ Tennessee Eastman Corporation Fellow, Brown University (1946–48). Present address: Department of Chemistry, State College of Washington, Pullman, Washington.

[1] L. Pauling, Phys. Rev. **36**, 430 (1930).

[2] J. Frenkel, Acta Physicochimica **3**, 23 (1935).

[3] A. W. Lawson, Phys. Rev. **57**, 417 (1940).

the heat capacity at constant volume (C_v) in the vicinity of the λ-point is strongly opposed to any rotation, or even near rotation, in either phase. His data seem incontrovertible. Earlier spectroscopic evidence which appeared to show rotational structure on at least one of the vibrational bands[4,5] has been shown to be definitely incorrect,[6] although recently it has been argued that Raman polarization measurements indicate rotation about a single threefold axis.[7]

The x-ray evidence of Smits and MacGillivry[8] and Ketelaar[9] has confirmed that the N and the Cl atoms are arranged in a CsCl lattice in both phases although the lattice expands by one percent as the temperature is raised through the transition at −30.5°C. It has been shown that below the transition point NH_4Cl exhibits a piezoelectric effect[10,11] which vanishes in the room temperature phase. Similarly, the Raman spectrographic investigations of Menzies and Mills[12] show a distinct lattice line at 183 cm^{-1} in the low temperature modification (Phase III)¶ which is absent in the room temperature modification (Phase II).¶ However, Krishnan[13] has found that this line (as well as several others) persists in Phase II although with much less intensity. None of these data are opposed to the structure of Phase III which is consistent with the x-ray evidence, namely a CsCl lattice with space group symmetry T_d^1, but they offer no definite evidence regarding the nature of the phase transition.

In the first paper of this series[14] it was shown that the fundamental vibrations of the crystal which may be active in the infra-red or Raman spectrum are those which are allowed under the crystallographic point group. The selection rules for the fundamentals of the NH_4^+ ion may also be obtained from the local symmetry of the ion in the crystal. Since the local symmetry of the ion is T_d if the space group is T_d^1, both of these statements lead to the conclusion that only those fundamental vibrations allowed under the tetrahedral group, T_d, should be active in either spectrum if the symmetry of the low temperature phase is indeed T_d^1. Since all of the fundamentals are then allowed in the Raman spectrum, it does not afford a critical test. However, only the two triply degenerate internal modes and one triply degenerate limiting lattice mode are allowed in the infra-red spectrum.

No such definite predictions can be made regarding Phase II. It seems clear from free energy considerations that the transition must consist of some sort of disordering process, in which case two possible effects can appear in the spectra: (1) Selection rules may be relaxed and the transitions not allowed in Phase III may become active in Phase II, and (2) degeneracies may be lifted and degenerate vibrations in Phase III may be spread out into narrow bands in Phase II.

The infra-red spectrum of NH_4Cl has been previously studies by several investigators and Pohlman[4] has most recently studies both phases. The spectra obtained have been used to argue either that the ammonium ion does not possess tetrahedral symmetry, or that the simple selection rules previously mentioned are incorrect.[15,16]

In order to throw further light on these questions the infra-red spectra of both NH_4Cl and ND_4Cl were studied in Phase III at −190°C and −78°C and in Phase II at 28°C on films essentially free of scattering and with considerably higher resolution than previously used. It appears that the difficulty was due to a consistent misinterpretation of the spectrum of the NH_4^+ ion. Since a torsional lattice vibration is observed in both phases, there can be no question of free rotation in either phase, and it appears that the λ-point transition is of the type suggested by Frenkel[2] and consists of a change from relative order to relative disorder of the equilibrium orientations of the NH_4^+ ions. A detailed theory of the Bragg-Williams type based on this idea has been developed for NH_4Cl by Nagamiya.[17]

II. EXPERIMENTAL METHODS AND APPARATUS

The ammonium salts employed in these investigations were reagent grade chemicals. Thin films of these salts on rocksalt plates were used in obtaining the spectra. The films were prepared by subliming the ammonium or deutero-ammonium halide through a loose glass wool plug onto a polished rocksalt plate which had been cleaned with the high frequency discharge of a vacuum leak tester. The sublimations were performed in a closed glass system under a pressure of about 10^{-2}-mm Hg at 110–130°C. Under such conditions the films obtained were quite clear. They exhibited only very little scattering in either visible or infra-red radiation provided that the thicknesses were less than about 0.6 micron. The majority of the films investigated had thicknesses, as estimated by the interference colors of reflected white light, of about 0.1 to 1.0 micron.

The deutero-ammonium halides were prepared by means of a simple exchange reaction[18] in which the

[4] R. Pohlman, Zeits. f. Physik **79**, 394 (1932).
[5] C. Beck, J. Chem. Phys. **12**, 71 (1944).
[6] E. L. Wagner and D. F. Hornig, J. Chem. Phys. **17**, 105 (1949).
[7] L. Couture and J. P. Mathieu, Proc. Ind. Acad. Sci. **28A**, 401 (1948).
[8] A. Smits and C. MacGillivry, Zeits. f. physik. Chemie **A166**, 97 (1933).
[9] J. A. Ketelaar, Nature **134**, 250 (1934).
[10] A. Hettich and A. Schleede, Zeits. f. Physik **50**, 249 (1928); Zeits. f. physik. Chemie **A168**, 353 (1934).
[11] S. Bahrs and J. Engl, Zeits. f. Physik **105**, 470 (1937).
[12] A. C. Menzies and H. R. Mills, Proc. Roy. Soc. London **148A**, 407 (1935).
¶ This is the designation used by A. Eucken, Zeits. f. Elektrochemie **45**, 126 (1939). In this system the phase (or modification) just below the melting point is designated by the number I and successive phases at lower temperatures are designated by successively increasing Roman numerals. In NH_4Cl Phase I has the NaCl structure which changes to Phase II at 184.3°C.
[13] R. S. Krishnan, Proc. Ind. Acad. Sci. **A26**, 432 (1947).
[14] D. F. Hornig, J. Chem. Phys. **16**, 1063 (1948).
[15] R. Ananthakrishnan, Proc. Ind. Acad. Sci. **5A**, 76 (1937).
[16] L. Couture, J. Chem. Phys. **15**, 153 (1947).
[17] T. Nagamiya, Proc. Phys. Math. Soc. Japan **24**, 137 (1942).
[18] K. F. Bonhoeffer and G. W. Brown, Zeits. f. physik. Chemie **B23**, 171 (1933).

corresponding ammonium salt was dissolved in the minimum amount of 99.6 percent D_2O at approximately 70°C and the exchange water evaporated off in a vacuum at room temperature. This process was repeated four or five times with fresh batches of D_2O. A conversion to 99.5 percent deuterated ammonium salt has been claimed for this procedure.[19] Our samples contained considerably more than 0.5 percent hydrogen at the time the spectra were obtained, possibly acquired in handling because of the somewhat more hygroscopic nature of the deuterated compounds.

The halide films were maintained at the appropriate temperature by means of the low temperature absorption cell illustrated in Fig. 1. This is a direct transmission type cell which can conveniently be inserted

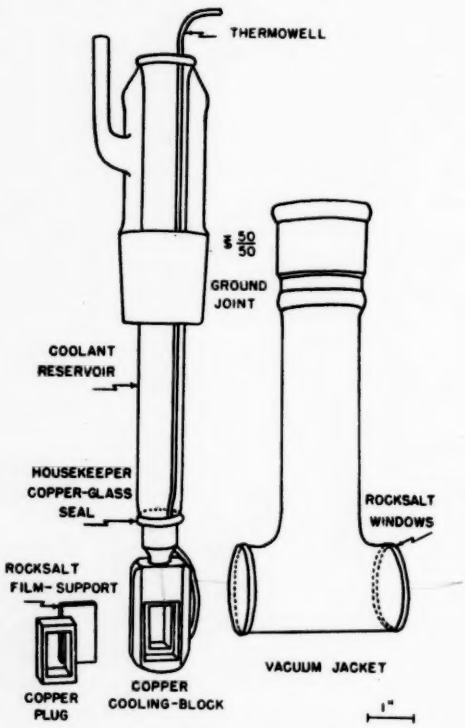

FIG. 1. Infra-red absorption cell for use at low temperatures.

into the beam of almost any infra-red spectrometer without changing the optical path. The cell was composed of a copper cooling block, a coolant reservoir, and an enveloping jacket. The cooling block consisted of a piece of solid copper through which a rectangular hole had been machined in such a way that a shoulder existed in the center of the block. The rocksalt plate on which the ammonium halide film had been sublimed rested against this shoulder and was held in position by means of an annular copper plug. A thin layer of vacuum grease between this shoulder and the rocksalt plate was found necessary to obtain adequate thermal contact. The temperature of the cooling block was measured by means of a fine thermocouple inserted into a thermowell which was embedded in the block, and the temperature of the rocksalt plate was measured by another fine thermocouple whose junction was embedded into a hole drilled halfway through the salt plate. The glass coolant reservoir was attached to the cooling block by means of a copper to glass Housekeeper seal which gave an extremely satisfactory vacuum-tight joint. The rocksalt or silver chloride windows were sealed onto the flat ground ends of the glass jacket with clear Glyptal lacquer.

Prior to cooling, the assembled cell was evacuated to a pressure of about 10^{-4}-mm Hg. Under such conditions it was found that the cooling block quickly attained the refrigerant temperature. However, at liquid nitrogen temperatures the rocksalt plate supporting the ammonium halide film was 5° hotter than the block. At −78°C no temperature difference between the block and the plate could be detected. In the radiation beam of the spectrometer the temperature of the rocksalt plate did not increase. Under the normal operating conditions of this cell less than 200 ml of liquid nitrogen were required to maintain the temperature of the rocksalt plate at −190°C for one hour. When the cooling block was maintained at liquid nitrogen temperature the exterior windows did not cool perceptibly.

The spectra were taken with a modified Perkin-Elmer Spectrometer Model 12B. The modification consisted of replacing the usual system for focusing the radiation source onto the entrance slit with a double beam arrangement for shifting the beam alternately through the sample and through a blank cell. With this instrument alternate point by point recordings of the transmissions of the sample and a blank were obtained. In addition, the instrument recorded the zero or base line positions after each transmission point. This has the advantage of essentially eliminating errors in transmission due to base line drift, a factor which may become significant in low temperature work.

The optical paths of the spectrometer were completely enclosed. Prior to recording a spectrum the housing was thoroughly flushed out with dry nitrogen gas until the CO_2 band at 4.26μ and the 2.67μ. H_2O band were hardly discernible. Under such conditions, the maximum absorption in the 6.3μ water vapor band was less than 10 percent. This procedure was adopted when it was ascertained that the point by point method of recording spectra leads to the appearance of spurious peaks in the plotted spectrum. This results from the paucity of points along the steep slopes of deep atmospheric absorption bands. These false peaks do not necessarily coincide with those of the atmospheric bands, but may be situated along one or both of the slopes depending upon their relative steepness.

Calcium fluoride and rocksalt prisms were utilized in these investigations. The slit widths employed were such that the theoretical widths of the frequency bands resolved were (for the fluorite prism) 9 cm^{-1} at 3μ,

[19] Clusius, Kruis, and Schanzer, Zeits. f. anorg. allgem. Chemie **236**, 24 (1938).

3.3 cm^{-1} at 7μ, (and for the rocksalt prism) 4.6 cm^{-1} at 8μ and 2.7 cm^{-1} at 10μ.

III. EXPERIMENTAL RESULTS

The spectra obtained for NH_4Cl are shown in Fig. 2. In these curves the noise level has not been smoothed out nor have they been corrected for scattering. All the data of these spectra pertain to a single film whose thickness, as estimated from the color of reflected light, was about 0.2 micron. In addition to the records reproduced here, spectra were also obtained for eight other NH_4Cl films, ranging in thickness from 0.1 to 1.0 micron. No difference between the various spectra could be detected except that in the thickest film the frequencies of maximum absorption seemed to be shifted to higher frequencies by 5 to 10 cm^{-1}. Since it has been shown that NH_4Cl smokes with particle sizes about equal to the thickness of our films have the bulk crystal structure,[20] the cause of the apparent frequency shift is probably not due to a change of crystal structure with thickness.

The corresponding spectra of ND_4Cl are given in Fig. 3. Three different films of ND_4Cl were studied. Unfortunately, the films of this salt were always contaminated with some ND_3H^+ and $ND_2H_2^+$ ions so that some of the observed peaks must be ascribed to these contaminations. This was done by analogy to the corresponding deutero-methanes, all of which have been studied,[21] and by comparison with the Raman spectra of the various deuterated ammonium chlorides.[22]

The observed frequencies of maximum absorption, the relative integrated peak intensities, and our assignments are given in Tables I and II. In the case of overlapping bands the intensities were partitioned in what seemed to be the most reasonable way but, particularly in the case of the 3.2μ region in NH_4Cl, this partitioning was undoubtedly inaccurate. The relative intensities of the bands are believed to be accurate to about 15 percent.

The most striking difference between the spectra of NH_4Cl and ND_4Cl is the contrast between the very strong single peak at 2336 cm^{-1} in ND_4Cl and the strong doublet at 3080 cm^{-1} in the corresponding NH_4Cl spectra. Relative to the sharp peaks at 1067 cm^{-1} in ND_4Cl and 1403 cm^{-1} in NH_4Cl, it is found that the total intensity of the doublet at 3080 cm^{-1} in NH_4Cl is about equal to the intensity of the strong single peak at 2336 cm^{-1} in ND_4Cl. This suggests strongly that the doubling is due to Fermi resonance between the strong fundamental, ν_3, and an almost coincident combination level.

The temperature behavior of the bands at 1760 and 2000–2100 cm^{-1} in the NH_4Cl spectrum is very interest-

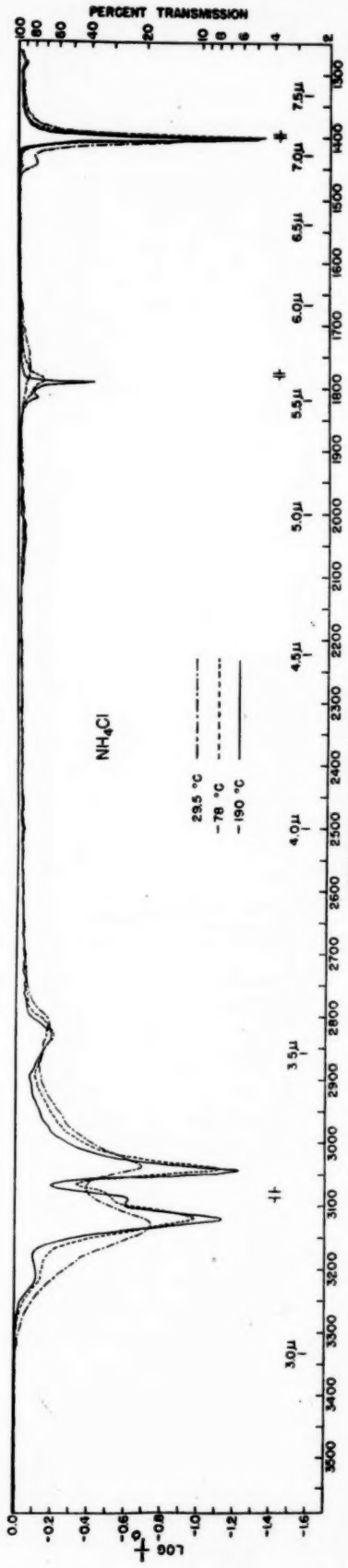

FIG. 2. Infra-red spectrum of NH_4Cl in Phase II at 29.5°C and Phase III at −78°C and −190°C.

[20] J. Trillat and A. Laloeuf, Comptes Rendus **227**, 67 (1948).
[21] See G. Herzberg, *Infra-Red and Raman Spectra of Polyatomic Molecules* (D. Van Nostrand Company, Inc., New York 1945), p. 309.
[22] R. Ananthakrishnan, Proc. Ind. Acad. Sci. **5A**, 175 (1937).

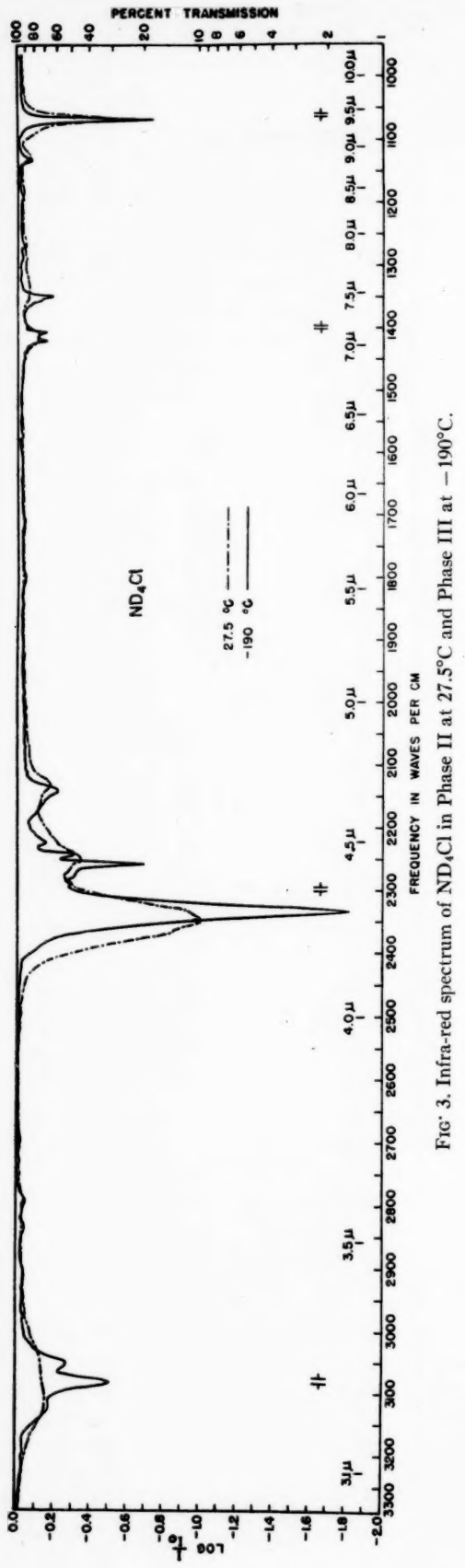

FIG. 3. Infra-red spectrum of ND_4Cl in Phase II at 27.5°C and Phase III at −190°C.

ing. They change from broad symmetrical bands at room temperature to curiously shaped multiple peak bands at −190°C. There is no evidence of discontinuities in their behavior at the λ-point. The details of the shape of the 1760-cm^{-1} band, determined on a thicker film, have been published in an earlier communication,[6] and those of the 2000–2100-cm^{-1} band are given in Fig. 4. It is interesting to note that these are the only two bands in the spectrum which are significantly shifted in the spectra of the heavier halides of ammonium.||

One of the most salient features of the NH_4Cl spectrum is the complete disappearance at low temperature of the subsidiary peak on the high frequency side of the 1403-cm^{-1} band. The intensity of this peak, which amounts to 10 percent of the main peak at room temperature, drops quite abruptly at the λ-point but apparently it does not completely disappear at this temperature.

All of the lines in the spectrum show a notable sharpening as the temperature is lowered and the weak peak in the center of the NH_4Cl doublet at 3080 cm^{-1} is only resolved at the lowest temperature. In general, the intensities of the fundamentals decrease by about 30 percent between room temperature and liquid nitrogen temperature, while the intensities of combination and overtone bands are relatively less affected by this temperature change.

IV. THE AMMONIUM ION FUNDAMENTALS

The fundamental ion frequencies of the NH_4^+ ion may be expected to lie slightly higher than those of methane. It seems apparent, therefore, that the low frequency bands at 1067 and 1403 cm^{-1} in the two chloride salts may be assigned with confidence to the triply degenerate bending mode, ν_4, of the tetrahedral model. Indeed, the ratio of these frequencies in ND_4^+ and NH_4^+, 0.7605, is very close to the corresponding ratio between CD_4 and CH_4, namely, 0.7622. The width at half-height of this line in both salts is only 6 cm^{-1} at −190°C. The sharpness of this degenerate vibration therefore affords strong evidence that the ion symmetry is genuinely tetrahedral at low temperatures.

Similarly, the very strong peak at 2336 cm^{-1} in the spectrum of ND_4Cl is certainly the triply degenerate stretching frequency, ν_3. The corresponding frequency in NH_4Cl must lie approximately at the 3080-cm^{-1} doublet mean. If it is assumed that the combination level "borrows" all of its intensity from the fundamental (certainly a good assumption since ν_3 is by far the strongest band in the spectrum), a more accurate estimate of the unperturbed frequencies of the two levels may be obtained from their relative intensities. A first-order perturbation calculation yields

$$\delta = S(R-1)/(R+1),$$

|| The data for the bromides and iodides will be presented at a later date in this Journal.

TABLE I. Observed frequencies, relative intensities, assignments, and inferred frequencies for NH_4Cl and ND_4Cl in Phase III.

Assignment	NH_4Cl Inferred freq. (cm^{-1})	NH_4Cl Obs. freq. at −78°C (cm^{-1})	NH_4Cl Obs. freq. at −190°C (cm^{-1})	ND_4Cl Inferred freq. (cm^{-1})	ND_4Cl Obs. freq. at −190°C (cm^{-1})
					3129*
					3089*
					3059*
$\nu_1+\nu_5$	3231	3228 (3)	3223 (6)	2331	
$2\nu_4+\nu_6$	3219			2315	
$\nu_3(F_2)$	[3086]†	3126 (34)	3126 (41)	[2325]†	2336 (94)
		3090 (1)	3089 (5)		2292
					2279*
$\nu_2+\nu_4$	[3086]†	3047 (38)	3050 (42)	[2272]†	2260 (16)
					2246*
					2224*
$\nu_1(A_1)$		(3048)§	(3048)§		
$2\nu_4$	2806	2833 (6)	2828 (8)	2134	2142 (12)
$\nu_2+\nu_6$	2074	2018††(1)	2005–2100††(2)	1486	
					1420*
					1405*
$\nu_4+\nu_6$		1788 (3)	1817 } (4)		1360 } (4)
			1794 }		1348 }
$\nu_2(E)$	1683		(1712)§	1205	
					1132*
$\nu_4(F_2)$		1447 (1)			
		1402 (10)	1403 (10)		1067 (10)
$\nu_6(F_1)$	391			281	
$\nu_5(F_2)$		(183)§	(183)§		

* ND_3H^+ and $ND_2H_2^+$.
† Computed unperturbed frequencies.
†† Broad band.
§ From Raman spectrum (see references 12 and 13).

TABLE II. Observed frequencies, relative intensities, assignments, and inferred frequencies for NH_4Cl and ND_4Cl in Phase II.

Assignment	NH_4Cl Inferred freq. (cm^{-1})	NH_4Cl Obs. freq. at 28°C (cm^{-1})	ND_4Cl Inferred freq. (cm^{-1})	ND_4Cl Obs. freq. at 28°C (cm^{-1})
$\nu_1+\nu_5$	3209	3200		3121*
$\nu_3(F_2)$	[3097]†	3138 (39)	[2337]†	2350 (84)
$\nu_2+\nu_4$	[3085]†	3044 (31)	[2265]†	2252 (13)
$\nu_1(A_1)$		(3041)§		(2214)§
$2\nu_4$	2806	2810 (6)	2132	2129 (12)
$\nu_2+\nu_6$	2041	2000††(1)	1469	
				1413*
$\nu_4+\nu_6$		1762 (3)		1335 (3)
$\nu_2(E)$	1682	(1710)§	1200	(1215)§
				1126*
$\nu_4(F_2)$		1445 (1)		1090 } (10)
		1403 (10)		1066 }
$\nu_6(F_1)$	359		269	
$\nu_5(F_2)$		(168)§		

* ND_3H^+ and $ND_2H_2^+$.
† Computed unperturbed frequencies.
†† Broad band.
§ From Raman spectrum.

where δ is the separation of the unperturbed levels, S is the observed separation of the peaks and R is the ratio of the observed intensities of the two branches of the resonating doublet. In this way the frequencies written in brackets in the inferred spectrum columns of Tables I and II were obtained. The Teller-Redlich frequency product ratio for the two F_2 species is then

$$\frac{\nu_3^D \nu_4^D}{\nu_3^H \nu_4^H} = 0.5725.$$

For comparison, the harmonic value of this ratio is 0.5528, while the corresponding observed ratio for CD_4 and CH_4 is 0.570. It is interesting that the frequencies of the two F_2 modes are essentially identical in the spectra of NH_4Cl, NH_4Br and NH_4I.

The band at 1794 cm^{-1} in NH_4Cl has sometimes been assigned[13] to the doubly degenerate bending vibration, ν_2. However, the corresponding band in ND_4Cl, which is plainly identified by its temperature behavior, occurs at 1348 cm^{-1}. The frequency ratio is then 0.7514, whereas if it were actually ν_2 the ratio would be closer to 0.707. The observed value of this ratio cited[21] for methane is 0.6906.** Thus, it seems unquestionable that the 1794-cm^{-1} band in NH_4Cl cannot be the doubly degenerate vibration, ν_2. If we assume that the level which resonates with ν_3 in NH_4Cl is $\nu_2+\nu_4$ (the only possible binary combination), and make a corresponding assignment to the peak at 2260 cm^{-1} in ND_4Cl, we obtain the frequencies 1683 and 1205 cm^{-1} for the values of ν_2 in NH_4Cl and ND_4Cl, respectively. The frequency ratio is then 0.7159 and the isotope check is good. A further check on this frequency, although a rough one, is supplied by the combination band at 2000–2100 cm^{-1} which we shall discuss in more detail later. The corresponding room temperature Raman lines occur at approximately 1710 and 1215 cm^{-1}. These values are probably more correct than the frequencies we have calculated.

V. COMBINATION AND OVERTONE BANDS

The selection rules for fundamental vibrations are exceedingly strict in that spectral activity is restricted to those fundamentals which are totally symmetric with respect to translation. This translational restriction is very much relaxed in the case of combinations and overtones since the only requirement is that the combining modes have the same wave number vector,[22] and it is not necessary that, in the individual normal vibrations, the vibrations of all cells be in phase. The resultant level, however, is totally symmetric with respect to translation. In the case of molecular modes, the frequencies will not in general be strongly affected by the phase shifts between neighboring molecules, since the interactions are usually weak. Thus all frequencies within the branch lie in a narrow region. Consequently, the entire band of allowed frequencies comprising the overtone or combination should lie close to the value computed in terms of the totally symmetric fundamentals. However, the resulting band *is* a distribution function and may therefore show structure,

** It should be noted that the ν_2-modes have never actually been observed in CH_4 and CD_4.

[22] M. Born and M. Bradburn, Proc. Roy. Soc. London 188A, 161 (1947).

including subsidiary peaks. The temperature behavior of many of the combination bands indicates that they may well be ternary bands where the third component is the Debye frequency distribution. No calculations on the detailed envelopes of such bands have yet been made.

The first overtone of ν_4 is observed as a band with a maximum at 2828 cm^{-1} in NH_4Cl and 2142 cm^{-1} in ND_4Cl. In each case the frequency of maximum absorption is slightly greater than $2\nu_4$ when ν_4 is taken as the limiting frequency which is itself allowed, If the frequency in the ν_4-branch increases in going from the completely in-phase to the completely out-of-phase motion, we expect the center of the overtone, $2\nu_4$, to be greater than twice the frequency of the in-phase motion (which we observe) and also to have a width approximately equal to twice the width of the ν_4-branch. The shape of the band changes appreciably with temperature, chiefly in that the low frequency side of the band tends to vanish as the temperature is reduced. The same phenomenon has been observed in the Raman spectrum.[15] It is interesting that the intensity of this overtone is just as great or greater than that of the fundamental. This may be caused by the fact that the number of transitions entering an overtone is enormously greater than in the case of a fundamental, so that although individual transitions may be exceedingly weak the integrated intensity may become quite considerable.

The combination $\nu_4+\nu_2$ has been discussed previously. Because it is so closely coupled to the intense fundamental ν_3, it is impossible to say anything about its envelope or intensity in NH_4Cl. However, if the ν_4-distribution increases we would expect the ν_2-distribution to decrease in going from in-phase to out-of-phase motion since the in-phase ν_2-motion has the same phase relation between adjacent N—H bonds as the out-of-phase ν_4-motion and *vice versa*. In this case the $\nu_4+\nu_2$-band would be relatively narrow since the width should be approximately equal to the difference between the two distributions. This is actually the case as may be seen from the ND_4Cl spectrum where the combination level does not resonate seriously with ν_3.

The bands observed at 1794 cm^{-1}, 2020 cm^{-1} and 3223 cm^{-1} cannot be accounted for in terms of intramolecular frequencies. The latter can, however, be interpreted as a combination between the totally symmetric mode of the NH_4^+ ion (which has been assigned to 3048 cm^{-1} on the basis of the Raman spectrum[12]) and the optical branch of the lattice spectrum whose greatest density of frequencies is in the vicinity of the Reststrahlen frequency, 183 cm^{-1}. The other two bands must involve still a different characteristic lattice frequency.

VI. TORSIONAL LATTICE VIBRATIONS

In addition to the vibrations of a CsCl type space-lattice, the NH_4Cl crystal lattice spectrum must also contain three branches arising from the coupled torsional oscillations of the NH_4^+ ion. The limiting frequency of this type of motion, which we shall designate ν_6, is of symmetry species F_1 so that it may be active the Raman spectrum as a fundamental but is forbidden in the infra-red spectrum. In order to consider combination bands which may involve these modes, an estimate of the frequency of torsional oscillation would be useful.

The purely electrostatic potential energy in the vicinity of a threefold axis in a CsCl structure is given by

$$V=\frac{e}{a}\Bigg\{\sum_l\sum_m\sum_n\Bigg[\Bigg\{(l-\alpha)+\alpha\left(\phi+\frac{\phi^2}{2}\right)\Bigg\}^2+\Bigg\{(m-\alpha)-\alpha\left(\phi-\frac{\phi^2}{2}\right)\Bigg\}^2+\{(n-\alpha)\}^2\Bigg]^{-\frac{1}{2}}-\sum_u\sum_v\sum_w\Bigg[\Bigg\{\left(\frac{u}{2}-\alpha\right)+\alpha\left(\phi+\frac{\phi^2}{2}\right)\Bigg\}^2+\Bigg\{\left(\frac{v}{2}-\alpha\right)-\alpha\left(\phi-\frac{\phi^2}{2}\right)\Bigg\}^2+\Bigg\{\left(\frac{w}{2}-\alpha\right)\Bigg\}^2\Bigg]^{-\frac{1}{2}}\Bigg\}, \quad (1)$$

where a is the lattice constant, α is the x, y, or z coordinate of a point on the threefold axis (the origin is taken at the center of the cube of eight chlorine atoms), ϕ is the angle (small) about the z axis by which the point in question is obtained from the point α, l, m, n are integers, and u, v, w are odd integers only. If as a rough model of the charge distribution on an NH_4^+ ion we assume a charge fe on each hydrogen atom, where e is the electronic charge, we find for the force constant of the torsional oscillation about the z axis

$$k_\phi=\frac{4fe^2\alpha}{a}\Bigg\{\sum_l\sum_m\sum_n\Big[3\alpha(l-m)^2\{(l-\alpha)^2+(m-\alpha)^2+(n-\alpha)^2\}^{-5/2}-(l+m)\{(l-\alpha)^2+(m-\alpha)^2+(n-\alpha)^2\}^{-\frac{3}{2}}\Big]-\sum_u\sum_v\sum_w\Bigg[3\alpha\left(\frac{u}{2}-\frac{v}{2}\right)^2\Bigg\{\left(\frac{u}{2}-\alpha\right)^2+\left(\frac{v}{2}-\alpha\right)^2+\left(\frac{w}{2}-\alpha\right)^2\Bigg\}^{-5/2}-\left(\frac{u}{2}+\frac{v}{2}\right)\Bigg\{\left(\frac{u}{2}-\alpha\right)^2+\left(\frac{v}{2}-\alpha\right)^2+\left(\frac{w}{2}-\alpha\right)^2\Bigg\}^{-\frac{3}{2}}\Bigg]\Bigg\}. \quad (2)$$

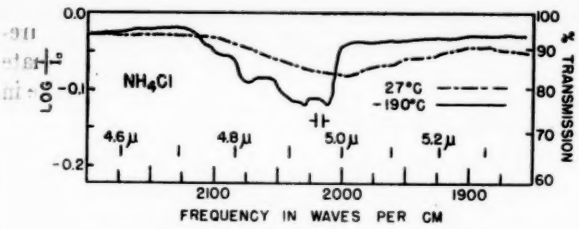

FIG. 4. 4.9 micron band of NH_4Cl in Phase II at 27°C and Phase III at −190°C.

Using the value $f=0.2$ which was estimated by Pauling,[24] the values $a=3.86$A and $r_{NH}=1.0$A, we then calculate for the torsional oscillation frequency, by considering the contributions of 180 surrounding ions, the value

$$\nu_6=262 \text{ cm}^{-1}.$$

It is interesting to note that considering only the 14 nearest neighbor ions this frequency comes out to be 265 cm^{-1}. If instead we use the values suggested by Nagamiya,[17] $f=0.277$ and $r_{NH}=1.13$A we obtain

$$\nu_6=360 \text{ cm}^{-1}.$$

These estimates neglect entirely the effects of repulsion (which would lower the frequency), of the polarizability of the halogen and NH_4^+ ions (which would raise the frequency), and of multipolar terms due to the non-spherical charge distribution in the NH_4^+ ions other than the one considered (which would be small). Since the frequency of oscillation is determined almost entirely by the nearest neighbor halide ions, the frequency should not depend greatly on the relative phase of the torsional motion of the NH_4^+ ions. Hence the distribution of frequencies in this branch should cover only a narrow range compared, for example, to the acoustic branches of the lattice spectrum.

If the band at 1794 cm^{-1} in the low temperature ammonium chloride spectrum, to which no combination of internal modes can be assigned, is identified with the combination $\nu_4+\nu_6$, the torsional oscillation frequency is approximately 391 cm^{-1}. A corresponding assignment to the band at 1348 cm^{-1} in the deuterated salt yields 281 cm^{-1}. The ratio of these frequencies, 0.718, is in satisfactory agreement with the ratio predicted by the Teller-Redlich rule, 0.707.

Using our previously derived value of approximately 1680 cm^{-1} for ν_2, this same type of assignment accounts for the presence of the band at 2000–2100 cm^{-1} as $\nu_2+\nu_6$. Although this band also has a sharp low frequency edge at low temperature, it is quite broad and apparently possesses several maxima. Its detailed structure obviously requires further investigation. Nevertheless, a qualitative estimate of the width and shape of this as well as the $\nu_4+\nu_6$-band can be obtained in the following way. If we assume that in going from the in-phase to the out-of-phase motion the frequency of the torsional lattice mode, ν_6, decreases, we would expect the $\nu_4+\nu_6$-band to be narrow since we found previously that the overtone indicates that the ν_4-distribution increases. This is indeed the case. Also, since it has been shown earlier that the ν_2-distribution probably decreases, the $\nu_2+\nu_6$-band may be expected to have a width approximately equal to the sum of the two distributions and to be distributed to lower frequencies than the value predicted from the in-phase modes. This is consistent with the observed spectrum.

Furthermore, this one frequency, 390 cm^{-1}, can account qualitatively for a series of heretofore inexplicable Raman frequencies observed by Krishnan;[13] e.g., that at 560 cm^{-1} can be assigned to the limiting frequency $\nu_5+\nu_6$, where ν_5 is the Reststrahlen frequency; that at 760 cm^{-1} can be assigned to the first overtone $2\nu_6$, and the diffuse bands at 1065–1145 cm^{-1} and 1280–1335 cm^{-1} in the room temperature spectrum may be assigned to the difference bands $\nu_4-\nu_6$ and $\nu_2-\nu_6$, respectively. Finally, this frequency, on the basis of Eq. (2), should be sensitive to the lattice dimensions, and should therefore be lower in NH_4Br and NH_4I. It is found that the bands corresponding to the 1794 cm^{-1} and 2000–2100 cm^{-1} frequencies in NH_4Cl are the only ones in the spectrum which are significantly shifted; in NH_4Br both bands occur at frequencies about 60 cm^{-1} lower and in NH_4I they occur about 110 cm^{-1} lower. It seems inescapable, therefore, that the torsional frequency occurs at about 390 cm^{-1} in Phase III of NH_4Cl. If this conclusion is correct, this vibration occurs at about 360 cm^{-1} in Phase II. Consequently, there can be no question of free rotation in this phase in Pauling's sense.[1]

In order to interpret the envelope of the combinations involving ν_6 in detail it will be necessary to obtain the complete frequency distributions for the ν_6 branch and for the molecular branches as well as an intensity estimate for all the combinations between branches.

VII. THE RAMAN SPECTRUM

The Raman spectrum of NH_4Cl has been studied by Krishnan[13] over the same temperature range as in this work. Although Krishnan has listed a very large number of lines, his microphotometer tracings are in general very similar to the infra-red spectra published here. In particular, Krishnan has found ν_4 to be very sharp, but in his case it exhibits a double peak at low temperatures. It is not clear why this should be so, but it should be noted, first, that ν_4 has never been observed in the Raman spectrum of methane and, second, that the lines obtained by Krishnan are of relatively low intensity. The 3100 cm^{-1} region of the Raman spectrum is even more complicated than in the infra-red spectrum, since in addition to the strong resonance doublet it contains the even more intense totally symmetric fundamental, ν_1. The Raman spectrum in the vicinity of 1790 cm^{-1} and 2000–2100 cm^{-1} parallels the spectrum

[24] L. Pauling, *Nature of the Chemical Bond* (Cornell University Press, Ithaca 1944), p. 72.

reported here. Menzies and Mills[12] also observed a Raman line at 1712 cm^{-1} in the spectrum at $-150°C$ which may be the doubly degenerate vibration, ν_2, which we have placed at approximately 1680 cm^{-1}. However, this fundamental is also unobserved in the Raman spectrum of methane and, since its motion is quite similar to that of ν_4, it is surprising that its intensity should be so much greater than that of ν_4 in the ammonium halides. Krishnan has also observed a series of frequencies between 3200 cm^{-1} and 3500 cm^{-1}, all of which can be qualitatively accounted for in a variety of ways using the assignments obtained here.

Polarization measurements have not been obtained in Phase III, but Couture and Mathieu[7] have determined the polarization of all the main Raman lines at room temperature. In every case the reported polarization is consistent with the assignments obtained here on the basis of a tetrahedral model. Polarization measurements in Phase III as well as low temperature Raman spectra of the deuterated compounds would be of value in these interpretations.

VIII. THE NATURE OF THE λ-POINT TRANSITION

The simplest crystal structure of NH_4Cl consistent with the x-ray data is that of space group T_d^1. In this structure the ammonium ion tetrahedra are identically situated in every unit cell and the hydrogen atoms lie on the threefold axes. It is in terms of this structure that it has been possible to interpret the low temperature (Phase III) spectrum of NH_4Cl and ND_4Cl. With this symmetry the crystal may exhibit a piezoelectric effect, which has been found by Hettich,[10] may show a first-order Raman lattice spectrum, as has been observed by Menzies and Mills[12] and by Krishnan,[13] and should be optically isotropic, as is the case.[10]

In order to interpret the phase transition, a similar knowledge of the structure of the room temperature modification (Phase II) is necessary. Now it is clear for two reasons that the ammonium ions in this phase are not rotating. First, the narrow line due to the fundamental ν_4 is characteristic of a pure vibrational transition and shows no evidence of rotational structure, particularly on its low frequency side. (Rotational lines might be expected to be spaced at about 15 cm^{-1} intervals.) Second, the identification of a torsional oscillation frequency at a frequency much higher than rotational frequencies removes all of the degrees of freedom which might be available to rotation. However, it is apparent that there are two equivalent equilibrium orientations for the ammonium ion in a single unit cell of a body-centered structure. In both of these the hydrogen atoms lie on the threefold axes. If, therefore, the structure of Phase II is taken as one in which ammonium ions are randomly distributed between these two possible orientations, the infra-red spectrum can be satisfactorily interpreted.

Couture and Mathieu[7] have argued that a disordered phase should yield a depolarization ratio $\rho=6/7$ rather than the observed ratios which are characteristic of cubic crystals. This argument would be valid for *completely random* orientations such as would be obtained if there were free rotation, but for the model suggested above the depolarization ratios would be only slightly perturbed from those of an ordered cubic crystal, since none of the axes of the tetrahedra are shifted with respect to the crystal lattice.

In our Phase II structure the crystal symmetry is lowered and, consequently, the symmetry of the crystalline field about any ammonium ion is no longer genuinely tetrahedral. A variety of symmetrically non-equivalent configurations of nearest neighbor ammonium ions are possible. Some of these configurations slightly displace the chloride ions, and this, in turn, probably gives rise to the main perturbation on the NH_4^+ ion. The most obvious effect to expect is the destruction of the degeneracy of the triply degenerate vibrations, and, indeed, the most striking change of the Phase III to Phase II transformation is the shoulder which develops on the high frequency side of ν_4. This is illustrated by the spectra in Fig. 2.

It is interesting to compare this behavior with that of NH_4Br and NH_4I, which in Phase III do not possess tetrahedral NH_4^+ ion symmetry.††

In these compounds there is a sharp second peak which merges with the main peak as the temperature is raised through the transition point and the line assumes a shape which is almost identical with that of the chloride. The fact that the infra-red spectra of the three halides in Phase II are essentially identical is consistent with the idea that all three have the structure for Phase II discussed above. A more detailed discussion of this transition will be given at a later date. However, it is reasonable to expect that, as in disordered alloy structures, the near neighbor structures are chiefly those of the most stable crystalline forms although over any extended volume of the crystal there is complete randomness. In this case the Phase II structure might be expected to approximate locally a mixture of NH_4Cl and NH_4Br structures, which is consistent with the observed spectrum.

A further consequence of such a randomly oriented structure would be that the lattice vibrations of the crystal should be spread out by the destruction of much of the lattice symmetry. This has been qualitatively observed by Krishnan in the Raman spectrum and may be the reason for the very considerable broadening of the bands at 1794 cm^{-1} and 2000–2100 cm^{-1} which involve the torsional lattice vibration.

†† The x-ray symmetry of NH_4Br and NH_4I in Phase III is D_{4h}^7 so that the NH_4^+ ion symmetry is V_d. In Phase II all three halides have the CsCl structure.

The Vibrational Spectra of Molecules and Complex Ions in Crystals IV. Ammonium Bromide and Deutero-Ammonium Bromide* †

E. L. WAGNER‡ AND D. F. HORNIG
Metcalf Research Laboratory, Brown University, Providence, Rhode Island

(Received October 3, 1949)

The infra-red spectra of thin non-scattering films of NH_4Br and ND_4Br were obtained at 28°C, −78°C and −190°C. The spectra of both compounds in Phase III are in agreement with the x-ray symmetry, D_{4h}^7. The torsional oscillation frequencies occur at 319 cm^{-1} and 230 cm^{-1} in NH_4Br and ND_4Br, respectively. The spectra of Phase II are similar to those of the chloride and indicate a structure in which the NH_4^+ ions are disordered in their equilibrium orientations. There is no evidence of free rotation at any temperature studied. The spectra support x-ray evidence for a further transition at −100°C in ND_4Br to Phase IV which has symmetry T_d^1 as in NH_4Cl.

I. INTRODUCTION

IN the case of highly symmetrical ions in crystals it should be possible on the basis of present theory to obtain considerable information about the symmetry and structure of the crystals from the vibrational spectrum.[1]

In a previous paper[2] the infra-red spectra of NH_4Cl and ND_4Cl were used to obtain evidence regarding the structure of the two crystalline modifications and the nature of the λ-point transition between them. It was shown that in all probability the low temperature phase of each salt has the structure of symmetry T_d^1 in which the ion symmetry is tetrahedral, and that all of the evidence is consistent with a structure of the room temperature phase in which the equilibrium orientations of the NH_4^+ ions are disordered.

Ammonium bromide and deutero-ammonium bromide possess λ-point transitions similar to those of the chlorides at −38.1° and −58.4°C, respectively.[3,4]

However, the λ-point transitions of the bromide salts differ in several respects from those of the chlorides. The temperature of transition of the deuterated ammonium bromide is lower than that of the undeuterated bromide, while the reverse situation is true for the corresponding chloride salts. With the bromides, in contrast to the chlorides, the volumes decrease on raising the temperature through the transformation region.[5]

Furthermore, there is a difference in the reported x-ray crystal structure between the low temperature (Phase III) and the room temperature (Phase II) modifications of the bromides, but not between those of the chlorides. X-ray studies[6,7] indicate that the room temperature modifications of both the chlorides and the bromides have the CsCl type structure relative to the nitrogen and halogen atoms, but that below the transition points the bromide lattices are slightly distorted relative to the Phase II structures and possess the symmetry of the space group D_{4h}^7 with two molecules per unit cell. It is interesting and surprising that ND_4Br, apparently alone among all the ammonium halides, possesses an additional transition at about −100°C, below which it has been reported to revert again to the CsCl type structure.[8]

In addition, although the bromides are not piezoelectric either above or below the transition points, the low temperature (Phase III) modifications do possess optical axes and consequently exhibit double refraction.[9] The Reststrahlen frequency of the room temperature modification of NH_4Br has been observed

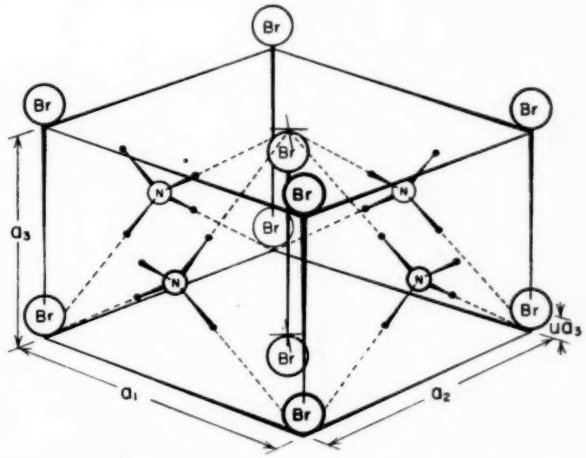

FIG. 1. The unit cell of Phase III of NH_4Br and ND_4Br.

* Based in part on a thesis submitted by Edward L. Wagner in partial fulfillment of the requirements for the Ph.D. degree at Brown University, 1948.

† This work was supported in part by the ONR under Contract N6ori-88, T.O. 1.

‡ Tennessee Eastman Corporation Fellow, Brown University, 1946–48. Present address: Department of Chemistry, State College of Washington, Pullman, Washington.

[1] D. F. Hornig, J. Chem. Phys. **16**, 1063 (1948).

[2] E. L. Wagner and D. F. Hornig, J. Chem. Phys. **18**, 296 (1950).

[3] Smits, Ketelaar, and Muller, Zeits. f. physik. Chemie **A175**, 359 (1936).

[4] Smits, Tollenaar, and Kroger, Zeits. f. physik. Chemie **B41**, 215 (1938).

[5] F. Simon and R. Bergmann, Zeits. f. physik. Chemie **B8**, 255 (1930).

[6] J. A. Ketelaar, Nature **134**, 250 (1934).

[7] J. Weigle and H. Saini, Helv. Phys. Acta **9**, 515 (1936).

[8] A. Smits and D. Tollenaar, Zeits. f. physik. Chemie **B52**, 222 (1942).

[9] A. Hettich, Zeits. f. physik. Chemie **A168**, 353 (1934).

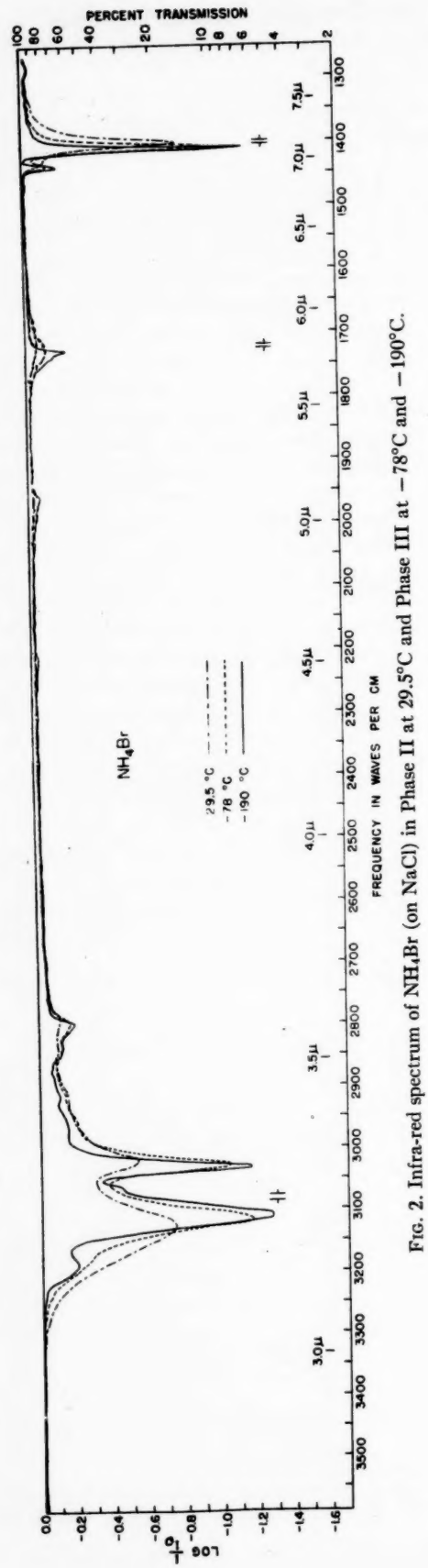

FIG. 2. Infra-red spectrum of NH_4Br (on NaCl) in Phase II at 29.5°C and Phase III at −78°C and −190°C.

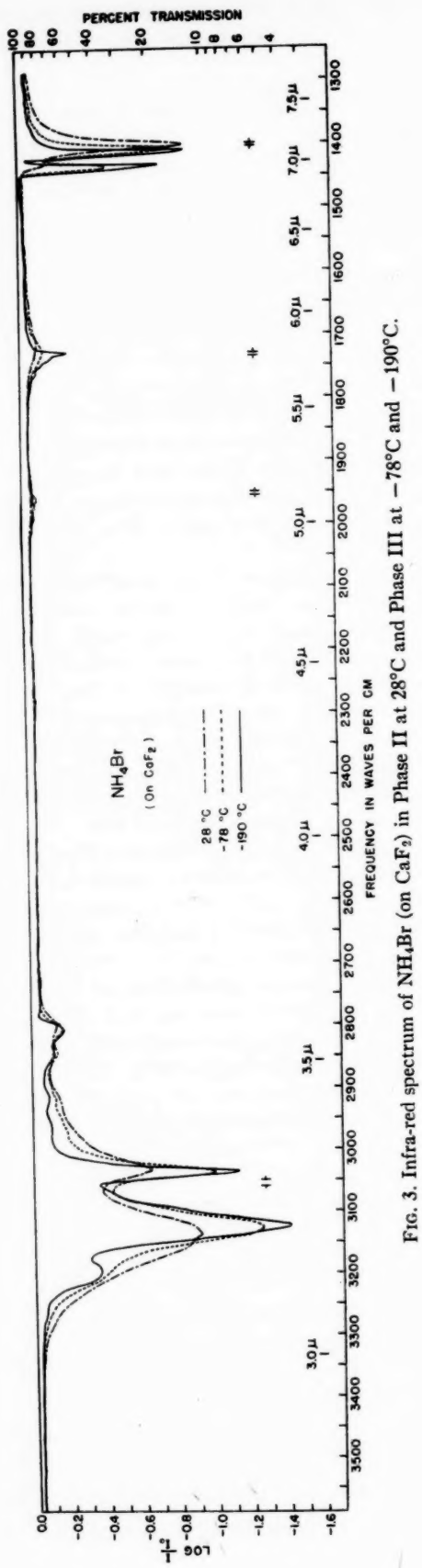

FIG. 3. Infra-red spectrum of NH_4Br (on CaF_2) in Phase II at 28°C and Phase III at −78°C and −190°C.

at 160 cm^{-1} in the reflection spectrum,[10] but the limiting lattice frequency has not been observed directly in the infra-red absorption spectrum. It presumably lies at a somewhat lower frequency. Although Menzies and Mills[11] could find no Raman line corresponding to the lattice line in NH_4Cl, Krishnan[12] and Couture and Mathieu[13] found a series of Raman lines, ascribed by them to lattice frequencies, which persisted considerably above the transition point. Pohlman[14] has studied the infra-red spectrum of NH_4Br at both room temperature and at $-80°C$. She found that the room temperature spectra of NH_4Br and NH_4Cl are essentially identical, but that the low temperature spectra differ primarily in the temperature behavior of the subsidiary peak on the high frequency side of the 7μ bands. This peak disappeared at low temperatures in the chloride spectrum but developed into a distinct second peak in the Phase III bromide spectrum.

All of the evidence is consistent with the structure for the low temperature bromide which possesses the space group symmetry D_{4h}^7 and the ammonium ion symmetry $V_d(\equiv D_{2d})$. This structure is illustrated in Fig. 1. On the basis of previous deductions[1] these symmetry classifications determine the selection rules for the fundamental vibrations of the crystal. We would then expect four internal modes and three limiting lattice modes to be allowed in the infra-red spectrum. In the Raman spectrum there would be seven internal modes and three limiting lattice modes. Since we can consider the ammonium ion in NH_4Br to be a slightly perturbed tetrahedron, we do not necessarily expect to find distinct lines for all the fundamental vibrations. Furthermore, since there is a center of symmetry in the unit cell, the mutual exclusion rule will apply and no frequency may occur in both Raman and infra-red spectra although if the coupling is weak, the frequencies may very nearly coincide.

In order to verify these predictions and to throw further light upon the nature of the λ-point transition in ammonium salts, the infra-red spectra of thin films of NH_4Br and ND_4Br were studied at $-190°C$ and $-78°C$ in Phase III and at 28°C in Phase II. These infra-red spectra are satisfactorily interpretable on the basis of the above model for the low temperature modification of ammonium bromide. Since, as in the chlorides, a torsional lattice mode is observed in both modifications there can be no question of free rotation of the ammonium or deutero-ammonium ions. In addition, the variation in the infra-red spectra of the bromides between the Phase III and Phase II modifications is consistent with the picture of the λ-point transition

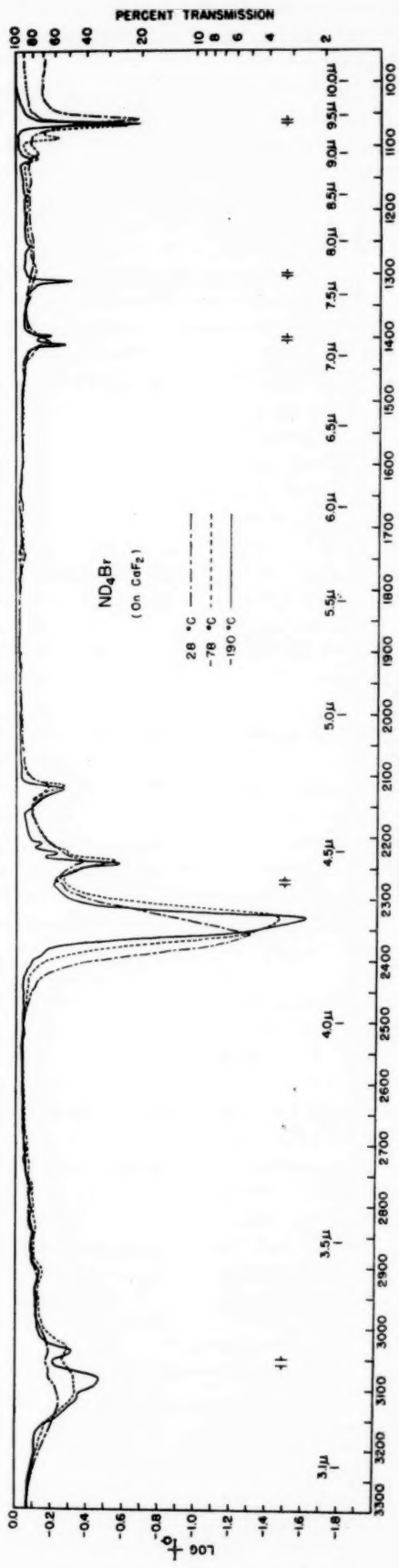

FIG. 4. Infra-red spectrum of ND_4Br (on CaF_2) in Phase II at 28°C, Phase III at $-78°C$ and Phase IV at $-190°C$.

[10] H. Rubens and H. V. Wartenberg, Sitz. preuss. Akad. Wiss. 169 (1914).
[11] A. C. Menzies and H. R. Mills, Proc. Roy. Soc. London **148A**, 407 (1935).
[12] R. S. Krishnan, Proc. Ind. Acad. Sci. **A27**, 321 (1948).
[13] L. Couture and J. P. Mathieu, Proc. Ind. Acad. Sci. **A28**, 401 (1948).
[14] R. Pohlman, Zeits. f. Physik **79**, 394 (1932).

as a change from relative order to relative disorder of the equilibrium orientations of the NH_4^+ ions as suggested by Frenkel.[15]

A detailed theory of such a transition in ammonium bromide has been advanced by Nagamiya.[16] The infrared spectrum of ND_4Br at −190°C (Phase IV) is consistent with the x-ray data and indicates that the structure is identical with that of the low temperature modification (Phase III) of NH_4Cl.

II. EXPERIMENTAL RESULTS

The apparatus and experimental techniques used were essentially identical with those described previously for the ammonium and deutero-ammonium chlorides.[2] The sublimed NH_4Br and ND_4Br films employed were necessarily somewhat thicker than those of the corresponding chloride salts since the absorption coefficients are somewhat less for the heavier halide salts because of the decreased NH_4^+ ion density. In

TABLE I. Observed frequencies, relative intensities, assignments and inferred frequencies for NH_4Br in Phase III and ND_4Br in Phases III and IV.

Assignments	NH_4Br Inferred freq. (cm^{-1})	NH_4Br Obs. freq. at −78°C (cm^{-1})	NH_4Br Obs. freq. at −190°C (cm^{-1})	ND_4Br Inferred freq. (cm^{-1})	ND_4Br Obs. freq. at −78°C (cm^{-1})	ND_4Br Obs. freq. at −190°C (cm^{-1})
					3107*	3115*
					3080*	3085*
					3035*	3040*
					2908*	2910*
					2840*	2845*
						2808*
$\nu_1+\nu_5$ $\nu_1+\nu_{5'}$		3200 (6)	3195 (9)			
$\nu_3(B_2)$ $\nu_{3'}(E)$	[3100]†	3126 (57)	3124 (65) 3075	[2321]†(IV) [2320]†(III)	2332 (135)	2331 (130)
						2257*
$\nu_2+\nu_4$ $\nu_2+\nu_{4'}$ $\nu_{2'}+\nu_{4'}$	[3060]†	3035 (22)	3035 (22)	2254† (IV) 2251† (III)	2239 (21)	2244 (17)
$\nu_1(A_1)$		(3037)¶	(3038)¶			
		2970	2965 (2)		2225*	2228*
		2915	2915 (2)			2212*
$\nu_4+\nu_{4'}$ $2\nu_{4'}$	2840 2812	2843 2802 (5)	2845 2805 (6)	2130 (IV) 2154 2134 (III)	2118 (6)	2124 (8)
						1748*
$\nu_2+\nu_{6'}$ $\nu_{2'}+\nu_{6'}$ $\nu_{2'}+\nu_{6'}$	1973	1950‡ (1)	1950– 2040‡ (1)	1436 (IV) 1414 (III)		
					1410*	1413*
						1400*
					1338*	1340*
$\nu_4+\nu_{6'}$ $\nu_{4'}+\nu_6$ $\nu_{4'}+\nu_{6'}$		1725 (3)	1728 (4)		1297 (1)	1313 (4)
					1257*	1260*
$\nu_2(A_1)$ $\nu_{2'}(B_1)$	1654	(1694)¶	(1690)¶	1189 (IV) 1184 (III)		
						1178*
					1119*	1121*
$\nu_4(B_2)$		1434 (3)	1433 (6)		1087 (2)	
$\nu_{4'}(E)$		1406 (10)	1408 (10)		1067 (10)	1065 (10)
$\nu_6(A_2)$ $\nu_{6'}(E)$	319	(328)¶	(335)¶	248 (IV) 230 (III)		
$\nu_5(B_2)$ $\nu_{5'}(E)$	160					

* ND_3H^+ and $ND_2H_2^+$ bands.
† Computed unperturbed frequencies.
‡ Broad band.
¶ From Raman spectrum.

[15] J. Frenkel, Acta Physicochimica **3**, 23 (1935).
[16] T. Nagamiya, Proc. Phys. Math. Soc. Japan **25**, 540 (1943).

TABLE II. Observed frequencies, relative intensities, assignments and inferred frequencies for NH_4Br and ND_4Br in Phase II.

Assignment	NH_4Br Inferred freq. (cm^{-1})	NH_4Br Obs. freq. at 28°C (cm^{-1})	ND_4Br Inferred freq. (cm^{-1})	ND_4Br Obs. freq. at 28°C (cm^{-1})
				3120*
				3075*
				3043*
				2920*
				2848*
				2795*
$\nu_3(B_2)$, $\nu_{3'}(E)$	[3110]†	3137 (46)	[2342]†	2358 (104)
				2277*
				2267*
$\nu_2+\nu_4$, $\nu_2+\nu_{4'}$, $\nu_{2'}+\nu_{4'}$	[3058]†	3031 (16)	[2256]†	2240 (16)
$\nu_1(A_1)$		(3037)‡		
$\nu_4+\nu_{4'}$, $2\nu_{4'}$	2830, 2802	2833, 2797 (3)	2116	2119 (4)
$\nu_2+\nu_{6'}$, $\nu_{2'}+\nu_{6'}$, $\nu_{2'}+\nu_6$	1968	1965¶	1436	
				1406*
$\nu_4+\nu_{6'}$, $\nu_{4'}+\nu_6$, $\nu_{4'}+\nu_{6'}$		1712 (2)		1275 (<1)
				1255*
$\nu_2(A_1)$, $\nu_{2'}(B_1)$	1657	(1686)‡	1198	
				1118*
$\nu_4(B_2)$, $\nu_{4'}(E)$		1429 (<1), 1401 (10)		1058 (10)
$\nu_6(A_2)$, $\nu_{6'}(E)$	311		217	

* ND_3H^+ and $ND_2H_2^+$ bands.
† Computed unperturbed frequencies.
‡ From Raman spectrum.
¶ Broad band.

addition to the standard sublimation procedure, films were sublimed onto a polished CaF_2 plate cooled to 0°C. This procedure was used to prevent possible halide exchange and also to obtain a backing with a less pronounced adsorbed water film.

The spectra obtained from an NH_4Br film approximately 0.5-micron thick on a rocksalt plate are shown in Fig. 2. The spectra of four additional NH_4Br films of varying thickness on rocksalt plates were also studied. Figure 3 shows the spectra of an NH_4Br film which had been sublimed onto a cooled CaF_2 plate. The spectra shown in these two figures are experimental curves which have not been corrected for scattering nor has the noise level been appreciably smoothed out.

In general, the NH_4Br spectrum is very similar to that of NH_4Cl. The only significant frequency differences occur for the bands appearing in NH_4Br at 1728 cm^{-1} and 1950–2040 cm^{-1}. These two bands occur at frequencies 60–65 cm^{-1} lower than the corresponding bands in NH_4Cl. The other bands appear at frequencies within 25 cm^{-1} of those in the chloride spectrum. The most striking difference between the spectra of NH_4Br and NH_4Cl is the materialization of a distinct separate peak at about 1435 cm^{-1} in the spectrum of NH_4Br at low temperature. With powdered material and with thick or strongly scattering films of NH_4Br on rocksalt, the intensity ratio in Phase III of the two peaks at 1400 cm^{-1} and 1435 cm^{-1} approaches 2:1. With thin non-scattering films on rocksalt this ratio is sometimes as high as 10:1, indicating a partial orientation of the NH_4Br film in Phase III in such a way that the unique axis of the D_{4h}^7 unit cell is perpendicular to the rocksalt surface. On the other hand, this ratio is less than 2:1 in the Phase III spectrum of NH_4Br on CaF_2, indicating that the orientation is such that the unique crystal axis lies parallel to the CaF_2 plate surface. However, for a given film this ratio is somewhat temperature-dependent, a fact for which we have no present explanation. There are also several additional weak absorption peaks in the bromide spectra that do not appear in the corresponding chloride spectra, particularly in the 2800–3000 cm^{-1} region. It is to be noted that the two strong bands near 3.2μ which are of equal intensity in NH_4Cl differ very considerably here. The intensity ratio of those two bands is also slightly different depending on whether the film is on a rocksalt or a CaF_2 plate.

The corresponding spectra of an ND_4Br film on a CaF_2 plate are shown in Fig. 4. One other film on CaF_2 and two other films on rocksalt were also studied. The films on rocksalt were considerably more contaminated with ND_3H^+ and $ND_2H_2^+$ than that shown in Fig. 4. The spectra of ND_4Br bear the same general relation to those of ND_4Cl as the NH_4Br spectra do to those of NH_4Cl, except at the lowest temperature shown here. The differences at low temperature are associated with the known additional phase transition of ND_4Br which occurs at about −100°C. In agreement with the x-ray data the spectrum of ND_4Br in Phase IV is very similar to that of ND_4Cl in Phase III.

The observed frequencies of maximum absorption, the relative integrated peak intensities and our assignments of the spectra of NH_4Br and ND_4Br on CaF_2 plates are given in Tables I and II. In these tables the vibrational modes are designated by the same subscripts as the corresponding NH_4Cl modes. Where splitting of the degeneracies occurs the additional components are indicated by primes. The assignments to ND_3H^+ and $ND_2H_2^+$ were made by analogy with the deutero-ammonium chlorides and deutero methanes. They were all checked experimentally by preparing films from ND_4Br which had been exposed to increasing

TABLE III.

T_d	Resolved into $V_d(D_{2d})$
A_1	A_1
A_2	B_1
E	A_1+B_1
F_1	A_2+E
F_2	B_2+E

amounts of water vapor and noting the changes in intensity. In addition to the frequencies listed, a film prepared from ND_4Br which had been exposed to water vapor showed peaks at 2275 cm^{-1} and 2307 cm^{-1} when it was cooled to −190°C.

III. DISCUSSION

If the space group of NH_4Br and ND_4Br in Phase III is D_{4h}^7, the local symmetry of the NH_4^+ and ND_4^+ ions is V_d so that only those fundamental vibrations which are allowed under the point group V_d may be active in either spectrum.[1] Each of the irreducible representations of V_d goes into two irreducible representations of D_{4h}, *gerade* and *ungerade* with respect to the center of symmetry. Accordingly, each normal vibration of the ammonium ion gives rise to two limiting vibrations of the crystal which correspond physically to the symmetric and anti-symmetric coupling of the vibrations of the two ions in the same unit cell. Only *gerade* vibrations may be active in the Raman spectrum and only *ungerade* vibrations in the infra-red spectrum. Consequently, the two spectra should not be expected to coincide unless the coupling between ammonium ions is very weak.

The primary distinction between ammonium ions with symmetry T_d as in Phase III of the chlorides and those with symmetry V_d as in Phase III of the bromides is that the latter have lost their threefold symmetry axes. One may thus expect that the tetrahedral degeneracies will be partially removed. Table III shows the resolution of the species of point group T_d into those of point group V_d. A tetrahedral ammonium ion would have two normal vibrations of symmetry species F_2, a stretching and a bending vibration. Under V_d these may be resolved into two components, polarized along and perpendicular to the S_4 axis of V_d which in this structure is parallel to the fourfold axis of the crystal. Similarly, the doubly degenerate bending vibration of the tetrahedral model is split but neither component is allowed in the infra-red spectrum. Finally, the totally symmetric stretching vibration is inactive under V_d as well as under T_d. As in NH_4Cl, all of the internal vibrations may be active in the Raman spectrum.

In addition, the T_d^1 lattice of NH_4Cl has two limiting lattice modes, one of species F_2 which consists of the vibration of the NH_4^+ sublattice against the Cl^- sublattice, and one of species F_1 which involves the torsional oscillations of the NH_4^+ ions. Under the point group V_d both of these lattice modes may be split. The two components of the F_2 (translational) lattice vibration and the E component of the torsional oscillation may be both infra-red and Raman active. The A_2 component of the torsional oscillation is forbidden in both spectra.

The infra-red spectra of the ammonium bromides in Phase III can be assigned by comparison with the corresponding spectra of NH_4Cl and ND_4Cl. The triply degenerate mode of the tetrahedral model ν_4, is split in both cases into two sharp lines which occur (−78°C) at 1406, 1434 cm^{-1} and 1067, 1087 cm^{-1} in NH_4Br and ND_4Br, respectively. In unoriented films the integrated intensity ratio of these two peaks is 2:1, in agreement with the expected ratio for E and B_2 components. Since the spectral lines corresponding to these two components are sharp and distinct, with no indication of further splitting, the ion symmetry in Phase III must be either V_d or C_{3v}. The fact that the fundamental, ν_2, has not been detected in the infra-red spectrum suggests that the symmetry is in fact V_d since ν_2 is allowed under C_{3v} but is forbidden under V_d.

At −190°C, where ND_4Br is known to exist in the Phase IV modification, ν_4 is no longer split and the infra-red spectrum is remarkably similar to that of ND_4Cl in Phase III. The symmetry of the ion in Phase IV must therefore be tetrahedral. The only possible structures for this phase based on a CsCl arrangement of N and Br are therefore T_d^1 with an NH_4Cl structure or T_d^5 with 4 molecules per unit cell. This conclusion is in accord with the x-ray data. Several face-centered lattices would also be in accord with our data.

Both in this and the preceding paper we have used the absence of splitting of the fundamental mode, ν_4, to demonstrate that the symmetry is such as to make it degenerate. This argument is valid only if ν_4 is in fact sensitive to small changes in its crystalline environment. In the case of NH_4Br it is known from x-ray data that the Br^- ions are displaced two percent of the lattice constant, or 0.09A, from their lattice position in a simple CsCl cubic lattice in which ν_4 would be degenerate. The resultant splitting is 28 cm^{-1}. Consequently, we can safely conclude that in the case of this particular mode the splitting is an extremely sensitive measure of the distortion of the crystal lattice.

On the other hand, it is apparent from a comparison of the very intense band at 2332 cm^{-1} in ND_4Br and 2336 cm^{-1} in ND_4Cl that the splitting of the other triply degenerate vibration, ν_3, is certainly not as great as 10 cm^{-1} since it cannot be detected in the spectra. In NH_4Br, just as in NH_4Cl, this fundamental resonates with the nearly coincident combination level, $\nu_2+\nu_4$, giving rise to the doublet at 3.25μ. The coincidence of the levels is not as exact as in NH_4Cl since the intensities of the two branches differ considerably. If, as in the previous paper,[2] it is assumed that all of the intensity in the band originates in the fundamental, the intensity ratio of the two branches can be used to compute a separation of about 40 cm^{-1} for the unperturbed levels. These calculated unperturbed frequencies are designated in Tables I and II by the numbers in brackets. The Teller-Redlich frequency product ratios for the two internal vibrations¶ of species E and B_2 of the bromides

¶ To use the product rule rigorously it would be necessary to include the lattice frequencies of appropriate symmetry. However, the frequency separation between the internal and lattice vibrations is so great that it is safe to assume that the interaction is negligible.

in Phase III at −78°C are

$$\frac{\nu_3'^{D}\nu_4'^{D}}{\nu_3'^{H}\nu_4'^{H}}=0.568$$

and

$$\frac{\nu_3{}^{D}\nu_4{}^{D}}{\nu_3{}^{H}\nu_4{}^{H}}=0.567,$$

respectively. These values are within the usual range of agreement with the harmonic approximation value, 0.5528.

The fundamental vibration, ν_2, is not observed directly in any of the spectra but its frequency may be inferred from the combination $\nu_2+\nu_4$. Three of the four components of the combinations $\nu_2+\nu_4$ are allowed but only one band is observed in each spectrum which can clearly be assigned to this combination band. In the case of NH_4Br these levels all resonate strongly with ν_3 so that a detailed discussion of the shape of the band is impossible. In ND_4Br the resonance with ν_3 is not serious but, because of the fact that in crystals all combination bands are themselves distributions of frequencies,[17,18] it is unreasonable to use the details of the band to assign components. From the position of the computed unperturbed levels of $\nu_2+\nu_4$ the frequency of ν_2 is found to be approximately 1654 cm^{-1} in NH_4Br and 1184 cm^{-1} in ND_4Br. A Raman line has been observed at 1694 cm^{-1} at this same temperature[11] which has been shown to have the proper polarization for ν_2 at room temperature[13] so that this Raman value is probably correct. The Raman spectrum of ND_4Br has not been studied but it is likely that the frequency inferred from the infra-red data is nearly correct in this case since the resonance correction to $\nu_2+\nu_4$ is small.

The same overtones and combinations are observed in NH_4Br and ND_4Br as in the chlorides. In this case there are three possible components of $2\nu_4$, two of which are allowed in the infra-red spectrum. In fact, the band, $2\nu_4$, has maxima at 2806 and 2845 cm^{-1} in NH_4Br but since the distribution function for a single component of the overtone may have several maxima it does not seem safe to infer that the maxima represent these components. Moreover, in Phase IV of ND_4Br only a single active component of $2\nu_4$ exists but the same two maxima are apparently observed.

The combination bands involving the torsional modes of the ammonium ions, $\nu_4+\nu_6$ and $\nu_2+\nu_6$, are very similar in appearance and temperature behavior to the corresponding bands in the chlorides. They occur at 1728 cm^{-1} and 1945–2040 cm^{-1} in Phase III of NH_4Br. The latter band has not been observed in ND_4Br because of overlying bands due to hydrogen contamination. It may, therefore, be inferred that the torsional lattice vibrations of the NH_4^+ and ND_4^+ ions in Phase III of the bromides have a frequency of 319 and 230 cm^{-1}, respectively, at −78°C. The ratio of these frequencies is 0.721, approximately the expected value. It is, of course, impossible to compare this ratio alone with theory since the E component of the F_2 lattice vibration is coupled with it. Krishnan has found a reasonably intense Raman line at 335 cm^{-1} which has not previously been accounted for. It seems likely that it is the torsional fundamental, ν_6, and that the lines at 660 cm^{-1} and 490 cm^{-1} are its first overtone and its combination with the limiting lattice mode, ν_5. In this case the limiting lattice frequency is approximately 155–165 cm^{-1} which compares well with the value 160 cm^{-1} obtained here from the combination $\nu_1+\nu_5$ at 3200 cm^{-1}. There are no data available from which the corresponding ND_4Br frequency may be obtained.

The Raman spectrum of a single crystal of NH_4Br has been obtained by Krishnan at a series of temperatures from +125°C to −188°C. Although Krishnan has tabulated a great many lines in the 1400–3500 cm^{-1} region his microphotometer tracings are quite similar, in general, to the infra-red spectra reported here except for the appearance of the strong line at 1690 cm^{-1} (ν_2), the comparative feebleness of ν_4 and the absence of the combination $\nu_4+\nu_6$ at 1728 cm^{-1}. It is interesting that there is essentially no discrepancy between the frequencies observed in the Raman and infra-red spectra since it indicates, as mentioned previously, that the coupling between the motions of adjacent ammonium ions is negligible. Krishnan has also observed a rich lattice spectrum for NH_4Br.

Polarization measurements[13] have been made in the Raman spectrum only in Phase II. The polarization measurements are entirely consistent with the assignment proposed here whereas it is difficult to reconcile them with any other.

IV. THE λ-POINT TRANSITION

The infra-red spectrum of Phase II of NH_4Br and ND_4Br is similar, in general, to that in Phase III and the same vibrational assignments may be made. The most conspicuous difference is that in both cases the second sharp component of ν_4 in Phase III is replaced in Phase II by a flat shoulder. Similarly, the sharp peak in the combination $\nu_4+\nu_6$ in Phase III is replaced by a broad diffuse band in Phase II. Although differing from the Phase III bromide spectra in these respects, the Phase II bromide spectra are almost identical with the Phase II chloride spectra. Consequently, it appears that the same model for the structure of Phase II applies in both gases, namely, one in which the equilibrium orientations of the ammonium ions are randomly distributed between the two orientations possible for a tetrahedron in a cubic cage of halide ions. In both orientations the hydrogen (or deuterium) atoms lie on the threefold axes.

Perhaps the strongest evidence, although they did not consider it so, for this structure of Phase II is the Raman depolarization data of Couture and Mathieu.[13]

[17] M. Born and M. Bradburn, Proc. Roy. Soc. **188A**, 161 (1947).
[18] H. Winston and R. S. Halford, J. Chem. Phys. **17**, 607 (1949).

They found that in this phase in both NH_4Cl and NH_4Br the depolarization ratios were essentially those of an ordered cubic crystal. The necessary condition that this be the case is that the symmetry axes of the cubic crystal remain intact or be only slightly perturbed. The model described is the only disordered structure in which this is the case. It is not the case, for example, in any model involving free rotation of the ammonium ions.

The infra-red spectra are also consistent with this model. It has been pointed out previously that the effect of coupling of neighboring ammonium ions is very small but that ν_4 is very sensitive to small displacements of the halide ions. The precise equilibrium position of each halide ion certainly depends on the orientation of the ammonium ions surrounding it. An example of such a displacement of the halide ions from their position in a cubic lattice is the D_{4h}^7 structure of Phase III (see Fig. 1) whereas a configuration in which they are not displaced is the T_d^1 structure of Phase III of NH_4Cl. In the disordered model the halide ions would be displaced by intermediate amounts and since the displacements vary statistically we might expect shifts in ν_4 varying from zero to a maximum value approximately equal to the splitting of ν_4 in Phase III of NH_4Br since this structure clearly gives a maximum halide displacement.

X-ray data might provide a further check on this model. If it is correct the halide ions are statistically distributed about their mean lattice positions in Phase II and some indications of disorder should be discernible. In any case, it is clear that the λ-point transition between Phase III and Phase II does not involve free rotation and it seems likely that it is a simple order-disorder transformation in the equilibrium orientations of the ammonium ions.

THE JOURNAL OF CHEMICAL PHYSICS VOLUME 18, NUMBER 3 MARCH, 1950

The Interchange of Translational and Vibrational Energy in an Asymmetric Molecular Potential Field*

GILBERT W. CASTELLAN† AND HUGH M. HULBURT
Department of Chemistry, The Catholic University of America, Washington, D. C.

(Received July 14, 1949)

Reflection coefficients are calculated for a matter wave in a parabolic channel and in a square channel, each channel closed at one end by a vertical plane tilted slightly from the normal to the axis of the channel. The number of collisions necessary to dissipate one quantum of vibrational energy is given in terms of $\lambda = \tan\theta$, where θ is the angular deviation of the plane end from the normal to the axis of the channel. Comparison with the data from measurements on sound dispersion shows good agreement for N_2O and CO_2. The temperature dependence of the average probability of transition per collision is compared with data for Cl_2 and a mixture of Cl_2 and CO.

I. INTRODUCTION

THE probability of exciting internal energy states of a molecule in a collision is a quantity of importance in several physico-chemical phenomena. The Lindemann theory of unimolecular reactions supposes that activation occurs by this mechanism and the relative rates of activation and dissociation of the excited molecule determine the apparent pressure dependence of the reaction.

The dispersion of sound in gases likewise is governed by the rate of exchange of energy between translational and internal degrees of freedom of the molecule. Anything which prevents the internal degrees of freedom from taking up their equilibrium share of the heat of compression of the sound wave will diminish the effective specific heat of the gas and increase the velocity of sound. As the frequency is increased, a point is reached where the time required to establish temperature equilibrium is of the same order as the period of the sound wave. An increase of sound velocity with frequency is then observed. From experimental data on dispersion, the number of collisions required to dissipate one quantum of vibrational energy can be calculated.

This problem of energy exchange between various degrees of freedom has been reviewed by Oldenburg and Frost.[1] The present discussion will be restricted to interchange between vibrational and translational energy. The simplest case is the collision of an atom with a diatomic molecule. This process can be represented classically by the motion of a mass-point on the appropriate energy surface in the configuration space of the triatomic complex. The surface upon which the complex moves during the collision is the same as that considered in the activated complex theory of chemical

* From a dissertation submitted by Gilbert W. Castellan to the Faculty of the Graduate School of Arts and Sciences of the Catholic University of America in partial fulfillment of the requirements for the degree of Doctor of Philosophy.

† Present address: Department of Physics, The University of Illinois, Urbana, Illinois.

[1] O. Oldenburg and A. Frost, Chem. Rev. **20**, 99 (1937).

reaction rates. In the case of a simple collision, however, there is not enough energy for the complex to reach the activated state and we consider only a surface consisting of a channel with a closed end. The point-mass representing the complex is reflected by the surface and returns along the channel through which it came, but not necessarily in its initial vibrational state. Irregularities in the channel will cause a change in the components of momentum parallel and perpendicular to the path of least potential energy, which we shall call briefly the reaction path. This change in the momentum components of the point-mass represents a change in vibrational energy of the system. Inspection of the potential energy surfaces which have been calculated[2] shows that as the complex approaches the barrier, the surface rises and becomes assymmetric about the reaction path. This assymmetry seems to bear the primary responsibility for the change in the vibrational energy of the system.

In quantum mechanics, the point-mass is replaced by a wave packet moving in the potential energy field represented by the surface. A steady stream of such packets is best treated by considering its Fourier plane-wave components in each vibrational state separately. The progressive wave is diffracted by irregularities in the potential energy (analogous to variations of the refractive index in the optical case) and is reflected and diffracted by the closed end of the channel. A particularly simple mathematical treatment is possible when the surface can be idealized to consist of two or more sections in each of which explicit solutions of the Schrödinger equation can be found. Boundary conditions and continuity conditions at the junctions of the several regions permit the solutions to be expanded in terms of eigenfunctions that represent plane waves incident and reflected in the incoming channel. The expansion coefficients give the relative transition probabilities for excitation to the higher vibrational states. This is similar to the "sudden" approximation in the quantum theory of the collisions of elementary particles.[3] A different approximation, based upon analytic continuation of the eigenfunctions, has been used by Hirschfelder and Wigner[4] for a continuous potential energy surface. Golden and Peiser[5] use still a different approach.

The energy surfaces shown in Figs. 1 and 2 represent collisions of hard spheres, one of which has a vibrational degree of freedom. They are of the same general type as that discussed qualitatively by Gershinowitz.[6] Zener[7] has used a more elaborate model. In a hard-sphere model, when the closing surface is normal to the channel axis, the Schrödinger equation separates into two equations for motion parallel and normal to the reaction path, respectively, and no vibrational transitions are induced by collision. Detailed reasons for this will be evident in the mathematical treatment that follows. The simplest modification that produces transitions is to incline the closed end slightly from the normal to the channel axis, as illustrated in Fig. 2. As atom A approaches diatomic molecule BC along the line of centers, the vibrations of BC become perturbed, being reduced in amplitude if no excitation occurs. This is effectively an anharmonicity introduced during the collision which induces an exchange of energy between translational and vibrational degrees of freedom. As might be expected, the reduced amplitude available favors transitions to higher energy levels in the case of a harmonic oscillator.

The parameter λ, the cotangent of the angle made by the closed end and the channel axis, measures the intensity of the interaction during the collision. If the angle is small, perturbation begins at large intermolecular distances. This model, however, allows no separate adjustment of both the anharmonicity and the duration of the perturbation. Thus a short range highly anharmonic interaction would have much the same representation as a long range, weakly anharmonic perturbation. Consequently, this model cannot be expected to give a quantitative account of the data, but may indicate important qualitative features of the interaction.

Both square and parabolic channels have been used

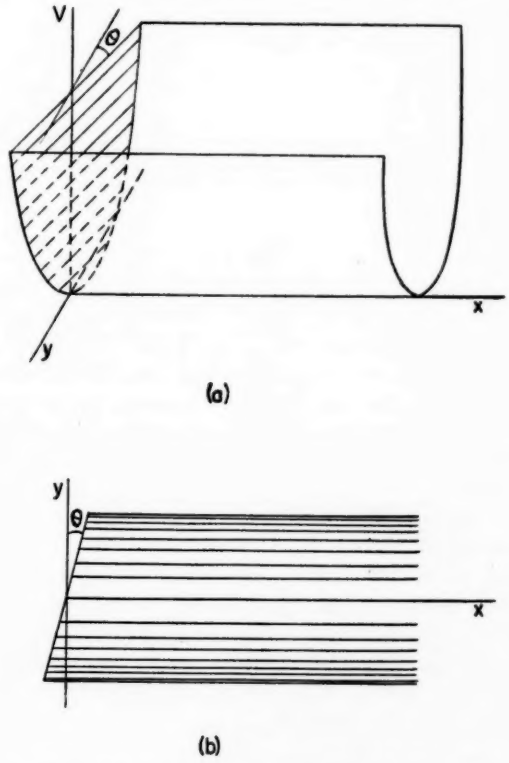

FIG. 1. The parabolic channel. (a) $V(x)$ is infinite on the plane $x=y\tan\theta$, and is zero everywhere else. (b) Contour.

[2] Glasstone, Laidler, and Eyring, *The Theory of Rate Processes* (McGraw-Hill Book Company, Inc., New York, 1941), Chapter III.

[3] Cf. L. I. Schiff, *Quantum Mechanics* (McGraw-Hill Book Company, Inc., New York, 1949), p. 207 ff.

[4] J. O. Hirschfelder and E. Wigner, J. Chem. Phys. **7**, 616 (1939).

[5] S. Golden and A. M. Peiser, J. Chem. Phys. **17**, 630 (1949).

[6] H. Gershinowitz, J. Chem. Phys. **5**, 54 (1937).

[7] C. Zener, Phys. Rev. **37**, 556 (1931).

to calculate reflection coefficients in detail. However, only the results from the parabolic channel will be used to interpret data.

II. CALCULATION OF THE REFLECTION COEFFICIENTS

The Parabolic Channel

The Schrödinger equation for the potential energy surface shown in Fig. 1 may be written

$$(-\hbar^2/2m)\nabla^2\psi+(k/2)y^2\psi=E\psi, \tag{1}$$

where ∇^2 is the two-dimensional Laplacian operator in rectangular coordinates. The solution to this equation is written in the form:

$$\psi_n=\sum_j [\exp(-ip_jx/\hbar)\delta_{nj}+R_{nj}\exp(ip_jx/\hbar)]H_j(\eta). \tag{2}$$

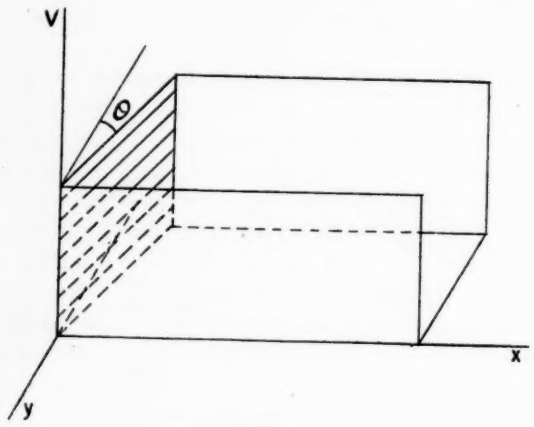

(a)

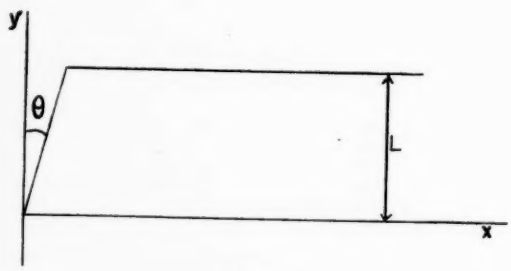

(b)

FIG. 2. The square channel. (a) $V(x)$ is infinite on the plane $x=y\tan\theta$, and is zero everywhere else. $V(y)$ is infinite on the planes $y=0$ and $y=L$ and is zero in-between. (b) Contour.

This solution represents a system in the nth state incident upon the barrier with unit amplitude; the system is reflected from the barrier in various states, j, with the amplitudes R_{nj}. In this expression, $H_j(\eta)$ is the normalized, weighted, jth Hermite polynominal; $\beta=(mk/\hbar^2)^{\frac{1}{4}}$; and $\eta=y\beta^{\frac{1}{2}}$. The energy equation corresponding to this solution is

$$E/E_0=r_j^2+2j+1, \tag{3}$$

where $E_0=(\frac{1}{2})h\nu_0$, $p_j=r_j\mathfrak{p}$, and $\mathfrak{p}=(mh\nu_0)^{\frac{1}{2}}$.

The boundary condition requires that $\psi_n=0$, when $y=x/\tan\theta$, that is, when $\eta=\beta^{\frac{1}{2}}x/\tan\theta$. Applying this condition and making the transformations: $\lambda=\tan\theta$, $\xi=\beta^{\frac{1}{2}}x/\lambda$, Eq. (2) becomes

$$\sum_j [\exp(-ir_j\lambda\xi)\delta_{nj}+R_{nj}\exp(ir_j\lambda\xi)]H_j(\xi)=0. \tag{4}$$

This equation must hold for all values of ξ.

The following expansions are then made:

$$\exp(-ir_j\lambda\xi)H_j(\xi)=\sum_k P_{jk}H_k(\xi) \tag{5}$$

$$\exp(ir_j\lambda\xi)H_j(\xi)=\sum_k Q_{jk}H_k(\xi), \tag{6}$$

where

$$P_{jk}=\int_{-\infty}^{\infty}\exp(-ir_j\lambda\xi)H_j(\xi)H_k(\xi)d\xi \tag{7}$$

$$Q_{jk}=P_{jk}^*=\int_{-\infty}^{\infty}\exp(ir_j\lambda\xi)H_j(\xi)H_k(\xi)d\xi. \tag{8}$$

Substitution of these expansions into Eq. (4) yields the result

$$\sum_j\sum_k [\delta_{nj}P_{jk}+R_{nj}Q_{jk}]H_k(\xi)=0. \tag{9}$$

Setting the coefficient of each $H_k(\xi)$ equal to zero, one obtains

$$P+RQ=0, \tag{10}$$

where the equation has been written in matrix form. This equation immediately yields the formal solution: $R=-PQ^{-1}$. However, finding the inverse of Q is not a convenient method for evaluating the matrix elements of R.

The integrals P_{jk} and Q_{jk} can be evaluated explicitly; this is done in Appendix I. It is to be noted that $P_{jk}=Q_{jk}^*$, where the asterisk indicates the complex conjugate. The explicit form of Q_{jk} is

$$Q_{jk}=\left(\frac{j!k!}{2^{j+k}}\right)^{\frac{1}{2}}(ir_j\lambda)^{j+k}$$

$$\times\exp[-(r_j\lambda/2)^2]\sum_{t=0}\frac{(-1)^t2^t(r_j\lambda)^{-2t}}{t!(k-t)!(j-t)!}, \tag{11}$$

where the sum is from zero to the smaller of the values j or k.

Since there is no simple method of obtaining the inverse of a matrix such as Q, it will be convenient to use an alternate method to obtain approximate values of the R_{nj} when lambda is small.

The exponential factor in the integrals P_{jk} and Q_{jk} is expanded before integrating and the resulting expression integrated term by term. This leads to an expansion of P and Q in powers of lambda with matrix coefficients. The matrix R is also expanded in powers of

lambda with undetermined coefficients.

$$P=\sum_{n=0} P^{(n)}\lambda^n \tag{12a}$$

$$Q=\sum_{n=0} Q^{(n)}\lambda^n \tag{12b}$$

$$R=\sum_{n=0} R^{(n)}\lambda^n. \tag{12c}$$

Substituting these expansions in Eq. (10) yields:

$$\sum_n P^{(n)}\lambda^n+\sum_n\sum_s R^{(n)}Q^{(s)}\lambda^{n+s}=0, \tag{13}$$

where

$$Q_{jk}{}^{(n)}=\frac{(ir_j)^n}{n!}\Phi_{jk}{}^{(n)}$$

$$P_{jk}{}^{(n)}=(-1)^nQ_{jk}{}^{(n)}$$

$$\Phi_{jk}{}^{(n)}=\int_{-\infty}^{\infty}\xi^nH_j(\xi)H_k(\xi)d\xi.$$

Again, Eq. (13) is an identity in lambda; consequently, the coefficient of each power of lambda must vanish. This gives the equation

$$P^{(n)}+\sum_s R^{(s)}Q^{(n-s)}=0 \tag{14}$$

or the series of equations

$$\begin{aligned}&P^{(0)}+R^{(0)}Q^{(0)}=0\\&P^{(1)}+R^{(0)}Q^{(1)}+R^{(1)}Q^{(0)}=0\\&P^{(2)}+R^{(0)}Q^{(2)}+R^{(1)}Q^{(1)}+R^{(2)}Q^{(0)}=0.\end{aligned} \tag{15}$$

Since $P^{(0)}=Q^{(0)}=E$, the unit matrix, we have immediately that $R^{(0)}=-E$. If this result is substituted in the second of Eqs. (15), $R^{(1)}$ is determined. $R^{(1)}=Q^{(1)}-P^{(1)}$, or, $R^{(1)}=2Q^{(1)}$. This procedure is repeated until the desired accuracy is obtained. Explicitly,

$$\begin{aligned}R_{jk}{}^{(0)}&=-\delta_{jk}\\R_{jk}{}^{(1)}&=ir_j\sqrt{2}[j^{\frac{1}{2}}\delta_{j-1,k}+(j+1)^{\frac{1}{2}}\delta_{j+1,k}]\\R_{jk}{}^{(2)}&=r_j\{[j(j+1)^{\frac{1}{2}}]r_{j-1}\delta_{j-2,k}\\&\quad+[jr_{j-1}+(j+1)r_{j+1}]\delta_{jk}\\&\quad+[(j+1)(j+2)]^{\frac{1}{2}}r_{j+1}\delta_{j+2,k}\}.\end{aligned} \tag{16}$$

These first three coefficients will be sufficient to give reflection coefficients correct to the power of λ^2.

The reflection coefficient is defined by the equation

$$\rho_{jk}=R_{jk}R_{jk}{}^*(r_k/r_j). \tag{17}$$

The value of ρ_{jk} is the probability that a system which strikes the barrier in the jth vibrational state will be reflected in the kth vibrational state. Conservation of matter as expressed by setting the probability current equal to zero—i.e.,

$$0=\frac{h}{2im}\left[\psi^*\frac{\partial\psi}{\partial x}-\psi\frac{\partial\psi^*}{\partial x}\right]$$

imposes the condition that $\sum_k\rho_{jk}=1$.

Using the definition of the reflection coefficient, one obtains the expression

$$\begin{aligned}\rho_{jk}=\delta_{jk}&+2\lambda^2r_k\{jr_j\delta_{j-1,k}\\&-[jr_{j-1}+(j+1)r_{j+1}]\delta_{jk}+(j+1)r_j\delta_{j+1,k}\}.\end{aligned} \tag{18}$$

This form of ρ_{jk} can be shown to obey the summation condition. Also, it is readily shown that $\rho_{jk}=\rho_{kj}$.

Several remarks may be made concerning the reflection coefficient. It will be noted that there is a selection rule; the quantum number may change only by plus or minus one. Secondly, the diagonal terms decrease with increase in j, while the off-diagonal elements increase with increasing j. In other words, a system in a high vibrational state will have less chance of staying there than a system in a lower state. Furthermore, the off-diagonal elements are proportional to the product of the incident and reflected momenta; this indicates that the chance of a large change in the vibrational quantum number is small—a further confirmation of the selection rule. The ratio of the chance of jumping from j to $j+1$, to that for jumping from j to $j-1$, is $(j+1)/j$. This last result was obtained by Landau and Teller[8] by consideration of a perturbation energy which depends linearly on the coordinate of the vibration.

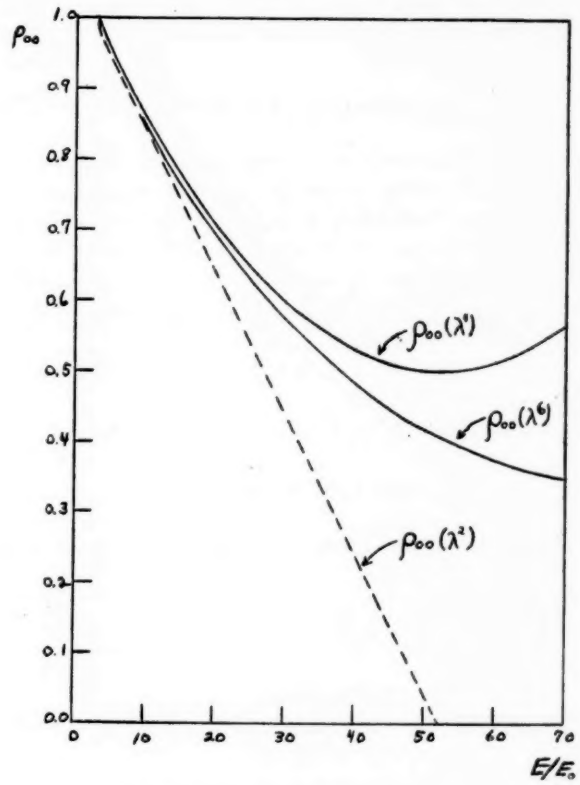

FIG. 3. Various approximations to ρ_{00}.

In Fig. 3 are plotted the curves for ρ_{00} corresponding to the first three approximations; that is, first including

[8] L. Landau and E. Teller as quoted by A. Eucken and H. Jaacke, Zeits. f. physik. Chemie **B30**, 96 (1935).

only the terms in λ^2, then adding the terms in λ^4, and finally adding the terms in λ^6. The various approximations diverge rapidly for large value of E/E_0, but lie closely together in the interesting range, 0–10 multiples of E/E_0. At very high energies, this approximation breaks down completely and another method must be employed. (See Appendix I.)

The Square Channel

The solution of the Schrödinger equation in the square channel (Fig. 5) has the form

$$\psi_n=\sum_j [\delta_{nj}\exp(-ip_jx/h) + R_{nj}\exp(ip_jx/h)]\sin(\pi jy/L). \quad (19)$$

Again, the boundary condition requires that $\psi_n=0$ when $y=x/\lambda$, where, as before, $\lambda=\tan\theta$. Applying this condition and expanding in terms of $\sin(k\pi x/L\lambda)$, we are led again to the matrix equation (10), where now

$$P_{jk}=Q_{jk}^*=\frac{2}{\pi}\int_0^\pi \exp(-ir_j\lambda z)\sin jz\sin kz dz \quad (19)$$

and

$$z=\pi x/L\lambda;\quad E/E_0=r_j^2+j^2;\quad E_0=\pi^2h^2/2mL^2$$

$$p_j=r_j\mathfrak{p};\quad \mathfrak{p}=\pi h/L.$$

The reflection coefficient, expanded in powers of λ, is

$$\rho_{jk}=\left(1-\frac{128\lambda^2}{\pi^2}j^2r_jS_{jj}\right)\delta_{jk} + \frac{128\lambda^2j^2k^2r_jr_k}{\pi^2(j^2-k^2)^4}[1-(-1)^{j+k}]\Delta_{jk}, \quad (20)$$

where

$$S_{jj}=\sum_{m=0}^{\infty} m^2r_m[1-(-1)^{j+m}]\Delta_{jm}/(j^2-m^2)^4 \quad (21)$$

and

$$\Delta_{jk}=0 \quad \text{if} \quad j=k;\quad \Delta_{jk}=1 \quad \text{if} \quad j\neq k.$$

This form for ρ_{jk} obeys the summation condition for j and k. The selection rule in this case allows only transitions between states of different symmetry. In addition, the resonance denominator effectively limits the transitions to those in which the quantum number changes by ±1. The general form for the reflection coefficient is much the same as for the parabolic case; however, the relative probability for an upward jump as compared to a downward jump does not have as simple a form as it did in the case of the parabolic channel. Figure 4 shows the variation of ρ_{jk} as a function of the energy ratio, E/E_0.

Because of the greater simplicity of the results and the more reasonable shape, only the results for the parabolic channel will be used in discussing experimental data.

III. THE AVERAGE PROBABILITY OF TRANSITION

The values of ρ_{jk} give the probability per collision for a system to leave the jth vibrational state and enter the kth vibrational state if the initial relative momentum is characterized by a given value of r_j. In order to calculate the average probability of transition per collision, the reflection coefficient must be multiplied by the number of collisions in the given velocity range and the resulting expression integrated over all possible values of the velocities.

The number of collisions between a molecule in state j, in the velocity range $\mathbf{c}_j$, $d\mathbf{c}_j$; and all other molecules (of the first kind), in the velocity range $\mathbf{c}_1$, $d\mathbf{c}_1$, is given by the expression[9]

$$f_1f_jgbdbd\epsilon d\mathbf{c}_1d\mathbf{c}_j, \quad (22)$$

where f_1 is the distribution function for molecules of the first kind; f_j is the distribution function for molecules in the jth state; g is the relative velocity along the line of centers of the colliding molecules; b is an encounter variable which specifies the range of molecular interaction and which may depend upon g; ϵ is the

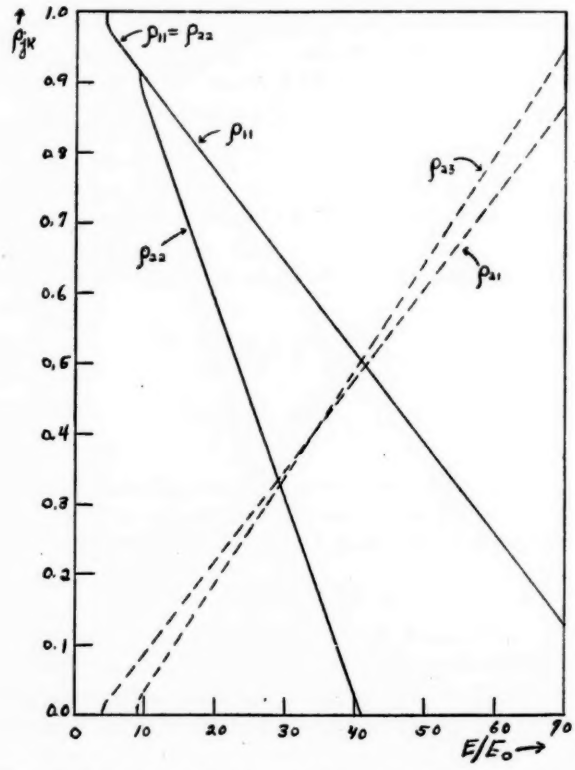

FIG. 4. Reflection coefficients as a function of the energy ratio (square channel).

[9] S. Chapman and T. G. Cowling, *The Mathematical Theory of Non-Uniform Gases* (Cambridge University Press, London 1939), p. 61.

azimuth of the plane containing the orbit of the center of mass of the colliding system relative to a fixed plane of reference; $\mathbf{c}_1$ and $\mathbf{c}_j$ are the velocities of the two colliding molecules.

The total number of molecules per cubic centimeter going from state j to stake k per second is:

$$\int\int\int\int \rho_{jk} f_1 f_j g b db d\epsilon d\mathbf{c}_1 d\mathbf{c}_j. \tag{23}$$

The average probability per collision of leaving j and entering k is given by the expression:

$$\frac{\int\int\int\int \rho_{jk} f_1 f_j g b db d\epsilon d\mathbf{c}_1 d\mathbf{c}_j}{\int\int\int\int f_1 f_j g b db d\epsilon d\mathbf{c}_1 d\mathbf{c}_j}. \tag{24}$$

If the expression (24) is summed over all values of k except j, then the result is the average probability per collision of leaving state j. This quantity will be designated P_j.

$$P_j=\frac{\int\int\int\int (1-\rho_{jj}) f_1 f_j g b db d\epsilon d\mathbf{c}_1 d\mathbf{c}_j}{\int\int\int\int f_1 f_j g b db d\epsilon d\mathbf{c}_1 d\mathbf{c}_j} \tag{25}$$

where the substitution $\sum_{k\neq j}\rho_{jk}=1-\rho_{jj}$ has been made.

For the case of hard-sphere molecules, b does not depend upon g; and, consequently, the integrations over b and ϵ may be carried out immediately.‡ Since this integral occurs as a factor in both the numerator and the denominator, it cancels out and the equation becomes

$$P_j=\frac{\int\int (1-\rho_{jj}) f_1 f_j g d\mathbf{c}_1 d\mathbf{c}_j}{\int\int f_1 f_j g d\mathbf{c}_1 d\mathbf{c}_j}. \tag{26}$$

The expressions for f_1 and f_j are now substituted; since any numerical and normalizing factors will cancel out, only the factors involving c_1 and c_j need be considered. The equation now becomes

$$P_j=\frac{\int\int (1-\rho_{jj}) \exp[-(mc_1^2+m^*c_j^2)/2kT] g d\mathbf{c}_1 d\mathbf{c}_j}{\int\int \exp[-(mc_1^2+m^*c_j^2)/2kT] g d\mathbf{c}_1 d\mathbf{c}_j}, \tag{27}$$

where m is the mass of the impinging molecule, and m^* is the mass of the oscillator—i.e., $m^*=m_A+m_B$, for a molecule $A-B$.

A change in variables is now effected; $\mathbf{c}_1$ and $\mathbf{c}_j$ are replaced by $\mathbf{g}$ and $\mathbf{G}$, which are defined through the relations

$$\mathbf{c}_1=\mathbf{G}-M_2\mathbf{g}$$
$$\mathbf{c}_j=\mathbf{G}+M_1\mathbf{g}$$
$$g=|\mathbf{g}|.$$

Substitution into Eq. (27) yields

$$P_j=\frac{\int\int (1-\rho_{jj}) \exp[-m_0(G^2+M_1M_2g^2)/2kT] g d\mathbf{g} d\mathbf{G}}{\int\int \exp[-m_0(G^2+M_1M_2g^2)/2kT] g d\mathbf{g} d\mathbf{G}} \tag{28}$$

where $m_0=m+m^*$, $M_1=m/(m+m^*)$, $M_2=m^*/(m+m^*)$. Since $\mathbf{g}$ is the relative velocity along the line of centers of the two colliding molecules, it is directly proportional to r_j, the velocity variable in the reflection coefficient. Since r_j and $\mathbf{G}$ are independent, the latter variable may be integrated out in both the numerator and denominator. Furthermore, the orientation variables in the vector differential, $d\mathbf{g}$, can be integrated out; this leaves only the integration over the scalar relative speed, g. Equation (28) reduces to

$$P_j=\frac{\int_0^\infty (1-\rho_{jj}) \exp(-\mu g^2/2kT) g^3 dg}{\int_0^\infty \exp(-\mu g^2/2kT) g^3 dg}, \tag{29}$$

‡ For details of these integrations, see reference 9, p. 89 ff.

where μ is the reduced mass of the colliding system—$\mu=mm^*/m_0$.

The numerator and denominator are now transformed by substituting for g its equivalent in terms of r_j; $g=p_j/\mu$, or $g=r_j\mathfrak{p}/\mu$. It is necessary to call attention to the fact that in the expression for E [Eq. (3)], the mass, m, which occurred there is actually the reduced mass of the three-body system, and hence is equal to μ.

The value of $1-\rho_{jj}$ is now substituted, with the result that

$$P_j=\frac{\int_0^\infty 2\lambda^2 r_j[jr_{j-1}+(j+1)r_{j+1}]r_j^3\exp(-ar_j^2)dr_j}{\int_0^\infty r_j^3\exp(-ar_j^2)dr_j} \tag{30}$$

where $a=E_0/kT$, $(E_0=\frac{1}{2}h\nu_0)$.

Use is made of Eq. (3) to derive the formulas:

$$r_{j-1}=(r_j^2+2)^{\frac{1}{2}}$$
$$r_{j+1}=(r_j^2-2)^{\frac{1}{2}}.$$

Substituting these expressions in the numerator and integrating the denominator directly leads to the result

$$P_j=4\lambda^2a^2\Big[j\int_0^\infty (r_j^2+2)^{\frac{1}{2}}r_j^4\exp(-ar_j^2)dr_j$$
$$+(j+1)\int_{\sqrt{2}}^\infty (r_j^2-2)r_j^4\exp(-ar_j^2)dr_j\Big]. \tag{31}$$

Since the second term on the right-hand side of the equation does not contribute for values of $r_j<\sqrt{2}$, the lower limit of the integral must be taken as $\sqrt{2}$. The lower limit of the first integral is zero. The equation may be simplified further by changing the variable of integration to $x=ar_j^2$ in the first integral, and to $x=a(r_j^2-2)$ in the second integral. The expression for P_j now is

$$P_j=(2\lambda^2/a)[jJ_1+(j+1)\exp(-2a)J_2] \tag{32}$$

where

$$J_1(a)=\int_0^\infty [x(x+2a)]^{\frac{1}{2}}x\exp(-x)dx \tag{33}$$

$$J_2(a)=\int_0^\infty [x(x+2a)]^{\frac{1}{2}}(x+2a)\exp(-x)dx. \tag{34}$$

These integrals will be approximated by the expressions

$$J_1(a)\approx 2(1+a)^{\frac{1}{2}} \tag{35}$$

$$J_2(a)\approx 2[(1+a)(1+2a+2a^2)]^{\frac{1}{2}}. \tag{36}$$

The basis of this approximation is explained in Appendix II.

This gives the final form of P_j:

$$P_j=(4\lambda^2/a)(1+a)^{\frac{1}{2}}$$
$$\times[j+(j+1)\exp(-2a)(1+2a+2a^2)^{\frac{1}{2}}]. \tag{37}$$

Since P_j is the average probability of transition per collision, $1/P_j$ is the average number of collisions which the molecule undergoes before leaving the jth state. In Fig. 5, $1/P_0$ is plotted against $a=E_0/kT$. The curve on the right is for a value of $1/\lambda^2=692$, while the curve on the left is for a value of $1/\lambda^2=24{,}600$. These values of $1/\lambda^2$ have been obtained for helium and argon colliding with other molecules such as chlorine, nitrous oxide, and carbon dioxide from data on sound dispersion. Figure 5 illustrates the strong temperature dependence of the collision number as well as the striking difference between the efficiency of helium and argon in dissipating vibrational energy.

IV. DISCUSSION AND COMPARISON OF THE THEORY WITH EXPERIMENTAL DATA

From their measurements of the dispersion of sound in gas mixtures, Eucken and Becker[10] calculated values for the number of collisions necessary to dissipate one quantum of vibrational energy. This collision number depends markedly on the partner in the collision. For example, chlorine at 18°C requires 900 collisions with an atom of helium in order to dissipate one quantum of vibrational energy, while, at the same temperature, 32,000 collisions with an argon atom are required.

One can interpret these collision numbers in terms of P_j [Eq. (37)], or, rather, in terms of $1/P_0$. P_0 represents the average number of molecules leaving the zeroth level per collision. Since the average number leaving the zeroth level must be equal to the average number entering the zeroth level from the first level (cf. the selection rule in the reflection coefficient), P_0 also represents the average number of quanta dissipated per collision; it is assumed that the number of molecules in higher levels is so small that contributions from this source may be neglected. Accordingly, $1/P_0$ is the average number of collisions necessary to dissipate one quantum of vibrational energy.

In Table I, the parameter λ has been assumed to depend only upon the impinging molecule, i.e., the data for helium colliding with chlorine has been used to calculate a value of λ, which is then assumed to be characteristic of helium only. This value of λ is then used to calculate the number of collisions needed to

[10] A. Eucken and R. Becker, Zeits. f. physik. Chemie **B27**, 235 (1934). See also A. Eucken and E. Neumann, Zeits. f. physik. Chemie **B36**, 163 (1937).

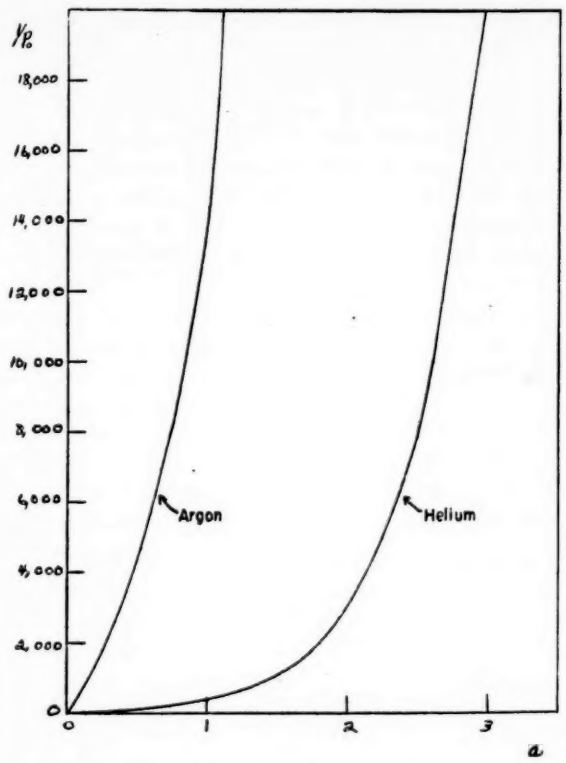

FIG. 5. Variation of the collision number as a function of a.

dissipate one quantum when helium collides with carbon dioxide and nitrous oxide. The same procedure is repeated for argon-chlorine to calculate collision numbers for the systems argon-carbon dioxide, and argon-nitrous oxide.

In all three cases, helium has a much lower collision number. This has been explained heretofore by Eucken and Becker as being due to a deeper penetration of the structure of the oscillator by the small helium molecule. In terms of the above treatment the same explanation holds, of course. A larger value of λ in the case of helium as compared to argon simply means that the perturbation is larger in the case of helium. The calculated values in Table I are within the experimental error which is estimated to be between ten and thirty percent.

There is an obvious reason why the agreement should be better in the case of carbon dioxide than in the case of nitrous oxide. The vibration which is excited is the doubly degenerate bending vibration. Since carbon dioxide is symmetrical, the bending vibration is separable from the stretching vibrations—a fact which allows the use of the very simple surface which has been chosen (cf. Fig. 4). This energy surface pictures the collision as taking place between a helium molecule and a molecule of carbon dioxide, with the helium approaching the carbon dioxide molecule along a perpendicular bisector of the molecular axis; this configuration presumably represents an optimum condition for the excitation of the vibration.

The Temperature Dependence of the Collision Number

Equation (37) also shows the temperature dependence of $1/P_0$. Unfortunately, experimental data are not available for systems involving rare gases; however, if it is assumed that in the collision of two molecules of chlorine, for example, that only one of them can be excited, then a comparison of theory and experiment can be made. The difficulty which presents itself is the choice of a value for the parameter λ. This choice can only be made by curve-fitting.

The curve-fitting has been done simply by averaging the values of λ calculated from experimental data at various temperatures. The average value of λ is used to draw the theoretical curve. For pure chlorine, the results are shown in Table II. The calculated values of P_0 were obtained by using $\lambda_{Av}^2=4.58\times10^{-5}$. The results for chlorine colliding with carbon monoxide are given in Table III. Here $\lambda_{Av}^2=6.31\times10^{-3}$. These results are plotted in Figs. 6 and 7, respectively. All of the data are taken from Eucken and Becker.[10]

It is interesting to note that in the case of chlorine colliding with chlorine, the values of λ^2 differ from the average value by an average of 14.7 percent; while in the case of chlorine and carbon monoxide, λ^2 is more nearly constant, the values differing from the average value by an average of 6.4 percent. The theory seems to be better for the more reactive gas, although it might have been expected to be worse because of the use of a hard-sphere model.

It is difficult to associate the values of λ with features of known energy surfaces, chiefly because of the highly

TABLE I.

Oscillator	ν_0[a]	T	a	Helium $1/\lambda^2=692$ Obs.[b]	Calc.	Diff.	Argon $1/\lambda^2=24{,}600$ Obs.[b]	Calc.	Diff.
N_2O	588.8 cm^{-1}	291°K	1.44	1700 1400[c]	1000	41% 29%	—	36,000	—
CO_2	667.3 cm^{-1}	291°K	1.64	1700	1500	12%	47,000	53,000	13%

[a] G. Herzberg, *Infrared and Raman Spectra* (D. Van Nostrand Company, Inc., New York, 1945), pp. 274, 278.
[b] A. Eucken and R. Becker, see reference 10.
[c] A. Eucken and E. Neumann, see reference 10.

TABLE II. Chlorine-chlorine.

T°K	a	λ^2	P_0(exp.)	P_0(calc.)
241	1.685	3.92×10^{-5}	1.66×10^{-5}	1.94×10^{-5}
291	1.396	3.90×10^{-5}	2.94×10^{-5}	3.45×10^{-5}
347	1.170	4.65×10^{-5}	5.55×10^{-5}	5.47×10^{-5}
415	0.979	5.86×10^{-5}	10.5×10^{-5}	8.21×10^{-5}

TABLE III. Chlorine-carbon monoxide.

T°K	a	λ^2	P_0(exp.)	P_0(calc.)
241	1.685	5.77×10^{-3}	2.56×10^{-3}	2.67×10^{-3}
291	1.396	6.04×10^{-3}	4.35×10^{-3}	4.76×10^{-3}
347	1.170	6.45×10^{-3}	7.70×10^{-3}	7.54×10^{-3}
415	0.979	6.98×10^{-3}	12.5×10^{-3}	11.3×10^{-3}

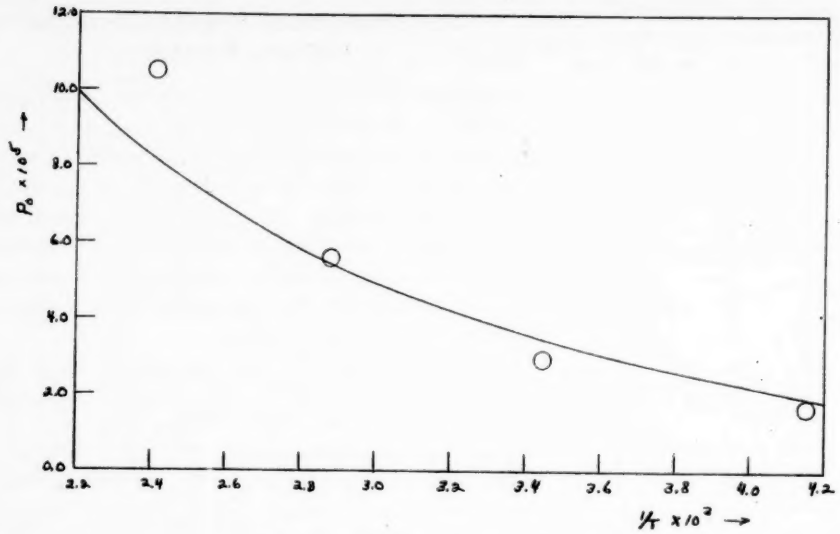

FIG. 6. Temperature variation of P_0. Chlorine-chlorine.

idealized nature of the model. As pointed out earlier, a weak interaction extending over a longer range than a strong interaction leads to the same value of λ. It is this circumstance, no doubt, which permits us to treat λ as a property of the rare gas, rather than of the colliding pair. The second virial coefficients of helium and argon show argon atoms to interact much more strongly than helium atoms, though at a somewhat greater distance. Our λ is much smaller for argon than for helium, suggesting that the penetration of the diatomic molecule is relatively more important for vibrational excitation than the strength of the van der Waals forces. However, we do not wish to push the quantitative significance of the model too far.

V. UNIMOLECULAR DECOMPOSITIONS

One can use the method of the preceding sections to derive explicit expressions for the various rate constants which appear in the Lindemann mechanism for unimolecular decompositions. However, several difficulties arise in the application of these expressions to an actual chemical reaction. The value of λ is undetermined. Presumably, it can be determined by independent measurements on sound dispersion. However, one finds that for a unimolecular reaction to occur at a measurable rate at ordinary pressures, the values of λ which must be taken are several orders of magnitude larger than those which are found in sound dispersion. This result immediately breaks down the approximation which was used to derive values of the reflection coefficients.

Another difficulty presents itself if the results of the measurements of the inhibition of unimolecular reactions by foreign gases are considered. In the case of fluorine monoxide at 250°C it is found that argon is

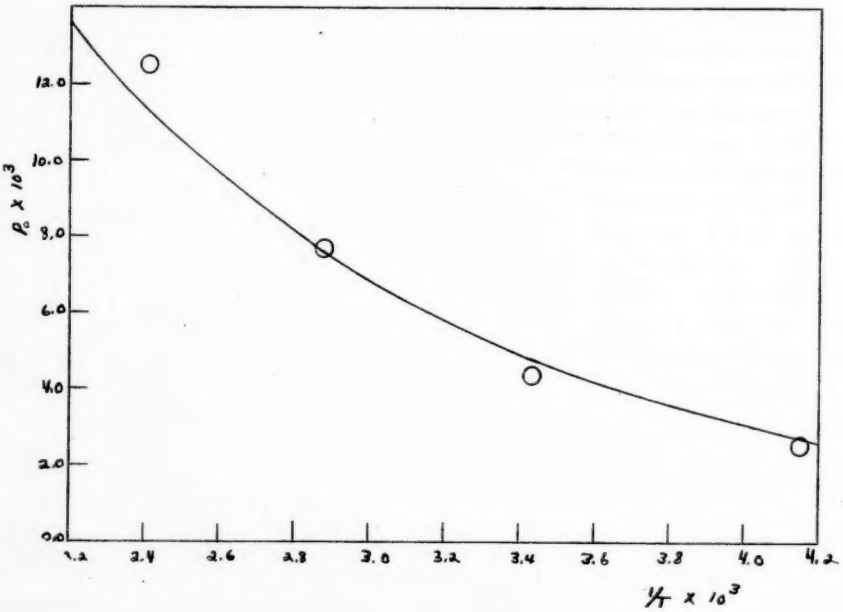

FIG. 7. Temperature variation of P_0. Chlorine-carbon monoxide.

twice as efficient as helium in producing excitation.[11] In the case of sound dispersion, the effect was in the opposite direction and helium was found to be 35 times as efficient as argon. In the case of nitrous oxide, helium is found experimentally to be three times as efficient as argon in chemical activation at least in this case the variation is in the same direction as for sound dispersion, although it differs by one order of magnitude. As Gershinowitz[6] has pointed out, there is no reason to expect that the collision efficiencies should be the same for sound dispersion as for activation. In sound dispersion the pertinent vibrational level is the first or, at most, the second, while in chemical activation the higher levels are involved. Furthermore, the individuality of the energy surface exerts a specific effect upon the collision process in activation; this is evidence by the change in the order of magnitude of the ratio of helium efficiency to that of argon in the case of nitrous oxide and the reversal in the case of fluorine monoxide.

It may thus be concluded that although the simple collision model considered here provides a fair representation of the collision process as it occurs in sound dispersion, it is much too idealized to represent the activation process in a chemical reaction. In addition, the process in sound dispersion is concerned mainly with the lowest vibration frequency in the molecule, while in the activation process the contributions of the other degrees of freedom to the activation of a particular bond may be considerable.

APPENDIX I

Evaluation of P_{jk} and Q_{jk}

Integrals such as P_{jk} and Q_{jk} can be evaluated through the use of the generating function for the Hermite polynomials. If the integrals are stripped of normalizing coefficients and complicated notation, they can be written in the form

$$K_{jk}=\int_{-\infty}^{\infty}\exp(i2bx-x^2)H_j(x)H_k(x)dx, \qquad (38)$$

where $H_j(x)$ is the ordinary Hermite polynomial. The generating function for the Hermite polynomials is such that

$$\exp[x^2-(z_1-x)^2]=\sum_{n=0}H_n(x)z_1{}^n/n!. \qquad (39)$$

If two equations such as (39) are multiplied together, the result multiplied on both sides by $\exp(i2bx-x^2)$, and the integral taken on both sides of the resulting equation, one obtains

$$\exp(-z_1{}^2-z_2{}^2)\int_{-\infty}^{\infty}\exp[-x^2+2(z_1+z_2+ib)x]dx = K_{ns}z_1{}^nz_2{}^s/n!\,s!. \qquad (40)$$

[11] See, for example, reference 2, p. 291.

The variable of integration on the left-hand side of the equation is replaced by $y=x-(z_1+z_2+ib)$. This reduces the integral to a very simple form which integrates immediately to give

$$\exp(-b^2+2z_1z_2+i2bz_1+i2bz_2)=\sum_n\sum_s K_{ns}z_1{}^nz_2{}^s/n!\,s!. \qquad (41)$$

The exponential factors on the left are now expanded in powers of z_1 and z_2.

$$\exp(i2bz_1)=\sum_{p=0}(i2bz_1)^p/p!$$

$$\exp(i2bz_2)=\sum_{r=0}(i2bz_2)^r/r!$$

$$\exp(2z_1z_2)=\sum_{t=0}(2z_1z_2)^t/t!.$$

These expansions are substituted on the left for the exponentials with the result

$$(\pi)^{\frac{1}{2}}\exp(-b^2)\sum_p\sum_r\sum_t(i2b)^{p+r}2^tz_1{}^{p+t}z_2{}^{r+t}/p!\,r!\,t! = \sum_n\sum_s K_{ns}z_1{}^nz_2{}^s/n!\,s!. \qquad (42)$$

Since Eq. (42) is an identity, the coefficients of $z_1{}^k$ must be equal on both sides of the equation. On the right side this coefficient is

$$\sum_{s=0}K_{ks}z_2{}^s/k!\,s!.$$

On the left side, the sums are over all values of r, and over all values of p and t consistent with the relation: $p+t=k$. Thus, p is set equal to $k-t$, the sum over p disappears and the sum over t becomes a finite sum from 0 to k. Hence, setting the coefficients equal, one obtains the relation

$$(\pi)^{\frac{1}{2}}\exp(-b^2)\sum_{r=0}^{\infty}\sum_{t=0}^{k}(i2b)^{k-t+r}2^tz_2{}^{t+r}/(k-t)!\,t!\,r! = (1/k!)\sum_{s=0}^{\infty}K_{ks}z_2{}^s/s!. \qquad (43)$$

Applying the same argument to the coefficients of $z_2{}^j$, on the right side this coefficient is $K_{kj}/k!\,j!$; while on the left, it is seen that for each value of t, $r=j-t$. This leads to the equation

$$(\pi)^{\frac{1}{2}}\exp(-b^2)\times\sum_{t=0}^{k}(i2b)^{j+k-2t}2^t/(k-t)!\,(j-t)!\,t!=K_{kj}/k!\,j!. \qquad (44)$$

This yields immediately the value of the integral.

$$K_{kj}=(\pi)^{\frac{1}{2}}\exp(-b^2)(i2b)^{j+k}\times\sum_{t=0}^{k}(-1)^tt!\binom{k}{t}\binom{j}{t}(\tfrac{1}{2}b^2)^t \qquad (45)$$

TABLE IV.

J_1: a	Error	J_2: a	Error
0	0.0 percent	0	0.0 percent
½	+2.0	½	+2.2
1	+2.9	1	+3.8
2	+6.4	2	+6.6
∞	+6.4	∞	+12.8

where $\binom{k}{l}$ is the binomial coefficient. It can be shown that this formula for the integral satisfies the differential equation of the integral. The integral is symmetric in j and k, i.e., $K_{kj}=K_{jk}$.

In order to obtain Q_{jk}, the substitutions: $b=r_j\lambda/2$, and

$$H_j(x)\exp(-x^2/2)=[2^j j!\,(\pi)^{\frac{1}{2}}]^{\frac{1}{2}}H_j(x)$$

are made.

The High Energy Region

For very high energies, the power series expansion of the matrices, P and Q, breaks down. To obtain an approximation in this region, Eq. (11) may be written

$$Q_{jk}=(2^{j+k}j!k!)^{-\frac{1}{2}}(ib_0)^{j+k}[1-j(j+k)/\epsilon]\times[1-2kj/b_0^2]\exp(j\lambda^2/2) \quad (46)$$

where

$$r_j\lambda=b_0(1-j/\epsilon);\quad b_0=\lambda\epsilon^{\frac{1}{2}}\gg 1. \quad (47)$$

In the set, Eq. (9), since $P=Q^*$, all multiplicative factors independent of j cancel. Hence we may write

$$Q'_{jk}=F_j\cdot(1-G_{jk})=\sum_m F_{jm}(1-G_{mk})\delta_{jm}=(P'_{jk})^* \quad (48)$$

where

$$\left.\begin{aligned}F_{jm}&=(2^j j!)^{-\frac{1}{2}}(ib_0)^j\delta_{jm}\exp(j\lambda^2/2)\\ G_{mk}&=[\lambda^2 m(m+k)+2km]/b_0^2\end{aligned}\right\}. \quad (49)$$

Thus

$$R=-PQ^{-1}=-P'(Q')^{-1}=-F^*F^{-1}=\|(-1)^{j+1}\delta_{jk}\|.$$

At very high energies, therefore, vibrations are not excited. Similar results are known for electronic excitation by electron impact.

APPENDIX II

Evaluation of the Integrals J_1 and J_2

The integral J_1 is given by

$$J_1=\int_0^\infty [x(x+2a)]^{\frac{1}{2}}x\exp(-x)dx. \quad (50)$$

It is obvious that, since a is always positive,

$$\int_0^\infty x^2\exp(-x)dx<J_1<\int_0^\infty (x+2a)x\exp(-x)dx. \quad (51)$$

The following substitutions are made:

$$g(x)=x\exp(-x)$$
$$f(x)=x$$
$$h(x)=(x+2a).$$

The inequality now becomes

$$\int_0^\infty fgdx<\int_0^\infty (fh)^{\frac{1}{2}}gdx<\int_0^\infty hgdx. \quad (52)$$

Since the integrand in J_1 is the geometric mean of the integrands at the two bounds of the interval, J_1 has been approximated by taking the geometric mean of the two bounding integrals which are easily integrated. The same type of argument is used to evaluate J_2.

It will be noted that using this argument of the geometric mean is ambiguous in the case of J_2; two different approximate formulas can be gotten. However, since the difference in the arithmetical values given by the two different approximations is less than 0.6 percent in the interesting range of values of a, the more convenient approximation given in Eq. (36) will be used.

Both integrals have been measured with a planimeter for values of $a=\frac{1}{2}$, 1, and 2. For $a=0$, the approximation becomes exact in both cases. A comparison of the measured and calculated values of the integrals is given in Table IV.

ACKNOWLEDGMENT

One of us (G.W.C.) wishes to express his sincere thanks to Mrs. Ella Mullen Weckbaugh of Denver, Colorado, and to the Catholic University of America for the award of a John K. Mullen Scholarship for the years 1945–1949.

Specific Magnetic Susceptibilities and Related Properties of Manganese-Activated Zinc Fluoride*

PETER D. JOHNSON† AND FERD E. WILLIAMS†
Chemistry Department, University of North Carolina, Chapel Hill, North Carolina

(Received July 25, 1949)

The specific magnetic susceptibilities of manganese-activated zinc fluoride phosphors of diverse activator concentration, and prepared by various crystallization procedures, have been measured from −60°C to 200°C. A trivial Weiss constant, except for phosphors of inordinately high manganese concentration, demonstrates the absence of appreciable exchange demagnetization of adjacent paramagnetic activator ions and suggests that there exists negligible departure from a random distribution of manganese ions over cation sites. Utilizing this distribution, and recognizing that only manganese ions not having other manganese ions at any of the nearest cation sites are capable of luminescence, an expression for the dependence of luminescent efficiency on activator concentration is derived and found to be in quantitative agreement with experiment.

INTRODUCTION

IN previously reported work[1] on the magnetic properties of manganese-activated zinc fluoride, it was found that there exists a difference in multiplicity between the unexcited and the emitting states of the activator. Preliminary specific susceptibility measurements indicated that the unexcited activator is predominantly in the divalent state of maximum multiplicity, most probably the ^6S state. The susceptibility of one phosphor of moderate activator concentration was slightly below the theoretical value; and this fact was tentatively interpreted as being evidence for exchange demagnetization. Since the possibility of exchange interaction and a resulting departure from the random distribution of activator would be of considerable importance to the understanding of luminescence phenomena, and in particular to the problem of explaining luminescent efficiency as a function of activator concentration, it was decided to study the problem in greater detail.

TEMPERATURE DEPENDENCE OF MAGNETIC SUSCEPTIBILITY

First, the magnetic susceptibilities of a number of ZnF_2:Mn phosphors of various activator concentrations were measured as a function of temperature in order to determine the Weiss constant, which is a direct measure of the interaction energy. Measurements were made from −60°C to +200°C by use of the Gouy method.[2] Since only the Weiss constant and not the precise absolute susceptibility is needed, the only data required are the temperature dependence of the force on the sample produced by its interaction with the magnetic field. The observed forces are corrected for the non-temperature dependent diamagnetic susceptibility of the host lattice, and that of the Pyrex sample tube. The experimental procedure eliminated the effect of the change in buoyancy of air with temperature. The sample tube, half-filled with the tightly packed powdered phosphor, was thoroughly flushed out with carbon dioxide, whose volume susceptibility is negligible, before being sealed. The temperature was measured by a calibrated thermocouple and controlled, by use of an electrically heated oven and a Variac to within 0.5°C in the range from 20° to 200°C. Measurements near −60°C were obtained by using dry ice-acetone-water as a coolant. Provision was made for the continual circulation of coolant in the jacket surrounding the chamber in which the sample was suspended.

Figure 1 shows the corrected results of the measurements. For convenience the molar susceptibility of the activator in each phosphor is normalized at 20°C to the theoretical "spin only" value for divalent manganese, and the ordinate scale is displaced for each phosphor. The force, f, on a sample using the Gouy method is given by the relation:[2]

$$f=\tfrac{1}{2}(k_1-k_2)(H_1^2-H_2^2)A,$$

where k_1 and k_2 are the volume susceptibilities of the sample and the surrounding atmosphere, respectively. H_1 is the maximum field located at one end of the sample, and H_2 is the minimum field located at the other. A is the cross-sectional area of the sample. Since k_2 is negligible, and H_1, H_2, and A are constant in a series of measurements, the force on the sample at a given temperature resulting from the interaction of the sample with the applied field is proportional to the volume susceptibility at that temperature. The volume susceptibility is proportional to the molar susceptibility because there is negligible change in density of the sample with temperature.

The 0.97 ZnF_2:0.034 MnF_2 was prepared by fusion in a "glow bar" furnace for 45 min. The other samples were prepared by fusion of the ingredients in an atmosphere of ammonium fluoride for 5 min. and allowed to

* Supported by the ONR through Contract N7onr-284, Task Order I.

† Present address: Research Laboratory, General Electric Company, Schenectady, New York.

[1] P. D. Johnson and F. E. Williams, J. Chem. Phys. **17**, 435 (1949).

[2] P. W. Selwood, *Magnetochemistry* (Interscience Publishers, Inc., New York, 1943).

cool over a period of 15 min., except for one of the 0.85 ZnF_2:0.15 MnF_2 samples which was quenched.

It is seen that all samples except 0.75 ZnF_2:0.25 MnF_2 obey the Curie law, indicating that in these cases there is negligible exchange demagnetization. Differences in time of firing or methods of cooling have no detectable effect on the Weiss constant. If one attempts to draw a straight line through the points obtained for 0.75 ZnF_2:0.25 MnF_2 it is seen that the Curie law is not obeyed. Upon calculation of the Weiss constant of this material using a number of different pairs of experimental points as checks, substituting in expressions of the form:

$$\chi = C/(T+\Delta),$$

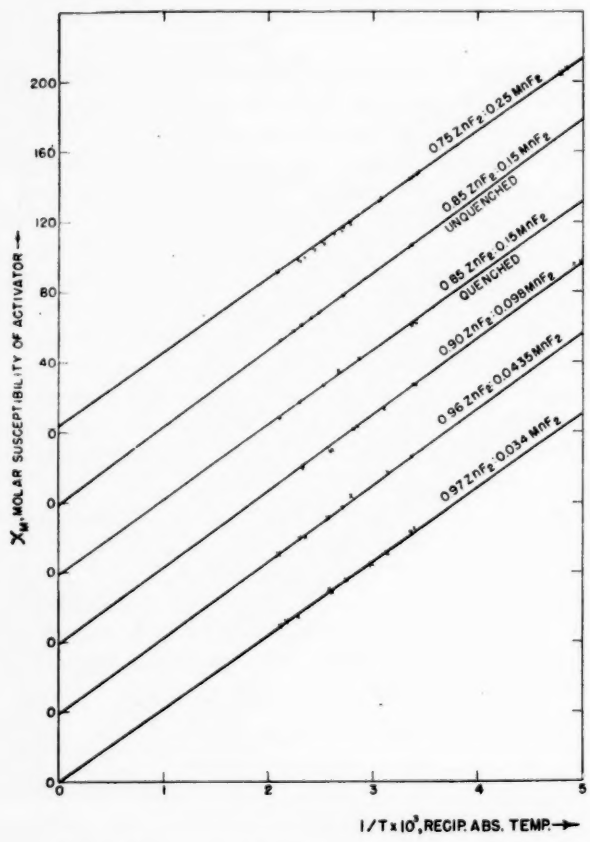

FIG. 1. Temperature dependence of susceptibilities of ZnF_2:Mn phosphors.

it is found that the Weiss constant is $+7\pm2$. By considering the Weiss constant proportional to the number of interactions per mole phosphor, the 25 mole percent phosphor is calculated to have a Weiss constant in qualitative agreement with the observed value. For phosphors containing 15 mole percent or less of activator, Debye-Sherrer x-ray data indicate only one phase and agreement with Vegard's rule, as would be expected for a random distribution of activators over cation sites.

These results demonstrate the absence of measurable magnetic interaction in phosphors of usual activator concentration and a lack of a departure from the random distribution detectable by conventional magnetic and x-ray measurements.

TABLE I.

Sample	Obs. spec. susc. of phosphor $\chi\times10^6$	$\chi_M\times10^4$ for activator
0.995 ZnF_2:0.00505 MnF_2	0.40	163
0.98 ZnF_2:0.0194 Mn	2.60	159
0.957 ZnF_2:0.0435 Mn	6.34	158
0.902 ZnF_2:0.098 Mn	13.2	146
0.976 ZnF_2:0.0335 Mn	4.20	140*
ZnF_2	−0.40	
MnF_2 theoretical		147

* Different heat treatment.

CONCENTRATION DEPENDENCE OF MAGNETIC SUSCEPTIBILITY

In order to determine whether the previously observed specific susceptibilities of manganese-activated zinc fluoride are characteristic of the phosphor, a more extensive study of the precise room temperature susceptibilities was undertaken.

The experimental procedure for the determination of the mass susceptibility was a modification of the Faraday method used previously.[1] The method of analysis of the manganese content of the phosphors consists in the oxidation of the manganese to permanganate with periodate and colorimetric comparison of the resulting solution with standards in the Evelyn photoelectric colorimeter. The mean error of an analysis is about one percent.

Table I shows for 20°C the results of the measurements. The combined errors of analysis, standardization, and measurement of the susceptibilities involved in calculation of the molar susceptibility of the activator give a probable error of about two percent for the values in the last column. The molar susceptibilities tabulated are calculated using the susceptibility of the host lattice, the susceptibility of the phosphor, and assuming the additivity of the susceptibilities of the components.

The third, fourth, and fifth phosphors are the same as those on which the data for the bottom three curves in Fig. 1 were obtained. The phosphor with high activator concentration has nearly the theoretical value of susceptibility. Also a sample of the same material which had been quenched had precisely the same susceptibility. The 0.97 ZnF_2:0.034 MnF_2, which was prepared by the same method as the phosphor previously reported as having a lowered susceptibility, again shows a lower than theoretical paramagnetic susceptibility. Chemical tests similar to those of Kroger,[3] Haayman, and Bol fail to show any manganese in higher than the divalent state, which could account for the effect in this phosphor. However, the phosphor reduces both chlorine water and potassium permanganate solution to an extent corresponding to the oxidation of approximately 10^{18}

[3] F. A. Kroger, *Some Aspects of the Luminescence of Solids* (Elsevier Publishing Company, Inc., New York, 1948).

atoms of a divalent metal per cc of phosphor. It is likely that there is this quantity of metallic zinc atoms in the lattice and that the valence electrons of this metallic zinc become paired with the unpaired *3d* electrons of the activator with a corresponding lowering of susceptibility. This mechanism can account for the lowering quantitatively.

It will be noticed that at low activator concentrations, the susceptibility of the activator appears to be higher than the theoretical value. There are several possible considerations which might contribute to the observed effect. One possibility is that the diamagnetic susceptibility of the lattice is reduced by the condition of local compression arising from the presence of the activator. The maximum reduction possible by this mechanism is only a small fraction of the 25 percent decrease in susceptibility of the host lattice which must be postulated to explain the observed data. Another possibility is that the introduction of activator causes the generation of a feeble paramagnetism due to incomplete quenching of the high frequency elements of the orbital moments of neighboring ions of the host lattice. It is likely that the observed high paramagnetic susceptibility is due to some effect such as this rather than to the generation of a new paramagnetic species such as Zn^{+}.

LUMINESCENCE EFFICIENCY *VERSUS* ACTIVATOR CONCENTRATION

On the basis of the conclusion that there is no departure from the random distribution of activator in ZnF_2:Mn, it is possible to develop from theoretical considerations an expression relating luminescent efficiency to activator concentration. The efficiency, η, is equal to the ratio of the probability of capture of an exciting photon by activators capable of emission to the total probability of capture by any component of the phosphor. For the present formulation it is assumed that (1) the emission is not absorbed; (2) the activators which are adjacent to each other are not capable of emission; and that (3) the non-adjacent activators are 100 percent efficient. σ, σ', and σ'' are defined as the capture cross sections of the host lattice, activators capable of emission, and activators incapable of emission, respectively. If C is the mole fraction of all activators in the phosphor and z is the number of nearest neighbor cation sites, it is obvious that the mole fraction of non-adjacent activators is $C(1-C)^z$. Similarly the mole fraction of adjacent activators is $C[1-(1-C)^z]$ and that of the host lattice is $(1-C)$.

Recognizing that the probability of capture by any one of the three species present is proportional to the mole fraction multiplied by the capture cross section, the following expression is readily deduced:

$$\eta = P_{\text{capture for emission}}/P_{\text{total capture}} \qquad (1)$$

or:

$$\eta = \frac{C(1-C)^z\sigma'}{(1-C)\sigma + C(1-C)^z\sigma' + C[1-(1-C)^z]\sigma''}. \qquad (2)$$

The same expression may be derived by considering the exponential attenuation of the excitation on passage through the phosphor and by recognizing that the capture cross sections and the concentrations of the various components are independent of the depth to which the excitation penetrates. The modifications which apply in case any one of the three original assumptions are not valid are obvious. An additional term in the denominator would take care of the effect of impurities which might act as poisons.

Figure 2 demonstrates satisfactory agreement between the experimental efficiencies of a series of ZnF_2:Mn phosphors at 25°C for 1849A excitation and the theoretical expression (2) using reasonable ratios of capture cross sections. The cross sections are, of course, dependent on temperature and wave-length of excitation. At the higher activator concentration the theoretical efficiency is greater than the experimental because the same cross section is used for dimer, trimer, tetramer, etc. activator ions. A more precise treatment would involve increasing capture cross sections for larger activator aggregates whose mole activator fractions are given by the successive terms of the expansion:

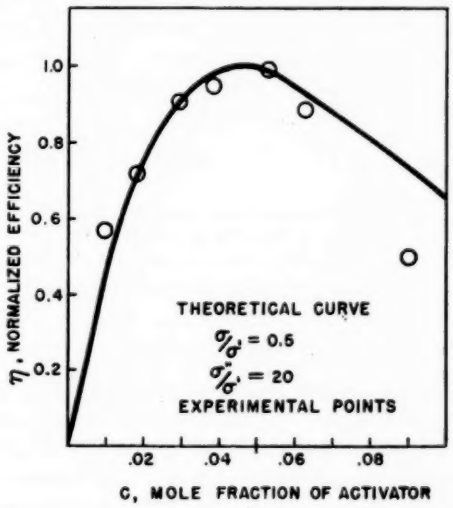

FIG. 2. Dependence of luminescence efficiency of ZnF_2:Mn on manganese concentration.

$$[(1-C)+C]^z = (1-C)^z + z(1-C)^{z-1}C + [z(z-1)/2!](1-C)^{z-2}C^2 + \cdots. \qquad (3)$$

Further study of the dependence of luminescence efficiency on activator concentration for other phosphors is in progress. For sulfide phosphors it is expected that next-nearest cation sites are important because of the large activator orbitals and that σ/σ' is small so that the maximum efficiency occurs at very low activator concentrations and the absolute efficiency is quite high.

CONCLUSIONS

From measurements of the temperature dependence of specific magnetic susceptibilities of a series of

manganese-activated zinc fluoride phosphors, it is concluded that there is negligible exchange demagnetization of adjacent paramagnetic activator ions and therefore that the manganese ions are distributed at random over the cation sites. Using this distribution and recognizing that only manganese ions not having other manganese ions at any of the nearest cation sites are capable of luminescence, the dependence of luminescence efficiency on activator concentration has been successfully computed.

THE JOURNAL OF CHEMICAL PHYSICS VOLUME 18, NUMBER 3 MARCH, 1950

Infra-Red and Raman Spectra of Fluorinated Ethylenes. I. 1,1-Difluoroethylene*

D. C. SMITH
Naval Research Laboratory, Washington, D. C.

AND

J. RUD NIELSEN AND HOWARD H. CLAASSEN
Department of Physics, University of Oklahoma, Norman, Oklahoma

The infra-red absorption of $CF_2:CH_2$ gas has been investigated between 2 and 22.7μ with a prism spectrometer of high resolution. The Raman spectrum of the compound in the gaseous state has been photographed with a three-prism glass spectrograph of linear dispersion 15A/mm at 4358A. The 12 fundamental vibration frequencies have been assigned and the observed spectra have been interpreted in detail.

INTRODUCTION

BECAUSE of the extreme electronegativity of the fluorine atom, fluorinated hydrocarbons have unique physical and chemical properties which make the investigation of their infra-red and Raman spectra of considerable interest. While a considerable number of workers have studied the spectra of fluorinated methanes, little work has been done on fluorinated ethylenes.

Hatcher and Yost[1] obtained the Raman spectrum of $CF_2:CCl_2$ in the liquid state. Torkington and Thompson[2] have investigated the infra-red spectra of six fluorinated ethylenes and have made partial assignments of fundamentals. Very recently Edgell and Byrd[3] have obtained the Raman spectrum of liquid $CF_2:CH_2$ and have made a complete assignment of fundamentals.

As a part of a larger project on the spectroscopic properties of fluorocarbons and fluorinated hydrocarbons, we have investigated the infra-red and Raman spectra of $CF_2:CH_2$, $CF_2:CCl_2$, perfluoroethylene, $CF_2:CFCl$, and perfluoropropene. In the present paper the results obtained with gaseous $CF_2:CH_2$ will be reported.

EXPERIMENTAL

The sample of 1,1-difluoroethylene was prepared and purified in the Jackson Laboratory of E. I. du Pont de Nemours and Company. No information was available about its purity. Although it is believed that a few very faint infra-red absorption maxima are caused by impurities, the fact that it has been possible to interpret practically all of the observed infra-red and Raman bands indicates that the purity of the sample is high.

The infra-red absorption spectrum of gaseous $CF_2:CH_2$ was measured over the range from 2 to 23.7μ by means of a prism spectrometer of high resolution.[4] The cell length was 10 cm. The entire spectrum was recorded at a pressure of 775 mm and the regions of strong absorption at several lower pressures. Through the courtesy of Dr. E. K. Plyler of the National Bureau of Standards, the region from 22 to 38μ was surveyed with a KRS-5 prism instrument.

The Raman spectrum of gaseous $CF_2:CH_2$ was photographed by means of a high speed spectrograph recently developed by the Lane-Wells Company. The dispersive system of this instrument consists of three 60° prisms, with faces 153 mm wide and 75 mm high, of extra dense flint glass. The camera consists of a correcting shell, designed by P. Swings, a spherical mirror of diameter 200 mm and radius of curvature 737 mm, and a curved film holder designed so as to obstruct only ten percent of the light. A narrow mask was added, so as to prevent the 4358A mercury light from striking the film. The linear dispersion is 15A/mm near 4358A and 34 A/mm at 5000A. The entire spectrograph is enclosed in a thermostat.

The irradiation apparatus employs two high current low pressure mercury lamps with internally water-cooled electrodes of the kind developed by Welsh and Crawford at the University of Toronto.[5] The lamps, which operate on 110 volts d.c. and draw 15 amperes each, are folded, so as to have two effective straight

* This work has been supported by the ONR under Contract N7-onr-398, Task Order I.

[1] J. B. Hatcher and D. M. Yost, J. Chem. Phys. **5**, 992 (1937).
[2] P. Torkington and H. W. Thompson, Trans. Faraday Soc. **41**, 236 (1945).
[3] W. F. Edgell and W. E. Byrd, J. Chem. Phys. **17**, 740 (1949).
[4] Nielsen, Crawford, and Smith, J. Opt. Soc. Am. **37**, 296 (1947).
[5] H. L. Welsh and M. F. Crawford (private communication).

columns. The radiation is concentrated on a 30 cm length of the Raman tube by means of a polished aluminum reflector, the cross section of which is made up of four segments of ellipses. The Raman tube is encircled by a filter jacket through which a filter solution circulates. To remove the heat generated in the lamp columns, air is drawn through the space between the filter jacket and the reflector by means of a blower.

The Raman tube, filled to a pressure of 7 atmospheres, was placed with its window immediately in front of the spectrograph slit. Exposures up to 70 hours were made on Eastman Tri X Panchromatic films, which were developed in DK 60a developer.

RESULTS

The infra-red absorption of 1,1-difluoroethylene gas between 2 and 22.7μ is shown in Fig. 1, which gives a complete percent transmittance curve for a pressure of 775 mm and partial transmittance curves for lower pressures. The wave numbers of the observed absorption maxima are given in the first column of Table I. In the second column the relative intensities are indicated by means of the following abbreviations *vs* very strong, *s* strong, *m* medium, *w* weak, etc. For bands having more or less typical contours, the contour type in Badger and Zumwalt's notation[6] is also given in this column. Unusually sharp or diffuse bands of un-

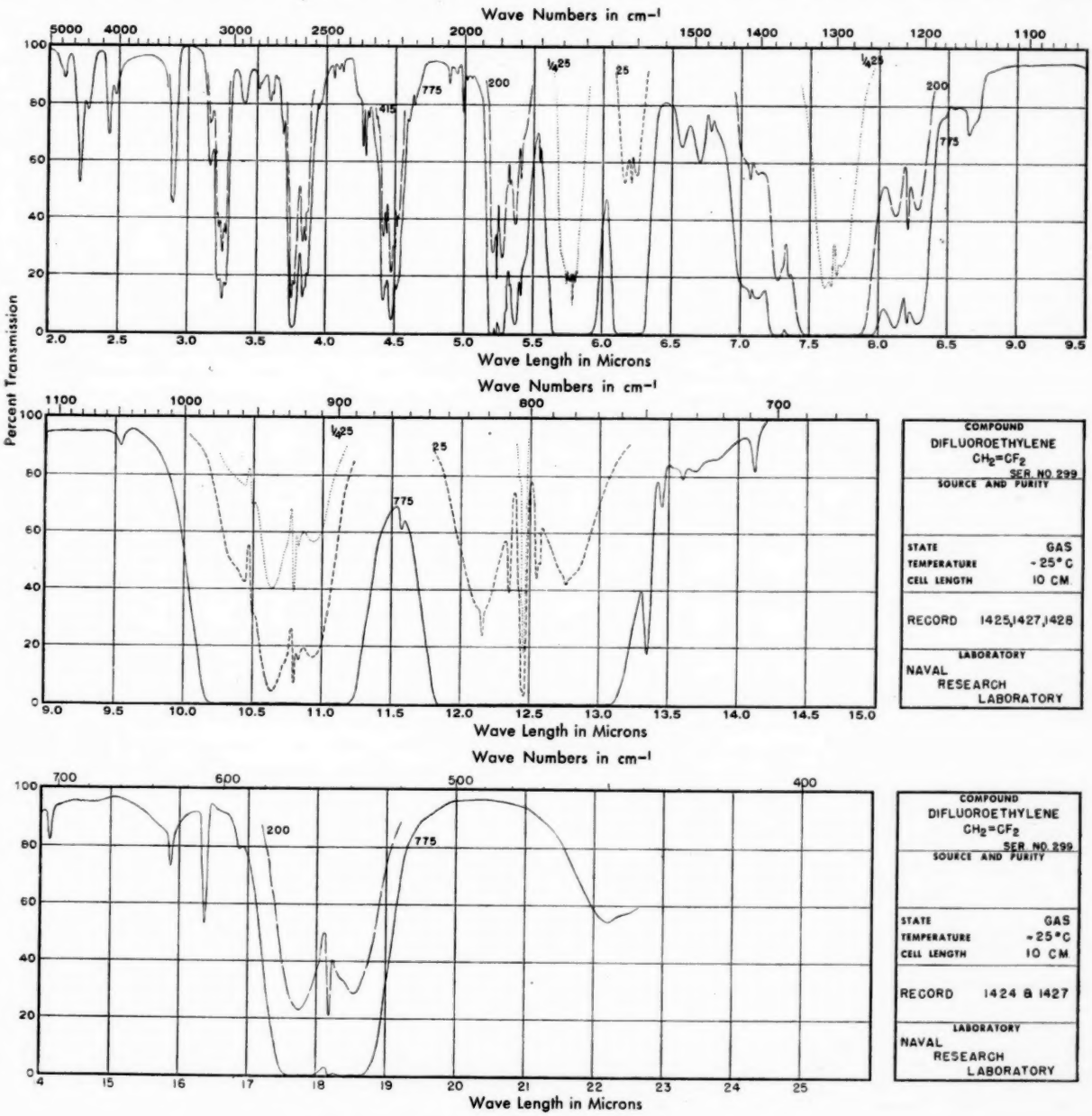

FIG. 1. Infra-red absorption spectrum of 1,1-difluoroethyene gas.

[6] R. M. Badger and L. R. Zumwalt, J. Chem. Phys. **6**, 711 (1938).

TABLE I. Infra-red spectrum of $CF_2:CH_2$ (gas).

Wave number	Description		Interpretation
429, 446 * cm^{-1}	m		B_1 Fundamental
~539			
550	m	Type A	A_1 Fundamental
~563			
593			
611	vw	Type C	B_2 Fundamental
630			
708	vvw	Type C	$1302-590=712(B_2)$
735	vvw		$550+803-611=742(A_1)$
743, 749	w	Type B	$1302-550=752(B_1)$
784			
796			
797			
803	vs	Type C	B_2 Fundamental
810			
822			
864	vvw		$1414-550=864(A_1)$; $1302-438=864(A_1)$
914			
923			
926	vs	Type A	A_1 Fundamental
940			
952, 958	s	Type B	B_1 Fundamental
1048	vvw	Type C?	$438+590=1028(B_2)$?
1156	vw		$550+611=1161(B_2)$
~1170	vw		$1728-550=1178(A_1)$
~1180	vw		$2\times590=1180(A_1)$
1208			
1218	m	Type A	$2\times611=1222(A_1)$
1232	m		
1294			
1299, 1305	vs	Type B	B_1 Fundamental
1314			
1361	w		$550+803=1353(B_2)$
1376	w	Type B?	$438+925=1363(B_1)$
1404			
1414	m	Type A	A_1 Fundamental
1425			
1475	vw	sh	$550+925=1475(A_1)$
1493	vw		$550+955=1505(B_1)$
1522	vw		$611+925=1536(B_2)$

TABLE I.—*Continued*

Wave number	Description		Interpretation
1602 cm^{-1}			
1611	s	Type A	$2\times803=1606(A_1)$
1623			
1720			
1724			$803+925=1728(B_2)$
1728	vs	Type A?	A_1 Fundamental
1733			
1738			
1740	vs	sh	$438+1302=1740(A_1)$
1804 cm^{-1}	vvw	Type C?	$2\times438+925=1801(A_1)$
1849	m	sh	$2\times925=1850(A_1)$; $550+1302=1852(B_1)$; $438+1414=1852(B_1)$
1863	m		$925+955=1880(B_1)$
1877	m	sh	$590+1302=1892(B_2)$
1896			
1909	s	Type A?	$2\times955=1910(A_1)$
1913			
1921			
1981	vvw		$550+1414=1964(A_1)$?
1996	vvw		
2000	vvw		
2004	vw	sh	
2023	vvw		$611+1414=2025(B_2)$
2045	vvw		$438+2\times803=2044(B_1)$
2155, 2174	vw, vw		$438+1728=2166(B_1)$
2208	w		
2216	w	sh	$803+1414=2217(B_2)$
2222	m		$925+1302=2227(B_1)$
2234	m		
2251	m	sh	$955+1302=2257(A_1)$
2263	m		
2285	vvw	sh	$550+1728=2278(A_1)$?
2290	vvw	sh	$438+550+1302=2290(A_1)$; $2\times438+1414=2290(A_1)$
2319			
2331	vw	Type C	$925+1414=2339(A_1)$; $611+1728=2339(B_2)$
2344	vw	sh	
2425	vvw	sh	$550+925+955=2430(B_1)$
2441	vvw	sh	$3059-611=2448(B_1)$
2467	vvw	sh	$2\times955+550=2460(A_1)$
2533	vvw	sh	$803+1728=2531(B_2)$
2584	w		$2\times590+1414=2594(A_1)$
2593	m	sh	$2\times1302=2604(A_1)$
2606	m		$3058-438=2620(B_1)$
2648	m		$925+1728=2653(A_1)$
2661	m	sh	$3100-438=2662(A_1)$
2709	vw	sh	$1302+1414=2716(B_1)$?

certain contour type are designated as *sh* or *d*, respectively.

The observed Raman shifts for $CF_2:CH_2$ gas are listed in Table II. The wave numbers corresponding to the frequency shifts are given in the first column. In the second column are given rough estimates of the relative intensities of the bands, as well as indications about unusual sharpness or diffuseness.

DISCUSSION OF RESULTS

Sharp infra-red absorption maxima lying below 1500 cm^{-1} have been measured to an accuracy of

± 1 cm^{-1}. With increasing wave number the accuracy of measurement decreases, being about ± 10 cm^{-1} for sharp maxima in the 3000 cm^{-1} region. Sharp Raman bands have been measured to 0.5 cm^{-1} or better, but the inaccuracy in wave numbers given for the most diffuse Raman bands may be as high as ± 10 cm^{-1}.

Two infra-red bands, at 677 and 1133 cm^{-1}, found by Torkington and Thompson[2] and interpreted by them as fundamentals were not observed in the present work. When the great difference in resolving power is considered, the agreement between the data given here and those of Torkington and Thompson is otherwise about as good as could be expected.

When the difference in state of aggregation is considered the agreement between our Raman data and those of Edgell and Byrd is fairly close, except for the bands in the 3000 cm^{-1} region. Edgell and Byrd observed five Raman bands for liquid $CF_2:CH_2$ which were not observed in the present work on gaseous $CF_2:CH_2$.

A few very faint infra-red absorption maxima near 2000 cm^{-1} have been observed also in other fluorinated hydrocarbons. They are probably caused by an impurity. The weak Raman bands at 3085 and 3112 cm^{-1} were observed only in the last exposure made after the $CF_2:CH_2$ gas had been irradiated for a total of 240 hours, half of this time without nitrite filter. Since evidence was observed of photo-chemical reaction, it is possible that these Raman bands are caused by a reaction product.

INTERPRETATION

(1) Determination of Fundamentals

If the $CF_2:CH_2$ molecule has a planar structure of symmetry C_{2v} the normal vibrations divide themselves into symmetry species as follows: There are five fundamentals of species A_1, one of species A_2, four of species B_1, and two of species B_2. All of the fundamentals are active in the Raman effect, the five totally symmetrical vibrations giving rise to polarized bands and the other vibrations to depolarized bands. With the exception of the single fundamental of species A_2 (the twisting mode), all of the fundamental vibrations are active in infra-red absorption.

The vibrations of species B_2, in which the atoms move perpendicular to the plane of the molecule, i.e., parallel to the axis of greatest moment of inertia, give rise to infra-red absorption bands of Type C. The contours of the bands belonging to species A_1 and B_1 will depend on whether the C=C bond is the axis of least or intermediate moment of inertia.

Recently Roberts and Edgell,[7] on the basis of microwave observations, have reported the following moments of inertia, 76.28, 80.47 and 156.99×10^{-40} g cm^2, for the $CF_2:CH_2$ molecule. The smallest moment belongs to an axis coinciding with the C=C bond.

[7] A. Roberts and W. F. Edgell, Phys. Rev. **76**, 178 (1949); J. Chem. Phys. **17**, 742 (1949).

Badger and Zumwalt's parameters

$$\rho=(a-b)/b \quad \text{and} \quad S=(2b-a-c)/(a-c),$$

where a, b and c are the reciprocals of the smallest, intermediate and largest moments of inertia, respectively, then have the following values $\rho=0.54$ and $S=0.80$. Badger and Zumwalt have given curves only for $\rho=\frac{1}{3}$, $\frac{1}{2}$ and $\frac{3}{4}$, $S=-\frac{1}{2}$, 0, $+\frac{1}{2}$. Using the curves for $\rho=\frac{1}{2}$ and $S=\frac{1}{2}$, we get for the spacing $\nu-\nu_0$ from the band center to the maxima of the rotational branches 13.5, 3.4 and 19 cm^{-1} for Type A, B, and C, bands, respectively. Extrapolation to $S=0.8$ gives 13 cm^{-1} for Type A, 2.9 cm^{-1} for Type B, and 18 cm^{-1} for Type C bands, in excellent agreement with the observed spacings.

The fairly strong Type A infra-red band at 550 cm^{-1}, although not observed in the Raman effect, is undoubtedly an A_1 fundamental. The corresponding vibration may be characterized roughly as a CF_2 deformation. The very intense band at 926 cm^{-1} definitely has Type A contour and is observed as a strong sharp band in the Raman effect. It must also be a totally symmetrical fundamental.

Going towards higher wave numbers, we must next account for the A_1 CH_2 deformation fundamental. In ethylene the symmetrical and unsymmetrical CH_2 deformation frequencies lie at 1342 and 1444 cm^{-1},

TABLE I.—*Continued*

Wave number	Description		Interpretation
2767 cm^{-1}	vw		$3\times925=2775(A_1)$; $550+925+1302=2777(B_1)$
2779	vw		$438+925+1414=2777(B_1)$
2817	vw		$2\times1414=2828(A_1)$
2844	vw		$3\times955=2865(B_1)$?
2929	vw	d	$590+611+1728=2929(B_1)$
3049			
3060	m	Type A?	A_1 Fundamental
3072	m	Type C?A?	$550+803+1728=3081(B_2)$
3088	m		
3099	m		B_1 Fundamental
3109	w		
3147	w		$1414+1728=3142(A_1)$; $803+925+1414=3142(B_2)$
3160	w		$438+1302+1414=3154(A_1)$
3453	w		$2\times1728=3456(A_1)$
3464	w		$438+3058=3496(B_1)$
4030	vw		$925+3100=4025(B_1)$?; $955+3100=4055(A_1)$
4120	w		$2\times550+3058=4158(A_1)$?
4390	w		$1302+3100=4402(A_1)$
4500	w		$1414+3100=4514(B_1)$; $1414+3058=4472(A_1)$
4740	w		$1728+3058=4786(A_1)$

* Observed by Dr. E. K. Plyler of the National Bureau of Standards.

TABLE II. Raman spectrum of $CF_2:CH_2$ (gas).

Wave number	Description	Interpretation
~440 cm^{-1}	vw vd	B_1 Fundamental
~590	vw vd	A_2 Fundamental
~615	vw d	B_2 Fundamental
799	vw vd	B_2 Fundamental
925.3	vs sh	A_1 Fundamental
1358.7	vw	$438+925=1363(B_1)$; $550+803=1353(B_2)$
~1405	w vd	A_1 Fundamental
1479.5	vw	$550+925=1475(A_1)$
1610	vw	$2\times803=1606(A_1)$
1728.5	s sh	A_1 Fundamental*
1740.6	s sh	$438+1302=1740(A_1)$
3058.3	s sh	A_1 Fundamental
3085.4	w	
3099.8	m	B_1 Fundamental
3112.2	w	

* Coincides with $803+925=1728(B_2)$.

respectively.[8] In isobutene Kilpatrick and Pitzer[9] have assigned 1390 cm^{-1} to this mode, and for $CCl_2:CH_2$ Kahovec and Kohlrausch[10] have assigned a value of approximately 1400 cm^{-1}. Most hydrocarbons of the form $CH_2:CHR$ have a characteristic frequency very close to 1416 cm^{-1}.[11] Thus, there can be little doubt that the Type A infra-red band at 1414 cm^{-1}, and the weak and very diffuse Raman band with a broad maximum at 1405 ± 10 cm^{-1}, represent the A_1 fundamental associated with the CH_2 deformation. It is somewhat disturbing, nevertheless, that these bands could also be explained as $611+803=1414(A_1)$.

While all olefinic hydrocarbons have a frequency near 1640 cm^{-1}, usually ascribed to a C=C stretching mode, it has been found by Hatcher and Yost[1] for $CF_2:CCl_2$, by Torkington and Thompson,[2] and in the present work that the corresponding frequency in fluorinated olefins lies at considerably higher values. In $CF_2:CH_2$ a very intense infra-red band is observed at 1728 cm^{-1}. Its abnormal contour indicates that it is not a single band. In the Raman spectrum two strong and sharp bands occur, at 1728.5 and 1740.6 cm^{-1}, respectively. One of these must be the A_1 fundamental in question. Since the lower value is the more useful in accounting for combination bands, and since the higher value can readily be explained as an A_1 combination band, $438+1302=1740$, it appears certain that 1728.5 cm^{-1} is the A_1 fundamental. The fact that the band at 1740 cm^{-1} is about as intense as the fundamental may be explained by the proximity of the two A_1 bands. The complexity of the infra-red contour is even greater than would be expected for two close A_1 bands. This appears to be the result of overlapping with a combination band $803+925=1728$ cm^{-1} of species B_2.

The last A_1 fundamental is essentially a C−H stretching mode and should lie between 2980 and 3080 cm^{-1}. It must be identified with the strong sharp Raman band at 3058 cm^{-1}. This probably corresponds to the infra-red absorption maximum at 3060 cm^{-1} rather than to the somewhat more intense maximum at 3072 cm^{-1} which appears to result from a B_2 combination band.

The two most intense infra-red bands with Type B contours, at 1302 and 955 cm^{-1}, must be fundamentals of species B_1. They may be characterized roughly as C−F stretching and CH_2 rocking modes. Although the higher frequency lies closest to the values for the CH_2 rocking frequency found for olefins, the greater intensity of the band at 1302 cm^{-1} would indicate that it is associated with a motion in which the fluorine atoms participate strongly. The transmittance curve given in Fig. 1 shows fairly strong absorption at the long wavelength limit of the spectral region investigated. Extending the observations by means of KRS-5 prism, Dr. E. K. Plyler of the National Bureau of Standards found two absorption maxima of medium intensity at 429 and 446 cm^{-1}. Although the contours are distorted because of the wide slit-width used, these undoubtedly represent a B_1 fundamental with center at 438 cm^{-1}. In the Raman spectrum a very diffuse and weak band is observed with maximum near 440 cm^{-1}. This fundamental may be designated roughly as a CF_2 rocking mode.

The remaining B_1 fundamental, which can be characterized rather accurately as the unsymmetrical C−H stretching mode, must lie somewhat higher than the corresponding A_1 fundamental. It must undoubtedly be identified with the medium intense Raman band at 3099.8 cm^{-1}. In the infra-red, absorption maxima have been observed at 3098 and 3109 cm^{-1}. Because of the low dispersion in this region and the proximity to the A_1 fundamental, and apparently also because of overlapping of combination bands, it is not possible to ascertain the band contour and obtain an accurate frequency value from the infra-red spectrum.

The single fundamental of species A_2, which corresponds to the twisting of the molecule, is active only in the Raman effect. If it is observed it must be 590 cm^{-1}. This value seems quite reasonable. In fact, if the twisting frequency for ethylene is taken to be 825 cm^{-1},[12] and if it assumed that 1,1-difluoroethylene has the same configuration and the same torsional force constant as ethylene, a simple calculation gives a value of 590 cm^{-1} for the twisting frequency. No other reasonable interpretation seems possible for the Raman band at 590 cm^{-1}. It is therefore assumed to be the A_2 fundamental. Recently, Arnett and Crawford[13] have shown that the twisting frequency of ethylene is 1027 rather than 825 cm^{-1}. This gives the higher value, 735 cm^{-1}, for the calculated twisting frequency of $CF_2:CH_2$. However, in view of the nature of the other assumptions upon which this calculation is based, this does not

[8] See G. Herzberg, *Infrared and Raman Spectra of Polyatomic Molecules* (D. Van Nostrand Company, Inc., New York, 1945) p. 326.

[9] J. E. Kilpatrick and K. S. Pitzer, J. Res. Nat. Bur. Stand. **38**, 1768 (1947).

[10] See K. W. F. Kohlrausch, *Ramanspektren* (Akademische Verlagsgesellschaft, Becker & Erler, Leipzig, 1945) p. 305.

[11] See J. H. Hibben, *The Raman Effect and Its Chemical Applications*, (Reinhold Publishing Corporation, New York, 1939), p. 165.

[12] See Reference 8, p. 326.

[13] R. L. Arnett and B. L. Crawford, Jr., O.N.R. Progress Report (N5 ori-147, T.O. 2), dated February 1, 1949.

TABLE III. Fundamental vibration frequencies for CF_2:CH_2.

Symmetry species	Approximate character*	Infra-red (gas) Wave number	Infra-red (gas) Description	Raman (gas) Wave number	Raman (gas) Description
A_1	C=C Stretching	1728	vs Type *A*	1728.5	s sh
A_1	CH Stretching	3060	m Type *A*	3058.3	s sh
A_1	CF Stretching	926	vs Type *A*	925.3	vs sh
A_1	CH_2 Deformation	1414	m Type *A*	1405	w vd
A_1	CF_2 Deformation	550	m Type *A*		
B_2	CH_2 Wagging	803	vs Type *C*	799	vw vd
B_2	CF_2 Wagging	611	w	615	vw vd
A_2	Twisting			590	vw vd
B_1	CH Stretching	3103	m	3099.8	m
B_1	CF Stretching	1302	vs Type *B*		
B_1	CH_2 Rocking	955	s Type *B*		
B_1	CF_2 Rocking	438**	w Type *B*	440	vw vd

* The terms in this column have only rough meaning, especially for vibrations involving the CF_2 group.
** Observed by Dr. E. K. Plyler, National Bureau of Standards.

materially weaken the argument. Edgell and Byrd[3] have recently observed a very weak Raman band at 714 cm^{-1} in liquid CF_2:CH_2 and have interpreted this as the A_2 fundamental. Further work is undoubtedly required before a final choice can be made between their value and ours.

There remain the two fundamentals of species B_2. One of these is certainly 803 cm^{-1}, which occurs as a very intense Type *C* band in the infra-red and as a faint very diffuse band in the Raman effect. This frequency must be associated with a wagging motion of the CH_2 group. While the contour of the infra-red band at 803 cm^{-1} is undoubtedly of Type *C*, the band appears to have two or perhaps four secondary zero branches, for which we have found no satisfactory explanation.

The other B_2 fundamental must lie below 803 cm^{-1}. The strongest Type *C* band observed here is the very weak band at 611 cm^{-1}. This could be interpreted as a difference band, $1414-803=611(B_2)$. However, this is not a plausible interpretation, especially since Edgell and Byrd have found a strong Raman band at 603 cm^{-1} in liquid CF_2:CH_2 at a low temperature. The possibility that the absorption maximum found by Dr. Plyler at 429 cm^{-1} is the B_2 fundamental has been considered, but its interpretation as one component of a Type *B* band seems more plausible. Thus, the infra-red band at 611 cm^{-1}, and the very weak and diffuse Raman band at 615 cm^{-1}, are assigned as the second B_2 fundamental.

The infra-red and Raman frequencies interpreted here as fundamental vibration frequencies for CF_2:CH_2 are listed in Table III. As already pointed out, the characterization of the vibration given in the second column has only very rough significance, except for vibrations limited largely to the CH_2 group.

Six of the fundamentals listed here were previously assigned by Torkington and Thompson.[2] When the large differences in some of the frequency values are disregarded, the assignment given here agrees with that of Edgell and Byrd,[3] except for the A_2 fundamental and for the A_1 CH_2-deformation frequency. Edgell and Byrd identify the latter with the Raman band at 1359 cm^{-1}, which here is interpreted as a combination band.

2. Interpretation of the Spectra

On the basis of the fundamental frequencies listed in Table III it has been possible to give a satisfactory interpretation, listed in the third columns of Tables I and II, of practically all of the observed infra-red and Raman bands. Of the 64 infra-red-active binary combination (sum or overtone) bands that can be formed from the 12 fundamentals, about two-thirds have been accounted for in the observed spectrum, although several bands coincide or overlap. Several binary combination bands are masked by fundamentals or lie outside the spectral range investigated. Other binary combination bands that could not be identified lie in the region beyond 3000 cm^{-1} where the dispersion is low and where bands are crowded together. Only one binary combination band, the overtone 2×550 cm^{-1}, is conspicuously absent. Six bands are interpreted as binary difference bands. For each of these the corresponding sum band appears to be present with the intensity to be expected from the Boltzmann factor for the excited initial level. However, because of overlapping of bands no accurate test of the intensity relations could be made. A dozen of the weakest bands are interpreted as ternary sum or difference bands. Because of the large number of possible combinations of this kind, the assignment of these bands must be regarded as tentative. For some bands more than one interpretation is given, but not all of the possible alternative assignments have been indicated.

The agreement between the calculated and the observed frequencies for the combination bands is on the whole very good, the most conspicuous exceptions being the bands at 1048 and 1522 cm^{-1}.

The peculiar contours of the fundamental bands at 803 and 1728 cm^{-1} have already been pointed out. The A_1 fundamental at 925 cm^{-1} apparently has a second zero branch at 923 cm^{-1}, which seems too intense to arise from molecules containing a C_{13} atom but may belong to a combination of form $925+\nu_z-\nu_x$ ("upper-stage band"). The high intensities of the overtone bands at 1218 and 1611 cm^{-1} is striking but may result from their proximity to the A_1 fundamentals at 1414 and 1728 cm^{-1}.

With the exception of the Raman bands at 3085 and 3112 cm^{-1}, which are believed to be caused by a photochemical reaction product, all of the observed Raman bands have been satisfactorily interpreted.

ACKNOWLEDGMENTS

The writers wish to acknowledge their indebtedness to E. I. duPont de Nemours and Company for the gift of the sample; to Dr. E. K. Plyler of the National Bureau of Standards for his valuable help in providing data for the long wave-length region; and to Professor W. F. Edgell for giving them his results for liquid 1,1-difluoroethylene before publication.

The Microwave Spectra of Isotopic Methyl Chloride*

G. MATLACK AND G. GLOCKLER
Department of Chemistry and Chemical Engineering
AND
D. R. BIANCO AND A. ROBERTS
Department of Physics
State University of Iowa, Iowa City, Iowa

(Received August 15, 1949)

The rotational transition $J=0\rightarrow J=1$ of the isotopic species $C^{13}H_3Cl$, $C^{12}H_2DCl$, and $C^{12}HD_2Cl$ have been investigated by microwave absorption. The data have been used to obtain the ground state dimensions of the methyl chloride molecule. The effects of zero-point vibration are rather large, and do not permit very accurate results for the dimensions of the methyl group: $C-H=1.103\pm0.006$A, $\measuredangle H-C-H=109.8°\pm0.5°$.

DATA on the pure rotational spectra of CH_3Cl^{35} and CH_3Cl^{37} in the microwave region have been reported by Gordy, Simmons, and Smith.[1] They observed the $J=0\rightarrow J=1$ transition for both molecules. The transition actually gives rise to three lines because of the hyperfine structure caused by the nuclear quadrupole coupling effects of the chlorine nucleus. By combining the microwave with previously known infrared absorption data,[2] they arrived at the following dimensions for methyl chloride:

$$C-Cl=1.779\text{A}; C-H=1.109\text{A}; H-C-H \text{ angle}=110°$$

The precision of these values depends upon the precision of the known value of I_A. The above dimensions were calculated using 5.52×10^{-40} g×cm² as the best value for I_A. Actually, this value of I_A has a probable error of $\pm0.16\times10^{-40}$ g×cm². This would introduce an uncertainty into the internuclear parameters of the following extent:

$$C-Cl=1.779\pm0.005\text{A}; \quad C-H=1.109\pm0.005\text{A}$$
$$H-C-H \text{ angle}=110°\pm1°30'.$$

TABLE I. Symmetric CH_3Cl frequencies for the $J=0\rightarrow J=1$ transition. Probable errors are ±0.1 mc.

	Freq. (mc/sec.)	Separation	Reference
$C^{12}H_3Cl^{35}$	26,604.57	15.08	a
	26,589.49		
	26,570.77	−18.72	
$C^{12}H_3Cl^{37}$	26,191.13	11.83	a
	26,179.30		
	26,164.57	−14.73	
$C^{13}H_3Cl^{35}$	25,577.40	−18.79	b
	25,596.19		
	25,611.09	14.90	
$C^{13}H_3Cl^{37}$	25,167.68	−14.82	b
	25,182.50		
	25,194.20	11.70	

[a] Gordy, Simmons, and Smith, Phys. Rev. **74**, 243 (1948).
[b] This work.

Since both C^{13} and deuterium have become readily available in high concentrations, it was hoped that the spectra of methyl chloride containing C^{13} and deuterium would help in further elucidation of the problem. The compounds reported here are $C^{13}H_3Cl$, CH_2DCl, and CHD_2Cl.

I. SYMMETRIC METHYL CHLORIDE

Experimental Procedure

Carbon dioxide, generated from one gram of barium carbonate containing 53 atom percent C^{13}, was dried and reduced to methyl alcohol by the method of Nystrom, Yanko, and Brown.[3] The methyl alcohol was then converted to methyl chloride by heating with aluminum chloride according to the procedure given by Norris and Sturgis.[4] The methyl chloride, as it was generated, was entrained in a slow stream of dry nitrogen and collected in a trap cooled with liquid air.

The microwave spectrometer was of the Hughes-

TABLE II. Hypothetical unsplit frequencies, $J=0\rightarrow J=1$, for symmetric CH_3Cl and corresponding I_B.

	Freq. (mc/sec.)	$I_B(10^{-40}$ g×cm²)	Reference
$C^{12}H_3Cl^{35}$	26,585.77	63.114	a
$C^{12}H_3Cl^{37}$	26,176.37	64.101	a
$C^{13}H_3Cl^{35}$	25,592.43	65.562	b
$C^{13}H_3Cl^{37}$	25,179.54	66.640	b

[a] Gordy, Simmons, and Smith, Phys. Rev. **74**, 243 (1948).
[b] This work.

TABLE III. Internuclear parameters for methyl chloride.*

Model	C−Cl	C−H	H−C−H angle
I	1.779A	1.094A	109°28′
II	1.779	1.109	110°
III	1.781	1.098	110°

* Dailey, Mays, and Townes, Phys. Rev. **76**, 136 (1949) give C−Cl 1.781A°, C−H 1.12A° and angle HCH 110°50′.

* Supported in part by ONR.
[1] Gordy, Simmons, and Smith, Phys. Rev. **74**, 243 (1948).
[2] W. H. Bennett and C. F. Meyer, Phys. Rev. **32**, 888 (1928).
[3] Nystrom, Yanko, and Brown, J. Am. Chem. Soc. **70**, 441 (1948).
[4] J. F. Norris and B. M. Sturgis, J. Am. Chem. Soc. **61**, 1413 (1939).

Wilson[5] Stark modulation type, using an eight-foot K-band absorption cell.

The observed frequencies for $C^{12}H_3Cl$ and $C^{13}H_3Cl$, together with the triplet separations, are given in Table I.

Results

The hypothetical unsplit frequencies and the I_B values calculated from these frequencies are given in Table II.

Knowing the microwave data from three isotopic species of methyl chloride, it should be possible, theoretically, to obtain the three internuclear parameters of the molecule from microwave data alone. Equation (1) gives the expression for the moment of inertia about the principal axis perpendicular to the figure axis.

$$I_B = M_{Cl}R^2 + 3M_H(r\cdot\cos\alpha)^2 + \tfrac{3}{2}M_H(r\cdot\sin\alpha)^2 - \frac{(M_{Cl}R - 3M_H r\cdot\cos\alpha)^2}{M_C + M_{Cl} + 3M_H}, \quad (1)$$

where R is the C−Cl distance, r is the C−H distance, and α is the angle between the C−H bond and the figure axis. The relation between α and β (the H−C−H angle) is given by

$$\cos\alpha = \left(\frac{1+2\cos\beta}{3}\right)^{\frac{1}{2}}. \quad (2)$$

Using Eq. (1), an attempt was made to obtain an explicit solution for the three internuclear parameters, employing the above data and that given by Gordy, Simmons, and Smith.[1] A reasonable value for the C−Cl distance was obtained, but the results found for the methyl group were not very precise. Equation (1) contains the term $\frac{3}{2}M_H(r\cdot\sin\alpha)^2$. Its contribution to the total moment of inertia is too small to give reliable values for the distance from the figure axis to the hydrogens.

It is possible, however, by using Eq. (1) to check the accuracy of several models for methyl chloride. By using this method of approximation, it has been found that three different sets of internuclear parameters will predict the frequencies so far obtained from the four isotopic methyl chloride molecules within 1.0 mc/sec. They are shown in Table III. It is entirely possible that other reasonable sets could be found also.

II. ASYMMETRIC METHYL CHLORIDES ($C^{12}H_2DCl^{35}$, $C^{12}H_2DCl^{37}$, $C^{12}HD_2Cl^{35}$, and $C^{12}HD_2Cl^{37}$)

On the basis of the findings described above, it was felt that information of a more definite nature might perhaps be obtained by introducing one or two deuterium atoms into the methyl chloride molecule, thus converting the symmetric top structure to an asymmetric one.

[5] R. H. Hughes and E. B. Wilson, Jr., Phys. Rev. **71**, 562 (1947).

TABLE IV. Asymmetric CH_3Cl frequencies for $0_0 \rightarrow 1_{-1}$ transitions.

	Freq. (mc/sec.)	Separations
CH_2DCl^{35}	24,641.70	−18.63
	24,660.33	
	24,675.25	14.92
CH_2DCl^{37}	24,252.00	−14.68
	24,266.68	
	24,278.33	11.65
CHD_2Cl^{35}	23,035.00	−18.62
	23,053.62	
	23,068.51	14.89
CHD_2Cl^{37}	22,659,29	−14.51
	22,673.80	
	22,685.60	11.80

TABLE V. Hypothetical unsplit frequencies, $J=0_0 \rightarrow J=1_{-1}$, for $C^{12}H_2DCl^{35}$, $C^{12}H_2DCl^{37}$, $C^{12}HD_2Cl^{35}$, and $C^{12}HD_2Cl^{37}$, and frequencies calculated from the models of Table III.

Molecule	Freq. observed	Freq. cal. I	Freq. cal. II	Freq. cal. III
$C^{12}H_2DCl^{35}$	24,658	24,630	24,623	24,626
$C^{12}H_2DCl^{37}$	24,266	24,237	24,231	24,234
$C^{12}HD_2Cl^{35}$	23,054	22,994	22,986	22,997
$C^{12}HD_2Cl^{37}$	22,674	22,618	22,604	22,607

Experimental Procedure

Inasmuch as an unseparated mixture of CH_2DCl and CHD_2Cl is suitable for microwave examination, the deuterated methyl chlorides were made by the same general method as used for the symmetric methyl chlorides. To reduce the carbon dioxide from one gram of ordinary barium carbonate, a mixture of 0.3 g. $LiAlH_4$ and 0.3 g. $LiAlD_4$ in diethyl carbitol was used. The methyl alcohol thus obtained was then converted to methyl chloride by heating with aluminum chloride as described above.

Results

There are two transitions from the ground rotational state, for each asymmetric methyl chloride, permitted by the selection rules for an asymmetric top.[6] For CH_2DCl, these are the $0_0 \rightarrow 1_{-1}$ and the $0_0 \rightarrow 1_0$ transitions, corresponding to frequencies of $B+C$ and $A+C$, respectively. For CHD_2Cl, the transitions are $0_0 \rightarrow 1_{-1}$ and $0_0 \rightarrow 1_1$ with corresponding frequencies of $B+C$ and $A+B$. However, since the asymmetry due to the introduction of the deuteriums is small ($\kappa = -0.993$), the component of the dipole moment perpendicular to the axis of least moment of inertia is also quite small, and the intensities of the $0_0 \rightarrow 1_0$ and $0_0 \rightarrow 1_1$ transitions will

[6] G. Herzberg, *Infrared and Raman Spectra of Polyatomic Molecules*, (D. Van Nostrand Company, Inc., New York, 1945), pp. 50–55.

be very weak. Furthermore, both B and C are of the order of 12,000 mc/sec., while A is of the order of 100,000 mc/sec. Therefore, these latter transitions could not be reached with present equipment. Under these circumstances, the only transition one could expect to observe is the $0_0 \rightarrow 1_{-1}$ transition which corresponds to the $0 \rightarrow 1$ transition in the symmetric top case.

Table IV gives the observed triplets of the $0_0 \rightarrow 1_{-1}$ transition for each of the asymmetric methyl chlorides. In Table V the hypothetical unsplit frequencies are compared with frequencies calculated for the three models I, II, and III given in Table III.

The quadrupole coupling in a symmetric top molecule depends on the second derivative of the potential, q, along the symmetry axis only (for a nucleus on the symmetry axis) and therefore substitution of an isotopic carbon atom in methyl chloride should not affect the quadrupole coupling energy, at least to the first order terms in eqQ/B_0. The separation between the hyperfine components should therefore be the same in $C^{13}H_3Cl$ as in $C^{12}H_3Cl$, for corresponding chlorine nuclei. We are here supposing that we may neglect both second-order quadrupole terms and the additional terms which may be introduced into the molecular Hamiltonian by substituting the nucleus C^{13}, which has a spin $\frac{1}{2}$ and a nuclear magnetic moment, for the nucleus C^{12}, with zero spin and no magnetic moment. Such additional terms might include the mutual interaction of the nuclear magnetic moments, and the interaction of the C^{13} moment with the molecular rotation, both of which are very small.

In the slightly asymmetric molecules CH_2DCl and CHD_2Cl, the quadrupole coupling will in general be slightly altered because the C—Cl bond no longer lies exactly along a principal axis. Formulas for the quadrupole splitting in asymmetric rotors have been given by Bragg.[7] The quadrupole splitting of any level in an asymmetric top differs from that in the limiting symmetric top only by a scale factor which depends upon the second derivative of the potential, q_i, along the principal axes. In general, the q_i must be determined from the observed spectra. In the $0_0 \rightarrow 1_{-1}$ transitions of any molecule, the 0_0 level is of course unsplit by the quadrupole coupling, and the 1_{-1} level splitting can differ from that in the limiting symmetric top only by a scale factor. Hence the position of the unsplit line can be calculated without knowing the q_i.

For the 1_{-1} level, the Bragg formula shows that the splitting depends only on the derivative along the principal axis of least moment of inertia, q_a, and does not depend explicitly upon the asymmetry parameter. From the experimental fact (see Table IV) that the total quadrupole coupling of the 1_{-1} level is indistinguishable from that found in the symmetric tops, we may deduce the fact that q_a is independent of the small angular changes in the position within the molecule of the principal axis of least moment of inertia. This implies that q_a is an extremum along the symmetric top figure axis. Such a conclusion is what one expects for almost any type of chemical bond.

We have neglected throughout the further splitting of the hyperfine structure levels by the quadrupole moment of the deuteron. The deuteron quadrupole moment is quite small, and the coupling is experimentally insufficient to split the levels enough even to broaden the lines appreciably.

[7] J. K. Bragg, Phys. Rev. **74**, 533 (1948).

Discussion

The observed frequencies of the asymmetric methyl chlorides are higher than predicted for all three molecular models. It is interesting to note that the difference between the observed and calculated values nearly doubles when the mono-deutero compound is replaced by the dideutero compound. This doubling of the deviation would seem to indicate an effect caused by the difference in zero-point vibrational energy of the methyl chloride as the hydrogen atoms are replaced by deuterium atoms. The values of the internuclear parameters used in the calculations are the "effective" values for the molecule in the vibrational ground state, and are not the equilibrium values which would correspond to a vibrationless ground state. If the difference in zero point vibrational energy on going from hydrogen atoms to deuterium atoms, in methyl chloride, is the chief factor in this deviation, it might be expected that the CD_3Cl frequencies will prove to be about 100 megacycles higher than the predicted value.[8]

The fact that the three models all give a good fit for the data from the symmetric methyl chloride, and that the deviations from the observed frequencies of the asymmetric methyl chlorides are about the same for the three models, brings out the importance of obtaining a more accurate value of I_A than is available now. On the basis of the present data on the symmetric and asymmetric methyl chlorides, a clear-cut choice of the internuclear distances and angle does not seem possible.

It may well happen that even if the I_A value is accurately measured from microwave data, the relatively large effects of zero-point vibration on the parameters of the methyl group will prevent the evaluation of a more precise set of dimensions.

Making due allowance for all the above effects, it seems reasonable to propose the following values for the dimensions of methyl chloride in the ground vibrational state from microwave data:

$$\text{C—Cl: } 1.780 \pm 0.002\text{A}$$
$$\text{C—H: } 1.103 \pm 0.006\text{A}$$
$$\measuredangle \text{H—C—H: } 109.8° \pm 0.5°.$$

[8] *Note added in proof:* The observations of Simmons [Phys. Rev. **76**, 686 (1949)] on the frequencies of CD_3Cl show that this is indeed the case, the observed frequency for CD_3Cl^{37} being 21,325±5 mc, the calculated value from model I 21,243 mc.

The Properties of *n*-Pentforane and Its Mixtures with *n*-Pentane

J. H. SIMONS AND R. D. DUNLAP
Fluorine Laboratories, The Pennsylvania State College, State College, Pennsylvania

(Received August 22, 1949)

A sample of *n*-pentforane, C_5F_{12}, of high purity was made available by the operation of the electrochemical process for the production of fluorocarbons. The physical properties of this material were determined, and a study was made of the two-component, liquid-gas system of it with *n*-pentane, C_5H_{12}. Deviations from Raoult's law were found which were much greater than could be predicted by existing theories for solutions of nonpolar substances. In order to correlate the experimentally determined properties of these mixtures, it was necessary to extend the existing theories. This was done by assuming a new concept of possible significance in solubility relationships. This concept is pictured as the interpenetration of the molecules in the condensed state. For the particular system herein studied the interpenetration between hydrocarbon molecules is much greater than between fluorocarbon molecules, and the interpenetration between the fluorocarbon and hydrocarbon molecules is as small or smaller than that between fluorocarbon molecules. This additional concept has provided a means for correlating the measurements.

INTRODUCTION

THE properties of a two-component liquid system are necessarily related to the forces of interaction between both like and unlike molecules. Those between like molecules are responsible for the properties of the pure liquids; and it is, therefore, highly desirable to be able to predict the properties of the two-component system from those of the pure substances. The contributions of a number of factors to the properties of a mixture have been exhaustively treated. Examples of these are dipole moments, polarizability, molecular dimensions, structural formula, and tendencies toward chemical combinations. A preliminary consideration of the herein studied system indicated deviations from Raoult's law enormously greater than could be expected from consideration of the above factors. This led to a more detailed study of the system and to the introduction of the interpenetration concept as an important factor in solubility relationships.

The discovery of the fluorocarbons and the invention of processes for their production has provided a new family of chemical substances different from but roughly parallel to organic compounds, which now are available for comparison studies and tests of various theories. As the boiling points of the fluorocarbons are lower for their molecular weights than is true for almost all other molecular substances approaching in this respect the inert monatomic gases, it is conceivable that they will provide norms or basic points of references for the comparison of the properties of other substances, particularly in such concepts as those of ideal solutions.

n-Pentforane, C_5F_{12}, and *n*-pentane, C_5H_{12}, are very similar in many of their properties. They boil at approximately the same temperature and have approximately the same energy of vaporization. They both have negligible dipole moments, and the electron polarizability is essentially the same. They have approximately the same melting point. They each have the same number of atoms in the molecule and each have five carbon atoms per molecule arranged in a linear sequence. There is no apparent molecular association in the liquid state, and there is no apparent chemical interaction between these substances. Experimentally, however, deviations from Raoult's law much larger than existing theories would predict were found. The large difference in vapor density of the two components enables gaseous mixtures to be analyzed by the determination of this property and liquid mixtures by the same technique after evaporation.

PROPERTIES OF *n*-PENTFORANE, C_5F_{12}

This substance, free from major contamination of isomers, was obtained by the operation of the electrochemical process[1] using pyridine as the raw material. Chemical treatment and precision fractionation gave

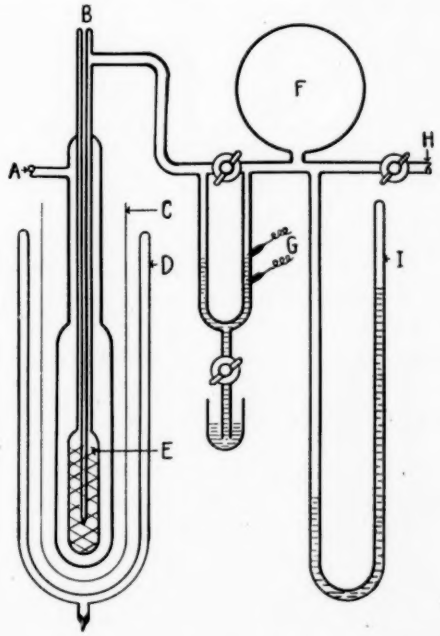

FIG. 1. Melting point and vapor pressure apparatus.

[1] J. H. Simons and co-workers, J. Electrochem. Soc. **95**, 47 (1949).

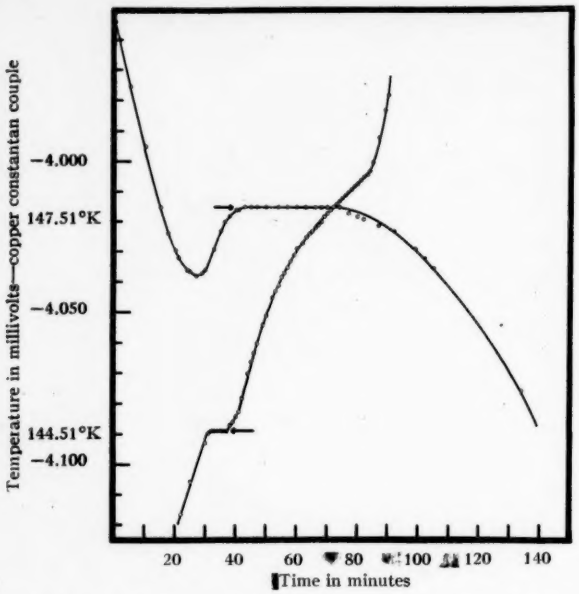

FIG. 2. Cooling and warming curves for pentforane.

1.9 kilograms of purified material from 5 kilograms of fluorocarbon raw material.

The freezing point, transition point, and vapor pressure were determined in the apparatus schematically shown in Fig. 1 by the standard and well-known laboratory techniques. On a 30 cm³ sample, warming and cooling curves were obtained. This was repeated after a six-stage fractional crystallization purification. The final curves duplicated the original ones indicating no separation or purification had occurred during the recrystallization. The rest point at 144.51±0.05°K is assumed to be a crystal transition, and the one at 147.51±0.05°K is taken as the freezing point. An estimate of the purity of the sample can be obtained from these curves.[2] Since there is no perceptible slope at the rest point, the precision of the temperature measurement is taken as the freezing point discrepancy assuming the heat of fusion of the order of magnitude of that for *n*-pentane.[3] The calculated purity of *n*-pentforane is 99.8 mol percent pure from solid insoluble material. Representative warming and cooling curves are given in Fig. 2.

It is interesting to note that a single isomeric species can be obtained by means of the electrochemical process. This is of greater importance for fluorocarbons than it would be for hydrocarbons, because structural isomers of the fluorocarbons boil within a few tenths of a degree apart, and separation by means of distillation is not feasible.

A drift method was used in the determination of vapor pressure. The sample was allowed to warm slowly and exert its vapor pressure against the balancing manometer *G* provided with electrical signalling devices. The rate of warming was such that 20 hours was required to produce 700 mm pressure. The curve obtained by warming was duplicated by slow cooling. By the method of least squares, the following equation was fitted to the experimental data:

$$\log_{10}p = -2108.0/T - 4.9814\log T + 22.2092.$$

p is in mm of Hg at standard gravity and 0°C, and T is the absolute temperature. The temperature at which p is equal to 760 mm of Hg is 302.35°K. The heat of vaporization at the boiling point, calculated from this equation and an approximate state equation for the gas is 6.38 kcal. per mol. The corresponding entropy of vaporization is 21.1 e.u.

A moderate pressure gas equation of the type $PV(1+BP)=RT$ was obtained by determining a series of gas densities at different pressures. B for *n*-pentforane was found to be 0.041 atmos.$^{-1}$.

The density of *n*-pentforane was determined in two different dilatometers at five different temperatures between 258° and 293°K. The ten points were found to fall on a curve which was noticeably convex towards the temperature axis. The following equation was fitted to the data by the method of least squares:

$$D_t = 1.6195 + 3.375\times10^{-3}(293.16-T) - 6.374\times10^{-6}(293.16-T)^2$$

D is in g per cm³ and T is the absolute temperature.

SOURCE OF *n*-PENTANE, C_5H_{12}

The *n*-pentane used in the solubility experiments was obtained from Phillips Petroleum Company. This material, labeled "Pure Grade," 99 mol percent minimum was fractionated in an efficient column, and a middle cut of constant refractive index of 1.3576 at 20°C was considered acceptable for the present purpose.

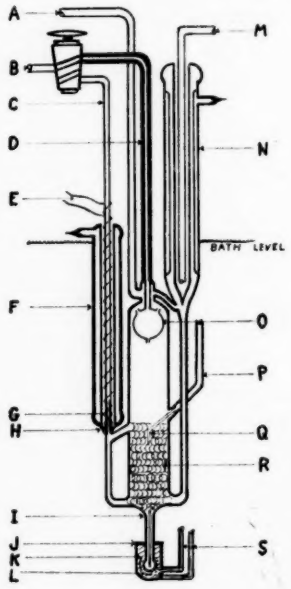

FIG. 3. Equilibrium still.

[2] W. J. Taylor and F. D. Rossini, J. Research Nat. Bur. Stand. 32, 197 (1944).
[3] G. H. Messerly and R. M. Kennedy, J. Am. Chem. Soc. 62, 2988 (1940).

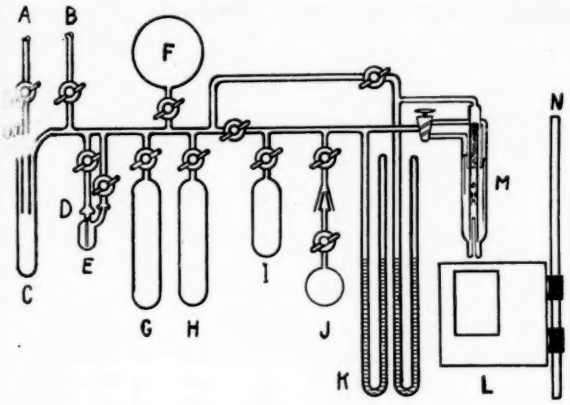

FIG. 4.

LIQUID VAPOR EQUILIBRIUM

Apparatus

In Fig. 3 is shown the equilibrium still employed for this study. The liquid containing vessel (*R*) was filled with multi-turn helices to discourage large size bubble formation. The liquid was boiled in *K* by means of heater (*L*), supplied with current through *S*, and bumping was prevented by means of the return tube (*I*). The vapor was condensed in the vacuum jacket condenser (*N*) and the liquid returned to the bottom of the vessel. Vapor sample was obtained through the capillary tube (*D*) and prevented from liquid splash by the splash guard (*O*). The liquid sample was withdrawn through *C* in the form of vapor. Evaporation was provided by heater (*E*) protected by the vacuum jacket (*F*). The thermocouple in the capillary tube (*Q*) provided the temperature reading. The remainder of the design is obvious from the diagram with the exception of the seals, *H* and *J*, which were made from asbestos and U. S. Stoneware Tygon Paint. This seal was found satisfactory over a considerable range of temperature and unaffected by the ethylene glycol-water solution used as the liquid in the thermostat. This still was connected to the apparatus shown in Fig. 4 at the location *M* of that figure. The thermostat (*L*) of Fig. 4 could be moved into position to surround the equilibrium still. This was regulated to within $\pm 0.05°$ at any temperature down to $-40°$C. In operation, the equilibrium still was a constant temperature device; the heater and condenser merely serve to provide circulation.

Procedure

The pure components were stored in the vessels (*G* and *H*), Fig. 4, and a mixture of the desired composition was prepared by withdrawing the vapors into the 5 liter bulb (*F*) and noting the pressures. Liquid samples of approximately 50 cm^3 volume obtained in this was condensed into the equilibrium still. Cold air was supplied to the condenser and current to the heater, and a satisfactory steady state was obtained in about two and one-half hours. At this time, the liquid sample was slowly removed and immediately afterwards the vapor sample was removed at such a rate that no observable change in the pressure was observed. The samples withdrawn were of sufficient size so that checked determinations were possible, and the operation was repeated at five different temperatures before the still was recharged.

Results

The experimental data obtained from the equilibrium still is tabulated in Table I, and the pressure-composition diagrams for each of the five different temperatures are shown in Figs. 5, 6, 7, 8, and 9. The data shown in Table II was taken from the pressure-composition plots. The partial molal heat of solution was calculated from the rate of change of $\ln p_1/p_0$ with temperature. For the purpose of this study, p_1/p_0 is assumed to be equal to the activity. The change in free energy in transferring a mol of one of the components from an ideal solution to an actual solution of the same concentration was calculated from the activity coefficients. The following thermodynamic relationships were used:

$$\bar{H}_1-\bar{H}_1{}^i=R\frac{d\ \ln a_1}{d(1/T)} \tag{1}$$

and

$$\bar{F}_1-\bar{F}_1{}^i=RT\ \ln a_1/n_1=RT\ \ln\gamma_1. \tag{2}$$

The values obtained for $\bar{H}_1-\bar{H}_1{}^i$ and $\bar{F}_1-\bar{F}_1{}^i$ are tabulated in Table III. The data were not sufficiently accurate to determine the rate of change of free energy with temperature, and therefore the average for the five temperatures was taken. These partial molal heats and free energies of solution are plotted against the quantity $\phi_2{}^2v_1$ where ϕ is the volume fraction and v is the molal volume. These plots are shown in Fig. 10. The fact that values for each of the components fall on the same straight line is evidence enough for the consistency of the experimental data. The data is

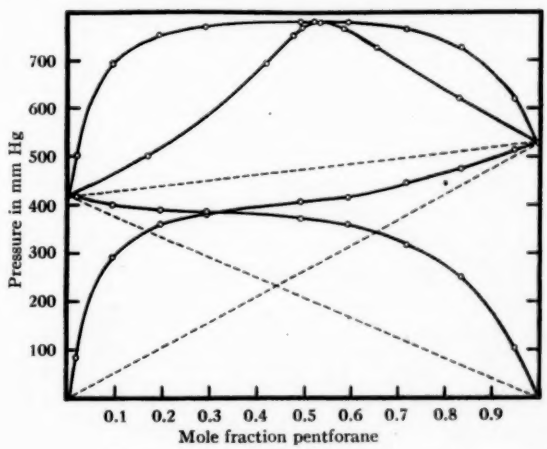

FIG. 5. $T-292.9°$K.

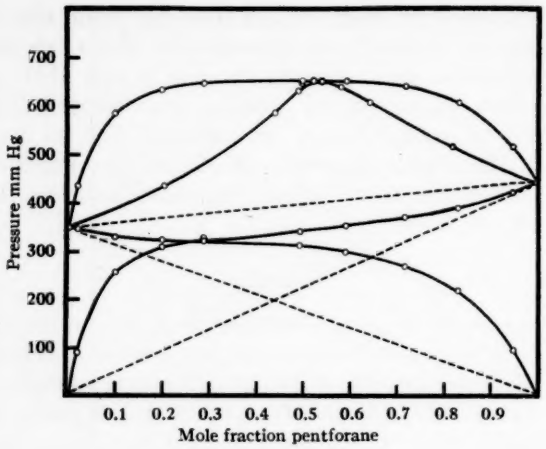

FIG. 6. $T-288.2°K$.

represented by the following equations:

$$RT \ln\gamma_1 = 7.69\phi_2^2 v_1 \quad (3)$$

and

$$RT \ln\gamma_2 = 7.69\phi_1^2 v_2, \quad (4)$$

where the subscripts 1 and 2 refer to *n*-pentforane and *n*-pentane respectively. The system was found to have a minimum boiling point at 292.2°K for one atmosphere. The corresponding azeotropic composition is 0.53 mol percent *n*-pentforane.

MUTUAL SOLUBILITIES OF *n*-PENTFORANE AND *n*-PENTANE

The mutual solubilities of *n*-pentforane and *n*-pentane were determined in the apparatus shown in Fig. 11 and at *M* in Fig. 4. *A* and *B* are leads to the sampling system and *D* is connected with the manometer. *C* and *I* are sampling probes through which samples from the less and more dense phases may be removed. With careful manipulation of the stopcock, the liquid sample may be completely converted to vapor in the superheated section and analyzed as such. An all glass pump (*J*) was designed to pump the upper layer through the lower one and was operated by intermittent activation

TABLE I. Experimental data for liquid-vapor equilibrium.

Temperature °K	Total pressure in mm of Hg	Average molecular weight of liq. samp.*	Average molecular weight of vap. samp.*	Partial pressure of *n*-pentforane	Partial pressure of *n*-pentane	Mole fraction of C_5F_{12} in liquid	Mole fraction of C_5F_{12} in vapor
292.9	503	76.1	108.7	85	418	0.018	0.169
288.2	434**			89**	345**	0.020	0.205**
278.6	293	75.7	115.2	58	235	0.016	0.199
283.1	360**			77**	283**	0.020	0.214**
262.4	145	75.3	120.4	32	113	0.014	0.223
293.6	705	92.6	163.1	296	409	0.095	0.421
278.2	407	93.1	170.5	185	222	0.097	0.455
262.4	204**			94**	110**	0.080**	0.458**
247.3	97	88.9	181.7	49	48	0.077	0.507
292.9	753	114.3	175.7	361	392	0.195	0.479
278.6	439	112.6	179.3	218	221	0.187	0.496
263.3	225	111.5	183.5	116	109	0.182	0.516
262.4	216	110.5	182.1	110	106	0.177	0.509
292.9	769	135.7	179.4	381	388	0.294	0.497
288.2	646	134.3	179.3	320	326	0.288	0.496
283.1	529	134.3	179.3	262	267	0.282	0.496
278.6	443	135.5	181.7	225	218	0.293	0.507
283.1	534	157.4	180.1	267	267	0.395	0.500
278.6	444	158.1	183.3	229	215	0.398	0.515
292.9	781	178.6	185.0	408	373	0.493	0.523
288.2	651	179.5	184.8	340	311	0.497	0.522
283.1	532	179.9	184.7	277	255	0.499	0.521
278.6	445	179.5	184.7	232	213	0.497	0.521
292.9	779	200.6	187.7	417	362	0.595	0.535
288.2	651	199.9	188.7	352	299	0.592	0.540
283.1	532	201.1	185.6	279	253	0.597	0.525
278.6	445	201.3	185.1	235	212	0.598	0.523
262.4	213	206.3	185.2	111	102	0.621	0.523
292.9	766	227.2	198.5	448	318	0.718	0.585
288.2	639	227.2	197.2	370	269	0.718	0.579
283.1	526	222.0	195.5	300	226	0.685	0.571
278.6	438	229.6	195.7	251	187	0.729	0.572
262.4	211	230.0	189.9	115	96	0.731	0.545
292.9	727	252.6	213.4	475	252	0.836	0.654
288.2	605	251.7	210.5	388	217	0.831	0.641
283.1	501	251.6	208.4	316	185	0.831	0.631
278.6	417	252.0	206.5	259	158	0.833	0.622
262.4	202	251.5	199.0	119	83	0.831	0.587
292.9	620	277.1	251.5	515	105	0.949	0.831
288.2	515	277.0	249.2	421	94	0.949	0.820
283.1	422	276.8	246.1	340	80	0.948	0.806
278.6	352	277.4	244.4	280	72	0.950	0.798
262.4	167	277.3	236.5	127	40	0.950	0.761

* Average from three determinations.
** Interpolated.

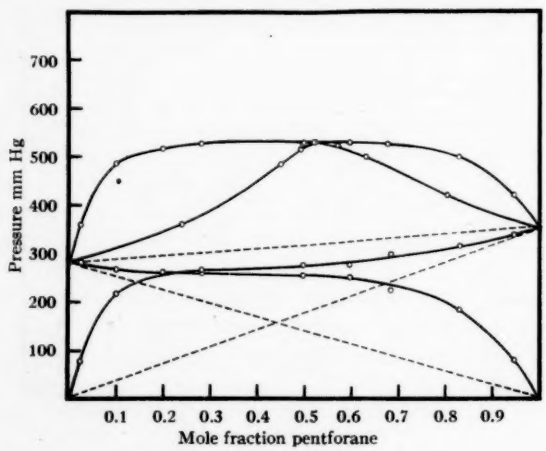

FIG. 7. $T-283.1°K$.

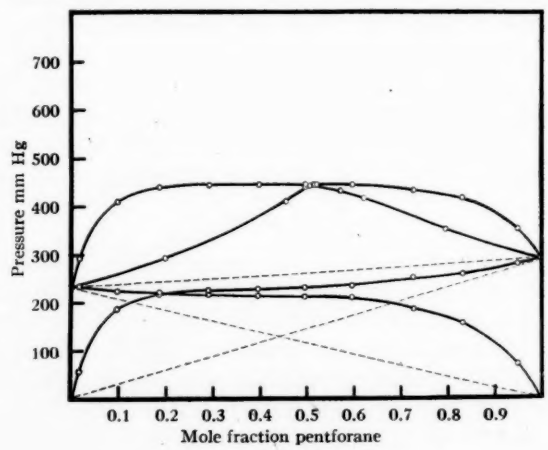

FIG. 8. $T-278.6°K$.

of the solenoid (E). G is a soft iron core sealed into the pump shaft and padded with pieces of asbestos (F). The inverted tube (L) serves two purposes; it displaces the liquid trapped under the valve (K) on the down stroke, and in doing so it acts as a shock absorber.

Procedure

A charge of 55 cm³ of approximately 40 mol percent of pentforane was placed in the above-mentioned apparatus. Two hours were allowed for equilibrium to be established. The pump was then stopped and a sample removed from each layer for analysis. The process was then repeated at other temperatures.

Results

The experimental data are tabulated in Table IV and are shown in Fig. 12. Smoothed data, taken from the graph, are given in Table V. The point obtained at 265.48°K was obtained by analyzing the homogeneous solution at 266°K, and then slowly cooling the system while agitating with the pump, until turbidity appeared. It was not possible to obtain separation into two layers above 265.2°K after agitation had ceased, and for this reason it is believed that a stable emulsion might be obtained with these substances.

The solubility of n-pentane in n-pentforane is about twice as large as the solubility of n-pentforane in n-pentane. The critical unmixing composition, calculated from the data by the law of rectilinear diameters is 37 mol percent n-pentforane.

THE CHANGE IN VOLUME ON MIXING

The densities for solutions of n-pentforane and n-pentane were measured over a 36° temperature range

TABLE II. Partial pressures of n-pentforane and n-pentane.

(a) Partial pressures of C_5F_{12} over $C_5F_{12}-C_5H_{12}$ solutions; concentration in mf of C_5F_{12}

Concentration temperature °K	0.1	0.2	0.3	0.4	0.5	0.6	0.7	0.8	0.9	1.0
292.9	298 mm Hg	363	384	396	408	419	442	466	496	565
288.2	256	308	322	332	342	353	366	383	405	466
283.1	216	256	266	271	276	282	296	312	328	380
278.6	188	218	226	228	232	238	247	256	269	315
262.4	100	110	110	110	110	111	113	116	123	149

(b) Partial pressures of C_5H_{12} over $C_5F_{12}-C_5H_{12}$ solutions; concentration in mf of C_5H_{12}

Concentration temperature °K	0.1	0.2	0.3	0.4	0.5	0.6	0.7	0.8	0.9	1.0
292.9	182	276	327	359	373	381	387	391	401	420
288.2	158	234	274	296	310	315	319	324	332	349
283.1	129	200	234	252	256	257	260	262	268	283
278.6	118	169	196	211	213	215	218	221	224	234
262.4	58	86	99	105	106	106	106	106	108	109

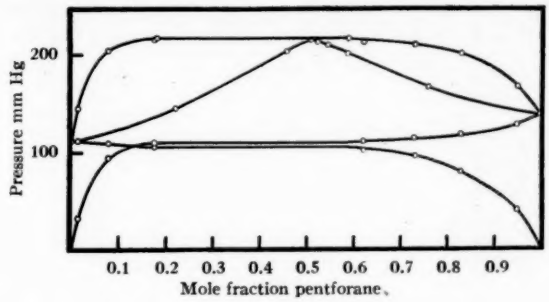

FIG. 9. $T-262.4$°K.

at nine different compositions. Equations for the total volume, V, of the solution as a function of the concentration of n-pentforane, n, were derived from the density-temperature data at two temperatures and are:

$$V_{293.16}=86.61n-21.60n^2+115.7 \quad (5)$$

and

$$V_{265.5}=75.90n-18.52n^2-110.5. \quad (6)$$

The change in volume on mixing is greater at 293.16° than at 265.5°K. The composition corresponding to maximum change for each temperature is 46.5 mol percent n-pentforane. The increases in volume on mixing at 293.16° and 265.5°K were found to be 3.5 percent and 3.2 percent respectively.

THE ANALYSIS OF MIXTURES OF n-PENTFORANE AND n-PENTANE

These determinations were accomplished by means of determination of the vapor density of the mixture. The large difference in molecular weights of the two components made this procedure a satisfactory one. A gas law $PV(1+BP)=RT$ was used for the pure vapors. By determining the vapor density of the pure vapors at different pressures, B was found to be 0.066 atm.$^{-1}$ for n-pentane and 0.041 atm.$^{-1}$ for n-pentforane. The error introduced into the molecular weight due to the uncertainty in B was 0.2 percent for the fluorocarbon and 0.4 percent for the hydrocarbon. B was found to be linear with the composition within the limits of the precision. For determination of the vapor density of the mixture the weighing bulb (J), Fig. 4, was used. This had an accurately determined volume slightly greater than 100 cm³. After filling this bulb at a noted temperature and pressure, it was removed from the system and weighed. Checked determinations were made with the sample at different pressures. The composition was then calculated from the vapor density using the above-mentioned gas law and the molecular weights for the two components of 288.0 and 72.15.

THE APPLICATION OF THE GENERAL THEORY OF SOLUBILITY OF NONPOLAR SUBSTANCES TO THIS TWO COMPONENT SYSTEM

A theory which should be applicable to this system is given by Hildebrand.[4] The so-called approximation

[4] J. H. Hildebrand, *Solubility* (Reinhold Publishing Corporation, New York, 1936), p. 66.

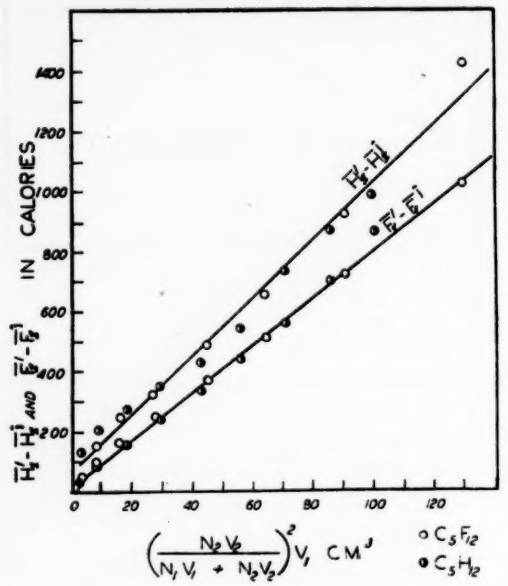

FIG. 10.

equation, relating the partial molal energy of solution to the composition and the internal pressures of the pure components has been given as:

$$\bar{E}_1-E_1^0=\left(\frac{n_2v_2}{n_1v_1+n_2v_2}\right)^2 v_1\left[\left(\frac{\Delta E_1}{v_1}\right)^{\frac{1}{2}}-\left(\frac{\Delta E_2}{v_2}\right)^{\frac{1}{2}}\right]^2. \quad (7)$$

The partial molal energy of solution may be equated to the partial molal heat of solution without serious error as the difference in these two terms is given by $P(\bar{v}-v)$. Values of $\bar{E}_1-E_1^0$, calculated from the physical properties of the pure components with the aid of the above equation, are tabulated in Table III for comparison with the partial molal heats of solution calculated from the experimental data.

In the derivation of Eq. (7), $V=n_1v_1+n_2v_2$ instead of the more exact $V=n_1\bar{v}_1+n_2\bar{v}_2$ was assumed. An equation similar to (7) may be derived in a similar manner using partial molal volumes instead of molal volumes. This is given as:

$$\bar{E}_1-\frac{v_1}{\bar{v}_1}E_1^0=\left(\frac{n_2\bar{v}_2}{n_1\bar{v}_1+n_2\bar{v}_2}\right)^2\bar{v}_1 \times\left[\left(\frac{v_1}{\bar{v}_1^2}\Delta E_1\right)^{\frac{1}{2}}-\left(\frac{v_2}{\bar{v}_2^2}\Delta E_2\right)^{\frac{1}{2}}\right]^2. \quad (8)$$

From this equation, Eq. (5), and the known physical properties of the pure components, the values for $\bar{E}_1-E_1^0$ were calculated and are tabulated in column 3 of Table III. It is readily seen from the table that while the refinement of partial molal volumes greatly improves the correlation with the experimental data, it alone is not enough, especially in the case of solutions with a large concentration of hydrocarbon.

TABLE III. The energy and volume changes which result from mixing *n*-pentforane and *n*-pentane.

(a) One mole of C_5F_{12} is added to an infinite quantity of solution

Mole fraction of C_5F_{12}	$\bar{E}_1-E_1^0$ from Eq. (7)	$\bar{E}_1-E_1^0$ from Eq. (8)	$\bar{H}_1-\bar{H}_1^i$ exp.	$\bar{F}_1-\bar{F}_1^i$ exp.	$\bar{v}_{C_5F_{12}}$ at20°C	$\left(\frac{n_2V_2}{n_1V_1+n_2V_2}\right)^2V_1$
0.1	220 cal.	940 cal.	1425 cal.	1025 cal.	194 cm³	130.0 cm³
0.2	155	650	925	725	191	90.8
0.3	110	450	655	515	187	64.5
0.4	80	265	490	370	184	45.0
0.5	45	175	320	255	182	27.4
0.6	30	65	250	165	180	16.2
0.7	15	25	150	100	179	8.4
0.8	6	0		50	178	3.5
0.9	1	0		15	177	0.8

(b) One mole of C_5H_{12} is added to an infinite qu antity of solution

Mole fraction of C_5H_{12}					$\bar{v}_{C_5H_{12}}$	
0.1	170	775	985	870	133	100.5
0.2	145	670	870	705	129	85.9
0.3	120	560	735	565	126	70.7
0.4	95	440	535	445	123	56.4
0.5	75	280	415	335	121	42.7
0.6	50	240	355	240	119	29.7
0.7	30	130	275	160	117	18.4
0.8	15	75	205	90	117	9.0
0.9	4	50	140	35	116	2.5

A regular solution has been defined by Hildebrand[5] as one in which thermal agitation is able to overcome any tendency towards molecular orientation, combinations, or association and gives the same completely random distribution as exists in ideal solutions. For solutions of this type, that is with ideal entropy of mixing, the following condition is valid:

$$\bar{E}_1-E_1^0\simeq\bar{H}_1-\bar{H}_1^i=\bar{F}_1-\bar{F}_1^i=RT\ln(a_1/n_1). \quad (9)$$

Upon substitution in Eq. (7), and differentiation with respect to n_1 and applying the conditions at the critical region of $d\ln a_1/dn_1=0$ and $d^2\ln a_1/dn_1^2=0$, Hildebrand

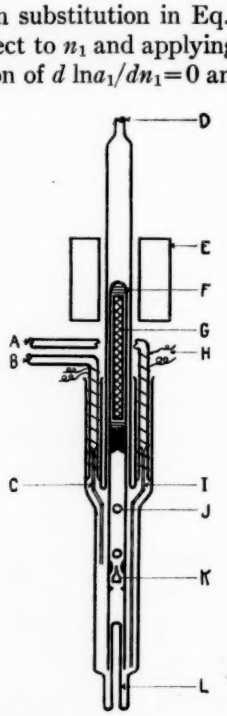

FIG. 11. Apparatus for liquid phase equilibrium.

[5] J. H. Hildebrand, J. Am. Chem. Soc. **51**, 66 (1929).

TABLE IV. Experimental data for mutual solutility of *n*-pentforane and *n*-pentane.*

Temperature °K	Pressure mm Hg	Molecular weight of sample from more dense phase	Molecular weight of sample from less dense phase	Mole fraction of C_5F_{12} in the more dense phase	Mole fraction of C_5F_{12} in the less dense phase
243.8	80	246.7	87.0	0.808	0.069
244.0	82	245.2	86.8	0.801	0.068
247.5	102	240.2	88.8	0.778	0.077
252.7	133	229.9	94.1	0.730	0.101
256.4	162	211.5	99.5	0.645	0.126
258.5	182	215.0	105.5	0.661	0.154
260.5	201	208.2	110.1	0.630	0.176
262.4	218	199.2	111.6	0.588	0.183
263.3	230	193.3	116.5	0.561	0.205
264.3	240	183.2	123.0	0.514	0.235
264.6	244	180.5	125.4	0.502	0.246
264.90	247	174.8	130.5	0.475	0.270
265.02	248	173.0	131.4	0.467	0.274
265.21	250	167.6	137.6	0.442	0.303

* 265.48 = turbidity point; composition 0.374, m.w. = 153.0.

has arrived at the following relationships for the critical unmixing temperature and composition for a binary system:

$$RT_c=\frac{2N_1N_2v_1^2v_2^2}{(N_1v_1+N_2v_2)^3}\left[\left(\frac{\Delta E_1}{v_1}\right)^{\frac{1}{2}}-\left(\frac{\Delta E_2}{v_2}\right)^{\frac{1}{2}}\right]^2 \quad (10)$$

and

$$N_1=1-N_2=\frac{(v_1^2+v_2^2-v_1v_2)^{\frac{1}{2}}-v_1}{v_2-v_1}. \quad (11)$$

When temperature is lowered to the critical unmixing temperature, the two species begin to unmix, but the temperature range in which aggregation occurs is assumed to be small, so that Eq. (10) may be applied where it is known that the statistical distribution must be other than that for a regular solution.

The difference in the square roots of the internal pressures may be calculated (a) with the aid of Eq. (7) and the slopes of the curves in Fig. 10, (b) from the critical unmixing temperature and composition and Eq. (10), and (c) from the physical properties of the pure components. The agreement among the values obtained by these different methods may be seen by inspection of Table VI. The values for ΔE were calculated from the vapor pressure equation, the Clapeyron equation, and a modified equation of state, for each of the components. The vapor pressure data used for *n*-pentane was that obtained by Messerly and Kennedy[6] and the density data for this substance was taken from the International Critical Tables.[7] The modified equations of state were obtained in this study for the analytical methods.

It is readily seen that the difference in the square roots of the internal pressures calculated from the physical properties of the pure components in the above manner is not large enough to account for the large deviation from Raoult's law. In fact, if the critical unmixing temperature is calculated from the physical properties of the pure components and Eq. (10), one would arrive at the value of 62°K as compared with the value 265.5°K determined from the experiment. The critical unmixing composition, 37 mol percent *n*-pentforane, is in excellent agreement with the value 35 mol percent, calculated from Eq. (11), and the molal volumes at 265.5°K.

[6] G. H. Messerly and R. M. Kennedy, J. Am. Chem. Soc. 62, 2988 (1940).
[7] Int. Crit. Tab., Vol. III, p. 29.

TABLE V. The mutual solubilities of *n*-pentforane and *n*-pentane.

Temperature °K	Solubility of C_5F_{12} in C_5H_{12} mole fraction	Solubility of C_5H_{12} in C_5F_{12} mole fraction
265.0	0.274	0.533
264.0	0.228	0.470
263.0	0.201	0.432
262.0	0.182	0.404
261.0	0.166	0.382
260.0	0.155	0.362
255.0	0.114	0.296
250.0	0.088	0.244
245.0	0.071	0.201

* 265.5°K = critical solution temperature at 0.37 mf C_5F_{12}.

Solutions containing fluorocarbons have been recently studied by Hildebrand and his co-workers.[8–10] The systems studied show excellent agreement with the existing solubility theory for regular solutions.

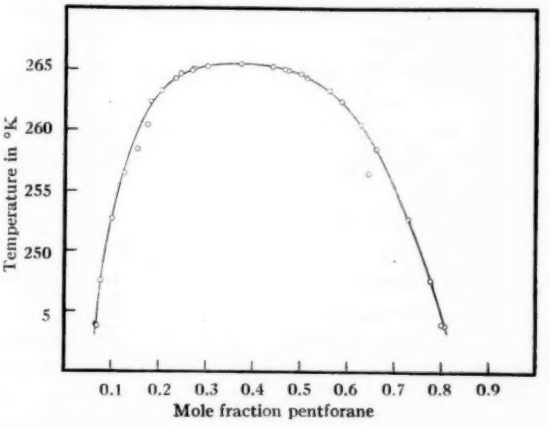

FIG. 12. Liquid phase temperature-composition diagram.

A COMPARISON OF THE PHYSICAL PROPERTIES OF *n*-PENTFORANE AND *n*-PENTANE

In view of the large deviation from Raoult's law and the inability for the existing solubility theory to correlate the observed data for the *n*-pentforane *n*-pentane system, some physical properties of these substances are compared in Table VII.

[8] H. A. Benesi and J. H. Hildebrand, J. Am. Chem. Soc. 70, 3978 (1948).
[9] R. L. Scott, J. Am. Chem. Soc. 70, 4090 (1948).
[10] J. H. Hildebrand and D. R. F. Cochran, J. Am. Chem. Soc. 71, 22 (1949).

TABLE VI. Solubility parameters for *n*-pentforane and *n*-pentane from physical properties and solubility.

Temperature °K	Vol. in cm³/mol C_5H_{12}	Vol. in cm³/mol C_5F_{12}	ΔE_v in kcal./mol C_5H_{12}	ΔE_v in kcal./mol C_5F_{12}	$(\Delta E/v)^{\frac{1}{2}}$ C_5H_{12}	$(\Delta E/v)^{\frac{1}{2}}$ C_5F_{12}	$(\Delta E_2/v_2)^{\frac{1}{2}}-(\Delta E_1/v_1)^{\frac{1}{2}}$ Phys. prop.	$(\Delta E_2/v_2)^{\frac{1}{2}}-(\Delta E_1/v_1)^{\frac{1}{2}}$ Solubility
293.2	115.3	177.8	5.83	5.97	7.11	5.80	1.31	2.89* 2.77**
265.5	110.5	168.7	6.22	6.44	7.50	6.18	1.32	2.74***

* From slope of $\bar{H}_1-\bar{H}_1^i$ *vs.* $\phi_2^2 v_1$ where ϕ is the volume fraction.
** From slope of $\bar{F}_1-\bar{F}_1^i$ *vs.* $\phi_2^2 v_1$.
*** From the critical unmixing temperature and composition and Eq. (7)

These compounds, which have a molecular weight ratio of four to one, boil at nearly the same temperature and melt at nearly the same temperature. The density temperature curve for *n*-pentforane is noticeably convex towards the temperature axis over the short range of temperature studied as compared to the very much straighter curve for *n*-pentane. If the difference in the molal volumes of these two components is plotted against the temperature, the curve would have a minimum. An interesting observation in connection with this is the change in volume when these components are mixed at different temperatures. A greater change in volume upon mixing was observed at 293.16°K than at 265.5°K. The molal volumes of these substances have a ratio of about two to three.

The values in Table VII for the differentials in the expression $(DE/dt)/(dV/dt)$ at 300°K were obtained from the vapor pressure equations and the thermal coefficients of expansion at 300°K. The electron polarizabilities were calculated from the refractive index and Clausius-Mosotti equation. The velocity of sound for C_5F_{12} was estimated from the molal sound velocity of *n*-heptforane given by R. T. Lagemann and his coworkers[11] and the bond value for C—C used was 4.25.[12] The Eyring free volume[13] was calculated from the velocity of sound in the liquid to the velocity of sound in the gas. The adiabatic compressibilities were calculated with the aid of the formula $B_{ad}=1/v^2d$, where v is the velocity of sound and d is the liquid density. This compressibility for the fluorocarbon is ninety percent larger than that for hydrocarbon.

An examination of the properties of *n*-pentforane and *n*-pentane would lead one to expect excellent agreement with the internal pressure theory for solu-

TABLE VII. Some physical properties of *n*-pentforane and *n*-pentane.

Property	*n*-Pentforane	*n*-Pentane
Molecular weight	288.0	72.15
Boiling point	302.4°K, 29.32°C[a]	309.22°K[b]
Freezing point	147.51°K	143.47°K[c]
Crystal transition	144.51°K	
Vapor pressure equation	$\log_{10}P=-2108.0/T$	$\log_{10}P=-2312.8/T-10.18859\log T$
P is in mm of Hg at 0°C and $g=980.665$	$-4.9814\log T+22.2092$	$+0.005000T+8.75\times10^{-7}(260-T)^2$
T is in °K	$\log_{10}P_{mm}=6.8838-\frac{961.19}{T}-\frac{7.5512^a}{T^2}$	$+34.18793^c$
Low pressure gas equation	$PV(1+0.041P)=RT$	$PV(1+0.066P)=RT$
Liquid density	$d_t=1.6195+a(293.16-T)$ $-b(293.16-T)^2$ $a=3.375\times10^{-3}$ $b=6.374\times10^{-6}$	$d_t=0.62624+a(293.16-T)$ $-b(293.16-T)^{2\,d}$ $a=0.9467\times10^{-3}$ $b=0.4495\times10^{-6}$
Molal volume at 20°C	177.8 cm³	115.3 cm³
ΔE_v at 300°K (uncorrected)	6080 cal.	5970 cal.
$\Delta E_v/V$ at 300°K	1390 atm.	2120 atm.
$\left(\frac{dE}{dt}\Big/\frac{dv}{dt}\right)$ at 300°K	1340	1660 atm.
Electron polarizability	10.94A³	10.00A³
Refractive index	1.245_{20}	1.35748_{20}
Dielectric constant	1.68[e]	1.83[f]
Velocity of sound in liquid at 20°C	471 meters/sec.	1052 meters/sec.[g]
Molal free volume from velocity of sound	1.45 cm³	0.75 cm³
Adiabatic compressibility calculated from velocity of sound	2.79×10^{-10} cm²/dyne	1.45×10^{-10} cm²/dyne

[a] E. J. Barber and G. H. Cady, presented at the Division of Physical and Inorganic Chemistry at the Meeting of the American Chemical Society, Portland, Oregon, September, 1948.
[b] B. J. Mair, J. Research Nat. Bur. Stand. **9**, 457 (1932).
[c] See reference 6.
[d] See reference 7.
[e] W. A. Wilson and J. H. Simons, unpublished work from the Fluorine Laboratories of The Pennsylvania State College.
[f] Internation Critical Tables VI, p. 89.
[g] See reference 12.

[11] Lagemann, Woolf, Evans, and Underwood, J. Am. Chem. Soc. **70**, 2994 (1948).
[12] R. T. Lagemann and J. E. Corry, J. Chem. Phys. **10**, 759 (1942).
[13] H. Eyring and J. Hirschfelder, J. Phys. Chem. **41**, 249 (1937).

tions of nonelectrolytes inasmuch as there are no obvious irregularities such as dipole moment, chemical interaction, etc. in their individual properties.

MODIFICATION OF THEORY TO INCLUDE CONCEPT OF INTERPENETRATION AND ITS APPLICATION TO THE SYSTEM *n*-PENTFORANE AND *n*-PENTANE

The general solubility theory may be regarded valid for any system of this type.

The general equation[14] from which Eq. (7) was derived is:

$$\bar{E}_1-E_1^0=2\pi N^2\left(\frac{n_2v_2}{n_1v_1+n_2v_2}\right)^2 v_1\left[\frac{2}{v_1v_2}\int_0^\infty e_{12}W_{12}r^2dr-\frac{1}{v_1^2}\int e_{11}W_{11}r^2dr-\frac{1}{v_2^2}\int_0^\infty e_{22}W_{22}r^2dr\right]. \quad (12)$$

N is the number of molecules in a mol; n and v represent the number of mols and molal volumes of components 1 and 2 respectively; W is a probability function used in counting the number of molecules around a central molecule at distance r; and e, which is a function of r, represents the interaction potential between pairs. In the derivation of Eq. (7) from Eq. (12) it will be recalled that Hildebrand neglected the repulsive potential and assumed a London type attractive potential between pairs. It was also assumed that the interaction constant for unlike molecules was a geometric mean of the constants for like molecules. The complete interaction potential for a pair of molecules may be represented by a bireciprocal equation of the following type:

$$e=j/r^m-k/r^6, \quad (13)$$

where the (j) term represents the repulsive potential and the (k) term represents the attractive potential. (r) is the distance between the pairs, and (m) is a number in the order of magnitude of twelve. When (r) is large, the first term is small and (e) is negative; but as (r) becomes smaller, the repulsive term becomes larger and the potential becomes positive and increases very rapidly. For this reason, (k) may be evaluated by assuming some value for the distance of closest approach of a pair of molecules and the potential function given by Eq. (14). In order, then, to evaluate k_{11}, k_{22}, and k_{12}, suitable values for the distance of closest approach must be selected for the various pairs involved.

The van der Waals' size for an atom is defined as one-half the internuclear distance of two adjacent atoms of the same element, when these atoms are attached to different molecules and in such a position that their attractive forces are balanced by their repulsive forces. This equilibrium distance is a function of the kinetic energy of the molecules and correspondingly a function of the temperature; and it may be measured by gas viscosity, surface films, crystal structure, scattering, etc. Each method gives a number which has significance only when the method of determination is also given.

As a convenient point of reference, the distance of closest approach of the centers of two carbon atoms, which are located in adjacent molecules, will be considered suitable for this work. The distance between the carbon center and some peripheral nucleus to which it is attached would be expected to be approximately the same for molecules in the liquid, gaseous, or crystalline state, and over a considerable range of temperature. The distance between carbon atoms on adjacent molecules would depend on the thermal motions of the molecules and the size and nature of the force field characteristic of the peripheral atoms. If we consider the peripheral atoms to have a definite size and add the radii of the peripheral atoms on adjacent molecules to the above-mentioned nuclear distance, an estimate of the value of the distances of closest approach of the carbon atoms on the adjacent molecules can be obtained. We shall call this the superior limit of approach of the molecules. A van der Waals' radius of 1.29A will be used for the hydrogen atom as has been assigned by Mack[15] to satisfy the requirements of hydrocarbon crystals at room temperature. A similar assignment for the fluorine atom has not yet been reported. Pauling[16] has shown in the case of chlorine that the ionic radius is essentially equal to half the distance between chlorine atoms attached to carbon atoms of adjacent molecules in the crystal. By analogy, he assigned a value to the radius to the fluorine atom the value measured for the fluorine ion in the sodium fluoride crystal. As the value so obtained is not unreasonable, it will be herein employed. Another value for the effective radius of the fluorine atom can be obtained by extrapolating the apparent molecular volume to absolute zero of temperature. The value so obtained is in good agreement with the value obtained from the measurements of the sodium fluoride crystal.

The distance of closest approach between two molecules calculated in this value is made on the assumption that the peripheral atoms always approach those on neighboring molecules along the line of centers of the carbon atoms and also that these peripheral atoms are highly resistant to compression. For this reason, this distance so calculated is probably the largest distance of closest approach "superior limit." It is conceivable that the peripheral atoms on adjacent molecules may approach in other directions than that in the line of centers of the carbon atoms or that there be some give to the structure, so that a slight change of angle or slight compression of the structures may allow for a closer approach. We shall designate this shortening of

[14] Reference 4, p. 71.

[15] E. Mack, Jr., J. Am. Chem. Soc. **54**, 2141 (1932).

[16] L. Pauling, *The Nature of the Chemical Bond* (Cornell University Press, Ithaca, New York, 1942), p. 188.

the distance of closest approach as interpenetration. As the hydrogen atoms forming the sheath of the carbon skeleton on the hydrocarbon can be considered smaller or more flexible than the fluorine atoms forming the sheath of the carbon skeleton of the fluorocarbons, one might expect a much greater interpenetration of the hydrocarbons than of the fluorocarbons. This idea is consistent with the difference in properties of the fluorocarbons and hydrocarbons. The lower surface tensions of the fluorocarbons than the hydrocarbons and the much greater resistance to chemical attack are consistent with the idea. As a crude mechanism picture, we may visualize a molecule in a two-dimensional domain as a toothed gear wheel. The teeth may be broad or narrow, tall or short, and the wheels may move with a variety of speeds. We must consider the radius to the outside of the teeth as the superior limit of the molecule. In case the gears do not mesh, the sum of the superior radii for the two wheels in the distance of approach of the centers. They may not mesh for several reasons. The teeth on adjacent wheels may be of different sizes, or the speed of rotation is so greatly different that meshing is impossible. Very little meshing also occurs if the teeth are very shallow. Applying this mechanical picture to our binary system, we visualize less meshing or interpenetration between the fluorocarbon molecules, because the fluorine atoms form a relative coherent sheath over the carbon skeleton, and the teeth are very shallow. There is an appreciable intermeshing in the case of two hydrocarbon molecules. Between the fluorocarbon molecule and a hydrocarbon molecule there is very little interpenetration, either because the rate of motion due to their difference in mass is greatly different or because there are no effective teeth on the fluorocarbon wheel. There may be some interpenetration between fluorocarbon molecules, although the present study is unable to evaluate it. A study of a binary system of a fluorocarbon with one of the monatomic inert gases would be of assistance in this evaluation. For the purposes of the present work, it is sufficient to assume essentially zero penetration between fluorocarbons and fluorocarbons and between fluorocarbons and hydrocarbons.

If the potential energy of the system is considered to be zero when the molecules are separated an infinite distance, the potential energy for one mol of liquid may be set equal to the energy of vaporization; and an equation suited to the calculation of the attraction constant between pairs is given by:

$$\Delta E_v = -\frac{2\pi N^2}{v}\int_{r=r_0}^{\infty} -(k/r^4)dr. \qquad (14)$$

A similar term may be written for each type of pair, and these may be substituted into Eq. (12) with the suitable values for the r_0's and k's for the different kinds of pairs. The values for r_0 which were chosen for this problem are:

r_0 for CFFC $= 2(\text{C}-\text{F})+2F_v$
$= 2(1.35)+2(1.35) = 5.40\text{A}$

r_0 for CFHC $= (\text{C}-\text{F})+F_v+(\text{C}-\text{H})+H_v$
$= 2.70+2.38 = 5.08\text{A}$

r_0 for CHHC $= 2(\text{C}-\text{H})+2H_v-d = 4.76-d.$

The symbols CFFC, CFHC, and CHHC represent fluorocarbon-fluorocarbon, fluorocarbon-hydrocarbon, and hydrocarbon-hydrocarbon pairs respectively. C−H and C−F represent the internuclear distance of the carbon to hydrogen and carbon to fluorine atoms respectively, and the F_v and the H_v are the superior limits for the van der Waals' radii. The interpenetration factor "d" for hydrocarbons may be calculated from the measured heats of solution with the aid of Eqs. (12) and (14). The following assumptions are used: (1) there is zero interpenetration of the force fields of a fluorocarbon and a hydrocarbon molecule, and zero interpenetration beyond the assigned limits of the force fields of two fluorocarbon molecules; (2) the attraction constant k, for unlike pairs is the geometric mean of the constants for like pairs; (3) the different molecular species were assumed to have the same general type of arrangement in the solution as in the pure components.

The interpenetration factor "d" for n-pentane was found to be 0.24A. This is purely a relative value based upon the above assumptions. The value "d" should be about the same for all normal hydrocarbons in similar systems, but this awaits further investigation. This factor, "d" may be different for cyclic compounds and aromatic derivatives, and thus solubility studies of this type may provide a way for obtaining evidence to support assumed structures.

The assigned superior limits for the sizes of these molecules and the interpenetration factor "d" for hydrocarbons derived from them receive added support from the relation between Eyring free volume and the velocity of sound in the liquid.[17] If (s) is the incompressible diameter of a molecule, (V) the total volume per molecule, and cubic packing is assumed, the free volume is given by:

$$v_F = 8(V^{\frac{1}{3}}-s)^3. \qquad (15)$$

If infinite velocity is assumed for a sound wave traveling through the molecules, then the rate determining factor for the velocity of sound through a liquid is the amount of free space between the molecules in the liquid. The velocity of sound in a liquid then gives us a reliable estimate of the distance $2V^{\frac{1}{3}}-2s$ that a central atom is free to move along each axis in its cell. The free volume per mol is then given by:

$$V_F = Nv_F = 8N(V^{\frac{1}{3}}-s)^3. \qquad (16)$$

[17] Glasstone, Laidler, and Eyring, *Theory of Rate* (McGraw-Hill Book Company, Inc., New York, 1941), p. 480.

A superior limit for the volume of a single molecule may be estimated from the upper limits of the van der Waals' dimensions and the internuclear distances. The distances between the carbon atoms in the fluorocarbon were assumed to be the same as that measured by electron diffraction in ethforane,[18] 1.45A. The distances between carbons in the hydrocarbons were taken as 1.54A.[19] In order to estimate the upper limit to their size, rod shaped molecules were assumed with a length equal to the length of the zig-zag chain with its end atoms and their van der Waals' radii included. The radius was assumed to be equal to the distance between the carbon and the peripheral atom plus the latter van der Waals' radius. The value (s) was then taken as the cube root of this superiority limit for the volume of a single molecule.

The free volumes calculated from Eq. (16) are 1.2 cm^3 and 0.075 cm^3 for n-pentforane and n-pentane respectively. The corresponding values calculated from the velocity of sound, as listed in Table VII, are 1.45 and 0.75 cm^3 respectively. In the case of the hydrocarbon, the values calculated by these two methods differ by a factor of ten. The difference may be reconciled by assuming an interpenetration of the hydrocarbon molecules resulting in a larger free volume. The interpenetration per molecule which must be assumed in order to obtain agreement between the two methods is 0.14A. This may be compared with the value obtained from solubility, that is $d/2=0.12$A.

The Entropy Change on Mixing

n-Pentforane and n-pentane do not form a regular solution. The quantity $T(\bar{S}_1-\bar{S}_1^i)$ may be calculated from the data in Table III and the thermodynamic relationship:

$$\bar{F}_1-\bar{F}_1^i=\bar{H}_1-\bar{H}_1^i-T(\bar{S}_1-\bar{S}_1^i). \qquad (17)$$

The change in entropy during mixing of nonpolar substances is usually greater than that for an ideal solution over the entire range of composition.[20,21] When two such substances are mixed, the entropy change in addition to that obtained in ideal mixing must be accompanied by an increase in randomness caused by destruction of some or all of the order existing in the pure components, and a decrease in randomness due to any new orientation of the components in the solution. The difference between the partial molal entropy of mixing and that for an ideal solution is greater for the fluorocarbon when dissolved in a concentrated solution of hydrocarbon, than for the hydrocarbon when dissolved in a concentrated solution of fluorocarbon. This is contrary to what one might expect on a free volume basis. The fluorocarbon has the larger free volume into which the hydrocarbon may be dispersed, and thus the hydrocarbon should have a larger partial molal entropy change on mixing than the fluorocarbon. The entropy of mixing, however, not only depends on volume, but upon the order-disorder relationships of the molecules in the liquid. If there were no order in each of the pure components, and no order in the solution, then the entropy of mixing would be ideal. It appears that the hydrocarbon has a greater order or liquid structure than the fluorocarbon, and that what structure does exist in the fluorocarbon is more completely destroyed in the presence of the stronger structure-preserving orientational forces of the hydrocarbon than is that of the hydrocarbon in the presence of a large concentration of fluorocarbon. This is consistent with the concept of interpenetration between molecules of hydrocarbons.

There is still another interesting observation which may be made in connection with the entropy of mixing of these components. The vertical distance between the two curves in Fig. 10 represents the quantity of heat which must be subtracted from the heat of solution to give the free energy of solution. This quantity, when divided by the temperature is the difference between the entropy of mixing and the ideal entropy of mixing at the concentration represented on the abscissa. Apparently, then, the partial molal entropy of mixing is the same for each component when

$$\left(\frac{n_2v_2}{n_1v_1+n_2v_2}\right)^2 v_1$$

has the same value for each component. This matter, however, needs further study on carefully selected species.

SUMMARY

The properties of n-pentforane and its solutions with n-pentane have been investigated. The binary system was found to have a large positive deviation from Raoult's law which could not be accounted for by the difference in internal pressures of the pure components. A method of correlating some properties of these solutions with their physical properties has been suggested. The difference in potential energy resulting from the removal of a molecule from its pure liquid and transferring it to an infinite quantity of its solution has been equated to the partial molal heat of solution. The change in potential may be calculated by assuming the same general type of arrangement in the solution as in the pure components, and that the attraction constant for unlike molecules is a geometric mean of the constant for like molecules.

In order to evaluate these constants in the interaction potential, suitable limits for the distances of closest approach of unlike and like pairs, and no interpenetra-

[18] Brockway, Secrist, and Lucht, Abstracts, Buffalo Meeting of the American Chemical Society, September 1942.
[19] Reference 13, p. 161.
[20] S. E. Wood, J. Chem. Phys. **15**, 358 (1947).
[21] J. R. Lacher, J. Am. Chem. Soc. **63**, 2422 (1949).

tion of unlike pairs was introduced. Assuming no interpenetration for the fluorocarbon pairs, and no interpenetration for the fluorocarbon-hydrocarbon pairs, an interpenetration factor, "*d*" was calculated for *n*-pentane. The value for "*d*" should be essentially the same for all normal hydrocarbons in similar fluorocarbon solutions, however, this awaits further experimental investigation.

ACKNOWLEDGMENT

The authors wish to thank Professor J. G. Aston for the loan of the Cryogenic Laboratory Standard Thermocouple #S-5 for use in calibrating the thermocouples used in this research. They wish to thank The Minnesota Mining and Manufacturing Company for sponsoring the program under which this work has been carried out.

THE JOURNAL OF CHEMICAL PHYSICS VOLUME 18, NUMBER 3 MARCH, 1950

Substituted Methanes. I. Raman and Infra-Red Spectral Data, Assignments, and Force Constants for Some Tribromomethanes*

ARNOLD G. MEISTER, SHIRLEY E. ROSSER,†‡ AND FORREST F. CLEVELAND
Spectroscopy Laboratory, Department of Physics, Illinois Institute of Technology, Chicago, Illinois

(Received August 17, 1949)

As a part of a systematic investigation of the vibrational spectra of substituted methanes and ethanes, Raman displacements, semiquantitative relative intensities, quantitative depolarization factors, and infra-red absorption frequencies in the region 700–5000 cm^{-1} have been obtained for CBr_2H, CBr_3Cl, and CBr_4. Details about the design of the infra-red spectrograph are given. The Raman and infra-red spectral data in the literature for CBr_3H, CBr_3D, CBr_3F, CBr_3Cl, and CBr_4 have been collected, tabulated, and critically examined in comparison with the present results and a decision was made as to the probable values of the Raman and infra-red data at the present time. Assignments of the observed Raman and infra-red bands, consistent with the selection rules, were made for all of the molecules. Finally, force constants were calculated for the five molecules, using a potential energy function containing all possible second degree terms.

INTRODUCTION

SUBSTITUTED methanes and ethanes in which the substituents are single atoms—not radicals—are being systematically investigated in this laboratory. It is hoped that Raman displacements, relative intensities, quantitative depolarization factors, infra-red absorption spectra in the region 400–5000 cm^{-1}, force constants, and thermodynamic properties may eventually be obtained for all such molecules for which the present information is incomplete and for which samples can be obtained. The present paper presents results obtained in an investigation of a series of methanes of the type CBr_3X.

EXPERIMENTAL DETAILS

The Raman displacements were obtained partly with a Hilger E-518 spectrograph having a dispersion of 307 cm^{-1}/mm (63A/mm) at 4500A, and partly with a two-prism spectrograph constructed in this laboratory which has a dispersion of 162 cm^{-1}/mm (33A/mm) at 4500A. The spectrograms were obtained on Eastman 103-J plates with Hg 4358A as the exciting line, using the experimental arrangement and technique previously described.[1]

The relative intensities were obtained with the aid of a Gaertner microdensitometer[2] by the formerly used method.[1,3] The relative intensities are only semiquantitative since no correction was made for variation in the sensitivity of the plates with wave length and since calibration marks were not placed upon each spectrogram but only upon a master calibration plate with the same type of emulsion.

The depolarization factors were obtained by a well-tested, quantitative method.[4] The two exposures corresponding to the vertical and horizontal components of the electric vector were obtained simultaneously, calibration marks were placed upon each spectrogram, and separate calibration curves were prepared for each Raman line; corrections were made for failure of the reciprocity law, for real or apparent polarization produced by the spectrograph or other optical parts in the path of the scattered beam, and for convergence errors.

The infra-red absorption spectra were obtained with a self-recording infra-red spectrometer constructed in this laboratory. The arrangement of the optical parts and the radiation path in this spectrometer are shown in Fig. 1. The source N is a Nernst glower. The mirrors

* Presented at the Chicago meeting of the American Physical Society, November, 1948, papers C1 and C2; abstract in Phys. Rev. **75**, 333 (1949).

† The experimental portion of this paper gives results obtained in an investigation carried out at the Illinois Institute of Technology by Mr. Shirley E. Rosser in partial fulfillment of the requirements for the degree of Master of Science at the University of Virginia.

‡ Present address: Department of Physics, Lynchburg College, Lynchburg, Virginia.

[1] Forrest F. Cleveland, J. Chem. Phys. **11**, 1 (1943).

[2] S. Jacobsohn and W. H. Kliever, J. Opt. Soc. Am. **25**, 244 (1935).

[3] Forrest F. Cleveland, J. Chem. Phys. **11**, 227 (1943); Year Book of the American Philosophical Society (1942), pp. 104–105.

[4] Forrest F. Cleveland, J. Chem. Phys. **13**, 101 (1945).

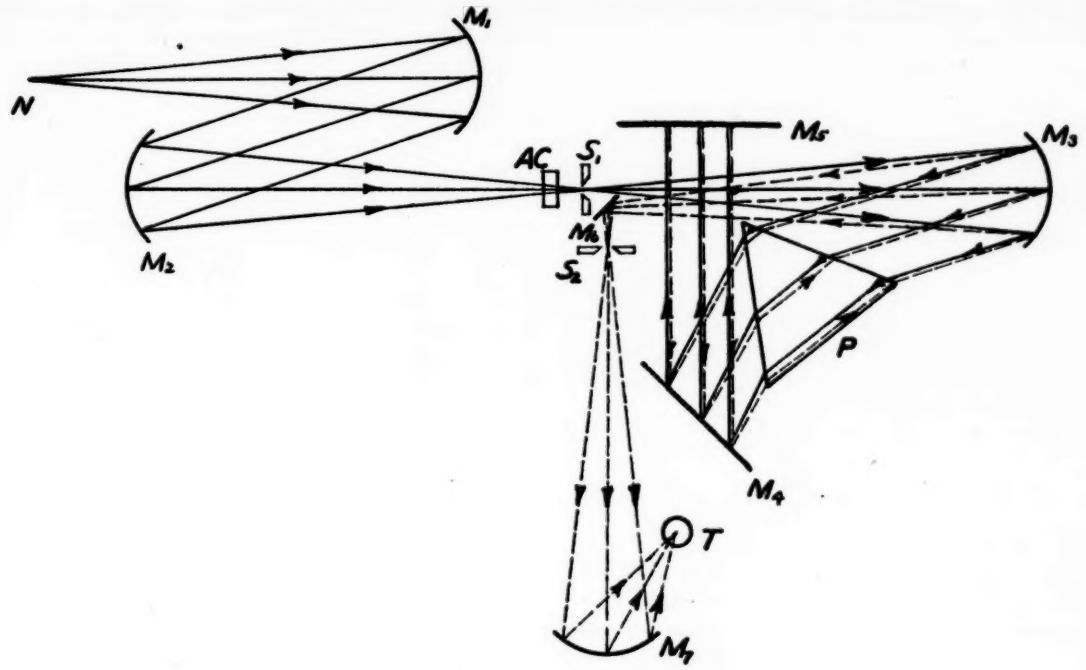

FIG. 1. Arrangement of the optical parts in the infra-red spectrometer.

M_1, M_2, and M_7 are spherical and are all 5 cm in diameter; for M_1 and M_2, the focal lengths were 30 cm, while for M_7 it was 10 cm. AC is the absorption cell and the entrance and exit slits S_1 and S_2 are Gaertner L162b bilateral slits. The collimating mirror M_3 is parabolic, 10° off-axis, and has a focal length of 30 cm and a diameter of 5 cm. M_4, M_5, and M_6 are plane mirrors and the prism P is of rocksalt with 6 cm base and 4 cm height; it can be replaced by a similar KBr prism. The thermocouple T is a compensated Weyrich thermocouple obtained from the Department of Physics of the University of Michigan through the courtesy of Professors H. M. Randall and E. F. Barker.

The slit-width varied from 0.30 mm near 3000 cm^{-1} to 3.00 mm in the 700–1000 cm^{-1} region. Since no amplification was used, the resolving power was not very good; it of course varies for different regions of the spectrum and depends upon the slit-width and the intensity of the bands, so that it is not possible to give a single value for all conditions; the most closely spaced bands that were resolved in the present investigation were 26 cm^{-1} apart (at 925 cm^{-1}), but no attempt was made to find whether this was the limit for resolution.

RAMAN AND INFRA-RED SPECTRAL DATA

For use in the force constant calculations to be discussed in a subsequent section, and in thermodynamic calculations to be discussed in a later paper, it was desired to have the best possible values of the Raman and infra-red spectral data. Consequently, all of the compounds for which samples could be obtained (CBr_3H, CBr_3Cl, and CBr_4) were reinvestigated. In addition, the previous data in the literature were collected, tabulated, and critically examined in comparison with the present results and finally a decision was made as to the probable values of the Raman and infra-red data.

Tribromomethane (Bromoform, CBr_3H)

The sample of tribromomethane was kindly furnished by the Dow Chemical Company, Midland, Michigan; it was originally of the "technical" grade, but was carefully purified by use of a distilling column. The spectrograms were obtained with the sample in the liquid state at approximately 30°C. The exposure time on the plate giving the best lines for depolarization measurements was 7 hr. at a slit-width of 0.09 mm. On this plate all previously reported lines were obtained, except for the one at 1439 cm^{-1} which has never been obtained with sufficient intensity to permit depolarization measurements, even qualitative ones. In fact, this line could not be obtained in the present investigation even on frequency spectrograms with very long exposures.

Raman spectral data have been obtained in ten previous investigations[5–14] and infra-red data have been

[5] A. S. Ganesan and S. Venkateswaran, Ind. J. Phys. **4**, 195 (1929).
[6] S. Bhagavantam and S. Venkateswaran, Proc. Roy. Soc. London **A127**, 360 (1930).
[7] S. Bhagavantam, Ind. J. Phys. **5**, 35 (1930).
[8] See reference 7, p. 59.
[9] S. Venkateswaran, Phil. Mag. **15**, 263 (1933).
[10] J. Cabannes and A. Rousset, Ann. de physique **19**, 229 (1933).
[11] J. T. Dahr, Ind. J. Phys. **9**, 189 (1934).
[12] O. Redlich and W. Stricks, Sitz. Akad. Wiss. Wien IIb, **145**, 192 (1936).
[13] A. A. Sidorova, Acta Physicochimica **7**, 193 (1937).
[14] V. Tatevsku, J. Phys. Chem. U.S.S.R. **20**, 129 (1946).

TABLE I. Raman and infra-red spectral data for liquid tribromomethane (CBr_3H), including calculated frequencies and assignments.*

Raman										Infra-red						Theoretical		
		$\Delta\nu$		I			ρ			ν	I		ν		I			
PR	N	PV	AD	PR	V	B	CR	PR	PS	PR	PR	N	PV	AD		ν_c	Assignment	Type
												1	128	—	—	*116*	$\nu_5-\nu_2$	E
155	10	154.3	0.5	45	0.8	0.78	0.77	0.85	D							**153.8**	ν_6	E
222	10	222.5	0.5	100	0.2	0.22	0.11	0.45	P			2	219.0	2.0	—	**222.5**	ν_3	A_1
												1	250	—	—	*(231)*	$(\nu_2-2\nu_6)$	A_1+E
												1	308	—	—	*308*	$2\nu_6$	A_1+E
												1	379	—	—	*376*	$\nu_3+\nu_6$	E
												2	390.0	2.0	—	*385*	$\nu_2-\nu_6$	E
												2	431.5	1.5	—	*433*	$\nu_5-\nu_3$	E
540	10	539.3	0.9	35	0.1	0.13	0.06	0.18	P			3	538.0	1.3	—	**540.4**	ν_2	A_1
655	10	655.5	1.0	15	0.7	0.5	0.53	0.72	D	(674)	w	3(4)	661.0	1.3	—	**652.3**	ν_5	E
										774	s	2	773.5	0.5	s	*761*	$\nu_2+\nu_3$	A_1
												1	797	—	—	*809*	$\nu_5+\nu_6$	A_1+A_2+E
										875	m	2(3)	872.5	2.5	m	*877*	$\nu_3+\nu_5$	E
												1	(969)	—	—	*990*	$\nu_4-\nu_6$	A_1+A_2+E
1143	7	1144.3	1.7	15	0.7	0.5	6/7	0.54	D	1143	vs	3(5)	1143.1	0.6	vs	**1147.2**	ν_4	E
										1309	m	2	1298.5	10.5	m	*1298*	$\nu_4+\nu_6$	A_1+A_2+E
—	4	(1439.0)	3.0	vw												*1416*	$\nu_2+\nu_3+\nu_5$	E
												1	2283	—	—	*2288*	$2\nu_4$	A_1+E
3017	8	3020.9	1.6	60	0.3	0.22	0.24	0.64	P	3004	vs	5	3010.4	12.7	vs	**3022.5**	ν_1	A_1
												1	4142.0	—	50	*4165*	$\nu_1+\nu_4$	E
												1	4326.0	—	52	*4319*	$\nu_1+\nu_4+\nu_6$	A_1+A_2+E
												1	4453.4	—	23	*4437*	$\nu_1+\nu_2+\nu_3+\nu_5$	E
												2	4463.9	0.1	22	*4473*	$\nu_1+\nu_4+2\nu_6$	A_1+A_2+2E
												1	4492.8	—	32	*4485*	$\nu_1+2\nu_5+\nu_6$	A_1+A_2+2E
												1	4680.1	—	26	*4704*	$\nu_1+\nu_2+\nu_4$	E
												3	4820.2	14.4	44	*4820*	$\nu_1+\nu_4+\nu_5$	A_1+A_2+E
												1	5240.4	—	77	*5243*	$\nu_1+2\nu_2+\nu_4$	E
												3	5314.9	40.8	66	*5309*	$\nu_1+2\nu_4$	A_1+E
												1	5775.0	—	45	*5820*	$2\nu_1-\nu_3$	A_1
												4	5950.6	37.4	81	*6042*	$2\nu_1$	A_1
												1	6128.9	—	6	*6196*	$2\nu_1+\nu_6$	E
												1	6334.3	—	20	*6264*	$2\nu_1+\nu_3$	A_1
												1	6442.0	—	17	*6486*	$2\nu_1+2\nu_3$	A_1
												2	6537.3	22.2	21	*6581*	$2\nu_1+\nu_2$	A_1
												3	6810.0	66.0	11	*6697*	$2\nu_1+\nu_5$	E
												3	7067.0	50.6	74	*7186*	$2\nu_1+\nu_4$	E
												1	7752	—	—	*7725*	$2\nu_1+\nu_2+\nu_4$	E
												2	8224.3	108.8	7	*8330*	$2\nu_1+2\nu_4$	A_1+E
												3	8688.3	10.2	51	*8687*	$3\nu_1-\nu_3-\nu_6$	E
												1	9524	—	—	*9507*	$3\nu_1+2\nu_3$	A_1
												4	9781.5	46.5	16	*9718*	$3\nu_1+\nu_5$	E
												1	9901	—	—	*9940*	$3\nu_1+\nu_3+\nu_5$	E
												1	10101	—	—	*10141*	$3\nu_1+2\nu_2$	A_1
												1	10417	—	—	*10373*	$3\nu_1+2\nu_5$	A_1+E
												2	11111	0.0	—	*11084*	$3\nu_1+\nu_3+\nu_4+\nu_6$	A_1+A_2+E
												3	11282.7	31.1	—	*11351*	$3\nu_1+2\nu_4$	A_1+E
												1	12453	—	—	*12460*	$4\nu_1+\nu_3+\nu_6$	E

* $\Delta\nu$ is the Raman displacement in cm^{-1}, I is the relative intensity, ρ is the depolarization factor of the Raman line, ν is the infra-red absorption frequency in cm^{-1}, ν_c is the calculated frequency in cm^{-1}; PR = present results, N = number of times the band has been observed in independent investigations, PV = the probable value of the Raman displacement or infra-red frequency, AD = the average deviation of the individual values from the mean, V = Venkateswaran (see reference 9), B = Bhagavantam (see reference 8), CR = Cabannes and Rousset (see reference 10), PS = the polarization state (depolarized D, polarized P); uncertain frequencies are enclosed in parentheses; under the infra-red intensities, w = weak, m = medium, s = strong, vs = very strong, and the numbers give percent absorption.

obtained in thirteen previous investigations.[15–27] The present results and the previous data are summarized and compared in Table I. The Raman displacements are given at the left and the fifth column gives the relative intensities of the Raman lines; the values listed are those obtained in the present investigation, the previously obtained values being only visual estimates. The depolarization factors obtained in four independent investigations are given in columns six to nine. It was thought best not to take a mean of these values, since the reliability of the experimental methods used in determining depolarization factors varies so widely, but rather to list the individual values side by side for comparison, and finally—as has been done in column ten—to decide from the polarization data which lines are depolarized (D) and which are polarized (P). Only four investigators[6–8, 13] have observed the very weak Raman line at 1439 cm^{-1}; this line failed to show on the spectrograms in the present study even after very prolonged exposures. It thus seems quite probable that this line may have been due to an impurity. Sidorova,[13] one of the four, also reported Raman lines for the liquid at 580, 695, and 1292 cm^{-1} with intensities of 30, 30, and 10 (on a basis of 100 for the strongest Raman line); since these three lines were not observed in any of the other nine investigations, it seems certain that they must have been due to impurities. Sidorova[13] also reported the following $\Delta\nu(I)$ values for the solid state: 42(5), 156(8), 220(10), 538(9), 654(7), 696(1), 1145(5), 1294(1), 1448(0), and 3020(6). These solid state data also include the four Raman displacements attributed above to impurities in the liquid sample.

[15] J. W. Ellis, Phys. Rev. **23**, 48 (1924).
[16] Easley, Fenner, and Spence, Astrophys. J. **67**, 185 (1928).
[17] J. Lecomte, Comptes Rendus **196**, 1011 (1933).
[18] B. Timm and R. Mecke, Zeits. f. Physik **98**, 363 (1935).
[19] E. Trabert and K. Schaum, Zeits. f. wiss. Phot. **35**, 153 (1936).
[20] A. Maione, Nuovo Cimento **14**, 361 (1937).
[21] G. Emschwiller and J. Lecomte, J. de phys. et rad. **8**, 130 (1937).
[22] Yeou Ta, Comptes Rendus **206**, 1371 (1938).
[23] A. Carrelli and P. Tulipano, Nuovo Cimento **15**, 1 (1938).
[24] P. Barchewitz and M. Parodi, J. de phys. et rad. **10**, 143 (1939).
[25] W. Gordy, J. Chem. Phys. **7**, 163 (1939).
[26] G. L. Jenkins and J. W. Straley, Phys. Rev. **68**, 99 (1945).
[27] E. K. Plyler, J. Chem. Phys. **16**, 1008 (1948).

TABLE II. Raman spectral data, calculated frequencies, and assignments for liquid deuterotribromomethane (CBr_3D).*

Observed $\Delta\nu$	I_e	Calculated ν_c	Assignment	Type
153.4	8	**153.4**	ν_6	E
221.6	10	**221.4**	ν_3	A_1
519.3	7	**517.6**	ν_2	A_1
628.5	5b	**631.8**	ν_5	E
840	3b	**844.6**	ν_4	E
856.5	3	*850*	$\nu_3+\nu_5$	E
2247	4b	**2247.6**	ν_1	A_1

* I_e = visually estimated relative intensity, b = broad; other symbols have the same meaning as in Table I.

TABLE III. Raman spectral data, calculated frequencies, and assignments for liquid fluorotribromomethane (CBr_3F).

Observed $\Delta\nu$	I_e	ρ	Calculated ν_c	Assignment	Type
150	14	6/7*	**150**	ν_6	E
218	20	0.1	**218**	ν_3	A_1
306	3.3	6/7*	**306**	ν_5	E
398	10	0.04	**398**	ν_2	A_1
743	m	6/7*	**743**	ν_4	E
1069	w	0.42	**1069**	ν_1	A_1

* Given as 6/7 in a later paper, M. L. Delwaulle and F. Francois, J. de physique **7**, 15 (1946).

The infra-red data are given in the central part of Table I. For the 661-cm^{-1} frequency, the band has been observed four times, but one of the values seemed unreliable and hence was not included in the mean value; likewise, one of the values for the 872.5-cm^{-1} band and two of the values for the 1143.1-cm^{-1} band seemed to differ from the other values by an amount greater than the expected experimental error, and were excluded in taking the mean. In general, the infra-red spectra have not been studied as frequently as the Raman spectra and the average deviations for the infra-red are greater than for the Raman, especially for the higher frequencies.

Jenkins and Straley[26] obtained infra-red frequencies for two of the bands for both the liquid and gaseous states; for the liquid they obtained 1142.4 and 3012.0 cm^{-1} and for the gaseous state they obtained 1147.7 and 3049.2 cm^{-1}.

Deuterotribromomethane (CBr_3D)

No infra-red data were found for deuterotribromomethane and Raman data have been reported only by Redlich and Stricks.[12] The values obtained by them are compared with the present calculated values in Table II. No depolarization factors were found for this molecule.

Fluorotribromomethane (CBr_3F)

Likewise, no infra-red data were found for fluorotribromomethane and Raman data have been reported only by Delwaulle and Francois.[28] Their values, the present calculated values, and the assignments are given in Table III.

Chlorotribromomethane (CBr_3Cl)

The sample of chlorotribromomethane also was furnished by the Dow Chemical Company. Since it was a solid at room temperature, the spectrograms were obtained with benzene and CCl_4 solutions; both solutions upon exposure to the light from the arcs developed a deep brown coloration, presumably due to the liberation of bromine; to keep them colorless during the exposure five percent by volume of *n*-amylene was added.

Previous spectral data have been reported in two[29,30] Raman and in one[29] infra-red investigations. The

TABLE IV. Raman and infra-red spectral data for chlorotribromomethane (CBr_3Cl, liquid or solution), including calculated frequencies and assignments.*

Raman								Infra-red			Theoretical		
		$\Delta\nu$		I		ρ		ν	I_e	ν			
PR	N	PV	AD	PR	DF	PR	PS	PR	PR	LVT	ν_c	Assignment	Type
141	3	140.3	0.9	70	7**	0.83	D				**140.3**	ν_6	E
210	3	211.3	1.8	100	0.5	0.64	P				**211.5**	ν_3	A_1
											211.3	ν_5	E
269	3	268.3	1.6	3	—	—					*281*	$2\nu_6$	A_1+E
326	3	326.7	0.9	100	0.05	0.35	P				**326.7**	ν_2	A_1
677	3	677.0	2.0	35	0.7	0.93	D			667	**677.0**	ν_4	E
748	2(3)	745.0	3.0	5	0.7	—				740	**744.9**	ν_1	A_1
								887	m		*888* or *885*	$\nu_3+\nu_4$ or $\nu_4+\nu_5$ or $\nu_1+\nu_6$	E or A_1+A_2+E or E
								(968)	m		*956*	$\nu_1+\nu_3$ or $\nu_1+\nu_5$	A_1 or E
								(1150)	m		*1167*	$\nu_1+2\nu_3$ or $\nu_1+2\nu_5$	A_1 or A_1+E
								(1310)	m		*1354*	$2\nu_4$	A_1+E

* DF = Delwaulle and Francois (see reference 30), LVT = Lecomte, Volkringer, and Tchakirian (see reference 29); other symbols have the same meaning as in Table I.

** Given as 6/7 in a later paper, M. L. Delwaulle and F. Francois, J. de phys. et rad. **7**, 15 (1946).

[28] M. L. Delwaulle and F. Francois, Comptes Rendus **214**, 828 (1942).
[29] Lecomte, Volkringer, and Tchakirian, Comptes Rendus **204**, 1927 (1937).
[30] M. L. Delwaulle and F. Francois, Comptes Rendus **214**, 226 (1942).

TABLE V. Raman and infra-red data for tetrabromomethane (CBr_4, solution), including calculated frequencies and assignments.*

Raman								Infra-red						Theoretical		
		$\Delta\nu$		I		ρ		ν	I_e		ν		I_e			
PR	N	PV	AD	PR	DF	PR	PS	PR	PR	N	PV	AD		ν_c	Assignment	Type
122	3(4)	122.5	0.3	100	7/8**	0.71	D							**122.5**	ν_2	E
										1	(164)	—	—		?	
182	4	182.5	0.5	40	7/8**	0.72	D			1	182	—	—	**182.5**	ν_4	F_2
										1	213	—	—	*221*	$\nu_3-\nu_1-\nu_4$	$A_1+E+F_1+F_2$
267	4	267.2	1.2	70	0.05	0.00	P			1	(266)	—	—	**267.2**	ν_1	A_1
										1	303	—	—	*306*	$\nu_2+\nu_4$	F_1+F_2
										1	365	—	—	*366*	$2\nu_4$	A_1+E+F_2
										1	454	—	—	*450*	$\nu_1+\nu_4$	F_2
671	4	670.7	1.8	10	7/8**	0.83	D			2	666	1.0	—	**670.7**	ν_3	F_2
								(734)	s	1	(734)	—	s	*794*	$\nu_2+\nu_3$	F_1+F_2
								931	w	1	931	—	w	*938*	$\nu_1+\nu_3$	F_2
								1118	w	1	1118	—	w	*1121*	$\nu_1+\nu_3+\nu_4$	$A_1+E+F_1+F_2$

* The symbols have the same meaning as in Table I.
** Given as 6/7 in a later paper, M. L. Delwaulle and F. Francois, J. de phys. et rad. 7, 15 (1946).

Raman and infra-red data, calculated frequencies, and assignments are given in Table IV. One of the previous Raman displacements was excluded in taking the mean for the 745.0-cm^{-1} frequency since it seemed to be considerably too low. The relatively few infra-red data are given in columns nine to eleven; of the four infra-red frequencies obtained in the present work, three are enclosed in parentheses as uncertain.

Tetrabromomethane (Carbon Tetrabromide, CBr_4)

This compound was included in the present investigation as still another molecule of the type CBr_3X, despite the fact that it represents the very special case in which X=Br. The sample was furnished by the Dow Chemical Company, and like CBr_3Cl, was a solid at room temperature; accordingly, it was investigated in an approximately saturated benzene solution. Initial attempts to obtain the Raman spectrum resulted in a marked formation of cloudiness in the solution when it was exposed to the mercury arcs, thus ruining the spectrogram. This difficulty was eliminated by renewing the solution in the Raman tube at half-hour intervals during the exposures. The infra-red spectrum was also obtained in benzene solution.

Previous Raman spectral data have been obtained in three[30–32] and infra-red data also in three[17,24,29] other investigations. Two of the previous Raman spectra were obtained with CCl_4 solution,[30,32] one with benzene solution.[31] One of the previous infra-red spectra[17] was obtained in CS_2 solution. The results are given in Table V.

Iodotribromomethane (CBr_3I)

Iodotribromomethane, CBr_3I, is a logical sixth member of this series, but no Raman or infra-red data could be found in the literature for this molecule and it was not possible to locate a sample for investigation.

[31] A. Dadieu and K. W. F. Kohlrausch, Sitz. Akad. Wiss. Wien IIa, **139**, 717 (1930).
[32] A. Langseth, Zeits. f. Physik **72**, 350 (1931).

ASSIGNMENTS

The CBr_3X Molecules

The CBr_3X molecule has a symmetry corresponding to the point group C_{3v}. According to the well-known selection rules,[33] the molecule should therefore have three non-degenerate, totally symmetrical vibrations of type A_1 and three doubly degenerate vibrations of type E. All of these are allowed in both the Raman and infra-red spectra and furthermore all binary combinations and all overtones are allowed in both spectra.

The assignments of the observed frequencies for CBr_3H, consistent with these selection rules, are given at the right in Table I.[34] It was possible to assign all of the Raman and infra-red frequencies in the region of the fundamental frequencies (128–3025 cm^{-1}) as fundamentals, first overtones, or binary combinations, with the exception of the infra-red frequency at 250 cm^{-1} and the doubtful Raman displacement at 1439 cm^{-1}. The assignment given for the 250-cm^{-1} frequency is not too certain, for difference tones should coincide more exactly with the observed frequency than is here the case. For the overtone and combination frequencies above 3100 cm^{-1}, the agreement of the calculated and observed values is generally not as exact as for the lower frequencies. This may be due partly to the influence of anharmonicity, but it is probably also due in large part to the greater inaccuracies in the experi-

[33] *Cf.* Meister, Cleveland, and Murray, Am. J. Phys. **11**, 239 (1943).
[34] The numbering of the vibrational frequencies follows the procedure of G. Herzberg, *Infrared and Raman Spectra of Polyatomic Molecules* (D. Van Nostrand Company, Inc., New York, 1945), which is also in line with the agreement of molecular spectroscopists at the Symposium on Molecular Structure and Spectroscopy, held at Ohio State University (1948). The largest frequency of the most symmetrical type (A_1 in this case) is designated ν_1, the next largest ν_2, and so on up to ν_n, where n is the number of frequencies of type A_1 (here $n=3$); one then proceeds to the next most symmetrical type (here type E), designating the first frequency of this type ν_{n+1}, the next ν_{n+2}, etc.; this process is continued until all of the fundamentals have been numbered. Thus, the lowest frequency of the most unsymmetrical type (here ν_6) is designated ν_m, where m is the number of distinct fundamental frequencies.

mental data since the values reported by different investigators are not in very good agreement in this region.

The assignments for the CBr_3D molecule are given in Table II. The 840, 856.5-cm^{-1} doublet appears to be due to Fermi resonance between ν_4 and the combination frequency $\nu_3+\nu_5$. All of the remaining observed frequencies are fundamentals.

The assignments for the CBr_3F molecule are given in Table III. For this molecule, all of the observed frequencies are fundamentals, no overtone or combination frequencies having been observed as yet.

The assignments for the CBr_3Cl molecule are given in Table IV. The point requiring the greatest comment in this assignment is that of the 211-cm^{-1} frequency. Simanouti[35] has carried out normal-coordinate treatments for 16 substituted methanes, including CBr_3Cl; 102 fundamental frequencies were calculated with 28 distinct force constants and the mean deviation of the calculated and observed values was 1.4 percent. According to his calculations, two fundamental frequencies fall together near 211 cm^{-1} for CBr_3Cl, one an A_1-, the other an E-type frequency. This is not inconsistent with the fact that in the present investigation the depolarization factor for the 211 line has an abnormally large value for a polarized line; this could be caused by the superposition of the polarized A_1 and the depolarized E frequencies.

If the 211-cm^{-1} line is indeed due to the coincidence of these two lines, the coincidence must be nearly exact (within about 5 cm^{-1}), for examination of the polarization spectrograms obtained by the authors shows no displacement or shading of the weak component relative to the strong component, as would be the case if a polarized and a depolarized line were nearly but not quite coincident. Furthermore, the width of the 211-cm^{-1} line is not abnormally great, which would indicate that if the line is double the superposition must be nearly exact.

If one assigns two fundamentals to the observed 211-cm^{-1} line, it is then necessary to assign the line observed at 268.3 cm^{-1} as the first overtone of the 140.3-cm^{-1} fundamental; this overtone would fall at 280.6 cm^{-1}, or 12.3 cm^{-1} from the observed value. While this may be the correct assignment, it seems doubtful that the combined effects of anharmonicity and experimental error in determining the Raman displacements would be greater than about 5 cm^{-1}; hence the 12.3-cm^{-1} difference seems rather large.

An alternative explanation would be to assign the observed Raman displacement at 268.3 cm^{-1} as the E fundamental and the 211.3-cm^{-1} line as the A_1 fundamental, ascribing its large depolarization factor to the fact that it is a deformation vibration; Wolkenstein and Eliashevich[36] have pointed out that the depolarization factors of pure deformation vibrations are usually large, even for totally symmetrical (A_1) vibrations. However, if this assignment is made, Simanouti's calculated value for the E fundamental would be in error by 57 cm^{-1} or 21 percent and this does not seem possible in view of the good agreement he has obtained for the large number of other frequencies in the extended series of similar molecules.

Consequently, it seems that the most probable assignment is the one given in Table IV, where—in agreement with Simanouti—the 211 line is considered to correspond to the two fundamentals in nearly exact coincidence. A clear-cut decision on the assignment of this E frequency must, however, await the investigation of the 211 frequency, in either the Raman or infra-red spectra, with sufficient resolution to obtain the rotational contour of the band, from which one should be able to determine whether it is a normal parallel (A_1-type) band or whether it is a superposition of a parallel and a perpendicular (E-type) band. Unfortunately, the spectrographs available to the authors do not have sufficient dispersion to make this test possible in their laboratory.

If the 268-cm^{-1} line were assigned as ν_5, rather than as $2\nu_6$ as suggested by Simanouti, the assignments given in Table IV would be changed otherwise only by the omission of the alternative combination bands which involve ν_5.

The CBr_4 Molecule

The CBr_4 molecule has a greater symmetry than the CBr_3X molecules, namely, that corresponding to the point group T_d. According to the well-known selection rules,[33] the molecule should therefore have one totally symmetrical type A_1 vibration, allowed in the Raman, forbidden in the infra-red; one doubly degenerate type E vibration, allowed in the Raman, forbidden in the infra-red; and two triply degenerate type F_2 vibrations, allowed in both the Raman and infra-red spectra. All binary combinations of these frequencies are allowed in the Raman spectrum, but only the ones $A_1\times F_2$, $E\times F_2$, and $F_2\times F_2$ are allowed in the infra-red. Moreover, while all overtones of these frequencies (at least up to the fourth overtone) are allowed in the Raman spectrum, only the overtones of the triply degenerate F_2 frequencies are allowed in the infra-red.

The assignments for CBr_4, consistent with these selection rules, are given in Table V. All of the observed Raman and infra-red frequencies have been accounted for as fundamentals, binary combinations, or first overtones, with the exception of the 213- and 1118-cm^{-1} infra-red bands, which had to be assigned as ternary combinations, and the 164-cm^{-1} infra-red band for which no explanation could be found.

The values of the fundamental frequencies of the five molecules which the authors regard as the most probable values at the present time are collected for ease of comparison and for ready reference in Table VI.

[35] T. Simanouti, J. Chem. Phys. **17**, 245 (1949).
[36] M. Wolkenstein and M. Eliashevich, Acta Physicochimica U.R.S.S. **20**, 525 (1945).

CALCULATION OF FORCE CONSTANTS

Although force constants have been given by other investigators for the molecules considered in this study, no single investigator considered all of the molecules of the CBr_3X set. In most cases, the sequence $CH_4 \rightarrow CBr_4$ was investigated in order to find a general set of force constants for the sequence. In this way, several atoms were changed in going from one molecule to another, while in the present investigation an attempt was made to determine the variation in force constants when only one atom was changed. In other cases interaction constants were omitted from the calculations which on the basis of the present work are quite large. Furthermore, the other investigators did not always agree on the values for the fundamental frequencies to be used in determining the force constants. So, for these reasons, it was felt that a consistent treatment of the CBr_3X molecules using the best known values of the fundamental frequencies would furnish information about the behavior of the force constants.

The Wilson *FG* matrix method[37] was used in the calculations. The potential energy function used for CBr_3H, CBr_3D, CBr_3F, and CBr_3Cl was the following:

$$
\begin{aligned}
2V = {} & k_D(\Delta D)^2 + k_d[(\Delta d_1)^2 + (\Delta d_2)^2 + (\Delta d_3)^2] \\
& + 2k_{dD}[(\Delta D)(\Delta d_1 + \Delta d_2 + \Delta d_3)] \\
& + 2k_{dd}[(\Delta d_1)(\Delta d_2 + \Delta d_3) + (\Delta d_2)(\Delta d_3)] \\
& + d^2k_\alpha[(\Delta\alpha_{12})^2 + (\Delta\alpha_{23})^2 + (\Delta\alpha_{13})^2] \\
& + d^2k_\beta[(\Delta\beta_1)^2 + (\Delta\beta_2)^2 + (\Delta\beta_3)^2] \\
& + 2dk_{D\alpha}[(\Delta D)(\Delta\alpha_{12} + \Delta\alpha_{23} + \Delta\alpha_{13})] \\
& + 2dk_{D\beta}[(\Delta D)(\Delta\beta_1 + \Delta\beta_2 + \Delta\beta_3)] \\
& + 2dk_{d\beta}[(\Delta d_1)(\Delta\beta_1) + (\Delta d_2)(\Delta\beta_2) + (\Delta d_3)(\Delta\beta_3)] \\
& + 2d^2k_{\alpha\alpha}[(\Delta\alpha_{12})(\Delta\alpha_{23} + \Delta\alpha_{13}) + (\Delta\alpha_{23})(\Delta\alpha_{13})] \\
& + 2dk_{d\beta}'[(\Delta d_1)(\Delta\beta_2 + \Delta\beta_3) + (\Delta d_2)(\Delta\beta_1 + \Delta\beta_3) \\
& \quad + (\Delta d_3)(\Delta\beta_1 + \Delta\beta_2)]
\end{aligned}
$$

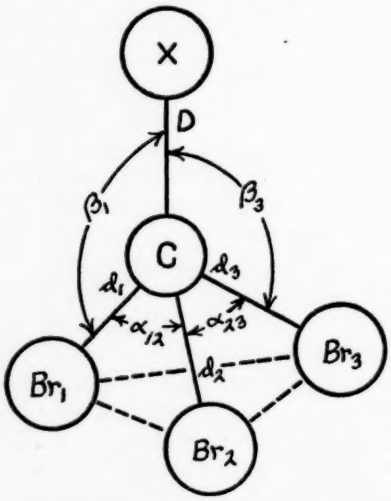

FIG. 2. Equilibrium bond distances and bond angles for a CBr_3X molecule.

[37] E. B. Wilson, Jr., J. Chem. Phys. **7**, 1047 (1939); **9**, 76 (1941).

TABLE VI. Probable values of the fundamental vibrational frequencies for the tribromomethanes (liquid or solutions).

Type	Degeneracy	Frequency in cm^{-1} CBr_3H	CBr_3D	CBr_3F	CBr_3Cl	CBr_4	Degeneracy	Type
A_1	1	3020.9	2247	1069	745.0			
A_1	1	539.3	519.3	398	326.7	267.2	1	A_1
A_1	1	222.5	221.6	218	211.3			
E	2	1144.3	848.2	743	677.0	670.7	3	F_2
E	2	655.5	628.5	306	211.3	182.5	3	F_2
E	2	154.3	153.4	150	140.3	122.5	2	E

$$
\begin{aligned}
& + 2dk_{d\alpha}[(\Delta d_1)(\Delta\alpha_{12} + \Delta\alpha_{13}) + (\Delta d_2)(\Delta\alpha_{12} + \Delta\alpha_{23}) \\
& \quad + (\Delta d_3)(\Delta\alpha_{13} + \Delta\alpha_{23})] \\
& + 2d^2k_{\beta\beta}[(\Delta\beta_1)(\Delta\beta_2 + \Delta\beta_3) + (\Delta\beta_2)(\Delta\beta_3)] \\
& + 2dk_{d\alpha}'[(\Delta d_1)(\Delta\alpha_{23}) + (\Delta d_2)(\Delta\alpha_{13}) + (\Delta d_3)(\Delta\alpha_{12})] \\
& + 2d^2k_{\alpha\beta}[(\Delta\beta_1)(\Delta\alpha_{12} + \Delta\alpha_{13}) + (\Delta\beta_2)(\Delta\alpha_{12} + \Delta\alpha_{23}) \\
& \quad + (\Delta\beta_3)(\Delta\alpha_{13} + \Delta\alpha_{23})] \\
& + 2d^2k_{\alpha\beta}'[(\Delta\beta_1)(\Delta\alpha_{23}) + (\Delta\beta_2)(\Delta\alpha_{13}) \\
& \quad + (\Delta\beta_3)(\Delta\alpha_{12})].
\end{aligned}
$$

The equilibrium bond distances and bond angles are shown in Fig. 2.

Because CBr_4 has greater symmetry than the other CBr_3X molecules, it was necessary to modify the potential energy function so that for this molecule one has

$$
\begin{aligned}
2V = {} & k_d[(\Delta d_1)^2 + (\Delta d_2)^2 + (\Delta d_3)^2 + (\Delta d_4)^2] \\
& + 2k_{dd}[(\Delta d_1)(\Delta d_2 + \Delta d_3 + \Delta d_4) \\
& \quad + (\Delta d_2)(\Delta d_3 + \Delta d_4) + (\Delta d_3)(\Delta d_4)] \\
& + d^2k_\alpha[(\Delta\alpha_{12})^2 + (\Delta\alpha_{13})^2 + (\Delta\alpha_{14})^2 \\
& \quad + (\Delta\alpha_{23})^2 + (\Delta\alpha_{24})^2 + (\Delta\alpha_{34})^2] \\
& + 2d^2k_{\alpha\alpha}[(\Delta\alpha_{12})(\Delta\alpha_{13} + \Delta\alpha_{14} + \Delta\alpha_{23} + \Delta\alpha_{24}) \\
& \quad + (\Delta\alpha_{13})(\Delta\alpha_{14} + \Delta\alpha_{23} + \Delta\alpha_{34}) \\
& \quad + (\Delta\alpha_{14})(\Delta\alpha_{24} + \Delta\alpha_{34}) \\
& \quad + (\Delta\alpha_{23})(\Delta\alpha_{24} + \Delta\alpha_{34}) + (\Delta\alpha_{24})(\Delta\alpha_{34})] \\
& + 2d^2k_{\alpha\alpha}'[(\Delta\alpha_{12})(\Delta\alpha_{34}) \\
& \quad + (\Delta\alpha_{13})(\Delta\alpha_{24}) + (\Delta\alpha_{14})(\Delta\alpha_{23})] \\
& + 2dk_{d\alpha}[(\Delta d_1)(\Delta\alpha_{12} + \Delta\alpha_{13} + \Delta\alpha_{14}) \\
& \quad + (\Delta d_2)(\Delta\alpha_{12} + \Delta\alpha_{23} + \Delta\alpha_{24}) \\
& \quad + (\Delta d_3)(\Delta\alpha_{13} + \Delta\alpha_{23} + \Delta\alpha_{34}) \\
& \quad + (\Delta d_4)(\Delta\alpha_{14} + \Delta\alpha_{24} + \Delta\alpha_{34})] \\
& + 2dk_{d\alpha}'[(\Delta d_1)(\Delta\alpha_{23} + \Delta\alpha_{24} + \Delta\alpha_{34}) \\
& \quad + (\Delta d_2)(\Delta\alpha_{13} + \Delta\alpha_{14} + \Delta\alpha_{34}) \\
& \quad + (\Delta d_3)(\Delta\alpha_{12} + \Delta\alpha_{14} + \Delta\alpha_{24}) \\
& \quad + (\Delta d_4)(\Delta\alpha_{12} + \Delta\alpha_{13} + \Delta\alpha_{23})].
\end{aligned}
$$

Since the symmetry coordinates and *G* matrices for a CY_3X and a CY_4 molecule have already been given in a previous publication,[38] they will not be repeated here. Also, because the *F* matrices are somewhat the same as those obtained previously[38] they will not be given again, because once the form of the potential energy function and the symmetry coordinates are known, these matrices can be found very simply by the method given in reference 38.

Tetrahedral angles were assumed and the following constants were used: for the reciprocals of the masses of

[38] A. G. Meister and F. F. Cleveland, Am. J. Phys. **14**, 13 (1946).

TABLE VII. Force constants for CBr_3H and CBr_3D (10^5 dynes/cm).

Type	CBr_3H	CBr_3D
k_D	4.8847	4.8809
k_d	2.8987	2.8965
k_{dd}	0.27567	0.32250
k_{dD}	0.058900	0.058900
$*k_{D\gamma}$	0.24448	0.24448
$k_{d\alpha}$	0.17662	0.17662
$k_{d\alpha}'$	−0.10884	−0.10884
$k_{d\beta}$	0.13597	0.13597
$k_{d\beta}'$	−0.079581	−0.079581
k_α	0.33399	0.33133
$k_{\alpha\alpha}$	0.067920	0.065377
$k_{\alpha\beta}$	0.021329	0.021329
$k_{\alpha\beta}'$	0.00000	0.00000
k_β	0.16044	0.16326
$k_{\beta\beta}$	−0.0013706	−0.0013706

$* k_{D\gamma}=k_{D\alpha}-k_{D\beta}$.

the atoms,

$$\mu_C=5.0153\times10^{22},$$
$$\mu_H=5.9762\times10^{23},$$
$$\mu_D=2.9905\times10^{23},$$
$$\mu_F=3.1702\times10^{22},$$
$$\mu_{Cl}=1.6988\times10^{22},$$

and

$$\mu_{Br}=7.5372\times10^{21}\ g^{-1};$$

and for the equilibrium values of the bond distances,[39]

C−Br=1.91A for CBr_3H, CBr_3D, CBr_3F, and CBr_3Cl;
C−Br=1.92A for CBr_4;
C−H =C−D=1.093A;
C−F =1.44A;
and
C−Cl=1.76A.

It will be noted that most of the force constants are expressed to five significant figures which is greater, in most cases, than the number of significant figures occurring in the frequencies used to determine force constants. This greater number of significant figures was retained in order to insure agreement in all cases between the observed and calculated frequencies to the nearest cm^{-1}. Since the error in the observed frequencies may be greater than one cm^{-1}, the force constants cannot, of course, be considered as having been reliably established to five significant figures.

In order to obtain force constants for the CBr_3 group, the CBr_3H and CBr_3D molecules were considered. Using the observed fundamental frequency values of Redlich and Stricks,[12] force constants for these two molecules were determined which gave calculated values for the frequencies that agreed to within 0.1 cm^{-1} of the observed values. These constants are given in Table VII. Since there are sixteen force constants and only twelve fundamental frequencies, it was necessary to make assumptions concerning the values of four of the force constants. The value of k_{dD} was taken from the work of Stepanov[40] while the value of $k_{\beta\beta}$ was obtained from the work of Decius.[41] However, no value could be found in the literature for $k_{\alpha\beta}'$ so it arbitrarily was assumed to be zero, although the value given for $k_{\alpha\beta}$ actually is for the difference $(k_{\alpha\beta}-k_{\alpha\beta}')$ which becomes $k_{\alpha\beta}$ when $k_{\alpha\beta}'$ is made zero. Finally, the linear combination $k_{D\alpha}-k_{D\beta}=k_{D\gamma}$ was used since the two constants $k_{D\alpha}$ and $k_{D\beta}$ occur only once in the F matrices and as this linear combination.

Although two sets of force constants were determined for these two molecules, this calculation is not presented as proof that the force constants for CBr_3H and CBr_3D are considerably different. Rather it indicates how the force constants are affected when anharmonicities are neglected and force constants are modified in order to get good agreement between the calculated and observed values of the fundamental frequencies. Actually, in the investigation of the other tribromomethanes, the mean values of the force constants of the two sets were used and the calculated

TABLE VIII. Force constants for some tribromomethanes (10^5 dynes/cm).

	CBr_3H and CBr_3D			CBr_3F	CBr_3Cl			CBr_4			
					Present						
Type	Present	Decius	Stepanov	Present	Set I	Set II	Simanouti	Present	Decius	Simanouti	Stepanov
k_D	4.8828	5.04	5.02	4.9531	2.9565	2.9565	2.7684	—	—	—	—
k_d	2.8976	2.840	2.886	2.8976	2.8976	2.8976	2.4073	2.8976	2.840	2.3379	2.945
k_{dd}	0.29910	0.186	0.147	0.29910	0.29910	0.29910	0.35465	0.15437	0.186	0.35465	0.147
k_{dD}	0.058900	0.000	0.0589	0.62654	0.20890	0.20890	0.41186	—	—	—	—
$*k_{D\gamma}$	0.24448	0.000	−0.168	−0.035300	−0.24818	−0.24818	−0.21094	—	—	—	—
$k_{d\alpha}$	0.17662	0.179	0.286	0.17662	0.17662	0.17662	0.19563	0.17662	0.179	0.19563	0.336
$k_{d\alpha}'$	−0.10884	−0.0995	0.000	−0.10884	−0.10884	−0.10884	0.00000	−0.12211	−0.0995	0.00000	0.000
$k_{d\beta}$	0.13597	0.160	0.286	0.13886	0.16567	0.29918	0.22952	—	—	—	—
$k_{d\beta}'$	−0.079581	−0.0796	0.000	−0.081027	0.094430	−0.16118	0.00000	—	—	—	—
k_α	0.33266	0.291	0.257	0.33266	0.33266	0.33266	0.34155	0.29473	0.291	0.33933	0.261
$k_{\alpha\alpha}$	0.066648	0.0367	0.0192	0.066648	0.066648	0.066648	0.053479	0.034934	0.0367	0.025999	0.0192
$k_{\alpha\beta}$	0.021329	0.000	0.0173	0.013707	0.021889	0.060851	0.053479	—	—	—	—
$k_{\alpha\beta}'$	0.00000	0.000	0.000	0.00000	0.00000	0.00000	0.00000	—	—	—	—
k_β	0.16185	0.161	0.187	0.30015	0.25468	0.44497	0.33795	—	—	—	—
$k_{\beta\beta}$	−0.0013706	−0.00137	0.0249	−0.049727	−0.019260	−0.036487	0.053479	—	—	—	—
$k_{\alpha\alpha}'$	—	—	—	—	—	—	—	0.010579	0.0106	0.00000	0.000
$k_{D\alpha}$	—	0.000	0.000	—	—	—	0.00000	—	—	—	—
$k_{D\beta}$	—	0.000	0.168	—	—	—	0.21094	—	—	—	—

$* k_{D\gamma}=k_{D\alpha}-k_{D\beta}$.

[39] L. R. Maxwell, J. Opt. Soc. Am. **30**, 374 (1940).
[40] B. I. Stepanov, Acta Physicochimica U.R.S.S. **20**, 174 (1945).
[41] J. C. Decius, J. Chem. Phys. **16**, 214 (1948).

fundamental frequencies given in Table I for CBr_3H and in Table II for CBr_3D were obtained using this mean set of force constants.

The above procedure served to establish the force constants of the CBr_3 group which were used for CBr_3F and CBr_3Cl. The values of k_D for these molecules were obtained by splitting out[37] the C—F and C—Cl stretching frequencies for the type A_1 vibrations. Other force constants were determined from the probable values of the observed fundamental frequencies given in Table VI. In Table VIII the force constants which were obtained for CBr_3F and CBr_3Cl are given as well as the mean set for CBr_3H and CBr_3D taken from Table VII.

It will be noted that two sets of force constants have been given for CBr_3Cl. This results from the fact that the value of one of the type E fundamental frequencies is uncertain as was mentioned previously in the section on assignments. The first set of force constants was obtained assuming that the value of the frequency was 211.3 cm^{-1} while the second set resulted when the value 268.3 cm^{-1} was used. Although the two sets of force constants appear to be reasonable, the much higher values of k_β, $k_{d\beta}$, and $k_{d\beta}'$ obtained in Set II might indicate that the force constants of Set I are to be preferred over those of Set II.

For CBr_4 the values of k_d and $k_{d\alpha}$ were taken from the mean set for CBr_3H and CBr_3D while the value of $k_{d\alpha}'$ was taken from the work of Decius.[41] The remaining force constants were determined from the probable values of the observed fundamental frequencies given in Table VI and in Table VIII the force constants for CBr_4 are indicated.

Force constants for the tribromomethanes determined by Decius,[41] Simanouti,[35] and Stepanov,[40] also are given in Table VIII for comparison. Simanouti used a Urey-Bradley type potential energy function but he gave relations between his force constants and those of the modified valence force type potential energy function used in this investigation. The values in the columns headed Simanouti were calculated using his equations and force constants. Decius assumed k_{dD}, $k_{D\alpha}$, $k_{D\beta}$, $k_{\alpha\beta}$, and $k_{\alpha\beta}'$ were zero while Stepanov neglected $k_{d\beta}'$, $k_{d\alpha}'$, and $k_{\alpha\alpha}'$. Since some of these interaction constants seem large when compared with the bending force constants, it seems that the present values of the force constants are to be preferred over those of these two investigators. The agreement between the present values of the force constants and those determined by the other investigators in most cases is good although it seems that all the other investigators used a value of k_D for CBr_3H and CBr_3D which was too high. The lower value obtained in this investigation is believed to be a better value since the other investigators found calculated values for the C—H and C—D frequencies which were greater than the observed values. This resulted from their attempt to determine a C—H stretching force constant which would remain the same in the sequence $CH_4 \rightarrow CX_3H$.

Finally, it should be indicated that Stepanov[42] calculated fundamental frequencies for the CBr_3F molecule using force constants which he obtained in an earlier work. However, the reference he gives to this work is in error and it was not possible to determine the values of the force constants he used since they were not given in the later paper.[42]

ACKNOWLEDGMENTS

The microdensitometer used in this investigation was obtained with a grant from the Penrose Fund of the American Philosophical Society; the Hilger E-518 spectrograph was obtained, in part, with a grant from the Permanent Science Fund of the American Academy of Arts and Sciences; and the optical parts for the two-prism spectrograph were obtained with a grant from The Society of the Sigma Xi.

The infra-red spectrometer was carefully constructed in the Illinois Institute of Technology shop by Mr. Max Schoenherr and was modified somewhat by Mr. Walter L. Hadlock, both of whom contributed many original ideas to its design. The samples used in the experimental part of the paper were furnished by the Dow Chemical Company, Midland, Michigan, through the courtesy of Mr. Walter W. Cooper. The drawing used for Fig. 1 was prepared by Mr. Dusan J. Ljubenko.

The authors are grateful for all of this assistance.

[42] B. I. Stepanov, Comptes Rendus U.R.S.S. **45**, 56 (1944).

Infra-Red Absorption Spectrum of Dimethyldiacetylene*

FORREST F. CLEVELAND
Spectroscopy Laboratory, Department of Physics, Illinois Institute of Technology, Chicago, Illinois

AND

KENNETH W. GREENLEE AND ELY E. BELL
Departments of Chemistry and Physics, Ohio State University, Columbus, Ohio

(Received August 23, 1949)

The infra-red absorption spectrum of freshly prepared dimethyldiacetylene has been obtained for the vapor existing above the solid or liquid at temperatures of 25°, 40°, 60°, 80°, 85°, and 110°C; for the gas at 130°C; and for CCl_4 and cyclohexane solutions. A Beckman IR-2 spectrophotometer with rocksalt optics was used. The observed values of the $\bar{A}_2$ frequencies were 940, 1369, 2157, and 2920, as compared with the calculated values 903, 1368, 2131, and 2946 cm^{-1} given previously by Meister and Cleveland. A frequency assignment based upon the D_{3h}' structure is given: One of the 20 distinct fundamental frequencies (10 non-degenerate, 10 doubly degenerate) corresponds to the internal free rotation; the other nine non-degenerate and seven of the doubly degenerate fundamentals are rather certainly assigned and tentative values are given for the remaining three. All of the other observed Raman and infra-red bands could be accounted for as binary combinations, except the 2225-cm^{-1} Raman line and the 2228-cm^{-1} infra-red band which seem to originate from the coincidence of a large number—43 and 40, respectively—of ternary combination frequencies. The sample used melted at 64.95±0.03°C, corresponding to a purity of 99.77±0.05 mole percent. A description of the method of preparation is given.

INTRODUCTION

DIMETHYLDIACETYLENE has been subjected to very few investigations by spectroscopic methods. Apparently the first such investigation was that of Meister and Cleveland[1] who obtained Raman displacements, relative intensities, and depolarization factors of the Raman lines, using a CCl_4 solution. Later, they reported[2] the results of a normal coordinate treatment, using the Wilson *FG* matrix method, for the non-degenerate vibrations of this molecule. The A_1 frequencies could be compared with the Raman spectral data, but the $\bar{A}_2$ frequencies were forbidden in the Raman spectrum and the infra-red spectrum had not been investigated. The present authors obtained the infra-red spectrum, using the Beckman IR-2 spectrophotometer in the Physics Department at Ohio State University, during the summer of 1947, but because of pressure of other work it has not been possible to publish the results until now. It was desired to obtain observed values of the $\bar{A}_2$ frequencies for comparison with the calculated values of Meister and Cleveland and to obtain other infra-red frequencies for use, together with the previously observed Raman displacements, in a later normal coordinate treatment of the degenerate frequencies and in calculations of the thermodynamical properties for the molecule.[3]

EXPERIMENTAL DETAILS

Preparation of Dimethyldiacetylene

The dimethyldiacetylene was prepared by the method of Griner[4] which has also been used by Conn, Kistiakowsky, and Smith[5] and by M. J. Murray in preparing the sample used by Meister and Cleveland;[1] it involves the oxidation of cuprous methylacetylide, $Cu_2(C{\equiv}CCH_3)_2$, by aqueous potassium ferricyanide solution. The essential reaction, represented ionically, is probably as follows:

$$CH_3-C{\equiv}C^-:+Fe(CN)_6^{-3}\rightarrow CH_3-C{\equiv}C\cdot+Fe(CN)^{-4}$$
$$2CH_3-C{\equiv}C\cdot\rightarrow CH_3-C{\equiv}C-C{\equiv}C-CH_3.$$

As might be predicted on the basis of this free radical mechanism and the use of water as a solvent, the yield was low, only 32 percent of theory; yields of 50 percent[4] and 42 percent[5] have been reported for operations on a much smaller scale than the present. This type of reaction has also been carried out in a non-aqueous solvent (diethyl ether); 60–72 percent yields[6,7] of homologous diacetylenes were obtained. Further study is expected to lead to an improved procedure for dimethyldiacetylene.

A solution of 10.5 moles of sodium acetylide was prepared[8] in three liters of liquid ammonia and reacted with an equivalent amount of dimethyl sulfate. When reaction was complete, five liters of water were added

* Presented at the Chicago meeting of the American Physical Society, November, 1948; abstract in Phys. Rev. **75**, 334 (1949).

[1] A. G. Meister and F. F. Cleveland, J. Chem. Phys. **12**, 393 (1944).

[2] A. G. Meister and F. F. Cleveland, J. Chem. Phys. **15**, 349 (1947).

[3] This work is now in progress at Illinois Institute of Technology and the results will be reported in a later paper.

[4] G. Griner, Ann. Chim. Phys. (6) **26**, 354 (1892).

[5] Conn, Kistiakowsky, and Smith, J. Am. Chem. Soc. **61**, 1868 (1939).

[6] V. Grignard and Tchéoufaki, Comptes Rendus **188**, 357 (1929).

[7] J. P. Danehy and J. A. Nieuwland, J. Am. Chem. Soc. **58**, 1609 (1936).

[8] K. W. Greenlee and A. L. Henne, *Inorganic Syntheses* (McGraw-Hill Book Company, Inc., New York, 1946), edited by W. C. Fernelius, Vol. II, Sections 21 and 38.

and the methylacetylene was distilled into an absorber containing an excess of ammoniacal cuprous chloride solution. Since no losses of gas were observed, it was assumed that the yellow precipitate obtained represented 5.25 moles of $Cu_2(C{\equiv}CCH_3)_2$. It was filtered out, washed, suspended in water, and oxidized by slow addition of a potassium ferricyanide solution in 75 percent excess; during the oxidation, 0.4 mole of methylacetylene escaped. The dimethyldiacetylene produced was distilled from this reaction mixture by a current of steam. The crude crystalline product was dissolved in *n*-pentane, whereupon a water layer separated; the net yield of dimethyldiacetylene was 130 g or 32 percent of theory.

To obtain the sample for spectral examination, a small portion of the *n*-pentane solution was chilled to 0°C; the crystals which separated were filtered and freed from solvent by keeping under low vacuum for 12 hr. A larger portion, similarly treated, gave crystals which melted at 64.95±0.03°C, corresponding to a purity of 99.77±0.05 mole percent. Later, the remainder of the material was freed from solvent by distillation and was fractionated at an efficiency of about 20 theoretical plates. A heart cut was found to boil at 129.51±0.03°C at 760 mm pressure, to freeze at 65.03±0.03°C, and to be 99.89±0.05 percent pure. The purities were estimated by the cryoscopic method[9] from a freezing point curve and from melting point lowering data; the ultimate freezing point (t_{f_0}) was estimated as 65.08±0.03°C, and the freezing point lowering was found to be 0.60±0.03°C per mole percent of added impurity (*n*-heptane).

Infra-Red Technique

The white solid, prepared as described, was placed in an absorption cell 20 cm in length, which was wrapped with a heater element and insulating tape. The junction of a previously calibrated thermocouple was placed in contact with the absorption cell in order to obtain a measure of the temperature of the cell, and the air was removed from the cell with a pump. Because there was some uncertainty as to whether the

TABLE I. The present infra-red spectral data, the previous Raman spectral data, calculated frequencies, and assignments for dimethyldiacetylene (2,4-hexadiyne, $H_3C-C{\equiv}C-C{\equiv}C-CH_3$).*

	Infra-red					Raman				Theoretical	
	Gas or vapor			CCl_4 solution		CCl_4 solution			Calc.	Assignment	Type
N	ν_g	AD	I_g	ν_s	I_s	$\Delta\nu_s$	I	ρ	ν_c		
						247	8	0.64		ν_{20}	$\bar{E}$
						475	22	0.64	473	ν_5	A_1
						(686)	vw		*692*	$\nu_3+\nu_{15}$	E
1	(721)		vw						*716*	$\nu_{13}-\nu_{14}$	$A_1+\bar{A}_2+E$
6	941	1	m	940	m				903	ν_{10}	$\bar{A}_2$
						(957)	vw		965	ν_4	A_1
						1020	vw			ν_{18}	$\bar{E}$
2	1030	1	vw	1016	m					ν_{13}	E
						(1151)	vw		*1158*	$\nu_{10}+\nu_{15}$	$\bar{E}$
						(1185)	vw		*1188*	$\nu_{10}+\nu_{20}$	E
						(1228)	vw		*1237*	$\nu_{15}+\nu_{18}$	$\bar{A}_1+\bar{A}_2+\bar{E}$
10	1254	6	m	1253	w	1253	2		*1247*	$\nu_{13}+\nu_{15}$	$A_1+\bar{A}_2+E$
15	1379	1	s	1369	s				1368	ν_9	$\bar{A}_2$
						1381	12	0.62	1375	ν_8	A_1
						1426	1			ν_{17}	$\bar{E}$
7	(1472)	2	m	1433	s	1458	vw			ν_{12}	E
9	2050	4	m	2037	w				*2050*	$\nu_{13}+\nu_{18}$	$\bar{A}_1+\bar{A}_2+\bar{E}$
11	2163	5	w	2157	m				2131	ν_8	$\bar{A}_2$
						2225	vw		*2224*	$\nu_4+\nu_{18}+\nu_{20}$	A_1+A_2+E
11	2234	7	m	2223	m				*2228*	$2\nu_4+\nu_{14}$	E
						2264	100	0.40	2265	ν_2	A_1
						2309	1		*2320*	$\nu_9+\nu_{10}$	A_1
						2502	vw		*2495*	$\nu_{16}-\nu_{19}$	A_1+A_2+E
1	2667		vw						*2650*	$\nu_{11}-\nu_{15}$	A_1+A_2+E
12	2782	8	m	2758	w				*2760*	$\nu_3+\nu_9$	$\bar{A}_2$
						2821	vw		*2807*	$\nu_3+\nu_{17}$	$\bar{E}$
				2867	m	2848	2			ν_{11}	E
						2914	40	0.17	2946	ν_1	A_1
9	2947	17	s	2920	s				2946	ν_7	$\bar{A}_2$
						2954	4			ν_{16}	$\bar{E}$
12	3277	16	w	3262	vw				*3268*	$\nu_{14}+\nu_{16}$	$\bar{A}_1+\bar{A}_2+\bar{E}$
15	4435	22	m	4352	w				*4380*	$\nu_{16}+\nu_{17}$	A_1+A_2+E
7	5845	28	w						*5861*	$\nu_1+\nu_7$	$\bar{A}_2$

* N is the number of times the band was measured on separate records; ν_g, the mean of the N readings, is the infra-red frequency in cm^{-1} for the gas or vapor; AD is the average deviation of the N readings from the mean; I_g is the estimated intensity (s = strong, m = medium, w = weak, vw = very weak); ν_s is the infra-red frequency for the solution in cm^{-1}; $\Delta\nu_s$ is the Raman displacement for the solution in cm^{-1}; I is the relative intensity of the Raman lines, upon the basis of 100 for the strongest Raman line; ρ is the depolarization factor of the Raman line; ν_c is the calculated frequency in cm^{-1}; and data in regard to which there is some uncertainty are enclosed in parentheses. ν_{14}, ν_{18}, and ν_{19} are assumed to be at 314, 217, and 459 cm^{-1}, respectively, and ν_8 is the internal free rotation.

[9] Glasgow, Streiff, and Rossini, J. Research Nat. Bur. Standards, **35**, 355 (1945).

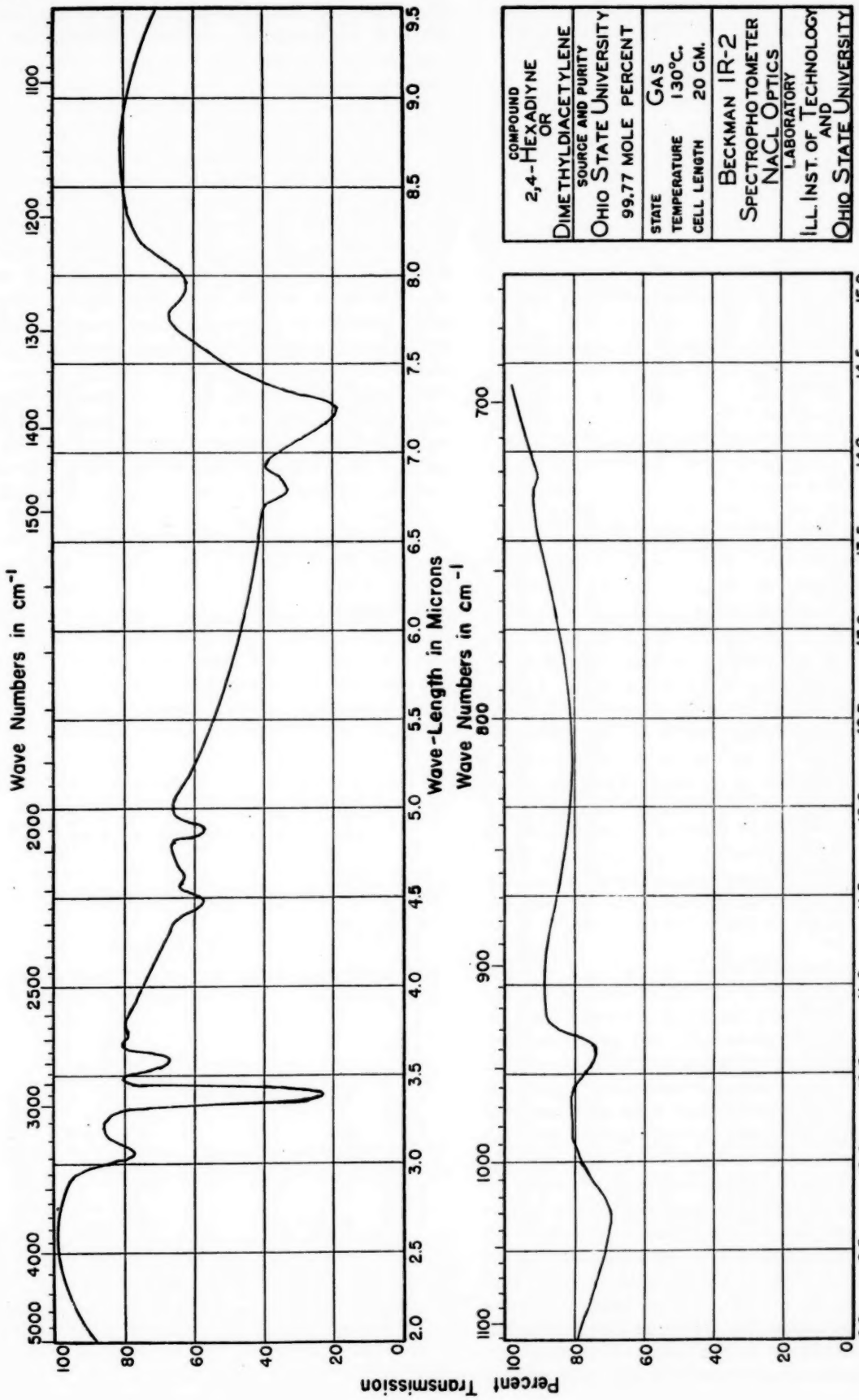

FIG. 1. Infra-red absorption curve for gaseous dimethyldiacetylene.

TABLE II. A tentative list of fundamental frequencies for dimethyldiacetylene.

Designation	Frequency (cm^{-1})	Degeneracy	Type
ν_1	2914	1	A_1
ν_2	2264	1	A_1
ν_3	1381	1	A_1
ν_4	957	1	A_1
ν_5	475	1	A_1
ν_6	Free rot.	1	$\bar{A}_1$
ν_7	2947	1	$\bar{A}_2$
ν_8	2163	1	$\bar{A}_2$
ν_9	1379	1	$\bar{A}_2$
ν_{10}	941	1	$\bar{A}_2$
ν_{11}	2867	2	E
ν_{12}	1458	2	E
ν_{13}	1030	2	E
ν_{14}	(314)*	2	E
ν_{15}	(217)*	2	E
ν_{16}	2954	2	$\bar{E}$
ν_{17}	1426	2	$\bar{E}$
ν_{18}	1020	2	$\bar{E}$
ν_{19}	(459)*	2	$\bar{E}$
ν_{20}	247	2	$\bar{E}$

* These frequencies are not established with certainty.

sealing wax holding the windows on the cell would withstand high temperatures, records were obtained first at 25°C, then at 40°, 60°, 80°, 85°, 110°, and finally for the gas at 130°C. Records were also obtained for CCl_4 and cyclohexane solutions, since the Raman spectra were obtained with CCl_4 solution. The Beckman instrument was equipped with rocksalt optics and the spectral range covered in the investigation was 675–6000 cm^{-1}. Records of the atmospheric absorption were obtained immediately before or after the other records in order to make possible the elimination of the atmospheric absorption bands from the results.

No evidence of decomposition was noted, though the runs were not checked downward through the temperature range, as they perhaps should have been.

RESULTS

The results obtained for the infra-red frequencies in the gas or vapor and in CCl_4 solution, and for comparison the previous Raman data and calculated frequencies,[1,2] are given in Table I; the assignment of the observed infra-red and Raman bands is also included but will not be discussed in detail until a later section. Also, a graphical presentation of the infra-red bands for the gas is given in Fig. 1. No useful results were obtained with the cyclohexane solution and hence no column corresponding to it appears in Table I. The infra-red frequencies were measured at that point in the band which corresponded to the maximum absorption. The 721-cm^{-1} band was very weak and the 1472-cm^{-1} band was in a region where there was some atmospheric absorption; hence these frequencies are not as well established as the others. The calculated values for the fundamentals are of course more reliable than those for the combinations and overtones; this has been emphasized in Table I by using **bold face** type for the fundamentals and *italics* for the combinations and overtones.

Since a point of special interest in the present investigation was a comparison of the observed values of the $\bar{A}_2$ frequencies with the previous calculated values,[2] it may be noted that the observed values are 940, 1369, 2157, and 2920 cm^{-1}, while the calculated values were 903, 1368, 2131, and 2946 cm^{-1}; the errors are 3.9, 0.1, 1.2, and 0.9 percent, respectively, or an average of 1.5 percent. This is excellent agreement, especially when one remembers that the calculated values were published before the observed values became available. The comparison is made with the infra-red frequencies obtained with the CCl_4 solution, since the force constants used in calculating the $\bar{A}_2$ frequencies were obtained from the A_1 frequencies in the Raman spectrum of a CCl_4 solution. If the infra-red frequencies for the gas had been used in the comparison, the average error would have been 1.6 percent, which is practically the same.

As usual, the frequencies for the gas or vapor are somewhat greater than the corresponding ones for the solution. For example, the frequencies which appeared at 940, 1016, 1369, 2157, and 2920 cm^{-1} in the infra-red spectrum of the solution were at 941, 1030, 1379, 2163, and 2947 cm^{-1} in the infra-red spectrum of the gas or vapor; thus, for these five frequencies, the average difference is 12 cm^{-1} or 0.7 percent.

On one record there was some indication that the 941 cm^{-1} frequency is a doublet with components at 935 and 947 cm^{-1}, but the reality of this doublet could not be established with certainty.

ASSIGNMENT OF FREQUENCIES

A tentative assignment of the Raman frequencies of dimethyldiacetylene was made by Meister and Cleve-

TABLE III. Binary and ternary combination frequencies for dimethyldiacetylene.

Observed (cm^{-1})	Number	Calculated Nearest one	Mean value
686	3	692	670
721	4	716	717
1151	7	1158	1144
1185	4	1188	1186
1228	3	1237	1219
1253	5(3)	1247	1261
2044	3(1)	2050	2052
2225*	43(5)	2224	2219
2228*	40(8)	2228	2219
2309	3(2)	2320	2342
2502	9	2495	2494
2667	6	2650	2646
2770	2	2760	2749
2821	5(3)	2807	2828
3270	3	3268	3296
4393	4	4380	4384
5845	6	5861	5834

* These two are ternary combinations, the others are all binary combinations.

land;[1] this assignment later was revised by them following their normal coordinate treatment[2] of the non-degenerate vibrations of this molecule. Now that infra-red spectral data have been obtained, it seems desirable to review again the assignments of the Raman frequencies and to make assignments of the newly obtained infra-red frequencies.

As in the previous assignment,[2] it is assumed that the structure of the dimethyldiacetylene molecule is that corresponding to the special group D_{3h}', introduced by Howard,[10] which of course presupposes free rotation about the central carbon-carbon single bond. For this symmetry, the selection rules predict five non-degenerate, totally symmetrical A_1-type vibrations, polarized lines in the Raman spectrum, forbidden in the infra-red; one non-degenerate $\bar{A}_1$-type vibration, forbidden in both Raman and infra-red (a torsional oscillation of one methyl group with respect to the other about the three-fold symmetry axis through the six carbon atoms if the rotation about the central carbon-carbon bond is hindered rather than free); four non-degenerate $\bar{A}_2$-type vibrations, parallel bands in the infra-red, forbidden in the Raman; five doubly degenerate E-type vibrations, perpendicular bands in the infra-red, depolarized lines in the Raman; and five doubly degenerate $\bar{E}$-type vibrations, forbidden in the infra-red, depolarized lines in the Raman spectrum. All binary combinations of these frequencies are allowed in the Raman spectrum, except $A_1\times\bar{A}_1$, $A_1\times\bar{A}_2$, and $\bar{A}_1\times\bar{A}_2$; and all such combinations are forbidden in the infra-red, except $A_1\times\bar{A}_2$, $A_1\times E$, $\bar{A}_1\times\bar{E}$, $\bar{A}_2\times\bar{E}$, $E\times E$, $E\times\bar{E}$, and $\bar{E}\times\bar{E}$. All overtones of the E and $\bar{E}$ fundamentals (at least up to the fourth overtone) are allowed in both the Raman and infra-red spectra; for the non-degenerate vibrations, however, the only overtones allowed in the infra-red are $(\bar{A}_2)^n$ (n odd), *i.e.*, the second, fourth, etc. overtones, while the only overtones forbidden in the Raman spectrum are $(\bar{A}_1)^n$ (n odd) and $(\bar{A}_2)^n$ (n odd).

An assignment of the observed Raman and infra-red frequencies, consistent with the above selection rules, is given at the right in Table I.[11] The symbol ν_6 is reserved for the forbidden $\bar{A}_1$ frequency, which will be an internal rotational frequency if the rotation is unhindered, as is assumed here.

Fundamentals

The present assignment of the A_1 fundamentals is the same as in the previous assignment[2] and the assignment of the $\bar{A}_2$ frequencies is in line with the calculated values given previously.[2] It thus appears that the frequencies of these two types are rather well established.

The E and $\bar{E}$ fundamentals cannot be assigned with as great a certainty since a normal coordinate treatment[3] has not been completed for the degenerate vibrations, since the infra-red spectrum has not been reported for the region below 700 cm^{-1}, and since the Raman spectrum has been obtained only in CCl_4 solution. The $\bar{E}$ frequencies are allowed only in the Raman spectrum. By analogy with dimethylacetylene,[12] the Raman frequencies at 2954, 1426, and 1020 cm^{-1}, which are frequencies involving the methyl group, may be assigned as $\bar{E}$ frequencies, as in the previous assignment.[2] The E frequencies are allowed in both the Raman and infra-red spectra. Again by analogy with dimethylacetylene, the three E frequencies involving the methyl group may be rather certainly assigned. The only strong line in the 3000 cm^{-1} region that has not been previously assigned and which occurs in both spectra is the one which occurs at 2848 (Raman), 2867 (infra-red); consequently, this frequency, as well as the one at 1458 (Raman), 1433 (infra-red), and the one at 1016 (infra-red, solution), 1030 (infra-red, gas), is assigned as an E frequency. The Raman line corresponding to the 1016 infra-red frequency was either too weak to be observed or was unresolved from the 1020 $\bar{E}$ frequency. This completes the assignment of the three E and the three $\bar{E}$ methyl group frequencies.

The remaining four doubly degenerate frequencies, two E and two $\bar{E}$, are deformation frequencies involving the carbon chain. Consideration of the similar frequencies of diacetylene and dimethylacetylene makes it appear improbable that these frequencies would be above 600 cm^{-1}; if this is true, the frequency at 1254 cm^{-1}, which seems strong enough to be considered as a fundamental, cannot be assigned as an E fundamental; and the frequencies at 721 (infra-red) and 686 cm^{-1} (Raman), which are rather too weak to be fundamentals, also cannot be assigned as E or $\bar{E}$ fundamentals. Below 600 cm^{-1}, however, the infra-red spectrum has not been reported and only two Raman lines have been observed, of which one (475 cm^{-1}) must be interpreted as an A_1 fundamental. While all four of the doubly degenerate vibrations are allowed in the Raman spectrum, it must be remembered that since the Raman spectrum was obtained only in CCl_4 solution, there may be dimethyldiacetylene lines at 217, 314, and 459 cm^{-1} where they would be obscured by the CCl_4 lines. Furthermore, it may be that one or more of the E or $\bar{E}$ fundamentals coincides with or is unresolved from the 247 and 475 cm^{-1} Raman lines.

If one assigns the 247 Raman line as an $\bar{E}$ fundamental and assumes that the other $\bar{E}$ fundamental coincides with the 459 cm^{-1} CCl_4 line and that the two E fundamentals coincide with the 217 and 314 CCl_4 lines, then one can interpret the 1254 line as the com-

[10] J. B. Howard, J. Chem. Phys. **5**, 442 (1937).

[11] The system used in numbering the frequencies is that agreed upon by molecular spectroscopists at one of the sessions of the 1948 Symposium on Molecular Structure and Spectroscopy, held at Ohio State University, whereby the largest fundamental frequency of the most symmetrical type is designated ν_1, after which one proceeds in order of decreasing frequency and decreasing symmetry, the smallest frequency of the least symmetrical type being designated ν_n, where n is the number of distinct fundamental frequencies (for the present molecule, $n=20$).

[12] B. L. Crawford, Jr., J. Chem. Phys. **7**, 555 (1939).

bination 217+1030=1247 cm^{-1}, which has the proper symmetry to gain intensity from the 1381 A_1 fundamental by resonance interaction, thus explaining the considerable intensity of the 1254 line. Also, the 686, 721, 1151, 1228, 2502, 2667, and 3270 frequencies can then be best interpreted as the binary combinations 217+475=692, 1030−314=716, 217+941=1158, 217+1020=1237, 2954−459=2495, 2867−217=2650, and 314+2954=3268, respectively; and the infra-red band at 2228 cm^{-1} can be interpreted as the ternary combination 2(957)+314=2228 cm^{-1}. Thus, the assumed fundamentals at 459, 314, and 217 cm^{-1} can be used to give the nearest calculated values for one, three, and five combination frequencies, respectively.

While the existence of fundamentals at 217, 314, and 459 cm^{-1} seems plausible when one considers the similar vibrations in diacetylene and dimethylacetylene, and while the fact that these frequencies can be used to give the best interpretation of nine combination bands is some evidence in favor of their existence, the assumption should be tested by obtaining the Raman spectrum in a solvent other than CCl_4 and by obtaining the infra-red spectrum[13] in the region below 700 cm^{-1}.

Upon the basis of the present information, then, the best values that can be given for the fundamental frequencies of dimethyldiacetylene are those listed in Table II. While these frequencies may be used for tentative calculations of thermodynamical properties, a more reliable determination of these properties must await further work.

Combination Frequencies

All of the observed Raman and infra-red frequencies not previously assigned as fundamentals can be accounted for as binary combinations, as indicated in Table I, except for the Raman line at 2225 cm^{-1} and the infra-red band at 2228 cm^{-1} which must be interpreted as ternary combinations. For all of these frequencies, more than one combination could have been used; the one given in Table I is the one whose value, calculated from the fundamentals listed in Table II, agreed most closely with the observed value. In Table III are given the number of binary or ternary combinations whose calculated frequency fell near the observed frequency, the nearest calculated value, and the mean of the calculated values, since all of these may have contributed to the intensity of the observed band. The numbers given in the parentheses in column two represent the number of combinations that have the proper symmetry for resonance interaction with a nearby fundamental, which would add to the intensity of the observed band, causing it to be stronger than is normal for an overtone or combination band.

While ternary combinations are expected to be less intense than binary combinations in general, the appearance of the ternary combinations at 2225 and 2228 cm^{-1} can be understood when one considers the large number—43 and 40, respectively—of ternary combinations whose calculated frequencies fall near 2226 cm^{-1}. The integrated intensity of all of these could easily give rise to an observable band, especially in view of the fact that several of them have the proper symmetry for resonance interaction with a nearby fundamental. Also, the fact that some of the allowed binary combinations were observed while others were not could be explained in a similar manner.

[13] In the laboratory of the first author, it is planned to obtain in the near future the Raman spectrum of dimethyldiacetylene in benzene solution and the infra-red spectrum in the region 400–700 cm^{-1}; no equipment is available in this laboratory, however, for the infra-red region below 400 cm^{-1}.

ACKNOWLEDGMENTS

One of us (F. F. C.) wishes to express his appreciation to Professor Harald H. Nielsen for making it possible for him to spend the summer of 1947 as Visiting Professor of Physics at the Ohio State University and for placing at his disposal the infra-red equipment needed to secure during that time the data reported in the present paper.

He also wishes to thank Mr. S. M. Ferigle, who is carrying out further investigations on dimethyldiacetylene, for several valuable discussions relative to the assignment of the frequencies.

Another one of us (K. W. G.) wishes to thank Mr. Walter H. Bolinger, Ohio State University, for assistance in the physical property studies on dimethyldiacetylene.

THE JOURNAL OF CHEMICAL PHYSICS VOLUME 18, NUMBER 3 MARCH, 1950

Hindered Rotation in Methyl Alcohol with Note on Ethyl Alcohol

J. O. HALFORD
Department of Chemistry, University of Michigan, Ann Arbor, Michigan
(Received August 24, 1949)

The potential barrier to the internal rotation in methyl alcohol is recalculated from the entropy with the aid of new molecular dimensions generously provided by Burkhard and Dennison. The barrier calculation is examined for temperature dependence and checked for reliability by recalculation with the Clapeyron equation substituted for parts of the data. The result is 1600±700 cal./mole, which includes the new spectroscopic barrier of Burkhard and Dennison at 326 cm^{-1}. Within the range covered by the result, a residual entropy up to 0.50 cal./mole deg. is possible, and the retention of 0.46 e.u. by the crystal is consistent with a reasonable simple assumption about the distribution of hydrogen bonds.

It is suggested, by analogy, that the barrier to the hydroxyl group rotation in ethyl alcohol should be about 1000 cal./mole.

THE height of the potential barrier restricting the internal rotation in methyl alcohol has now been evaluated from the entropy, the heat capacity at ordinary temperatures, the infra-red absorption spectrum and micro-wave data.

The most reliable published value from the entropy is near 2500 cal./mole.[1,2] (870 cm^{-1}). A much lower result (1350) by French and Rasmussen[3] is not acceptable because of the use of a heat of vaporization at room temperature which cannot be aligned in any reasonable way with the accurately known heat of vaporization at the boiling point. A higher barrier (3400) obtained by Crawford[4] from essentially the same data, appears to be the result of an erroneous calculation of the barrier from the entropy of the motion.

Barrier evaluations from the vapor heat capacity are very recent. From data obtained by means of a heat conductivity method, Eucken and Franck[5] found 1800 cal./mole. Rowlinson,[6] however, employed the velocity of supersonic waves to obtain a result near 1300 cal./mole.

All of the above evaluations are based upon essentially the same molecular model and the same normal frequencies for the remaining internal degrees of freedom. Since certain features of the model are gratuitously assumed, this is a possible source of error common to all the evaluations from thermal data. There is a secondary source of error, the effect of deviation from ideal gas behavior, which could be appreciable. The vapor heat capacities have been used over a range of temperatures because the barrier height is a double valued function of heat capacity in which the choice between the alternatives is based upon the temperature variation. None of the evaluations from the entropy, however, has been made over a range of temperatures to see if a single barrier height is consistent with the data at different temperatures.

Koehler and Dennison[7] have used the infra-red absorption data of Borden and Barker[8] and of Lawson and Randall[7] to make an estimate of the barrier height. When calculations of line spacings based upon a preliminary barrier of 770 cm^{-1} (2200 cal./mole) were compared with the data, the estimate was revised downward to 450 cm^{-1} (1300 cal./mole).

Burkhard and Dennison[9] have extended the infra-red observations to lower frequencies, with a resulting barrier estimate of 300 cm^{-1}, and have calculated an accurate barrier, 326 cm^{-1} (932 cal./mole), from microwave data. Thus the correct barrier is considerably less than any value derived from thermal data, showing that some serious error has been made in the calculation of entropy and heat capacity. In addition to the barrier height, Burkhard and Dennison have evaluated the moments of inertia from the data, including the value 1.01×10^{-40} g cm^2 as a close approximation to the moment of the OH group about an axis through the center of gravity of the molecule parallel to the symmetry axis of the methyl group. This is much lower than the value used in any of the previous barrier determinations, and corresponds to a COH angle in the neighborhood of 125°. Although, according to Professor Dennison, this value is still preliminary and, therefore subject to possible change upon further investigation, it will be used to obtain limiting barrier estimates.

In the present paper, the entropy of the internal rotation is recalculated with the new molecular dimensions, and barrier estimates are made from the data and a selected equation of state at a number of temperatures from 273 to 393°K.

From the required experimental data and the chosen equation of state the hypothetical perfect gas entropy can be calculated in four ways because it is possible to substitute the Clapeyron equation for parts of the data.

[1] J. O. Halford and B. Pecherer, J. Chem. Phys. **6**, 571 (1938).
[2] K. S. Pitzer, J. Am. Chem. Soc. **70**, 2140 (1948).
[3] F. A. French and R. S. Rasmussen, J. Chem. Phys. **14**, 389 (1946).
[4] B. L. Crawford, Jr., J. Chem. Phys. **8**, 744 (1940).
[5] A. Eucken and E. U. Franck, Zeits. f. Elektrochemie **52**, 195 (1948).
[6] J. S. Rowlinson, Nature **162**, 820 (1948).
[7] J. S. Koehler and D. M. Dennison, Phys. Rev. **57**, 1006 (1940).
[8] A. Borden and E. F. Barker, J. Chem. Phys. **6**, 553 (1938).
[9] D. G. Burkhard and D. M. Dennison (private communication).

TABLE I. Entropy of translation, rotation, and vibration for methyl alcohol at one atmosphere.

T(°K)	$S_{(t+r)}$	S(vib.)	$S°-S_{rr}$
273.2	54.581	0.138	54.719
293.2	55.143	0.201	55.344
313.2	55.667	0.278	55.945
333.2	56.159	0.370	56.529
353.2	56.623	0.478	57.101
373.2	57.060	0.599	57.659
393.2	57.475	0.729	58.504

TABLE II. Entropy of methyl alcohol vapor at the saturation pressure.

T(°K)	Liquid $S-S_{298.2}$	$\Delta H/T$	ST(vapor) $-S_0$
273.2	−1.625	33.646	62.281
293.2	−0.322	30.706	60.644
313.2	+0.959	28.009	59.228
333.2	2.233	25.509	58.002
353.2	3.511	23.167	56.938
373.2	4.803	20.945	56.008
393.2	6.117	18.816	55.193

The usual calculation uses the experimental heat of vaporization, the vapor pressure and a correction based upon the equation of state for deviation from ideal gas behavior. The heat of vaporization, however, can be calculated from the vapor pressure and the equation of state, a new equation of state can be derived and used, or a new vapor pressure curve can be calculated from the thermal data and the equation of state, provided that one point on the curve is known or assumed. Thus it is possible to set up a trial barrier as a function of the temperature in four ways, and, by comparing the results, to show which data are probably in error and where the true barrier should lie.

If all of the data, including the equation of state, were accurate, the same constant barrier would be obtained at all temperatures by any of the alternative calculations. In this connection it is safe to assume that any anharmonicity effect such as that proposed by Scott, Waddington, Smith, and Huffman[10] for the benzene case is negligible. It is necessary, however, to use the equation of state in the simplified form

$$pV=RT+Bp, \tag{1}$$

in which B is a function of the temperature alone and is evaluated from data taken at constant pressure. If the expression for B is used at other pressures an error will be introduced. The resulting entropy of gas imperfection, pdB/dT, should be nearly correct at low pressures, but will be low at high pressures, as the neglected terms in powers of the pressure become important. Consequently, trial barriers obtained with this form of the equation of state should increase with the temperature.

A qualitative idea of the effect can be obtained from the data for water vapor, for which the deviation entropy has been calculated[11] from the virial coefficients tabulated by Keyes.[12] The deviation volume at the saturation pressure is calculated from the same coefficients and the entropy effect is estimated as pdB/dT. The result is low to an increasing degree with increasing temperature. The effect for methyl alcohol, based upon a single isobar, should be in the same direction but of smaller magnitude. The trial barrier may then be expected to increase, slowly at first, but more rapidly later, with increasing temperature. It is a fair presumption that, if the barrier calculated from a selection of data behaves in this manner, the value obtained at the lowest temperature is near to the correct one.

The sum of the statistical contributions to the perfect gas entropy from all sources except the internal rotation is first calculated. This is subsequently compared with the third law value obtained in several different ways to give the entropy of the internal rotation, which is then translated into the equivalent potential barrier by reference to the tables of Pitzer and Gwinn.[13] The physical constants used throughout the calculations are taken from a circular distributed by the National Bureau of Standards, bearing the date December 31, 1947.

For the rotational entropy of the rigid molecule the product of the principal moments of inertia is required, while the determination of the potential barrier uses the reduced internal moment of inertia. Burkhard and Dennison[9] have evaluated the large principal moment (A) and have obtained a close approximation to the moment of the OH group (C_1) about an axis through the center of gravity parallel to the symmetry axis of the methyl group. The difference between them, $A-C_1=B$ is near to a second principal moment. The moment of inertia of the methyl group (C_2) is taken from the spectroscopic value for the methyl halides. For the present purpose, the effect of the small product of inertia due to the off-center location of the hydroxyl hydrogen is neglected, and the moments are taken as $A=35.1(\times 10^{-40}$ g cm$^2)B=34.1$, $C_1=1.01$, $C_2=5.50$, $C=C_1+C_2=6.51$, and, for the reduced internal moment $C_1C_2/C=0.845$.

The true moment product for the rigid molecule is slightly less than ABC. Also it is probably true that the ratio of two evaluations of Kassel's[14] determinant, respectively with and without the internal rotation, should be used for the internal moment. This ratio is 0.815×10^{-40}, but the larger internal moment is used here because of its prior use in determining the potential barrier. The correct product of principal moments and the lower internal moment would each lead to lower values of the potential barrier.

For the translational and rotational entropy at one

[10] Scott, Waddington, Smith, and Huffman, J. Chem. Phys. **15**, 565 (1947).
[11] J. O. Halford, J. Chem. Phys. **17**, 405 (1949).
[12] F. G. Keyes, J. Chem. Phys. **15**, 611 (1947).
[13] K. S. Pitzer and W. D. Gwinn, J. Chem. Phys. **10**, 428 (1942).
[14] L. S. Kassel, J. Chem. Phys. **4**, 276 (1936).

atmosphere, the equation is

$$S(t+r)=4.516+(\tfrac{3}{2})R\ln M+(\tfrac{1}{2})R\ln ABC+4R\ln T \quad (2)$$

in which M is the molecular weight in grams and A, B and C are moments of inertia in g cm$^2\times10^{38}$.

Vibrational frequencies have been assigned by Borden and Barker[8] and by Noether.[15] The differences introduced by Noether which are pertinent to the present calculation are the substitution, for two degrees of freedom, of the frequencies 1209 and 1260 for 1034 and 1340. The result is a small decrease of the vibrational entropy, relative to the Borden-Barker assignment, and a corresponding increase in the entropy available to the internal rotation. The effect of this increase upon the derived potential barrier is very small relative to other uncertainties. Noether's assignment has been used in the present calculations, merely because it is the later one, although it is not obvious that it is the correct one.

Table I shows, successively, for a range of temperatures, the entropy of translation and rotation, the vibrational entropy and their sum, S^0-S_{rr}, where S_{rr} is the entropy of the restricted rotation. Any error in the last column due to the moments of inertia is constant, while the effect of a wrong frequency will increase with the temperature.

The third law entropy is based upon Kelley's[16] value of 30.26±0.2 cal./mole deg. for the liquid at 298.2°K, which is combined with the heat capacity and heat of vaporization of Fiock, Ginnings, and Holton[17] as shown in Table II. Any correction of Kelley's value called for by the newer physical constants can be neglected. The last column gives the entropy increase above that retained at the absolute zero, S_0.

The correction for deviation from perfect gas behavior is based upon the equation for the second virial coefficient proposed by Eucken and Meyer,[18]

$$B(cc)=80-1.65\times10^{18}/T^6. \quad (3)$$

The gas imperfection entropy in cc atmos./deg. mole is $9.90\times10^{18}p/T^7$. Table III shows the increase of the hypothetical perfect gas entropy above the residual entropy, S_0, at one atmosphere.

TABLE III. Hypothetical perfect gas entropy of methyl alcohol at one atmosphere. (cal/mole deg.)

T(°K)	p(atmos.)	(S^*-S) (E and M)	$R\ln p$	$(S_T^0-S_0)$
273.2	0.0389	0.082	−6.452	55.911
293.2	0.1251	0.161	−4.131	56.674
313.2	0.3427	0.283	−2.128	57.383
333.2	0.8255	0.434	−0.381	58.055
353.2	1.764	0.617	+1.128	58.683
373.2	3.451	0.821	2.461	59.290
393.2	6.252	1.032	3.642	59.867

[15] H. D. Noether, J. Chem. Phys. **10**, 693 (1942).
[16] K. K. Kelley, J. Am. Chem. Soc. **51**, 181 (1929).
[17] Fiock, Ginnings, and Holton, J. Research Nat. Bur. Stand. **6**, 881 (1931).
[18] A. Eucken and L. Meyer, Zeits. f. physik. Chemie **5B**, 452 (1929).

It is unlikely that the vapor pressure will introduce a serious error. Consequently if a trial barrier has the predicted kind of temperature dependence, and the thermal data are accurate, it becomes probable that the deviation correction is accurate enough. This correction is independent of the constant term in Eq. (3).

The difference between the last columns of Tables I and III is $S_{rr}-S_0$. Table IV shows this quantity, together with two sets of trial barriers, for which, respectively, S_0 is assumed to be zero and 0.200. The expression

$$Q_f=2.7935(10^{38}IT)^{\frac{1}{2}}/3 \quad (4)$$

has been used for the partition function of the limiting free rotator. The barriers are subject to error, particularly at the lower temperatures, because they require an extended extrapolation beyond the limits of the entropy table of Pitzer and Gwinn. The writer is fully aware of the factors which determined these limits and of the implications of such an extrapolation. However, for the purpose of seeing in a semi-quantitative way how nearly the entropy-based barrier can be brought to agreement with the spectroscopic one, the adopted procedure should be adequate. In the extrapolation, the attempt was made to choose relations between the variables which would lead to high, rather than low barriers. This difficulty will be removed by calculations, now in progress, of the thermodynamic properties directly from the newly determined molecular constants.

The predicted rise of the trial barriers at high temperatures appears in both sets. There is also a presumably false increase at the lower temperatures which could be due entirely or in part either to the extrapolation or to a fault in the experimental data. Each column shows a minimum, and it becomes probable that the true barrier would be somewhat less than the minimum obtained in a similar calculation with the correct residual entropy.

Further indications of the reliability of the data are now sought with the aid of the Clapeyron equation. The gas imperfection correction is taken, for the first check, from the heat of vaporization and the vapor pressure curve. The resulting trial barrier, for zero residual entropy, starts at 1300 and ends at 2300 after passing through a minimum near 600, and a qualitatively similar situation would appear for other assumed residual entropies. If the heat data are correct, this

TABLE IV. Trial potential barriers for methyl alcohol (cal./mole deg.)

T(°K)	$S_{rr}-S_0$	$1/Q_f$	RT	$V(S_0=0)$	$V(S_0=0.200)$
273.2	1.192	0.7068	542.9	1730	1300
293.2	1.330	0.6823	582.6	1625	1080
313.2	1.438	0.6601	622.4	1630	1060
333.2	1.526	0.6400	662.1	1610	1010
353.2	1.582	0.6216	701.9	1650	1020
373.2	1.631	0.6047	741.6	1710	1090
393.2	1.663	0.5892	781.4	1830	1220

effect must be due to errors in the vapor pressures. It is possible, however, for dp/dT to be responsible without meaning that the pressures themselves are seriously wrong. The slope, in general, is too high, and, if the vapor pressure near the boiling point is assumed to be correct, it follows that the pressures are low at low temperatures and high at high temperatures. Correction for this effect would tend to decrease or eliminate the minima of Table IV, and would support the conclusion that the true barrier should be below the minimum one obtained with the data.

The next check omits the heat of vaporization and uses the vapor pressures and the equation of state. Here the trial barriers start at a low level and decrease with the temperature to the free rotation limit and beyond. The calculation follows the equation

$$S^0-S_l=RTd\ \ln p/dT+(B-V_l)dp/dT +R\ln p+pdB/dT, \quad (5)$$

in which the term containing V_l is negligible. The first term produces an effect in the observed direction, but could hardly be responsible for the extreme results obtained at higher temperatures. Consequently, since the last two terms have been used in preparing Table IV without coming under suspicion, it follows that the constant term in B is mainly responsible for the high entropy. This constant becomes an increasingly important part of the deviation volume with increasing temperature.

A third check can be made by combining the equation of state, the heat of vaporization, the Clapeyron equation and a single vapor pressure at 333.2°K, near the boiling point. The slope of the vapor pressure curve is calculated and new vapor pressures are found by graphical integration. They are not much different from the original vapor pressures and they lead to small decreases in the trial barriers at the lowest temperatures. These barriers are not reliable, however, because, as shown above, the constant term in B is probably inaccurate. If this constant were adjusted to a more reasonable value, the required change in the vapor pressures and the trial barriers would be decreased.

From these checks upon the data no reason appears for changing the conclusion drawn directly from Table IV. The errors revealed by the analysis appear to involve principally dp/dT and the constant term of Eq. (3), neither of which enters directly into the tabulated barrier calculation. The barrier estimate has also been made in the same manner for $C_1=1.4\times10^{-40}$, resulting in $V_0=2200\pm700$ cal. If it becomes necessary to revise C_1 to an intermediate value, it will be accurate enough to obtain the corresponding barrier by linear interpolation between the values given here.

French and Rasmussen[3] obtained a barrier of 1350 cal./mole by selecting from the literature a heat of vaporization favorable to their empirical scheme for predicting potential barriers. If their calculation were repeated with the new moments of inertia the result would be close to the spectroscopic barrier. Their selected heat of vaporization, however, cannot be aligned with that of Fiock, Ginnings, and Holton[17] at the boiling point to give an acceptable temperature variation of the calculated barrier. Since the Fiock, Ginnings, and Holton value at the boiling point checks earlier measurements of high reliability, it follows that the barrier calculation by French and Rasmussen is not a valid one. These authors have stated that the high barrier proposed by Crawford (3400) is due to the use of an older set of fundamental physical constants. Actually, the choice of constants could not affect the derived barrier by much more than 100 cal. Instead, the high result is due to an alternative relation between the entropy and the potential barrier proposed by Crawford. This relation has been disregarded in the present study because Pitzer and Gwinn[13] have stated that their tables are accurate for all molecules described as rigid frameworks with one symmetrical top attached. The writer has studied their theory and method of calculation in enough detail to be convinced that their statement is correct.

From the last column of Table IV it can be concluded that the barrier derived from the entropy will be below 1000 cal. if an error or residual entropy of 0.20 cal./mole deg. can be accounted for. Kelley's[16] estimate of the uncertainty of the liquid entropy (±0.20), combined with other errors to which the calculation is subject, can account for an uncertainty of at least ±0.25. It thus appears at the present writing that the spectroscopic barrier (932 cal.) lies near the lower limit of the range calculable from the entropy with the assumption that there is no retention of entropy by the crystal at the absolute zero. What has appeared heretofore to be a large and puzzling discrepancy becomes in these terms the result of an unfortunate combination of two large errors, one in the experimental data, the other in the molecular dimensions.

The barrier range derived from the entropy, 1600 $\pm$700 cal./mole, emphasizes that very accurate data are necessary for a barrier evaluation by this method. While the range includes the spectroscopic value, it also includes results corresponding to residual entropy at the absolute zero as high as 0.50 cal./mole deg. In the light of Pauling's[19] discussion of hydroxy compounds, including water, which possess entropy due to the random orientation of hydrogen bonds, a similar situation appears probable for methyl alcohol and for other alcohols as well. The crystal could contain units of n molecules arranged in chains or cycles which could assume two alternative forms, consistent with the presumption that each link between hydrogen and oxygen must be one of two kinds and that each atom of the OH groups is attached to its neighbors by two bonds, one of each kind. For this situation, if n is a

[19] L. Pauling, J. Am. Chem. Soc. **57**, 2680 (1935).

fixed constant, the entropy retained in the crystal is $(1/n)R\ln 2$ or $1.38/n$. The maximum deficiency from the data is not far from the value for $n=3$, which, for a cyclic unit, would produce an arrangement exactly like one face of the tetrahedron of the ice structure.

This explanation appeals to the writer as a more probable one than the case for zero retention of entropy.

Quantitative consideration of the vapor heat capacity data will be deferred until this property has been accurately calculated from the molecular constants. The present required extrapolation of the table of Pitzer and Gwinn[13] would introduce too large an uncertainty. Qualitatively, however, it is expected that the new dimensions will cause about the same decrease of the calculated barrier as in the case of the entropy. If this is true, the data of Eucken and Franck[5] will lead to a barrier around 1200 cal./mole, that of Rowlinson[6] to about 700 cal./mole.

Note on Ethyl Alcohol

In a recent analysis of the entropy of ethyl alcohol[20] it was found that, for zero residual entropy, the sum of the barriers opposing the rotation of the methyl and hydroxyl groups was approximately 6000 cal./mole, possibly a little lower. If the situation is like the methyl alcohol case, the true sum could be almost as low as 4000 cal. The arbitrary assignment of 3000 to the methyl group would then leave 1000 for the hydroxyl group, exactly the value derived by Eucken and Franck[5] from the vapor heat capacity.

The writer is indebted to Professor D. M. Dennison and Dr. D. G. Burkhard for permission to use their data and for stimulating discussions of this problem and related questions.

[20] J. O. Halford, J. Chem. Phys. **17**, 111 (1949).

THE JOURNAL OF CHEMICAL PHYSICS VOLUME 18, NUMBER 3 MARCH, 1950

On the Non-Orthogonality Problem Connected with the Use of Atomic Wave Functions in the Theory of Molecules and Crystals

PER-OLOV LÖWDIN
Institute of Mechanics and Mathematical Physics, University of Upsala, Trädgårdsgatan, Upsala, Sweden
(Received August 25, 1949)

The treatment of molecules and crystals by the Heitler-London method or by the collective electron model can be based on the atomic orbitals ϕ_μ of the system. These orbitals are in general overlapping, and the corresponding overlap integrals $S_{\mu\nu}$, given by (1), have almost universally been neglected in the literature as causing undesirable complications. Here we will take these overlap integrals into consideration and show that they, instead of being negligible, are of essential importance in molecules and in crystals. The problem is simply solved by considering the orthonormalized functions φ_μ, given by (21), as the real atomic orbitals. The solution is worked out in detail for (I) the molecular orbital method of treating molecules, (II) the Bloch orbital method of treating crystals, and (III) the Heitler-London method of treating both these systems in some simple spin cases. Some numerical applications are given for ionic crystals, showing that the overlap effects are responsible for all the repulsive forces in these solids. It is also shown that the overlapping adds interesting new features to the properties of molecules and crystals, namely the "many-orbital-effects," corresponding to certain "many-body-forces" in ionic solids.

I. INTRODUCTION

IN treating the properties of molecules and crystals (metals, ionic solids, etc.) by means of quantum mechanics two principal methods have been developed: the Heitler-London method using atomic orbitals (*AO*), and the collective electron model using molecular orbitals (*MO*) for the molecules and Bloch orbitals (*BO*) for the crystals. Even in the latter case the *MO* and the *BO* could be constructed by "linear combination of atomic orbitals" (*LCAO*), and hence the *AO* can constitute the starting point in both methods.

For the sake of simplicity we assume from the beginning that the atomic nuclei in the molecules and crystals under consideration have fixed positions. This means that we confine ourselves to the case of absolute zero of temperature and neglect the zero-point vibrations. Each *AO* is associated with an atomic nucleus and, if these nuclei are not too far from each other, the *AO* are then overlapping.

Let $\phi_\mu(\mu=1, 2, \cdots n)$ denote the complex or real atomic orbitals, which here are functions only of a space vector $\mathbf{r}$; the spin being excluded. They may be normalized, so that $\int \phi_\mu^* \phi_\mu d\tau = 1$, where $d\tau$ is the volume element, and the integration is to be carried out over the whole space. Then we define the "overlap integrals" by

$$S_{\mu\nu} = \int \phi_\mu^* \phi_\nu d\tau - \delta_{\mu\nu}, \tag{1}$$

with $S_{\mu\mu}=0$. These integrals are often small compared to unity, and, excepting some simple special cases, they have almost universally been neglected in the literature as causing undesirable complications. The existence of an overlapping problem has been pointed out by many

authors, e.g. Slater,[1] Inglis,[2] Van Vleck,[3,4] but a complete treatment, including the Heitler-London method as well as the collective electron model, has up till now not been given. The purpose of this paper is to develop a simple method of taking the overlap integrals into consideration. We wish to emphasize that the overlap effects, instead of being negligible, are often of essential importance for the properties of molecules and crystals.

II. CONSTRUCTION OF MOLECULAR ORBITALS

Let us first consider a molecule by means of the method of molecular orbitals developed by Lennard-Jones, Hund, Mulliken, and others. In this theory the overlap integrals have been taken into account in a few cases: e.g. for some unsaturated and aromatic molecules by Wheland,[5] for graphite by Bradburn, Coulson, and Rushbrooke,[6] and for the linear chain by Hoffmann and Kónya.[7] In some of his papers Mulliken[8] and his collaborators have also retained the S-integrals. A more complete treatment of the problem has recently been given by Chirgwin and Coulson[9] in connection with the theory of conjugated systems developed by Coulson and Longuet-Higgins,[10] and this paper will be discussed in greater detail below.

Let H_{op} be the *effective* Hamiltonian operator for one electron of the system, moving in the self-consistent field of the nuclei and the other electrons, with the matrix elements

$$H_{\mu\nu}=\int \phi_\mu^* H_{op}\phi_\nu d\tau, \tag{2}$$

with respect to the given AO. In the following we will denote matrices by the corresponding black type letters, and further we let $\mathbf{A}\dagger$ denote the hermitean adjointof $\mathbf{A}$, so that $A_{\mu\nu}\dagger=A_{\nu\mu}^*$. We note that the matrices $\mathbf{H}$ and $\mathbf{S}$, formed by the elements $H_{\mu\nu}$ and $S_{\mu\nu}$, are self-adjoint.

The molecular orbitals ψ_j $(j=1, 2, \cdots n)$ may be formed by linear combinations of the AO

$$\psi_j=\sum_{\mu=1}^{n}\phi_\mu x_{\mu j}, \tag{3}$$

where the coefficients $x_{\mu j}$ are determined by the conditions

$$E=\int \psi_j^* H_{op}\psi_j d\tau=\text{extreme value}, \tag{4}$$

$$\int \psi_j^*\psi_j d\tau=1. \tag{5}$$

The Eqs. (4) and (5) are equivalent to the n secular equations

$$\sum_{\nu=1}^{n} H_{\mu\nu}x_{\nu j}=\sum_{\nu=1}^{n}(\delta_{\mu\nu}+S_{\mu\nu})x_{\nu j}E_j, \tag{6}$$

$$\sum_{\mu\nu} x_{\mu j}^*(\delta_{\mu\nu}+S_{\mu\nu})x_{\nu j}=1. \tag{7}$$

which also can be written in the matrix form

$$\mathbf{Hx}=(\mathbf{1}+\mathbf{S})\mathbf{xE}, \tag{8}$$

$$\mathbf{x}\dagger(\mathbf{1}+\mathbf{S})\mathbf{x}=\mathbf{1}. \tag{9}$$

Here $\mathbf{x}$ and $\mathbf{E}$ are the matrices formed by the elements $x_{\mu j}$ and the diagonal elements E_j, respectively. Equation (9) is obtained by joining the normalization condition (7) with the orthogonality theorem, which is a consequence of (6) and the hermitean character of $\mathbf{H}$ and $\mathbf{S}$. The fundamental Eqs. (8) and (9) can now be essentially simplified by introducing the substitution

$$\mathbf{x}=(\mathbf{1}+\mathbf{S})^{-\frac{1}{2}}\mathbf{C}, \tag{10}$$

where $(\mathbf{1}+\mathbf{S})^{-\frac{1}{2}}$ means the matrix[11]

$$(\mathbf{1}+\mathbf{S})^{-\frac{1}{2}}=\mathbf{1}-\tfrac{1}{2}\mathbf{S}+\tfrac{3}{8}\mathbf{S}^2-\tfrac{5}{16}\mathbf{S}^3+-\cdots; \tag{11}$$

with the elements

$$(\mathbf{1}+\mathbf{S})_{\mu\nu}{}^{-\frac{1}{2}}=\delta_{\mu\nu}-\tfrac{1}{2}S_{\mu\nu}+\tfrac{3}{8}\sum_\alpha S_{\mu\alpha}S_{\alpha\nu}-\tfrac{5}{16}\sum_{\alpha\beta}S_{\mu\alpha}S_{\alpha\beta}S_{\beta\nu}+-\cdots.$$

Instead of (8) and (9) we now obtain

$$\mathbf{H}'\mathbf{C}=\mathbf{CE}, \quad \mathbf{C}\dagger\mathbf{C}=\mathbf{1}; \tag{12}$$

$$\mathbf{H}'=(\mathbf{1}+\mathbf{S})^{-\frac{1}{2}}\mathbf{H}(\mathbf{1}+\mathbf{S})^{-\frac{1}{2}}. \tag{13}$$

Hence the following theorem is valid: *The problem of solving the secular equations including the overlap integrals $S_{\mu\nu}$ can be reduced to the same form as it has in the simplified theory* ($\mathbf{S}$ *neglected*) *if the matrix* $\mathbf{H}$ *is replaced by the matrix* (*13*). This new matrix $\mathbf{H}'$ is also self-adjoint and can be expanded in the form

$$H_{\mu\nu}'=H_{\mu\nu}-\tfrac{1}{2}\sum_\alpha(S_{\mu\alpha}H_{\alpha\nu}+H_{\mu\alpha}S_{\alpha\nu})+\tfrac{3}{8}\sum_{\alpha\beta}(S_{\mu\alpha}S_{\alpha\beta}H_{\beta\nu}+\tfrac{2}{3}S_{\mu\alpha}H_{\alpha\beta}S_{\beta\nu}+H_{\mu\alpha}S_{\alpha\beta}S_{\beta\nu})-+\cdots. \tag{14}$$

[1] J. C. Slater, Phys. Rev. **35**, 509 (1930).
[2] D. R. Inglis, Phys. Rev. **46**, 135 (1934).
[3] J. H. Van Vleck and A. Sherman, Rev. Mod. Phys. **7**, 167 (1935).
[4] J. H. Van Vleck, Phys. Rev. **49**, 232 (1936).
[5] G. W. Wheland, J. Am. Chem. Soc. **63**, 2025 (1941).
[6] M. Bradburn, C. A. Coulson and G. S. Rushbrooke, Proc. Roy. Soc. (Edinb.) **62**, 336 (1948); C. A. Coulson and G. S. Rushbrooke, *ibid.*, **62**, 350 (1948).
[7] T. A. Hoffmann, and A. Kónya, J. Chem. Phys. **16**, 1172 (1948).
[8] See e.g. R. S. Mulliken, C. A. Rieke and W. G. Brown, J. Am. Chem. Soc. **63**, 41 (1941); R. S. Mulliken and C. A. Rieke, *ibid.* **63**, 1770 (1941); R. S. Mulliken, Phys. Rev. **74**, 736 (1948).
[9] B. H. Chirgwin and C. A. Coulson (in press). The author is indebted to them for the privilege of reading their manuscript before publication.
[10] C. A. Coulson and H. C. Longuet-Higgins, Proc. Roy. Soc. **A191**, 39; **192**, 16 (1947); **193**, 447 (1948); **193**, 456 (1948); **195**, 188 (1948).
[11] A more general definition of the matrix $(\mathbf{1}+\mathbf{S})^{-\frac{1}{2}}$ can be given by the methods developed in P. A. M. Dirac, *Quantum Mechanics* (Oxford University Press, New York, 1947), 3rd edition p. 41.

We can easily obtain the same result in another way, which at once gives an interpretation of the elements $H_{\mu\nu}'$. The *MO* ψ_j are formed from the *AO* by linear combinations, but in order to avoid the non-orthogonality difficulty we now first construct an orthonormalized set φ_μ from the set ϕ_μ, and then we build up our molecular orbitals with the aid of these new functions. Let $\boldsymbol{\phi}$, $\boldsymbol{\varphi}$, and $\boldsymbol{\psi}$ denote the row matrices of order n formed by the elements ϕ_μ, φ_μ, and ψ_j, respectively. It is easily verified by using (1) that the functions φ_μ given by the matrix relations

$$\boldsymbol{\varphi}=\boldsymbol{\phi}(1+\mathbf{S})^{-\frac{1}{2}}, \tag{15}$$

or

$$\varphi_\mu=\phi_\mu-\tfrac{1}{2}\sum_\alpha \phi_\alpha S_{\alpha\mu}+\tfrac{3}{8}\sum_{\alpha\beta}\phi_\alpha S_{\alpha\beta}S_{\beta\mu}-+\cdots, \tag{16}$$

are normalized and orthogonalized, i.e., that

$$\int \varphi_\mu^*\varphi_\nu d\tau=\delta_{\mu\nu} \tag{17}$$

The functions (16) seem to have been first introduced in a paper[12] by the author concerning the overlap effects in ionic solids. By means of these functions, it is then easy to construct the *MO* in the usual way. According to (3), (10), and (15) we now get

$$\boldsymbol{\psi}=\boldsymbol{\phi}\mathbf{x}=\boldsymbol{\phi}(1+\mathbf{S})^{-\frac{1}{2}}\mathbf{C}=\boldsymbol{\varphi}\mathbf{C}, \tag{18}$$

or

$$\psi_j=\sum_{\mu=1}^{n}\varphi_\mu C_{\mu j}. \tag{19}$$

Using (13) and (15) we further obtain

$$H_{\mu\nu}'=\int \varphi_\mu^* H_{op}\varphi_\nu d\tau, \tag{20}$$

i.e. that $H_{\mu\nu}'$ are the matrix elements with regard to the functions φ_μ. Since (19) also shows that $C_{\mu j}$ are the expansion coefficients with respect to the same functions, we get the following result: *The solution of the problem of constructing the molecular orbitals, when taking the overlap integrals into consideration, is the same as if we consider the orthonormalized functions*

$$\varphi_\mu=\phi_\mu-\tfrac{1}{2}\sum_\alpha \phi_\alpha S_{\alpha\mu}+\tfrac{3}{8}\sum_{\alpha\beta}\phi_\alpha S_{\alpha\beta}S_{\beta\mu}-+\cdots \tag{21}$$

as the real atomic orbitals.

We note that the functions φ_μ are reduced to the usual *AO* ϕ_μ when the distances between the atoms increase, but that these orbitals are essentially deformed when the overlap is appreciable.[13]

[12] P. O. Löwdin, Arkiv f. mat., astr. o. fysik, **35A**, 9 (1947). The first two terms and a part of the third term of (16) were given by R. Landshoff, Zeits. f. Physik **102**, 201 (1936). See also G. H. Wannier, Phys. Rev. **52**, 191 (1937), who has the first two terms.

[13] This property of the functions φ_μ makes it also probable that they are fit for use—at least to a certain degree of approximation—in treating the "ionized states" in the Heitler-London-Slater-Pauling theory of resonance valency.

Calculation of the Expansion Coefficients

Now we will consider the problem of calculating $\mathbf{C}$ in the case when the corresponding $\mathbf{C}_0$ for the simplified theory ($\mathbf{S}$ neglected) is already known. We have

$$\mathbf{HC}_0=\mathbf{C}_0\mathbf{E}_0, \quad \mathbf{C}_0\dagger\mathbf{C}_0=\mathbf{C}_0\mathbf{C}_0\dagger=\mathbf{1} \tag{22}$$

and

$$\mathbf{C}_0\dagger\mathbf{HC}_0=\mathbf{E}_0, \tag{23}$$

where $\mathbf{E}_0$ is the diagonal matrix formed by the elements ϵ_j, which are the characteristic numbers of the matrix $\mathbf{H}$. In the following we will use the theory of unitary transformations of matrices. Let us first introduce the new matrix

$$\mathbf{s}=\mathbf{C}_0\dagger\mathbf{SC}_0. \tag{24}$$

The matrix Eq. (12) can then by the substitution

$$\mathbf{C}=\mathbf{C}_0\mathbf{Q} \tag{25}$$

be put into the form

$$(\mathbf{1}+\mathbf{s})^{-\frac{1}{2}}\mathbf{E}_0(\mathbf{1}+\mathbf{s})^{-\frac{1}{2}}\mathbf{Q}=\mathbf{QE}, \tag{26}$$

$$\mathbf{Q}\dagger\mathbf{Q}=\mathbf{QQ}\dagger=\mathbf{1}. \tag{27}$$

For the further development it is convenient to distinguish between two cases:

(i) *The matrix* $\mathbf{S}$ *commutes with the matrix* $\mathbf{H}$. This important case has been treated in considerable detail by Chirgwin and Coulson,[9] but still the result obtained by the matrix method used here seem to be more surveyable and general. Now $\mathbf{S}$ can be expressed as a function of $\mathbf{H}$, and we assume that this function,[14] $\mathbf{S}=f(\mathbf{H})$, is of a simple polynomial type or can be expanded in a series of positive (and eventually negative) powers of $\mathbf{H}$. Using (24) and general theorems concerning unitary transformations we immediately obtain

$$\mathbf{S}=f(\mathbf{H}), \quad \mathbf{s}=f(\mathbf{E}_0), \quad s_j=f(\epsilon_j). \tag{28}$$

We note that $\mathbf{s}$ here is a *diagonal matrix* formed by the elements s_{jj} $(=s_j)$. The relations (13) and (14) can now be simplified:

$$\mathbf{H}'=(\mathbf{1}+\mathbf{S})^{-1}\mathbf{H}=\mathbf{H}(\mathbf{1}+\mathbf{S})^{-1}, \tag{29}$$

$$H_{\mu\nu}'=H_{\mu\nu}-\sum_\alpha H_{\mu\alpha}S_{\alpha\nu}+\sum_{\alpha\beta}H_{\mu\alpha}S_{\alpha\beta}S_{\beta\nu}-+\cdots. \tag{30}$$

The Eq. (26) has the solution $\mathbf{Q}=\mathbf{1}$, $\mathbf{C}=\mathbf{C}_0$, and we note that the necessary and sufficient condition for the existence of this solution is that $\mathbf{s}$ is a diagonal matrix, i.e. that $\mathbf{S}$ commutes with $\mathbf{H}$—as has already been found by Chirgwin and Coulson in another way.

If F denotes an arbitrary polynomial or power series function, we get, by using (10), (24), and the laws of unitary transformations, that

$$F(\mathbf{S})\mathbf{C}=\mathbf{C}F(\mathbf{s}), \quad F(\mathbf{S})\mathbf{x}=\mathbf{x}F(\mathbf{s}). \tag{31}$$

According to (10), (18), (25), and (26), we then obtain

[14] Wheland, Chirgwin, and Coulson and others have been mainly interested in the case of a linear connection between $\mathbf{S}$ and $\mathbf{H}$.

the matrix relations

$$\begin{aligned} \mathbf{C}&=\mathbf{C}_0, & \mathbf{x}&=\mathbf{C}(1+\mathbf{s})^{-\frac{1}{2}},\\ \mathbf{E}&=\mathbf{E}_0(1+\mathbf{s})^{-1}, & \boldsymbol{\psi}&=\boldsymbol{\phi}\mathbf{C}(1+\mathbf{s})^{-\frac{1}{2}}, \end{aligned} \tag{32}$$

or in components

$$C_{\mu j}=(C_0)_{\mu j},\quad x_{\mu j}=\frac{C_{\mu j}}{(1+s_j)^{\frac{1}{2}}},$$

$$E_j=\frac{\epsilon_j}{1+s_j},\quad \psi_j=(1+s_j)^{-\frac{1}{2}}\sum_\mu \phi_\mu C_{\mu j}. \tag{33}$$

The relation for the energy E_j in (33) can be considered as a generalization of the expressions found by Wheland[5] and Chirgwin-Coulson[9] for the case of a linear connection between **S** and **H**. The formula for ψ_j shows that the *MO* obtained in the simplified theory (**S** neglected) are quite correct but for a normalization constant $(1+s_j)^{-\frac{1}{2}}$ depending on the overlapping.

(ii) *The matrix* **S** *does not commute with the matrix* **H**. If the non-diagonal elements of the matrix **s** are very small, it will often be convenient to solve the Eq. (26) by the usual perturbation theory, treating

$$\mathbf{V}=(1+\mathbf{s})^{-\frac{1}{2}}\mathbf{E}_0(1+\mathbf{s})^{-\frac{1}{2}}-\mathbf{E}_0 \tag{34}$$

as the perturbation and $\mathbf{E}_0$ as the unperturbed matrix. The formulas needed may be put up without difficulties. If the non-diagonal elements of **s** are not so small, it seems better to solve the secular Eqs. (12) directly. We will therefore finish this part with a more detailed investigation of the matrix elements $H_{\mu\nu}'$.

Treatment of the Matrix H'

The fundamental matrix $H_{\mu\nu}'$ has been naturally introduced into the theory by considering the orthonormalized functions φ_μ given by (16) as the real atomic orbitals. The matrix $\mathbf{H}'$ is *self-adjoint* $(H_{\mu\nu}'^*=H_{\nu\mu}')$ and for real atomic orbitals this gives the simple symmetry relation

$$H_{\mu\nu}'=H_{\nu\mu}', \tag{35}$$

which is of importance for the interpretation of the theory.

Another property of $\mathbf{H}'$ may also be emphasized. From the expansion (14) we can see that $H_{\mu\nu}'$ depends on the *AO* ϕ_μ and ϕ_ν, but also on all the other atomic orbitals $\phi_\alpha(\alpha=1, 2, \cdots n)$ of the system. Hence the quantities $H_{\mu\nu}'$ have a certain *many-orbital-character* arising from the overlapping of the *AO* of the free atoms. The author has pointed out the importance of such "many-orbital-effects" in some earlier papers,[15,16] where it was shown that these effects could be considered responsible for the well-known failure of the Cauchy relations for the elastic constants in ionic crystal. More details about this question will be given in the later part of this paper.

[15] P. O. Löwdin, Arkiv f. mat., astr. o. fysik, **35A**, 30 (1948).

[16] P. O. Löwdin, *A Theoretical Investigation into Some Properties of Ionic Crystals* (thesis) (Almquist & Wicksell, Uppsala, 1948).

Here we will also show a transformation property of $\mathbf{H}'$. The effective Hamiltonian operator H_{op}, belonging to the system under consideration, contains various electrostatic potentials having zero-points which may be chosen arbitrarily. Changing the zero-point of H_{op} totally by an amount k we get the transformation

$$H_{op}\rightarrow H_{op}+k. \tag{36}$$

All energy quantities of the system, which are dependent on this zero-point, must then have the same change, whereas all other physical quantities must be *invariant*. Using (1), (2), and (36) we now immediately obtain

$$\mathbf{H}\rightarrow\mathbf{H}+k(1+\mathbf{S}), \tag{37}$$

which shows that H cannot possibly have a direct physical interpretation. On the other hand, we get for our matrix $\mathbf{H}'$:

$$\mathbf{H}'\rightarrow\mathbf{H}'+k\cdot\mathbf{1}, \tag{38}$$

or

$$H_{\mu\mu}'\rightarrow H_{\mu\mu}'+k,\quad H_{\mu\nu}'\rightarrow H_{\mu\nu}'\ (\mu\neq\nu), \tag{39}$$

which means that the diagonal elements are changed by k and that the non-diagonal elements are invariant. The hermitean character of $\mathbf{H}'$ and the transformation property (38) therefore show that it is possible that $\mathbf{H}'$ has a direct physical significance, i.e. that there exist some close connections between the elements $H_{\mu\nu}'$ and experimentally determined quantities.

Let us now introduce the notations

$$H_{\mu\mu}=\alpha_\mu,\quad H_{\mu\nu}=\beta_{\mu\nu}\ (\mu\neq\nu), \tag{40}$$

$$H_{\mu\nu}-H_{\mu\mu}S_{\mu\nu}=\gamma_{\mu\nu}\ (\mu\neq\nu). \tag{41}$$

Here $\gamma_{\mu\nu}$ is a generalization of the quantity γ originally introduced by Mulliken-Rieke-Brown[8] in 1941. The importance of this quantity has later been stressed by several authors. Using (37) we get

$$\alpha_\mu\rightarrow\alpha_\mu+k,\quad \beta_{\mu\nu}\rightarrow\beta_{\mu\nu}+kS_{\mu\nu}, \tag{42}$$

$$\gamma_{\mu\nu}\rightarrow\gamma_{\mu\nu}. \tag{43}$$

Here we emphasize that $\gamma_{\mu\nu}$ is invariant, and, as far as the author knows, this transformation property has never been pointed out before. Because of (42) and (43) it seems convenient to express the matrix $\mathbf{H}'$ only in terms of the quantities α_μ and $\gamma_{\mu\nu}$. Starting from the expression (13) and using the identity $(1+\mathbf{S})^{-\frac{1}{2}}\equiv(1+\mathbf{S})^{+\frac{1}{2}}-\mathbf{S}(1+\mathbf{S})^{-\frac{1}{2}}$, we easily derive the formula

$$H_{\mu\nu}'=\sum_\kappa\{(1+\mathbf{S})^{-\frac{1}{2}}{}_{\mu\kappa}\alpha_\kappa(1+\mathbf{S})^{+\frac{1}{2}}{}_{\kappa\nu}+\sum_{\lambda\neq\kappa}(1+\mathbf{S})^{-\frac{1}{2}}{}_{\mu\kappa}\gamma_{\kappa\lambda}(1+\mathbf{S})^{-\frac{1}{2}}{}_{\lambda\nu}\}. \tag{44}$$

In the special case(i) when **S** commutes with **H**, we start instead from (29) and by using the identity $(1+\mathbf{S})^{-1}\equiv\mathbf{1}-\mathbf{S}(1+\mathbf{S})^{-1}$ we get the result

$$H_{\mu\nu}'=\alpha_\mu\delta_{\mu\nu}+\sum_{\kappa\neq\mu}\gamma_{\mu\kappa}(1+\mathbf{S})^{-1}{}_{\kappa\nu}. \tag{45}$$

For small **S** the formulas (44) and (45) are very convenient for numerical computations, and in the case of (44) the result can be checked by the transformation property of **H′** given by (39). As examples we have calculated the matrix $H_{\mu\nu}'$ for butadiene and benzene; considering only the interaction between nearest neighbors and taking $S=0.25$, we have got the same result as given by Chirgwin and Coulson in another way.

Applications to the Theory of Conjugated Systems

The conjugated system has been investigated by many authors, but here we will follow the treatment given in a series of papers by Coulson and Longuet-Higgins.[10] For the simplified theory (**S** neglected) they have introduced some useful concepts, as charge density, bond order, and polarizabilities, and now we will show how it is possible to generalize these concepts even to the more general theory with the overlap effects taken into account. The total energy ϵ of the mobile electrons (π-electrons) is in the usual approximation given by

$$\mathcal{E}=\sum_{j=1}^{m} n_j E_j, \tag{46}$$

where we have to sum over all occupied *MO* ($j=1, 2, \cdots m$), and n_j is the number of electrons in the jth orbital. By using (4) and (18) we obtain

$$E_j=\int \psi_j^* H_{op}\psi_j d\tau=(\mathbf{C}\dagger\mathbf{H}'\mathbf{C})_{jj}, \tag{47}$$

$$\mathcal{E}=\sum_{j=1}^{m}\sum_{\alpha,\beta=1}^{n} n_j C_{j\alpha}\dagger H_{\alpha\beta}' C_{\beta j}.$$

Now we define a new matrix **P** by the relation

$$P_{\mu\nu}=\frac{\partial \mathcal{E}}{\partial H_{\mu\nu}'}, \tag{48}$$

where we assume that all elements $H_{\mu\nu}'$ are formally independently varied. If we consider only real functions ϕ_μ and employ the symmetry relation (35), we must replace (48) by the two equations

$$P_{\mu\mu}=\frac{\partial \mathcal{E}}{\partial H_{\mu\mu}'}, \quad P_{\mu\nu}=\frac{1}{2}\frac{\partial \mathcal{E}}{\partial H_{\mu\nu}'} \ (\mu\neq\nu). \tag{49}$$

Using the condition (4), giving $\partial\epsilon/\partial C_{\mu j}=0$, we have at once from (48) that

$$P_{\mu\nu}=\sum_{j=1}^{m} n_j C_{j\mu}\dagger C_{\nu j}=\sum_{j=1}^{m} n_j C_{\mu j}^* C_{\nu j}, \tag{50}$$

and for real functions

$$P_{\mu\nu}=\sum_{j=1}^{m} n_j C_{\mu j} C_{\nu j}. \tag{51}$$

Here **P** is in general a self-adjoint matrix. In the following we will denote $P_{\mu\mu}$ as the charge density of the π-electrons at the atom μ, and $P_{\mu\nu}(\mu\neq\nu)$ as the total mobile order of the bond $\mu-\nu$, noting that both quantities include many-orbital effects. Using the formulas (19) and (20) in Coulson and Longuet-Higgins (reference 10, Part I), we find that these concepts may be considered as convenient generalizations of the corresponding quantities of the simplified theory (**S** neglected), for in the case **S**$\rightarrow$**0** they are reduced to q_μ and $p_{\mu\nu}$, respectively.

Since $C_{\mu j}$ are the coefficients of the *MO* ψ_j in their expansions (19) with regard to φ_μ, we can also give another simple interpretation of the matrix **P**: The quantities $P_{\mu\mu}$ and $P_{\mu\nu}(\mu\neq\nu)$ constitute the charge densities and the bond orders in the sense of Coulson and Longuet-Higgins, if the orthonormalized functions φ_μ given by (21) are considered as the real atomic orbitals.

This result is in complete agreement with the theorem found on page 367, and it indicates the simplest way of transforming concepts from the simplified theory to the more general one including overlap effects. Hence the latter can be treated without further complications. All the theorems, for instance the useful integral formulas and the equations for the polarizabilities given by Coulson and Longuet-Higgins, are still valid: *One has only to replace the matrix $H_{\mu\nu}$ with the new matrix $H_{\mu\nu}'$ in the fundamental secular determinant, and then to employ the characteristic values E_j and the expansion coefficients $C_{\mu j}$ derived from this determinant.*

The Connection with the Theory of Chirgwin and Coulson

Here we have also to investigate the connection between our theory and the treatment of the overlap effects given by Chirgwin and Coulson.[9] Their theory is based on a "mixed tensor" $H_\mu{}^\nu$, which in our notations has the form $(\mathbf{1}+\mathbf{S})^{-1}\mathbf{H}$, and they define the new charge densities q_μ and bond orders $p_{\mu\nu}$ by

$$q_\mu=\sum_{j=1}^{m} n_j x_{\mu j} y_{\mu j},$$

$$p_{\mu\nu}=\frac{1}{2}\sum_{j=1}^{m} n_j(x_{\mu j}y_{\nu j}+x_{\nu j}y_{\mu j}), \tag{52}$$

where **y** is the matrix $\mathbf{y}=(\mathbf{1}+\mathbf{S})\mathbf{x}$. At first we consider the case (i) when **S** commutes with **H**. The relations (29) immediately show that the "mixed tensor" $H_\mu{}^\nu$ is now identical with our matrix **H′**; further we obtain, by using (31) and (33), that

$$x_{\mu j}=\frac{C_{\mu j}}{(1+s_j)^{\frac{1}{2}}}, \quad y_{\nu j}=C_{\nu j}(1+s_j)^{\frac{1}{2}},$$

$$x_{\mu j}y_{\nu j}=C_{\mu j}C_{\nu j}, \tag{53}$$

which shows that their definitions of charge densities

and bond orders are in agreement with ours. In this case both theories seem to give identical results.

In the general case (ii) when **S** and **H** do not commute, the circumstances are, however, quite different. Instead of our simple generalization, based on the concept that the orthonormalized functions φ_μ are the real atomic orbitals, Chirgwin and Coulson have a considerable work to carry out e.g. new formulas of the integral type and new equations for the polarizabilities. These complications seem to be closely connected with the fact that their "mixed tensor" $H_\mu{}^\nu$ has lost the fundamental symmetry property, i.e. that $H_\mu{}^\nu \neq H_\nu{}^\mu$ for real *AO*. For complex atomic orbitals, $H_\mu{}^\nu$ has a *non-hermitean* character which, of course, renders the physical interpretations more difficult. We note that no such complications occur in our treatment of the problem.

Even if the theory by Chirgwin and Coulson treats the simple case (i) in a very good way, our theory seems therefore to have considerable advantages in the general case (ii), for instance as regards the applications to heteromolecules.

III. CONSTRUCTION OF BLOCH ORBITALS IN A CRYSTAL

Let us now consider a crystal, where the atomic nuclei have fixed positions, forming a perfect and infinite lattice. The construction of crystal orbitals $\chi(\mathbf{r})$ by *LCAO* was first given by Bloch,[17] but, since he neglected all overlap-effects, we will here take up the problem again, taking these effects into full account. There is a close connection between the theory of Bloch orbitals and the theory of molecular orbitals, and in order to examine this in greater detail, we will again use the variation principle.[18] However, there is a slight complication, since the integrals (4) and (5) over the whole space, in the following indicated by (∞), are divergent for an infinite crystal. They have therefore to be replaced by integrals over a cyclic domain—the microcrystal—denoted by (G), which is defined below. The fundamental conditions for the *BO* then have the form

$$E=\int_{(G)} \chi^* H_{op}\chi d\tau = \text{extreme value}, \tag{54}$$

$$\int_{(G)} \chi^*\chi d\tau = 1. \tag{55}$$

For the sake of simplicity we will at first assume that only *one* atomic orbital is associated with each nucleus. Let $\phi_\mu=\phi(\mathbf{r}-\mathbf{\mu})$ be the normalized *AO* connected with the nucleus at the lattice point $\mathbf{\mu}=\mu_1\mathbf{a}_1+\mu_2\mathbf{a}_2+\mu_3\mathbf{a}_3$, where $\mathbf{a}_1$, $\mathbf{a}_2$, $\mathbf{a}_3$ are the basic vectors of the space lattice and μ_1, μ_2, μ_3 are integers between $-\infty$ and $+\infty$. The microcrystal is then defined by the Born-von Karman boundary condition

$$\chi(\mathbf{r}+G\mathbf{a}_\kappa)=\chi(\mathbf{r}), \quad \kappa=1, 2, 3 \tag{56}$$

where G is a very large integer. At the same time we introduce the ordinary **k**-vectors,

$$\mathbf{k}=(1/G)(k_1\mathbf{b}_1+k_2\mathbf{b}_2+k_3\mathbf{b}_3), \tag{57}$$

where $\mathbf{b}_1$, $\mathbf{b}_2$, $\mathbf{b}_3$ are the basic vectors of the reciprocal lattice, and k_1, k_2, k_3 are integers. In summations over the lattice points $\mathbf{\mu}$ and **k** in the ordinary space and the **k**-space, respectively, we let an index (∞) denote a summation over *all* lattice points and an index (G) a summation only over the *ground points*, i.e. the G^3 lattice points of each type, satisfying the condition

$$-\frac{G}{2}\leq\mu_\kappa<+\frac{G}{2}, \quad -\frac{G}{2}\leq k_\kappa<+\frac{G}{2}, \quad \kappa=1, 2, 3. \tag{58}$$

In order to take the overlap effects into consideration from the beginning, we start from the *orthonormalized AO*:[19]

$$\varphi_\mu=\phi_\mu-\tfrac{1}{2}\sum_\alpha^{(\infty)}\phi_\alpha S_{\alpha\mu}+\tfrac{3}{8}\sum_{\alpha\beta}^{(\infty)}\phi_\alpha S_{\alpha\beta}S_{\beta\mu}-+\cdots, \tag{59}$$

where S are the usual overlap integrals

$$S_{\mu\nu}=\int_{(\infty)}\phi_\mu{}^*\phi_\nu d\tau-\delta_{\mu\nu}, \tag{60}$$

and the indices μ, ν, α, β, k, $\cdots$ correspond to the vectors $\mathbf{\mu}$, $\mathbf{\nu}$, $\mathbf{\alpha}$, $\mathbf{\beta}$, $\mathbf{k}$, $\cdots$, respectively. Then we construct our *BO* by means of *LCAO*:

$$\chi_k=\sum_\mu^{(\infty)}\varphi_\mu C_{\mu k}, \tag{61}$$

where the coefficients $C_{\mu k}$ according to (56) satisfy the periodicity condition

$$C_{\mu+a\mathbf{G}_\kappa,k}=C_{\mu,k} \quad \kappa=1, 2, 3. \tag{62}$$

For each operator F, having the periodicity of the crystal, we obtain after some simple reductions the useful identity

$$\int_{(G)}\chi_k{}^*F_{op}\chi_{k'}d\tau=\sum_{\mu\nu}^{(G)}C_{k\mu}\dagger\bar{F}_{\mu\nu}{}'C_{\nu k'}, \tag{63}$$

$$\bar{F}_{\mu\nu}{}'=\sum_\lambda^{(\infty)}F_{\mu,\nu+G\lambda}{}'=\sum_\gamma^{(\infty)}\int_{(\infty)}\varphi_\mu{}^*F_{op}\varphi_{\nu+G\lambda}d\tau, \tag{64}$$

where $F_{\mu\nu}{}'$ is the usual matrix element with respect to the functions (59), and $\bar{F}_{\mu\nu}{}'$ is the result of a summation, in which generally only *one* term is of real importance (because of the large magnitude of G). The fundamental Eqs. (54) and (55) are now equivalent with the

[17] F. Bloch, Zeits. f. Physik **52**, 555 (1929).

[18] We note that Bloch instead employed a certain "orthogonality principle" in constructing the secular equations.

[19] Here each function is characterized by three integers, but, since the lattice points are enumerable, they can also be characterized by only one integer, as before; See Eq. (21).

relations

$$E_k=\sum_{\mu\nu}^{(G)} C_{k\mu}\dagger\bar{H}_{\mu\nu}'C_{\nu k}=\text{extreme value}, \tag{65}$$

$$\sum_{\mu}^{(G)} C_{k\mu}\dagger C_{\mu k}=1, \tag{66}$$

giving the secular equations

$$\sum_{\nu}^{(G)} \bar{H}_{\mu\nu}'C_{\nu k}=C_{\mu k}E_k, \quad \mu \text{ in } (G). \tag{67}$$

We note that, because of the periodicity condition (62), our secular problem is now reduced to the *finite* order G^3; the indices being referred only to the ground points of $\mathfrak{y}$ and $\mathbf{k}$.

Since we here are treating atomic orbitals $\varphi_\mu=\varphi(\mathfrak{r}-\mathfrak{y})$ of only *one* type, the matrix elements $\bar{H}_{\mu\nu}'$ depend only on the difference $\mathfrak{x}=\mathfrak{v}-\mathfrak{y}$ between their indices. It is therefore convenient to introduce the new notation

$$J_\kappa=\bar{H}_{\mu,\,\mu+\kappa}'=\sum_{\lambda}^{(\infty)} H_{\mu,\,\mu+\kappa+G\lambda}'. \tag{68}$$

Now it is well known (see Bloch, reference 17) that each cyclic matrix, having elements characterized only by the difference between their indices, can be transformed to the diagonal form by means of a similarity transformation $\mathbf{C}$, given by

$$C_{\mu k}=G^{-\frac{1}{2}}e^{2\pi i\mathbf{k}\cdot\mu}. \tag{69}$$

When the indices are referred only to the ground points of $\mathfrak{y}$ and $\mathbf{k}$, $\mathbf{C}$ is also a unitary matrix. Hence we obtain

$$\mathbf{E}=\mathbf{C}\dagger\bar{\mathbf{H}}'\mathbf{C}, \tag{70}$$

and

$$E_k=J_0+\sum_{\kappa\neq 0}^{(G)} J_\kappa e^{2\pi i\mathbf{k}\cdot\kappa}. \tag{71}$$

It is easily verified that the expressions (69) and (71) really satisfy the secular problem, i.e. the Eqs. (67) and (66). Introducing (69) into (61), we get the corresponding crystal functions

$$\chi_k(\mathbf{r})=G^{-\frac{1}{2}}\sum_{\mu}^{(\infty)} e^{2\pi i\mathbf{k}\cdot\mu}\varphi_\mu(\mathbf{r}), \tag{72}$$

the *Bloch orbitals*, which are automatically normalized and orthogonalized with respect to the ground domain (G), i.e.

$$\int_{(G)} \chi_k{}^*\chi_{k'}d\tau=\delta_{kk'}. \tag{73}$$

Besides they fulfill exactly the general Bloch condition

$$\chi_k(\mathbf{r}+\mathbf{a}_\kappa)=e^{2\pi i\mathbf{k}\cdot a_\kappa}\chi_k(\mathbf{r}), \quad \kappa=1,\,2,\,3. \tag{74}$$

At first sight it seems to be somewhat surprising that we here got exactly the same coefficients (69) as Bloch obtained in his simplified theory ($\mathbf{S}$ neglected). In order to examine this fact we now try to construct our Bloch orbitals directly from the *AO* ϕ_μ, given originally:

$$\chi_k=\sum_{\mu}^{(\infty)} \phi_\mu x_{\mu k}. \tag{75}$$

The fundamental conditions (54) and (55) again give a secular problem of the finite order G^3 by introducing the matrices

$$\bar{H}_{\mu\nu}=\sum_{\lambda}^{(\infty)} H_{\mu,\,\nu+G\lambda}=\sum_{\lambda}^{(\infty)}\int_{(\infty)} \phi_\mu{}^*H_{op}\phi_{\nu+G\lambda}d\tau, \tag{76}$$

$$\bar{S}_{\mu\nu}=\sum_{\lambda}^{(\infty)} S_{\mu,\,\nu+G\lambda}=\sum_{\lambda}^{(\infty)}\int_{(\infty)} \phi_\mu{}^*\phi_{\nu+G\lambda}d\tau. \tag{77}$$

Since $\bar{H}_{\mu\nu}$ as well as $\bar{S}_{\mu\nu}$ depend only on the difference $\mathfrak{x}=\mathfrak{v}-\mathfrak{y}$, they can both be transformed to a diagonal form by the unitary transformation (69). This means that our matrices $\bar{\mathbf{H}}$ and $\bar{\mathbf{S}}$ *commute*, i.e. that our crystal problem belongs to the simple case (i) treated before. Here we have the explanation why the coefficients (69) are identical with the coefficients of the simplified theory. We note that the functions

$$G^{-\frac{1}{2}}\sum_{\mu}^{(\infty)} e^{2\pi i\mathbf{k}\cdot\mu}\phi_\mu \tag{78}$$

given by Bloch, are really the correct crystal functions except for a normalization factor, which, however, is of essential importance. The normalization of (78) is a rather delicate problem (see Eq. 33), and in practical investigations it is therefore much better to start from the automatically normalized functions (72).

The Band Structure

Equation (71) gives the energy band in the crystal associated with the atomic orbitals under consideration. The quantities J_κ characterize the band structure, and here we will consider them in greater detail.

Between the fundamental matrix elements $H_{\mu\nu}'$, $H_{\mu\nu}$, and $S_{\mu\nu}$ there is a relation of the form (14). Using (64), (76), (77), and the transformation

$$\sum_{\alpha}^{(\infty)} F_{\mu\alpha}=\sum_{\alpha}^{(G)} \bar{F}_{\mu\alpha}, \tag{79}$$

we obtain, after some simple reductions, for the finite matrices of order G^3:

$$\bar{\mathbf{H}}'=(\mathbf{1}+\bar{\mathbf{S}})^{-\frac{1}{2}}\bar{\mathbf{H}}(\mathbf{1}+\bar{\mathbf{S}})^{-\frac{1}{2}}, \tag{80}$$

or, since $\bar{\mathbf{S}}$ commutes with $\bar{\mathbf{H}}$:

$$\bar{\mathbf{H}}'=\bar{\mathbf{H}}(\mathbf{1}+\bar{\mathbf{S}})^{-1}. \tag{81}$$

In analogy to (42) and (43) we now introduce the notations

$$\alpha=\bar{H}_{00}, \quad \gamma_\eta=\bar{H}_{0\eta}-\bar{H}_{00}\bar{S}_{0\eta}. \tag{82}$$

In the same way as in deriving (45) we then get

$$J_\kappa=\alpha\delta_{0\kappa}+\sum_{\eta\neq 0}^{(G)} \gamma_\eta(\mathbf{1}+\bar{\mathbf{S}})^{-1}{}_{\eta\kappa}, \tag{83}$$

where we also have neglected a term containing the quantity $\bar{S}_{00}$, which is practically zero. The formula (83) seems to be the best for practical purposes. The further development of the theory can be given in the usual way.

We note that, unlike the simplified theory (**S** neglected), the theory of band structure based on (59) and (83) is *invariant* with respect to the transformation (36), i.e. to an arbitrary change of the zero-point of the Hamiltonian operator. This is important, because in the simplified theory a very small change in the atomic potentials could cause considerable changes in the whole band structure.

Numerical applications[20] of the simplified theory (**S** neglected) have given rather bad results, and from this fact one has usually drawn the conclusion that the whole *LCAO*-method represents a relatively bad and rough approximation for crystals. However, actual calculations in the complete theory, including overlap effects, show that the overlap integrals are of essential importance for the results, and therefore the whole problem must be reexamined. Numerical calculations on some typical crystals are now in progress, and the results will be published later.

Finally, we will say a few words about the connection between our orthonormalized atomic orbitals φ_μ, given by (59), and the functions introduced by Wannier.[21] He has treated the reverse problem, namely the construction of orthonormalized atomic orbitals by means of linear combinations from Bloch orbitals, which are given from the beginning (e.g. calculated by the "cellular method"). Introducing the notation

$$\bar{\varphi}_\mu = \sum_{\lambda}^{(\infty)} \varphi_{\mu+G\lambda}, \tag{84}$$

and using the unitary property of (69), we obtain directly from (72) the two relations

$$\chi_k = G^{-\frac{1}{2}} \sum_{\mu}^{(G)} e^{2\pi i \mathbf{k}\cdot\mu} \bar{\varphi}_\mu, \tag{85}$$

$$\bar{\varphi}_\mu = G^{-\frac{1}{2}} \sum_{k}^{(G)} e^{-2\pi i \mathbf{k}\cdot\mu} \chi_k. \tag{86}$$

Here (86) shows that, except for the different starting points, there is a very close connection between the functions $\bar{\varphi}_\mu$ and Wannier's functions, since the latter are just given by a relation of this type. Slater[22] has employed Wannier's functions in his theory of ferromagnetism, and now it is possible to reconsider this theory, starting from given atomic orbitals ϕ_μ.

The theory of ferromagnetism, developed by Heisenberg, Bloch, Slater, and others, is based on the properties of certain "exchange integrals." It may here be pointed out that these integrals, referred to the orthonormalized atomic orbitals φ_μ, are invariant with respect to an arbitrary change of the zero-point of the Hamiltonian operotor. This does not apply to the corresponding quantities in the simplified theory (*S* neglected).

Here we have confined ourselves to the simple case when each unit cell $\mathfrak{y}$ contains only *one* atomic orbital ϕ_μ, but we note that the theory is easily generalized even to the case when each unit cell $\mathfrak{y}$ contains p different atomic orbitals $\phi_\mu^{(1)}$, $\phi_\mu^{(2)}$, $\cdots\phi_\mu^{(p)}$, which may be associated with the same or different atomic nuclei in the cell $\mathfrak{y}$. The corresponding energy matrix

$$\bar{H}'_{\mu\nu}{}^{(rs)}(r, s=1, 2, \cdots p)$$

can be essentially simplified by the unitary transformation (69), but instead of (71) we now get a determinant equation of the order p. For each value of $\mathbf{k}$ we then have p different values of the energy E_k, giving the p different energy bands belonging to the problem. It is not necessary to give more details, since the further development can be carried out following the conventional methods (see Mott and Jones, reference 20).

IV. THE NON-ORTHOGONALITY PROBLEM IN THE HEITLER-LONDON METHOD

Let us now consider a molecule or crystal, which contains N electrons having N atomic orbitals $\phi_\mu(\mu=1, 2, \cdots N)$ at their disposal, by means of the Heitler-London method. As before the nuclei are assumed to be fixed; further we let Z_g be the atomic number of the nucleus situated at the point g. The fundamental energy operator [23] H_{op}—different from the "effective" Hamiltonian in the theory of molecular orbitals—has now the form

$$H_{op} = W + \sum_{i=1}^{N} H_i + \sum_{i,k}{}' G_{ik}. \tag{87}$$

Here W represents the interaction between the nuclei, H_i the kinetic energy of the electron i plus its potential energy in the field of the nuclei, and G_{ik} the Coulomb interaction between the electrons i and k:

$$W = \frac{e^2}{2} \sum_{gg'} \frac{Z_g Z_{g'}}{r_{gg'}}, \qquad H_i = \frac{1}{2m}\mathbf{p}_i^2 - e^2 \sum_g \frac{Z_g}{r_{ig}}, \quad G_{ik} = \frac{e^2}{2r_{ik}}. \tag{88}$$

In the one-electron-approximation the wave function of each state of the system can be represented by a determinant of order N, each element being a product of an AO ϕ_μ and a spin factor, η^+ or η^-. In the case under consideration we have a complicated spin degeneracy, which can be treated by the Heitler-London-Slater-

[20] See e.g. Sommerfeld and Bethe, Handbuch der Physik **XXIV**: 2, p. 405. Mott and Jones, *The Theory of Properties of Metals and Alloys* (Oxford University Press, London, 1936).

[21] G. H. Wannier, Phys. Rev. **52**, 191 (1937).

[22] J. C. Slater, Phys. Rev. **52**, 198 (1937).

Note added in proof.—J. C. Slater, Phys. Rev. **76**, 1592 (1949), has recently shown that it is possible to treat electrons even in perturbed periodic lattices by means of Wannier's functions in a simple way.

[23] Relativistic effects being neglected.

TABLE I. Overlap integrals for LiCl and NaCl.*

LiCl	$a_0=5.07\ L_H$			
	1s0/3p0	1s0/3s0		
$S=$	0.0450	0.0092		
NaCl	$a_0=5.20\ L_H$			
Cl/Na	1s0	2s0	2p0	2p1
3p0	0.0047	−0.0555	0.0378	—
3s0	0.0007	−0.0116	0.0129	—
3p1	—	—	—	−0.0099

* 1s0/3p0 etc. give the quantum numbers of the overlapping oribitals.

Pauling resonance theory. Here we are mainly interested in the overlapping effects, and, for the sake of simplicity, we will therefore confine ourselves to the simplest spin state, where all electrons have *parallel spin*. This state has the wave function

$$\Psi=\frac{1}{(N!)^{\frac{1}{2}}}\begin{vmatrix}\phi_1(1) & \phi_2(1) & \cdots\phi_N(1)\\ \phi_1(2) & \phi_2(2) & \cdots\phi_N(2)\\ \cdot & \cdot & \cdot\\ \cdot & \cdot & \cdot\\ \phi_1(N) & \phi_2(N) & \cdots\phi_N(N)\end{vmatrix}\times\eta^+(1)\eta^+(2)\cdots\eta^+(N). \quad (89)$$

The corresponding energy E is then given by

$$E=\frac{\int\Psi^*H_{op}\Psi d\tau_1'\cdots d\tau_N'}{\int\Psi^*\Psi d\tau_1'\cdots d\tau_N'}, \quad (90)$$

where the integrations over $d\tau'$ include also summations over the spins. In (90) the calculation of the integrals is complicated by the non-orthogonality of the *AO* ϕ_μ. Again we will use the formulas (15) and (16), giving

$$\boldsymbol{\phi}=\boldsymbol{\phi}(\mathbf{1}+\mathbf{S})^{+\frac{1}{2}},$$

or

$$\phi_\mu=\sum_{\alpha=1}^{N}\varphi_\alpha(\mathbf{1}+\mathbf{S})^{\frac{1}{2}}{}_{\alpha\mu}. \quad (91)$$

Introducing the "overlap determinant"

$$\Delta=\det\{\delta_{\mu\nu}+S_{\mu\nu}\}=\begin{vmatrix}1 & S_{12} & S_{13}\cdots S_{1N}\\ S_{21} & 1 & S_{23}\cdots S_{2N}\\ \cdot & \cdot & \cdot\\ S_{N1} & S_{N2} & S_{N3}\cdots 1\end{vmatrix} \quad (92)$$

and using the law of determinant multiplication, we immediately obtain

$$\det\{\phi_\mu(\nu)\}=\det\{\varphi_\alpha(\nu)\}\cdot\det\{(\mathbf{1}+\mathbf{S})^{\frac{1}{2}}{}_{\alpha\mu}\}=\Delta^{\frac{1}{2}}\cdot\det\{\varphi_\mu(\nu)\}, \quad (93)$$

and

$$\Psi=\left(\frac{\Delta}{N!}\right)^{\frac{1}{2}}\det\{\varphi_\mu(\nu)\eta^+(\nu)\}. \quad (94)$$

Here the elements of the determinant are really orthonormalized functions, and hence we can directly employ the well-known formulas in the theory developed by Hartree-Slater-Fock. This simplification depends on the fact that a linear transformation of the *AO* changes the determinant only by a constant factor.[24] By using (94) we get directly

$$\int\Psi^*\Psi d\tau_1'\cdots d\tau_N'=\Delta=\det\{\delta_{\mu\nu}+S_{\mu\nu}\}. \quad (95)$$

For $N=2$ we have $\Delta=1-|S_{12}|^2$, and, for small values of S_{12}, the second term may be neglected in comparison to unity; i.e. the wave function is approximately normalized. However, this does not apply to higher values of N, since for increasing N we get a rapidly increasing number of S-terms, which therefore no longer may be neglected in comparison to 1. For a crystal, where N is an immense number, these terms are dominating.

TABLE II. Survey of the various energy contributions in kcal./mol for LiCl, NaCl, and KCl.

Crystal	Electrostatic energy	Exchange energy	S-energy	Cohesive energy	Experimental value
LiCl	−210.4	−12.7	+35.4	−187.7	−198.1
NaCl	−218.5	−34.4	+69.7	−183.2	−182.8
KCl	−206.3	−53.7	+93·1	−166.9	−164.4

The importance of the S-terms in this connection was first pointed out by Slater.[1] Later Inglis[2] stressed that for the theory of ferromagnetism the overlap integrals seemed to cause a real "non-orthogonality-catastrophe," but Van Vleck[4] reexamined the problem and showed that probably the simplified theory (**S** neglected) gives the best approximation. The latter also derived a semiquantitative formula for the error due to the non-orthogonality. Here we can now obtain a simple solution of the problem concerning the S-integrals.

In the energy expression (90) the numerator as well as the denumerator contains the factor Δ, which therefore cancels. Now we will introduce the following matrix elements:

$$[\mu|H|\nu]=\int\varphi_\mu^*(1)H_1\varphi_\nu(1)d\tau_1,$$
$$[\mu\nu|G|\kappa\lambda]=\int\varphi_\mu^*(1)\varphi_\nu^*(2)G_{12}\varphi_\kappa(1)\varphi_\lambda(2)d\tau_1d\tau_2. \quad (96)$$

In the same manner we let brackets of the type ( ) denote the corresponding elements associated with the original set ϕ_μ:

$$(\mu|H|\nu)=\int\phi_\mu^*(1)H_1\phi_\nu(1)d\tau,$$
$$(\mu\nu|G|\kappa\lambda)=\int\phi_\mu^*(1)\phi_\nu^*(2)G_{12}\phi_\kappa(1)\phi_\lambda(2)d\tau_1d\tau_2. \quad (97)$$

[24] This idea of treating the non-orthogonality problem seems to have been first introduced by Landshoff, Zeits. f. Physik **102**, 201 (1936), in an approximate way.

By using (94) and (96), we now get for the energy (90), according to a well-known formula in the Hartree-Slater-Fock theory,

$$E=W+\sum_{\mu}[\mu|H|\mu]+\sum_{\mu\nu}\{[\mu\nu|G|\mu\nu]-[\mu\nu|G|\nu\mu]\}. \quad (98)$$

In order to express the energy (98) in terms of the original matrix elements (97), we will use the matrix

$$\mathbf{T}=(\mathbf{1}+\mathbf{S})^{-1}. \quad (99)$$

If $\Delta_{\mu\nu}$ is the cofactor of the determinant (92) associated with the element (μ, ν), we have

$$T_{\mu\nu}=\Delta_{\nu\mu}/\Delta. \quad (100)$$

According to (91) we get $\varphi=\phi\mathbf{T}^{\frac{1}{2}}$, and, using the law of matrix multiplication, we then directly obtain

$$\begin{aligned}\sum_{\mu}[\mu|H|\mu]&=\sum_{\mu\nu}T_{\nu\mu}(\mu|H|\nu),\\ \sum_{\mu\nu}[\mu\nu|G|\mu\nu]&=\sum_{\mu\nu\kappa\lambda}T_{\kappa\mu}T_{\lambda\nu}(\mu\nu|G|\kappa\lambda), \quad (101)\\ \sum_{\mu\nu}[\mu\nu|G|\nu\mu]&=\sum_{\mu\nu\kappa\lambda}T_{\kappa\nu}T_{\lambda\mu}(\mu\nu|G|\kappa\lambda).\end{aligned}$$

Putting (101) into (98), we get the result

$$E=W+\sum_{\mu\nu}T_{\nu\mu}(\mu|H|\nu)+\sum_{\mu\nu\kappa\lambda}(T_{\kappa\mu}T_{\lambda\nu}-T_{\kappa\nu}T_{\lambda\mu})(\mu\nu|G|\kappa\lambda). \quad (102)$$

The last term can be transformed by using Jacobi's formula

$$\Delta_{\mu\kappa}\Delta_{\nu\lambda}-\Delta_{\nu\kappa}\Delta_{\mu\lambda}=\Delta\cdot\Delta_{\mu\nu,\,\kappa\lambda}, \quad (103)$$

where $\Delta_{\mu\nu,\,\kappa\lambda}$ is the determinant, obtained by striking out from Δ the rows μ and ν together with the columns κ and λ, multiplied by a sign factor $(-1)^{\mu+\nu+\kappa+\lambda}$. From (100) and (102) we then get the final expression

$$E=W+\frac{1}{\Delta}\sum_{\mu\nu}\Delta_{\mu\nu}(\mu|H|\nu)+\frac{1}{\Delta}\sum_{\mu\nu\kappa\lambda}\Delta_{\mu\nu,\,\kappa\lambda}(\mu\nu|G|\kappa\lambda), \quad (104)$$

which has a very simple symmetry.[25]

We note that there is no "non-orthogonality-catastrophe," because the critical determinant Δ does not appear alone but only in the connection

$$T_{\mu\nu}=\frac{\Delta_{\nu\mu}}{\Delta}=\delta_{\mu\nu}-S_{\mu\nu}+\sum_{\alpha}S_{\mu\alpha}S_{\alpha\nu}-+\cdots. \quad (105)$$

Putting the expansion (105) in (102), we get an energy expression which is well fitted for numerical computations. However, we wish to emphasize that, even if there is no "S-catastrophe," the overlap integrals are still of essential importance for the results, which will be shown by the following examples.

[25] See W. Bleick and J. E. Mayer, J. Chem. Phys. **2**, 252 (1934).

Applications to Ionic Crystals

The ionic crystals in their ground states give another simple system without spin complications. Here we have $2N$ electrons in N atomic orbitals, each AO containing two electrons with opposite spin. Even this state has a wave function which can be represented by a single determinant of order $2N$, and the calculations can then be carried out in the same way as in the preceding section—we have only to include the spin factors explicitly in the elements of the determinant (89) and in the corresponding matrix elements (96) and (97). The essential difference is that these matrix elements are different from zero only for electron states with parallel spins.

The first treatment of ionic crystals by the Heitler-London method was given by Hylleraas[26] on LiH, and by Landshoff[24] on NaCl. Later the present author has treated a series of alkali halides by the method mentioned above. We have based our computations on atomic orbitals ϕ_μ belonging to the self-consistent fields with exchange, which are numerically given for various free ions by Hartree-Hartree and Fock-Petrashen. Here we will stress only some numerical results connected with the overlap integrals, and for details we will refer the reader to the original papers.[12, 15, 16]

The overlap integrals $S_{\mu\nu}$, defined by (1), are really rather small compared to unity, and as examples we will give the following values (Table I) referred to the equilibrium distances between the ions in the normal crystals.

The total energy is given by the formulas (102) and (105)—see the remark on the spin above—and the cohesive energy of the crystal can then be obtained by subtracting the total energy of the free ions. This cohesive energy, expressed in integrals containing the original atomic orbitals ϕ_μ, has been split in three terms:

$$E_{coh}=\text{electrostatic energy}+\text{exchange energy}+S\text{-energy}, \quad (106)$$

where in the S-energy we have collected all terms with one or more overlap integrals as factors; the first two terms have their conventional form. Table II gives a survey of the various energy contributions in the equilibrium state. At first sight it is perhaps somewhat surprising that the S-energy is relatively so large (see Table I with the small values of S itself), but we must remember that the cohesive energy in reality is a "small" quantity, being the difference between two "large" quantities, namely the total energy and the total energy of the free ions.

We note that the S-energy in all these crystals corresponds to the repulsive forces between the ions. This means that in the simplified theory (**S** neglected) we should not get any repulsive forces at all; that is the whole approximation should have broken down. This fact shows how important it is to include the overlap

[26] E. A. Hylleraas, Zeits. f. Physik **63**, 771 (1930).

effects in the calculations, before one draws any conclusion as to the accuracy of the *LCAO*-method.

Now we will treat another property of the ionic crystals, closely connected with the overlap effects. Because of the perfect spherical symmetry of the complete electron-shells of the free ions, it has earlier often seemed to be natural to assume that the ions in the crystal, too, interact with central forces. As has been shown by the author,[15,16] this is, however, not true because of the overlap effects.

The electrostatic energy as well as the exchange energy in (106) can be expressed in the form

$$\tfrac{1}{2}\sum_{gg'} E_{gg'}(r_{gg'}), \tag{107}$$

where $E_{gg'}$ is a function which depends only on the distance $r_{gg'}$ between the nuclei of *two* ions. In the following we will therefore call forces, corresponding to potentials of this type, *two-body-forces*.[27]

In an ionic crystal even the S-energy is a function only of the distances between the nuclei of the ions:

$$E_S = E_S(r_{12}, r_{13}, \cdots r_{23}, \cdots), \tag{108}$$

but this energy is now of a more complicated form than (107), since the corresponding expansion in addition to the two-body-terms also contains terms depending on the distances between the nuclei of *three* and more ions. The S-energy is therefore said to correspond to *many-body-forces*, and these forces add interesting new features to the properties of ionic crystals, e.g. as regards the elastic constants, the relative stability of different lattice types, and so on.[28]

Let us here consider the problem of the elastic constants c_{ij} ($i, j = 1, 2, \cdots 6$). It is well known that if the forces in a general crystal are of two-body type, then these constants satisfy the six additional Cauchy relations[29]

$$\begin{array}{lll} c_{12}=c_{66} & c_{23}=c_{44} & c_{31}=c_{55} \\ c_{14}=c_{56} & c_{25}=c_{64} & c_{36}=c_{45} \end{array} \tag{109}$$

On the other hand, in references (15) and (16) the author has shown that these relations are no longer valid for the many-body potential derived there.[30] This is of some interest, since experiments have shown that the Cauchy relations in reality are not valid for the crystals in nature. A comparison between the theoretical values of c_{ij}, derived from the expression (106), and the experimental data would therefore also be a good test on the validity of our theoretical discussion concerning the overlap effects.

TABLE III. Survey of the various contributions to the elastic constants c_{12} and c_{44} of some alkali halides in the unit 10^{11} dyne/cm^2. (The exchange energy gives no contribution in the approximation under consideration). The theoretical values are related to the absolute zero of temperature.

Crystal	Elastic constant	Electrostatic part	S-energy part	Theoretical value	Experimental value
LiCl	c_{12}	1.895	−0.396	1.499	
	c_{44}	1.895	+0.120	2.015	
NaCl	c_{12}	1.399	−0.417	0.982	1.10*
	c_{44}	1.399	+0.126	1.525	1.339
KCl	c_{12}	0.885	−0.284	0.601	0.6*
	c_{44}	0.885	+0.063	0.948	0.669
LiF	c_{12}	5.009	−1.247	3.762	4.04**
	c_{44}	5.009	+0.691	5.700	5.54

* M. A. Durand, Phys. Rev. **50**, 449 (1936), at low temperature.
** H. B. Huntington, Phys. Rev. **72**, 321 (1947), at room temperature.

The alkali halides constitute the simplest case; they have only three independent elastic constants c_{11}, c_{12}, and c_{44} with the Cauchy relation

$$c_{12} = c_{44}. \tag{110}$$

The calculations have been carried out for some of them, starting from the atomic orbitals ϕ_μ, numerically given by Hartree-Hartree and Fock-Petrashen. Table III gives a survey of the importance of the overlap effects for the elastic constants.

The agreement between the theoretical and experimental values are almost better than one could really expect with regard to the approximations involved in the starting point as well as is the Heitler-London method. Hence, it seems probable that, in ionic crystals, the overlap effects with their many-body-forces are able to give an explanation of the well-known failure of the Cauchy relations.

As a summary of this paper we can thus draw the conclusion that, even if there is no "non-orthogonality-catastrophe," the overlap integrals are of essential importance in treating molecules and crystals by the *LCAO*-method.

ACKNOWLEDGMENT

Part of this work was carried out during a stay at H. H. Wills Physical Laboratory, University of Bristol, and I wish to express my gratitude to Professor N. F. Mott for his great hospitality and for fruitful discussions concerning crystal problems. Further, I take this opportunity of thanking Professor T. Waller, Upsala, for pointing out to me the problem connected with the elastic constants of the ionic crystals and the usefulness of Landshoff's work[24] as a starting point for treating this problem. I am also indebted to Professor C. A. Coulson, London, for valuable discussions as to the conjugated systems. Finally, I should like to thank Dr. G. Wyllie, Bristol, for his kind help in reading the manuscript.

[27] The classical name "central forces" is not so good, since even the more complicated forces—the many-body-forces—can be constituted by components along the central lines between the nuclei.

[28] The elastic constants corresponding to a general potential have previously been considered by e.g. G. H. Begbie and M. Born, Proc. Roy. Soc. **188**, 179 (1947).

[29] The validity of the Cauchy relations has been discussed by many authors. A simple derivation, based on the stress-strain law for finite strains, may be found in Löwdin (reference 16), Sec. 18 and the Appendix.

[30] Previously, many authors have taken the failure of the Cauchy relations just as a criterion for the existence of non-central forces, but, as far as we know, this is the first time such forces have been explicitly derived for the alkali halides by means of quantum mechanics.

The Electrical Charge of 18-Min. Br^{80} from Isomeric Transition†

S. WEXLER
Argonne National Laboratories, Chicago, Illinois

AND

T. H. DAVIES
Institute for Nuclear Studies, University of Chicago

(Received August 29, 1949)

The space between two concentric copper-amalgam electrodes was filled to several microns pressure with ethyl bromide containing 4.4-hr. Br^{80*}. The distribution between electrode surfaces of 18-min. Br^{80} dissociated from ethyl bromide in consequence of the isomeric transition process was determined. The results establish the presence of positively charged 18-min. Br^{80} species among the decay products. At least 50 percent of the dissociations yield positive Br^{80} species. The remainder yield uncharged Br^{80} species.

IN the isomeric transition of 4.4-hr. Br^{80*} to its 18-min. ground state, accompanying chemical changes are often noted. For example, organic bromides marked with Br^{80*} when extracted with aqueous solutions yield only 18-min. Br^{80} as inorganic bromine to the water layer.[1,2] The fraction of the nuclear transitions which yield inorganic bromine varies with experimental conditions, but it is high for gaseous bromine compounds and approaches unity for CH_3Br marked with Br^{80*}.[2,3]

The molecular dissociation observed here is regarded as the end result of the internal conversion process by which the isomeric transition of Br^{80*} seems always to occur.[4–6] De-excitation of the nucleus by emission of a K (or L) electron will leave the atom or molecule in an electronically excited state. An "Auger process" should follow in which the cascade of electrons toward the vacancy produces ionization of additional electrons as well as x-radiation. On the basis of x-ray fluorescence yields and the K and L conversion coefficients of the Br^{80*} transition, DeVault and Libby[2] estimate the electron loss as follows: "At least 15 percent of the isomeric transitions cause loss of all the valence electrons, over 60 percent cause loss of four or more, less than 10 percent lose only two, and less than 2 percent lose only one." In an approximate quantum mechanical calculation for the transition in HBr, Cooper[7] finds +4.7 as the average charge after transition. If the transformed nucleus is part of a molecule, the large positive charge accumulated should lead to dissociation of the molecule.

However, positively charged daughter species from isomeric transition with internal conversion are not yet reported. In fact, Capron, Crèvecoeur, and Faes[8] have subjected neutron-bombarded liquid C_6H_5Br to an electric field after bombardment and report an enrichment relative to Br^{80*} of Br^{80} (from isomeric transition) on the gold foil employed as *anode*.

In the study to follow, we shall describe an effect of electric field upon the distribution between electrodes of Br^{80} from Br^{80*} present as gaseous C_2H_5Br. Very low pressures are employed to minimize the effect of collisions intervening between the creation of the Br^{80} atom and its approach to an electrode. The techniques used are discussed in more detail elsewhere.[9]

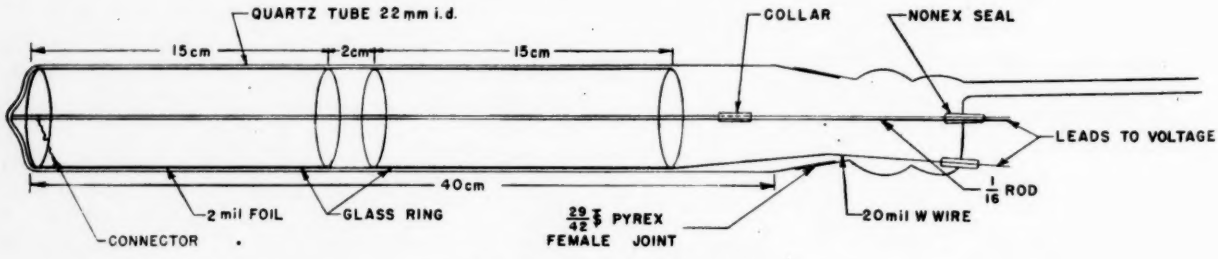

FIG. 1. The electrode chamber.

† This paper is based on work performed at the Argonne National Laboratory, Chicago, Illinois, operated by the University of Chicago for the AEC.

[1] Segrè, Halford, and Seaborg, Phys. Rev. **55**, 321 (1939).
[2] D. C. DeVault and W. F. Libby, Am. Chem. Soc. **63**, 3216 (1941).
[3] W. H. Hamill and H. A. Young, J. Chem. Phys. **17**, 217 (1949).
[4] J. E. Willard, J. Am. Chem. Soc. **62**, 256 (1940).
[5] Seaborg, Friedlander, and Kennedy, J. Am. Chem. Soc. **62**, 1309 (1940).
[6] For details of the Br^{80*} decay scheme read: E. Segrè and A. C. Helmholz, Rev. Mod. Phys. **21**, 291 (1949).
[7] E. P. Cooper, Phys. Rev. **61**, 1 (1942).
[8] Capron, Crèvecoeur, and Faes, J. Chem. Phys. **17**, 349 (1949).
[9] S. Wexler and T. H. Davies, "The dissociation of ethyl bromide by neutron capture," Brookhaven National Laboratory Report No. C-7 (1948); in preparation for journal publication.

TABLE I. Distribution of 18-min. Br^{80} between rod and wall electrodes.

Expt.	Radius of central rod	Electrodes analyzed	Field	Br^{80} (cts/min.) Rod	Wall	Ratio $\left(\frac{\text{wall}}{\text{rod}}\right)$	Fraction Br^{80} on rod
1	0.795 mm	left	none	53	1127	21	0.045
		right	Rod−3000 v	709	252	0.36	0.74
2	0.795 mm	left	none	50	847	17	0.055
		right	Rod+3000 v	16	1437	90	0.011
3	5.5 mm	left	none	192	445	2.3	0.30
		right	Rod−2500 v	356	191	0.54	0.65
4*	5.5 mm	left	none	790	4700	6.0	0.14
		right	Rod−2500 v	1910	1230	0.64	0.61

* In experiment 4, the electrodes were not analyzed radiochemically for Br^{80} but the wall foils and the foil wrapped (in this experiment) around the central rod were placed around a "Raythion" glass tube counter and counted immediately following removal of the C_2H_5Br.

PROCEDURE AND RESULTS

The electrode chamber used is sketched in Fig. 1. In it are three collecting surfaces: a central rod either 0.795 mm or 5.5 mm in radius, surrounded by two tandem concentric cylinders of foil. The two cylinders are of 20 mm inside diameter and fit snugly in the cylindrical quartz container with near edges 2 cm apart. The left-hand cylinder is electrically connected to the central rod. A potential difference of several thousand volts is placed across the central rod and the right-hand cylinder. Thus the left annular gas space is field free while the nearly identical right-hand space is subjected to the full field. The electrode surfaces were of amalgamated copper prepared by dipping copper foil and rod briefly in dilute HNO_3 solutions of a mercury salt. After exhaustive washing in distilled water, the foils and rod were placed in the chamber and the water and excess Hg driven off in vacuum by heating. Surfaces thus prepared were shown in previous work[9] to hold Br^{80*} recoils from neutron capture apparently at first collision.

Purified HBr was bombarded in a neutron flux of approximately 10^{12} neutrons/cm²/sec. to partial saturation of the 4.4-hr. Br^{80*} activity. Radioactive C_2H_5Br of very high specific activity was prepared by photochemical addition of the HBr to C_2H_4. The carefully outgassed decay chamber was filled to a pressure of about 4 microns with a purified sample of the C_2H_5Br and the voltage was imposed. After an hour's decay, the C_2H_5Br was removed and the chamber disassembled. The central rod was cut into left- and right-hand parts. The four surfaces were separately washed with 1N HNO_3 containing Br^- carrier and then with 2 percent $(NH_4)_2CO_3$ solution. The two washings of each electrode were combined and analyzed radiochemically for bromine by a standard method. Counting of the final AgBr mounts with a G-M tube and scaling circuit began about 70 min. after termination of the experiment and six hours after bombardment of the HBr. Each sample decayed initially with an 18-min. half-life followed finally by decay with a 4.4-hr. half-life. Extrapolation of the last part of the decay curve to the time of removal of the C_2H_5Br from the decay chamber showed that only several percent of the initial activity on the electrodes was due to the 4.4-hr. Br^{80*} activity. The counting data corrected to a constant elapsed time after removal of the C_2H_5Br, corrected for variation in the chemical yield of the analysis and for counter background appear in Table I. The ratios listed are the activities from the indicated wall foil divided by the activity from the appropriate section of the central rod.

CALCULATIONS AND DISCUSSIONS

In the absence of intermolecular collisions in the field free annular gas space, the probability that the Br^{80} species will strike the rod before the wall foil is $2\theta/2\pi$ where θ is the angle between the normal to the rod from the point of origin of the Br^{80} and the tangent to the rod in the same plane. Integrating over the gas space, we find the fraction of all Br^{80} species striking the rod first to be

$$F=\frac{r_r}{\pi(r_w^2-r_r^2)}\left[\frac{r_w^2}{r_r}\arcsin\frac{r_r}{r_w}+(r_w^2-r_r^2)^{\frac{1}{2}}-\frac{\pi}{2}r_r\right],$$

where r_r and r_w are the radii of rod and wall foil respectively. If the Br^{80} sticks to the surface at first collision, then F above predicts the distribution of activity between rod and left-hand foil. For $r_r=0.795$ and $r_w=10$ mm the calculated F is 0.045; for $r_r=5.5$ and $r_w=10$ mm, F is 0.26. The observed F values (Table I) of the first three experiments for the left-hand surfaces agree well with those predicted,‡ suggesting that gas space collisions and re-emission of Br^{80} from the foils are relatively unimportant. Gas space collisions should increase the F values toward 0.074 and 0.36, calculated from the ratio of the exposed surface areas of wall foil

‡ Using similar foils in a similar chamber to collect Br^{80*} recoils from neutron capture by C_2H_5Br at 1–3-microns pressure, we find, with no electric field, F values of 0.037, 0.037, 0.036, 0.040, 0.038, 0.036, 0.040, 0.052, and 0.031 compared to a calculated F of 0.043; with a thicker central rod 0.35, 0.33, and 0.35 *vs.* a calculated value of 0.26[9]. The recoils from neutron capture probably have a higher kinetic energy and certainly are less often charged than the Br^{80} from isomeric transition.

and rod. The effect of re-emission from the surfaces cannot be assessed without information on the angular distribution of the re-emitted species.

The data may be used to estimate the distribution of Br^{80} among species of positive, negative, and neutral provided collection efficiencies of the electrodes for the charged species can be assumed. This requires in turn an estimate of the kinetic energies of the Br^{80} following the transition. Recoil energies from the conversion electrons will be less than 0.5 ev. However, if a large positive charge accumulates on the C_2H_5Br through the Auger process, the molecule will dissociate fragments with substantial kinetic energies. The kinetic energy of a Br^{+2} ion dissociated from a molecule of initial charge +4 will be about 10 ev. However, the larger charge of the Br^{80} will increase collection efficiency. Obviously the concentration of the electric field about the central rod will repel all but a vanishing fraction of similarly charged Br^{80} of less than 10-ev kinetic energy when the voltage difference of rod and wall is several thousand volts. Thus the collection efficiency of the wall foil for oppositely charged Br^{80} can be taken as unity. In the thin rod experiments, the fraction of Br^{80} species which originate at points less than 10 ev from the wall foil is less than 1 percent when the wall-rod potential difference is 3000 volts. Accordingly, the collection efficiency of the rod for Br^{80} of opposite charge can be taken as unity also. A small fraction of the more energetic Br^{80} species may spiral about the rod until sufficient angular momentum relative to the rod is lost via gas space collisions to permit the Br^{80} to reach the rod. Collection efficiencies for the thick rod experiments will approach unity still more closely.

The distribution among species of different charge can be obtained by simultaneous solution of the following relations:

$$R^-=\frac{N_w{}^0+N^-}{N_r{}^0+N^+},\qquad R^+=\frac{N_w{}^0+N^+}{N_r{}^0+N^-},\qquad R^0=\frac{N_w{}^0}{N_r{}^0},$$

and $N_w{}^0+N_r{}^0+N^++N^-=1$, where R^0 is the wall-rod ratio of Br^{80} in the absence of a field, R^- is the same ratio when the rod is negative, R^+ is the same ratio when the rod is positive, $N_r{}^0$ is the fraction of Br^{80} which is uncharged and found on the rod, $N_w{}^0$ is the fraction of Br^{80} which is uncharged and found on the wall foil, and N^+ and N^- are fractions of all Br^{80} which carry positive and negative charges, respectively.

With the R^-, R^+, and R^0 (average) values from experiments 1 and 2, one obtains $N^+=0.72$, $N^-=-0.003$, and $N^0=0.28$. If N^- is zero, from experiment 3, $N^+=0.50$ and $N^0=0.50$. Experiment 4 is given for qualitative confirmation only since the data for the left foil differs markedly with the other results here and in the neutron capture studies.

The experiments then demonstrate the positive Br^{80} species anticipated in previous discussions of the internal conversion process. However, uncharged Br^{80} is certainly found also, although the magnitude of this fraction is not yet accurately determined. The yield of uncharged Br^{80} from HBr^{80*} should be nearly zero provided internal conversion is complete.[2,7] With $C_2H_5Br^{80*}$, however, some cancellation of the high Br charge by electrons from the ethyl radical should occur prior to dissociation. Another source of the neutral Br^{80} observed here could be electron transfer in gas space collisions. The mean free path at 4-microns pressure of C_2H_5Br is approximately 1.6 cm for Br^+ and 3.3 cm for Br^{5+}. When the 0.795-mm rod is several thousand volts negative to the wall, approximately 35 percent of the Br^+ and 18 percent of any Br^{5+} ions should collide with C_2H_5Br molecules. With wall negative, collisions should be reduced by a factor of two. The cross section for electron exchange with C_2H_5Br may be larger than that for van der Waal collisions, however. The free energy change in the oxidation of a C_2H_5Br molecule by Br^+ is favorable by nearly 1 ev.[10,11]

If the precision of the technique can be improved, we shall study this and related questions by observing the effect of variation in pressure, potential, and bromine compounds used upon the fraction of Br^{80} which is charged.

[10] W. M. Latimer, *Oxidation Potentials* (Prentice-Hall Inc., New York, 1938) p. 14.
[11] W. C. Price, Ann. Rep. Chem. Soc. **36**, 55 (1940).

Concerning the Work of Polarization in Ionic Crystals of the NaCl Type. III. Numerical Results for a Single Charge in the Rigid Lattice*

F. K. du Pré, R. A. Hutner, and E. S. Rittner
Philips Laboratories, Inc., Irvington-on-Hudson, New York

(Received October 3, 1949)

Numerical results determined from the theory presented in Part I are given for thirty-three substances.

In this paper, as in Parts I[1] and II,[2] the work of polarization, W, is defined as the change in electrostatic energy resulting from the removal of a positive or negative charge from a lattice point in an ionic crystal. The term "rigid lattice" means that the removal is effected so rapidly that there is no displacement of any ion as a whole.

In Part I the Mott-Littleton[3] method of calculating W was extended with some modification to a higher order approximation. This consisted of a nearly exact solution for the induced dipole moments on the ions in the first eight shells and an application of the Mott-Littleton zero order approximation to the remainder of the crystal.

The same method was employed in the present paper to calculate W for all substances of the NaCl-type structure, for which the required data were available. The data for the lattice constant, a, were taken from Wyckoff;[4] those for the optical dielectric constant, κ_0, from Højendahl,[5] Spangenberg,[6] and Haase;[7] and the

TABLE I.

Substance	Data used a Å	κ_0	R_+ cm³	R_- cm³	Results α_+ 10^{-24} cm³	α_- 10^{-24} cm³	W_+ ev	W_- ev	(W_++W_-) ev
LiF	2.009	1.92	0.074	2.65	0.025	0.884	2.92	1.81	4.73
LiCl	2.565	2.75	0.074	9.30	0.023	2.95	3.14	1.89	5.03
LiBr	2.745	3.16	0.074	12.14	0.025	4.11	3.18	1.91	5.09
LiI	3.000	3.80	0.074	18.07	0.025	6.20	3.17	1.89	5.06
NaF	2.310	1.74	0.457	2.65	0.171	0.993	2.13	1.50	3.63
NaCl	2.814	2.25	0.457	9.30	0.147	2.98	2.43	1.53	3.96
NaBr	2.980	2.62	0.457	12.14	0.161	4.27	2.60	1.61	4.21
NaI	3.231	2.91	0.457	18.07	0.155	6.11	2.57	1.57	4.14
KF	2.670	1.85	2.12	2.65	0.892	1.12	1.75	1.66	3.41
KCl	3.139	2.13	2.12	9.30	0.750	3.29	1.96	1.42	3.38
KBr	3.293	2.33	2.12	12.14	0.779	4.46	2.06	1.43	3.49
KI	3.526	2.69	2.12	18.07	0.792	6.75	2.18	1.44	3.62
RbF	2.820	1.93	3.57	2.65	1.45	1.08	1.64	1.76	3.40
RbCl	3.270	2.19	3.57	9.30	1.32	3.43	1.86	1.48	3.34
RbBr	3.427	2.33	3.57	12.14	1.34	4.56	1.91	1.44	3.35
RbI	3.663	2.63	3.57	18.07	1.36	6.90	2.02	1.42	3.44
AgCl	2.773	4.01	4.33	9.30	1.62	3.48	3.12	2.55	5.67
AgBr	2.884	4.62	4.33	12.14	1.65	4.62	3.24	2.49	5.73
MgO	2.101	2.95	0.238	9.88	0.041	1.70	3.98	2.43	6.41
MgS	2.595	5.11	0.238	26.0	0.044	4.78	4.05	2.41	6.46
MgSe	2.725	5.95	0.238	26.8	0.053	5.96	4.02	2.38	6.40
CaO	2.398	3.28	1.19	9.88	0.306	2.54	3.59	2.37	5.96
CaS	2.840	4.49	1.19	26.0	0.257	5.62	3.52	2.17	5.69
CaSe	2.955	5.04	1.19	26.8	0.301	6.77	3.51	2.15	5.66
CaTe	3.172	6.79	1.19	35.6	0.325	9.71	3.53	2.14	5.67
SrO	2.572	3.45	2.18	9.88	0.660	2.99	3.33	2.37	5.70
SrS	2.935	4.36	2.18	26.0	0.493	5.88	3.34	2.12	5.46
SrSe	3.115	4.80	2.18	26.8	0.607	7.46	3.25	2.06	5.31
SrTe	3.235	5.60	2.18	35.6	0.565	9.22	3.29	2.04	5.33
BaO	2.761	3.83	3.94	9.88	1.39	3.49	3.12	2.47	5.59
BaS	3.175	4.64	3.94	26.0	1.10	7.28	3.10	2.07	5.17
BaSe	3.310	4.97	3.94	26.8	1.26	8.60	3.04	2.03	5.07
BaTe	3.493	5.66	3.94	35.6	1.23	11.1	3.02	1.95	4.97

* This work was carried out with the support of the Air Materiel Command under Contract W33-038 ac-15141 with Philips Laboratories, Inc., and under Contract W19-122 ac-24 with Harvard University.

[1] Rittner, Hutner, and du Pré, J. Chem. Phys. **17**, 198 (1949).
[2] Hutner, Rittner, and du Pré, J. Chem. Phys. **17**, 204 (1949).
[3] N. F. Mott and M. J. Littleton, Trans. Faraday Soc. **34**, 485 (1938).
[4] R. W. G. Wyckoff, *Crystal Structure* (Interscience Publishers, Inc., New York, 1948).
[5] K. Højendahl, Kgl. Danske Vid. Sels. **16**, 59 (1938).
[6] K. Spangenberg, Naturwiss. **15**, 206, 266 (1927).
[7] M. Haase, Zeits. f. Krist. **65**, 510 (1927).

values of the ionic polarizabilities, α_+ and α_-, were calculated in the following way from the mole refractions, R_+ and R_-, given by Pauling:[8]

$$\alpha_+/\alpha_- = R_+/R_-,$$
$$(\alpha_+ + \alpha_-) = (3a^3/2\pi)[(\kappa_0 - 1)/(\kappa_0 + 2)].$$

The numerical computations which required the solution of sets of ten simultaneous linear equations (see Part I,[1] Table I) were carried out by J. O. Gadd of the Harvard Computation Laboratory using the Mark I Computer.

The data employed and the results obtained are shown in Table I, where W_+ refers to the removal of a positive charge, and W_- to the removal of a negative charge.

It will be noted that the results for NaCl differ somewhat from those given in Table VIII of Part I. The reason for this is that in Part I we employed the same value of κ_0 as that used by Mott and Littleton to permit comparison with their results, whereas in the present work we consistently used the κ_0's given by Højendahl.

Although we realize that some of the substances listed in Table I may not be completely ionic, we believe that the results in such cases may be useful estimates. At the present time there does not appear to be an alternative method of computing the work of polarization in these compounds.

[8] L. Pauling, Proc. Roy. Soc. **A114**, 191 (1927).

ACKNOWLEDGMENTS

We wish to express our appreciation to Dr. E. P. Little, Chief, Computation Branch, Office of Air Research, Harvard University, for his kind cooperation and to Mr. J. O. Gadd of the Harvard Computation Laboratory for carrying out the involved numerical computations.

THE JOURNAL OF CHEMICAL PHYSICS VOLUME 18, NUMBER 3 MARCH, 1950

Critique of the Free Volume Theory of the Liquid State*

JOHN G. KIRKWOOD
Gates and Crellin Laboratories of Chemistry, California Institute of Technology, Pasadena, California
(Received August 29, 1949)

A deduction of the free volume theory of the liquid state from the general principle of statistical mechanics and certain well-defined approximations is undertaken. The Gibbs configuration integral is expressed as a sum of integrals corresponding to single and multiple occupancy of the cells of a reference lattice. The integral corresponding to single occupancy is evaluated with the approximate probability density, expressed as a product of functions of the coordinates of individual molecules, which leads to minimum free energy under the restraints of constant temperature and volume. The minimization of the free energy gives an integral equation for the probability density within each cell of the lattice. A first approximation of the solution of this equation yields a partition function identical with that of the Lennard-Jones-Devonshire free volume theory.

THE free volume theories of the liquid state developed by Eyring[1] and his co-workers and by Lennard-Jones and Devonshire[2] have provided a useful approximate description of the thermodynamic properties of liquids in terms of intermolecular forces. In these theories, a free volume v_f is defined in terms of the Gibbs phase integral Z_N in the configuration space of N molecules by the relation,

$$Z_N/N! = e^N v_f^N \exp(-\langle V_N\rangle_{Av}/kT),$$

where $\langle V_N\rangle_{Av}$ is the mean potential energy. The free volume v_f is then calculated without reference to the exact Gibbs theory by means of intuitively plausible models, in which each molecule is supposed to execute gas-like thermal motion in a cage formed by the average intermolecular force field of its neighbors.

Since the free volume theory yields explicit results with less labor than do the more exact treatments of the liquid state based upon the theory of distribution functions,[3] it seemed worth while to the author to investigate the possibility of placing it on a sounder and less empirical basis by deriving it from the general principles of statistical mechanics by means of well-defined approximations. The results of this investigation are the subject of the present article.

It is shown that the Lennard-Jones free volume theory is a first approximation to a general free volume theory in which the probability density in configuration space is approximated by a product of functions of coordinates of individual molecules which yields the

* This work was supported by the USONR.
[1] H. J. Eyring and O. Hirschfelder, J. Chem. Phys. **41**, 250 (1937).
[2] Lennard-Jones and Devonshire, Proc. Roy. Soc. **A163**, 53 (1937); **165**, 1 (1938).
[3] J. G. Kirkwood, J. Chem. Phys. **3**, 300 (1935); J. E. Mayer, J. Chem. Phys. **15**, 187 (1947); M. Born and H. S. Green, Proc. Roy. Soc. **A188**, 10 (1946).

lowest free energy under the restraint of single occupancy of the cells of a reference lattice.

The free energy A_N of a closed system of N monatomic molecules is given by the theory of the classical canonical ensemble in the form,

$$e^{-\beta A_N}=\left(\frac{2\pi mkT}{h^2}\right)^{3N/2}\frac{Z_N}{N!}$$

$$Z_N=\int^v\cdots\int^v e^{-\beta V_N}\prod_{k=1}^{N}dv_K \qquad (1)$$

$$\beta=1/kT$$

$$V_N=\sum_{\substack{i=k\\=1}}^{N}V(R_{ik}),$$

where Z_N is the Gibbs phase integral in configuration space, v the volume, T the temperature, k the Boltzmann constant, h Planck's constant, and V_N the potential of intermolecular force. If we span the volume v by a virtual lattice of N cells $\Delta_1\cdots\Delta_N$, each of volume Δ, and express the integral over v in the configuration space of each molecule as a sum of integrals over the individual cells, we may write

$$Z_N=\sum_{l_1=1}^{N}\cdots\sum_{l_N=1}^{N}\int^{\Delta l_1}\cdots\int^{\Delta l_N}e^{-\beta V_N}\prod_{k=1}^{N}dv_k. \qquad (2)$$

The choice of the lattice is entirely arbitrary and it is not necessary to choose the number of cells equal to the number of molecules in the system, although we choose to do so here. The N^N integrals of the sum of Eq. (2) may all be expressed in terms of integrals of the type $Z_N^{(m_1\cdots m_N)}$ where $m_1\cdots m_N$ are the numbers of molecules occupying the respective cells $\Delta_1\cdots\Delta_N$ in the given term, with the result

$$\frac{Z_N}{N!}=\sum_{\substack{m_1\cdots m_N\\=0\\\Sigma m_s=N}}^{N}\frac{1}{\prod_{s=1}^{N}m_s!}Z_N^{(m_1\cdots m_N)}. \qquad (3)$$

If we denote the integral corresponding to single occupancy of each cell by $Z^{(1)}$,

$$Z^{(1)}=Z^{(1,1,\cdots 1)}=\int^{\Delta_1}\cdots\int^{\Delta_N}e^{-\beta V_N}\prod_{k=1}^{N}dv_k, \qquad (4)$$

and define a parameter σ by the relation,

$$\sigma^N=\sum_{\substack{m_1\cdots m_N\\=0\\\Sigma m_s=N}}^{N}\frac{1}{\prod_s m_s!}\frac{Z^{(m_1\cdots m_N)}}{Z^{(1)}} \qquad (5)$$

we may write in a formal way

$$\frac{Z_N}{N!}=\sigma^N Z^{(1)}. \qquad (6)$$

We remark that σ has the value unity, if, as at high densities, intermolecular repulsive forces exclude multiple occupancy by causing all $Z^{(m_1\cdots m_N)}$ except $Z^{(1)}$ to vanish. On the other hand σ approaches the value e when all $Z^{(m_1\cdots m_N)}$ become equal, as the density tends to zero. The communal entropy of Eyring is equal to $R\log\sigma$. In the empirical free volume theories σ has been assigned the value e without adequate justification, as has been pointed out by Rice. We will not attempt to resolve the communal entropy problem in the present investigation but will confine ourselves to the analysis of the free volume approximation to the phase integral $Z_N^{(1)}$ corresponding to single occupancy of each cell of the reference lattice.

The phase integral $Z_N^{(1)}$ is related to the relative probability density in configuration space $P_N^{(1)}$, subject to the restraint of single occupancy, in the following manner,

$$P_N^{(1)}=\exp(\beta[A_N^{(1)}-V_N])$$

$$\exp(-\beta A_N^{(1)})=Z_N^{(1)}$$

$$A_N^{(1)}=E_N^{(1)}-TS_N^{(1)}$$

$$E_N^{(1)}=\int^{\Delta_1}\cdots\int^{\Delta_N}V_N P_N^{(1)}\prod_{K=1}^{N}dv_k \qquad (7)$$

$$S_N^{(1)}=-k\int^{\Delta_1}\cdots\int^{\Delta_N}P_N^{(1)}\log P_N^{(1)}\prod_{K=1}^{N}dv_k.$$

From Eqs. (1), (6) and (7) we obtain for the total free energy A_N,

$$A_N=-NkT\log\left[\left(\frac{2\pi mkT}{h^2}\right)^{\frac{3}{2}}\sigma\right]+A_N^{(1)}. \qquad (8)$$

We now introduce the approximation, similar to that employed by Hartree in the solution of the Schrödinger equation for several particles,

$$P_N^{(1)}=\prod_{s=1}^{N}\varphi(\mathbf{r}_s)$$

$$\int^{\Delta}\varphi(\mathbf{r})dv=1 \qquad (9)$$

where $\varphi(\mathbf{r}_s)$ depends only on the position of molecule s in cell s, referred to some convenient origin in that cell. In this approximation, the free energy $A_N^{(1)}$ per mole becomes,

$$\frac{A_N^{(1)}}{RT}=\int^{\Delta}\varphi(\mathbf{r})\log\varphi(\mathbf{r})dv$$

$$+\tfrac{1}{2}\int^{\Delta}\int^{\Delta}E(\mathbf{r}-\mathbf{r}')\varphi(\mathbf{r})\varphi(\mathbf{r}')dvdv' \qquad (10)$$

$$E(\mathbf{r})=\sum_{l=2}^{\infty}V(\mathbf{R}_{1l}+\mathbf{r})$$

where V is the potential of intermolecular force, say of the Lennard-Jones form, for a pair of molecules, and with the neglect of surface contributions, the sum defining $E(\mathbf{r})$ extends over all cells of an infinite lattice exterior to an arbitrary cell, labeled 1, $\mathbf{R}_{1l}$ being the lattice vector joining the origin of cell 1 and the origin of cell l. The choice of $\varphi(\mathbf{r})$ leading to the best approximation to the free energy under the given restraints is that which minimizes the free energy $A_N^{(1)}$ at constant T and Δ. Regarding $A_N^{(1)}$ as a functional of φ we obtain for the extremalization condition,

$$\delta A_N^{(1)} = \int^{\Delta} \Big\{ \log\varphi(\mathbf{r}) + \int^{\Delta'} E(\mathbf{r}-\mathbf{r}')\varphi(\mathbf{r}')dv' \Big\} \delta\varphi dv = 0 \quad (11)$$

$$\int^{\Delta} \delta\varphi dv = 0$$

where the restraint is imposed by the normalization condition, Eq. (9). Using Lagrange multipliers, we obtain from Eq. (11) the following integral equation,

$$\begin{aligned} \varphi &= e^{\beta(\alpha-\psi)} \\ e^{-\beta\alpha} &= \int^{\Delta} e^{-\beta\psi(\mathbf{r})} dv \\ \psi(\mathbf{r}) &= \int^{\Delta} w(\mathbf{r}-\mathbf{r}') e^{\beta[\alpha-\psi(\mathbf{r}')]} dv' \qquad (12) \\ w(\mathbf{r}) &= E(\mathbf{r}) - \bar{E} \\ \bar{E} &= \int^{\Delta}\int^{\Delta} E(\mathbf{r}-\mathbf{r}')\varphi(\mathbf{r})\varphi(\mathbf{r}')dvdv' \end{aligned}$$

which determines the best approximation to $P_N^{(1)}$ in the form of a product of functions of the coordinates of individual molecules.

Equations (8), (10) and (12) lead at once to the following expression for the free energy A_N of the system,

$$\begin{aligned} A_N/RT &= -\log\left[\left(\frac{2\pi mkT}{h^2}\right)^{\frac{3}{2}} \sigma v_f\right] + \bar{E}/2kT \qquad (13) \\ v_f &= \int^{\Delta} e^{-\beta\psi(r)} dv \end{aligned}$$

where the free volume v_f is determined by the function $\psi(\mathbf{r})$ satisfying the integral equation, Eq. (12). The precise value of the parameter σ, determining the communal entropy is of course left open in the present theory, as is the choice of reference lattice leading to the lowest free energy, subject to the restraint of single cell occupancy. For molecules interacting through central forces, the face-centered cubic structure is presumably the most favorable.

If $\varphi(\mathbf{r})$ is sharply peaked in the vicinity of the cell origin, it may be set equal to $\delta(\mathbf{r})$ in zero approximation. Equation (12) then leads to a first approximation,

$$\begin{aligned} \psi_1(r) &= w_0(\mathbf{r}) \\ \bar{E} &= E_0 = \sum_{l=2}^{N} V(\mathbf{R}_{1l}) \qquad (14) \\ w_0(\mathbf{r}) &= \sum_{l=2}^{N} [V(\mathbf{R}_{1l}+\mathbf{r}) - V(\mathbf{R}_{1l})]. \end{aligned}$$

If the sums defining E_0 and $w_0(\mathbf{r})$ are extended only over nearest neighbor sites, and if the nearest neighbor sum is replaced by an integral over a sphere of radius equal to the distance between neighbors, $w_0(\mathbf{r})$ becomes identical with the smoothed potential of the Lennard-Jones-Devonshire theory. To achieve an improvement on their theory, a second approximation to $\psi(\mathbf{r})$ might be obtained in the form

$$\psi_2(\mathbf{r}) = \int^{\Delta} w_0(\mathbf{r}-\mathbf{r}') e^{\beta[\alpha_0 - w_0(r')]} dv'. \qquad (15)$$

If convergent, a continuation of this scheme of approximation might be employed to obtain a numerical solution to the integral equation, Eq. (12), leading to a refinement of the Lennard-Jones-Devonshire theory. Whether this would be worthwhile in the absence of a solution of the communal entropy problem is open to question.

The present considerations allow the deductions of the free volume theory of the liquid state from the fundamental principles of statistical mechanics on the basis of well-defined approximations. The limitations of the free volume theory are clearly exhibited. Without a solution to the communal entropy problem, it is doubtful whether such a theory could ever distinguish between the liquid and solid state.

A Photoelectric Investigation of the Cool Flame of Ether

LUDOVIC OUELLET, EDOUARD LEGER, AND CYRIAS OUELLET
Département de Chimie, Université Laval, Québec, P. Q., Canada.

(Received October 3, 1949)

A method is described, in which the light from a cool flame under the form of a static, uniform glow is measured as a function of time by means of a multiplier photo-tube and a single-sweep cathode-ray oscillograph. The circuit embodies an a.c.–d.c. amplifier and a slow sweep. Cool flames of diethylether-oxygen mixtures in a Pyrex cylinder 4.6 cm in diameter have been studied under the following range of conditions: 180–250°C, 0–150 mm and 5–95 percent ether. The pulsating glow, which lasts about 1 second, shows two and sometimes more maxima. The generally accepted lower pressure limits appear as regions of feeble but smoothly decreasing intensities. Under the conditions of our experiments, the temperature coefficient is negligible. Both intensity and integral emission increase regularly with the concentrations of the reactants and are maximum at 50 percent ether by volume, the variations being roughly symmetrical with respect to the partial pressures of either component. Variations of pressure and composition cause regular but considerable changes in the shapes of the oscillograms. Light and pressure pulses follow each other closely, suggesting that the latter are of mainly thermal origin and that the light intensities reflect the instantaneous reaction rates. The glow lasts longer in the wider vessels. In the presence of the reaction products, it either fails to appear or emits the normal amount of light. A preliminary analysis of the quantitative data is given and possible interpretations, in terms of oxidation mechanisms, are discussed.

1. INTRODUCTION

THE faint glow or "cool flame" which accompanies the low temperature oxidation of certain substances in the gas phase has received the attention of most investigators of combustion processes.[1] Among the numerous papers on the cool flames of hydrocarbons, aldehydes, and ethers, only a few can be mentioned here as a key to the literature.[2–11] The phenomena observed with different substances are qualitatively the same. The glow takes place within certain temperature-pressure-composition limits and is accompanied by moderate pressure pulses.[12] The spectrum, which extends from 3400 to 4500A, is reported to be identical with that of excited formaldehyde[13] and the quantum yield is estimated to be of the order of one photon per 10^6 reacting molecules,[14] indicating that the luminescence probably originates in a side reaction. The products are mainly combustion intermediates.

Visual observations or long photographic exposures necessitating dynamic systems have long been the only available methods for the study of this luminescence. As shown in a recent note[15] by the authors, the use of a multiplier photo-tube and recording oscillograph now permits a more detailed investigation. This new method and some of the results obtained with cool flames of diethylether-oxygen mixtures are described in the present paper.

2. EXPERIMENTAL

To eliminate most complicating factors not connected with the chemical process itself, the quiet luminescence of a gaseous mixture at rest and in thermal equilibrium was chosen as the object of these first experiments and is believed to have been reasonably well approximated, as shown by the tests described below. This choice also simplified the requirements of the optical and light-recording systems.

a. Production of the Glow

The glow was produced by rushing the cold gaseous mixture through stopcock A (Fig. 1) into the evacuated and pre-heated reaction vessel U, generally a Pyrex

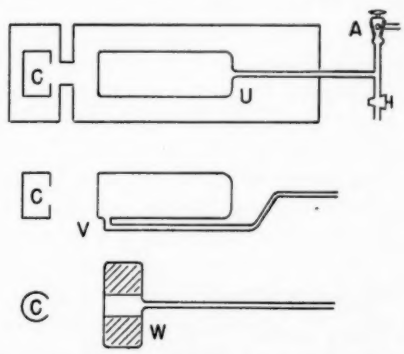

FIG. 1. Positions of multiplier photo-tube C and reaction vessels with gas inlets at U, V, or W (cylinder seen from above, screened except at the middle).

[1] B. Lewis and G. von Elbe, *Combustion, Flames and Explosions of Gases* (Cambridge University Press, London 1938); W. Jost, *Explosionen—und Verbrennungsvorgänge in Gasen* (Verlag. Julius Springer, Berlin, 1939).
[2] H. J. Emeléus, J. Chem. Soc. 2948 (1926); 1733 (1929).
[3] Gill, Mardles, and Tett, Trans. Faraday Soc. **24**, 574 (1928).
[4] Pope, Dykstra, and Edgar, J. Am. Chem. Soc. **51**, 1875 (1929).
[5] R. N. Pease, J. Am. Chem. Soc. **51**, 1839 (1929).
[6] M. Prettre, Bull. Soc. Chim. France **51**, 1132 (1932); Comptes Rendus **207**, 532 (1938).
[7] D. T. A. Townend, Chem. Rev. **21**, 259 (1937); E. A. C. Chamberlain and D. T. A. Townend, Proc. Roy. Soc. **A158**, 415 (1937); M. Maccormac and D. T. A. Townend, J. Chem. Soc. 155 (1940).
[8] B. Aivazov and M. B. Neuman, Zeits. f. physik. Chemie **B33**, 349 (1936); Acta Phys. Chim. U.R.S.S. **4**, 575 (1936); **6**, 279 (1937).
[9] D. M. Newitt and L. S. Thornes, J. Chem. Soc. 1656 (1937).
[10] L. Guibiansky, Acta Phys. Chim. U.R.S.S. **9**, 621 (1938).
[11] A. D. Walsh, Trans. Faraday Soc. **42**, 269 (1946); **43**, 297, 305 (1947).
[12] K. I. Ermakova, J. Phys. Chem. U. S. S. R. **14**, 148 (1940).
[13] A. R. Ubbelohde, Proc. Roy. Soc. **A152**, 354, 378 (1935).
[14] J. E. C. Topps and D. T. A. Townend, Trans. Faraday Soc. **42**, 345 (1946).
[15] Ouellet, Leger, and Ouellet, J. Chem. Phys. **17**, 746 (1949).

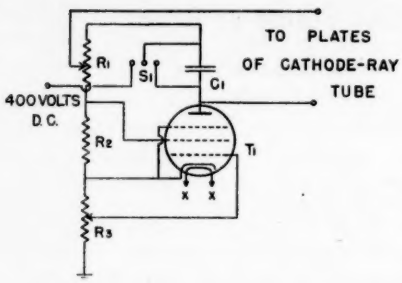

FIG. 2. Slow sweep generator for the cathode-ray tube. R_1—30K (Potentiometer position control). R_2—10K. R_3—1K (10 steps speed control). C_1—4μf, 1000 v. oil. T_1—6SJ7. S_1—S.P.D.T. (switch).

cylinder 13 cm long and 4.6 cm in diameter, enclosed in a brass furnace in which the temperature was constant and uniform within ± 1°C. The vessel was connected to the pumping system, including liquid air traps, a VMF5 oil diffusion pump and a Hyvac pump, and also to a mercury manometer which was cut off during a flame to prevent spurious pressure fluctuations. All stopcocks and ground joints were lubricated with Apiezon *M* grease. The ether used was Ether Absolute Merk, distilled once over an acid solution of potassium permanganate to destroy the peroxides, dried over metallic sodium and stored in vacuum. Mixtures of known compositions were prepared by evaporating some of this ether into an evacuated Pyrex reservoir, adding oxygen from a commercial cylinder to the required partial pressure and allowing to stand for one or two hours to ensure homogeneous mixing. Before each run, an adequate amount was transferred to an auxiliary flask, from which it was rushed into U by opening A. The Pyrex reservoirs were placed in metal cages packed with asbestos sheets. Whenever a detonation destroyed the apparatus, it originated in U, which was left intact in every case, and propagated through the manifold to reduce one or another section of it to glass powder. No explosions occured at pressures below 150 mm.

b. Light-Recording System

An 1P28 Multiplier Photo-tube, available in this laboratory, was used as radiation detector. It was placed at C (Fig. 1) and, to keep its temperature below 40°C, was enclosed in a water-cooled brass jacket bearing a narrow window through which the photocathode could see the reaction vessel U. It was operated under a 1200-v stabilized and frequently checked d.c. voltage, applied to the successive plates of the phototube through nine 10K resistances in a cascade arrangement. The current drawn from the last anode caused a potential drop in a resistance variable in steps of 20, 10, 5, and 1.3 meg., to provide four different sensitivities. This potential drop was amplified and applied to the deflection plates of a cathode-ray tube. The dark current was 1–3 percent of the photoelectric currents measured.

The problem being to record, on a single curve and

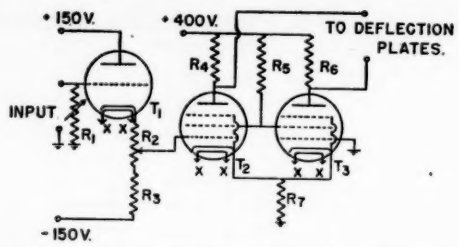

FIG. 3. A.c.-d.c. cathode-ray tube deflection amplifier (similar to amplifiers in Dumont, 208 oscillograph). R_1—20M, 10M, 5M in steps. R_2—20K potentiometer. R_3—100K. R_4—R_6—27K. R_5—150K. R_7—400 ohm. T_1—6J5. T_2—T_3—6V6—G.

without distortion, voltage surges lasting about one second, it was necessary to use a slow, single sweep and d.c.–a.c. amplificaion so that a conventional cathode-ray oscillograph could not be employed. To meet the first requirement, a slow linear sweep circuit was designed (Fig. 2), in which a 4μF condenser was charged through a constant-current device, in this case a 6SJ7 pentode tube. The terminals of the condenser were connected directly to the plates of the cathode-ray tube. The grid-bias of the pentode, at constant screen voltage, was made variable by steps to obtain a series of sweep periods extending from 0.1 to 12 seconds and provisions were made to permit a single sweep and a stationary position.

In the d.c.–a.c. amplifier (Fig. 3), two 6V6 beam-power tubes, connected as push-pull voltage amplifiers, provided a symmetrical deflection of the cathode-ray tube beam. The input of one of the tubes consisted of a cathode-follower circuit, permitting the high impedance input necessary for the amplification of the current surges due to the low level transient pulses, and the introduction of a positioning control. The voltage output was connected directly to the deflection plates of a 5-inch, blue screen Du Mont cathode-ray tube. Most of the circuits in the recording system were fed by independent, stabilized power supplies.

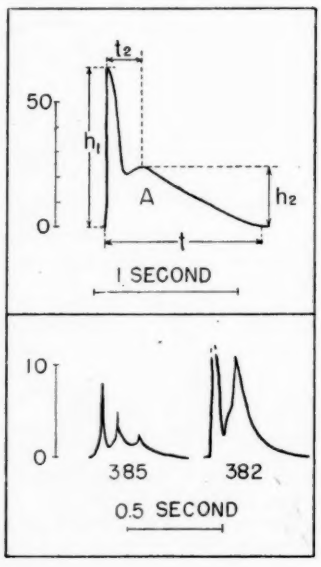

FIG. 4. Typical oscillogram, illustrating parameters h_1, h_2, t_2, t and A. Below, two oscillograms of flames at 5 percent ether, showing periodicity.

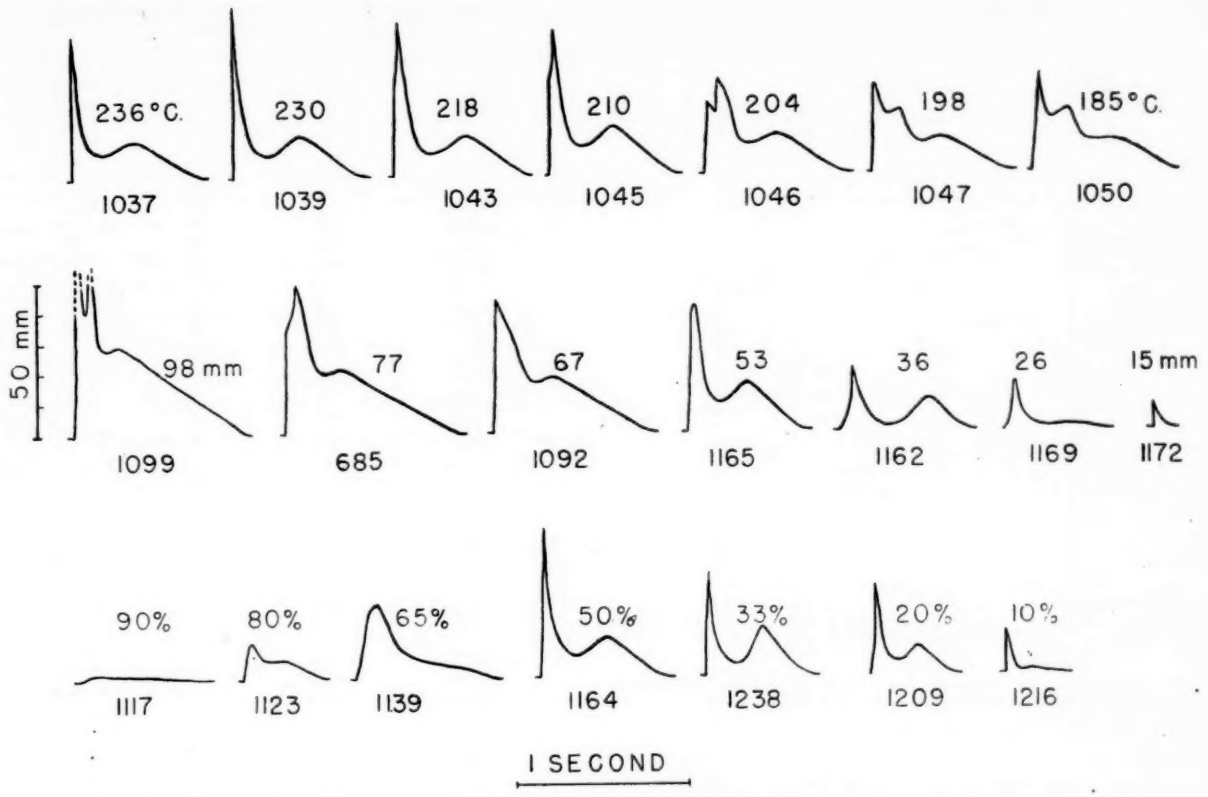

FIG. 5. Families of oscillograms showing the influence of temperature (first row), pressure (second row) and composition (third row). The numbers refer to Table I.

Photographic records of the oscillograms were made by the crude but convenient method of applying Velox rapid F-4 paper directly on the screen of the cathode-ray tube. The loss in definition was compensated by the advantage of immediately obtaining records of suitable size for direct examination and transcription on co-ordinate paper.

c. Performance

The reproducibility of the glow and the fidelity of the recording system are shown by the agreement, generally within 5 percent, of oscillograms obtained from identical runs, repeated subsequently or at intervals of several months. A preliminary survey of the field of experimental conditions provided a variety of oscillograms against which one member of almost every new series of experiments could be checked. The oscillograms in Figs. 5 and 8, and the points from which each curve in Figs. 6, 7, 9, 10, 11, and 13 was constructed, were collected from several different series of runs. The results were not affected by varying the period of evacuation between flames, discarding the diffusion pump, cleaning the reaction vessel with either chromic or nitric acid and distilled water, coating it with potassium chloride, or replacing it with another one of the same geometry.

The pulses in the recorded light-intensities could be attributed to spurious dynamic effects such as traveling flames. However, visual observations in the dark, using a Pyrex furnace instead of the one described above, failed to reveal any localization or movement in the faint bluish glow which seemed to fill the reaction chamber uniformly. Opening stopcock A more or less brusquely or changing the position of the gas inlet (Fig. 1) from U to V to W, did not alter the oscillograms. These tests, and the general regularity and reproducibility exhibited by the results, make it appear very probable that the observed pulses essentially reflect the course of the chemical reaction.

3. RESULTS

Most of the results described in this paper have been obtained in a 4.6×13 cm Pyrex cylinder, with diethyl-ether-oxygen mixtures of compositions expressed in percent ether by volume, at pressures and temperatures not exceeding 150 mm Hg and 250° C. All light intensities are arbitrarily expressed in millimeters deflection of the cathode-ray spot and the integral light emissions are given as the areas in square millimeters covered by the oscillograms. No absolute light-measurements have been attempted at this stage. Although the initial pressures could be estimated, the values given here are those of the measured final pressures.

a. General Features

A typical oscillogram, showing the light intensity against time, is given in Fig. 4 (above), together with

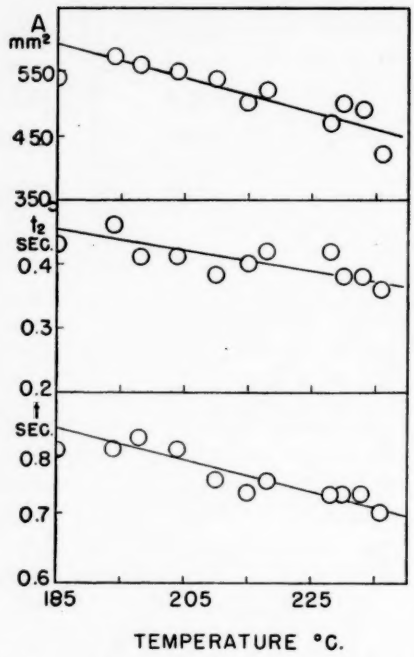

FIG. 6. Influence of temperature on total emission A, position t_2 of last maximum and total duration t, for series of flames at 50 percent ether and 50-mm total pressure.

the parameters which have been found useful in the description of the majority of our oscillograms: h_1 and h_2 the heights of the two maxima, t_2 the time of appearance of the second or last maximum, t, the approximate total duration of the glow, and A, the area. As shown in the lower half of Fig. 4, several sharp peaks may appear under certain conditions, especially at the extreme compositions, *viz.* 5 percent ether (No. 385). Some apparently minor details, for instance the small peak on the left of No. 1046 (Fig. 5), are reproducible with astonishing fidelity and should be considered significant. The data concerning all oscillograms shown in the figures are collected in Table I.

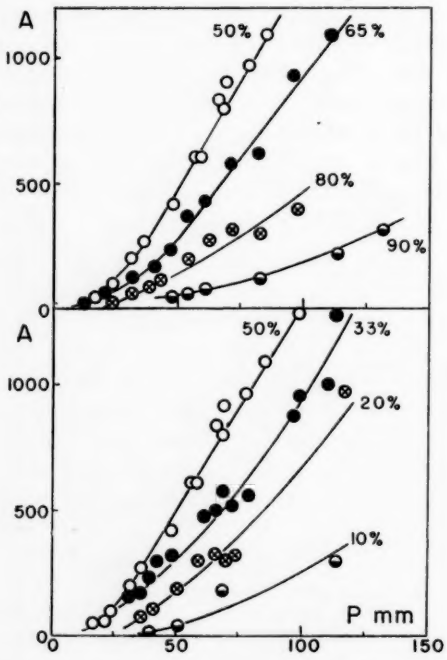

FIG. 7. Total emission at 215°C as a function of total pressure, for mixtures of various compositions (percent ether by volume).

TABLE I. Conditions under which the oscillograms of Figs 5 and 6 were obtained.*

Run No.	Temperature °C	Composition % ether	Pressure mm Hg
1037	236	50	51
1039	230	50	50
1043	218	50	50
1045	210	50	52
1046	204	50	50
1047	198	50	52
1050	185	50	52
1099	215	50	98
685	215	50	77
1092	215	50	67
1165	215	50	53
1167	215	50	36
1169	215	50	26
1172	215	50	15
1117	215	90	48
1123	215	80	46
1139	215	65	53
1164	215	50	48
1238	215	33	49
1209	215	30	51
1226	215	10	51
1232	215	33	114
683	215	50	76
1138	215	65	60
1123	215	80	46
752	215	50	70[a]
686	215	50	69
656	215	50	72[b]
764	215	50	71[c]

* Reaction vessel: 46-mm Pyrex cylinder, except
[a] 70-mm sphere.
[b] 34-mm cylinder.
[c] 21-mm cylinder.

b. Influence of the Variables

Generally, only the initial and final values of the variables temperature, pressure and composition are known, since all three undergo unpredictable and mutually dependent variations during the reaction. Fortunately, it will be seen that a number of simplifying factors operate.

The temperature coefficient is small, especially between 210 and 240°C, as shown by the top horizontal row of oscillograms in Fig. 5, all from mixtures with 50 percent ether at a total pressure of 50-mm Hg. Note the gradual merging of the two first maxima as the temperature passes from 185 to 210°C. The curves in Fig. 6 show slightly negative temperature coefficients for the parameters A, t_2, and t. This effect is real for t_2 and t; in the case of A, it can be attributed mainly to the decrease in concentration resulting from a temperature rise at constant pressure.

In the second row of Fig. 5 it is seen, from right to

left, that the main result of increasing the pressure i.e., concentration, at constant temperature and composition, is to enlarge the diagram in all directions and reduce the distance between the two main maxima, a naturally expected acceleration of part of the process. The second maximum appears only above about 20-mm Hg and the first one becomes composite at the higher pressures, where the onset of the glow is most sudden and its final decay linear. The curves in Fig. 7 show the rates of increase of the total emission as a function of the final pressure at various constant compositions.

The shape of the oscillogram is affected by changes in the composition of the mixture, as indicated by the bottom row in Fig. 5. Figure 8-A (reading up) shows the effect of increasing the pressure of oxygen when that of ether is kept constant at 38 mm. When the partial

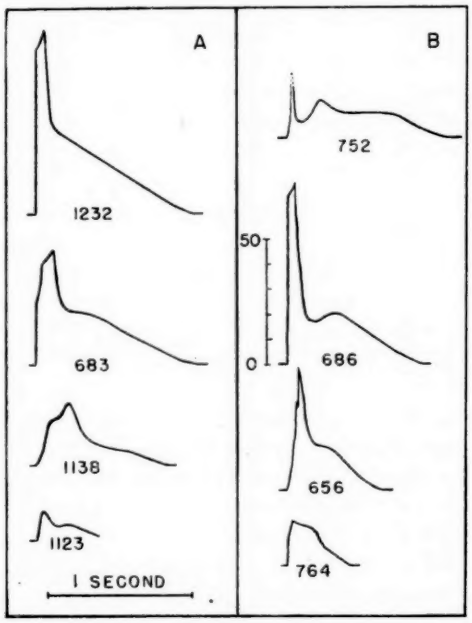

FIG. 8. (Read up). *A*—Effect of increasing oxygen pressure at constant ether pressure. *B*—Effect of increasing the diameter. The numbers refer to Table I.

pressures of ether and oxygen are increased one at a time, the influence on the total emission is that shown by the curves in Fig. 9. The saturation effect is more pronounced when ether is in excess. It is interesting to note that Cullis and Hinshelwood[16] have found a similar saturation, but only with excess oxygen, for the rates of oxidation of pentane and hexane.

It is clear, from the curves in Fig. 7, that at all total pressures the total emission is maximum at a composition of 50 percent ether, the composition effect being roughly symmetrical with respect to both reactants. In fact, all the points in this figure can be gathered about a single approximately straight line by plotting

[16] C. T. Cullis and C. N. Hinshelwood, Faraday Soc. Discussions 2, 117 (1947).

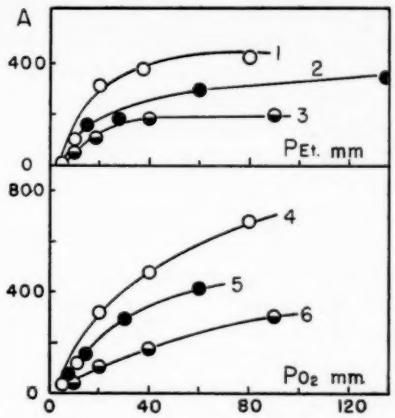

FIG. 9. Effect of partial pressure of each reactant on total emission *A*. Constant pressures of oxygen (1) 20 mm, (2) 15 mm (3) 10 mm; of ether (4) 20 mm, (5) 15 mm and (6) 10 mm.

the empirical function

$$A=K\left(\frac{P_{Et}}{P_{Et}+P_{O_2}}\right)P_{O_2} \quad \text{or} \quad A=K\left(\frac{P_{O_2}}{P_{Et}+P_{O_2}}\right)P_{Et}$$

(for $Et>50$ percent) (for $Et<50$ percent),

where P_{Et} and P_{O_2} are the partial pressures of ether and oxygen respectively and K is a constant having the same value in both cases. This approximate symmetry is clearly brought out in Fig. 10, where the total emission at three values of the total pressure is plotted against the composition. Numerous other experiments also indicate that, for given initial concentrations of the reactants, the total emission is remarkably independent of all other factors including the deformation of the oscillograms, either accidental or caused by the addition of certain gases. Figure 9, however, shows the limitations of that symmetry.

The complicated diameter effects will not be described in the present paper. Their general trend is shown by the second vertical row in Fig. 8. From top to bottom are oscillograms obtained at 215°C, 50 percent ether and 70-mm Hg in a Pyrex sphere 70 mm in diameter and in cylinders 46, 34 and 21 mm in diameter. The intensities are not comparable, owing to differences in the quantities of reactants and geometrical factors. The main effect is a shortening of the second part of the flame as the diameter is decreased. Complications arise above 230°C.

The empirical analysis given above is by no means exhaustive. A condensed set of elementary data, listed in Table II, may be used in seeking further relations.

Concerning the interdependence of the variables, the results show that the temperature coefficient is so small, in the region studied, that a rise of 50°C resulting from the reaction would exert little effect on the luminescence. In a series of experiments, pressure pulses were damped by adding to the system a dead volume of one-half that of the reaction vessel. Identical oscillograms were ob-

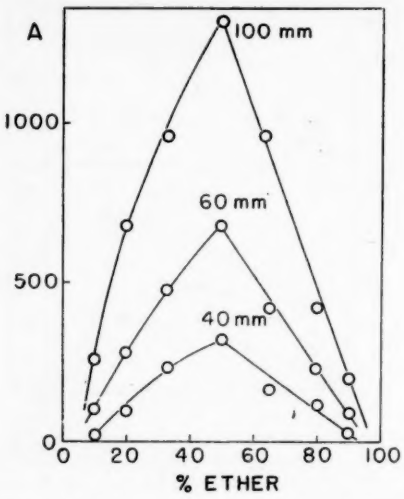

FIG. 10. Total emission A at 215°C, plotted against percent ether at three values of the total pressure: 40, 60 and 100 mm.

tained with and without that dead space, proving that pressure as such exerts no appreciable influence. The pressure effects described above are therefore genuine concentration effects.

One possible source of the pulsations would be an inhibition of the glow by its own products. In a few experiments, the reaction vessel was incompletely evacuated after a flame, and a fresh mixture was rushed in. According to the residual pressure in the vessel, the flame either failed to appear or, when it did, it gave off the normal amounts of light although the oscillograms were distorted and induction periods of several seconds were observed.

c. The Lower Pressure Limit

It has been generally accepted that cool flames take place above more or less defined pressure limits, but the values given by different authors show discrepancies which have been attributed to differences in the experimental conditions. It is clear that the concept of sharp explosion limit is inadequate to describe the complex state of affairs observed in this work. The curves of Figs. 7 and 9 show no important discontinuities as the pressure is lowered. The height h_1 of the first maximum levels off gradually and has been followed, as shown in Fig. 11, down to a pressure of 6 mm, which corresponds roughly to the limit found by Ermakova.[12] That of the second maximum, h_2, vanishes at about 20 mm without any previous sign of collapse (Fig. 11). The limit of sensitivity of the eye is likely to depend upon the distribution of intensities over the short period of the glow, so that the relatively rapid and simultaneous loss in both intensity and duration at the lower pressures may cause the illusion of a breakdown.

d. Manometric Measurements

It is obviously desirable to correlate the pulses of the glow with the concomitant pulses in temperature and pressure. A few pressure diagrams were obtained by means of a new recording manometer designed and built by Dr. P. A. Bricout and Mr. M. Boisvert,[17] to

TABLE II. Condensed set of data for flames at 215°C, showing values of integral emission A, heights h_1 and h_2 of first and second maxima, times of second maximum t_2 and total durations t.

Run No.	Comp. % ether	Pressure mm Hg	Area mm²	h_1 mm	h_2 mm	t_2 sec.	t sec.
224	90	132	320	9	8	0.52	1.13
222	90	114	220	9	6	0.43	1.06
1113	90	83	120	5	3	0.38	0.82
1115	90	63	80	3	3	0.33	0.78
1116	90	54	60	2	2	0.38	0.87
270	80	97	400	19	16	0.26	0.80
1121	80	63	280	14	17	0.19	0.49
1124	80	43	120	8	4	0.30	0.49
1126	80	32	65	6	2	0.16	0.49
1129	80	21	35	3	0	—	0.49
1308	65	127	1340	63	30	0.26	0.90
1310	65	96	930	33	21	0.35	0.82
1313	65	61	430	20	18	0.23	0.77
1141	65	41	160	20	3	0.30	0.63
1148	65	20	60	8	0	—	0.26
1299	50	100	1320	46	30	0.26	1.02
684	50	81	1050	65	24	0.26	1.03
1044	50	58	610	70	18	0.33	0.84
1168	50	33	200	15	6	0.52	0.80
1170	50	22	55	16	1	0.35	0.63
1234	33	99	960	55	23	0.24	1.05
899	33	79	550	60	18	0.21	0.87
1236	33	61	480	40	15	0.35	0.75
1240	33	39	240	12	12	0.42	0.64
567	33	31	12	12	0	—	0.12
1204	20	117	975	78	24	0.23	1.15
1206	20	72	340	80	16	0.23	0.64
1208	20	59	300	53	12	0.24	0.57
1211	20	36	70	23	1	0.35	0.43
1218	10	113	300	70	7	0.30	0.66
1224	10	68	88	27	5	0.19	0.37
1228	10	40	10	12	0	—	0.37

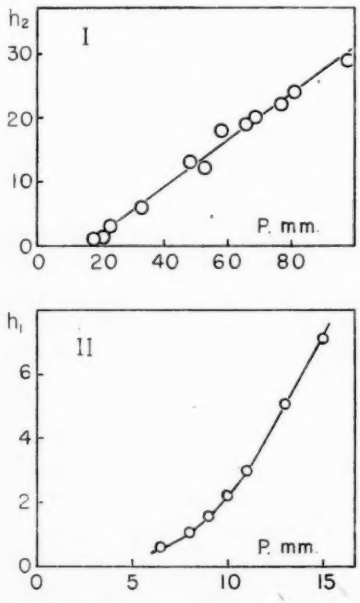

FIG. 11. Heights of last (I) and first (II) maxima against total pressure at 215°C and 65 percent ether, showing disappearance of h_2 at ~20 mm and absence of sharp lower limit.

[17] P. A. Bricout and M. Boisvert, Rev. Sci. Inst. **21**, 98 (1950); Revue Générale d'Electricité (in press); M. Boisvert, thèse, Université Laval (1949).

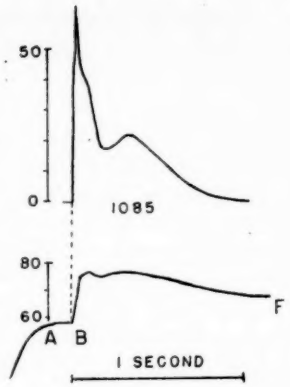

FIG. 12. Coincidence of light and pressure pulses at 199°C and 50 percent ether. Pressure scale (lower curve) in mm Hg. Note short induction period AB after thermal equilibrium at A.

whom we are indebted for the loan of their instrument and their help in carrying out the measurements. The core of the apparatus is a pressure box closed by a thin steel diaphragm, whose displacements cause frequency variations in an oscillating circuit. These are detected by a discriminator practically insensitive to the amplitudes of the oscillations, amplified and recorded on the moving film of a G.E. oscillograph. By scale adjustment, it is possible either to cover the whole pressure range or to obtain an enlarged record of the pulses. The results of these experiments are given as preliminary indications only.

Such a pressure diagram is compared, in Fig. 12, to the corresponding luminescence curve for a flame at 199°C, 50 percent ether and 67-mm final pressure. Thermal equilibrium is reached near A, before the end B of the induction period, a situation which seems to obtain only at temperatures lower than about 230°C. Starting from B, luminescence and pressure pulses follow each other rather closely, the pressure remaining constant for at least several seconds after the extinction of the glow at F. From a number of such manograms for 50 percent ether, the final pressures P_f, corrected for the dead volume of the manometer and its connections, have been plotted (Fig. 13) against the initial pressures P_0, giving a straight line of slope 1.5 which, by extrapolation, cuts the abscissa at $P_0 = 20$ mm, i.e., at the pressure under which no second maximum is observed (Fig. 11–I). The slope of this curve is taken as a temporary indication that the numbers of molecules before and after the reaction are roughly in the ratio of 2 to 3. Only poor correlation, based on too few data, has been found so far between the final pressure increase and the total amount of light emitted.

Other observations and relations, bearing mainly on flames in the lower and higher temperature ranges, diameter effects and the influence of added gases, will be published later. Supplementary data can also be found elsewhere.[18]

4. DISCUSSION

The validity of the results reported in this paper is obviously limited to the relatively narrow range of conditions covered in this preliminary survey. The significance of the relations involving h_1, h_2, t_2 and t is also linked with that of these arbitrarily chosen parameters. These circumstances, however, have no bearing on a few immediate observations such as the existence and chemical origin of the pulses, the absence of sharp lower limits, the coincidence between light and pressure pulses, and the remarkably symmetrical influence of the concentrations of both reactants. With respect to the pulses, it is assumed that the light intensity is a measure of the instantaneous reaction velocity. This is also reflected by the pressure pulses, which are due in part to temperature rises proportional to the rate of heat evolution. A detailed comparison of light and pressure curves could, therefore, yield information on the degrees of exothermicity of the various stages of the reaction. The symmetry with respect to composition exhibited by the total emission, and its relative independence of the complicated sequence of events, suggest that it is governed mainly by the available amount of an intermediate formed from ether and oxygen in the ratio of one molecule of each, during the short induction period.

For the purpose of this discussion, we adopt as a

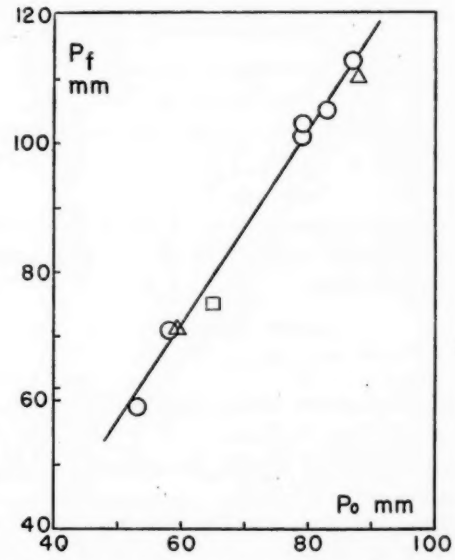

FIG. 13. Final pressures P_f against initial pressures P_0 for flames at 50 percent ether and 199°C (○), 215°C (△) and 225°C (□).

frame of reference the current ideas on the low temperature oxidation of hydrocarbons,[11,16,19] which is in many respects similar to that of ether. Following a simplified scheme susceptible of many variations, a peroxide or hydroperoxide accumulates during the induction period through a chain reaction such as:

$$RH + O_2 \rightarrow R + HO_2 \quad (1)$$

$$R + O_2 \rightarrow ROO \quad (2)$$

$$ROO + RH \rightarrow ROOH + R \quad (3)$$

[18] L. Ouellet, thèse, Université Laval (1949).

[19] M. F. R. Mulcahy, Trans. Faraday Soc. 45, 575 (1949).

(or even by a more direct reaction), up to a concentration where its rapid decomposition by branching sets in, giving rise to free radicals which

$$ROOH \rightarrow RO + OH \quad (4)$$

$$OH + RH \rightarrow R + H_2O \quad (5)$$

catalyze its own formation and also to aldehydes which accelerate its disappearance by condensing with it to form more labile hydroxyperoxides. The excited formaldehyde probably responsible for the luminescence would result from the recombination of two free radicals, for instance,

$$RCH_2O + OH \rightarrow ROH + HCHO^* \quad (6)$$

$$HCHO^* \rightarrow HCHO + h\nu \quad (7)$$

a type of process capable of supplying the 90 kcal. required[11] and sufficiently improbable to account for the low photon yield.

Frank-Kamenetskii[20] and Walsh have shown how a scheme of the above type can give rise to periodically varying reaction velocities. The sequence of autocatalytic steps,

$$A + X \xrightarrow{k_1} B + 2X$$

$$X + Y \xrightarrow{k_2} B + 2Y$$

$$A + Y \xrightarrow{k_3} B$$

where A is an original reactant, X and Y intermediates and B an inactive product, leads to the system of differential equations,

$$dx/dt = k_1ax - k_2xy$$
$$dy/dt = k_2xy - k_3ay$$

the solution of which shows that x and y can vary periodically in time. Intermediates X and Y have been tentatively identified with a hydroperoxide and aldehyde respectively.

Although none of our results could be considered as a confirmation of this or another mechanism, points of qualitative agreement are found. The central role played by an intermediate of composition ROOH (or ROO) receives support from the sharp maximum observed when ether and oxygen are present in the same proportion as in this compound. If the intermediate is reformed through a chain such as that given in Eqs. (2) and (3), necessitating the alternate intervention of RH and O_2, one would expect the same symmetry in the height h_2 of the second maximum. This is confirmed by data not included in this paper. The absence of a sharp lower limit and the gradual, initial rise in intensity at the lower pressures indicate that the concentration of intermediate at which branching or some other process sets in is not so critical as has been generally assumed. That few instances of evident periodicity are found in our oscillograms may be due to the fact that we have not, in this first survey, concentrated upon the conditions under which this phenomenon is produced in its purest form. According to Frank-Kamenetskii, the frequency of the oscillations should be given by

$$\nu = \frac{(k_1k_3)^{\frac{1}{2}}}{2\pi} a$$

where a is a function of the concentrations of the reactants. The reciprocal of ν, i.e., the distance between successive maxima, should decrease as the concentration increases. This effect, as evidenced by the middle row in Fig. 5, is found in practically all our results. A lengthening of the period, as the concentrations of the reactants decrease in the course of a single reaction, can also be seen on a few oscillograms bearing more than two maxima, such as 385 (Fig. 4), 1046, 1047, 1050 (Fig. 5), 1138, 752 (Fig. 8).

The later phase of the reaction seems to be predominantly affected by the walls. Among other possibilities it is conceivable, as already suggested,[15] that both ROO and ROOH accumulate, the first suffering a homogeneous decomposition, the second a mainly heterogeneous one. Whatever the species involved, the final decay is prolonged when diffusion to the walls is retarded, either by increasing the diameter or by raising the pressure.

The interpretation of these results obviously requires their correlation with analytical data obtained at the various stages of this rapid reaction. With this in view, a mass-spectrometer involving injection by molecular streaming and rapid scanning is under construction in this laboratory.

ACKNOWLEDGMENTS

Our thanks are due to the National Research Council of Canada for a grant in aid of this research and for studentships to two of us (L.O. and E.L.). We are also indebted to Dr. P. Bricout and Mr. M. Boisvert for the measurements carried out with their recording manometer.

[20] D. A. Frank-Kamenetskii, Comptes Rendus USSR **25**, 671 (1939); J. Phys. Chem. U.S.S.R. **14**, 30 (1940).

Letters to the Editor

THIS section will accept reports of new work, provided these are terse and contain few figures, and especially few half-tone cuts. The Editorial Board will not hold itself responsible for opinions expressed by the correspondents. Contributions to this section should not exceed 600 words in length and must reach the office of the Managing Editor not later than the 15th of the month preceding that of the issue in which the letter is to appear. No proof will be sent to the authors. The usual publication charge ($8.00 per page) will not be made and no reprints will be furnished free.

The Crystal Structures of CeB_4, ThB_4, and UB_4

ALLAN ZALKIN AND D. H. TEMPLETON
Department of Chemistry and Radiation Laboratory, University of California, Berkeley, California
January 9, 1950

THE compounds CeB_4, ThB_4, and UB_4 have been shown to crystallize in a new structure, which has been worked out from x-ray diffraction patterns. This structure is designated as the "UB_4 type structure," since that was the compound first observed. After the original preparation of this manuscript, we learned of the work of Andrieux,[1] who confirmed the identity of UB_4 by chemical analysis, and of Bertaut and Blum,[2] who found the unit cell dimensions and uranium coordinates for UB_4 crystals. They did not report the positions of the boron atoms. Their results are in agreement with ours reported here (with change of origin).

These borides were prepared by D. L. Sawyer and L. Brewer of this laboratory, who heated the metals and boron together in vacuum at about 1500°C. Powder diffraction patterns were obtained of the three compounds. Rotation and Weissenberg patterns were obtained for [110] and [001] axes of a small single crystal of ThB_4. The patterns were indexed on tetragonal lattices whose dimensions are listed in Table I ($CrK\alpha_1 = 2.2896$A).

TABLE I. Lattice parameters.

	a	c	c/a	X-ray density
CeB_4	7.205±0.008A	4.090±0.005A	0.568	5.74 g/cm³
ThB_4	7.256±0.004	4.113±0.002	0.567	8.45
UB_4	7.075±0.004	3.979±0.002	0.562	9.38[a]
UB_4[b]	7.066	3.97	0.562	

[a] Andrieux (see reference 1) reports 9.32 as the experimental density.
[b] Bertaut and Blum (see reference 2).

Consideration of the intensities leads to the following structure for the metal atoms:

Space group $D_{4h}^5 - P4/mbm$
4 Ce, Th, U in 4 (g): $\pm(u, 1/2+u, 0; 1/2-u, u, 0)$
$u = 0.31$.

These metal atoms are coplanar, with each having five nearly equidistant neighbors in the plane. Each metal atom has two neighbors in adjacent planes, but these are at a greater distance. This structure has holes, between the layers, which are best filled by boron atoms as follows:

4 BI in 4(e): $\pm(0, 0, v; 1/2, 1/2, v)$
$v = 0.2$
4 BII in 4(h): $\pm(w, 1/2+w, 1/2; 1/2-w, w, 1/2)$
$w = 0.1$
8 BIII in 8(j): $\pm(x, y, 1/2; 1/2+x, 1/2-y, 1/2; \bar{y}, x, 1/2; 1/2+y, 1/2+x, 1/2)$
$x = 0.2$
$y = 0.04$

Thus the compounds were assigned formulas of the type MB_4 in agreement with the deduction, from the phases observed in various preparations, that the composition is between MB_2 and MB_6.

This structure can be considered as a combination of two other more simple structures. Each atom BII is in a hole bounded by six metal atoms at corners of a triangular prism, as is the case with boron in the isostructural compounds AlB_2,[3] ZrB_2,[4] TiB_2,[5] CrB_2, NbB_2, TaB_2,[6] VB_2,[7] and UB_2.[8] The atoms BI and BIII are grouped together as octahedra in holes bounded by metals at the corners of square prisms, analogous to the arrangement in the compounds CaB_6, CeB_6, ThB_6, and others,[9] in which a simple cubic array of metal atoms is interpenetrated by boron octahedra. The interatomic distances in the MB_4 compounds are in reasonable agreement with the corresponding ones in the MB_2 and MB_6 compounds.

A more detailed account of this work will be published subsequently. We are indebted to Professor Brewer and Mr. Sawyer for their cooperation in preparing the samples, to Mrs. Lee Jackson for taking the powder patterns, and to Mrs. Carol Dauben for some of the calculations. This research was supported by the United States AEC.

[1] J. L. Andrieux, Ann. Chim. Phys. **12**, 423 (1929); J. L. Andrieux and P. Blum, Comptes Rendus **229**, 210 (1949).
[2] F. Bertaut and P. Blum, Comptes Rendus **229**, 666 (1949).
[3] W. Hofmann and W. Jäniche, Zeits. f. physik. Chemie (B) **31**, 214 (1936).
[4] P. McKenna, Ind. Eng. Chem. **28**, 767 (1936).
[5] P. Ehrlich, Angew. Chem. **59**, 163 (1947).
[6] R. Kiessling, Acta Chem. Scand. **3**, 90 (1949).
[7] Norton, Blumenthal, and Sindeband, J. Inst. Metals **1**, 749 (1949).
[8] A. Daane and N. C. Baenziger, USAEC Report ISC-53, July, 1949 (not yet published).
[9] G. Allard, Bull. Soc. chim. France **51**, 1213 (1932); M. v. Stackelberg and F. Neumann, Zeits. f. physik. Chemie (B) **19**, 314 (1932).

Carrier-Free Radioisotopes from Cyclotron Targets. VI. Preparation and Isolation of $Ag^{105, 106, 111}$ from Palladium*

HERMAN R. HAYMOND, KERMIT H. LARSON, ROY D. MAXWELL,** WARREN M. GARRISON, AND JOSEPH G. HAMILTON
Crocker Laboratory and Divisions of Medical Physics, Experimental Medicine, and Radiology, Radiation Laboratory, University of California, Berkeley, California
January 23, 1950

RADIOACTIVE silver, produced by bombardment of palladium with 19-Mev deuterons, has been isolated without added isotopic carrier. Four long-lived radioisotopes of silver† are produced in a thick target by (d, n) and $(d, 2n)$ reactions with deuterons of this energy: 45-day Ag^{105}, 8.2-day Ag^{106}, 225-day Ag^{110}, and 7.5-day Ag^{111}. Radioactive rhodium and radioactive ruthenium are also produced by (n, p) and (n, α) reactions respectively. The carrier-free radio-silver was separated from the target element and from the radioisotopes of rhodium and palladium by a precipitation technique using mercurous chloride as the co-precipitant.

A C.P. palladium metal target ($\frac{1}{4}$ in. Pd strip, soldered to a water-cooled copper plate with a silver-free hard solder) was bombarded with 19-Mev deuterons for a total of 200 μa-hr. at an average beam intensity of 20 μa. The irradiated surface was milled off (approximately 0.5 g of Pd) and dissolved in aqua regia. The solution was evaporated to dryness and dissolved in 500 ml of 0.5N HCl containing 50 mg each of rhodium and ruthenium hold-back carrier.

0.5 ml of a saturated solution of mercurous nitrate was added while the solution was stirred vigorously. The precipitate of Hg_2Cl_2 containing over 95 percent of the radio-silver was centrifuged, washed with 0.5N HCl and dissolved in a minimum volume of 16N HNO_3. 200 mg of Na_2SO_4 were added and the solution was evaporated to dryness in a porcelain dish which was then heated to 450°C for two hours to drive off the mercury

carrier. The activity was quantitatively soluble in 10 ml of distilled water to give an isotonic saline solution of carrier-free radio-silver which was used in subsequent biological experiments.

The radio-silver was identified by half-life determinations, absorption measurements and by chemical separation with carrier. The decay was followed for 200 days and showed the approximately 8-day[1,2] period of $Ag^{106,111}$ and the 45-day[3] period of Ag^{105}. One month after bombardment the activity showed only the 45-day period. After 150 days the decay curve began to level off, presumably into the 225-day[4] period of Ag^{110}; aluminum absorption measurements one week after bombardment showed the approximately 1.0-Mev beta-particle previously reported[5,6] for Ag^{106} and Ag^{111}; a tracer amount of activity added to a solution of Pd, Rh, Ru, and Ag in carrier amounts was quantitatively precipitated with the AgCl fraction.

We wish to thank the 60-inch cyclotron crew for the bombardments and target preparations, and Professor G. T. Seaborg for helpful suggestions.

* This document is based on work performed under the auspices of the AEC, Contract No. N-7405-eng-48-A.
** Lieutenant Colonel, U. S. Army, now stationed at Walter Reed Hospital, Washington, D. C.
† G. T. Seaborg and I. Perlman, Rev. Mod. Phys. **20**, 585 (1948).
[1] J. D. Kraus and J. M. Cork, Phys. Rev. **52**, 763 (1937).
[2] M. L. Pool, Phys. Rev. **53**, 116 (1938).
[3] T. Enns, Phys. Rev. **56**, 872 (1939).
[4] J. J. Livingood and G. T. Seaborg, Phys. Rev. **54**, 88 (1938).
[5] N. Feather and J. V. Dunworth, Proc. Roy. Soc. (London) **A168**, 566 (1938).
[6] E. P. Steinberg, Plutonium Project Report, cc-1331 (February, 1944), p. 23.

Absence of Spectroscopic Evidence for Rotational Isomerism in 2-Thiabutane*

D. H. Rank, E. R. Shull, and D. W. E. Axford
Spectroscopy Laboratory, Department of Physics, The Pennsylvania State College, State College, Pennsylvania
January 25, 1950

In view of the recent unequivocal evidence[1,2] for the existence of rotational isomers in normal butane it seems reasonable to expect similar behavior in similar small organic molecules. At the suggestion of Dr. H. M. Huffman of the United States Department of the Interior Bureau of Mines, Bartlesville, Oklahoma, we have investigated the Raman and infra-red spectrum of 2-thiabutane as a function of temperature.

The results of our experiments are conclusive in that they do not show the slightest evidence for the existence of two rotational isomers having an appreciable energy difference.

The relative intensity of lines in the Raman spectrum of the liquid remains strictly constant over a temperature range from 177° to 306°K. We have also investigated the infra-red spectrum of liquid and solid 2-thiabutane in the rocksalt region and find no change in the spectrum going from liquid to solid.

The sample furnished us by Dr. Huffman was stated to have an impurity of approximately 0.002 mole percent. In view of the fact that polarization data are lacking in the earlier work of Meyer[3] we are including our measurements for the sake of completeness. In general, our results agree with those of Meyer. We did not obtain the 1098 cm^{-1} frequency reported by him and with better resolution we have split the 1060 and 1430 frequencies into doublets. The Raman frequencies obtained are in cm^{-1}:

216 W.B.	Dep.	1042 M.	0.3
273 W.B.	0.5	1060 M.	0.3
355 S.	0.5	1259 W.	0.5
622 V.W.		1311 W.	0.5
656 V.V.S.	P.	1415 S.	
679 S.	P.	1429 S.B.	Dep.
727 V.S.	Dep.	2918 S.	P.
756 V.W.	Dep.	2922 S.	P.
975 M.B.	Dep.	3010 S.	Dep.

It should be mentioned that the infra-red spectrum of 2-thiabutane which we have obtained agrees in all particulars with the spectrum of this molecule obtained by the Bartlesville Laboratory of the U. S. Bureau of Mines.[4] It is to be noted that most of the stronger Raman lines coincide with strong infra-red bands. A complete analysis of this spectrum must probably await further experimental data in the *KBr* region and correlation with the heat capacity data. This data has recently been obtained by Donald W. Scott of the Bartlesville Laboratory and will appear in a separate publication.

* This research was carried out on Contract N6onr-269, Task V, of the ONR.
[1] Szasz, Sheppard, and Rank, J. Chem. Phys. **16**, 704 (1948).
[2] D. W. E. Axford and D. H. Rank, J. Chem. Phys. **17**, 430 (1949).
[3] J. Meyer, Z. Anorg. Chem. **203**, 146 (1931).
[4] Infra-Red Spectral Data, American Petroleum Institute Research Project 44, National Bureau of Standards, 2-thiabutane contributed by the U. S. Bureau of Mines, Bartlesville, Oklahoma.

Hydrazine Formation in the Photolysis of Ammonia at 1849A, and in the Reaction of Ammonia with Hg $6(^3P_1)$ and Hg $6(^1P_1)$ Atoms*

A. Kahn and H. E. Gunning
Department of Chemistry, Illinois Institute of Technology, Chicago, Illinois
January 6, 1950

Several investigators[1-3] have detected, as a product of the photolysis of ammonia, small amounts of a reducing substance which has been assumed to be hydrazine. However, only Gedye and Rideal[4] have actually identified hydrazine in the products of the photolysis. In their method ammonia is distilled from a dry ice-acetone trap to a liquid air trap via a quartz reaction cell illuminated with a quartz mercury arc. Under these conditions they report a yield of approximately 0.7 cc of gaseous hydrazine in 125 minutes of irradiation, at a flow rate of about 80 cc per minute.

We have attempted to duplicate the results of Gedye and Rideal; but only trace quantities of hydrazine were obtained.

Since ammonia shows maximum absorption in the region of 1850A, we have undertaken studies of the photolysis of ammonia, in a fast-flow system, using the high energy resonance line of mercury at 1849A. For this purpose a special U-shaped mercury-rare gas resonance discharge tube was fabricated, using very thin optical quartz to obtain maximum transmission at 1849A. The lamp is di-chromatic, emitting both at 1849A and 2537A. The 2537 line is not absorbed by ammonia. Using ammonia as an actinometer, it was found that the light intensity at 1849A was $1\text{–}2\times10^{-5}$ einstein per minute, depending upon the pressure of argon used in the lamp. The lamp was operated by a "neon sign" type transformer, with a 5000 v, 120 ma secondary. The electrodes of the lamp were ring-sealed into a large male quartz standard taper so that the lamp could be easily connected into the flow system.

In the fast-flow system ammonia is flowed past the resonance lamp, at atmospheric pressure, onto a cold finger trap containing dry-ice acetone, where it condenses, together with any hydrazine formed, and collects in a reservoir below. At the end of the run the liquid ammonia is evaporated to a small volume, after which water is added and the solution is acidified with concentrated hydrochloric acid. The amount of hydrazine formed is determined by titration with potassium iodate solution after the method developed by Penneman and Audrieth.[5] Hydrazine was positively identified by characterizing the benzaldehyde derivative. Blank experiments, made by injecting a known amount of hydrazine into the ammonia stream, with the lamp turned off, showed that hydrazine recovery was quantitative.

In one run, made at a flow rate of 5 liters per minute, with the lamp operating at 355 volts and 119 milliamperes, 19 milligrams

of hydrazine were obtained in 7 hours. Since great care was taken to exclude mercury vapor, photolysis must have been due almost exclusively to the mercury resonance line at 1849A.

When the ammonia was presaturated with mercury vapor, so that reaction occurred through collision of ammonia molecules with Hg $6(^3P_1)$ and Hg $6(^1P_1)$ atoms, only 6 milligrams of hydrazine were obtained in 7 hours, under flow conditions identical with the photolysis. It should be noted here that the effective light intensity has been increased by a factor of approximately twenty owing to the absorption of the 2537A by the mercury vapor.

In the direct photolysis, when hydrazine was passed through the lamp at a flow rate of 150 milligrams per hour, using either ammonia or nitrogen as a carrier gas, 40 milligrams of hydrazine were destroyed per hour. Under similar flow conditions, with mercury vapor in the stream, the hydrazine was completely destroyed, using nitrogen or helium as a carrier gas; and only 0.7 milligram of hydrazine were recovered per hour when ammonia was used as a carrier gas. The carrier gases were at atmospheric pressure.

These preliminary results are of interest for several reasons:

(1) The direct photolysis of ammonia is due almost exclusively to absorption of the 1849A line of mercury; and the photochemical effects of this line are of considerable fundamental interest. From our data on the photolytic decomposition of hydrazine, assuming a quantum yield of 1.25 for the decomposition,[6] we obtain a light intensity at 1849A, of 1.7×10^{-5} einstein per minute. A similar value was obtained from actinometric studies in a static system, using ammonia. Consequently the source is of sufficiently high intensity to be used for studying both photolyses at 1849A, and also for studying the reactions of molecules with Hg $6(^1P_1)$ atoms.

(2) In the photolysis of ammonia, the appearance of substantial quantities of hydrazine has been definitely established. Taking our value of 1.7×10^{-5} einstein per minute, for the light intensity of 1849A, a minimum quantum yield of 0.08 is obtained for hydrazine formation in the ammonia photolysis. In view of the fact that it has been shown that hydrazine undergoes some decomposition in passing through the irradiated zone, the quantum yield of formation must be much greater than 0.08.

(3) It has been generally assumed that hydrazine is formed by the recombination of NH_2 radicals. Since the primary processes in both the photolysis and the photosensitized reactions are generally agreed to involve the formation of NH_2 and H, the amount of hydrazine formed under photosensitizing conditions would be expected to be substantially greater than in the photolysis, owing to the higher quantum utilization. However the converse is true.

Further investigations on the photolyses at 1849A, and of the Hg $6(^1P_1)$ and Hg $6(^3P_1)$ reactions of ammonia and other molecules are in progress in this laboratory and more extensive reports will be submitted at a latter date.

* This work was supported in part by contract No. N7-onr-32908, with the Office of Naval Research, U. S. Navy, and in part by contract AT(11-1)-43 with the U. S. Atomic Energy Commission.

[1] J. R. Bates and H. S. Taylor, J. Am. Chem. Soc. **49**, 2438 (1927).
[2] A. Koenig and T. Brings, J. Phys. Chem. 541 (1931).
[3] H. J. Welge and A. O. Beckmann, J. Am. Chem. Soc. **58**, 2462 (1932).
[4] G. R. Gedye and E. K. Rideal, J. Chem. Soc. **135**, 1158 (1932).
[5] R. A. Penneman and L. F. Audrieth, Anal. Chem. **20**, 1058 (1948).
[6] Ogg, Leighton, and Bergstrom, J. Am. Chem. Soc. **56**, 318 (1934).

Rotational Isomerism in Substituted Ethanes Possessing Asymmetric Carbon Atoms

G. J. Szasz
U. S. Office of Naval Research, London, England
January 23, 1950

THE accumulated evidence of recent work[1–8] on rotational isomerism in substituted ethanes all points to the conclusion that the staggered configurations are always preferred to the eclipsed ones in these compounds. Furthermore, in 1,2-disubstituted ethanes, where two large groups dominate, the trans-configuration, in which these groups are farthest apart is the one with minimum potential energy, and in the solid state becomes the sole configuration present. The number of rotational isomers depends on the number of distinguishable substituents, while their actual occurrence in measurable concentrations depends on Boltzmann factors involving the energy difference between the isomers. These energy differences are determined principally by various interactions between the substituents, but are also sensitive to the state of aggregation. Large amounts of available spectral data[4] provide illustrations of rotational isomerism, generally in agreement with expectations based on the above factors.

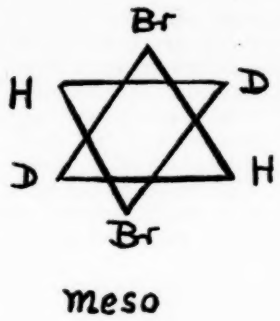

FIG. 1.

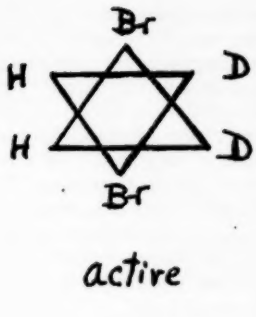

FIG. 2.

The substituted ethanes of types X_2YC-CXYZ and XYZC-CXYZ deserve special attention as they possess one and two asymmetric carbon atoms respectively. Thus study of the optical activity can yield relevant information regarding their rotational isomeric composition. It was in fact on the basis of such data, on tartaric acid and its esters, that R. Lucas[5] suggested the occurrence of a then new kind of isomerism, due to the existence of several different potential energy minima during a complete rotation around a C—C single bond. More recently Bernstein and Pedersen have applied this method to a quantitative study of secondary butyl alcohol.[6] The number of different rotational isomers to be expected in molecules of the type X_2YC-CXYZ is three. XYZC-CXYZ can exist both in the active and in the meso form; these two forms are not rotational isomers of one another, but rather each one may exhibit rotational isomerism of its own.[7] The active form will theoretically consist of three rotational isomers, while in the meso form two rotational isomers would be expected.[8,9] The relative abundance of the rotational isomers will again depend on the various factors mentioned earlier.

Due to their complexity, most of the data in the literature do not give definite indications regarding rotational isomers in compounds belonging to the two types discussed here. De Hemptinne[10] has, however, published valuable Raman spectra of a number of bromoethanes in which some or all hydrogens were replaced by deuterium. These included the compounds BrH_2C-CHDBr (I), BrD_2C-CHDBr (II), and BrDHC-CHDBr (III), which were studied in the liquid state; the Raman spectra of compounds (I) and (III) were obtained also in the solid state. The results can be shown to confirm the above, qualitative conclusions in a striking manner, even without a detailed interpretation of the spectra. The C-Br stretching frequencies, which occur in the 500–700 cm^{-1} region provide the simplest means of elucidating the number of rotational isomers present; among these the symmetrical C-Br stretching mode of the configurations in which the two bromine atoms are in the transposition should produce a very strong Raman shift. In agreement with this, it is noted that in compounds (I) and (II) there is one predominantly strong line in this region (640 cm^{-1} and 617 cm^{-1} respectively), which persists in the spectrum of compound (I) in the solid state. In compound (III) there are two predominantly strong Raman shifts of essentially equal intensity at 610 cm^{-1} and 626 cm^{-1}, both of which

persist in the solid state. These are undoubtedly caused by the two transforms shown in Figs. 1 and 2. The sample in question was prepared by the reaction $C_2H_2+2DBr \rightarrow BrDHC\text{-}CHDBr$ and no details are given[11] regarding separation and purification of the product into meso and *dl* (active) forms. Since both the steric and dipole effects of hydrogen and deuterium must be closedly alike,[12] there would be a very small energy difference between these two configurations. Thus they will probably be formed in approximately equal amounts during synthesis. The nearly equal observed intensity of their analogous vibrations is in good qualitative agreement with this picture.

I am indebted to Dr. N. Sheppard for helpful discussions.

[1] Szasz, Sheppard, and Rank, J. Chem. Phys. **16**, 704 (1948).
[2] J. R. Thomas and W. D. Gwinn, J. Am. Chem. Soc. **71**, 2785 (1949).
[3] Mizushima, Morino, Watanabe, Simonouti, and Yamaguchi, J. Chem. Phys. **17**, 591 (1949).
[4] K. W. F. Kohlrausch, *Ramanspektren* (Akademische Verlagsgesellschaft, Leipzig, 1943), pp. 173, 231.
[5] R. Lucas, Ann. de physique **9(X)**, 380 (1928).
[6] H. J. Bernstein and E. E. Pedersen, J. Chem. Phys. **17**, 885 (1949).
[7] K. L. Wolf, *The Structure of Molecules*, edited by P. Debye (Blackie and Son, Limited, London, 1932), p. 6.
[8] Weissberger, J. Org. Chemie **2**, 245 (1937).
[9] Taufen, Murray, and Cleveland, J. Am. Chem. Soc. **65**, 1130 (1943).
[10] M. De Hemptinne, Vol. Comm. V. Henri (Desoer, Liége 1948), p. 150.
[11] M. De Hemptinne and C. Velghe, Physica **5**, 958 (1938).
[12] A. Langseth and B. Bak, Kgl. Danske Vid. Sels. Math.-Fys. Medd. **13 (XXIV)**, 3 (1947).

Errata: Temperature Coefficients for the Mass Spectra of a Number of Hydrocarbons

[J. Chem. Phys. **17**, 1164 (1949)]

CLIFFORD E. BERRY
Research Department, Consolidated Engineering Corporation, Pasadena 4, California

THE value for the temperature coefficient of the sensitivity of 2-4-dimethyl hexane in Table I should be -0.4 rather than -1.0. Also, the compound labeled 2,2,3-tetramethylbutane should be 2,2,3,3-tetramethylbutane.

On the Quantum Theory of Kinetics

MITSUO SHIMOJI
Chemical Institute, Faculty of Science, Hokkaido University, Sapporo, Japan
January 9, 1950

IN a recent paper Golden[1] has given a general consideration of the quantum mechanics of chemical kinetics, in which some slight modifications of the time-dependent perturbation theory of Dirac has been used to determine the probability of transition from the stable configuration A to the other stable configuration B. As is well known, this solution obtained by an iterative procedure is limited to a comparatively short interval of time. This difficulty can be excluded easily as follows.

Schrödinger's time-dependent wave equation is

$$H\Psi = i\hbar(\partial\Psi/\partial t), \tag{1}$$

where H is the total Hamiltonian of the system and is independent of time, Ψ is defined all over the configurational space and time. Since the configurations of A and B are non-orthogonal, the following relations are obtained.

$$\Psi = a_0{}^A(t)\Psi_0{}^A \exp[-(i/\hbar)E_0{}^A t] + \sum_{m\neq 0} a_m{}^A(t)\Psi_m{}^A \exp[-(i/\hbar)E_m{}^A t], \tag{2}$$

$$\Psi = \sum_n a_n{}^B(t)\Psi_n{}^B \exp[-(i/\hbar)E_n{}^B t]. \tag{3}$$

Of course

$$H^A\Psi_0{}^A = E_0{}^A\Psi_0{}^A, \quad H^B\Psi_n{}^B = E_n{}^B\Psi_n{}^B, \quad \text{etc.} \tag{4}$$

Golden's treatment corresponds to $a_0{}^A(t)=1$, $a_m{}^A(t)=0$.

In order to evaluate the decrease of the configuration A with time appropriately, the following equation may be introduced.

$$d(|a_0{}^A(t)|^2)/dt = -\Gamma(|a_0(t)|^2) \tag{5}$$

with the initial condition

$$a_0{}^A(0)=1, \quad a_m{}^A(t)=0,$$

where $|a_0{}^A(t)|^2$ describes the probability of the zeroth state of the configuration A, Γ is a constant, which corresponds to the rate constant. Using some modifications of Weisskopf-Wigner method[2] in the radiation theory, these equations may be solved.

Substitute (2) and (3) respectively into (1) and multiply them by the complex conjugate of each wave function, which forms respectively a complete orthogonal set being normalized to unity.

$$i\hbar\dot{a}_0{}^A(t) = \int \Psi_0{}^{A*}(H-H^A)\Psi d\tau \exp[(i/\hbar)E_0{}^A t], \tag{2'}$$

$$i\hbar\dot{a}_n{}^B(t) = \int \Psi_n{}^{B*}(H-H^B)\Psi d\tau \exp[(i/\hbar)E_n{}^B t]. \tag{3'}$$

From (2), (5), and (3'), one obtains

$$a_n{}^B(t)-a_n{}^B(0) = \int \Psi_n{}^{B*}(H-H^B)\Psi_0{}^A d\tau \times \frac{1-\exp[(i/\hbar)(E_n{}^B-E_0{}^A)t-\Gamma t/2]}{E_n{}^B-E_0{}^A+i\hbar\Gamma/2} + \sum_m (\text{contributions from } m\neq 0). \tag{6}$$

Substituting (6) into (2'),

$$i\hbar\Gamma/2 = \sum_n \left\{ |H'|_{BA}{}^2 \times \frac{1-\exp[-(i/\hbar)(E_n{}^B-E_0{}^A)t+\Gamma t/2]}{E_n{}^B-E_0{}^A+i\hbar\Gamma/2} - |H'|_{BA}\int \Psi_n{}^{B*}\Psi_0{}^A d\tau \exp[-(i/\hbar)(E_n{}^B-E_0{}^A)t+\Gamma t/2] \right\} \tag{7}$$

can be obtained by inserting (3), since

$$\int \Psi_n{}^{B*}(H^A-H^B)\Psi_0{}^A d\tau = E_0{}^A \int \Psi_n{}^{B*}\Psi_0{}^A d\tau - \sum_i \left[\int \Psi_n{}^{B*}H^B\Psi_i{}^B d\tau\right]\left[\int \Psi_i{}^{B*}\Psi_0{}^A d\tau\right] = (E_0{}^A-E_n{}^B)\int \Psi_n{}^{B*}\Psi_0{}^A d\tau. \tag{8}$$

If the transition from the configuration A to the specified region of the configuration B is considered, one can carry out the integration with respect to (7) upon the possible energy values of the configuration B. As the result one has

$$\Gamma = (2\pi/\hbar)\int \rho_B(\alpha^B)|H'|_{BA}{}^2 d\alpha^B d\Omega, \tag{9}$$

where ρ_B is the density of B configuration, α^B is the characteristic value of B except energy and Ω is the solid angle.

Accordingly, the average rate of the transition $A \rightarrow B$ which is deduced from averaging Γ over the statistical equilibrium states of the configuration A is expressed as follows.

$$\bar{\Gamma} = \delta_A/D_A, \tag{10}$$

where

$$\delta_A = \frac{1}{h^{3i}}\sum_j \exp(-E_j{}^A/kT) \times \int dp_1{}^A \cdots dp_{3i}{}^A dq_1{}^A \cdots dq_{3i}{}^A \Gamma \exp(-E_2{}^A/kT),$$

$$D_A = \frac{1}{h^{3i}}\sum_j \exp(-E_j{}^A/kT) \times \int dp_1{}^A \cdots dp_{3i}{}^A dq_1{}^A \cdots dq_{3i}{}^A \exp(-E_2{}^A/kT).$$

If Born-Oppenheimer approximation, wave functions of free particles for nuclei, and relative coordinates with respect to the

center of mass of the system etc., in (10) are adopted, one obtains the same results as Golden's. Thus the absolute rate of reaction can be calculated theoretically as long as the matrix elements of (9) can be given accurately.

The author is grateful for the kind guidance of Professor K. Niwa.

[1] S. Golden, J. Chem. Phys. **17**, 620 (1949).
[2] Weisskopf and Wigner, Zeits. f. Physik **63**, 54 (1930); W. Heitler, *Quantum Theory of Radiation* (Oxford University Press, London 1944).

On the Mean Amplitudes of Thermal Vibrations in CO_2 Molecule

YONEZO MORINO
Chemical Laboratory, Faculty of Science, Tokyo University, Tokyo, Japan
January 3, 1950

IN the November issue of this Journal, I. L. Karle and J. Karle[1] reported a very interesting result obtained by electron diffraction investigation. They evaluated the mean amplitudes of atomic distances from the radial distribution function obtained by their sector method. Their result for CO_2 is shown in the first column of Table I. They used the following formulas in comparing their

TABLE I. The mean amplitudes of thermal vibrations in CO_2 molecule.

	Karle's observed values	Karle's computed values	Corrected values
C−O	0.034±0.003A	0.034A	0.034A
O−O	0.040±0.007A	0.029A	0.041A

experimental values with those calculated from the spectroscopic data,

$$\langle \Delta r_{CO}{}^2 \rangle_{Av} = (\mu_1+\mu_2)/2\alpha, \tag{1}$$

and

$$\langle \Delta r_{OO}{}^2 \rangle_{Av} = \mu_1/\alpha, \tag{2}$$

where μ_1 and μ_2 are the average energies of the oscillators of the normal coordinates, and α the force constant for the C−O bond. In this letter the author wishes to point out that the factor 2 should be added to the right-hand side of Eq. (2) as explained in the following.

When we transform the internal coordinates Δr_1, Δr_2 (the displacements from the equilibrium distances of the two C−O bonds), and $\Delta\theta$ (that of the angle OCO) into normal coordinates

$$\begin{cases} q_1=(\Delta r_1+\Delta r_2)/\sqrt{2}, \\ q_2=(\Delta r_1-\Delta r_2)/\sqrt{2}, \\ q_3=\Delta\theta, \end{cases} \tag{3}$$

the kinetic and potential energy functions of CO_2 molecule (assuming a simplified valence force field) are expressed as follows:

$$2T = m\dot{q}_1{}^2+\frac{mM}{2m+M}\dot{q}_2{}^2+\tfrac{1}{2}\cdot\frac{mM}{2m+M}r^2\dot{q}_3{}^2 \tag{4}$$

and

$$2V = \alpha q_1{}^2+\alpha q_2{}^2+\delta q_3{}^2,$$

where m and M are the masses of oxygen and carbon atoms, respectively, and δ is the force constant for the angle COC.

The mean amplitudes of each coordinate thus become

$$\langle q_1{}^2\rangle_{Av} = \mu_1/\alpha, \quad \text{and} \quad \langle q_2{}^2\rangle_{Av} = \mu_2/\alpha, \tag{5}$$

where

$$\mu_1 = \tfrac{1}{2}h\nu_1+h\nu_1/(e^{h\nu_1/kT}-1),$$

and

$$\mu_2 = \tfrac{1}{2}h\nu_2+h\nu_2/(e^{h\nu_2/kT}-1). \tag{6}$$

Therefore, the mean amplitudes of the thermal displacements from the equilibrium distances are

$$\langle \Delta r_{CO}{}^2 \rangle_{Av} = \langle \Delta r_1{}^2 \rangle_{Av} = \langle [(1/\sqrt{2})(q_1+q_2)]^2 \rangle_{Av} = (\langle q_1{}^2\rangle_{Av}+\langle q_2{}^2\rangle_{Av})/2 = (\mu_1+\mu_2)/2\alpha, \tag{7}$$

and

$$\langle \Delta r_{OO}{}^2 \rangle_{Av} = \langle (\Delta r_1+\Delta r_2)^2 \rangle_{Av} = \langle (\sqrt{2}q_1)^2 \rangle_{Av} = 2\langle q_1{}^2\rangle_{Av} = 2\mu_1/\alpha. \tag{8}$$

In the latter equation the term containing $\Delta\theta$ was neglected, since it is of a second-order magnitude. The value of $\langle \Delta r_{OO}{}^2 \rangle_{Av}{}^{\frac{1}{2}}$ calculated by this formula with the same numerical constants as those used by Karle, is 0.041A, which is in better agreement with the observed value than the one computed from Eq. (2) (see Table I). As to their result Karle and Karle stated that the difference between the electron diffraction and the spectroscopic values of $\langle l^2 \rangle_{Av}{}^{\frac{1}{2}}$ for the O-O distance may be attributed mainly to the fact that the O-O peak in the radial distribution curve is small which makes the determination less accurate. However, according to the view of the present author Karle's experiment is excellent and it affords us a new method for the study of molecular structure.

It may be said in this connection that the formula $\langle \Delta r_{OO}{}^2 \rangle_{Av} = \mu_1/2\alpha$ used by Debye[2] for the discussion of the thermal motion should also be corrected as stated.

Rigorous treatment with Urey-Bradley field does not improve the result so much, for it gives the values of 0.033A and 0.040A instead of 0.034A and 0.041A. A detailed argument will be published in the near future.

[1] I. L. Karle and J. Karle, J. Chem. Phys. **17**, 1052 (1949).
[2] P. Debye, J. Chem. Phys. **9**, 55 (1941).

The Electrolytic Separation Factor of Tritium*

JURO HORIUTI AND TAKASHI NAKAMURA
Research Institute for Catalysis, Hokkaido University, Sapporo, Japan
December 29, 1949

THE measurement of the tritium's separation factor S_T by Eidinoff[1] stimulated us to extend our previous theoretical calculation[2(b), 2(e)] of the deuterium's separation factor S_D to that case. The expression for S_T is similarly obtained as that,

$$S_T = (d\mathrm{H}/\mathrm{H})/(d\mathrm{T}/\mathrm{T}) = (q_H{}^*/q_T{}^*)\cdot\{Q(\mathrm{HTO})/Q(\mathrm{H_2O})\}\cdot K,$$

where the second member defines S_T as the ratio of $d\mathrm{H}/\mathrm{H}$, the relative rate of decrease of protium concentration H in the solution by electrolysis, to that for tritium $d\mathrm{T}/\mathrm{T}$. The $q_H{}^*$ is the Boltzmann factor $\exp(-\epsilon/k\mathrm{T})$ of the reversible work ϵ required to bring up the critical complex[3] of the rate-determining step of the hydrogen electrode reaction,

$$2\mathrm{H}^+ + 2e \rightarrow \mathrm{H_2}, \tag{1}$$

from its standard state up to a preliminary cleared definite site on the electrode, $q_T{}^*$ that for the critical complex derived from the above complex by replacing one constituent protium atom by a tritium atom, $Q(\mathrm{H_2O})$ or $Q(\mathrm{HTO})$ the partition function of a gaseous H_2O or HTO molecule respectively, and K the equilibrium constant of the reaction,

$$\mathrm{HTO}(g)+\mathrm{H_2O}(l) = \mathrm{HTO}(l)+\mathrm{H_2O}(g).$$

The rate-determining step of (1) is $2\mathrm{H}(a)\rightarrow\mathrm{H_2}$ or $\mathrm{H_2}^+(a)\rightarrow\mathrm{H_2}$ respectively according to the catalytic or the electrochemical mechanism,[2a] which has hitherto been evidenced to be operative respectively on hydrogen electrodes of Ni, Ag, Pt, etc., or on those of Hg, Sn, etc., where $\mathrm{H}(a)$ or $\mathrm{H_2}^+(a)$ denotes a hydrogen atom or a hydrogen molecule-ion adsorbed on the electrode.

In the case of the catalytic mechanism the potential function required for calculating $q_H{}^*/q_T{}^*$ was simply quoted from the

previous work[2(b)] for Ni electrode, whereas derived for Pt electrode similarly according to the so-called semi-empirical method from the following data: $D_e=60.0$ kcal., $a=1.50A^{-1}$, $r_e=1.65A$ for the Pt-H Morse function; 26 percent the Morse function for the Pt-H Coulomb energy; 10.0 kcal. and 6.0 kcal. respectively for the exchange and Coulomb energies of the Pt−Pt bond with Pt−Pt distance 3.93A. In the case of the electrochemical mechanism the potential function for a Hg electrode, polarized against the N calomel electrode by −1.26 volt in $N/10$ HCl, was derived from the paper[2(c)] dealing extensively with the electrochemical mechanism.

The calculation of $Q(H_2O)$, $Q(HTO)$ was based on Libby's recent analysis of the isotopic water molecules,[4] which seems most reliable. The value of K having not been measured so far, it was simply taken unity regarding the corresponding value for deuterium which had been found almost unity (1.04 at 25°C[5]). Wigner's correction for the quantum mechanical tunneling effect[6] (as considered in reference 2(b)) was not included here, inasmuch as it is invalidated, as remarked by R. P. Bell,[7] in the present case of large ν^*,† the imaginary frequency of the critical complex appropriate to the mode of motion normal to the barrier.

The S_T thus calculated are given in Table I, and compared with observed ones, if available, given in parentheses. Table I includes also the revised calculations of S_D for Ni and Hg electrodes based on the new data of the water molecules as well as new one for Pt electrode calculated using the potential energy data given. The coincidence seems satisfactory considering the possible lowering of observed S_D or S_T by local heating at the electrode, due to the negative temperature coefficient of the separation factor,[8] in the case of larger current density. The observation of the predicted S_T is desirable.

TABLE I. Separation factors (at 20°C).

	Catalytic mechanism		Electrochemical mechanism
	Ni electrode	Pt electrode	Hg electrode
S_D	6.8 (6.7[a])	7.2 (6.9[a])	3.8 (3.1[a])
S_T	15.1 (none)	16.1 (14.0[b])	5.8 (none)

[a] See reference 2(a).
[b] See reference 1.

* The detailed account will be given in J. Research Inst. Catalysis, Hokkaido University.
[1] Eidinoff, J. Am. Chem. Soc. **69**, 2507 (1946).
[2] (a) Horiuti and Okamoto, Sci. Pap. Inst. Phys. Chem. Research, Tokyo **28**, 231 (1936); (b) Okamoto, Horiuti and Hirota, *ibid.* **29**, 223 (1936); (c) Horiuti, Hirota and Keii, J. Research Inst. Catalysis (to be published); (d) Hirota and Horiuti, Sci. Pap. Inst. Phys. Chem. Research, Tokyo **30**, 151 (1936).
[3] Horiuti, J. Research Inst. Catalysis **1**, 8 (1948).
[4] D. M. Dennison and B. T. Darling, Phys. Rev. **57**, 128 (1940); W. F. Libby, J. Chem. Phys. **11**, 101 (1943).
[5] Horiuti and Okamoto, Bull. Chem. Soc. Japan **10**, 503 (1935).
[6] Wigner, Zeits. f. physik. Chemie **B19**, 203 (1932).
[7] R. P. Bell, Trans. Faraday Soc. **34**, 259 (1938).
† In our case, $\nu^*\approx 1000$ cm^{-1}.
[8] Wolfenden and Walton, Trans. Faraday Soc. **34**, 436 (1938).

On the Anomalous Thermal Diffusion Observed in the Solution of Mixed Electrolytes

KOZO HIROTA
Research Institute of Applied Electricity, Hokkaido University, Sapporo, Japan
January 31, 1950

THE negative effect of the thermal diffusion of aqueous solutions in which electrolytes are consisted of AX and BX, i.e., enrichment of A or B ion at the hotter region of the Clusius-Dickel's apparatus, was found by Gillespie and Breck[1] and independently by the present writer.[2] By the investigation made thereafter,[3] it was found that, though the effect seemed anomalous, it is brought about by a kind of diffusion potential as a result of the difference of diffusion velocity between ions.[4]

Recently, Guthrie and others proposed a theory on the separation of electrolyte solution in general and, standing on the same viewpoint, could explain the negative effect quantitatively. Slightly modifying their formula, separation ratio of A-ion in the solution of AX-BX type (R_a), defined by its concentration at the bottom reservoir of the Clusius-Dickel's apparatus to that at the top, is given by

$$R_a=R_{ax}+\frac{c_b(u_b+u_x)(R_{ax}-R_{bx})}{c_a(u_a+u_x)+c_b(u_b+u_x)}\cdot\frac{u_a}{u_x}, \qquad (1)$$

where R_{ax} and R_{bx} are separation ratios of AX and BX, respectively, while u_i is ionic mobility of i-ion and c_a and c_b concentration of AX and BX, respectively.

TABLE I.

Exper. number	Concentration in normal c_a	c_b	Separation ratio at 50°C A (obs)	A (calc.)	B (obs)	B (calc.)	Remark
I. HCl (A)−NaCl (B)							
1	0.50	0.50	1.34	1.39	0.97	0.96	—
2	0.050	0.53	1.47[7]	1.78 (1.51)	1.02[9]	1.02 (1.03)	$R_{ax}=1.16$, $R_{bx}=1.046$
3	0.350	2.54	1.47[8]	1.70 (1.78)	1.03[3]	1.01 (1.02)	$R_{ax}=1.25$, $R_{bx}=1.06$
4	0.130	2.79	1.56	1.81 (1.68)	1.05[4]	1.03 (1.05)	$R_{ax}=1.20$, $R_{bx}=1.06$
5	0.0186	2.51	1.65	1.88 (1.59)	1.05[5]	1.04 (1.05)	$R_{ax}=1.17$, $R_{bx}=1.06$
II. NH_4Cl (A)−NaCl (B)							
6	0.10	0.10	1.00[4]	0.99 (1.02)	1.04[4]	1.06 (1.05)	$R_{ax}=1.026$, $R_{bx}=1.044$
7	1.00	0.96	0.99*	0.99	1.05[2]*	1.06	—
III. HCl (A)−NH_4Cl (B)							
8	0.50	0.50	1.42	1.46	0.89	0.86	—
IV. NaOH (A)−NaCl (B)							
9	0.044	0.087	1.42	1.75	1.13	0.86	—

* $\mathbf{R}_i$'s interpolated at the second hours are used. Note (a) Calculated separation ratios parenthesized are calculated by use of R_i's described in the last column of the corresponding line. (b) Slight difference from those of Guthrie and others (No. 1 and No. 8) will be due to the difference of ionic mobilities used in the calculation.

As shown in Table I, the observed values at 50°C[5] are described together with the calculated according to Eq. (1) by use of the following constants.

The ionic mobilities used are H^+ 450, Cl^- 116, NH_4^+ 115, Na^+ 82, and OH^- 280. Separation ratios of each electrolyte are of one normal and that at the second hours, if otherwise not stated: i.e., HCl 1.22, NaCl 1.047, NH_4Cl 1.010, and NaOH 1.30. In order to check the concentration effect, $\mathbf{R}_i$'s which correspond to the concentration of the system concerned[3] are also used, the results being parenthesized in Table I.

Generally speaking, agreement of the theory with experiment is good also in other systems not yet discussed by Guthrie and others who applied their formula only to Nos. 1 and 8. It is remarkable that the agreement is improved, if the concentration dependency of R_i is taken into account. The positive effect of Cl^- ion in NaOH-NaCl, perfectly opposite to the theory, cannot be explained at all, because Eq. (1) does not give such a case that separation ratios of both R_a and R_b become larger than R_{ax} and R_{bx}.

Extended discussion will be published in Bull. Chem. Soc. Japan.

[1] K. Hirota, Bull. Chem. Soc. Japan **16**, 232 (1941).
[2] L. J. Gillespie and S. Breck, J. Chem. Phys. **9**, 370 (1941).
[3] K. Hirota, J. Chem. Soc. Japan (printed in Japanese) **64**, 16 and 112 (1943); cf. Chem. Abst. **41**, 3346 (1947).
[4] Guthrie, Wilson, and Schomaker, J. Chem. Phys. **17**, 310 (1949).
[5] The specification of the apparatus used: equidistant annular space 1.5 mm, its length 94 cm, volume of reservoirs 23 cc, higher temperature 76°C and lower temperature 25°C. Cf. Bull. Chem. Soc. Japan **16**, 475 (1941).

Application of Ursell and Mayer's Treatment for Imperfect Gases to Adsorption

SYÛ ONO
Institute of Applied Science, Faculty of Engineering, Kyushu University, Fukuoka, Japan
December 28, 1949

MANY attempts to derive the adsorption isotherm from a knowledge of the intermolecular forces have been made, based upon the idea of lattices. It seems, however, to be doubtful that the lattice theories of adsorption lead to really satisfactory results. To make further progress the author made the general development of the Gibbs phase integral for a system consisting of adsorbate molecules and an adsorbent according to Ursell[1] and Mayer's[2] method for treating imperfect gases.

We will denote the potential energy of the system containing n adsorbate molecules alone by the symbol $U_n(\{\mathbf{n}\}, 0)$ and the potential energy of the system containing n adsorbate molecules and an adsorbent by $U_n(\{\mathbf{n}\}, 1)$, where the boldface symbol $\{\mathbf{n}\}$ indicates the coordinates of n molecules. We define $F_n(\{\mathbf{n}\}, \epsilon)$ by

$$F_n(\{\mathbf{n}\}, \epsilon) = \exp\left(-\frac{U_n(\{\mathbf{n}\}, \epsilon)}{kT}\right), \tag{1}$$

where ϵ assumes the value 1. According to the result proved by Mayer and Montroll,[3] we may write the expansion of $F_M(\{\mathbf{M}\}, \epsilon)$ in the form

$$F_M(\{\mathbf{M}\}, \epsilon) = \sum \{k\{\mathbf{m}_i\}_M\}_u \prod_{i=1}^{k} [g_m\{\mathbf{m}_i\}_M + \epsilon h_m\{\mathbf{m}_i\}_M], \tag{2}$$

where $\sum \{k\{\mathbf{m}_i\}_M\}_u$ is used to indicate summation over all unconnected sets of subsets. The inverses of (2) are

$$g_m\{\mathbf{m}\} = \sum \{l\{\mathbf{M}_j\}_m\}_u (-)^{l-1}(l-1)! \prod_{j=1}^{l} F_M(\{\mathbf{M}_j\}_m, 0), \tag{3}$$

and

$$h_m\{m\} = \sum \{l\{\mathbf{M}_j\}_m\}_u (-)^{l-1}(l-1)! \times [\prod_{j=1}^{l} F_M(\{\mathbf{M}_j\}_m, 1) - \prod_{j=1}^{l} F_M(\{\mathbf{M}_j\}, 0)]. \tag{4}$$

The grand partition function of the system at the fugacity z is given by

$$\Xi(T, z, \epsilon) = \sum_{n=0} \frac{z^n}{n!} \int\int\cdots\int F_n(\{\mathbf{n}\}, \epsilon) d\{n\}, \tag{5}$$

$d\{\mathbf{n}\}$ being the configuration element of n molecules, where ϵ assumes 0 or 1 according as the system contains the adsorbent or not. Using the expression (2) we obtain

$$\Xi(T, z, \epsilon) = \exp[\sum_{l=1} Vb_l z^l + \sum_{l=1} a\gamma_l z^l], \tag{6}$$

in which V is the volume of the system and a is the area of the surface of the adsorbent. Here b_l and γ_l are the cluster integrals respectively defined as

$$b_l = \frac{1}{Vl!} \int\int\cdots\int g_l\{\mathbf{l}\} d\{\mathbf{l}\}, \tag{7}$$

and

$$\gamma_l = \frac{1}{al!} \int\int\cdots\int h_l\{\mathbf{l}\} d\{\mathbf{l}\}, \tag{8}$$

the integration being extended over a region bounded by the volume of the container. From (6) we at once have the expression for the average number of the molecules contained in the system. And the increase in the number of molecules per unit area of the surface of the adsorbent due to insertion of the adsorbent will be expressed by

$$\theta = \sum_{l=1} l\gamma_l z^l, \tag{9}$$

which gives the equilibrium number of adsorbed molecules as a function of the fugacity. The pressure can be expressed as a function of the fugacity by means of Mayer's equation:

$$p = kT \sum_{l=1} b_l z^l. \tag{10}$$

From (9) and (10) we can, in principle, calculate the adsorption isotherm.

The details of the theory will appear in the Memoirs of Faculty of Engineering, Kyushu University **12**, No. 1.

[1] H. D. Ursell, Proc. Camb. Phil. Soc. **23**, 685 (1927).
[2] J. E. Mayer, J. Chem. Phys. **5**, 67 (1937).
[3] J. E. Mayer and E. W. Montroll, J. Chem. Phys. **9**, 2 (1941).

"Vapor Snake" Phenomenon and "Plastic Crystals"

SYÛZÔ SEKI
Department of Chemistry, University of Osaka, Osaka, Japan
January 19, 1950

IN a recent communication, M. K. Phibbs and H. I. Shiff have reported the "vapor snake" phenomenon in cyclohexane.[1] They concluded from their experiments that this phenomenon was attributed to the high vapor pressures of cyclohexane (35 mm Hg at the melting point). However, judging from their description, one may receive an impression that they do not necessarily regard this condition as the decisive one. Indeed, they suggest also that this phenomenon is due to the highly symmetrical molecular structure of this substance. This latter condition, probably, may be rather essential in such a sense as will be given.

Quite independently, we have found just the same phenomenon in cyclohexanol and carbon tetrachloride during the course of fractional distillation in high vacuum and have already reported the results as well as some explanation in a Japanese scientific journal in 1948.[2] As this was written in Japanese and discussed in a somewhat different way from the above authors, we should like to explain the results and interpretation briefly in the present letter.

According to Timmermanns,[3] the so-called plastic crystals are generally composed of molecules of spherical shape and they form solid solutions with each other in wide range of concentrations regardless of the difference of chemical properties of component molecules. He pointed out, furthermore, the fact that the entropy change at the melting point is much smaller than that at the transition point between this plastic crystalline and ordinary crystalline phases and that the remarkable plastic property is characteristic of this phase. Plastic crystals are thus in an intermediate state between the solid and the liquid states.

In our Laboratory, under the direction of Professor Nitta, we have been studying the structure and properties of this sort of crystal for several years. The substances investigated with x-rays are pentaerythlitol,[4] tetranitromethane,[5] cyclohexanol,[6] cyclohexane,[7] and berylliumoxyacetate.[8] The analysis of the Laue effect and the diffuse scattering of x-rays of these crystals have revealed that, whereas the centers of mass of molecule are truly so arranged as to form an ordinary crystal lattice, a part or the whole of the molecule is no longer fixed and undergoes violent thermal motions.

This fact stands in contrast to the liquid crystal—the well-known intermediate phase between the solid and the liquid—in which the molecules have ordinarily rod-like shape and stack themselves together to form swarms, but do not constitute an ordinary crystalline lattice.

The vapor pressures of cyclohexanol and carbon tetrachloride measured by the present author at their melting points are only 0.7 mm Hg and 7 mm Hg, respectively.[5,9] They are much lower in comparison with that of cyclohexane; nevertheless they show this vapor snake phenomenon. In our opinion, therefore, the high vapor pressure of the crystal is not the necessary condition for the occurrence of this anomalous phenomenon, but the state of plastic crystal (not of the super-cooled liquid!) is a more essential factor. An ordinary liquid, when solidified, going to the polycrystalline phase, forms cracks in every direction. We can obtain this polycrystalline state of these substances without observing any vapor snake phenomenon, if we solidify them rapidly down below their transition points by immersing into the liquid air. Accordingly, the violent thermal motion of the molecules in the crystalline lattice seems to play an important rôle in this phenomenon. Thus, it is to be expected that the crystal of $C(SCH_3)_4$, of which the crystal structure has been determined recently and is known that the molecules are in violent thermal motion,[10] will also show this vapor snake phenomenon.

[1] M. K. Phibbs and H. I. Shiff, J. Chem. Phys. **17**, 843 (1949).
[2] S. Seki, Kagwaku **18**, 277 (1948).
[3] Timmermanns, J. Chim. Phys. **35**, 331 (1938).
[4] I. Nitta and T. Watanabe, Sci. Papers Inst. Phys. Chem. Research, Tokyo **34**, 1669 (1938); I. Nitta and T. Watanabe, Bull. Chem. Soc. Japan **13**, 28 (1938).
[5] Oda, Iida, and Nitta, J. Chem. Soc. Japan **64**, 616 (1943); T. Oda and T. Watanabe, *ibid.* **65**, 154 (1944); S. Seki and I. Nitta, *ibid.* **62**, 907 (1941).
[6] T. Oda, X-Rays **5**, 21 (1948).
[7] See reference 6, p. 2; S. Seki and I. Nitta, J. Chem. Soc. Japan **69**, 141 (1948).
[8] T. Watanabe and Y. Saito, Nature **163**, 225 (1949); Seki, Momotani, and Chihara, *ibid.* **163**, 226 (1949).
[9] I. Nitta and S. Seki, J. Chem. Soc. Japan **69**, 85 (1948).
[10] H. J. Backer and W. G. Pedrok, Rec. trav. Chim. **62**, 533 (1943).

Synthetic SiO_2 Prism in the Infra-Red

MANSEL DAVIES
Department of Chemistry, University College, Aberystwyth, Wales
January 20, 1950

THE use of synthetically grown crystals (NaCl, KBr, LiF, CaF_2, etc.) as prism materials in the infra-red is well known. Lithium fluoride, for instance, is much sought after as it offers good dispersive power in the 3000 cm^{-1} region of the O—H, N—H, etc. absorption frequencies. It is equally well known that, to the limits of its transmission in this region, quartz provides significantly higher dispersion before its absorption becomes too strong at (or before) 2800 cm^{-1} (3.5μ). From 2800 to 4000 cm^{-1}, although somewhat less effective than the crystalline material, the dispersive power of fused silica is still about 50 percent greater than that of LiF.

The purpose of this note is to indicate that transparent fused silica, available in this country from Thermal Syndicate Ltd., Wallsend-on-Tyne, is admirably suited for infra-red work in this region. A prism, height 8 cm, length of face 10 cm, angle 45°, although containing minute air bubbles, transmits adequate radiation for intensity measurements to within a few percent in the Grubb-Parsons single beam instrument down to 2850 cm^{-1}. The radiation scattered by the prism in this region is not significantly larger than that for clear NaCl. An approximate indication of the over-all performance in the spectrometer mentioned can be made by stating that the 2.6μ atmospheric water record approaches in detail Sleator's plot using a grating and slit widths of 31A (4.5 cm^{-1}).[1] With solutions, the details in Fox and Martin's careful grating spectra[2] are recorded, e.g., the 3111 cm peak in dilute CCl_4 solutions of $C_6H_5 \cdot CH_2OH$.[3]

To the British purchaser the relative costs of LiF (without import duties) and SiO_2 prisms of the mentioned size are about 8:1.

[1] Sleator, Astrophys. J. **48**, 125 (1918).
[2] Fox and Martin, Proc. Roy. Soc. **A162**, 419 (1937).
[3] See reference 2, Fig. 3.